

# **Risk Based Design, Maintenance and Inspection of Marine and Offshore Structures with Particular Reference to Fatigue Analysis**

**A Thesis Submitted to Liverpool John Moores  
University for the Degree of Doctor of Philosophy**

**Echezonachukwu Chukwuemeka Chukwuka**

**Liverpool Logistics, Offshore and Marine (LOOM) Institute  
School of Engineering, Technology and Maritime Operations  
June 2011**

---

## Summary

Risk, in many ramifications, cuts across all industries. It is acknowledged that risk cannot be eliminated completely but must be managed. A risk assessment embodies a framework by which decisions are made not only to mitigate risks but also to explore new possibilities while optimizing resources.

The recommendation of the Lord Cullen report on the Piper Alpha disaster has led to the use of the Formal Safety Assessment (FSA) framework in the maritime and offshore industries. The FSA framework provides a thorough risk assessment procedure by which potential hazards in human activities, transportation, structures, systems, etc. could be mitigated. The FSA is a five-step procedure consisting of: system definition, hazard identification, risk quantification (qualitative or quantitative), evaluation of Risk Control Options (RCOs)/Cost Benefit Analysis (CBA) and decision making. This framework also enables optimal utility of resources.

This research focuses on the incorporation of the FSA techniques in the design and maintenance of structures in the marine and offshore industries. The risk quantification stage of the FSA is perhaps the most challenging as the presence of uncertainty in several aspects poses a serious problem. The risk quantification is usually the main theme of most FSAs and will be the main focus of this research. As a result of the varying complexity and configuration of these structures, a FLEXible Structural RELiability algorithm (FLEXSTREM) is introduced. This methodology is based on the well known Monte Carlo simulation (a quantitative method) for the quantification of the risk associated with these structures. The increasing capacity of computers enabled the implementation of the procedure in FORTRAN 95 for increased robustness and efficiency.

The FLEXSTREM utilizes structural parameters and limit states in a semi-probabilistic manner to establish the reliability of a structure. A demonstration was first carried out on a single-member structure (SMS) in the form of a marine jib crane. Successful demonstration on the simple case of an SMS led to further development of the technique to accommodate multi-member structures (MMS) and complex

---

configurations. The Monte Carlo finite element method – a stochastic finite element analysis technique, formed the basis of this development. Successful demonstration and validation were carried out on an offshore crane (lattice jib).

Upon successful completion of the risk quantification stage, RCOs were sought. With the cost and safety (CBA) as guiding parameters, two RCOs were introduced: FLEXOPT – a FLEXSTREM based optimization method and STOFLEX – a stochastic implementation of the FLEXSTREM for maintenance and repair scheduling. Using the pre-existing offshore crane case study, several combinations of the different structural parameters were carried out in FLEXOPT to determine the optimal structural configuration. STOFLEX brings the time-variation effect into consideration. The main aim was to enable optimal scheduling of inspections and repair in order to mitigate risks and maximize productivity and structural life.

The main findings of this research are the developed methods of implementing the FSA in the context of structures. Several other significant findings pertaining to the methods are also denoted with possible future improvements identified.

---

## Acknowledgements

Firstly my thanks firstly go to God almighty for seeing me through this project. The project was impossible without Him. My inspiration and strength came from Him; my only regret is that I was too slow and lazy to implement all that came to me from Him in this thesis. My hearty thanks also go to my parents (Engr. and Dr. Mrs Chukwuka) to whom this project is dedicated for all their sacrifice towards our education. My father, Engr. Chukwuka (the bigger engineer), kept giving me ideas and scenarios which constantly challenged me to do more. I am also grateful to my brothers (Chukwunonso and Chukwunyelu) and only sister (Chinelo) for their help, advice and support and also to my twin sister (Adaeze aka ejima'm).

This research is not conceivable without Professor Jin Wang who guided me with hands sky high, thus giving me room for expression in this thesis not to mention the financial assistances. I am grateful. Dr. Zaili Yang and Dr. Keith Metcalfe have also been tremendously instrumental in making sure attention-to-detail has been kept for the technical chapters.

Finally my appreciation extends to Boehler Markus of Liebherr Cranes, Austria for the case study especially in the circumstances where no other company could oblige due to contractual issues and also to Hyundai Heavy Industries (HHI), South Korea for the standards provided. Also Marek Skowronek is not left out; his illustration of the Monte Carlo method set me up for so many implementations.

Dr. Andrew Cunningham (brother in Monte Carlo), Dr. Chidi Nwaoha, Dr. Hristos Karahalios, Dr. Darshana Godaliyadde, Dr. Steven Chen and other members of the LOOM research institute have also contributed in no small ways to the outcome of this thesis.

*E. Chukwuka*

---

## Table of Contents

Summary .....	i
Acknowledgements.....	iii
List of Figures.....	xi
List of Tables.....	xvi
Abbreviations .....	xix
List of Notations .....	xxi
Chapter 1: Introduction .....	1
Summary .....	1
1.1 Background of the Research .....	1
1.2 Statement of the Problem.....	3
1.3 Research Aims and Objectives .....	5
1.4 Research Methodology and Scope .....	5
1.5 Structure of the Thesis.....	6
Chapter 2: Literature Review .....	12
Summary .....	12
2.1 Risk Assessment.....	12
2.2 Risk-Based Design .....	19
2.3 Structures in the Marine and Offshore Environment .....	26
2.4 Reliability.....	29
2.4.1 Uncertainty.....	29
2.4.2 Structural Reliability.....	31
2.4.3 Deterministic Analysis/Modelling vs. Probabilistic Analysis/Modelling	31
2.4.4 Review of Methods of Handling Uncertainty .....	33
2.5 Monte Carlo Methods.....	34
2.5.1 Distributions.....	38
2.5.1.1 Expected Value .....	38
2.5.1.2 Uniform Distribution.....	39
2.5.1.3 Exponential Distribution .....	39
2.5.1.4 Normal (Gaussian) Distribution.....	40

---

2.5.1.5	Lognormal Distribution.....	41
2.5.1.6	Gumbel Distribution.....	41
2.5.2	Limit State Modelling.....	42
2.6	Maintenance.....	43
2.7	Justification for the Research.....	46
Chapter 3: Beta-Flexible Structural Reliability Algorithm (BETA-FLEXSTREM):		
A Risk Quantification Tool for Single-Member Structures (SMS).....		
	Summary .....	48
3.1	Introduction.....	48
3.2	Background/Review .....	49
3.2.1	Fatigue (Structural).....	49
3.2.2	Failure Prevention .....	51
3.2.2.1	Safety Factor Approach.....	51
3.2.2.2	Example I.....	52
3.3	Methodology .....	54
3.4	BETA-FLEXSTREM Overview.....	55
3.5	Analysis for Single-Member Structures (SMS).....	59
3.5.1	Option S – Determination of Analysis Type.....	59
3.5.2	Process A – Variable Initialization and Storage.....	60
3.5.3	Process B – Load and Stress Derivation.....	61
3.5.4	Process C – Stress Transformation.....	64
3.5.5	LM I – Stress Limit State Analysis .....	64
3.5.6	Process D – Crack Length Transformation.....	65
3.5.7	Process E – Crack Length Estimation .....	66
3.5.8	Process F – Stress Intensity Factor Computations .....	68
3.5.9	LM II – Stress Intensity Factor Limit State Analysis.....	70
3.5.10	Process G – Determination of Minimum Crack Length.....	71
3.5.11	LM III – Crack Length Limit Analysis.....	71
3.5.12	Process H – Structural Life Estimation.....	72

---

---

3.5.13	LM IV – Life Limit Analysis .....	73
3.5.14	Process I – Hierarchical Data Recording .....	73
3.5.15	Process J – Reliability Computation.....	74
3.5.16	Process M – S-N reliability analysis.....	75
3.6	Numerical Example (BETA-FLEXSTREM Application) .....	75
3.7	Results and Discussion .....	79
3.8	Sensitivity Analysis .....	88
3.8.1	Result Comparison for Number of Simulations.....	88
3.8.2	Sensitivity Analysis .....	89
3.8.2.1	Base Model as a Sensitivity Standard .....	89
3.8.2.2	Fracture Toughness .....	90
3.8.2.3	Defect (crack) Size .....	92
3.8.2.4	Planned Life.....	93
3.8.2.5	Loading.....	95
3.9	Conclusion .....	97
Chapter 4: Environmental, Structural and Operational Data Requirements for Structural Analyses including Demonstrational Case Studies .....		99
Summary .....		99
4.1	Environmental, Structural and Operational Data Requirements.....	99
4.2	Secondary (Derived) Data .....	103
4.3	Data Distribution Sources.....	103
4.4	Reliability Value Implication and Notation.....	104
4.5	Case Studies in this Research .....	104
4.5.1	Case Study 1: Offshore Crane Boom.....	105
4.5.2	Case Study 2: 25-Bar Truss System .....	109
Chapter 5: Flexible Structural Reliability Algorithm (FLEXSTREM): A Risk Quantification Tool for Marine/Offshore Structures .....		111
Summary .....		111
5.1	Introduction.....	111

---

---

5.2	Background .....	112
5.2.1	The Stochastic Finite Element Method/Analysis (SFEM/SFEA) .....	113
5.2.2	SFEA Background.....	114
5.2.3	Monte Carlo Finite Element Method.....	114
5.3	Methodology .....	117
5.4	FLEXSTREM Overview .....	118
5.5	FLEXSTREM Preface.....	123
5.5.1	Coefficient of Variance (COV) and Safety Factors .....	123
5.5.2	Coefficient of Variance (COV) and Number of Random Variables .....	124
5.5.3	Coefficient of Variance (COV), Number of Simulations and Reliability 125	
5.5.4	Blind Design Concept.....	127
5.5.5	Design Guides/Standards .....	127
5.5.6	Algorithm Sources.....	130
5.5.6.1	The Iwakuma Tetsuo FEA Code.....	130
5.5.6.2	Gmsh .....	130
5.6	FLEXSTREM Analysis for Structures.....	131
5.6.1	Process A – Type I Pre-MCS Process .....	131
5.6.2	Process B – Type II Pre-MCS Process .....	131
5.6.2.1	Validation of the FEA-Block Output .....	136
5.6.2.2	The Successive Over-Relaxation (SOR) method.....	139
5.6.2.3	B4 – Reference Variable (Shielding Factor) for Wind Force Estimation 140	
5.6.3	Process C – MCS Process .....	141
5.6.4	Process D – Wind Force Computation .....	141
5.6.5	Process E – Loading Combination and Determination of Load Increment Factors 142	
5.7	Type I (SMS Processes).....	145
5.7.1	Process F – Bending Stress Analysis.....	145
5.7.2	Process G – Tensile Stress Analysis.....	145

---



---

5.7.3	Process H – Compressive Stress .....	146
5.7.4	Process I – Multiaxial Stress Analysis.....	146
5.7.5	Process J – Crack Length Estimation .....	147
5.7.6	Process K – Stress Intensity Factor Analysis.....	147
5.7.7	Process L – Minimum Crack.....	148
5.7.8	Process M – Fracture Analysis.....	148
5.7.9	Process N – Life Cycle Assessment .....	148
5.8	Type II (Multi-Member Processes).....	150
5.8.1	Process O – Member Analyses.....	150
5.8.2	Process P – Node (Joint) LEFM Analyses.....	153
5.8.3	Process S – Reliability Estimation .....	161
5.9	Results/Discussion.....	162
5.9.1	Sensitivity Analysis .....	166
5.9.1.1	Fracture Toughness .....	166
5.9.1.2	Defect Size (Crack Length) .....	168
5.9.1.3	Planned/Design Life.....	170
5.9.1.4	Load Factor.....	171
5.9.2	The COV-Number of Simulations-Reliability Relationship.....	173
5.10	Conclusion.....	176
Chapter 6: FLEXSTREM Optimization (FLEXOPT): A FLEXSTREM Based		
	Structural Optimization Tool for Risk Control using Cost-Safety Criteria.....	178
	Summary .....	178
6.1	Introduction.....	178
6.2	Background.....	179
6.2.1	Sizing Optimization.....	180
6.2.2	Shape Optimization .....	180
6.2.3	Topology Optimization.....	180
6.3	Methodology .....	182

---

---

6.4	FLEXOPT Overview.....	184
6.4.1	Level Convergence Criteria .....	185
6.5	FLEXOPT Structural Analysis .....	186
6.5.1	Level Convergence Specification.....	187
6.5.2	Specification of the Number of Combinations to Perform .....	187
6.5.3	Specification of the Upper and Lower Boundaries of Optimization Percentage.....	187
6.5.4	Designation of the Target Reliability and Tolerance.....	189
6.5.5	Generation and Shuffling of the Optimization Coefficient Arrays .....	190
6.5.5.1	A1 – Generation of the Positive Optimization Coefficients.....	190
6.5.5.2	A2 – Generation of Negative Optimization Coefficients.....	191
6.5.5.3	A3 – Shuffling of Optimization Coefficient Arrays .....	192
6.5.6	FLEXOPT Loop .....	194
6.5.7	FLEXSTREM FEA Block Modification .....	194
6.5.8	Convergence Conditions.....	197
6.5.9	Result Sorting Operations .....	198
6.6	Result/Discussion.....	199
6.6.1	Optimization of Crane Boom .....	199
6.6.2	Optimization and Comparison of the 25-bar Truss Tower .....	200
6.6.3	Recommendation for a New Crane Boom Configuration .....	204
6.7	Conclusion .....	205
Chapter 7: Stochastic FLEXSTREM (STOFLEX): A Stochastic Implementation of FLEXSTREM for Risk Control in Structural Maintenance and Repair Scheduling .....		
		206
Summary .....		
		206
7.1	Introduction.....	206
7.2	Background.....	207
7.3	Methodology .....	211
7.4	STOFLEX Overview.....	213

---

---

7.4.1	Process S-S: Stochastic Initialization .....	216
7.4.2	Process S-J and SR3; LEFM Crack Growth Process .....	217
7.4.3	Perfect and Imperfect Repair.....	219
7.4.4	STOFLEX for existing structures.....	220
7.5	Results/Discussion.....	221
7.5.1	Crack Propagation .....	221
7.5.1.1	Crane Configuration 1 .....	222
7.5.1.2	Crane Configuration 2.....	223
7.5.1.3	Crane Configuration 3 (Optimal Configuration) .....	224
7.5.2	Stress Intensity Factor Analysis .....	225
7.5.3	Inspection and Maintenance Scheduling .....	229
7.6	Conclusion .....	234
Chapter 8: Discussion and Conclusion .....		235
Summary .....		235
8.1	Introduction.....	235
8.2	Findings .....	235
8.3	Research Contribution.....	236
8.4	Limitations and Future Work.....	237
References .....		238
Appendices .....		252
Appendix A.....		252
Appendix B.....		278
Appendix C.....		325

---

## List of Figures

Figure (1.1) – Modified FSA framework for structural design, maintenance and inspection.....	6
Figure (1.2) – Expanded (modified) framework showing the first three steps. ....	8
Figure (1.3) – Expanded (modified) framework showing the last two steps. ....	9
Figure (2.1) – Interrelations of five phases in the design for safety framework (Wang (2000)). ....	24
Figure (2.2) – Crack propagation. ....	32
Figure (2.3) – Generic limit state model. ....	42
Figure (3.1) – Simple cantilever. ....	52
Figure (3.2) – Plot of the strength (right) and stress (left) distributions. ....	53
Figure (3.3) – Methodology. ....	54
Figure (3.4) – Methodology. ....	54
Figure (3.5) – BETA-FLEXSTREM outline.....	57
Figure (3.6) – Fault tree representation of key variables. ....	58
Figure (3.7) – Decision S. ....	59
Figure (3.8) – Analysis selection process. ....	60
Figure (3.9) – Process A.....	60
Figure (3.10) – Process B.....	61
Figure (3.11) – Process B3.1 – load sampling. ....	62
Figure (3.12) – Uniform distribution of load selection process. ....	63
Figure (3.13) – Stress limit state analysis. ....	64
Figure (3.14) – Process E. ....	66
Figure (3.15) – The ‘dartboard’ illustration of the Monte Carlo integration method....	66
Figure (3.16) – Single-edge crack in a pure bending specimen (Tada et al (2000)). ....	69
Figure (3.17) – Stress intensity factor limit state analysis. ....	70
Figure (3.18) – Crack length limit analysis.....	71
Figure (3.19) – Life limit analysis. ....	73
Figure (3.20) – Process I. ....	73
Figure (3.21) – Data recording sequence at I1. ....	74
Figure (3.22) – Process M. ....	75
Figure (3.23) – Marine jib crane.....	77
Figure (3.24) – Area of high stress concentration. ....	79

---

Figure (3.25) – Gaussian distributed stresses.....	81
Figure (3.26) – Various load classes.....	81
Figure (3.27) – Gaussian distribution of material yield stress. ....	82
Figure (3.28) – Stress limit state.....	82
Figure (3.29) – Lognormal distribution of material fracture toughness. ....	83
Figure (3.30) – Lognormal distribution of the stress intensity factor.....	83
Figure (3.31) – Stress intensity factor limit state.....	84
Figure (3.32) – Lognormal distribution of the critical crack length.....	84
Figure (3.33) – Exponential distribution of the critical crack length. ....	85
Figure (3.34) – Gaussian distribution of the logarithm of operational life. ....	85
Figure (3.35) – Lognormal distribution of planned life.....	86
Figure (3.36) – Gaussian distribution of the logarithm of planned life. ....	87
Figure (3.37) – Life limit state. ....	87
Figure (3.38) – Reliability result comparison for different number of trials. ....	88
Figure (3.39) – Failure mode count comparison for different number of trials. ....	89
Figure (3.40) – Local sensitivity analysis of fracture toughness.....	91
Figure (3.41) – Local sensitivity analysis of the defect (crack) size. ....	93
Figure (3.42) – Local sensitivity analysis of the planned life. ....	95
Figure (3.43) – Local sensitivity analysis of the load.....	97
Figure (4.1) – System definition parameters highlighted. ....	100
Figure (4.2) – Crane outline. ....	105
Figure (4.3) – Boom outline.....	106
Figure (4.4) – Lateral view and top view of idealized crane boom.....	108
Figure (4.5) – Isometric view of the idealized crane boom. ....	108
Figure (4.6) – Restraints and loading schematic. ....	109
Figure (4.7) – 25-bar truss (Park and Sung (2002)).....	110
Figure (4.8) – Gmsh representation of the 25-bar truss.....	110
Figure (5.1) – Methodology. ....	117
Figure (5.2) – Methodology. ....	118
Figure (5.3) – FLEXSTREM.....	122
Figure (5.4) – Fault tree representation.....	123
Figure (5.5) – Uncertainty at 40% and uncertainty at 20% each.....	124
Figure (5.6) – Uncertainty at 13.3% each and uncertainty at 10% each.....	125

---

---

Figure (5.7) – Small COV and Large COV. ....	126
Figure (5.8) – Bar element. ....	133
Figure (5.9) – Space truss.....	136
Figure (5.10) – <i>Gmsh</i> representation of the space truss.....	137
Figure (5.11) – Process F. ....	141
Figure (5.12) – Generic structure. ....	143
Figure (5.13) – Generic limit state.....	144
Figure (5.14) – Member analysis.....	150
Figure (5.15) – Member analysis illustration. ....	151
Figure (5.16) – Joint (node) analyses.....	153
Figure (5.17) – Node analyses illustration. ....	154
Figure (5.18) – External circumferential crack in a thick walled cylinder (Tada et al (2000))......	156
Figure (5.19) – Plot of the function in Equation (5.61) (Tada (2000))......	157
Figure (5.20) – Gumbel distribution of wind speed. ....	165
Figure (5.21) – Gumbel distribution of wind force. ....	165
Figure (5.22) – Highly stressed points on crane boom. ....	166
Figure (5.23) – Local sensitivity analysis of the fracture toughness. ....	168
Figure (5.24) – Local sensitivity analysis of the defect (crack) size. ....	169
Figure (5.25) – Local sensitivity analysis of the planned life. ....	171
Figure (5.26) – Local sensitivity analysis of the load.....	172
Figure (5.27) – Constant COV(R) vs. increasing COV(D).....	174
Figure (5.28) – Reliability at different COV(D)s.....	175
Figure (6.1) – FLEXOPT algorithm. ....	183
Figure (6.2) – FLEXOPT algorithm. ....	186
Figure (6.3) – Level convergence specification. ....	187
Figure (6.4) – Narrow search distance between optimization percentage boundaries. ....	188
Figure (6.5) – Wide search distance between optimization percentage boundaries.....	188
Figure (6.6) – Generation of positive optimization coefficients. ....	190
Figure (6.7) – Generation of negative optimization coefficients. ....	191
Figure (6.8) – Initial coefficients array (before shuffling).....	192
Figure (6.9) – Shuffling of optimization coefficient arrays. ....	193
Figure (6.10) – Shuffled coefficients.....	194

---

---

Figure (6.11) – Level 1 convergence flow.....	197
Figure (6.12) – Level 2 convergence flow.....	198
Figure (7.1) – Methodology.....	212
Figure (7.2) – FLEXSTREM adaptation to STOFLEX.....	215
Figure (7.3) – STOFLEX daily loading pattern.....	216
Figure (7.4) – Crack growth/propagation algorithm.....	218
Figure (7.5) – Proposed concept of fatigue crack management in a welded structure (Okawa and Sumi (2008)). .....	219
Figure (7.6) – Crack propagation (all phases).....	222
Figure (7.7) – Crack propagation (all phases).....	223
Figure (7.8) – Crack propagation (all phases).....	224
Figure (7.9) – Fatigue crack propagation rate (da/dN) vs. the stress intensity factor ( $\Delta K_I$ ) (crane configuration 1). .....	226
Figure (7.10) – Fatigue crack propagation rate (da/dN) vs. the stress intensity factor ( $\Delta K_I$ ) (crane configuration 2). .....	227
Figure (7.11) – Fatigue crack propagation rate (da/dN) vs. the stress intensity factor ( $\Delta K_I$ ) (crane configuration 3 (optimal configuration)). .....	228
Figure (7.12) – Inspection and perfect repair scenario.....	231
Figure (7.13) – Inspection and perfect repair scenario.....	232
Figure (7.14) – Inspection and repair (none) scenario.....	233
Figure (A.1) – Uniform distribution of the load increment factor.....	257
Figure (A.2) – Normal distribution of the axial stress in structural member.....	257
Figure (A.3) – Normal distribution of the member (material) strength.....	258
Figure (A.4) – Normal distribution of the nodal stress.....	258
Figure (A.5) – Lognormal distribution of the nodal stress intensity factor.....	259
Figure (A.6) – Lognormal distribution of the nodal material fracture toughness.....	259
Figure (A.7) – Exponential distribution of the nodal defect.....	260
Figure (A.8) – Lognormal distribution of the nodal critical crack length.....	260
Figure (A.9) – Lognormal distribution of the expected life of the node.....	261
Figure (A.10) – Lognormal distribution of the node resultant life.....	261
Figure (A.11) – Constant COV(D) vs. Increasing COV(R).....	262
Figure (A.12) – Reliabilities at different COVs.....	263
Figure (A.13) – Simultaneously increasing COVs.....	264

---

---

Figure (A.14) – Reliabilities at different COVs.....	264
Figure (A.15) – Simultaneously decreasing COVs. ....	265
Figure (A.16) – Reliabilities at different COVs.....	266
Figure (A.17) – Constant COV(R) vs. decreased COV(D). ....	267
Figure (A.18) – Reliabilities at different COV(D)s.....	267
Figure (A.19) – Constant COV(D) vs. decreased COV(R). ....	268
Figure (A.20) – Reliabilities at different COVs.....	269
Figure (A.21) – Increasing COV(D) vs. decreasing COV(R).....	270
Figure (A.22) – Reliabilities at different COVs.....	270
Figure (A.23) – Increasing COV(D) vs. decreasing COV(R).....	271
Figure (A.24) – Reliabilities at different COVs.....	272
Figure (A.25) – Crack propagation phase 1.....	273
Figure (A.26) – Crack propagation phase 2.....	273
Figure (A.27) – Crack propagation phase 3.....	274
Figure (A.28) – Crack propagation phase 1.....	274
Figure (A.29) – Crack propagation phase 2.....	275
Figure (A.30) – Crack propagation phase 3.....	275
Figure (A.32) – Crack propagation phase 1.....	276
Figure (A.33) – Crack propagation phase 2.....	276
Figure (A.34) – Crack propagation phase 3.....	277



---

## List of Tables

Table (3.1) – Sample results of Monte Carlo simulation.....	53
Table (3.2) – The relationship between number of trials and accuracy.....	68
Table (3.3) – Validation of the stress intensity correction factor.....	70
Table (3.4) – Material properties/dimensions. ....	78
Table (3.5) – Material parameters/variables. ....	78
Table (3.6) – Sample results produced by BETA-FLEXSTREM.....	80
Table (3.7) – Failure counts and reliability for different number of trials.....	88
Table (3.8) – Base failure mode frequencies.....	90
Table (3.9) – Effect of fracture toughness decrease on reliability.....	90
Table (3.10) – Effect of fracture toughness decrease on reliability.....	90
Table (3.11) – Trended change in reliability (fracture toughness).....	91
Table (3.12) – Effect of crack length increase on reliability.....	92
Table (3.13) – Effect of crack length increase on reliability.....	92
Table (3.14) – Trended change in reliability (crack length). ....	92
Table (3.15) – Effect of planned life increase on reliability. ....	94
Table (3.16) – Effect of planned life increase on reliability. ....	94
Table (3.17) – Trended change in reliability (planned life). ....	95
Table (3.18) – Effect of load increase on reliability.....	96
Table (3.19) – Effect of load increase on reliability.....	96
Table (3.20) – Trended change in reliability (loading).....	96
Table (4.1) – Data required for FLEXSTREM analysis.....	101
Table (4.2) – Node data.....	102
Table (4.3) – Member data.....	102
Table (4.4) – Constraint data.....	102
Table (4.5) – Loading data.....	103
Table (4.6) – Derived data.....	103
Table (4.7) – Data distribution and sources.....	103
Table (5.1) – Percentage error in the stress results for each element by the FEA block. .....	138
Table (5.2) – Validation of the stress intensity correction factor for $r/r_o$ ratio: 0.0 – 0.5. .....	159

---

Table (5.3) – Validation of the stress intensity correction factor for $r_i/r_o$ ratio: 0.6 – 1.0. .....	160
Table (5.4) – FLEXSTREM result for crane boom.....	162
Table (5.5) – Sample result table from FLEXSTREM. (a).....	163
Table (5.6) – Sample result table from FLEXSTREM. (b) .....	164
Table (5.7) – Effect of fracture toughness decrease on reliability. (a) .....	167
Table (5.8) – Effect of fracture toughness decrease on reliability. (b) .....	167
Table (5.9) – Trended change in reliability (fracture toughness).....	167
Table (5.10) – Effect of crack length increase on reliability. (a) .....	168
Table (5.11) – Effect of crack length increase on reliability. (b).....	169
Table (5.12) – Trended change in reliability (crack length). .....	169
Table (5.13) – Effect of planned life increase on reliability. (a).....	170
Table (5.14) – Effect of planned life increase on reliability. (b).....	170
Table (5.15) – Trended change in reliability (planned life). .....	170
Table (5.16) – Effect of load factor increase on reliability. (a).....	171
Table (5.17) – Effect of load factor increase on reliability. (b).....	172
Table (5.18) – Trended change in reliability (load factor).....	172
Table (5.19) – Keeping COV(R) constant and increasing COV (D) at different numbers of simulations.....	174
Table (6.1) – Levels of design.....	185
Table (6.2) – Minimum material requirement for application Z.....	195
Table (6.3) – Material property X against minimum requirements for application Z..	195
Table (6.4) – Material property Y against minimum requirements for application Z..	195
Table (6.5) – Structural group identification.....	196
Table (6.6) – FLEXOPT optimization result. (a) .....	199
Table (6.7) – FLEXOPT 25-bar truss optimization result. (a) .....	200
Table (6.8) – FLEXOPT 25-bar truss optimization result. (b).....	201
Table (6.9) – FLEXOPT 25-bar truss optimization result. (c).....	202
Table (6.10) – Optimization comparison for 25-bar truss. ....	203
Table (6.11) – FLEXOPT optimization for new crane section configuration. ....	204
Table (7.1) – Crack propagation data for the 3 crane configurations.....	222
Table (7.2) – Repair operations for crane configuration 1.....	229
Table (7.3) – Repair operations for crane configuration 2.....	230

---

---

Table (7.4) – Repair operations for crane configuration 3.....	230
Table (A.1) – COV(D) constant; increasing COV(R).....	262
Table (A.2) – COV(D) and COV(R) simultaneously increased.....	263
Table (A.3) – COV(D) decreasing; COV(R) decreasing.....	265
Table (A.4) – COV(R) constant; COV(D) decreased.....	266
Table (A.5) – COV(D) constant; COV(R) decreased.....	268
Table (A.6) – COV(D) increased; COV(R) decreased.....	269
Table (A.7) – COV(D) decreased; COV(R) increased.....	271

---

## Abbreviations

AFORM	Advanced First Order Reliability Method
ALARP	As Low As Reasonably Practicable
ANN	Artificial Neural Network
ASD	Allowable Stress Design
ASM	Advanced Second Moment
ASORM	Advanced Second Order Reliability Method
BN	Bayesian Network
BRM	Boolean Representation Method
CCA	Cause Consequence Analysis
CFD	Computational Fluid Dynamics
CLT	Central Limit Theorem
DOF(s)	Degree(s) Of Freedom
ETA	Event Tree Analysis
FAR	Fatal Accident Rate
FEA/FEM	Finite Element Analysis/Method
FFEA	Fractal Finite Element Method
FLEXOPT	FLEXSTREM Optimization
FLEXSTREM	Flexible Structural Reliability Algorithm
FMECA	Failure Mode Effect and Criticality Analysis
FORM	First Order Reliability Method
FOSM	First Order Second Moment
FPSO	Floating Production, Storage and Offloading Unit
FTA	Fault Tree Analysis
FSA	Formal Safety Assessment
GA	Genetic Algorithms
HAZOP	Hazard and Operability Analysis
IEA	International Energy Agency
IM	Inspection and Monitoring
LEFM	Linear Elastic Fracture Mechanics
MCS/MCM	Monte Carlo Simulation/Method
MMS	Multi-Member Structure

---

NLFE	Non-Linear Finite Element
NPD	Norwegian Petroleum Directorate
PDF	Probability Density Function
PEM	Point Estimation Method
PHA	Preliminary Hazard Analysis
PLL	Probability of Loss of Life
PR	Perfect Repair
QRA	Quantitative Risk Assessment
RBI	Risk Based Inspection
RBLM	Risk Based Life Management
RBSA	Reliability Based Structural Analysis
RBSA-OPT	Reliability Based Structural Analysis Optimization
RCM	Reliability Centred Maintenance
RNG	Random Number Generator
RSM	Response Surface Method
SA	Simulated Annealing
SFE	Stochastic Finite Element
SFEA/SFEM	Stochastic Finite Element Analysis/Method
SSFEA	Spectral Stochastic Finite Element Analysis
SMS	Single Member Structure
SOFM	Second Order First Moment
SOR	Successive Over-Relaxation
SORM	Second Order Reliability Method
SSFEA	Spectral Stochastic Finite Element Analysis
STOFLEX	Stochastic FLEXSTREM

---

## List of Notations

<i>Notations</i>	<i>Variables</i>
* <sub>(mem)</sub>	(subscript) - pertaining to structural members
* <sub>(nd)</sub>	(subscript) - pertaining to structural nodes
a	crack (defect) length
a <sub>c</sub>	critical crack (defect) length
a <sub>d</sub>	detectable crack length
a <sub>f</sub>	final crack (defect) length
a <sub>i</sub>	initial crack (defect) length
c	centroidal distance
C <sub>A</sub>	cross-sectional area
C <sub>f</sub>	force coefficient
COV	coefficient of variance
C <sub>SA</sub>	area of sheltered members
E	Young's modulus (elasticity)
F <sub>cr</sub>	average compressive stress
F <sub>n</sub>	nominal strength
F <sub>ten</sub>	uniaxial tensile strength
F <sub>y</sub>	uniaxial yield strength
H <sub>gt</sub>	height
H <sub>T</sub>	highest temperature
I	integer
I <sub>mont</sub>	second moment of the closed section area of the beam
INS	inspection interval
K <sub>I</sub>	stress intensity factor (mode I)
K <sub>IC</sub>	critical stress intensity factor (fracture toughness)
K <sub>th</sub>	threshold driving force
L	length (m)
L <sub>cy</sub>	loaded daily cycles
LD	load
LD <sub>dead</sub>	dead load
LD <sub>struct</sub>	total mass of structure

---

<i>Notations</i>	<i>Variables</i>
$LD_w$	wind load
$LD_{ws}$	wind load on sheltered components
$L_T$	lowest temperature
$M$	moment of force
$mat_c$	crack growth rate coefficient
$mat_d$	material density
$mat_m$	crack growth exponent
$mat_\beta$	stress intensity correction factor
$Max_{RL}$	maximum rated load
$N$	integer limit
$N_{COM}$	number of combinations
$N_{mem}$	number of structural members
$N_{node}$	number of structural nodes
$N_{OP}$	operational/resultant life
$N_{PL}$	design/planned life
$NSIM$	number of simulations
$N_{STL}$	loaded cycles per year
$N_{STU}$	unloaded cycles per year
$N_{TL}$	total structural life (loaded and unloaded)
$N_{YRS}$	number of years in service
$P_{cr}$	compressive strength
$P_d$	dynamic pressure
$PFC$	process failure counters
$POF$	probability of failure
$q$	dynamic wind pressure
$R$	reliability
$r$	radius of gyration
$r_i$	inner radius of section
$r_o$	outer radius of section
$T$	temperature ( $^{\circ}K$ )
$thk$	thickness
$T_{len}$	total length

---

---

<i>Notations</i>	<i>Variables</i>
U	uniform random number
u	standard normal variate
$U_{cy}$	unloaded daily cycles
V	mean of variate (non standard )
$V_{trans}$	non standard variate (all distributions)
w	width of material geometry containing a crack, $a$
$W_{dh}$	width
$W_{fl}$	average wind force on live load
$w_s$	wind speed on structure
x	random variable
$X_{exp}$	exponential random number
$X_G$	normal (Gaussian) random number
$X_{gb}$	Gumbel random number
$X_{LG}$	log-normal random number
$y_m$	yield moment
$\alpha$	coefficient of expansion
$\beta$	rate (exponential distribution)
$\gamma$	wind design application coefficient
$\mu$	mean
v	air velocity
$\rho$	fluid density
$\sigma$	standard deviation
$\sigma_{bend}$	bending stress
$\sigma_{comp}$	compressive stress
$\sigma_{mul}$	multiaxial stress
$\sigma_{str}$	stress
$\sigma_{ten}$	tensile stress
$\sigma_{tor}$	torsion
$\varphi$	shielding factor
$\omega$	load increment factor

This list is only applicable to chapters 3, 4, 5 (with the exception of sections 5.2 and 5.6.2), and 7.



## Chapter 1: Introduction

### Summary

*This chapter presents the background to this research. It highlights some of the problems encountered by engineers pertaining to the design of structures in the marine/offshore environment. The aims and objectives of this research with respect to the aforementioned problems are stated. Also the methodology and scope of this research is outlined.*

### 1.1 Background of the Research

At about 22.30 hours on 6 July 1988, the ignition of a low-lying condensate cloud in the compression unit of the Piper Alpha platform initiated a sequence of events that led to the total loss of 167 lives including the loss of the platform (Shaw (1992)). This incident shocked the offshore industry worldwide and thus highlighted the importance of safety in the design, construction, installation and operation of offshore facilities.

Since offshore petroleum exploration and developments began, the two largest accidents in the North Sea, Piper Alpha in the UK sector (167 fatalities) and Alexander L. Kielland in the Norwegian sector (123 fatalities), contributed about half of the total number of fatalities in the offshore industry by 1994 (Tveit (1994)).

In the Pre-Piper Alpha era many developments in quantitative risk assessment (QRA) took place in the onshore industries during the 1980s, particularly in the UK (Brandsæter (2002)). QRA was also present in other parts of the world in the late 70s (Vinnem (1997)). Many UK operators used QRA methods as an integral part of the design process. However, the QRA methods were applied to only specific risk aspects

of the design, rather than to overall risks. The Piper Alpha accident in 1988 provided tragic confirmation that the major accidents/top events predicted by risk analyses were indeed realistic, and that QRA could be an effective tool for reducing risks. The Formal Safety Assessment (FSA) – a framework for the QRA – was proposed by Lord Cullen in the report on the Piper Alpha disaster public enquiry (Shaw (1992)). The FSA consists of the following stages (Wang (2000)):

- system definition;
- hazard identification;
- risk quantification;
- risk control options;
- evaluation/ decision making.

This confirmation prompted the application of QRA techniques to many UK Sector platforms, as operators attempted to discover the extent of their exposure to fire and explosion hazards (Brandsæter (2002)). Operators were requested to re-evaluate emergency isolation arrangements for risers and subsea pipelines, thus concentrating studies on riser hazards and effects of installing sub-sea isolation valves. QRA was found to be an appropriate tool for evaluating the relevant hazards (fire and explosion, dropped objects, valve reliability, diving risks, etc.).

As a result of various QRA activities, significant reductions in risk were achieved on many platforms by moving or installing isolation valves on risers and sub-sea pipelines or, in extreme cases, by relocating accommodation (Brandsæter (2002)). This success persuaded multi-national oil companies to apply similar safety evaluation to all their offshore operations. This effect was not confined to the UK Sector; in the few years following the Piper Alpha accident, QRA was applied to platforms in areas as diverse as Australia, New Zealand, Malaysia, Brunei and Canada.

Offshore oil production accounts for about 35% of total world oil production (IEA, 2003). Structures operating in this environment experience a combination of conditions unique to the offshore industry. The remoteness of facilities combined with the inherent environmental challenges leads to inevitably large investments in construction, transportation and operations.

As worldwide demand for oil continues to increase, exploration and hence discovery of new reserves pose more challenges as they are located in exposed deep water environments (Grime and Langley (2008)). Structures deployed in this environment are subject to significant random loading. Despite this, structures still have to be deployed in there and must be designed to operate productively. Consequently, a third of existing offshore platforms require life extension (Schoefs (2008)). The strength of these structures degrades with time due to cracks, dents and corrosion (Shi (1991)). Modelling and thus reliability estimation is compounded by the long-term variation in environmental conditions and model uncertainties (Grime and Langley (2008)).

## **1.2 Statement of the Problem**

The presence of uncontrollable random variables in the marine/offshore environment significantly increases offshore drilling costs compared to similar activities onshore. The remoteness of the operation and effects of the immediate environment give rise to limited space for facilities and personnel. This poses increased difficulty in mitigation of hazards.

The availability and performance of equipment, transportation and work conditions result in delay often leading to financial impacts. Emergency manoeuvres, unscheduled maintenance and non-routine operations increase the number of personnel, driving costs further up.

Kaiser (2007) presented a detailed analysis of energy loss events from 1972 to 2004 using the Willis Energy Loss database. The costs were inflation-adjusted to give reasonable values to the losses incurred.

Willis, a global insurance broker provides the most comprehensive database of energy losses in the world. The database is used widely by businesses and insurance organisations within the energy industry. The Willis Energy Loss database provides an in-depth review of the financial impacts of the dominant variables in the offshore environment from 1972 to present.

The data is presented in four categories. They are: regional category, type vessel or structure lost, loss type (i.e. physical damage, etc.) and hazard (or event leading to loss).

Focus is drawn to Europe and North America (for the regional category) and structural related events/hazards for the purpose of this research. From the analysis, it was shown that regionally, North America, Europe and the Far East have the highest incidents and offshore losses totalling about 80% of the total recorded loss.

In North America, the second most frequent cause of loss is windstorm. This is followed by design problems, heavy weather and mechanical failure (in descending order). The windstorm causes the second highest financial average loss (total loss/event). This is followed by heavy weather, mechanical failure (fatigue, etc.) and design.

In Europe, the most frequent cause of loss is design, heavy weather and mechanical failure (in descending order). Heavy weather is the third highest cause of financial loss followed by design and mechanical failure.

North America, Europe and Far East contribute over 90% of the losses caused by weather globally. The FPSOs (Floating Production Storage and Offloading unit) are the highest casualties as a result of weather.

The problem of design in Europe is 10 times more costly than Far East and North America due to hostile conditions present in the North Sea. Although it is impossible to entirely eliminate these risks (hazards), certain aspects could be reduced significantly.

Design frameworks which consider the risk and cost within a QRA framework are needed to reduce the risks in these structures. Several aspects pertaining to design require specialized knowledge. Thus such frameworks need to accommodate these specializations in order to indentify to a high degree, modes of failures on these structures. Identification of these often neglected areas lead to an increase in system definition and thus a decrease in system uncertainty.

### **1.3 Research Aims and Objectives**

The main aim of this research is to develop an overarching framework based on the FSA for use in the design, operation and maintenance of offshore structures with respect to one of the most dominant failure modes in marine/offshore structures – fatigue (Aghakouchak and Steiner (2001)). Such a framework should have the following objectives:

1. to give adequate definition of the inherent interaction(s) between the structure and its environment with respect to fatigue failure (and possibly other common failure modes);
2. to formulate a robust and comprehensive means of assessing the performance of structures with respect to fatigue failure (and possibly other common failure modes);
3. to provide better design options for new structures and give options for modification to already existing structures with respect to cost and safety;
4. to present possible solutions for scheduling of cost effective maintenance activities to ensure structural integrity (for both old and new structures) and extend the lives of already existing structures.

Demonstrations on a selected case study are carried out after achievement of each of the outlined objectives.

### **1.4 Research Methodology and Scope**

The research is conducted based on a modified FSA framework. In each step of the framework, novel methodologies are introduced and demonstrated on case studies. Partial validation is carried out on the foundational methodology (the methodology on which the subsequent methodologies are built).

The case studies presented are depictions of real scenarios and would be dealt with as such. The development of a realistic framework, which would be applicable to basic cases and has prospects for further development to deal with more complex scenarios, is the goal of this research.

### 1.5 Structure of the Thesis

The structure of the research is set out following a modified FSA methodology based on the FSA outlined in the Lord Cullen report in Wang, (2000).

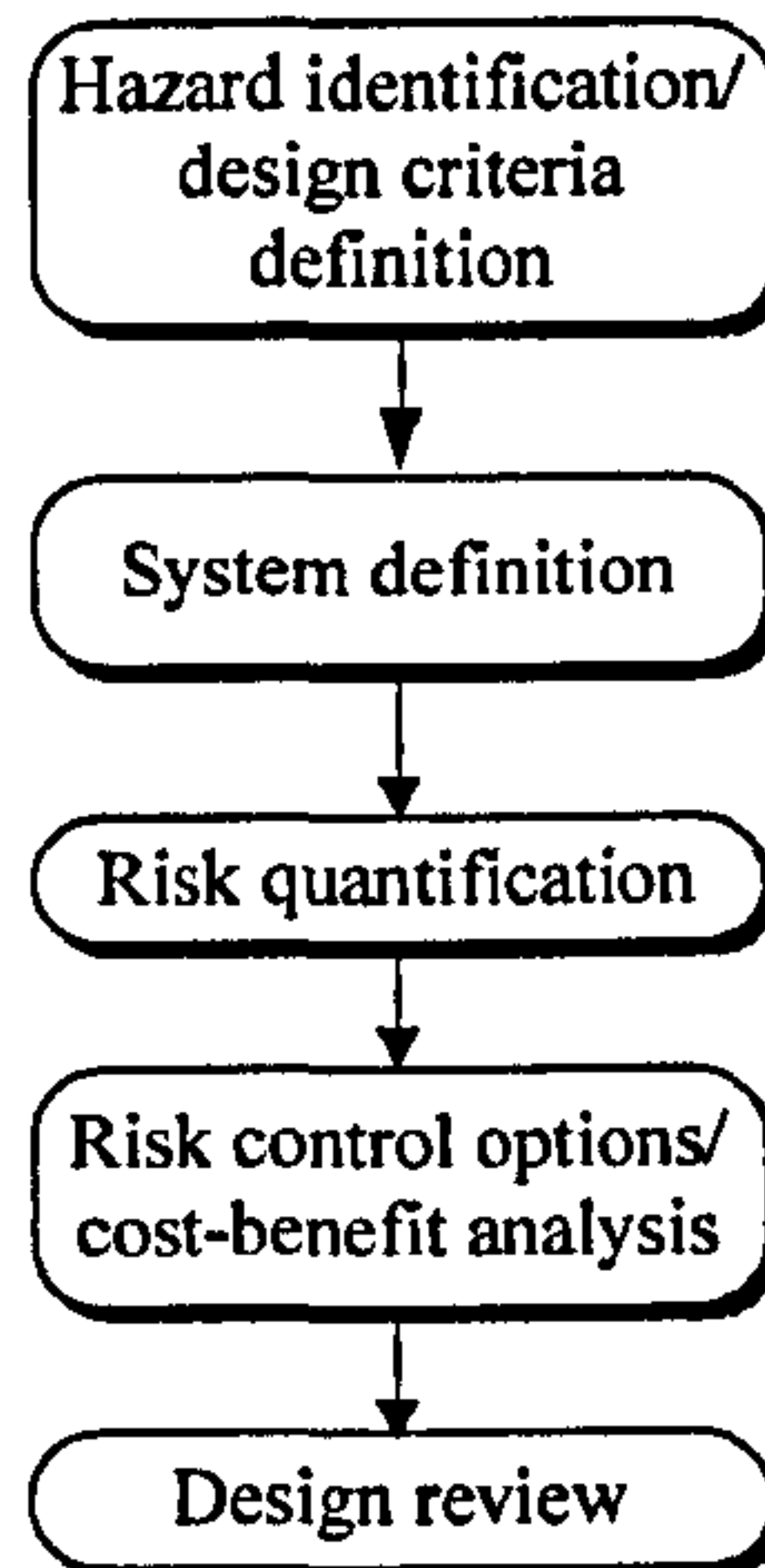


Figure (1.1) – Modified FSA framework for structural design, maintenance and inspection.

Figure (1.1) shows the modifications required to adapt the FSA framework of Wang (2000) for the design maintenance and inspection scheduling for marine and offshore structures. The first step (hazard identification phase) is necessarily concerned with gathering of information pertaining to the event(s) that could lead to the damage/loss of life, property or environmental degradation (i.e. top event(s)). Still at this step (design criteria definition phase), causal analysis is carried out to identify a focal area(s) within the fields of design and maintenance that is critical to the occurrence of the top event(s) identified from the previous phase (hazard identification). These focal areas are numerous within the field of design (e.g. fatigue, stress, corrosion, etc.). In the second step (system definition), the system (consisting of the structure and the environment) is defined around the focal area(s) identified. The third step (risk quantification) sets parameters to measure the structure's performance in the focal area(s) identified. This is perhaps the most important step as the subsequent methods introduced are based on the results obtained here. Having evaluated the structural performance, the fourth step (risk control options/cost benefit analysis) attempts to improve this performance through proposed methods which take cost and safety into consideration. The fifth step (design

review) is simultaneously carried out with the previous step (step four) as different solution scenarios are reviewed.

This modified FSA framework is expanded upon in the various chapters of this research. For the most part, a step/phase of the modified FSA is comprehensively dealt with in a chapter.

The first chapter provides an introduction to the scope of the research and identifies the areas that need to be addressed. The second chapter is the literature review chapter which takes a detailed view at the history of QRA within the industry and in relation to structures. Also, previous researches on QRA are outlined. Finally the proposed methods and the justification for the research are stated. Collectively both chapters deal with the first step (hazard identification/ design criteria definition) of the modified FSA framework as failure events and design goal/criteria are identified.

The third chapter is a precursor of the foundational methodology (step three) for use with a simple case – the single-member structure (SMS). The chapter partially combines step two (system definition) – as it seeks to establish the basic interactions between a structure and its environment with its relationship to fatigue, and step three (risk quantification) – as it attempts to measure the performance of the SMS with respect to fatigue, for the simple case of an SMS. A partial validation via sensitivity analyses was also presented. Expected trends/conformities in the sensitivity analyses allow for the adaptation of such a method to suit more realistic cases of multi-member structures (MMSs), which are necessarily more complex. The contents of each of the first three steps within the modified FSA and the interactions between them is illustrated in Figure (1.2).

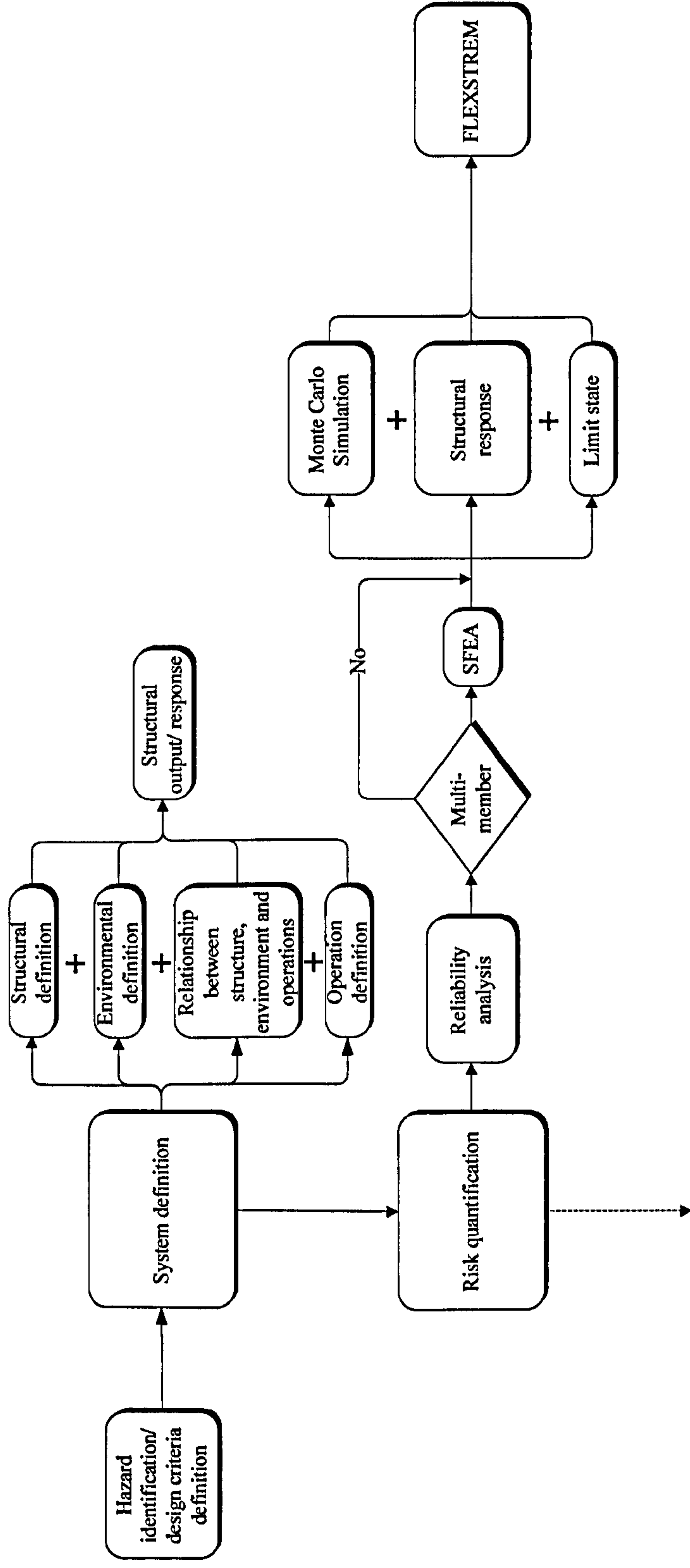


Figure (1.2) – Expanded (modified) framework showing the first three steps.



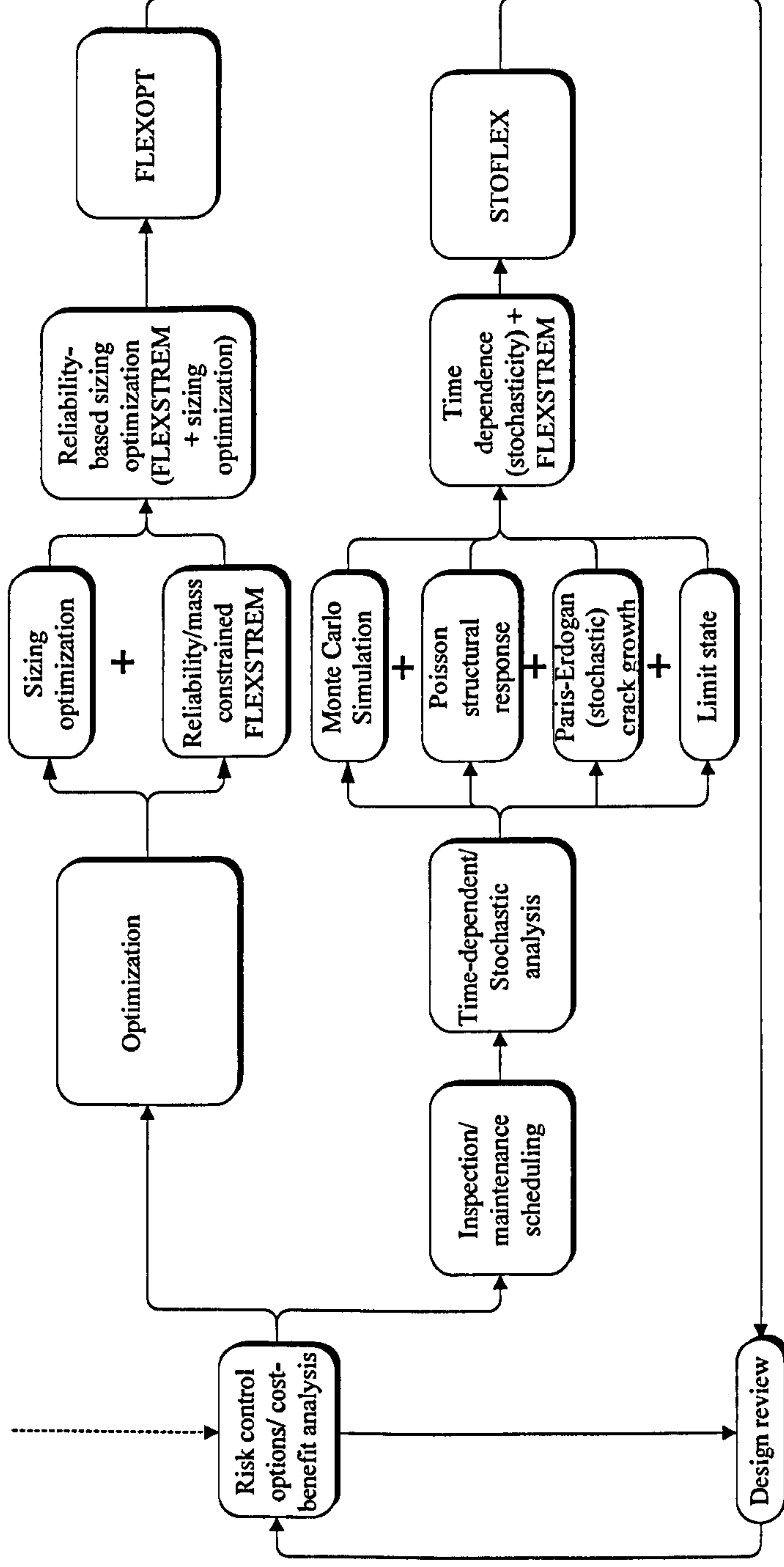


Figure (1.3) – Expanded (modified) framework showing the last two steps.

The fourth chapter is a detailed emphasis of the second step in the modified FSA (system definition). It is outlined in Figure (1.2). It comprehensively defines the structural, environmental and operational parameters required for the holistic analysis of structures with respect to fatigue (focal area). Also, case studies on which the latter stages of the modified FSA would be demonstrated, alongside all relevant data pertaining to the structure, the immediate environment and relevant operations, are presented. Furthermore, the characteristics of most variables from the supplied data are outlined. The chapter also ensures an orderly research structure free of unnecessary bulk repetitions.

Chapter 5 in its entirety deals with the third step in the modified FSA framework (risk quantification) (also outlined in Figure (1.2)). It is an improvement of the pre-existing test-method developed in the third chapter. In this chapter, the interactions between more realistic parameters obtained in the fourth chapter (second step in modified FSA) are modelled in addition (where necessary) to the pre-existing method. The method is further developed to cater for MMSs (and thus the incorporation of the stochastic finite element method/analysis (SFEA)) as well as the pre-existing SMSs. The method is then demonstrated on the case study stated in the fourth chapter. A partial validation is also presented to verify the method and its outcomes.

The sixth chapter is a hybrid of the fourth and fifth steps in the modified FSA (risk control options/cost benefit analysis and design review) in that it provides possible ways in which the reliability of a structural configuration could be increased with a healthy trade-off between the cost and the safety. The optimization method proposed is entirely based on the method in chapter 5 as shown in Figure (1.3). The case study, whose performance has been evaluated in chapter 4, is then analysed in order to provide possible configurations with better performance. A separate benchmarking case study (also stated in chapter 4) is also analysed for comparison purposes. Finally a proposed configuration to the pre-existing case study (previously analysed in chapters 5 and 6) is outlined.

Chapter 7 is a hybrid of the fourth and fifth modified FSA steps. The proposed method is also based entirely on the validated method presented in chapter 5. Its uniqueness to

the former is the implementation of time dependence as shown in Figure (1.3). This helps to assess the performance of structures as well as propose maintenance practices that would maintain/enhance the structure's integrity. The case study, whose performance has been evaluated in chapter 4, is then analysed in order to provide possible inspection/repair regimes that would maintain/enhance the structure's integrity. This case study is contrasted by its variants provided in the solution proposals by the method introduced in the sixth chapter. A feel for what structural configurations to adopt with respect to cost and safety (structural) integrity could be obtained from the results produced by the method proposed in this chapter.

The eighth chapter draws conclusions on the entire research. It lists the contribution to research with respect to the outlined aims and objectives given in the first chapter together with the limitations thereof. Finally future recommendation for improvement to the current research is stated.

## Chapter 2: Literature Review

### Summary

*This chapter gives an overview of risk assessment and reliability, their history, current status and the important roles they play within the marine/offshore industry. Structures within the offshore environment form the focal point of the applications of risk assessment techniques in this research. Discussions would also centre on the problems faced in the design and operation of these structures. Finally the justification for this research would also be presented.*

### 2.1 Risk Assessment

It is widely viewed by the public and within the oil industry, particularly, that the North Sea offshore is subject to very high risks: risk of loss of life, loss of assets and a risk of damage to the environment (Tveit (1994)). This impression may be based on various factors such as (Tveit (1994)):

- The remoteness from the shore.
- The rough weather (increasing the unpredictability of environmental loads and impacts).
- The explosions and toxic emissions in the event of loss of containment.
- The notion of technical complexity and size, and possible distrust in the industry's ability to manage such complex systems.
- 'Facts' in terms of accidents offshore, as they are perceived through the influence of the media.

One characteristic feature of the offshore industry in comparison with most onshore industries is that major accidents are far more prominent (Tveit (1994)).

There have been major changes in the UK and Norwegian offshore safety regimes in the last quarter century (Smith (1995)). The loss of the *Alexander Kielland* in 1980, followed by the loss of the *Ocean Ranger* in 1982, led to additional prescriptive technical requirements, as well as improved techniques of risk assessment for semi-submersibles (Brandsæter (2002)). On the basis of accumulated experience (including some major accidents), there has been a move away from these rigid, prescriptive approaches to setting safety standards to more flexible “goal-setting” approaches which also aid in achieving cost-effective solutions to offshore safety (Smith (1995)).

There are still advances by authorities around the North Sea towards a “goal-setting regime”, implying that the regulations specify the goals for the prevention and protection against accidents, rather than specifying step-by-step solutions to reach these goals (Vinnem (1997)). In order to adapt to this approach, offshore operators are increasingly using quantitative risk assessment (QRA) techniques as part of their risk management programmes (Aven et al (2007), Smith (1995)). The advantage of a goal-setting approach is that (Vinnem (1997)):

1. The industry has considerably more flexibility with respect to fulfilling the regulations, and should be able to choose the optimum solution considering the circumstances.
2. Preventive and protective systems and actions may be tailored to the hazards that are relevant for the installation, equipment and operations in question.
3. In order to take advantage of the potential of the goal-setting approach it is required that models are available to distinguish between different levels of threats, and to tailor the solutions to the circumstances.

The use of risk analysis has become increasingly important in the offshore industry, especially in the countries involved on the North Sea (Vinnem (1997)). Risk is defined as the combination of the two basic parameters: consequences and uncertainties (Aven et al (2007)).

It is widely acknowledged that risk cannot be eliminated but must be managed (Aven et al (2007)). Risk assessment could assume a pivotal role in providing advice on safety, environmental protection and reliability issues (Shaw (1992)). Risk management in the

offshore industry is focused primarily on the safety of personnel onboard the installation, prevention of environmental damage and production regularity (Brandsæter (2002)).

The principles of risk assessment are similar for both onshore and offshore studies; however some of the applied techniques are necessarily different (Shaw (1992)). Risk assessments are required by authorities in order to document the risk level to be within specified acceptance criteria. Initially, this is believed to have been that main reason for doing risk assessments (Brandsæter (2002)). Through the years, QRA has been taken into active use as support for decisions, regarding design, construction as well as operation of offshore installations.

The objectives of a QRA may include (Brandsæter (2002)):

- Estimating risk levels and assessing their significance (thus aiding decisions on whether or not to reduce risks).
- Identifying the main risk contributors (to aid understanding of the nature of the hazards and to suggest possible targets for risk reduction measures).
- Defining design accident scenarios. These can be used as a design basis for emergency equipment, or for emergency planning and training.
- Comparing design options. This gives input on risk issues for the selection of a concept design.
- Evaluating risk reduction measures. QRA can be linked to a cost-benefit analysis, to help choose the most cost-effective ways of reducing the risk.
- Demonstrating acceptability to regulators and the workforce. QRA can show whether the risks have been made as low as reasonably practicable (ALARP).
- Identifying safety-critical procedures and equipment. These are critical for minimizing risks, and need close attention during operation.
- Identifying accident precursors, which may be monitored during operation to provide warning of adverse trends in incidents.

Thus today, it is now widely acknowledged that a proper risk management is the right framework for obtaining a healthy balance between maximizing opportunities whilst meeting safety requirements (Aven et al (2007)). Safety policies often have to be adopted and executed under resource constraints and uncertainties (Pate-Cornell (1994)),

Aven et al (2007)). These uncertainties are a reflection of either randomness (among individuals and systems) or lack of knowledge about the fundamental hazard mechanisms (Pate-Cornell (1994)). This state of knowledge is subjected to constant updating as one gains experience with the problem. An overall risk management strategy, therefore, involves technical, organizational, ethical, social, legal, and economic factors. Risk analyses and related tools leave decision makers to apply decision processes outside the direct applications of the analyses (Aven et al (2007)).

Nonetheless it is necessary that a robust decision-making framework is made available for situations involving high risks and large uncertainties. Attainment of considerable consistency in decision-making processes is the ultimate objective of such a framework. This framework exists in various fields but could be improved (Aven et al (2007)). The objective of such a framework relates, but is not limited to (Aven et al (2007)):

- the fundamental understanding of the framework for decision making, involving the use of statistical expected values and treatment of uncertainties;
- the use of various tools for risk and decision analysis, including analysis of sensitivity and robustness;
- the structure for categorizing situations and the decision problems to tune the decision and risk analysis process and optimize the time and cost involved in the process;
- the way of performing trade-offs for prioritizing objectives and balancing various attributes (costs, safety, etc.);
- the way of reflecting interactions and dependencies between decision problems at various stages of a project and various authority levels (political institutions, regulatory bodies, company, management and staff);
- the overall presentation and communication of the decision support.

The basic structure of a risk assessment study is fundamentally the same with slight variations. The formal safety assessment (FSA) introduced by Lord Cullen following the Piper Alpha disaster consists of the following stages (Shaw (1992)):

- hazard identification;
- frequency estimation;
- consequence prediction;

- risk summation;
- evaluation.

A variant to the former risk assessment structure is (Brandsæter (2002)):

- Step I – hazard identification
- Step II – event scenario assessment
- Step III – consequence assessment
- Step IV – risk evaluation: Consists of two parts:
  - Step IV(A) – risk assessment.
  - Step IV(B) – risk comparison.
- Step V – decision making.

Another variant is as follows (Wang (2000)):

- problem definition
- hazard identification
- risk estimation
- risk evaluation and
- design review.

QRA is one of the most important techniques used to identify major accident hazards and to show that the risks have been made ALARP, and is explicitly required under most offshore regulations. Several other countries have followed this approach, greatly increasing the requirement for offshore QRA worldwide (Brandsæter (2002)).

Risk refers to the likelihood of a specific effect originating from a certain hazard occurring within a specified period or in specified circumstances (Brandsæter (2002)). Hazard refers to the property of a substance or physical situation, with a potential for creating damage to human health or the environment. Typical major hazard accidents (top events) on an offshore structure include (but are not limited to) (Brandsæter (2002), Shaw (1992)):

- Accommodation module fire
- Attendant vessel accidents
- Aviation fuel storage tank fire



- Blowouts
  - Blowout subsea
  - Blowout surface (through the annulus)
  - Blowout surface (through the tubing)
- Collision events
- Construction accidents
- Diesel storage tank fire
- Diving accidents
- Dropped objects
- Earthquake
- Electrical equipment fire
- Extreme wind and wave
- Failure within design
- Gas leak
- Helicopter crash
- Hydrocarbon release
- Marine events
- Non-process fires
- Non-process spills
- Passing vessel collision
- Personal (or occupational) accidents
- Pipeline failure
- Process events
- Process leaks
- Riser and pipeline failures
- Riser failures
  - Riser failure above sea
  - Riser failure subsea
- Riser/pipeline leaks
- Stabilized well fluid leak
- Structural events
- Supply boat collision
- Transport accidents

- Unstabilized well fluid leak etc.

Selected structural events may include (Brandsæter (2002)):

- Structural failure due to fatigue, design error, scour, corrosion, etc.
- Extreme weather
- Earthquakes
- Foundation failure (including punch-through)
- Bridge collapse
- Derrick collapse
- Crane collapse
- Mast collapse
- Disintegration of rotating equipment.

Authorities and operators are increasingly basing their regulations and designs respectively on the use of risk analysis as a tool to determine which preventive and mitigative systems are needed as well as to dimension loads and requirements (Vinnem (1997)). QRA could be used for new installations as well as for existing ones. For the latter, it is often a case for evaluation of required improvements. Thus the accuracy and robustness of the QRA is critically important as it may influence extensive and costly upgrading projects. New installations are more and more often limited and simplified in size and function, and rely on QRA to direct the level of protection, prevention and mitigation that is required for the possible scenarios on the installations. The use of risk analysis for these provides the feasibility for a profitable development concept. Thus, the QRA studies are also very vital for these installations.

The QRA is an overarching framework and is undoubtedly technically related to the use of reliability analysis – whether it is used in structural reliability or mechanical reliability (Smith (1995)). A reliability/vulnerability analysis is required for specified systems critical to safety on an installation (Brandsæter (2002)). Acceptability criteria for these systems are as follows (Brandsæter (2002)):

- single faults should not cause critical incidents;
- vital systems should be redundant;
- the degree of redundancy should be related to the degree of hazard.

Probabilistic risk analysis is employed to assess the relative contribution of different factors to the overall risk (Pate-Cornell (1994)). The results can be utilized in various ways:

- to minimize the costs of achieving a target safety level;
- to optimize the allocation of a fixed safety budget;
- to guarantee (to corporate managers, regulators, interest groups, etc.) that a facility is "safe enough" or safer than its previous state.

The Norwegian Petroleum Directorate (NPD) had adopted for a while an explicit severe accident criterion of a maximum  $10^{-4}$  per year for the probabilities of major initiators of platform failure (Pate-Cornell (1994), Brandsæter (2002)). They also adopted an annual individual risk threshold of  $10^{-4}$  per worker on new platforms for any of the major hazards (probably resulting in a total individual risk of about  $10^{-3}$  per year) (Pate-Cornell (1994)). In the U.K., the government authorities have adopted for offshore platforms a criterion similar to the Norwegians': a maximum annual individual risk per worker of  $10^{-3}$ .

Risk assessment studies have been conducted in many areas in the marine and offshore environment. Sharp et al (2001) demonstrated the importance of QRA in the design of offshore production jack-ups. Ruud and Mikkelsen (2008) utilized the QRA safety and reliability of crane safety systems. Wang (2000) carried out a comprehensive FSA for marine vessels. Falck et al (2000) addressed the use of QRA with other activities on an offshore oil production installation.

## **2.2 Risk-Based Design**

Having been actively utilized in the offshore industry especially in the North Sea for more than 20 years, QRA was initially used primarily as a verification tool (Falck et al (2000)). The risk analyses were often carried out in isolation from the main design process and the overall planning, while the implementation of the findings and results was not effective. However, it was useful in directing attention to safety critical

elements such as escape routes and emphasizing the importance of safe shelter integrity TR (i.e. Temporary Refuge).

Today QRA is gradually becoming a tool to be actively utilized throughout the planning and design activities period (Falck et al (2000)). It is also utilized in decision-making as well as exploration of the safety implications of the choices made. The QRA activities are closely integrated with the design processes and are in many respects considered as routine.

Risk assessment could be utilized at all stages of a project life-cycle (Smith (1995)). At the design stage (concept and detailed design), these techniques are valuable in ensuring that resources are wisely spent on safety-related systems. Design for safety is a vital component in the overall design process (Wang (2000)). Reliability analysis in design generally focuses on the subject of assessing the effectiveness of a system to meet its design objectives (Wu and Lewins (1992)). Such an analysis would indicate weak areas in a system and point out where new measures in design, construction, maintenance and operation could improve its reliability.

Design for safety provides a systematic approach to the identification and control of high risk areas. It would therefore be beneficial to integrate it into the design process from the initial stages to reduce or eliminate major hazards (Wang (2000)).

Typical marine/offshore structures/facilities are expensive, large and complex engineering structures, made up of several subsystems which must be well integrated to form a complete working system (Wang (2000)). However, due to the complexity of the safety assessment these structures/facilities and the lack of a concise framework for a design for safety methodology, design for safety has not generally been integrated into the design process for such products.

It should be noted that faults in these structures/facilities have generally been corrected only after accidents (which could have been prevented if greater attention had been paid to safety in the initial design stages) have occurred (Wang (2000)). Even with these events, only a handful of organized design for safety programmes devoted to marine and

offshore products have been implemented to date. There is therefore a perceived need for a design for safety methodology for large marine and offshore structures/facilities in order to improve their safety.

It is noteworthy to stress that risk assessment on its own does not guarantee a safe or efficient structure; this is achieved by good design and good operational/engineering practices (Shaw (1992)). Risk assessment could support the achievement of safe designs and also the establishment of 'best practice' and contingency plans, but not when it is done in isolation. It is crucial, therefore, that such studies are integrated into the design process or involve key operational personnel. Furthermore, it should be noted that risk assessment studies do not equate only negative advice (i.e. requiring additional expenditure). Risk assessments are to be realistic and also recognize that there are limits (optimum safety) beyond which additional levels of protection are not appropriate (i.e. uneconomical or having little effects). Risk assessment studies ought to identify the major risk factors and take decisions that promote effective (optimal) utilization of resources.

Currently there is considerable pressure on operators to reduce the costs of developments at the design stage (Smith (1995)). Also for new developments, there are moves towards concurrent engineering (compressed design periods). However, cost reductions cannot be allowed to impact significantly on installation safety or equipment availability. Risk assessment during the design process is a vital tool in ensuring cost-effective safety solutions.

Marine and offshore product design is a broad-based activity; the design process combines creativity, empiricism, theory and practice (Wang (2000)). There are also inherent influencing factors and diversity of applications which may require the latest technology to be utilized.

Marine and offshore products often have difficulties in their general design process. Some of these problems are (Wang (2000)).:

- a) the non-existence of historical data on design aspects;
- b) the impracticability of full-scale experimentation with many design aspects;

c) difficulty of replacing or modifying them once on location and in operation.

Engineering design is a creative process; it begins with a requirement and defines a system (and the methods of its realization) in order to satisfy requirements. Three broad categories of design related to the design of various large marine and offshore products have been identified (Wang (2000)). They are:

- (a) Original design: involves the production of an original solution for a system to carry out a new task.
- (b) Adaptive design: involves adapting a known system to a different task.
- (c) Variant design: involves varying the size and/or arrangement of certain aspects/components of a system whilst its function(s) and solution principle(s) remain the same.

Although the concept of design for safety was introduced in the aerospace, nuclear and chemical industries several years ago, a series of standards, covering the general use of safety and reliability through other industries, were used from the 1980s (Wang (2000)). Today, the design for safety of most marine and offshore structures/facilities is usually based on British standards and classification society requirements (or their equivalent), which incorporate the necessary rules and codes implemented over the years. These rules and codes are sometimes updated following catastrophic accidents. Unfortunately, safety analysis is still mostly applied (if applied at all) at the final stages of the design mainly for verification purposes, although many of the decisions having the greatest impact on product safety may be taken at the earlier design stages.

The growing technical complexity of large marine and offshore structures/facilities and the public concern regarding safety have aroused great interest in the development and application of safety assessment procedures (Wang (2000)). This is espoused by the conclusions and recommendations of the public inquiries of the Piper Alpha and Herald of Free Enterprise accidents.

FSA in ship design and operation may offer great potential incentives. The application of it may (Wang (2000)):

1. Improve the performance of the current fleet, be able to measure the performance change and ensure that new ships are good designs.

2. Ensure that experience from the field is used in the current fleet and that any lessons learned are incorporated into new ships.
3. Provide a mechanism for predicting and controlling the most likely scenarios that could result in incidents.

A design for safety framework should be developed to allow various safety assessment tools such that as the design process advances, and the available information increases in detail, safety assessment can move from a qualitative basis to a quantitative basis. This should also be done to enable safety move from an assessment function to a decision making function, and finally to a verification function, ensuring that a final design meets explicitly defined levels of safety (Wang (2000)).

As the design progresses, the level of detail in the design increases, thus causing a reduction in the uncertainties (Falck et al (2000)). The risk analysis needs to reflect this in order to address decisions simultaneously as the design progresses. It is therefore necessary to aim for a living QRA, i.e. a risk model of the platform that is updated and refined in detail as required. Assumptions being made at an early stage to compensate for missing information need to be followed up and eventually replaced by factual information when available.

A design for safety framework could assume the stages of a risk assessment procedure. A representation could be thus:

EXCLUDED  
UNDER  
INSTRUCTION  
FROM  
UNIVERSITY



Figure (2.1) – Interrelations of five phases in the design for safety framework (Wang (2000)).

In the problem definition phase the following items may be specified (Wang (2000)):

1. Sets of rules and regulations made by the national authorities and classification societies.
2. Deterministic requirements for the life of the product, reliability, availability, etc.
3. Criteria referring to probability of occurrence of serious system failure events and possible consequences (i.e. frequency–consequence curve).

The hazard identification process identifies all potential hazardous conditions or events, and respective causes and possible consequences (Wang (2000)). Experience in the marine/offshore industry has shown that a large proportion of critical failures result from ignoring potential system failure events. In the hazard identification phase, the combined experience and insight of engineers is required to systematically identify all potential failure events with a view to assessing their influences on system safety and performance. Various safety analysis methods may be used individually or in combination to identify the potential hazards of a system. Such typical methods include (Wang (2000)):

- (a) preliminary hazard analysis (PHA);
- (b) fault tree analysis (FTA);
- (c) event tree analysis(ETA);
- (d) cause–consequence analysis (CCA);

- (e) failure mode, effects and criticality analysis (FMECA);
- (f) hazard and operability analysis (HAZOP);
- (g) Boolean representation method (BRM);
- (h) simulation analysis.

While the overall process of ensuring safety should be a process of optimization (Shaw (1992)) the design for safety stage is an iterative process (Wang (2000)). For instance, the hazard identification phase may make use of the information produced from design review, converging to safety design goals defined in the problem definition phase.

Risk estimation should precede the design procedure in order to process the information produced from the hazard identification phase (Wang (2000)). In the risk estimation phase, the likelihood of occurrence of each identified system failure event and possible consequences can be assessed on either a qualitative or a quantitative basis.

As the design advances more information regarding safety is acquired (Wang (2000)). Once the minimal cut sets leading to a top event have been identified, the failure data of the basic events associated with the minimal cut sets could then be obtained. Finally, a quantitative risk estimation can be undertaken. The typical methods used in carrying out quantitative risk estimation include fault tree analysis (FTA), event tree analysis (ETA), cause consequence analysis (CCA), Boolean representation method (BRM) and simulation. The results produced from the risk estimation phase may be used during the risk evaluation phase and design review, and may also be used to assist designers in developing maintenance and operation policies.

QRA results need to be “translated” into engineering terms (Falck et al (2000)). Risk is measured in terms outlined by the risk acceptance criteria (e.g. potential loss of life (PLL), fatal accident rate (FAR), etc.) and required risk reduction will typically be specified as, e.g. reduction in PLL. This is not valuable information for the engineering team. The requirements must be specified as, e.g. design loads for explosion barriers or location of critical equipment.

The risk analysis needs to be sufficiently detailed to address the effects of engineering solutions and assessment of possible alternatives (Falck et al (2000)). Therefore, the risk analysis needs to be closely integrated with detailed engineering studies to enable it to provide more detailed information.

### **2.3 Structures in the Marine and Offshore Environment**

A structural system is an assembly of components – which themselves are subject to local failure. These components could be beam sections, connections or any other sections of the structures (Rashedi and Moses (1986)). Structural failure in this context is defined as the violation of one or more limit states (Gray and Melchers (2001)).

The limit state function defines the structural and/or component integrity into a safe and failure domain (Wu and Moan (1991)). Most reliability methods rely on the limit state function of a component and/or structure (Rashedi and Moses (1986)). Formulation of limit states has been an outcome of high idealization of structures. The variability in the limit states stems from the uncertainty in the loads and material resistance, thus the expression of the reliability as probability (Gray and Melchers (2001)).

Uncertainties exist in parameters such as structural dimensions, boundary conditions and section properties from manufacture, material stiffness and construction processes which cause the deterministic model of the structure to deviate from reality. The deterministic models are therefore insufficient (Du et al (2005)).

Reliability analysis is the main tool in quantifying the numerous uncertainties that exist in civil engineering systems (Ching and Hsu (2008)). Structural reliability methods aid in the rational quantification of structural reliability in the design process as well as having a great impact on the decision making process involved in the inspection and maintenance of the structure (Wu and Moan (1991)). Reliability analysis forms the basis of research fields such as performance-based engineering, design and optimization, life-cycle engineering, etc. (Ching and Hsu (2008)). Also updating of additional information and relative change in safety levels (compared with existing levels) could be achieved via structural reliability analyses (Schoefs (2008)).

For simple structures like bars and frames, structural analyses could be performed in a simple and perhaps analytical manner (Brenner and Bucher (1995)). These analytical methods (deterministic) could also be used in conjunction with randomness (semi-probabilistic or semi-analytical) to determine failure limits quite accurately (Du et al (2005)). Reliability assessment of single structural components has been well developed (Rashedi and Moses (1986)). In structural reliability, the study of failure of an individual element or a structural system could be undertaken.

Evaluation of overall structural reliability is essential as it differs from the reliability of individual components (Rashedi and Moses (1986)). Considerable effort is required for larger and more complex structures due to the large amount of components, vast number of random variables as well as complex system response under random loading (Brenner and Bucher (1995)). The nature of the structure could cause a complete miscue in the description of system behaviour and accurate quantification of load and system parameters. Such systems with significant dependencies between members (components) require a holistic assessment with regards to reliability to ensure system integrity, which is distributed amongst the members (Yang and Younis (2005)). There is need for flexible methods that address these complex designs.

Although in recent years efforts have been directed at developing methods and software packages for structural reliability analysis, the actual challenge lies in the provision of natural procedures and decision aid tools for the reassessment of offshore structures where the structural and mechanical integrities are paramount (Schoefs (2008)).

Various methods for handling uncertainty (and thus estimating reliability) in complex structures have been developed. Some conventional methods include (Yang and Younis (2005)), (Liu and Tang (2004)):

- Point Estimation Method (PEM).
- Response Surface Method (RSM).
- Monte Carlo Simulation (MCS).
- Petri nets.
- Bayesian Networks (BN).
- Markov modelling.

- Moment-based methods (FORM, SORM, FOSM, SOFM, etc.).

The disadvantage of methods like Petri nets is the oversimplification of the dynamic loading subject to the structure (Yang and Younis (2005)). Markov chains are event based with assigned failure rates which inadequately represent the effects of the elementary components on the failure mechanisms. The moment based methods are not adaptable to stochasticity.

Despite being computationally costly, MCS is a highly accurate method and unlike moment based methods, it could be applied where explicit limit state functions are unavailable (Wong et al (2005)). A large area in Monte Carlo research is dedicated to reducing computational costs e.g. importance sampling.

Tasks in structural reliability analyses may be grouped into two (Wu and Moan (1991)):

- Probabilistic modelling of the physical processes.
- Computation/determination of the overall structural system reliability.

The structural reliability analysis could be time-variant (stochastic) or time-invariant (random variable) depending on the nature of the load and the objective of the analysis (Gray and Melchers (2001)).

A certain structural behaviour or response could be modelled as a system output. This output varies in response to the changing levels of various input variables i.e. loads (Schoefs (2008)). Under limit state parameters, structures often exhibit non-linear behaviour. This behaviour could be extreme in the event of dynamic loading (Brenner and Bucher (1995)). Structural loading varies randomly (Floris (1998)) with time and space (Mori et al (2003), Wataru (1993)).

Loads having small variations with time and space may be conveniently modelled as random variables. A larger variation would require stochastic modelling (Floris (1998)). Modelling is usually based on the statistics of load subjection throughout the proposed life of the structure (Mori et al (2003)). Complexity inherent in the estimation of the extreme value of these combined loading effects means that approximate methods need to be developed (Naess and Royset (2000)).

In the design of civil engineering structures, realistic and practical means of estimating the load effect processes resulting from simultaneous loading is of utmost importance (Naess and Royset (2000)). For reliability limit state design, the maximum effect of the load combination must be appropriately modelled (Wataru (1993)). Turkstra's rule is one of the most prominent methods applied in load combination (Naess and Royset (2000)). It is often employed due to its simplicity (Mori et al (2003)). The limitation of this method is the non-conservative nature due to ignorance of the fact that the maximum loading effect is not only attained when each loading process is at the 'maximum' but could also be attained when these processes are at their 'near maximum' values (individually). Conventional allowable stress design (ASD) models (in use in most standards) are simple additive operations augmented by factors based on engineering experiences and judgements (Wataru (1993)). These methods become insufficient for complex cases.

A credible reliability assessment is one that entails a non-linear dynamic approach to modelling the loading parameters (Brenner and Bucher (1995)). The effect of randomness inherent in loading processes as well as structural parameters must be taken into consideration. The loads experienced by offshore structures are often Gaussian distributed in nature (Beck and Melchers (2004)), (Shi (1991)).

## **2.4 Reliability**

### **2.4.1 Uncertainty**

The analysis of marine and offshore structures involves the development of a representation model. The resulting model remains an abstraction of the entire structure in question as it is up to the engineer(s) to decide what to include or exclude as regards the characteristics of the structure. The following are some uncertainties that occur in the modelling of a structure characteristic or behaviour (Ayyub and McCuen (2003)):

- Physical randomness.
- Modelling uncertainty.
- Statistical uncertainty.
- Vaguely defined parameters, measurements and relations.
- Conflict and confusion in information.

- Human organisational errors.
- Extent of deviations between model and real system.

These uncertainties, to name a few, could make structural modelling difficult. Uncertainty in the context of this research is defined as “knowledge incompleteness due to intrinsic deficiencies with acquired knowledge”.

Uncertainties may be due to all or some of the reasons listed. Moreover, the overall characteristics of the structure may not be completely described by the latest technology advancements available. The background of the engineer or analyst also plays an important role in modelling certain characteristics of the structure. These factors increase the overall uncertainty of the structure.

In summary, most uncertainties encountered within structural modelling are attributed to ambiguity or vagueness in the definition of the characteristic variables or parameters and their governing relations (Ayyub and McCuen (2003)). The ambiguity factors consist of:

- Physical randomness.
- Model uncertainties due to simplified assumptions in analytical and prediction models, simplified methods and idealized representations of real processes.
- Statistical uncertainty due to the use of limited information to synthesize variable or parameter characteristics.

The vagueness factors include:

- Definition of interrelationships between parameters or variables of the structure in question especially of those with multiple components or complicated links.
- Definition of certain parameters like structural performance (failure or survival), quality, skill and experience of engineers, environmental impact of certain operations, structural condition, etc. to name a few.
- Human factors.

Fatigue modelling presents a range of uncertainties to be resolved by means of techniques gained from probability and reliability studies.

### **2.4.2 Structural Reliability**

Virtually all marine and offshore structures and facilities are composed of steel. These structures and facilities have an average service life of 20 years (Moan (2005)). Due to the inherent random nature of the conditions experienced by these structures, reliability analysis becomes essential in the design, inspection, repair, and maintenance of these structures (Pillai and Prasad (2000)).

The reliability of a structure may be defined as the probability that the structure maintains its integrity while fulfilling its service requirements throughout its service life (Kececioglu (2003)). Structural reliability as the name implies requires a broad knowledge of structural modelling as well as reliability analysis. This combination provides an essential criterion for engineers in the design, cost estimation, inspection, maintenance (and repair) and most importantly safety and reliability of structures.

### **2.4.3 Deterministic Analysis/Modelling vs. Probabilistic Analysis/Modelling**

Basic fatigue formulations are deterministic in nature i.e. all parameters are considered fixed at the time of calculation (Shigley et al (2004)). However, given the random nature of several engineering applications – fatigue included, several ambiguity-related uncertainties would render the results unrealistic. This would lead to underestimation or overestimation of cost and resources. Also the safety of the structure would differ from the predetermined value or criteria. This could be of catastrophic consequences especially in harsh or hazardous environments. This is often deterred by assuming upper-bound (extreme) values and incorporation of safety factors. These, as will be shown later on, are inadequate, as failures could still occur (and very likely in some cases). Also, the availability of data (partial or complete) – which is central to modelling, is not always guaranteed. This places a major limitation in the utility of this kind of modelling. Further uncertainties are introduced into the model by approximations of key parameters (Mao and Mahadevan (2000)). Deterministic modelling requires considerable amount of data to justify a value – which in itself is an approximation. These approximation errors become very significant in large scale representations.



Fatigue models of marine and offshore structures based on a deterministic approach would reflect these limitations which could lead to severe consequences. Therefore a model which takes the random behaviour of the structures, materials, processes and conditions into account will provide a realistic interpretation of the underlying interactions. This is a probabilistic approach. In place of data, suitable probability distributions are utilized.

Various materials exhibit different properties at different conditions. In the offshore environment, significant variation in these properties is a common phenomenon. The variations are considerably greater than those which occur in onshore conditions. Therefore, fatigue of marine and offshore structures – a random process – is best suited to the probabilistic approach. This approach provides criteria for cost effective decisions by engineers while required safety levels are maintained.

#### *Stress Intensity Factor*

The stress intensity factor is a test to measure the damage tolerance of the node/joint in a structure. The fracture toughness otherwise known as the critical stress intensity factor  $K_{IC}$ , is the property of a material to resist fast fracture. It is the value that the stress intensity factor (in a structure node) should not be allowed to attain or exceed in order to prevent fast fracture. The  $da/dN - \Delta K_I$  (where  $a$  is the crack length,  $N$  is the number of cycles and  $K_I$  is the stress intensity factor) curve is plotted on a log-log scale. The general format of this graph is shown in Figure (2.2):

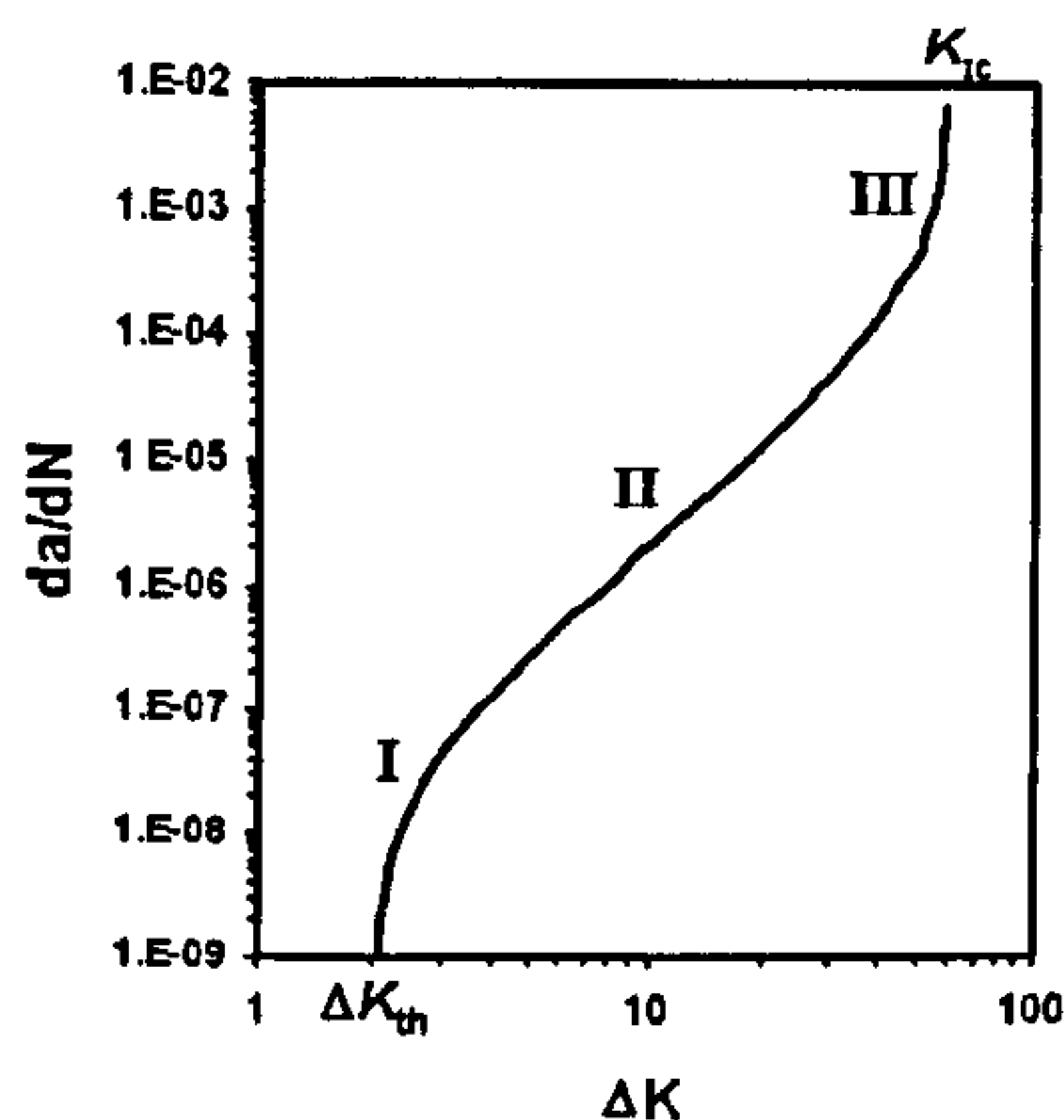


Figure (2.2) – Crack propagation.

The generic  $da/dN - \Delta K_I$  curve plotted on a log-log scale shows 3 regions which are considered in the modelling of the fatigue of a material/structure. Region I is the “near threshold” region in which no crack propagation occurs below a threshold value of a driving force denoted  $\Delta K_{th}$ . Region II shows a region where the crack growth rate experiences near linear change with the changes in stress intensity factor amplitude. Region III holds data that shows that small increments in the stress intensity factor amplitude leads to relatively large increases in crack growth rate as the material approaches fast fracture. The linear region (region II) of the curve has been modelled in this research.

#### ***2.4.4 Review of Methods of Handling Uncertainty***

Various methods have been developed by engineers, scientists and mathematicians in modelling structures more accurately. They include fuzzy logic, genetic algorithm and Monte Carlo simulation, reliability methods (FORM, SORM), regression analysis, Bayesian methods, sensitivity analysis, etc. Each of these methods possesses advantages unique to the type of scenario/uncertainty presented.

Uncertainty estimation and reduction has been a challenge in structural modelling over the years. An array of techniques has been formulated and applied in industries ranging from enormous structures onshore to locking mechanisms offshore. There have been considerable contributions made towards the development of comprehensible fatigue modelling for various conditions over the past decades.

Manners (1989) used the first order method to determine the reliability of offshore structures subjected to Ferry Borges – Castanheta type load histories. Hanna and Karsan (1991) carried out experiments and used probability distributions to determine the reliability of an offshore platform with reference to its tubular connections and defects. Jiao and Moan (1992) incorporated limit states based on S-N curves (S- stress and N- number of cycles to failure) and fracture mechanics. They further combined limit state modelling with FORM, SORM and Monte Carlo simulation to estimate the reliability of a structure.

Zhu et al (1992) compared fatigue crack growth obtained from deterministic procedures to those obtained from Monte Carlo simulation. The results were proved to be very reliable when compared with the theoretical and particularly, the experimental result. Pillai and Prasad (2000) investigated the reliability of fixed offshore platforms. Using Advanced Second Moment (ASM) method with respect to fatigue and stress, a reasonable result was obtained.

Faber (2000) used the Bayesian method to optimize the cost and reliability of a structure. Mori et al (2003) used the Advanced First Order Second Moment (AFOSM) method to predict the design point and hence the cumulative probability function of the maximum load acting on a structure. Gray and Melchers (2006) applied directional simulation techniques in determining the reliability of structures with reference to load combinations and configurations.

Amadio et al (2006) investigated the performance of a restrained steel frame structure using the Latin Hypercube method to synthesize the distribution of the joint parameters. Chryssanthopoulous and Righiniotis (2006) incorporated uncertainty parameters in the process of investigating the fatigue reliability of welded structures with respect to time. From the results obtained, inspection and decision making strategies were implemented. Grooteman (2008) utilized a combination of FORM, SORM and Monte Carlo simulation to predict the lifetime and implement inspection schemes for an aircraft component.

## **2.5 Monte Carlo Methods**

It is acknowledged that reliability analysis is important and should be an integral component of the planning, design and operation of all engineering systems, from the smallest and simplest to the largest and most complex (Wu and Lewins (1992)). Also, it is acknowledged that all engineers involved with such systems should be aware of, not only the benefits which could be accrued from reliability studies, but also the method of those studies.

The main quantities often sought after in reliability analysis of engineering systems include mean time to failure, reliability, availability, and average availability (Wu and Lewins (1992)). Also, since the system behaviour in time is inherently random, all of the above quantities represent an average rather than a strictly deterministic value. Therefore, in principle, the only way to measure these quantities is through experiment by operating several systems under conditions that simulate the real life of the system. Unfortunately, extensive testing is not always possible as it results in large expenditure of money and time. Thus cheap, quick and effective alternatives become attractive. Such alternatives should be able to describe system behaviour in time in a probabilistic sense and express the probability of various events during the entire life of a system i.e., from the moment that system is initially put in service until termination (i.e. system fails or passes its mission time).

Major techniques used in reliability studies summarily fall into two categories: analytical methods and simulation methods. Analytical methods are best applicable in the study of simple systems; they become very limited and time-consuming when applied to the study of complex systems (Wu and Lewins (1992)). Therefore, the use of other techniques that enable comprehensive studies of systems to become achievable and more efficient is required in today's complex engineering systems.

A Monte Carlo modelling usually consists of building, with a computer program, a probabilistic model of the engineering system under investigation (Wu and Lewins (1992)). The model is then run a large number of times (each time represents one history of the modelled system), to generate a large number of histories. From this all the reliability indices required about the system are retrieved.

A Monte Carlo method is “any method which solves a problem by generating suitable random numbers and observing that fraction of the numbers obeying some property or properties” (Yang (2002)). The term “Monte Carlo” was coined by Stanislaw Ulam in 1946 and is commonly used in physics and other fields that require solutions for problems that are impractical or impossible to solve by traditional analytical or numerical methods.

The Monte Carlo method is an attractive alternative to be used to analyse the reliability of complex engineering systems since it involves no complex mathematical analysis (Wu and Lewins (1992)). In addition, it can be used not only to analyse the present state of the system but also to predict change in reliability for changes in system design. This kind of prediction is vital in the system design optimisation process, thus making the Monte Carlo method even more attractive.

The only obstacle to using the Monte Carlo simulation in system reliability studies is the "rareness" of the event to be evaluated (Wu and Lewins (1992)). A rare event requires Monte Carlo simulation to run a lot of simulated histories (in other words, a long computer CPU time) before a reasonable accuracy of estimation can be achieved. However, many variance reduction techniques could be used to overcome the difficulty caused by the rare event.

The name and development of Monte Carlo methods (MCM) dates from about 1944 (Wu and Lewins (1992)). There are however a number of isolated and undeveloped instances that utilized the Monte Carlo principle on much earlier occasions (centuries earlier). The real use of Monte Carlo methods as a research tool stemmed from work on the atomic bomb during the Second World War. Since then, Monte Carlo methods have been applied in many fields such as particle transport (nuclear sciences), management sciences, econometrics, industrial planning and system reliability. MCM, also referred to as "stochastic simulation", based on the laws of probability and the use of random numbers, handles two types of problems, both probabilistic and deterministic. In probabilistic problems, the random nature of physical phenomena makes a simulation possible without elaborate mathematical formulation other than a mathematical description of the individual basic events. In deterministic problems (e.g. the evaluation of multiple integrals) Monte Carlo techniques have been used when conventional theoretical methods have proven to be inadequate.

Data from real systems and structures are often used by engineers and scientists to understand and establish certain underlying characteristics or behaviours (Ayyub and McCuen (2003)). For example a climatic/environmental parameter such as temperature, wind velocity, wave height, etc. is measured and analysed by engineers. The result of

these analyses reveals the material properties to be used in the construction of an offshore structure in that environment. Unfortunately, real world data may be inadequate. It may not cover extreme conditions which are very critical in design decisions. For example the wave-height or wind-velocity records may not include the extreme values needed in making design decisions.

A basic Monte Carlo simulation involves the use of the characteristic distribution of a particular dataset in conjunction with random number generation to produce a portion or a complete outlook of the original dataset – a pseudo-dataset. This gives possibilities of further analysis or synthesis of new characteristics. An advantage of the Monte Carlo simulation is that complex sets of data generation could be handled simultaneously (Rubinstein (1981)).

Prior to the 21st century, computing limitations implied that only the Monte Carlo simulation was constrained to a relatively low level of complexity. In recent years, however, rapid advancements in computer technology have facilitated extensive applications of Monte Carlo simulation for complex models and datasets.

Monte Carlo simulation takes strong advantage of the stochastic nature of fatigue in failure prediction as well as reliability assessment. Prevalent conditions in the offshore environment combined with operating parameters present important analyses and results to be utilized in reliability assessment.

Several methods and solutions have been delivered via Monte Carlo methods (MCM). Kreiner and Putcha (1994) utilized MCM in determining the probability of failure of shafts subjected to reverse bending. Rahman and Wei (2006) utilized the MCM in presenting a univariate method to predict the failure probability of structural and mechanical systems subject to random loads, material properties, and geometry. Neal (1991) showed that Bayesian inference from data modelled by a mixture distribution could feasibly be performed via Monte Carlo simulation. Lindt and Goh (2004) used the MCM to provide a basic method to better estimate the effect of earthquake duration on structural reliability. Aua et al (2007) used the MCM to develop a stochastic simulation approach for quantitative fire risk analysis. Naess et al (2007) utilized the MCM in

estimating the extreme response statistics of a drag-dominated offshore structure exhibiting a well-defined dynamic behaviour when subjected to harsh weather conditions. Zou et al (2007) presented a MCM for simulating rough surfaces with fractal behaviour. Siddiqui and Ahmad (2001) utilized the MCM while performing a non-linear dynamic analysis of an offshore platform for response calculations. Guoliang et al (1993) developed a Monte Carlo finite element method for performing the reliability analysis of any structure. Carassale and Solari (2006) utilized the MCM in the simulation of wind velocity fields over large domains in zones characterised by complex topography. Melchers and Ahammed (2004) utilized the numerical results from a Monte Carlo reliability estimation to carry out a structural reliability analysis.

### 2.5.1 Distributions

The use of random numbers sampled from various distributions is one of the highlights of the Monte Carlo simulation. The distributions used in this research are emphasized in this section. The inverse transform method is employed for the generation of random numbers for the uniform, exponential and Gumbel distributions while the Box-Muller method is used for random number generation for the normal and lognormal distributions.

#### 2.5.1.1 Expected Value

If  $x$  is a random variable with a probability density function (PDF),  $Q(z)$ , the expected value can be computed as:

$$E(x) = \int_{-\infty}^{\infty} zQ(z)dz \quad (2.1)$$

It can also be written as:

$$\langle X \rangle = \int_{-\infty}^{\infty} zQ(z)dz$$

When an arbitrary function of  $x$ ,  $F(x)$ , has a PDF  $Q(z)$ , the expected value is computed as:

$$E[F(x)] = \int_{-\infty}^{\infty} F(x)Q(z)dz \quad (2.2)$$

The expected value of a given distribution is often referred to as the mean of the data set.

### 2.5.1.2 Uniform Distribution

This is one of the most common distributions used as it forms the base of other distributions in computing. FORTRAN has an in-built congruential generator, which produces uniform random numbers between 0 and 1 using the following equation:

$$U_{i+1} = (a_{mul}U_i + c_{inc}) \bmod(m_{mod}) \quad (2.3)$$

where  $U_{i+1}$  is the uniform random number,  $U_i$  is the seed value,  $a_{mul}$  the multiplier,  $c_{inc}$  the increment and  $m_{mod}$  the modulus. It is implemented as:

$$V_{trans} = V \times U_{i+1} \quad (2.4)$$

where  $V$  is the variable to be transformed and  $V_{trans}$  is the transformed variable.

### 2.5.1.3 Exponential Distribution

This distribution is widely employed in the engineering world (Ayyub and McCuen (2003)). A variable  $x_{exp}$  or function  $f_x(x_{exp})$  is said to be exponentially distributed if it has the PDF:

$$f_x(x_{exp}) = \begin{cases} \frac{1}{\beta_r} e^{-\frac{x}{\beta_r}}, & 0 \leq x \leq \infty, \beta_r > 0 \\ 0, & otherwise \end{cases} \quad (2.5)$$

where  $\beta_r$  is a parameter of the distribution (a non zero value) sometimes called the rate.

Exponentially distributed random numbers are produced using the inverse transform method. The inverse transform method involves:

- generating the inverse of the desired cumulative distribution function (CDF) (integral of the PDF),  $F^{-1}_{(x)}$ ;
- generating a uniform number from the uniform distribution  $U$ ;
- obtain the value of  $x = F^{-1}_{(x)}(U)$ .

Thus, the exponentially distributed random numbers are obtained as follows:

Given that the integral of  $f_x$  is denoted as  $F_x$ ,

$$x_{exp} = F^{-1}(U) \quad (2.6)$$

hence,

$$U = F_x(x_{exp}) = 1 - e^{-\frac{x}{\beta}} \quad (2.7)$$

$$x_{exp} = -\beta_r \ln(1 - U) \quad (2.8)$$



Since  $(1-U)$  possesses a distribution similar to  $U$ , Equation (2.8) may be rewritten as:

$$x_{exp} = -\beta_r \ln U \quad (2.9)$$

The expected value is the product of the mean of an exponential variable or function and an exponentially distributed random number. It is implemented as:

$$V_{trans} = V \times x_{exp} \quad (2.10)$$

#### 2.5.1.4 Normal (Gaussian) Distribution

A variable or function is said to be normally distributed if it has the PDF:

$$f_x(x_G) = \frac{1}{\sigma\sqrt{2\pi}} e^{-\frac{(x_G-\mu)^2}{2\sigma^2}} \quad (2.11)$$

where  $\sigma$  is the standard deviation of the function  $f_x(x_G)$ , and  $\mu$  the arithmetic mean.

The inverse transform method cannot be applied in the case of a normal distribution. Box and Muller (1958) proposed a method to generate normally distributed random numbers for computation. This method was computationally exhaustive as it made several calls to the computer's library (cosine, sine, log, etc.). This was later modified to an algorithm less tasking for the computer. This is known as the polar form of the Box-Muller algorithm.

First two uniform random numbers,  $n_1$  and  $n_2$  are generated. The variables  $x_1$ ,  $x_2$ , and  $y$  are defined as:

$$x_1 = 2n_1 - 1 \quad (2.12)$$

$$x_2 = 2n_2 - 1 \quad (2.13)$$

$$y = x_1^2 + x_2^2 \quad (2.14)$$

For every positive outcome of the operation  $y > 1$ , new uniformly distributed random numbers  $n_1$  and  $n_2$  are generated and  $x_1$ ,  $x_2$  and  $y$  re-evaluated. Otherwise ( $y \leq 1$ ),  $x_{G1}$  and  $x_{G2}$  are pairs of standard normal variates by:

$$x_{G(i)} = \sqrt{\frac{-2 \ln y}{y}} x_1 \quad (2.15)$$

$$x_{G(i+1)} = \sqrt{\frac{-2 \ln y}{y}} x_2 \quad (2.16)$$

It is implemented as:

$$V_{trans} = V + (x_G \times \sigma) \quad (2.17)$$

$$\sigma = V \times COV \quad (2.18)$$

where  $\sigma$  is the standard deviation.

### 2.5.1.5 Lognormal Distribution

A variable or function is said to be lognormally distributed if it has the PDF:

$$f_x(x_{LG}) = \frac{1}{\sigma\sqrt{2\pi}} e^{-\frac{(\ln x_{LG} - \mu)^2}{2\sigma^2}} \quad (2.19)$$

The random number generation process is similar to the normally distributed random number up until the evaluation of the expected value. Essentially, the expected value of a lognormally distributed variable or function is the exponent of the Gaussian (normal) expected value of the variable or function. The implementation is as follows:

$$V_{trans} = e^{y_{LG}} \quad (2.20)$$

$$y_{LG} = [\ln(V) - 0.5x_{LG}] + [x_G \times \sqrt{x_{LG}}] \quad (2.21)$$

$$x_{LG} = \ln(1 + (COV)^2) \quad (2.22)$$

### 2.5.1.6 Gumbel Distribution

The (PDF) of the Gumbel (maximum) distribution is given (according to Gumbel (1947)) as:

$$f(x_{gb}) = e^{-x_{gb}} \cdot e^{-e^{-x_{gb}}} \quad (2.23)$$

Integrating the PDF gives the CDF:

$$F = e^{-e^{-x_{gb}}} \quad (2.24)$$

Using the inverse transform method, Gumbel random numbers are generated as follows:

$$U = F_{(x_{gb})}(x_{gb}) = e^{-e^{-x_{gb}}} \quad (2.25)$$

$$U = e^{-e^{-x_{gb}}} \quad (2.26)$$

rearranged,

$$-e^{-x_{gb}} = \ln(U)$$

$$e^{-x_{gb}} = -\ln(U) \quad (2.27)$$

rearranged,

$$-x_{gb} = \ln(-\ln(U))$$

$$x_{gb} = -\ln(-\ln(U)) \quad (2.28)$$

where  $x_{gb}$  is the Gumbel distributed random number and  $U$  is a uniform random number. It is implemented as:

$$V_{trans} = V + (\sigma \times x_{gb}) \quad (2.29)$$

### 2.5.2 Limit State Modelling

This proposes that a component possesses a certain resistance (strength) factor  $R$ , and is subjected to certain demand (stress)  $D$ . The survivability of this component is dependent on the outcome of  $y$ , where  $y$  is defined by the following equation:

$$y = R - D \quad (2.30)$$

The component survives if  $y > 0$  and fails otherwise. The  $R$  and  $D$  characteristics could be viewed as building blocks of a larger  $R$  and  $D$  component property (Shoorman (1990)). These building blocks are not entirely equal and exhibit variations or imperfections and hence form a statistical distribution.

The building blocks of  $R$  and  $D$ ;  $(R_1, R_2, \dots, R_i)$  and  $(D_1, D_2, \dots, D_i)$  respectively may be independent or dependent on other factors external or internal. Hence it could be assumed that the central limit theorem would hold for the relationship between these factors. This would mean that the resulting distributions of  $R$  and  $D$  would most likely be normal or lognormal (Ayyub and McCuen (2003)).

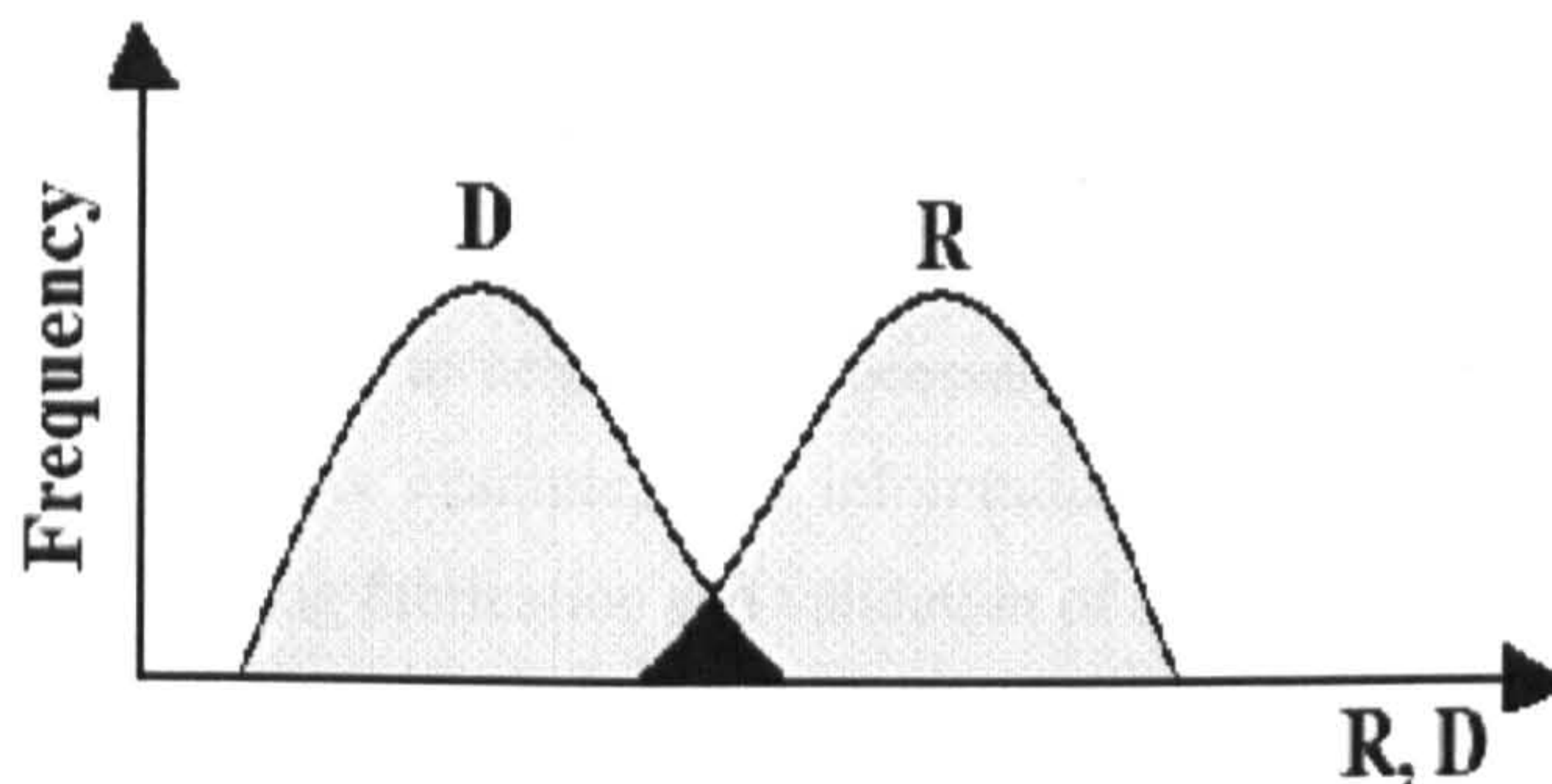


Figure (2.3) – Generic limit state model.

The area of overlap represents the probability of failure. Assuming the distribution in Figure (2.3) is normally distributed, the failure probability  $P$  could be computed as:

$$P = \int_{-\infty}^0 \phi(y) dy \quad (2.31)$$

where  $\phi(y)$  represents the value(s) of  $y$  according to a specified distribution. Thus, the reliability  $G$  is expressed as:

$$G = \int_0^{\infty} \phi(y) dy \quad (2.32)$$

## 2.6 Maintenance

In the last half century, maintenance policies have undergone a paradigm shift (Khan and Haddara (2003)). The concept of maintenance management has evolved from a necessary evil – performed primarily as corrective action – into an integrated part of a total management system, actively participating in the achievement of an organization's main objective.

Majority of the 5000 fixed offshore production platforms in the world have been in operation for more than the initially planned service life of 20 years. Approximately 40% of mobile drilling platforms have exceeded their planned service life (Moan (2005)).

It has been stated earlier that it is more important to know and manage the risk, than to necessarily reduce or eliminate it by all means (Jovanovic (2003)).

Since modifications to maintain an acceptable safety level within a structure are much more expensive to perform during the lifetime than at the initial design stage (before fabrication) other strategies to achieve the necessary safety for existing structures are pursued (Moan (2005)). For example, more information about material and geometrical properties collected during fabrication and validation of structural response made during operation, implies reduced uncertainties (by virtue of more information) in predicted resistance and load effects. Hence smaller safety margins than those used at the design stage could be demonstrated (with more certainty) to be acceptable.

Another strategy to compute an adequate safety for existing structures is to use more refined analysis methods for loads, load effects and strength than the often simple and conservative ones used in the initial design (Moan (2005)).

However, to achieve consistency in design and inspection criteria, fatigue design should be calibrated to reflect the consequences of failure and inspection plan (Moan (2005)).

Since this calibration is done on the basis of information available at the design stage, it would be beneficial to utilize more information obtained, e.g. by inspections during operation, to update the inspection plan (Moan (2005)).

It is often more economical to use existing structures than to build new ones (Moan (2005)). Therefore, there is a need to reassess existing offshore structures for a possible extension of the service life. This need for life extension may arise as a result of a planned change of function or the occurrence of damage.

Inspection and monitoring (IM), and, if necessary, maintenance and repair (MR) are vital measures for maintaining an adequate safety level, especially in terms of fatigue and other degradation phenomena (Moan (2005)). Improvements to reliability may be achieved through a robust inspection and maintenance program (Khan and Haddara (2003)).

The integration of risk considerations into the daily practice of maintenance has not been a straightforward and easy process (Jovanovic (2003)). There have been a number of stages through which maintenance practices have evolved. They include (Jovanovic (2003)):

- corrective maintenance;
- scheduled maintenance;
- condition-based maintenance.

This has finally led to concepts known today as reliability-centred maintenance (RCM), risk-aware maintenance and similar (Jovanovic (2003)).

First and most natural approach to maintenance is the corrective maintenance. It is based on the “fix it when it breaks” principle, i.e. on the repair when necessary, when a part is broken (Jovanovic (2003)). Although historically the oldest (and in many instances replaced by the consequent practices), the approach of corrective maintenance still lives in the daily practice, mainly for “non-critical” components. The corrective approach (especially in the maintenance of “critical” systems and components) has been widely replaced later by the concept of scheduled/planned maintenance. The scheduled/planned maintenance concept essentially recommends that everything related to design and maintenance of “critical components” (e.g. pressurized components) should be done as prescribed. By following prescribed routines, safety would be achieved (exclusion of failures). The scheduled/planned maintenance assumes that (Jovanovic (2003)):

- (a) the nature and extent of degradation of components can be predicted (e.g. based on the inspection history of those components or of other components in similar service) and
- (b) that the equipment, which has been proven not to degrade, need not be inspected further.

Unfortunately, real life in most cases cannot be prescribed. Whilst the prescription-based approach is well established in design, its application in inspection is much less suitable as state of the component depends strongly on mode and overall boundary conditions of operation. In such a situation, inspection of components at fixed time intervals can (Jovanovic (2003)):

- impair plant safety by diluting inspection resources;
- induce unnecessary costs;
- give a false impression of the damage state of the facility.

The solution for the problem has been proffered by the concepts of condition-based maintenance, RCM and risk-aware maintenance, risk-based inspection (RBI), risk-based life management (RBLM) and others (Jovanovic (2003)).

These risk-centred solutions recommend a necessary move away from the traditional (prescribed and time-based) practices to the adoption of strategies based on the

condition of the component and related risk (Jovanovic (2003)). Thus, the overall safety, reliability and economy of the structure can be improved and the resources optimally utilized by ensuring that inspection is focused on the critical components.

In order to achieve safe and efficient performance, it is essential to minimize and, if possible, eliminate unscheduled breakdowns (failures). This could be achieved through effective and efficient inspection and maintenance management (Khan and Haddara (2003)).

To derive the probability of failure or survival of a given system, detailed knowledge of the continuous (stochastic) degradation mechanisms, which affects the components is required (Jovanovic (2003)). This knowledge must be based on a thorough evaluation of the component itself (“condition assessment”), its operating environmental conditions and its relationship (as detailed as possible) with the overall structure.

## **2.7 Justification for the Research**

From the literature review it was noted that the use of QRA and thus reliability analyses of structures is ongoing today. Several methods have been utilized to these ends. There have been QRA methods proposed for structures (mostly for a specified type) usually addressing various subjects of risk generically. The reliability analyses have also focused solely on the quantification of risks within structures with current trends utilizing specialist software. While some of the reliability methods focus on a singular scenario, others focus on singular sections within a whole structure. There are still only a handful of reliability methods that address whole structures (complex). There has been no introduction of QRA frameworks that holistically address issues related to structural risk in a “root-to-fruit” fashion, thoroughly engaging specialist techniques in adequate instances and thus offering a complete solution platform.

This research attempts to provide an entire solution platform using a modified FSA framework (Figure (1.1)). The goal of such a platform would be to provide support, totally or partially, in the design of structure from concept to commissioning, operation and maintenance. Specialized methods are employed throughout the modified FSA

framework. Finally the methods are built for flexibility such that constant improvements could be implemented to provide solutions to a huge range of structures under different scenarios.



## **Chapter 3:**

# **Beta-Flexible Structural Reliability Algorithm (BETA-FLEXSTREM): A Risk Quantification Tool for Single-Member Structures (SMS)**

### **Summary**

*This chapter presents a beta version of a FLEXible STructural REliability algorithm (BETA-FLEXSTREM) for quantifying the risk (obtaining the reliability) of single-member structures (SMS). The methodology models major physical conditions present with appropriate limits and distributions. The principle of limit states is employed in modelling the interactions between the material and environmental parameters and the operating conditions of the structure. Four limit states are introduced. These act as the failure governing parameters in the widely acknowledged Monte Carlo simulation. Linear elastic fracture mechanics formulations form the basis of the fatigue life estimation. This procedure is executed by means of the scientific programming package – FORTRAN. A numerical application is presented for demonstration and validation.*

### **3.1 Introduction**

Structures in the marine and offshore environment are frequently subjected to several loads that vary randomly. This implies that structures to be deployed in these environments must be specially adapted in order to fulfil service requirements.

The conditions experienced by these structures are numerous and cut across several engineering fields. These conditions are present due to the nature of the external environment as well as the ongoing operations of the structures. High pressure

processes, corrosion, hazardous materials, temperature gradient, weather (climatic) variation, forces of wind and wave, etc., are some of the conditions present. Cumulatively, these conditions advance beyond the scope of a single engineering discipline. This presents a challenging design adaptation procedure for any structure or facility to be deployed in the offshore environment.

The safety of onboard personnel – and the structures eventually – is of utmost priority to major global operators in the marine and offshore industry. Risk assessment techniques not only ensure safety in the design and operation of these structures, they also bring about significant optimization of materials and resources.

This chapter presents a beta version of a flexible structural reliability algorithm (BETA-FLEXSTREM). The primary aim of the algorithm is to ascertain the reliability of a given structure with respect to specified failure criteria (limit states). The algorithm is designed in such a way that relevant failure criteria could be introduced or removed if irrelevant for a given analysis.

In the algorithm, there are several child models strongly interlinked in a Markov-like chain. While some of the child models are independent, others derive their values from preceding processes. They however serve as means (structural response) to an end (reliability) in a given scenario (loading/load input). The version is beta as the algorithm is still a “strait jacket” that handles only the stated case study as a case for single member structures (SMSs). A successful demonstration of this algorithm would lead to improvements that would also encompass multi-member structures (MMSs).

## **3.2 Background/Review**

### **3.2.1 Fatigue (Structural)**

Structures in the offshore environment are predominantly subjected to oscillatory environmental forces; hence fatigue characterizes a primary failure mode (Pillai and Prasad (2000)). These structures differ from onshore structures whose analysis or modelling is chiefly assumed to be static in nature. Analysis of this type (onshore

structures) closely approximates the actual conditions experienced by these structures (Shigley et al (2004)).

A fatigue failure is defined as the progressive and localized damage that occurs when a material is subjected to cyclic stress. A fatigue failure unlike a static failure reveals no signs and is often below the yield strength of the material. Studies have shown that failures resulting from fatigue are usually associated with poor design (Moan and Jiao (1992)).

While static modelling and analysis have been fully developed presently and are relatively easy to perform, a fatigue analysis is only partially understood and hence requires in-depth knowledge to be performed (Shigley et al (2004)). Fatigue failures at any point in offshore structures are closely patterned with the stress history during its service life. Estimation of the stress history and its effect on structural/material integrity is an extremely complex task. The random nature of sea, size of structure, calculation of stress concentration factors in welded joints, dynamic effects, etc., make the estimation of fatigue life challenging (Pillai and Prasad (2000)).

Generally, either of two approaches may be applied in fatigue modelling (Shigley et al (2004)). The first is the S-N approach in conjunction with Miner's damage accumulation rule. The second is the fracture mechanics approach in conjunction with a failure criterion (i.e. crack length/depth, stress intensity factor, etc.) (Chryssanthopoulos and Righiniotis (2006)). These approaches may be utilized based on data availability and classification of the fatigue i.e. high cycle (1000 cycles and above) or low cycle (1000 cycles and below).

Many sources of uncertainty arise during the fatigue analysis of any given structure/material. These include the fatigue process itself, the extrapolation from laboratory test results and application in real structures, loading conditions, environmental factors (temperature, presence of water, chemistry of the water, etc.), dynamic effects, etc.

These uncertainties are assigned different priorities depending on the structure and its applications. Further joint analysis of fatigue and any associated uncertainties may be needed for critical structures as relationships leading to severe consequences will need to be established.

### 3.2.2 Failure Prevention

Fatigue failure is the most common cause of failure in the field of engineering (Shigley et al (2004)). Reoccurrence of fatigue failures in several engineering fields has led to research and investigation into methods that reduce the likelihood of failure.

#### 3.2.2.1 Safety Factor Approach

The method of safety factors is the most prominent method of failure prevention in engineering. Kececioglu (2003) identifies the most common definitions or formulations of safety factors. They are (Kececioglu (2003)):

##### *Central Safety Factor*

Here the mean values of the stress induced and the strength of the material are the governing factors. Mathematically, the central safety factor ( $\overline{SF}$ ) is expressed as:

$$\overline{SF} = \frac{\text{mean strength}}{\text{mean stress}} \quad (3.1)$$

##### *Median Safety Factor*

The median values of the material strength and the stress induced are the governing parameters. Mathematically, the median safety factor (SF) is expressed as:

$$SF = \frac{\text{median strength}}{\text{median stress}} \quad (3.2)$$

##### *Extreme Safety Factor*

This method assumes a worst case scenario. It takes lowest material strength value against the highest induced stress. Mathematically, the extreme safety factor (SFe) is expressed as:

$$SF_e = \frac{\text{minimum strength}}{\text{maximum stress}} \quad (3.3)$$

For each safety factor definition, variations in reliability exist i.e. the reliability of a structure or component could vary from a high value to a low value, while maintaining a given safety factor value. This observation is illustrated in example I.

### 3.2.2.2 Example I

A simple cantilever problem is presented (Figure (3.1)). The beam is 3m long and weighs 200kg. The beam has a yield strength of 150MPa. The beam is subjected to repeated stresses ranging from 45MPa to 70MPa. The beam is designed with a safety factor (central safety factor) of 2.

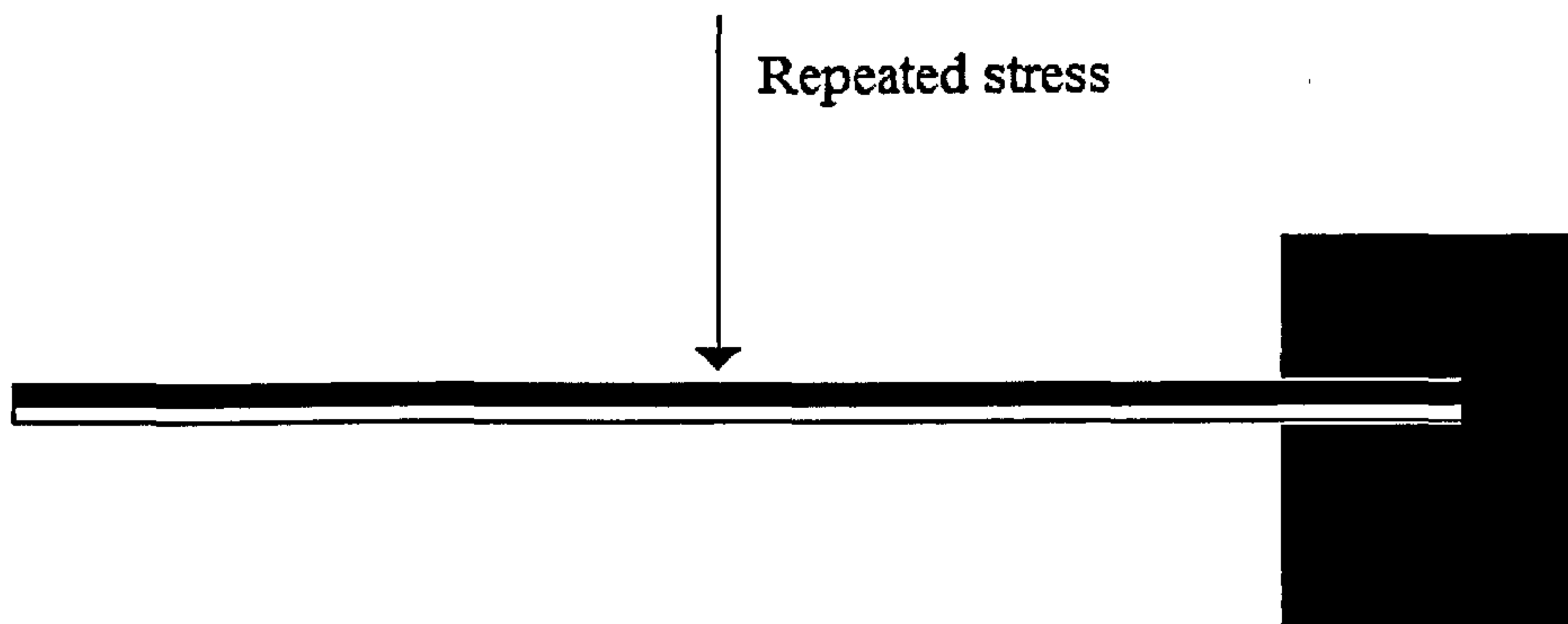


Figure (3.1) – Simple cantilever.

The (stress) reliability  $R$ , for the beam is defined mathematically as:

$$R = P(F_y > \sigma_{str}) \quad (3.4)$$

where  $F_y$  is the yield strength of the material and  $\sigma_{str}$  is the induced stress. The values of the coefficient of variation (COV) of both the stress and yield strength (material property) are 0.35 (i.e. 35%). Based on this relation (Equation (3.4)), the reliability will be estimated using simple Monte Carlo simulation techniques (10,000 trials). It is assumed that both the nominal and yield stresses are normally distributed.

Induced Stress ( $\sigma_{str}$ )	Yield Strength ( $F_y$ )
45	150
70	120
83.5	82

Table (3.1) – Sample results of Monte Carlo simulation.

Table (3.1) shows a sample of the variation in both the strength and stress parameters. The result of the simulation is represented graphically as in Figure (3.2).

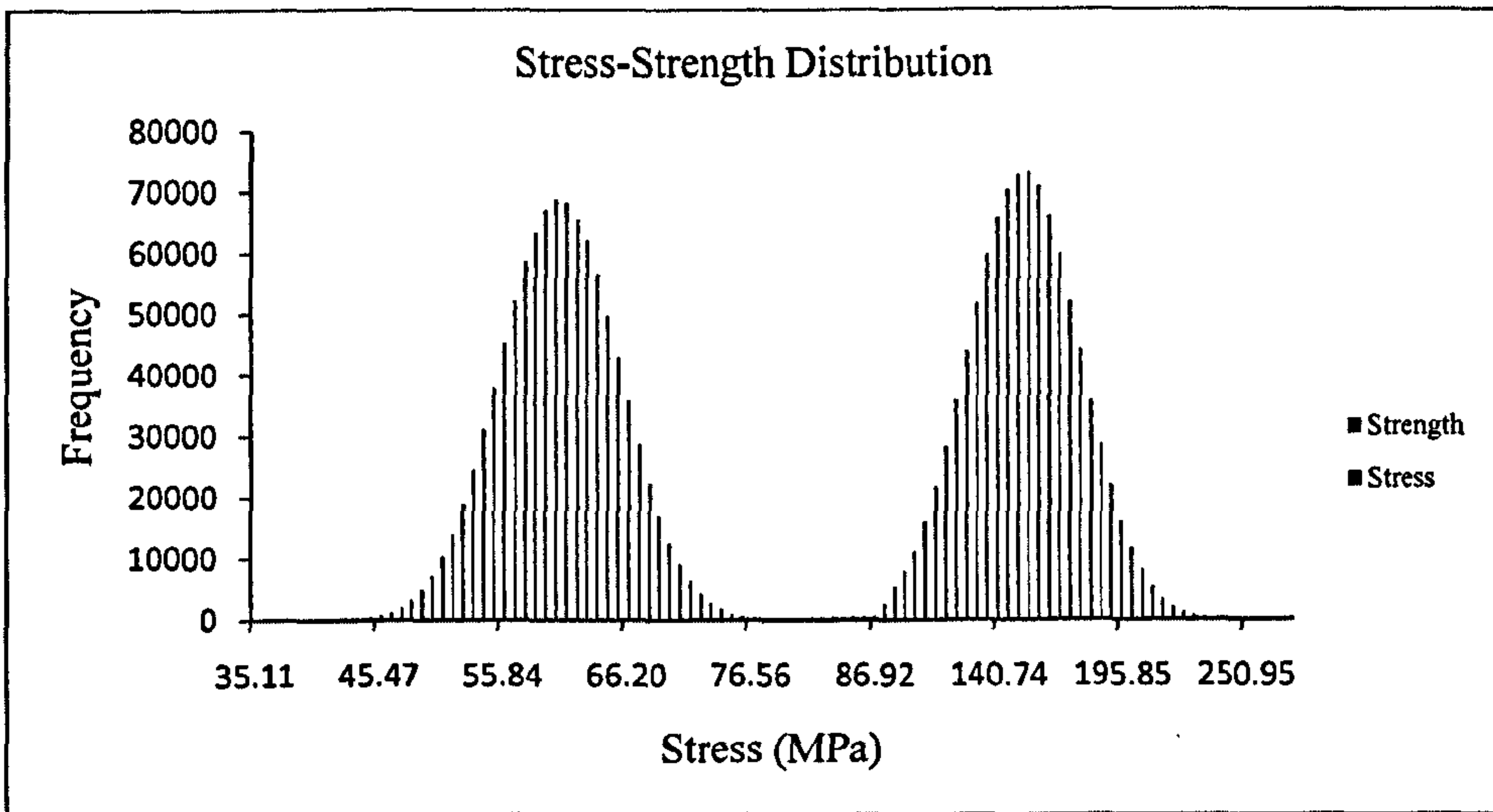


Figure (3.2) – Plot of the strength (right) and stress (left) distributions.

The simulation produced a reliability of 0.9925 despite the central safety factor of 2.

### 3.3 Methodology

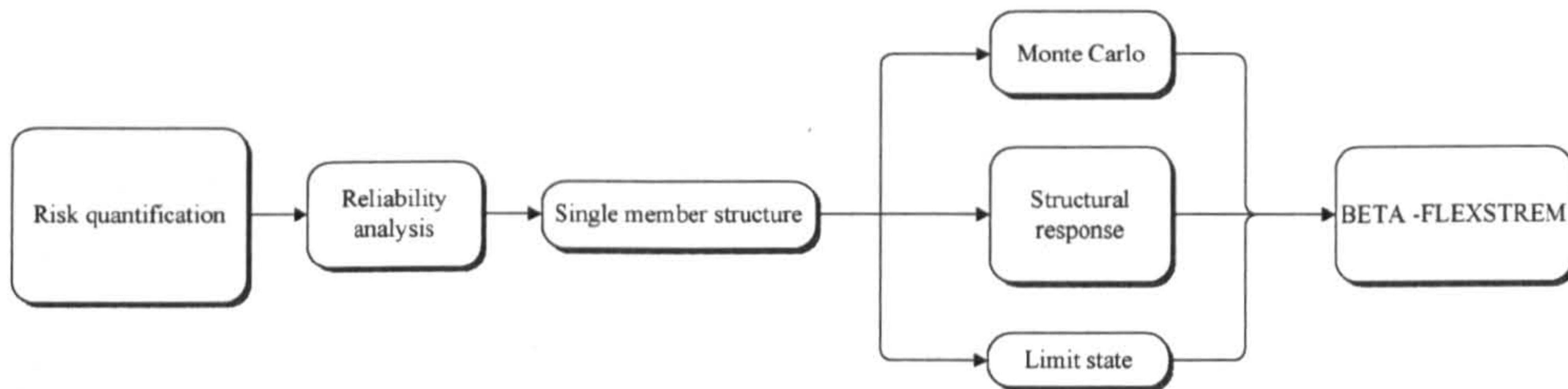


Figure (3.3) – Methodology.

Figure (3.3) is drawn from the modified FSA methodology developed in chapter 1. The risk quantification is perhaps the most rigorous of all the steps in most risk analyses in general. In the context of this research, methods by which the performance of a structure (or structural integrity) could be measured or quantified are required in order to successfully carry out the risk quantification. The structural reliability as a measure performs this function.

In dealing with SMSs, a novel methodology which involves the use of the structural response in conjunction with the MCS and limit states is introduced. The structural response is obtained from the interactions between three key groups: the users, the structure and the environment. Though these three groups are part of the system definition (which is not fully emphasized at this stage) as shown in Figure (3.4), the interactions between them are modelled in the risk quantification stage.

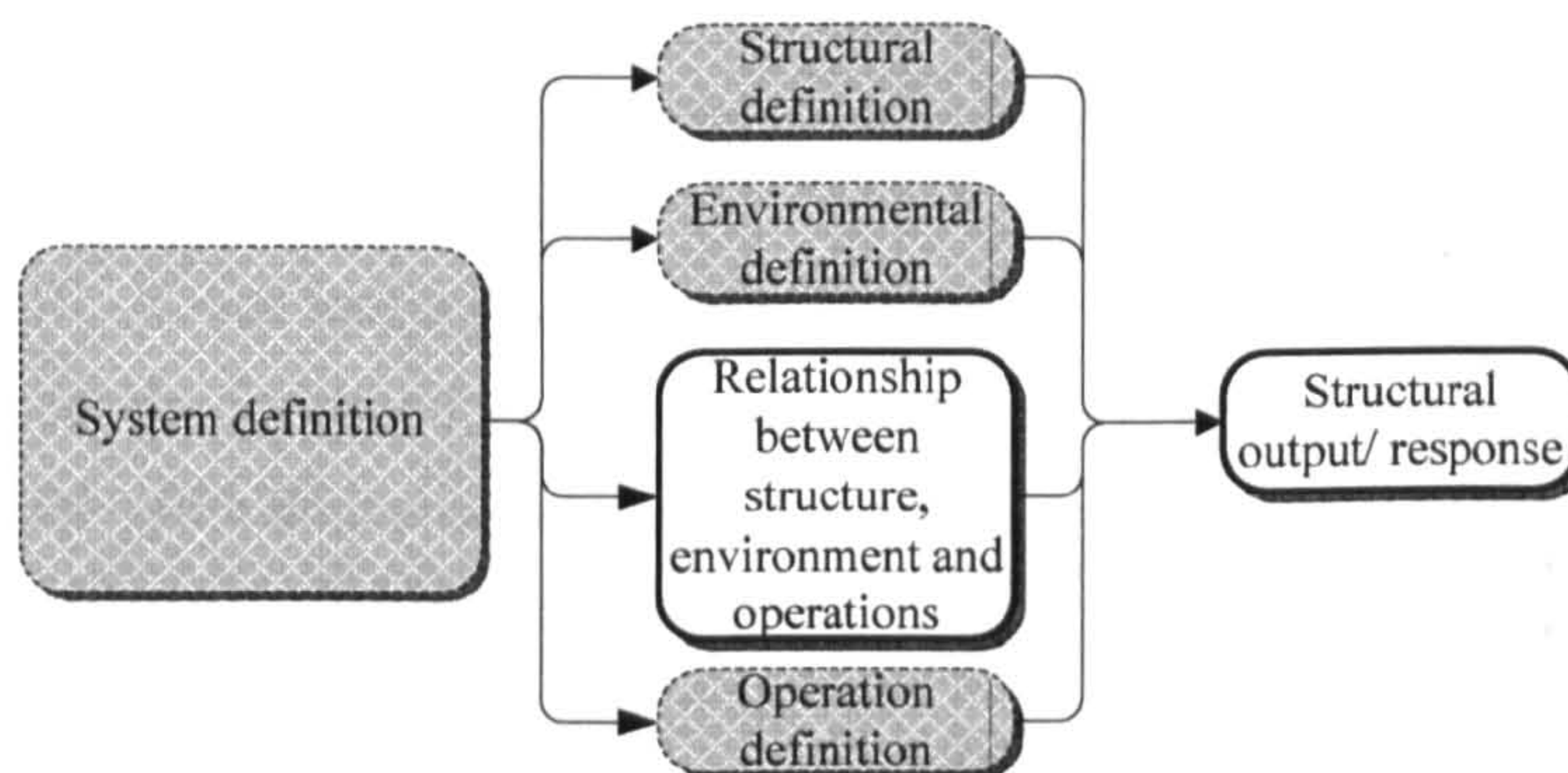


Figure (3.4) – Methodology.

The method introduced is a FLEXible STructural RELiability algorithm (BETA), shortened to BETA-FLEXSTREM. It is an algorithm that implements the use of the structural response in conjunction with the MCS and limit states to measure the reliability of structures. It is designed specifically for use on computers. The algorithm has been coded in the well known scientific language – FORTRAN. The flexibility and perhaps robustness comes from the fact that several components of the system (the structure, the environment, the operation by users and the relationships between all three) could be incorporated. It is still at beta stage as it only deals with a certain kind of SMS for now. A successful demonstration would provide for further development of the robustness of FLEXSTREM to deal with other kinds of structure especially MMSs.

### **3.4 BETA-FLEXSTREM Overview**

The BETA-FLEXSTREM consists of various limit states common to structures. The sizes of the block shapes in Figure (3.5) give a rough scale of the magnitude of the procedures relative to each other. The labelled blocks in the BETA-FLEXSTREM in Figure (3.5) refer to the following:

- Option S – Determination of analysis type
- Process A – Variable initialisation and storage
- Process B – Load and stress derivation
- Process C – Stress transformation
- LM I – Stress limit state analysis
- Process D – Crack length transformation
- Process E – Crack length estimation
- Process F – Stress intensity factor computations
- LM II – Stress intensity factor limit state analysis
- Process G – Determination of minimum crack length
- LM III – Crack length limit analysis
- Process H – Structural life estimation (as a result of the loading hitherto)
- LM IV – Life limit analysis
- Process I – Hierarchical data recording
- Process J – Reliability computation
- Process M – S-N reliability analysis



Processes B and C (LM I included) are typical mechanical procedures while processes D – H (LM IV included) are linear elastic fracture mechanic (LEFM) procedures. The two alternate processes (A-J or M-J) outlined are run repeatedly (looped) a certain amount of times in order to produce a value. This value is an average of specified instances within the body of the program (algorithm) where the failure criteria are satisfied. This value may be known as the reliability or probability of failure depending on the context the engineer chooses. The process of deducing this value is known as a simulation process. The Monte Carlo simulation method involves the use of distributions in this loop for the determination of reliability of structures and systems in the engineering world. This is also the key difference between ‘simulation’ and ‘Monte Carlo simulation’. Let us assume that a variable  $x$  in a given function  $F(x)$  has a distribution  $Q(x)$ , the Monte Carlo simulation of this variable may be represented mathematically as follows:

$$E[F(x)] = \frac{1}{n} \sum_{i=1}^n [F(x_1)Q(x) + F(x_2)Q(x) + \dots + F(x_n)Q(x)] \quad (3.5)$$

where  $E[F(x)]$  is the expected value of the function. This is the simplest case of a Monte Carlo simulation. The complexity of the simulation process increases with the introduction of limits. These limits may be the form of iterative limits of certain numerical processes (e.g. calculus), limit for cumulative processes (e.g. growth) or logical operation feedback in a limit state analysis.

The illustration in Figure (3.5) shows the various underlying processes of the BETA-FLEXSTREM that deduce the reliability of a single-member structure (SMS) in the marine or offshore environment.

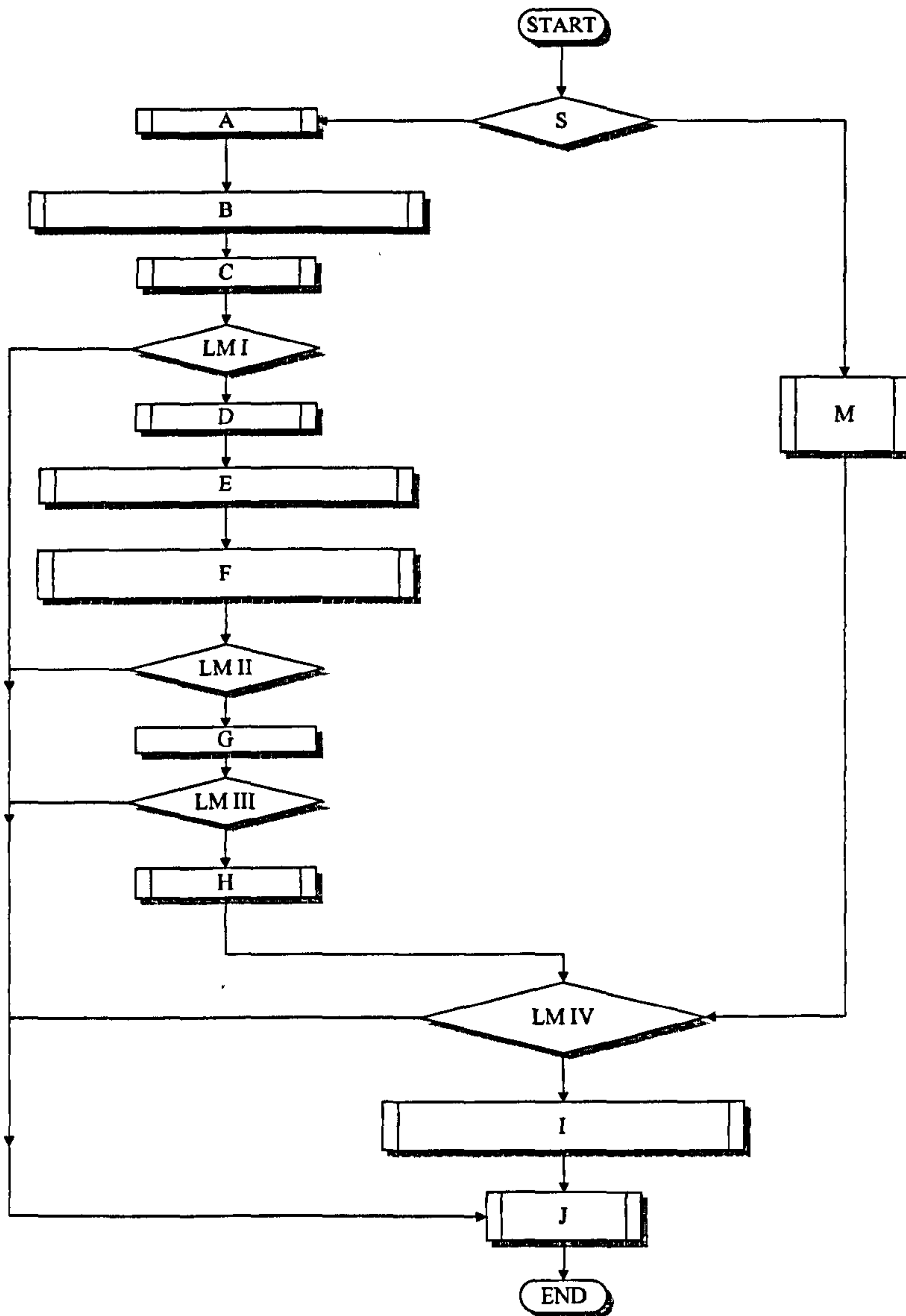


Figure (3.5) – BETA-FLEXSTREM outline.

The model represented in Figure (3.5) returns the probability of failure and thus reliability of an offshore structure. This model is essentially a Monte Carlo algorithm of the limit state analysis of four key variables which determine the failure or survival of the structure in question. In risk assessment terms, these four variables are referred to as basic events. These basic events would have a fault tree representation as shown in Figure (3.6).

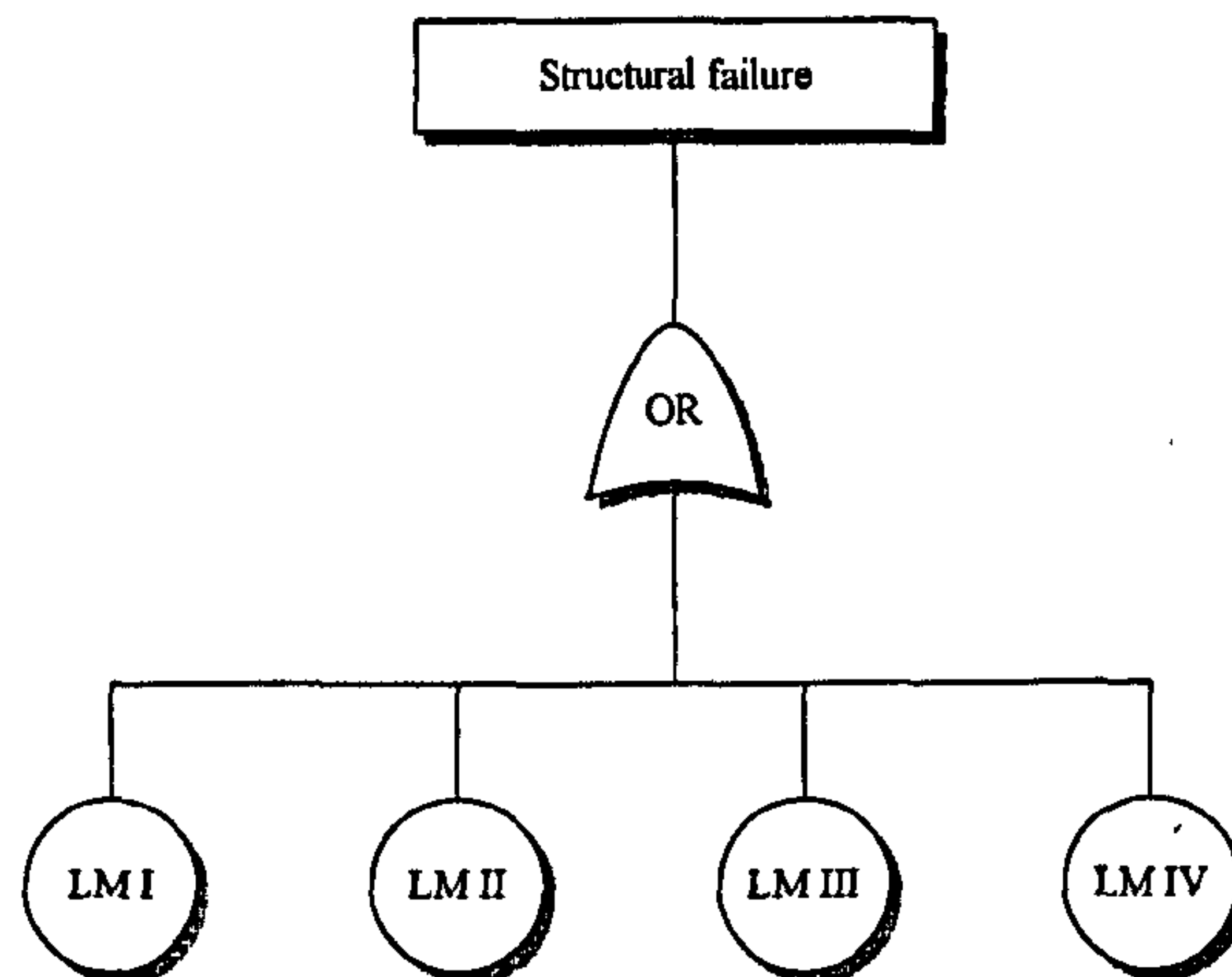


Figure (3.6) – Fault tree representation of key variables.

The basic events in Figure (3.6) (LM I-IV) model the relationship between the structural material and the load it is subjected to. The need for a high degree of accuracy cannot be over emphasized in analyses of this kind due to the frequent encounter of minute numbers. This gives rise to the use of large iterations that may be larger given the consequence, importance or uncertainty involved. 100,000 iterations will be used for this simulation.

BETA-FLEXSTREM is modelled such that updates on stresses and limit states could be incorporated easily to give results that reflect a target set of input parameters. Limits states such as environmental and accidental limits states and stresses like torsion, compression, buckling effects, wind action, etc. are examples to name a few that could be incorporated into the future versions of FLEXSTREM for analyses.

On robustness, the BETA-FLEXSTREM ideally handles high cycle fatigue (1000 cycles and above) and low cycle fatigue (1000 cycles and below). It is also capable of dealing with direct S-N approach, or Linear Elastic Fracture Mechanics (LEFM) as will be demonstrated in the case study. As mentioned earlier, on successful demonstration of BETA-FLEXSTREM, the algorithm would be further developed to handle more structure-types and scenarios.

The LEFM process has been carefully developed to a high level of accuracy accounting for several mechanical processes in order to produce highly reliable values. Most of the

blocks illustrated in Figure (3.5) are predefined processes. Processes A-J and M-J are looped processes in the Monte Carlo simulation.

The model is run as an algorithm written in FORTRAN 95 on a windows based platform. All utilized units are in S.I. The blocks in Figure (3.5) are subroutines. In this way, the flexibility, robustness and maintainability of the BETA-FLEXSTREM is achieved.

Though the algorithm is meant for implementation on a computer programming language, much emphasis is laid on the algorithm itself and the ideas behind it rather than the programming technique(s). The programming technique(s) could be accessed in any standard texts dealing with mathematics and computing. However, it is inevitable that terms related to programming would be used in the current discourse.

### 3.5 Analysis for Single-Member Structures (SMS)

#### 3.5.1 Option S – Determination of Analysis Type

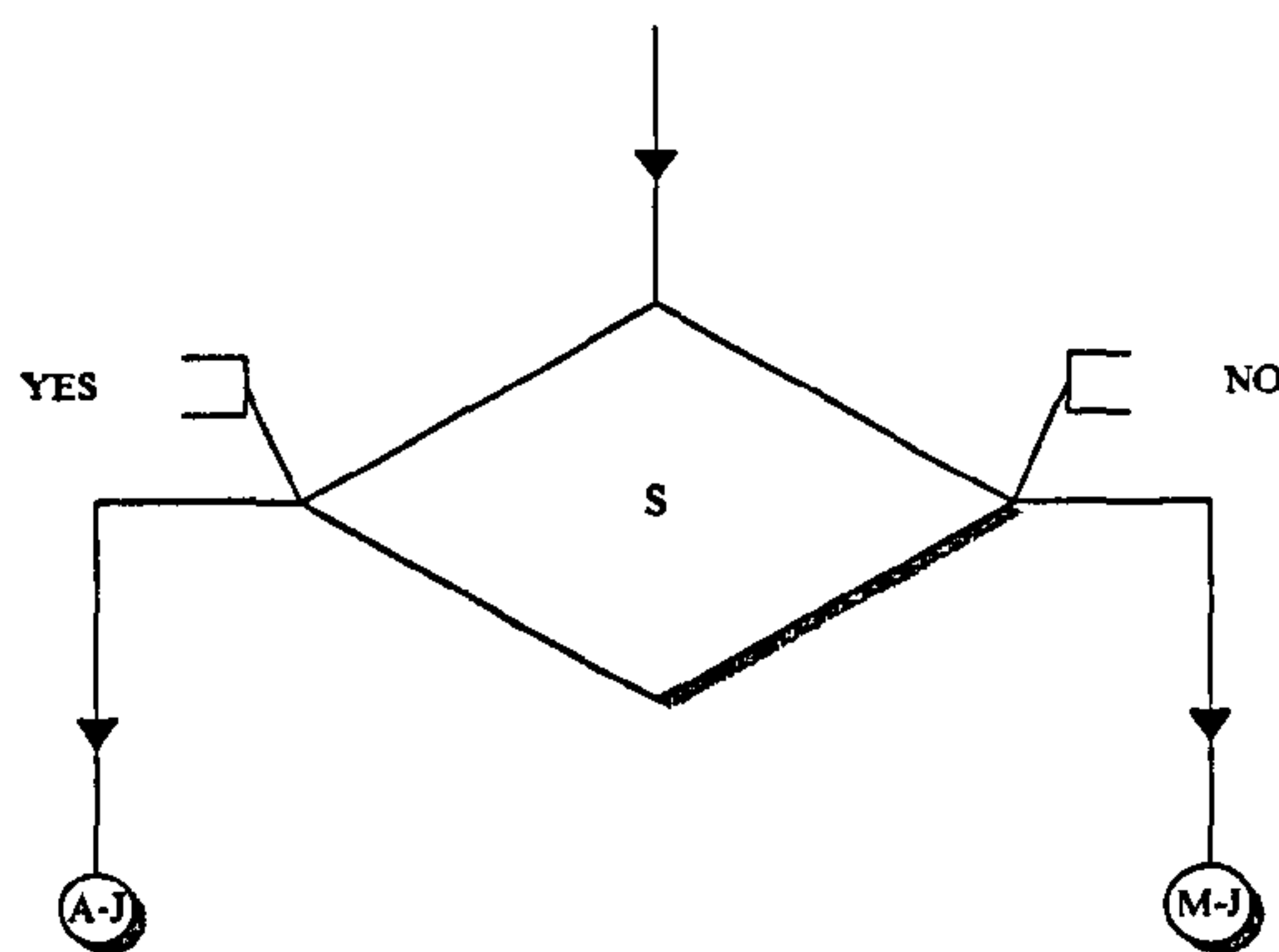


Figure (3.7) – Decision S.

This is a decision process (Figure (3.7)) mainly dependent on availability of data. Shigley et al (2004) suggested that the S-N approach is mainly suited to low-cycle fatigue (below 1000 cycles). The S-N data is only made available by testing at specific conditions. The cost of these tests hinders the availability of information on S-N data of different materials at different conditions. The LEFM approach however relies on data that is readily available or data that can be reasonably approximated. Figure (3.8) illustrates the methodology selection process:

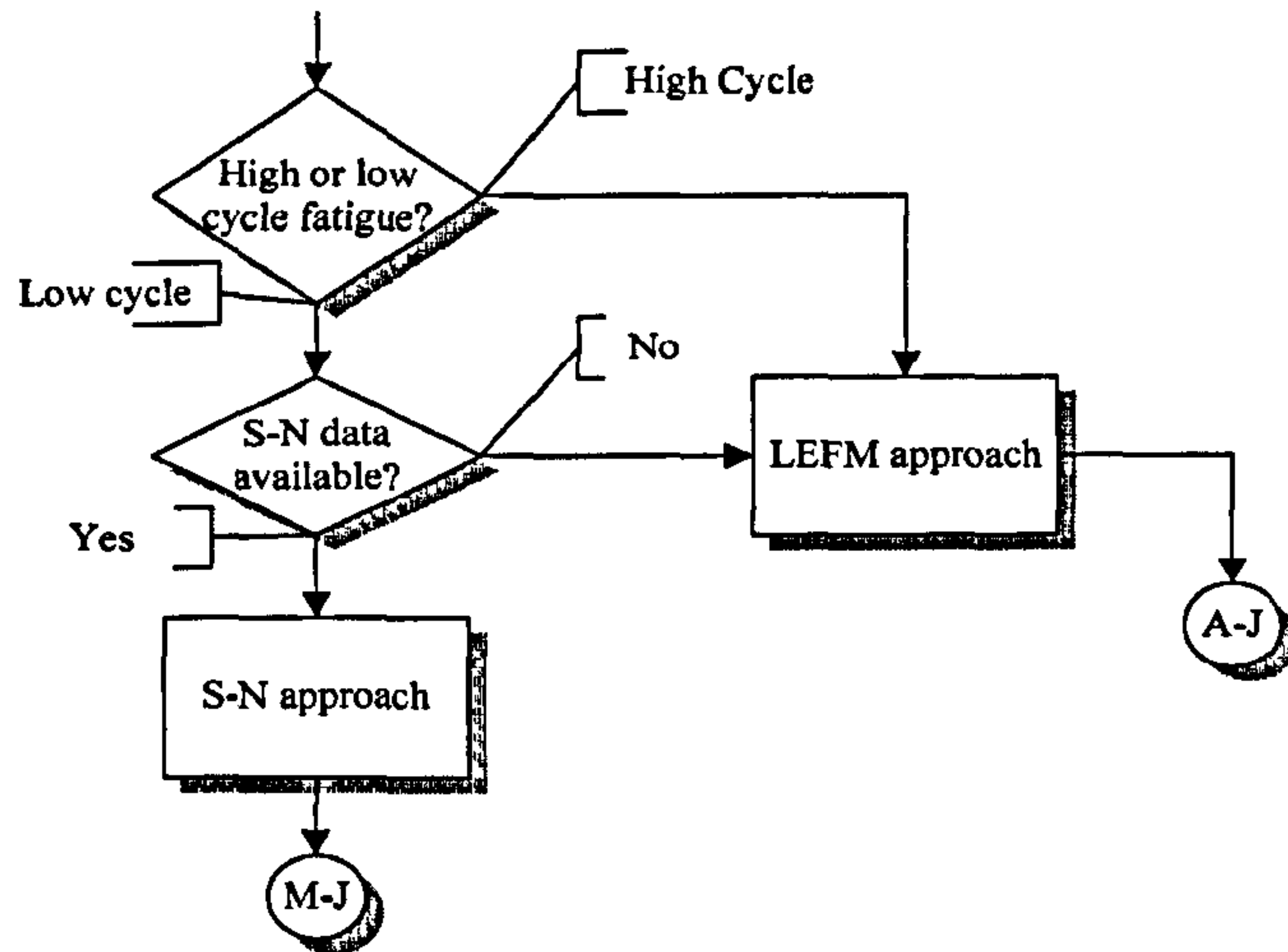


Figure (3.8) – Analysis selection process.

### 3.5.2 Process A – Variable Initialization and Storage

Process A is further divided into two sub-processes (Figure 3.9):

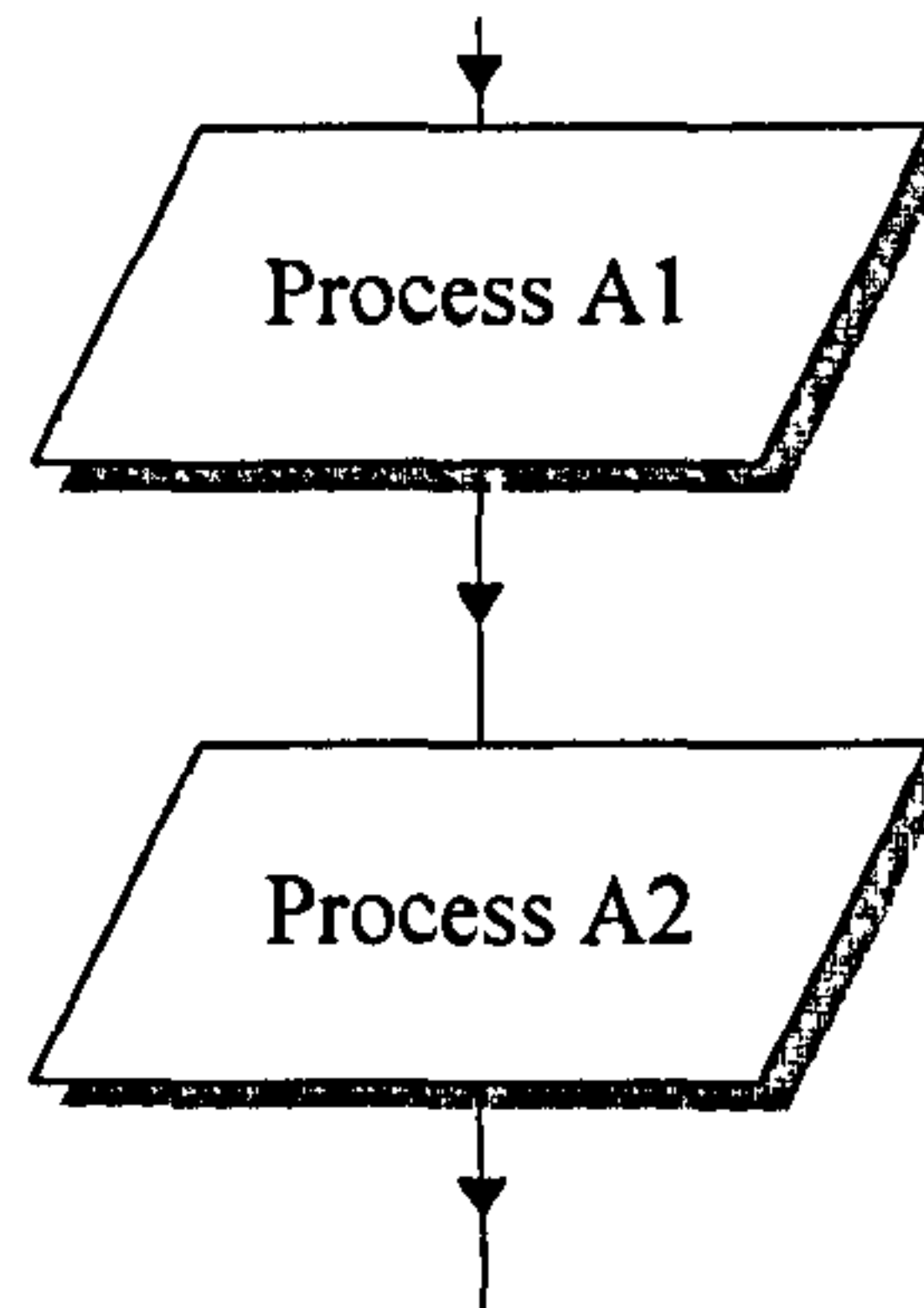


Figure (3.9) – Process A.

Sub-process A1 is the initialization of the variables (obtained from the system definition data) to be used in the Monte Carlo simulation (MCS). These variables are the materials properties, loads (operations) and environmental parameters present during the operational life of the structure.

Sub-process A2 is the initialization of random number generators (RNGs). These RNGs produce random numbers with a mean of 0 and standard deviation of 1 for the various

distributions utilized by the model. Four kinds of distributions are utilized by BETA-FLEXSTREM:

- Uniform distribution.
- Exponential distribution.
- Normal (Gaussian) distribution.
- Lognormal distribution.

### 3.5.3 Process B – Load and Stress Derivation

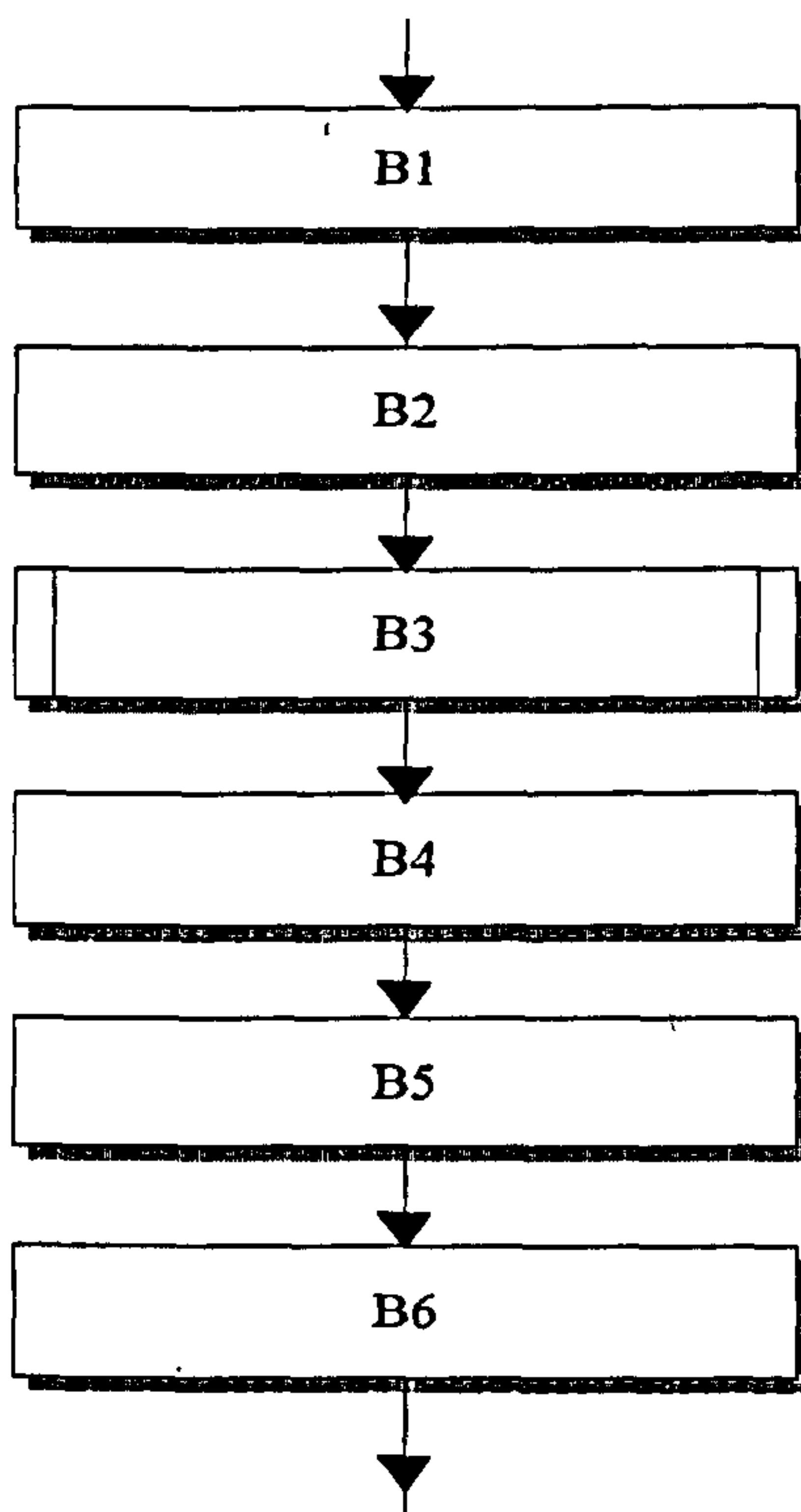


Figure (3.10) – Process B.

Figure (3.10) shows the processes involved in deriving loading and stress patterns in the structure. At sub-process B1, the model takes the temperature difference into consideration as this is a critical factor that governs behaviour of a material. The mean temperature is denoted as  $T_1$  (in Kelvin).  $T_2$ , the final temperature has its highest value at  $H_T^\circ K$  and its lowest value at  $L_T^\circ K$ . These values are chosen based on the characteristic temperatures of the environment where the structure is deployed. This is

particularly essential for extreme climates where material properties exhibit significant variations.

Sub-process B1 performs a linear transformation to produce uniformly distributed temperatures by the following equation:

$$T_2 = (U(H_T - L_T) + L_T)^\circ K \quad (3.6)$$

where  $U$  is a uniformly distributed random number. The linear transformation process is utilized based on the assumption that the effective temperature distribution is uniform throughout the year.

Sub-process B2 utilizes the values of  $T_2$ ,  $T_1$ ,  $\alpha$  (the coefficient of linear expansion) and  $L$  (the original length) of the focal structure (SMS) to estimate the change in its dimensions. A material/structure-member experiences a change in length  $\Delta L$  by the following equation:

$$\Delta L = L \times (\alpha \times (T_2 - T_1)) \quad (3.7)$$

Sub-process B3 is a load selection process. This process is defined as a reflection of the practices in the marine and offshore industry i.e. the rating of loads and lifting equipment. The full process is illustrated in Figure (3.11):

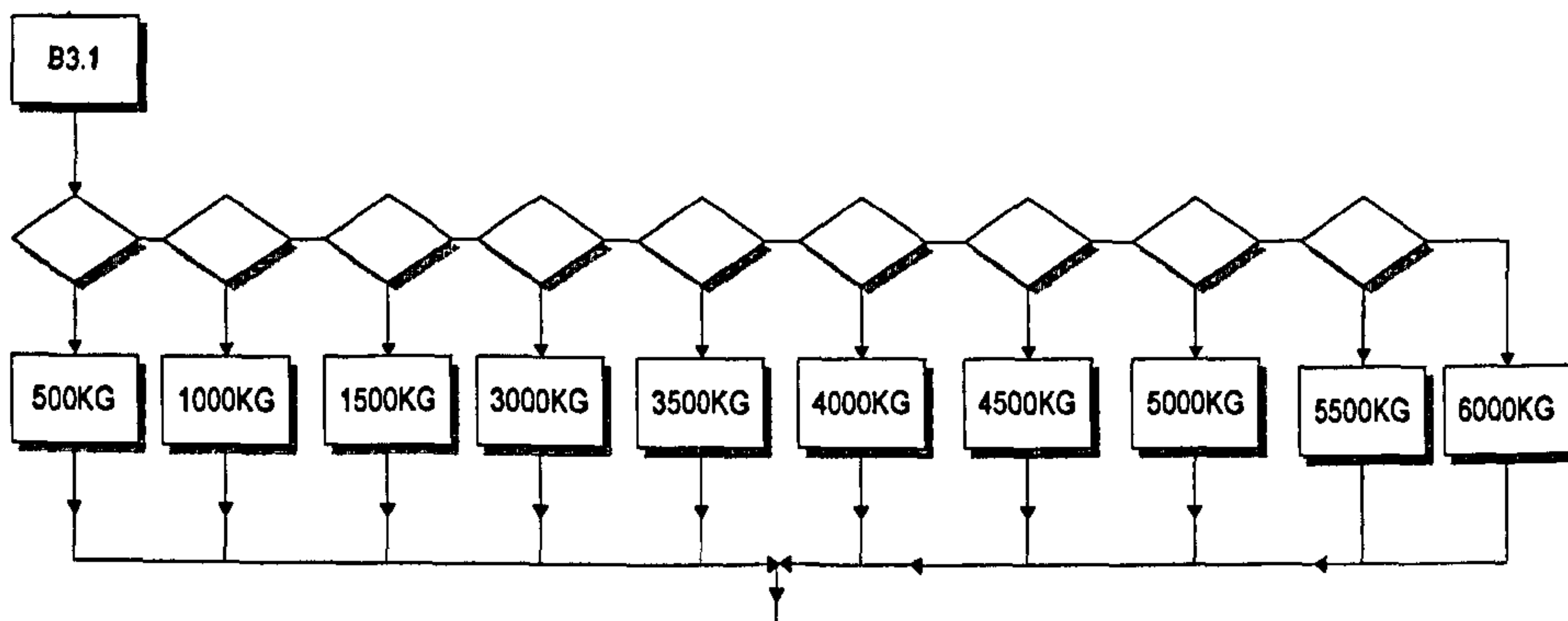


Figure (3.11) – Process B3.1 – load sampling.

A uniform load selection process takes place here. This process is illustrated in Figure (3.12):

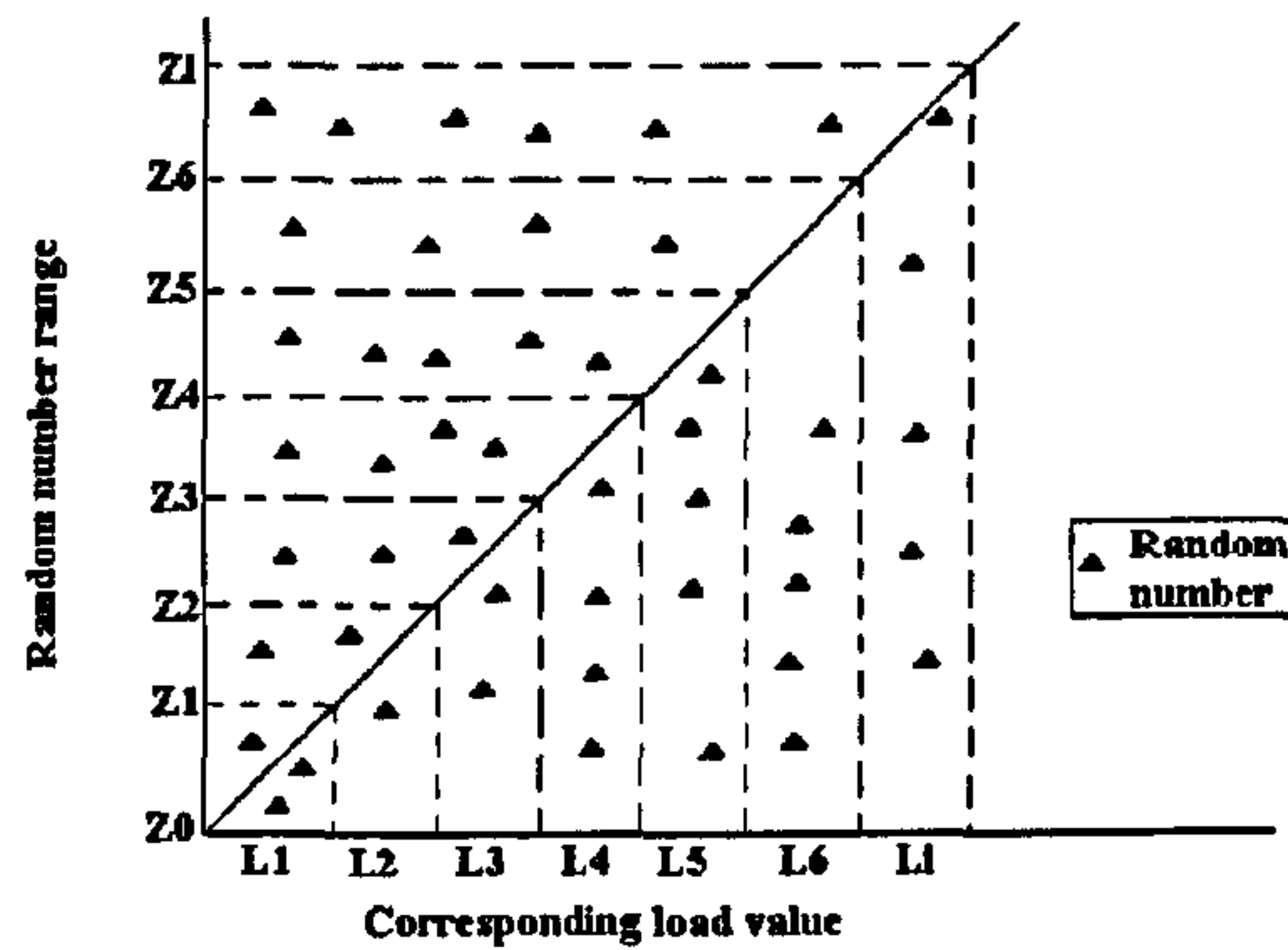


Figure (3.12) – Uniform distribution of load selection process.

Figure (3.12) shows uniformly distributed random numbers sampled in a range from  $Z_0$  to  $Z_i$ , where  $Z_0$  represents the lower bound of the range (initial seed value) and  $Z_i$ , the upper bound of the sampling range. Values within consecutive ranges on the y-axis correspond to the adjacent values on the x-axis, i.e. range  $Z_0$ - $Z_1$  corresponds to the load value  $L_1$  and so forth. This is one of the many numerical sampling methods available. This is a vital step in the analysis of the interactions between certain load classes and the material (SMS) strength.

Sub-process B4 is the calculation of the moment. This differs from structure to structure and is dependent on the load direction and structural shape and configuration. It is a necessary step towards estimating the nominal stress acting on a certain member.

Sub-process B5 is the calculation of the second moment of the closed section area of the beam. This is also another step in estimating the nominal stress acting on a member.

Sub-process B6 is the calculation of the nominal stress range acting on a given member. This is given by the following equation:

$$\Delta\sigma_{str} = \frac{M \times c}{I_{mont}} \quad (3.8)$$

where  $\Delta\sigma_{str}$  is the nominal stress range acting on a member,  $M$  the moment of the forces estimated from sub-process B4 and  $c$ , the centroidal distance from the neutral axis – dependent on the geometry and configuration of the member.  $I_{mont}$  is the second moment of the closed section area of the beam derived from sub-process B5. The determination of the nominal stress range is essential in the estimation of the reliability of the SMS.



### 3.5.4 Process C – Stress Transformation

Process C1 is a transformation process. Huajian and Yongchang (1995)) pointed out the statistical convergence of the stress (both nominal stress and yield stress) with the normal (Gaussian) distribution. Sub-process C1 is the transformation of the nominal stress range value to the normal distribution. This is done to take into account loads that have been ignored or are unmodelable but effectively play a vital role in the integrity of the structure. This process also takes several occasional stress scenarios into consideration, for example, the difference in loading experienced by a crane while moving a load through different angles of elevation. Although the loads experienced at different angles could be estimated, the computational task is reduced as it could be validly assumed that the successive load values tend towards the normal distribution. Also loads exerted by environmental forces such as wave and wind could be successfully integrated into the overall stress by this process.

Sub-process C2 is the yield stress transformation to the normal distribution (Equation (2.18)). Again this is done to account for changes in material property as a result of conditions modelled partially, ignored, or totally unmodelable.

### 3.5.5 LMI – Stress Limit State Analysis

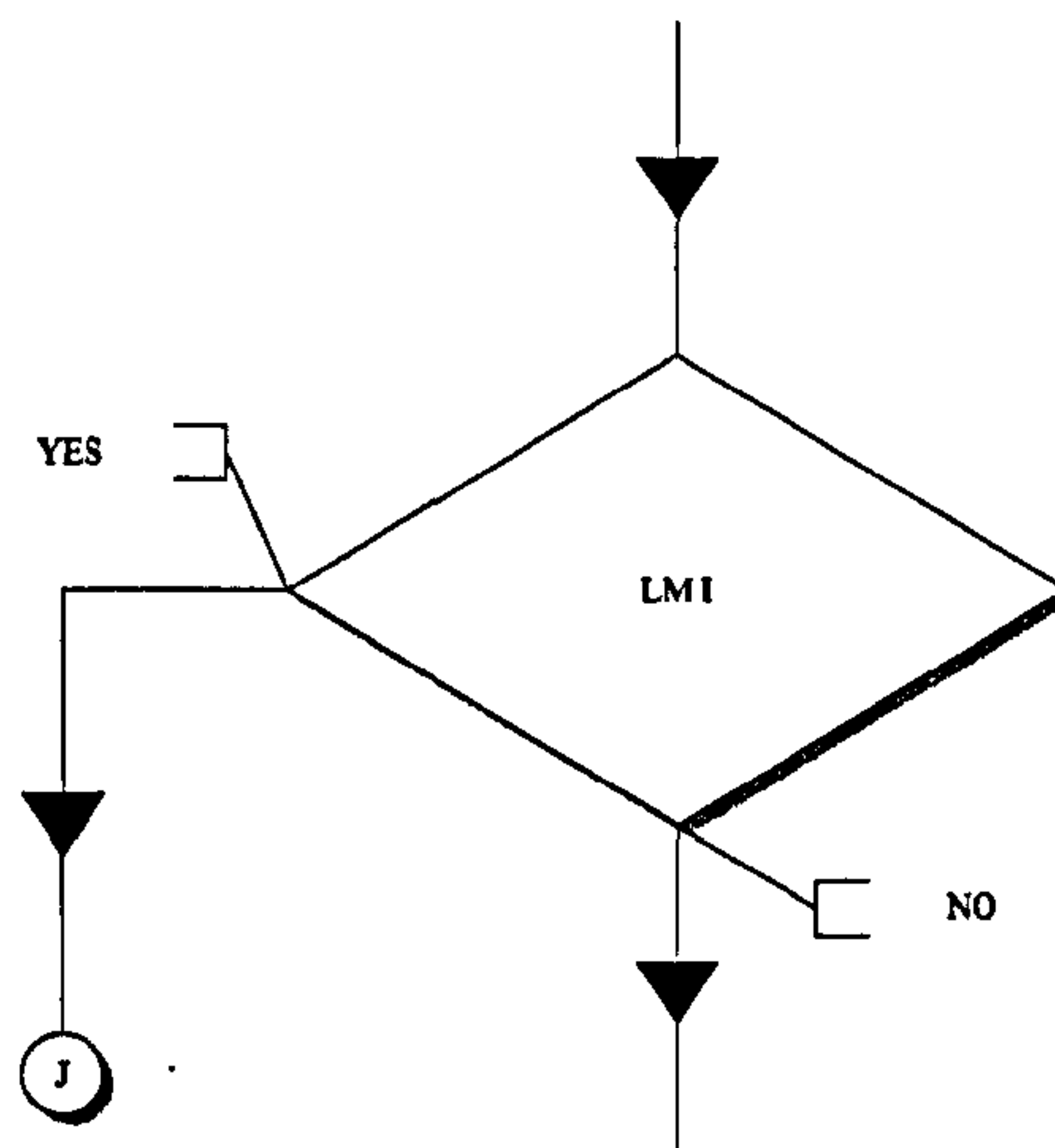


Figure (3.13) – Stress limit state analysis.

Figure (3.13) shows the logic flow for the stress limit state analysis. This is an important parameter of the simulation as it is a key factor to the reliability and hence integrity of the structure. This stress limit state analysis is defined as:

$$R = P(F_y > \sigma_{str}) \quad (3.9)$$

$$R = \int_{\sigma_{str}}^{\infty} f(F_y) dF_y \quad (3.10)$$

where  $F_y$  is the yield stress of the material and  $\sigma_{str}$  the stress (normally distributed) acting on the structure. The structure fails if the yield stress is equal to, or lower than the nominal stress. On failure, the flow of the code is stopped, values are recorded (at process I) and the next cycle (next simulation step) is initiated.

### 3.5.6 Process D – Crack Length Transformation

Process D marks the start of the investigation into the crack length to be used in the fatigue life formulation. It was shown by the research of Karamchandani et al (1991), Moan (2005), Chryssanthopoulos and Righiniotis (2006) that the crack length follows an exponential distribution.

Sub-process D1 is the transformation of the upper bound of the crack length value to the exponential distribution by Equation (2.10) as recommended by Karamchandani et al (1991). In the works of Balasubramanian and Guha (1999), it was observed that most fatigue failures result from imperfections in welds. Values of the upper bound of the crack length are determined empirically or carefully assumed depending on the material and the geometric parameters. Defect types (and hence crack length) differ as a result of different weld types and methods. This creates a degree of uncertainty in the determination of this value. The transformation process takes these uncertainties into account.

Sub-process D2 is similar to process D1 in importance and application. It is the transformation of the lower bound of the crack length value to the exponential distribution. This transformed value together with the transformed upper bound of the crack length value helps provide a defined boundary for the crack continuum.

The crack length plays a very vital role in the integrity of a structure as undetected cracks could reach a critical value at which fast fracture would occur.

### 3.5.7 Process E – Crack Length Estimation

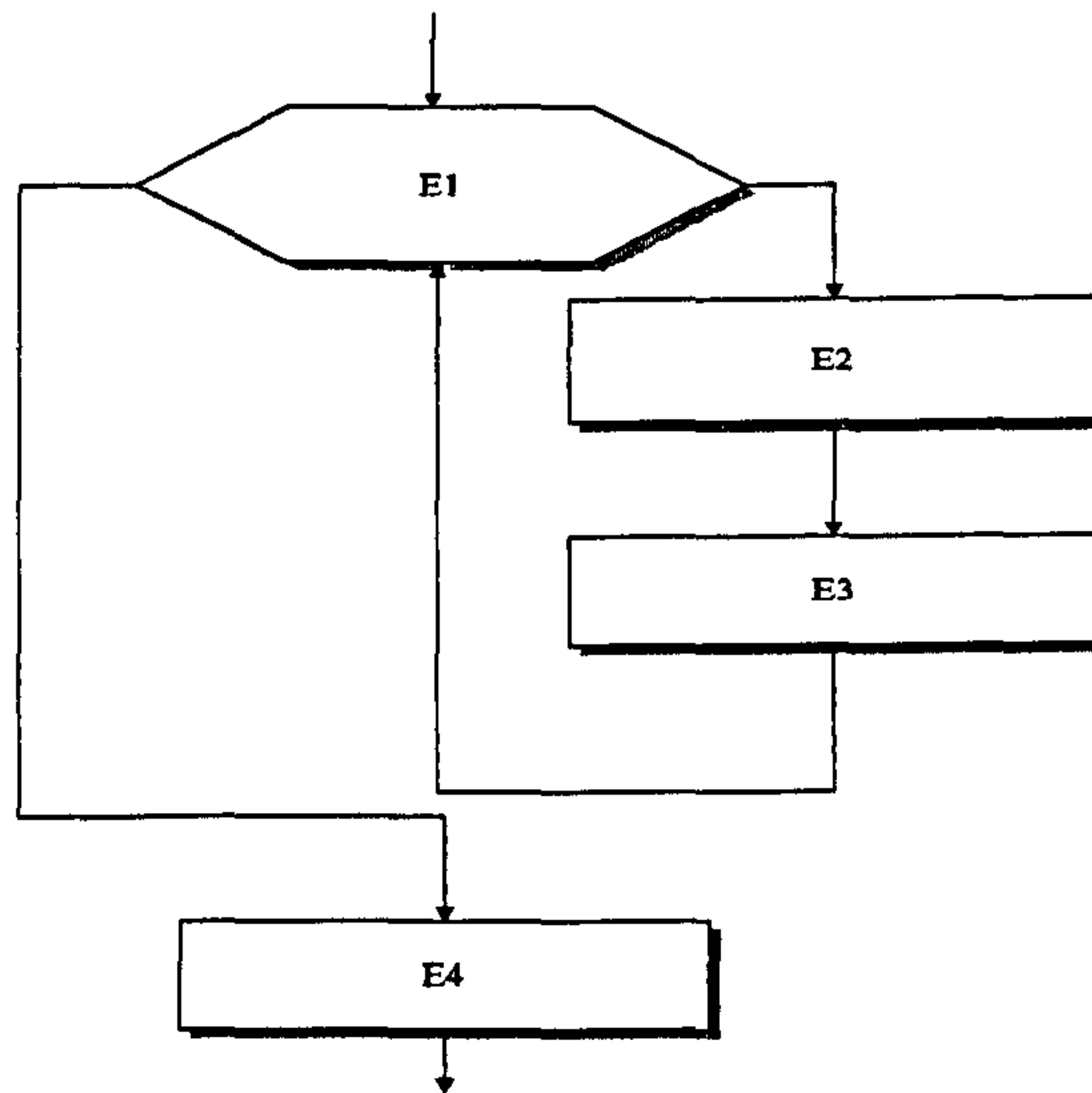


Figure (3.14) – Process E.

Process E (Figure (3.14)) is geared towards the estimation of the defect (crack) length. This is done utilizing the Monte Carlo integration procedure by Yang (2002).

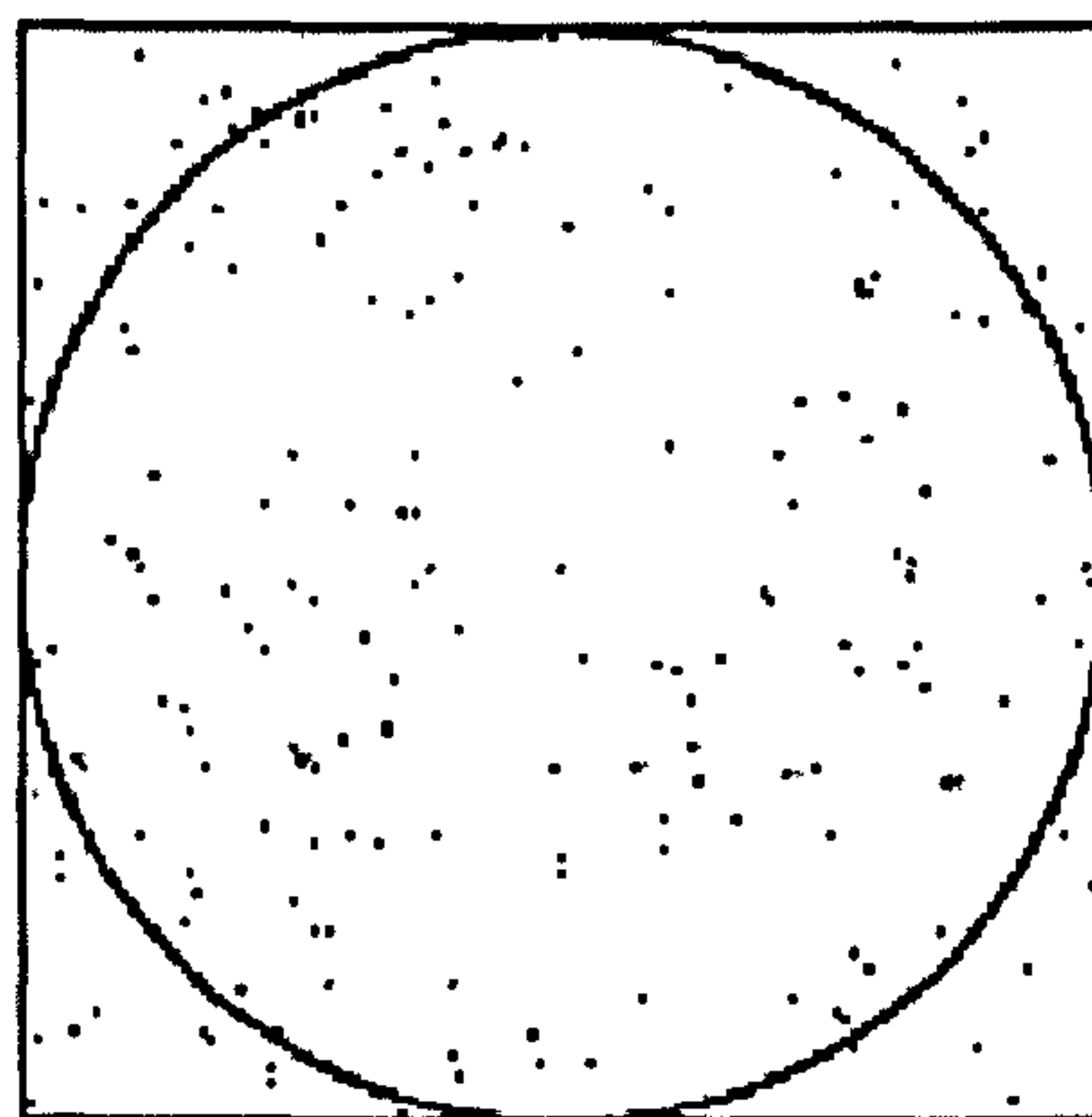


Figure (3.15) – The ‘dartboard’ illustration of the Monte Carlo integration method.

This procedure is based on the theory of large numbers. Figure (3.15) shows a dartboard illustration of the estimation of the area of a circle. It is assumed that the darts thrown are uniformly distributed over the entire surface of the box. As Figure (3.15) shows, the area of the circle, is the difference between the number of darts that fall *in the box* and the number of darts that fall *in the circle*. A more accurate value would require a higher number of darts thrown. The number of darts thrown is indicative of the number of trials needed in a Monte Carlo simulation. Also, the boundaries of the circle represent the limits of the variable. An acceptance-rejection method is employed in setting the boundaries of the circle. The process may be mathematically represented as:

$$\langle x \rangle = \int_c^d f(x) dx \quad \forall c \leq x \leq d \quad (3.11)$$

Where  $\langle x \rangle$  is the expected value depicting the area of the circle,  $f(x)$  is a function of the area of the circle (the darts) within limits  $d$  and  $c$ . This is simplified to:

$$\langle x \rangle \approx \frac{d-c}{n} \sum_{i=1}^n f(x_i) \quad (3.12)$$

where  $n$  is the number of MCS trials/iterations.

In the algorithm shown in Figure (3.14), Equation (3.12) is broken down further. Sub-process E1 is the MCS loop. Sub-process E2 is a selection process. Here random values are chosen between the upper and lower limits of the crack length. This may be mathematically represented as:

$$f(a) = U(a_f - a_i) + a_i \quad (3.13)$$

where  $U$  is a random number between 0 and 1,  $a_f$  the exponentially distributed upper bound of the crack length and  $a_i$  the exponentially distributed lower bound of the crack length. Sub-process E3 is mathematically represented as:

$$\sum f(a) = \sum_{i=1}^n (a_i + a_{i+1} + a_{i+2} + a_{i+3} + a_{i+4} + \dots + a_f) \quad (3.14)$$

Sub-process E4 is the evaluation of the crack length  $a$ . This is mathematically represented as:

$$\langle a \rangle = \frac{1}{n} \sum f(a) \quad (3.15)$$

The value of  $a$  is also known as the expected value as it is an arithmetic mean.

This process becomes very demanding computationally when the Monte Carlo integration is a sub-process (subroutine). Table (3.2) shows the level of accuracy achieved with respect to the number of trials employed for the integration of the function:

$$y = \int_0^1 x^2 dx \quad (3.16)$$

Number of simulations	Value of Integral ( $x^2$ ) i.e. $y$
1000	0.35128
10000	0.33179
100000	0.33443
1000000	0.33318

Table (3.2) – The relationship between number of trials and accuracy.

From Table (3.2) trials between  $10^5$  and  $10^6$  are the best options available and further decision is taken with regards to the importance of the function or variable to be integrated. However  $10^5$  will be most suitable in an effort to balance accuracy with efficiency (with respect to computation time).

### 3.5.8 Process F – Stress Intensity Factor Computations

Process F is the evaluation of the stress intensity factor,  $K_I$  utilizing the LEFM fast fracture Equation:

$$K_I = mat_{\beta} \Delta \sigma_{str} \sqrt{\pi a} \quad (3.17)$$

$$mat_{\beta} = F\left(\frac{a}{b}\right) \quad (3.18)$$

where  $mat_{\beta}$  is stress intensity correction factor,  $\Delta \sigma_{str}$  the stress intensity factor range obtained from process B6,  $a$  the crack length estimated from process E and  $b$  the width of the material cross-section.

Thereafter, the transformation of the  $K_{IC}$  value (the critical stress intensity factor or the material fracture toughness) of the material to the lognormal distribution (Equation (2.20)) is done. This assumption is made in accordance with the central limit theorem.

### Stress Intensity Correction Factor

The stress intensity correction factor  $mat_{\beta}$ , is a very important parameter in the determination of the stress intensity factor and the fatigue life of a structure. It is a function of a number of factors most notably the crack length and the width of the material geometry (Boresi et al. (1993)). At this stage of the research (risk estimation for SMSs), the crack geometry is assumed to be that of a single edge crack in a pure bending specimen:

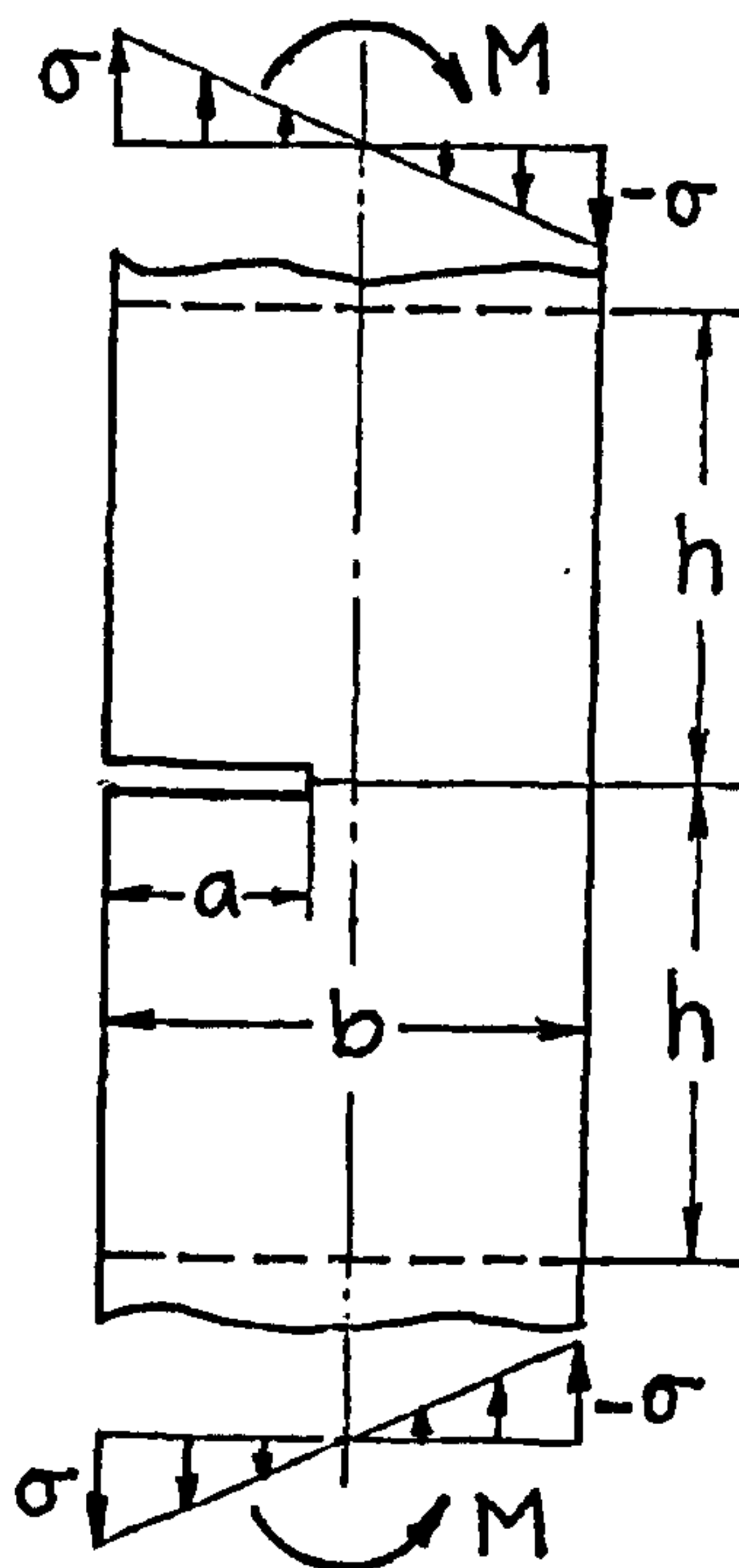


Figure (3.16) – Single-edge crack in a pure bending specimen (Tada et al (2000)).

where  $M$  is the bending moment,  $\sigma$  is the stress due to the bending moment,  $b$  is the section width,  $h$  is the length of the section from the crack, and  $a$  is the crack length. The stress intensity correction factor  $mat_{\beta}$ , can be evaluated by Equation (3.19) provided by Tada et al (2000):

$$F\left(\frac{a}{b}\right) = \sqrt{\frac{2b}{\pi a} \tan \frac{\pi a}{2b} \frac{0.923 + 0.199 \left(1 - \sin \frac{\pi a}{2b}\right)^4}{\cos \frac{\pi a}{2b}}} \quad (3.19)$$

Equation (3.19) provides for accuracy better than 0.5% for any  $a/b$  (Tada et al (2000)).

*Validation of the Stress Intensity Correction Factor*

Given a section width of 1 m (constant), the  $mat_{\beta}$  values from the assigned BETA-FLEXSTREM module are validated with those obtained by inserting Equation (3.19) in an excel spreadsheet. This is demonstrated in Table (3.3):

Crack length (a(m))	BETA-FLEXSTREM $mat_{\beta}$	Excel $mat_{\beta}$
0.1	1.040827	1.040827
0.2	1.03549	1.03549
0.3	1.097809	1.097809
0.4	1.234468	1.234468
0.5	1.475232	1.475232
0.6	1.898198	1.898198
0.7	2.716291	2.716291
0.8	4.674411	4.674411
0.9	12.46901	12.46901

Table (3.3) – Validation of the stress intensity correction factor.

From Table (3.3), the values obtained from the BETA-FLEXSTREM module are in good agreement with those obtained from the excel spreadsheet.

**3.5.9 LM II – Stress Intensity Factor Limit State Analysis**

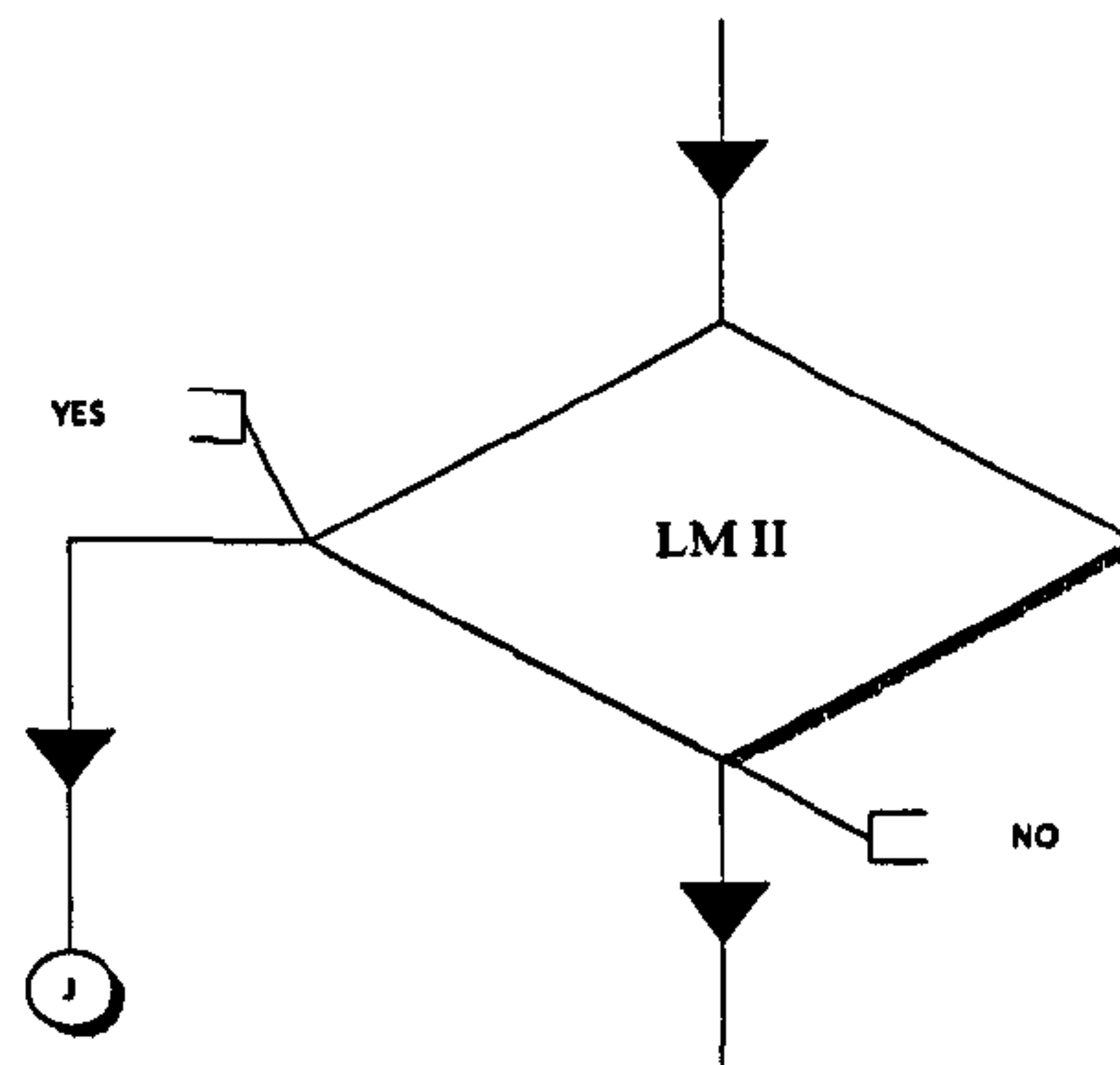


Figure (3.17) – Stress intensity factor limit state analysis.

Figure (3.17) shows the logic flow of LM II. LM II represents another failure criterion for the structure – the stress intensity factor limit. This is a limit state defined as:

$$R = P(K_I < K_{IC}) \tag{3.20}$$

$$R = \int_{K_I}^{\infty} f(K_{IC})dK_{IC} \tag{3.21}$$

This implies that the fracture toughness of the material should always be greater than the stress intensity factor. Any other condition will lead to fast fracture and ultimately failure.

### 3.5.10 Process G – Determination of Minimum Crack Length

This process deals with the estimation of the minimum length that a crack would have to grow to (due to a given stress), in order to cause structural failure. This may be represented as:

$$a_c = \frac{1}{\pi} \left( \frac{K_{IC}}{mat_{\beta} \sigma_{str}} \right)^2 \quad (3.22)$$

where  $a_c$  is the critical crack length. It is a variant of the LEFM fast-fracture equation. These values obtained would give good understanding of the distribution and properties (mean and standard deviation) of  $a_c$  as a product of various parameters with different distributions. The outcome is expected to follow the lognormal distribution trend according to the central limit theorem. The critical crack length may also be specifically indicated as certain values or ratios.

### 3.5.11 LM III – Crack Length Limit Analysis

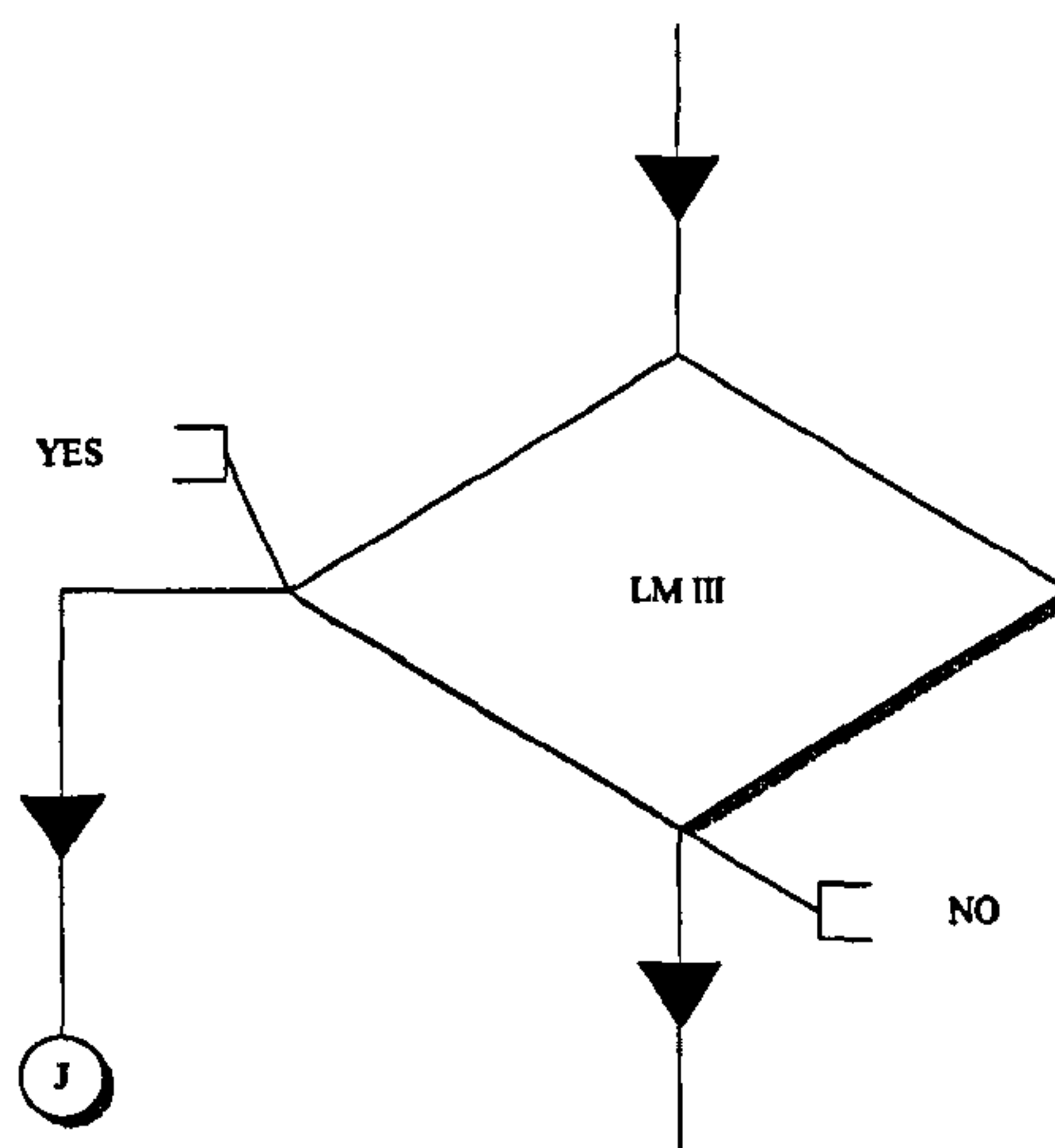


Figure (3.18) – Crack length limit analysis.



The estimation of the critical crack length enables the establishment of a third limit state – the crack length limit (Figure (3.18)). Mathematically,

$$R = P(a < a_c) \quad (3.23)$$

$$R = \int_a^{\infty} f(a_c) da_c \quad (3.24)$$

where  $a$  is the crack length and  $a_c$  the critical crack length.

It is necessary that the crack length does not reach or exceed the critical crack length of a defect or discontinuity in a structure. The values obtained from these variables could be further used for the scheduling of inspection and repair intervals.

### 3.5.12 Process H – Structural Life Estimation

Process H is essentially the estimation of the planned life and operational life of the structure. The works of Karamchandani and Dalane (1991), Moan (2004), Skjong and Torhaug (1991), Chryssanthopoulos and Righiniotis (2006), and Pillai and Prasad (1997), showed that the crack growth rate coefficient  $mat_C$  (a material property) follows a lognormal distribution. It is the final factor required in the estimation of the planned life of a structure. Sub-process H1 is the transformation of this  $mat_C$  value to the lognormal distribution.

Sub-process H2 is the estimation of the operational life of the structure using all the estimated values derived from the preceding processes according to the LEFM fatigue life estimation:

$$N_{OP} = \frac{1}{mat_C} \int_{a_l}^{a_f} \frac{da}{(mat_{\beta} \sigma_{str} \times \sqrt{\pi a})^{mat_m}} \quad (3.25)$$

where  $N_{OP}$  is the operational life of the structure,  $mat_C$  the crack growth rate coefficient,  $a_f$  the upper bound of the crack length,  $a_l$  the lower bound of the crack length,  $mat_{\beta}$  a stress intensity correction factor property,  $\Delta\sigma_{str}$  the stress intensity factor range, and  $mat_m$  the crack growth exponent. It has been observed that the number of cycles to failure ( $N_{PL}$ ) varies log-normally with the applied stress (Chryssanthopoulos and Righiniotis (2006)). Sub-process H3 is the transformation of the planned life  $N_{PL}$  of the structure to the lognormal distribution.

### 3.5.13 LM IV – Life Limit Analysis

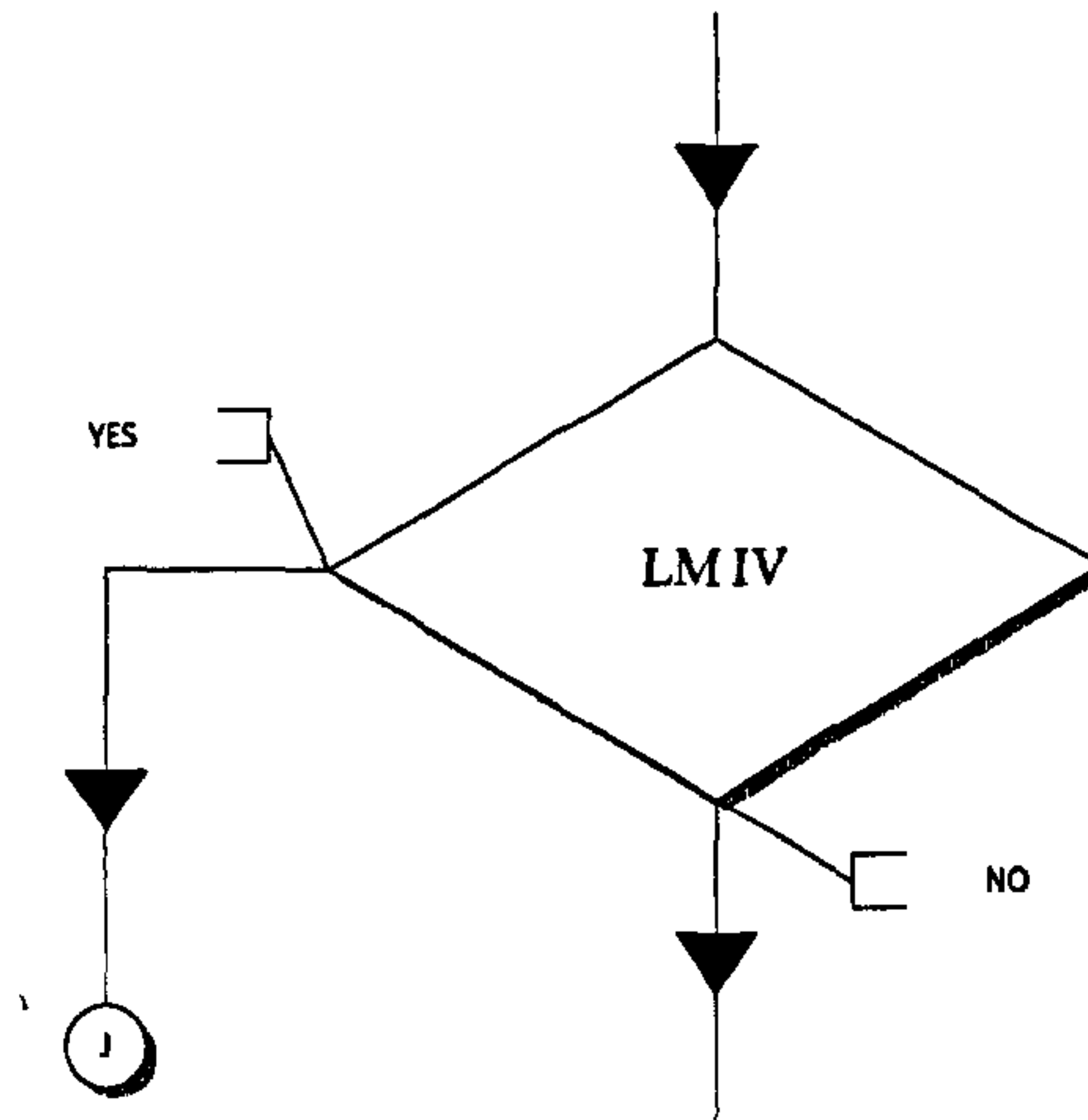


Figure (3.19) – Life limit analysis.

The estimated variable in process H sets up the final limit state – the life limit (Figure (3.19)). This limit state is defined by the following equation:

$$R = P(N_{OP} > N_{PL}) \quad (3.26)$$

$$R = \int_{N_{PL}}^{\infty} f(N_{OP}) dN_{OP} \quad (3.27)$$

where  $N_{OP}$  is the operational life of the structure and  $N_{PL}$  the planned life of the structure. It is important that the operational life always exceeds the planned life of the structure. Structural failure occurs on violation of the limit state.

### 3.5.14 Process I – Hierarchical Data Recording

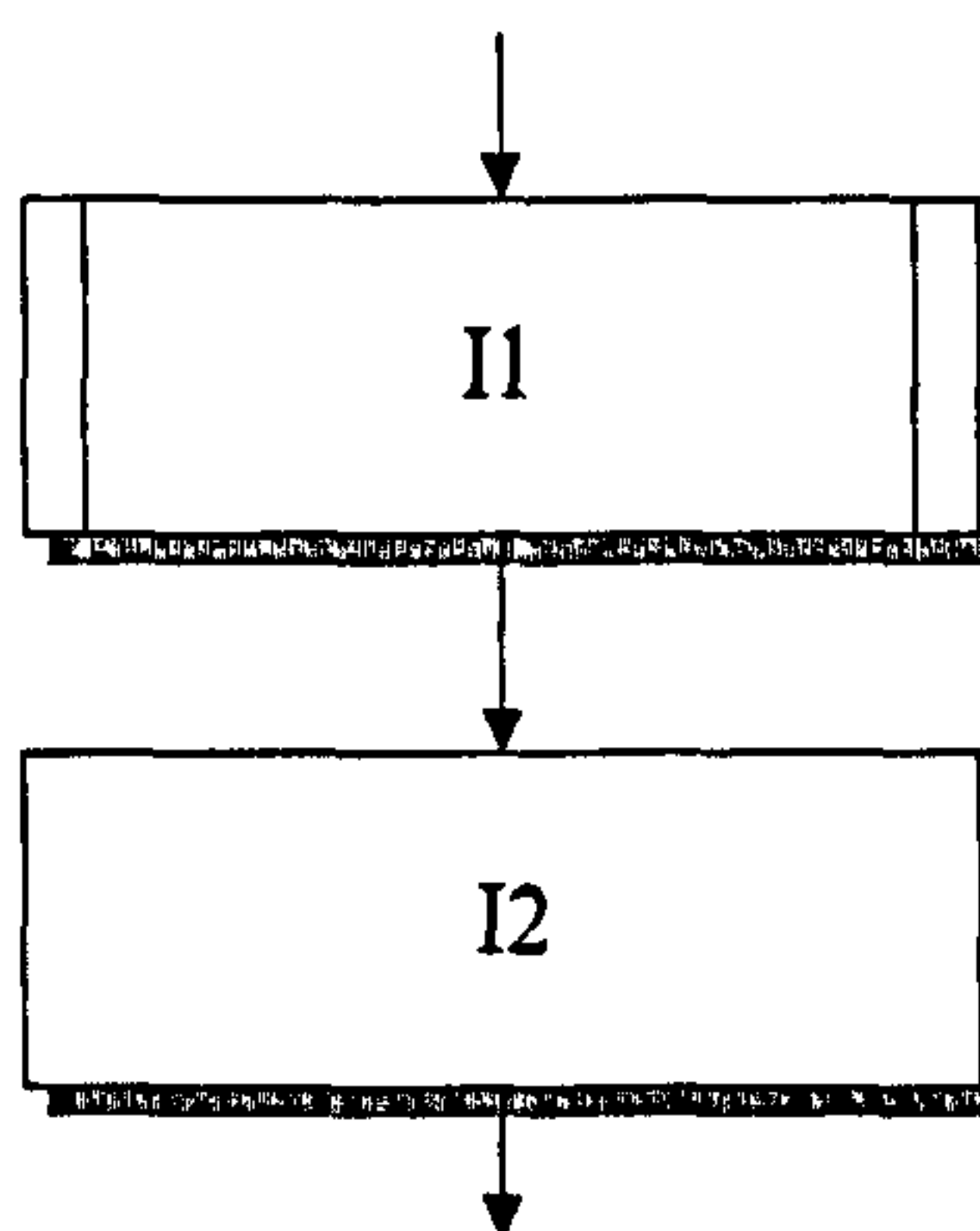


Figure (3.20) – Process I.

Here data collection is selectively done for clear data presentation for analysis. The process is in two steps as shown in Figure (3.20). Sub-process I1 is a defined data recording sequence of the four limit states in the following order (Figure (3.21)):

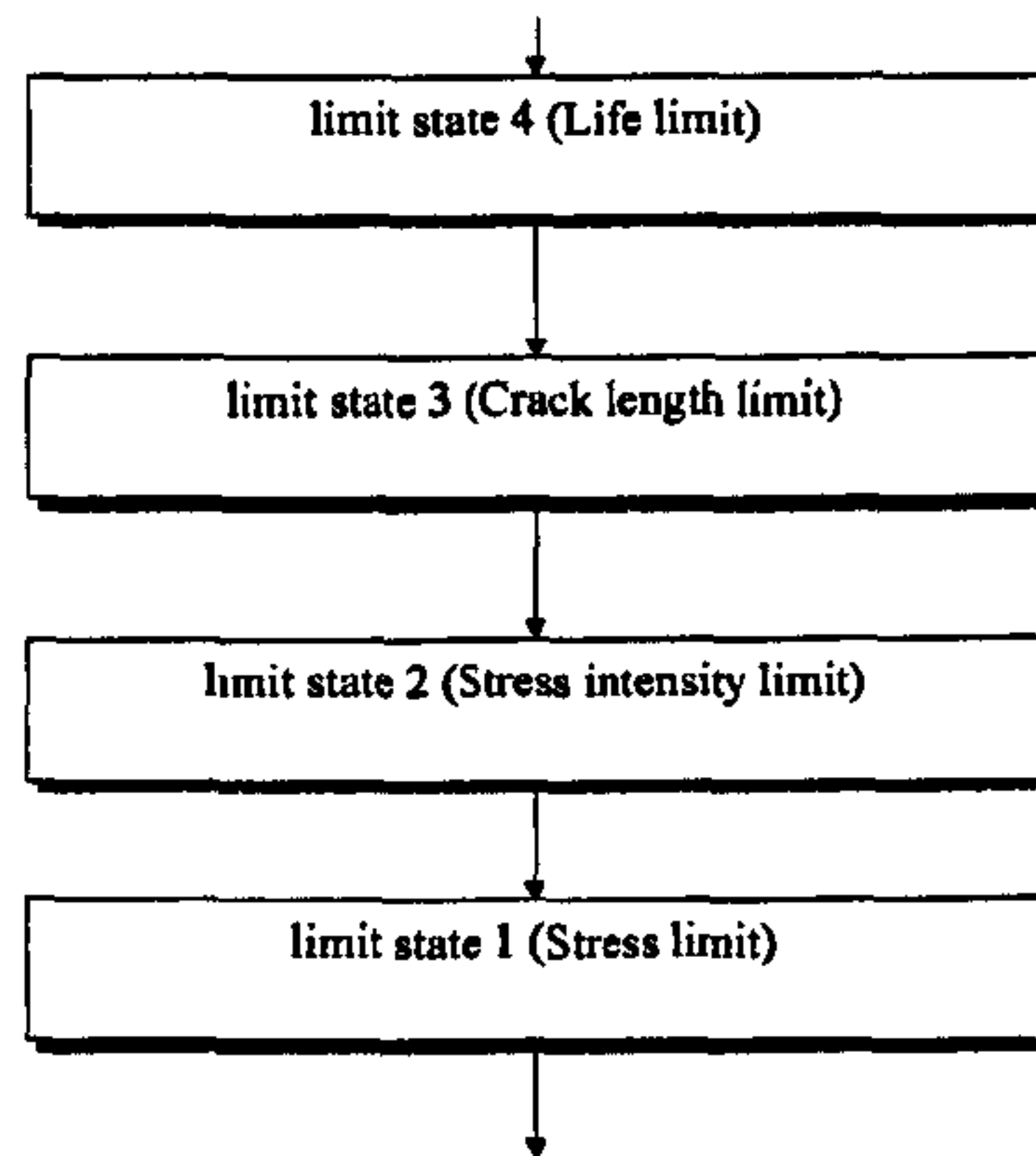


Figure (3.21) – Data recording sequence at I1.

Upon violation of any of the limit states, data is collected at the corresponding limit state as the algorithm progresses. In this way valid data is kept and non-numbers which could pose significant difficulties in analysis are ignored. Sub-process I2 is the collection of other important data (apart from the limit states) that may be used to improve design and reliability.

### 3.5.15 Process J – Reliability Computation

This computation utilizes the data containing the frequency of violation of any of the four limit states. This data is recorded in the Monte Carlo simulation process by the use of separate counters for each limit state. On violation of a limit state, the assigned counter adds 1 to the pre-existing data. The failure probability computation is expressed as:

$$POF = \frac{\sum PFC}{NSIM} \quad (3.28)$$

where  $POF$  is the probability of failure of the structure,  $PFC$  (process failure counter) is the limit state violation record for all four limit states and  $NSIM$  is the number of simulations. The reliability,  $R$  is thus,

$$R = 1 - POF \quad (3.29)$$

### 3.5.16 Process M – S-N reliability analysis

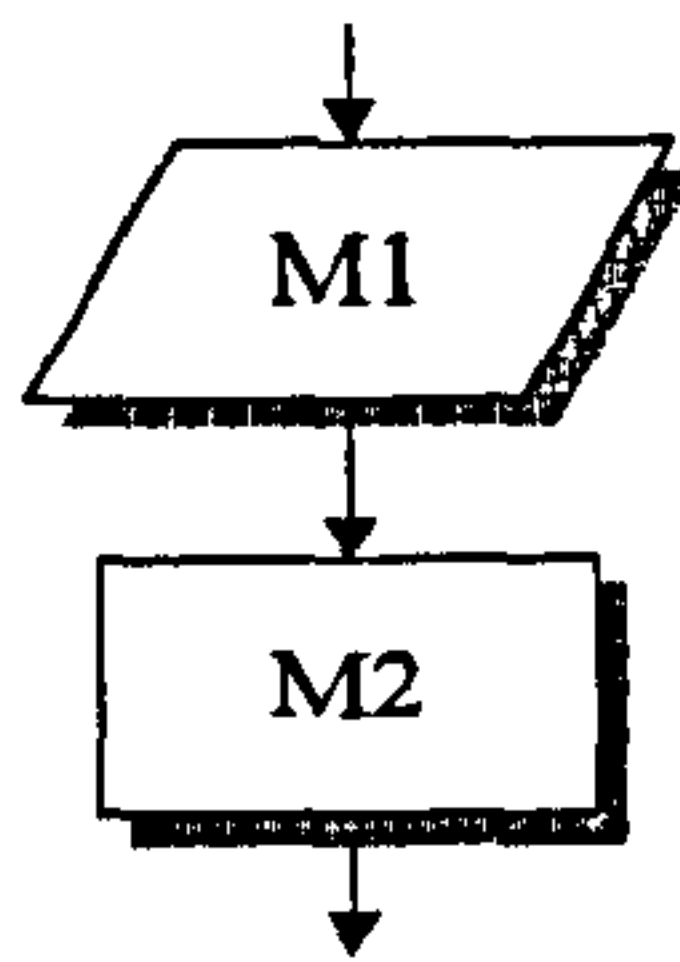


Figure (3.22) – Process M.

This is divided into two sub-processes as shown in Figure (3.22). M1 is the data initialization process for the S-N variables used in the S-N modelling. M2 is the transformation of the data to the lognormal distribution. Although this S-N data is rarely available, it presents a useful tool in the estimation of the fatigue life of a structure. Also less time is required for this modelling. The data provided is transformed to the lognormal distribution at process H. After the simulation, the results are collected at process I.

### 3.6 Numerical Example (BETA-FLEXSTREM Application)

A marine jib crane (Figure (3.23)) is considered. The crane information is from a haulage company in the Netherlands who wish to remain anonymous. The jib crane consists predominantly of AISI20 steel with a yield stress of 351.571MPa, fracture toughness of 70MPa and thermal expansion coefficient of  $15 \times 10^{-6}/K$  (at 20°C).

The overall height of the crane is 3 m with the jib boom extending 4.5 m. The total length of the jib boom is 5 m and is pivoted 300 mm from the non-load bearing end. The jib boom is an I-section beam with web width 30 mm, web height 500 mm, flange height 40 mm and flange width 300 mm.

The crane has a maximum load rating of 5 tonnes with a maximum slewing height of 60° and a minimum slewing height of 45°. The jib boom weighs 3.5 tonnes and the overall weight of the jib crane assembly is about 8 tonnes. The jib column, the lifting mechanism and the jib boom are assembled mainly by fillet welding. The welds contain defects ranging from 1.75 mm to 10 mm.

The crane is located on a large cargo ship that operates all year round on a very busy schedule. The loads handled are tailored to the crane capacity (5 tonnes) in increments of 0.5 tonnes, the lowest being 1 tonne.

The annual mean temperature of ship's exterior is assumed to be 10°C (283K) with a minimum annual temperature of -10°C (263K) and a maximum annual temperature of 30°C (303k).

It is assumed that:

- Service loads do not undergo any form of non-vertical lift hence zero torsion effects.
- There are no lateral compression forces and thus zero buckling effects.
- The distributions used in the analysis are well established in literature unless stated otherwise.
- The data provided emulates generic marine and offshore conditions as it is developed adhering to the codes provided by the DNV (DET NORSKE VERITAS (2004)) and ABS (American Bureau of Shipping (1991)).
- The standard deviations are taken to be 0.1 of the variable mean unless specified (i.e.  $COV=0.1$ ).

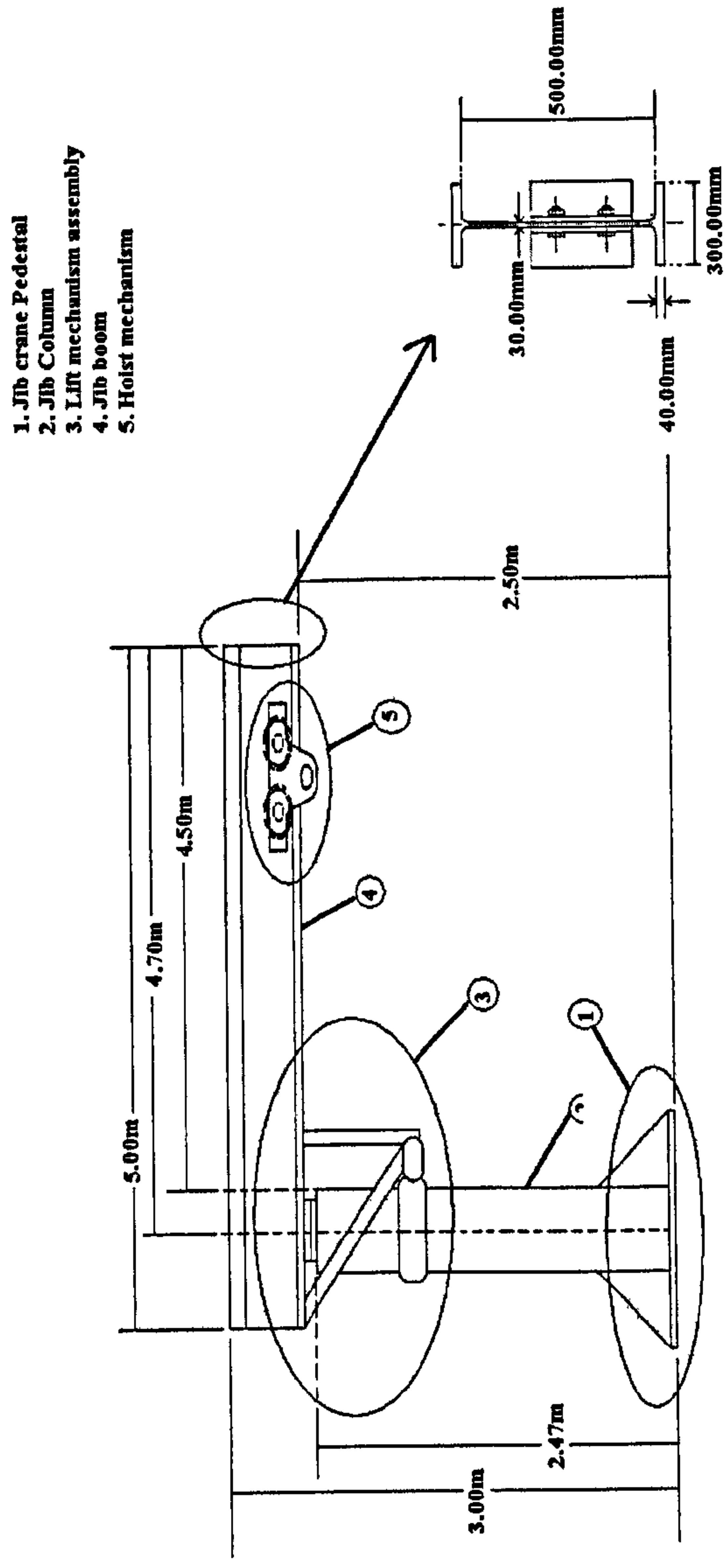


Figure (3.23) – Marine jib crane.

The properties of the material and the dimensions are shown in Table (3.4). These values will be used by BETA-FLEXSTREM in the reliability analysis.

Material dimensions	
Thermal expansion coefficient	$15 \times 10^{-6}/K$ (at 20°C)
Weight of jib boom	34 kN
Average temperature	20°C (293 K)
Web width	30 mm
Web height	420 mm
Flange width	300 mm
Flange height	40 mm
Jib boom length	5 m

Table (3.4) – Material properties/dimensions.

Particular distributions from literature have been assigned to the variables in Table (3.5). This will also be used by BETA-FLEXSTREM in the reliability analysis.

Parameter/ variable	Distribution	Mean	Coefficient of variation
$F_y$ (yield stress)	Gaussian	351.571 MPa	0.1
$K_{IC}$ (fracture toughness)	Lognormal	70 MPa	0.1
$a$ (crack length)	Exponential	0.05875 m	–
$a_c$ (critical crack length)	CLT	–	–
$mat_c$ (crack growth rate coefficient)	Lognormal	$4 \times 10^{-11}$	0.1
$K_I$ (stress intensity factor)	CLT	–	–
$mat_m$ (crack growth exponent)	Fixed	3	–
$N_{OP}$ (operational life)	CLT	–	–
$N$ (planned life)	Lognormal	108000	0.1

Table (3.5) – Material parameters/variables.

In the distributions column, CLT indicates derived distributions (from the interaction of fundamental variables) that obey the central limit theorem (CLT).

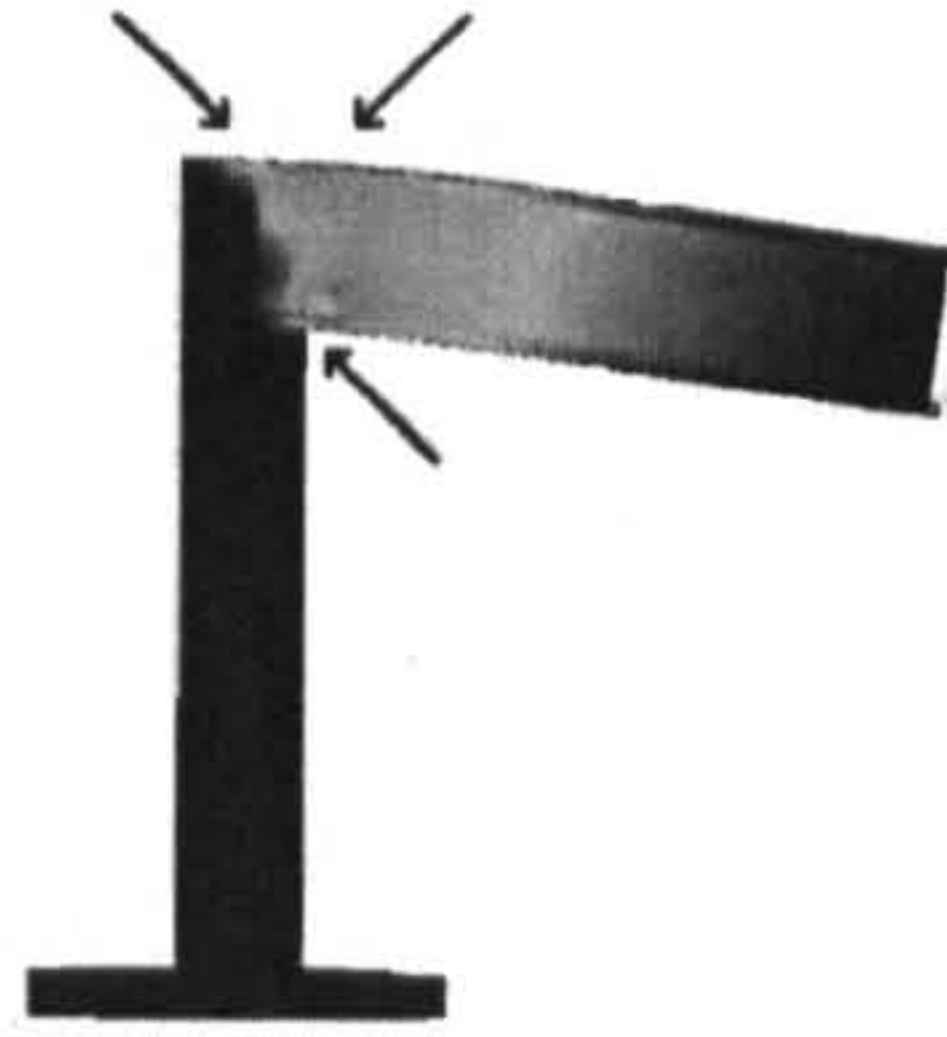


Figure (3.24) – Area of high stress concentration.

Figure (3.24) shows the area of the highest stress concentration. This is expected as it is an edge (or discontinuity). This area of high stress concentration is critical to the overall survivability of the structure. The main source of fatigue is imperfections (defects) (Balasubramanian and Guha (1999)). These imperfections could be subject to residual stresses which could (together with the working load) widen the imperfection (crack/defect size) and ultimately cause failure. Good manufacturing practices cannot be overemphasized here as the chances of failures are increased with poor material finishing. Material treatments such as shot-peening, grinding and dressing could decrease the presence of residual stresses. The application and transformation of the nominal stress in the BETA-FLEXSTREM prompts the monitoring of each limit state. Both dead and live loads are considered in the estimation of the nominal stress.

### 3.7 Results and Discussion

The results generated by the BETA-FLEXSTREM for a million trials were accumulated and analysed. Based on the analysis plots were produced. These plots form the crux of the analysis as results could be better appreciated with graphical representation of the interaction and relationships of the input variables.

Table (3.6) shows a sample of the results produced by BETA-FLEXSTREM. Interactions between the various load classes and the effect on the various limit states could be analysed effectively. The column to the extreme left shows the various load classes handled by the jib crane. These loads are fed into the BETA-FLEXSTREM alongside other system (SMS) definition parameters to produce the values in the subsequent columns.



Load (KN)	Critical crack length (m)	Crack length (m)	Crack growth rate coefficient	Fracture toughness (MPa $\sqrt{m}$ )	Stress intensity factor ( $\sqrt{m}$ )	Nominal stress (MPa)	Yield stress (MPa)	Operational life (cycles)	Planned life (cycles)
25	0.888	0.005	4.16E-11	76.645	3.121	29.664	398.953	2.552E+07	1.124E+05
40	2.182	0.068	4.05E-11	54.347	11.287	21.417	323.922	9.658E+07	1.095E+05
45	1.547	0.024	3.74E-11	65.607	3.235	25.483	360.915	1.860E+07	1.010E+05
40	1.347	0.016	4.46E-11	77.787	8.831	20.110	312.027	7.106E+07	1.205E+05
35	1.375	0.005	3.45E-11	67.174	13.719	23.481	342.697	3.036E+07	9.320E+04
50	0.840	0.016	4.62E-11	62.864	6.491	23.635	344.104	3.690E+07	1.247E+05
30	0.996	0.075	3.85E-11	76.591	10.241	24.555	352.470	2.187E+07	1.040E+05
25	1.814	0.029	3.73E-11	77.369	13.071	21.906	328.372	8.314E+08	1.008E+05
45	0.820	0.023	3.91E-11	74.403	12.862	30.356	405.250	3.353E+07	1.056E+05
35	2.342	0.035	4.36E-11	72.790	0.224	26.864	373.475	4.398E+06	1.176E+05
50	1.325	0.004	4.44E-11	74.599	7.034	32.431	424.125	7.181E+06	1.198E+05
40	0.762	0.024	4.06E-11	65.579	10.625	23.810	345.690	1.252E+08	1.096E+05

Table (3.6) – Sample results produced by BETA-FLEXSTREM.

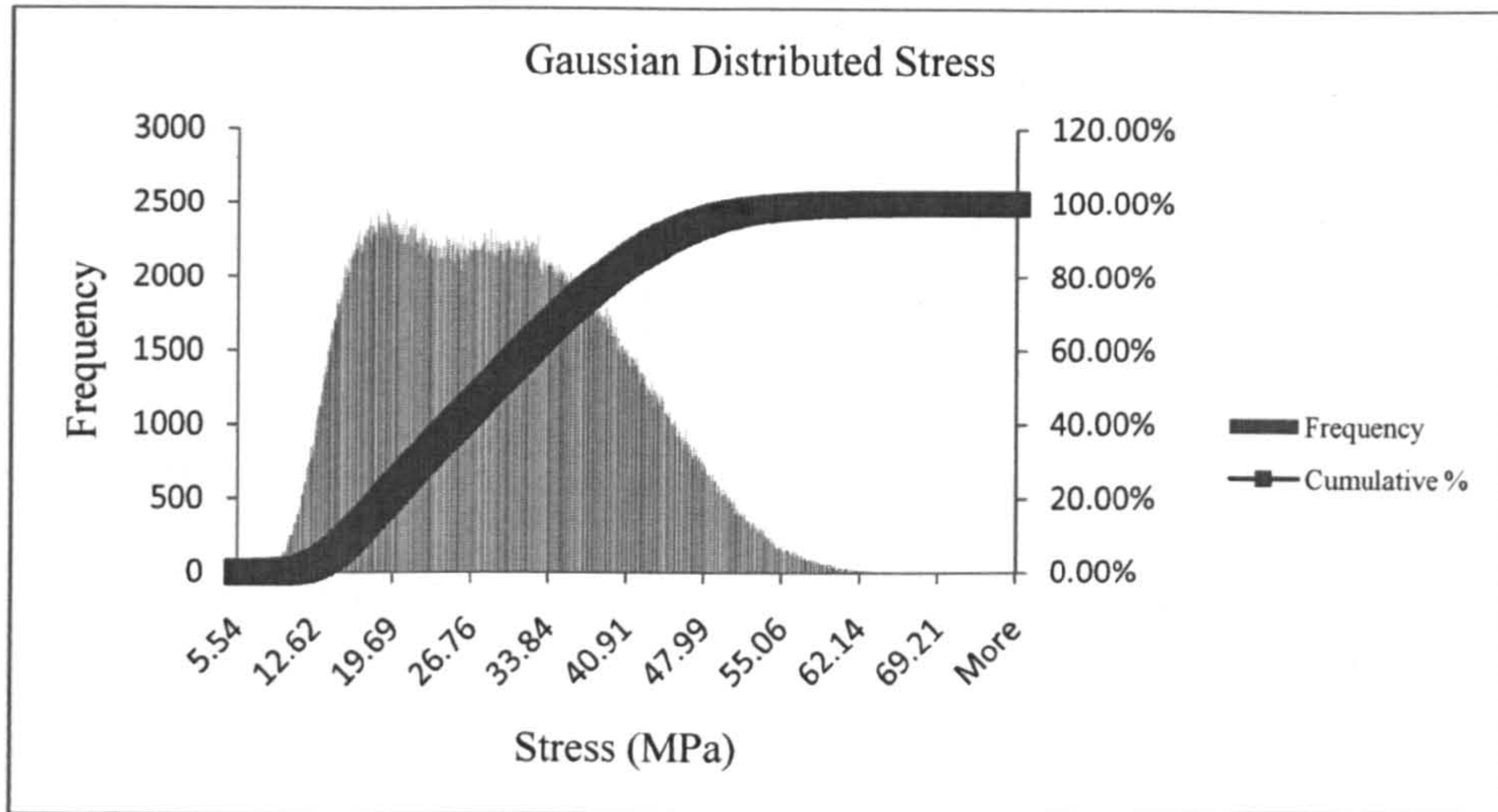


Figure (3.25) – Gaussian distributed stresses.

The outcome of a million trials (simulations) produced normally distributed data shown in Figure (3.25). The distribution is actually a culmination of several stresses brought about by the load classes as shown in Figure (3.26).

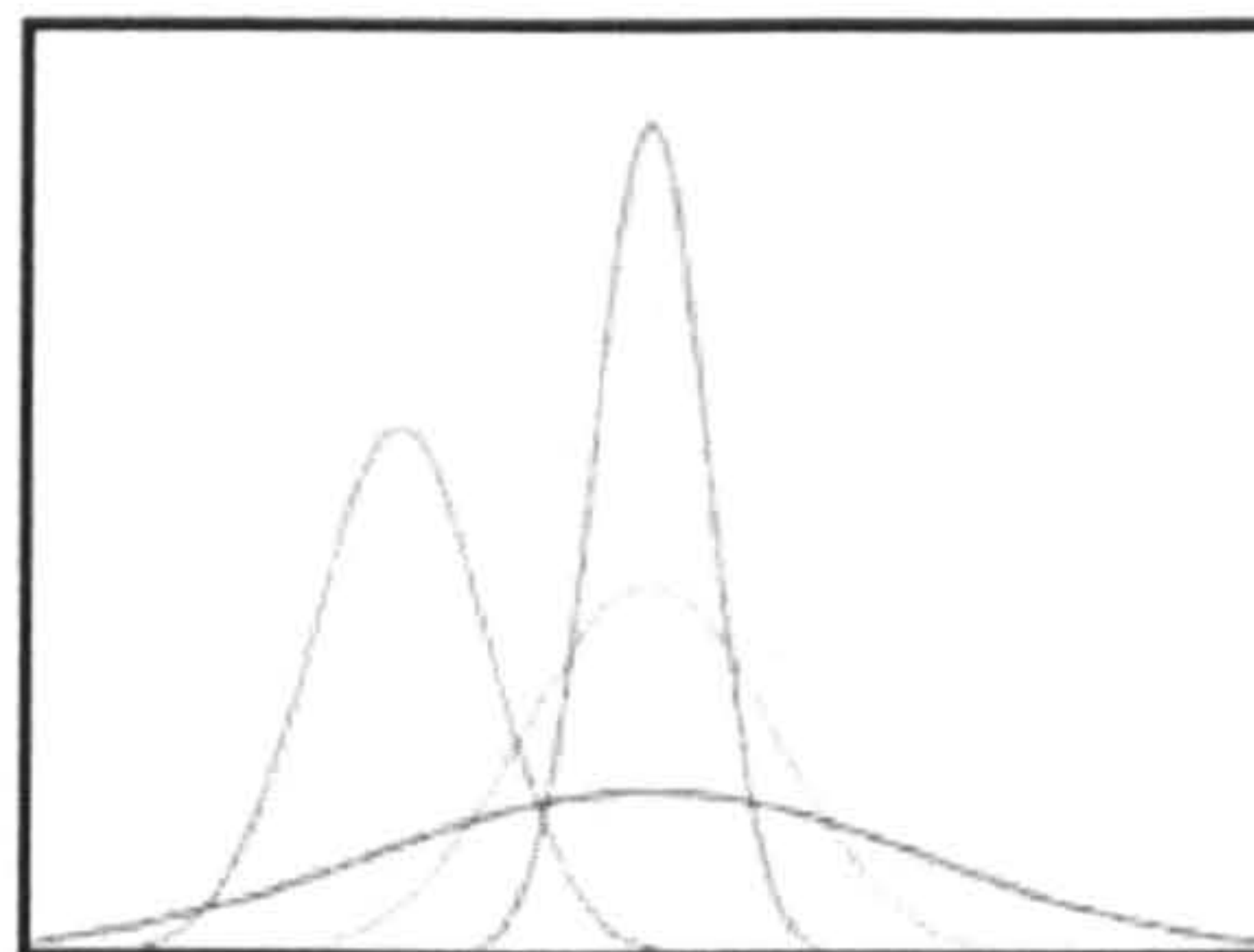


Figure (3.26) – Various load classes.

The various curves represent the various load classes that make up the distribution in Figure (3.26). A sensitivity analysis emphasizing the effect of each load class is presented in section 3.8.

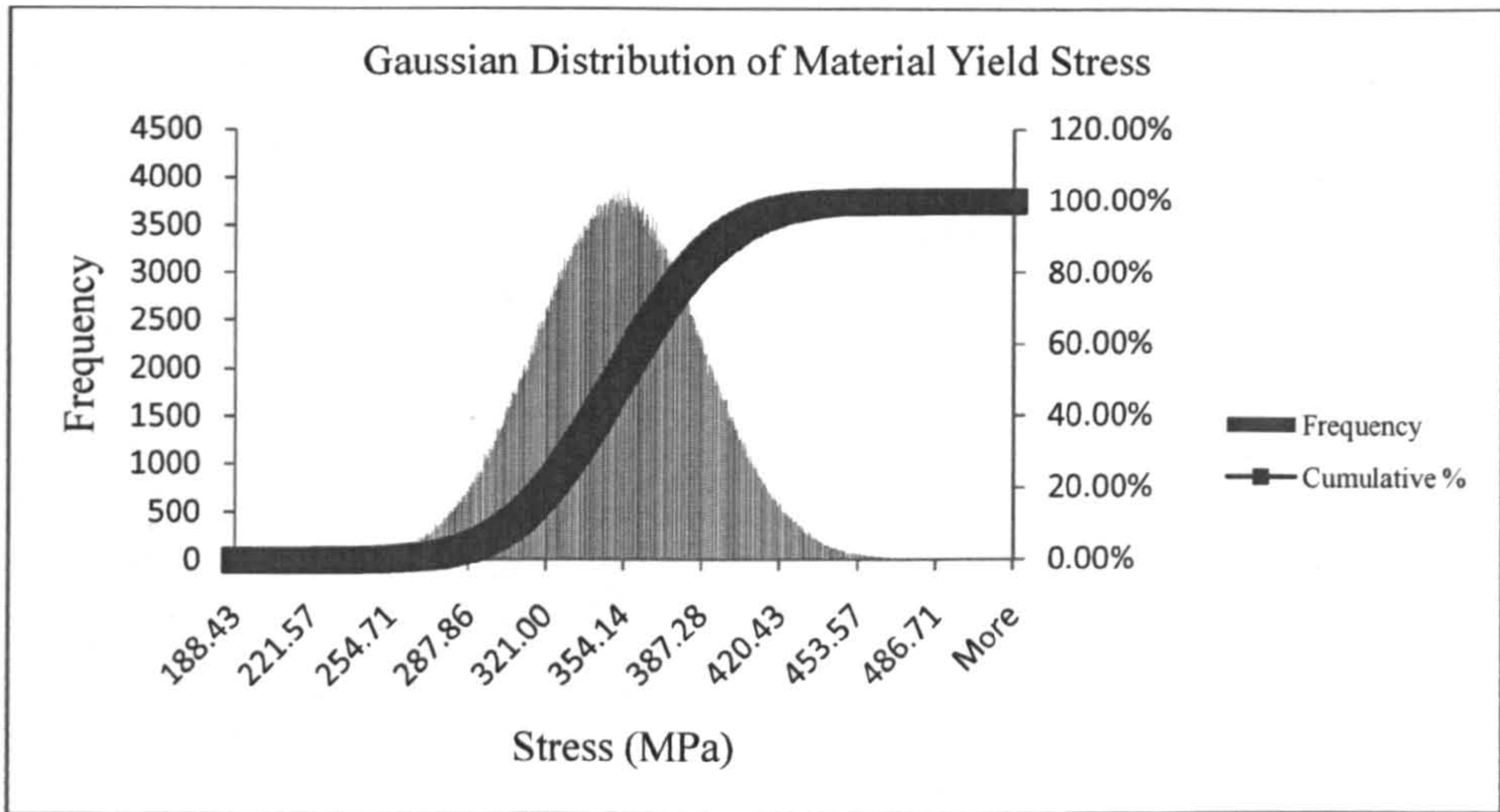


Figure (3.27) – Gaussian distribution of material yield stress.

The material yield stress for a million trials is shown in Figure (3.27). The normal distribution shown has a comparatively smaller variance. The values strongly occur around the mean and the standard extreme values occur rarely.

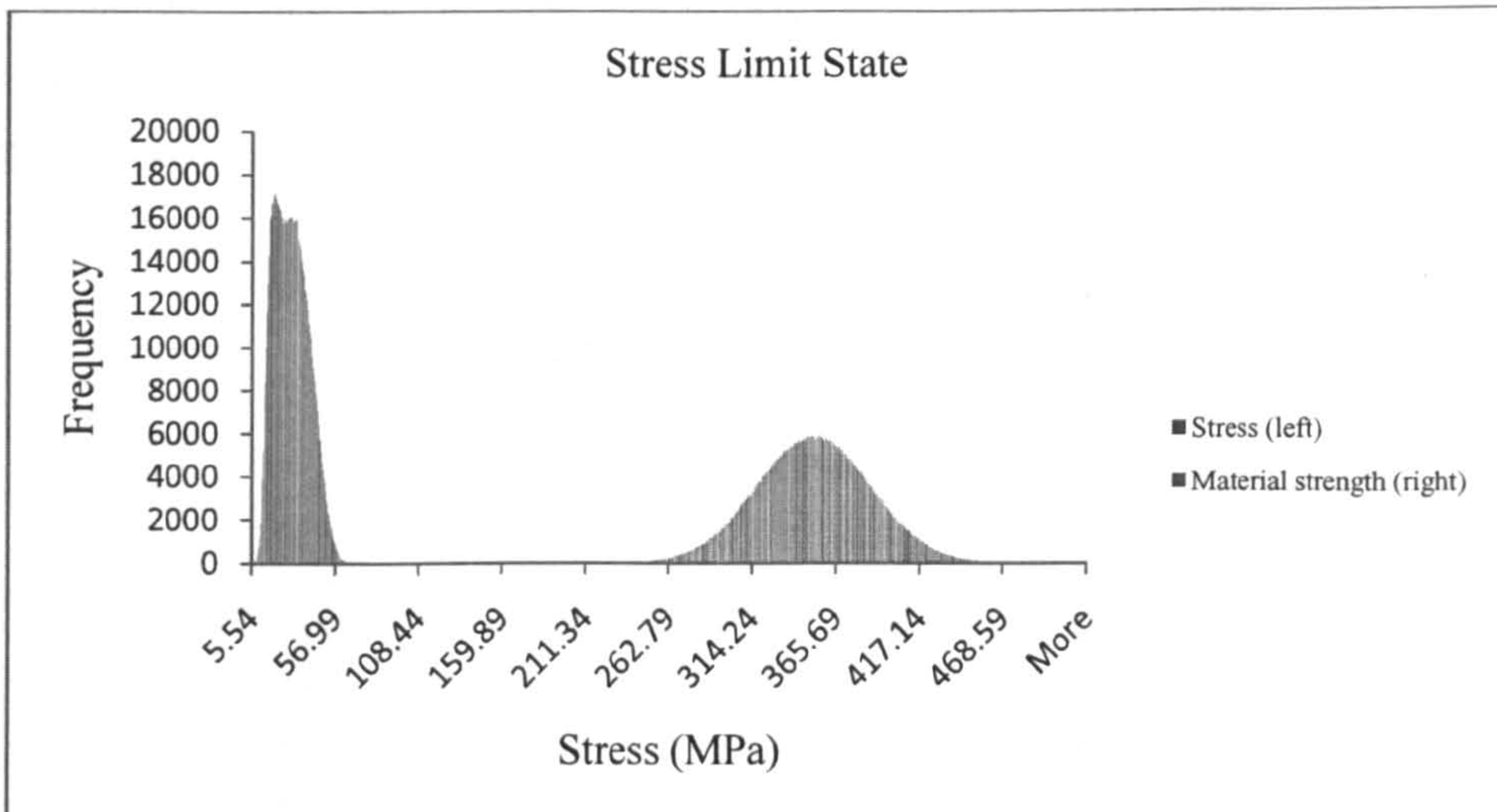


Figure (3.28) – Stress limit state.

The load limit is shown in Figure (3.28). A considerable stress range difference exists between the nominal stress range and the yield stress range. It could be statistically inferred that the safety factors introduced in the design of this component was significantly high and thus presents a good case of over-design.

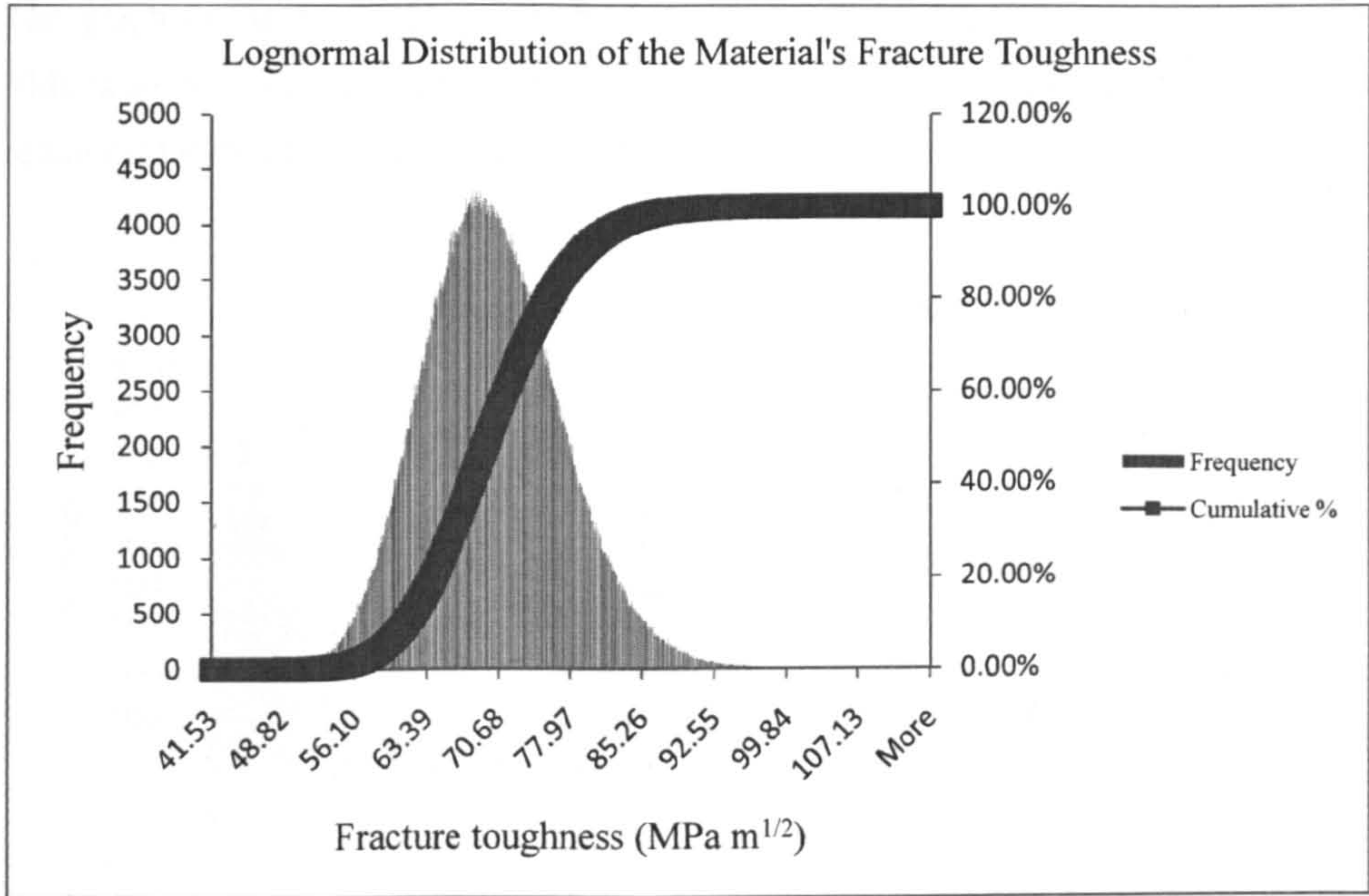


Figure (3.29) – Lognormal distribution of material fracture toughness.

Figure (3.29) shows the lognormal distribution of the material fracture toughness. This distribution unlike the Gaussian distribution has an increasingly wider “bell-shape” (graphically) as the variance reduces. Most of the values are close to the mean as a result of a low (relatively) COV.

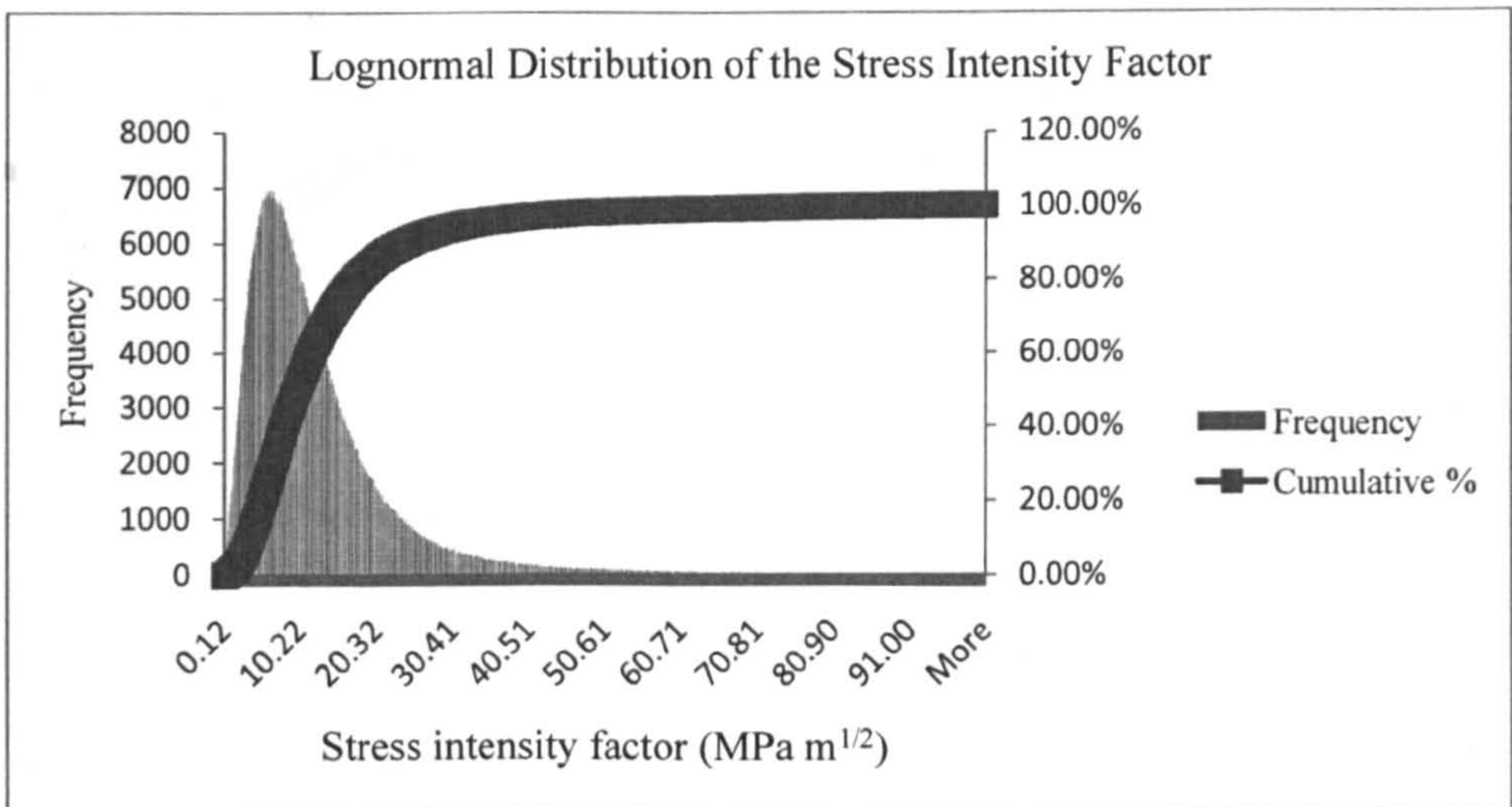


Figure (3.30) – Lognormal distribution of the stress intensity factor.

The graph in Figure (3.30) shows the lognormal nature of the stress intensity factor. This is a result of the central limit theorem as the data represented are derived from relationships of other fundamental (primary) values.

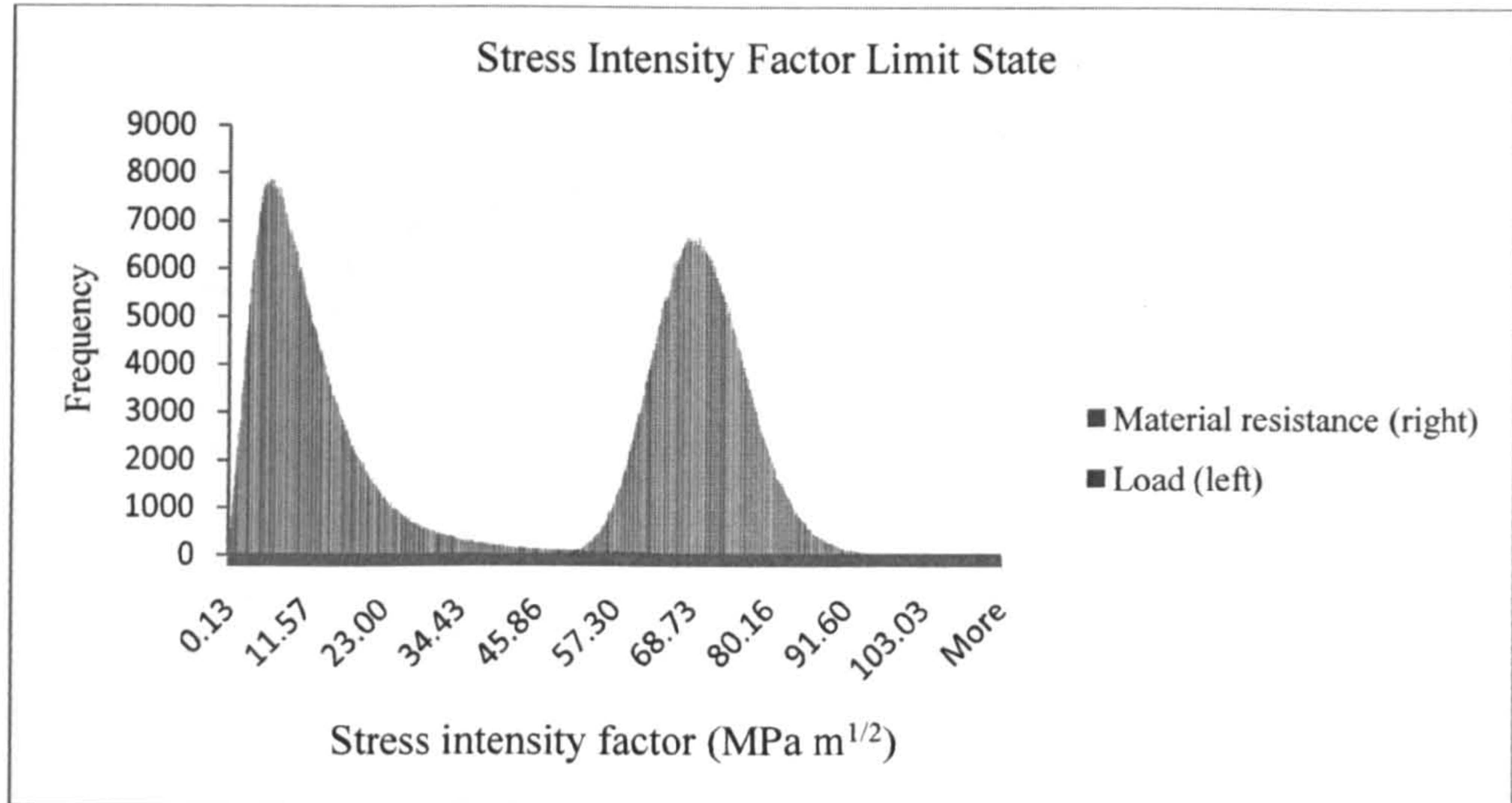


Figure (3.31) – Stress intensity factor limit state.

The second limit state – the fracture limit is presented in Figure (3.31). The overlap in values (failures) is also illustrated.

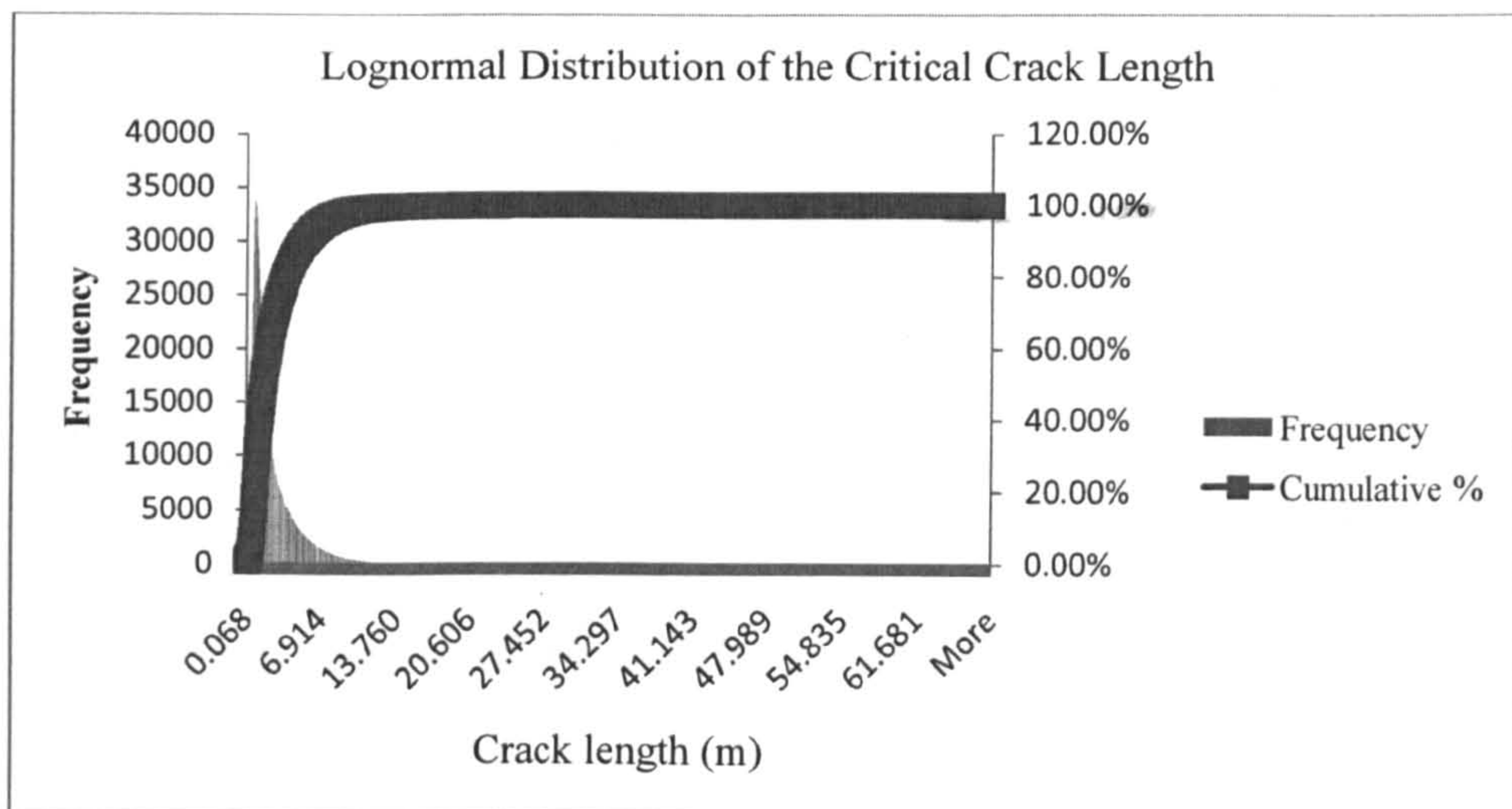


Figure (3.32) – Lognormal distribution of the critical crack length.

Here, the data represented in Figure (3.32) are derived from the stress intensity factor computations. Following the central limit theorem, the result is lognormally distributed. The stretch and skew of the distribution is relatively large.

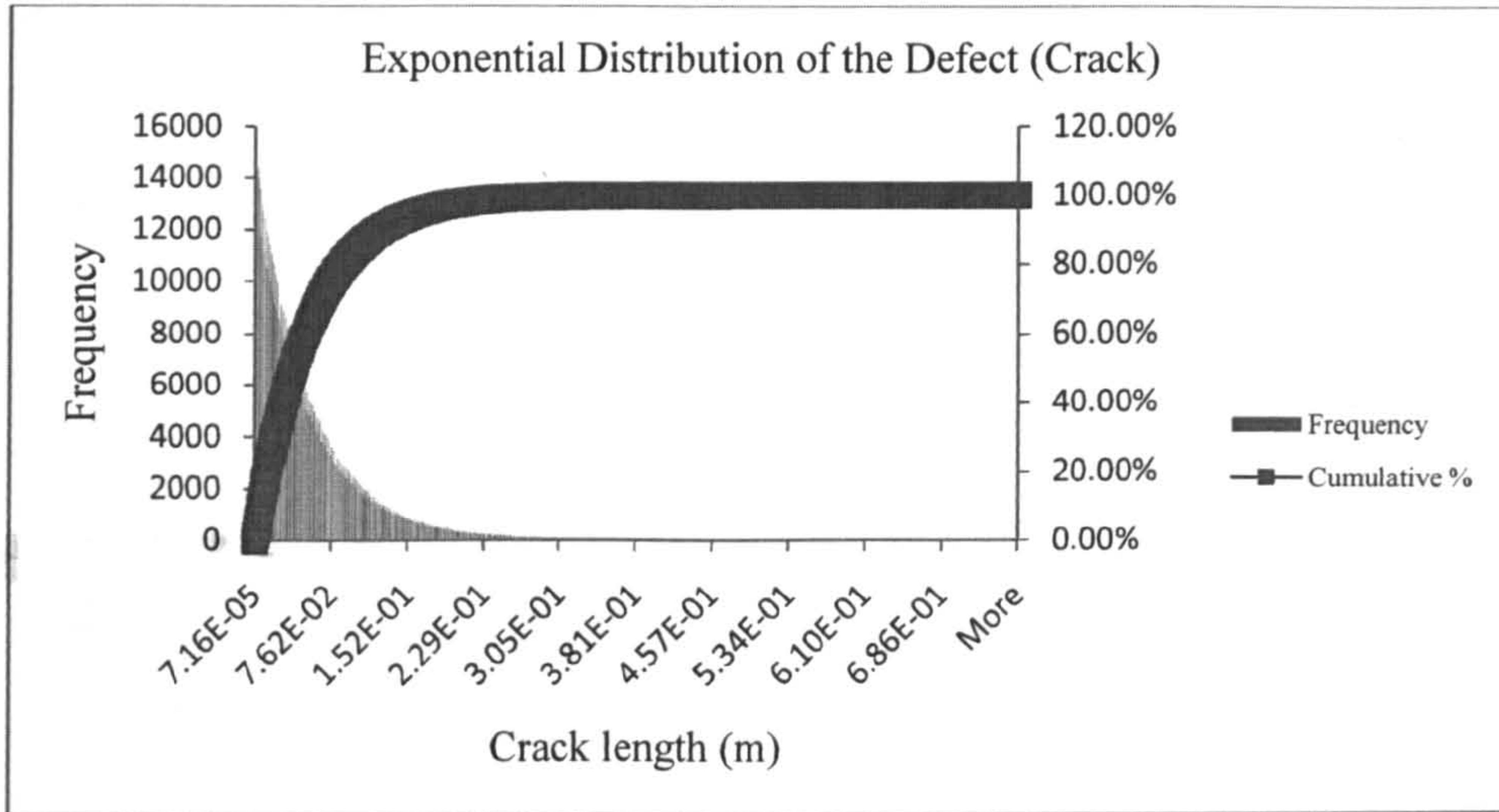


Figure (3.33) – Exponential distribution of the critical crack length.

The defect (crack) length is exponentially distributed as shown in Figure (3.33). Unlike the critical crack length values, these defect length values are fundamental (primary) i.e. not derived from any prior computations from the preceding processes S-D.

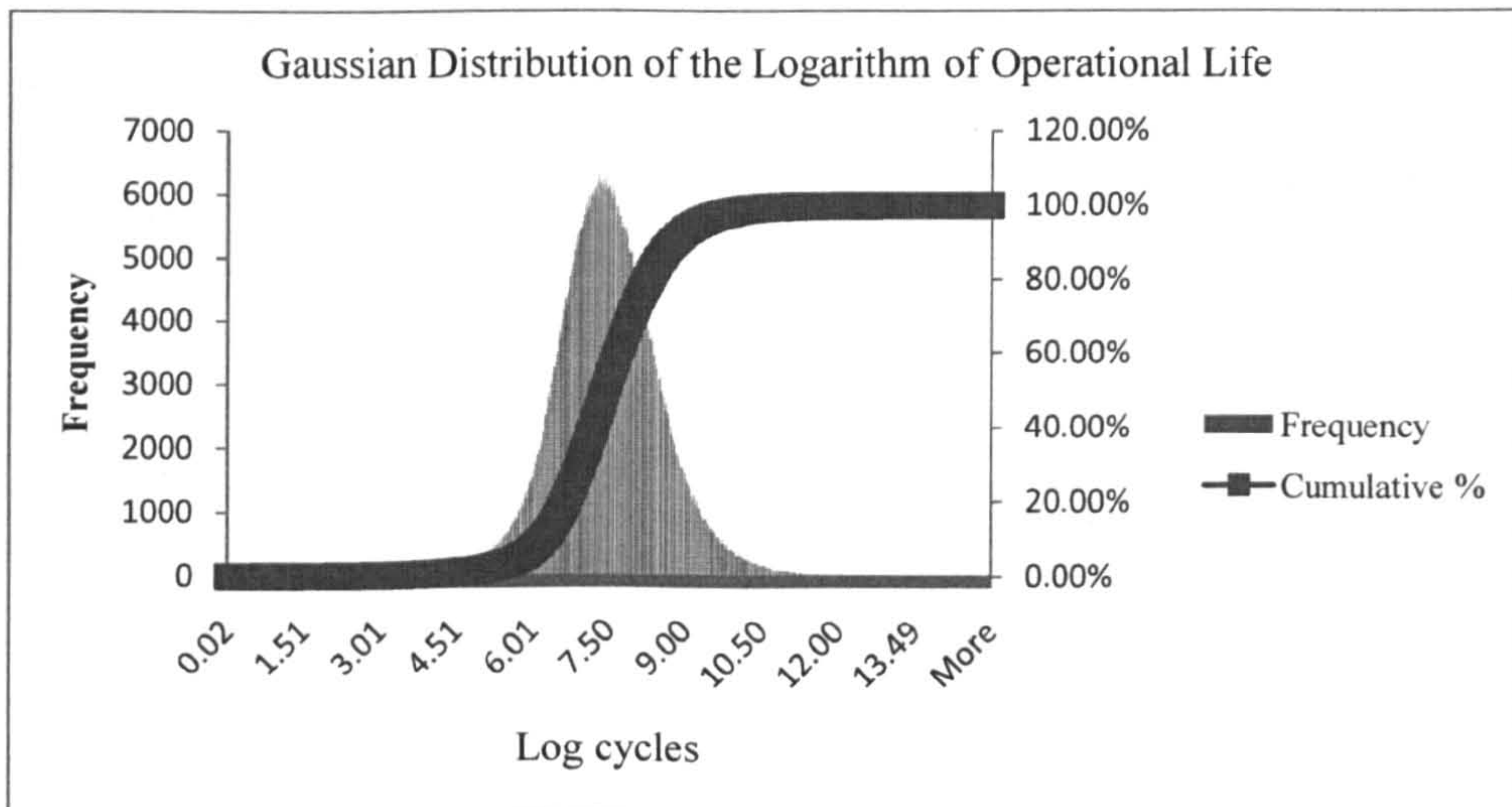


Figure (3.34) – Gaussian distribution of the logarithm of operational life.

High variance restricts the clearer presentation of the lognormal distribution of the estimated operational life of the component. The high variance is due to the several derived values (thus multiple variances) used in the estimation. However the logarithms of these values present a clearer illustration as shown in Figure (3.34). The conversion of the real values to logarithmic values is the reason for the Gaussian nature of this graph.

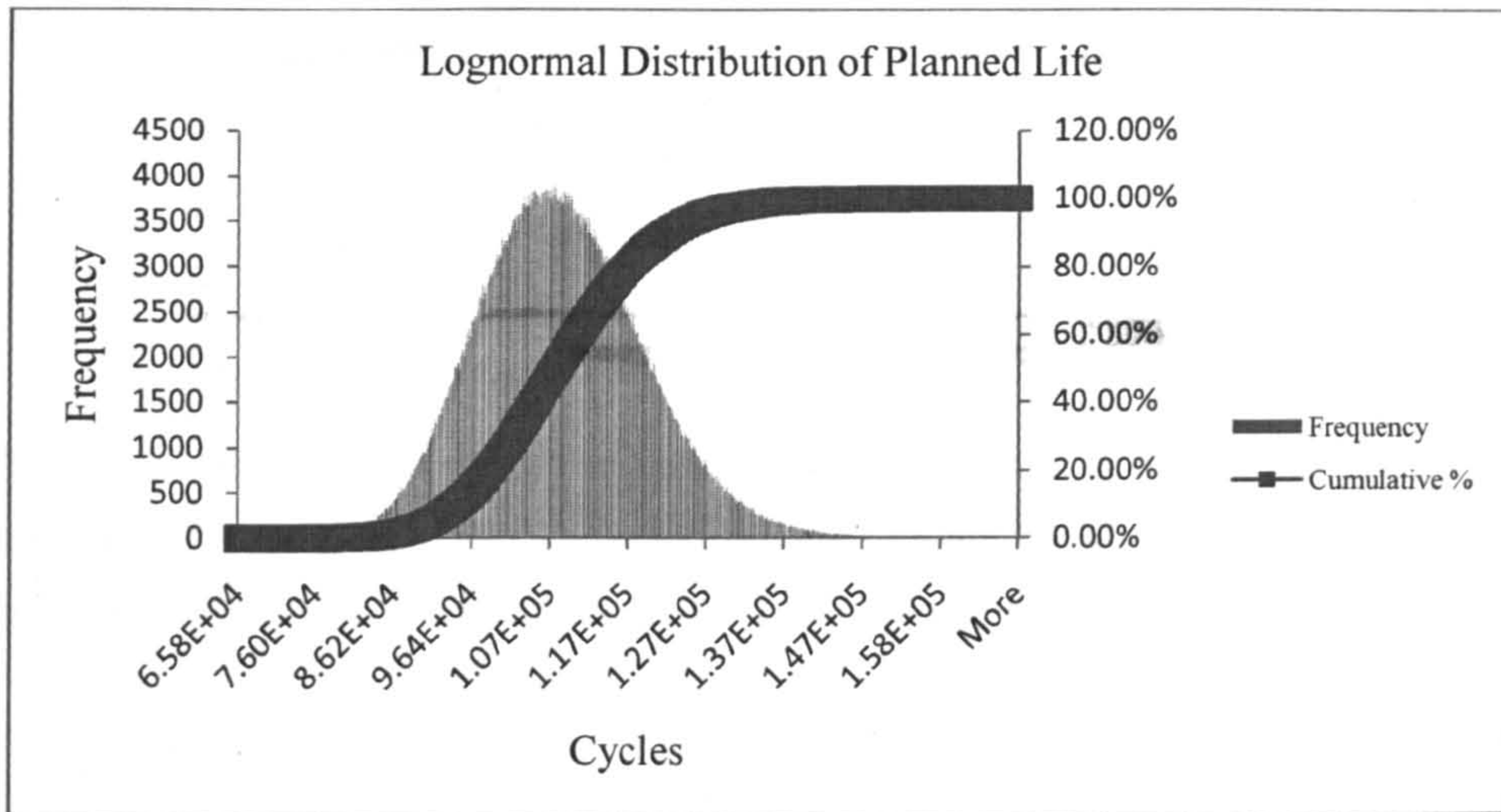


Figure (3.35) – Lognormal distribution of planned life.

The planned/design life, unlike the operational/resultant life, is a fundamental (primary) value. As mentioned before, the planned life is lognormally distributed. Figure (3.35) shows the variation in values of the planned life.

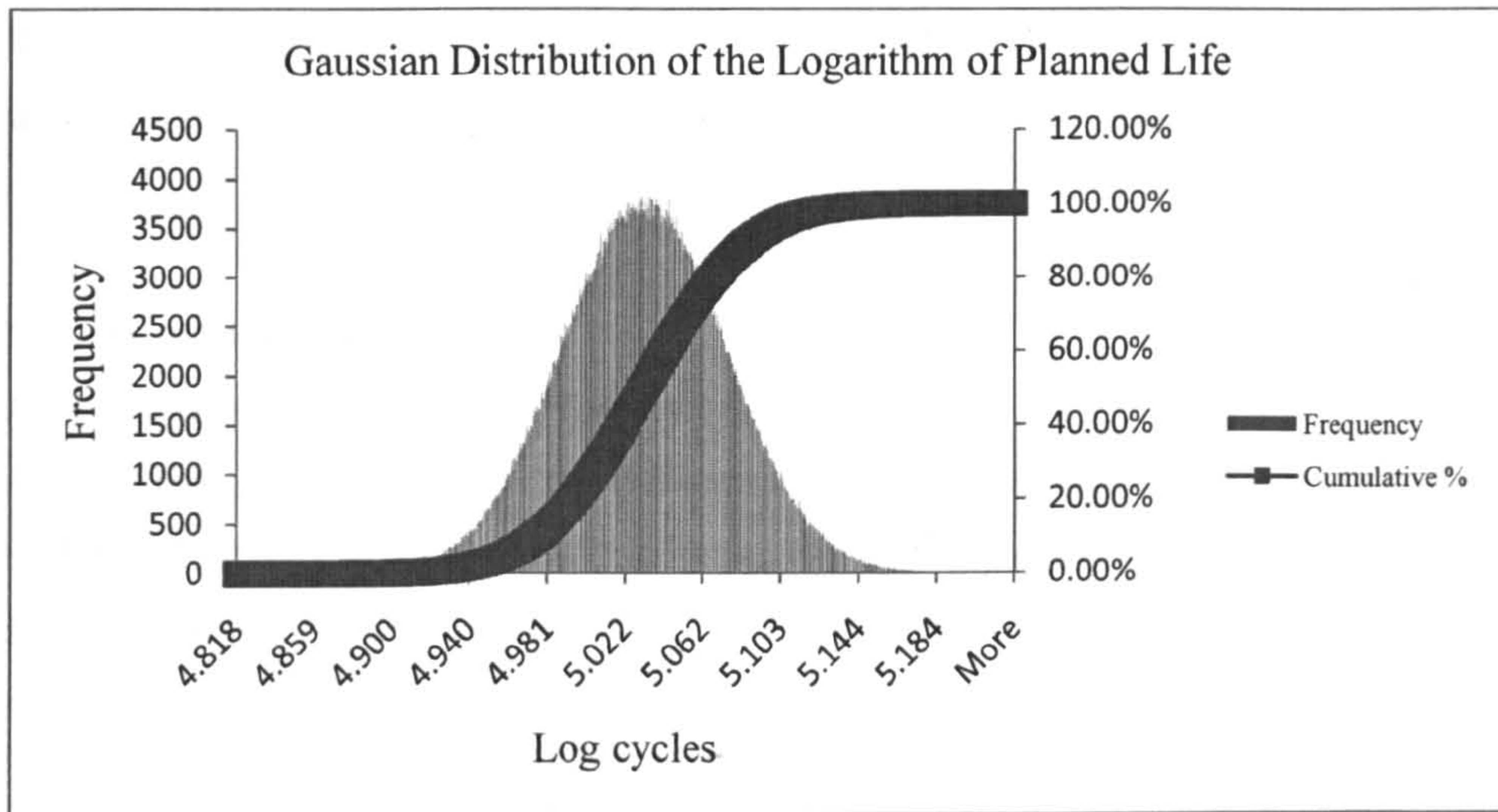


Figure (3.36) – Gaussian distribution of the logarithm of planned life.

The logarithmic conversion of the planned life values yields a normal distribution as shown in Figure (3.36). This conversion is done to aid the comparison between the planned life and the estimated operational life of the component.

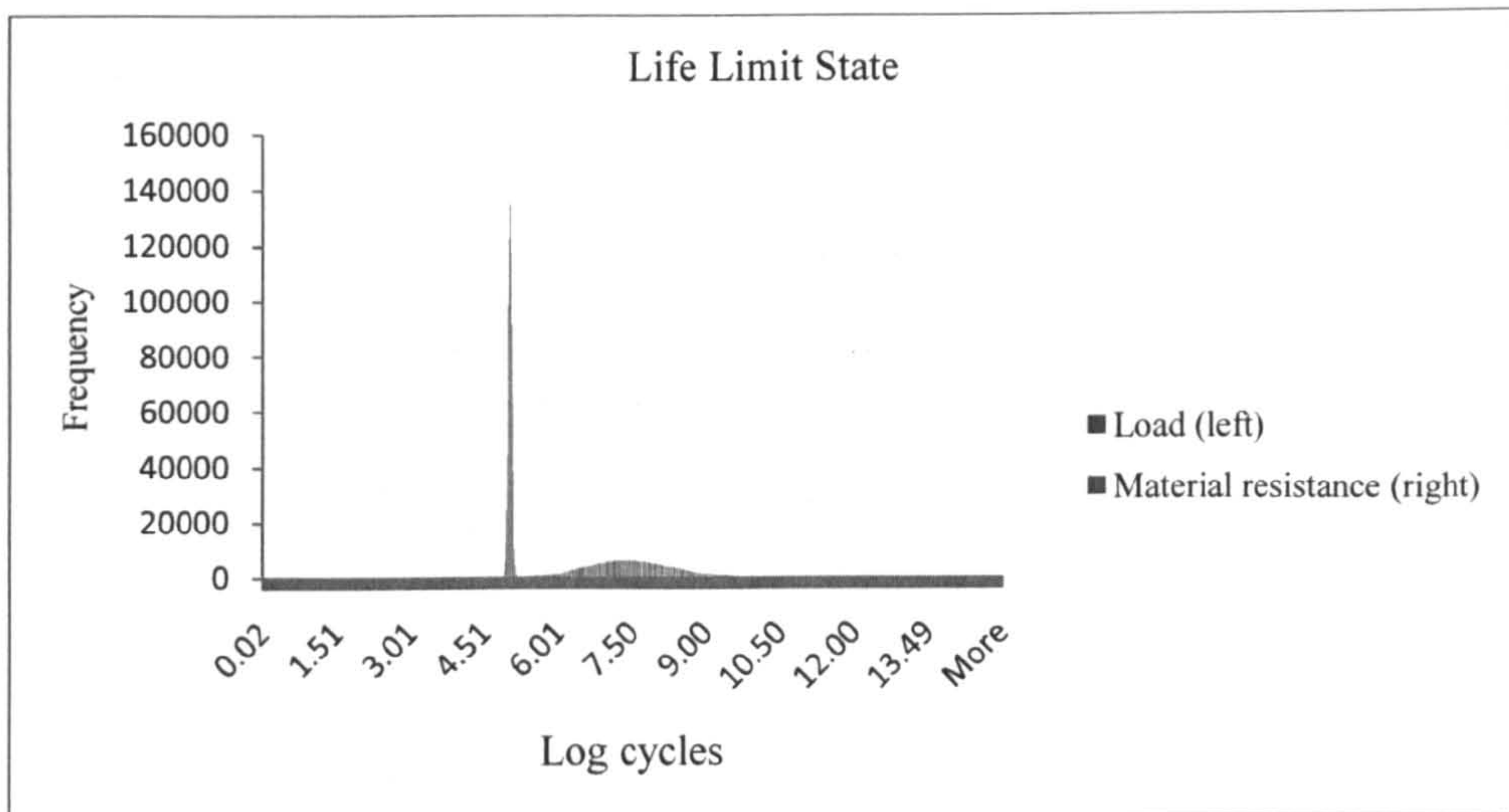


Figure (3.37) – Life limit state.

The fourth limit state – the life limit is illustrated in Figure (3.37). This shows a very good illustration of the variance of the planned and operational lives. The operational life has a huge range – compared to that of the planned life. This is due to the several



stress ranges brought about the different load classes. The region of overlap (failure) can also be seen (although the scale could be increased for a clearer visual appreciation).

### 3.8 Sensitivity Analysis

#### 3.8.1 Result Comparison for Number of Simulations

A result comparison was done for different numbers of simulations (trials) done in the BETA-FLEXSTREM. This was aimed at assessing the consistency of the results from different numbers of simulations. Table (3.7) shows the results plotted in Figures (3.38) and (3.39).

No of trials	Stress limit failure	Fracture limit failure	Critical crack limit failure	Life limit failure	Total number of failures	Reliability	Probability of failure
10,000	0	161	66	189	416	0.9584000	$4.16 \times 10^{-2}$
100,000	0	1645	676	1897	4218	0.9578200	$4.218 \times 10^{-2}$
500,000	0	8336	3191	9724	21251	0.9574980	$4.250 \times 10^{-2}$
1,000,000	0	16842	6254	19414	42510	0.9574370	$4.256 \times 10^{-2}$
10,000,000	0	168538	63155	193718	425411	0.9574589	$4.254 \times 10^{-2}$

Table (3.7) – Failure counts and reliability for different number of trials.

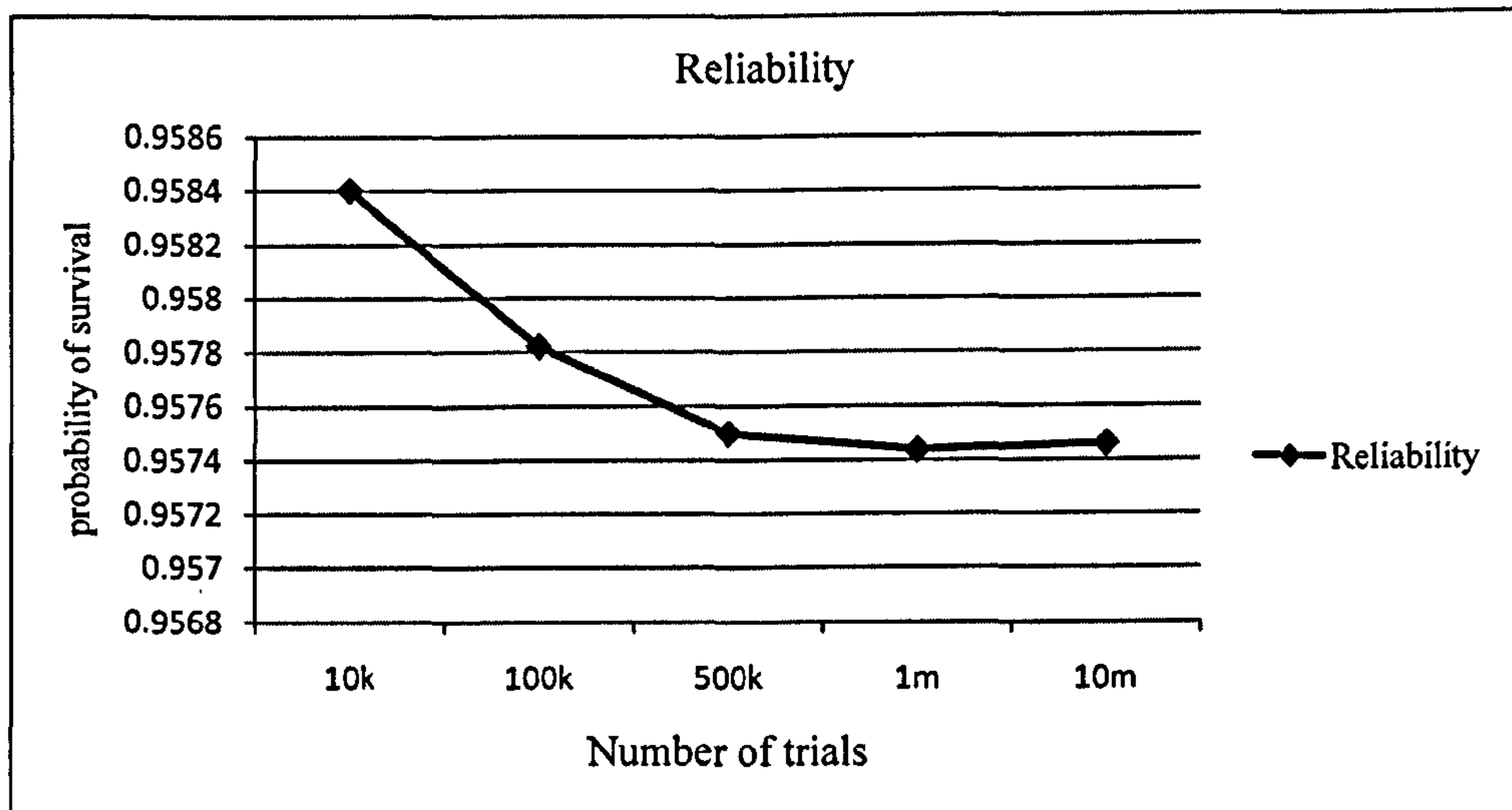


Figure (3.38) – Reliability result comparison for different number of trials.

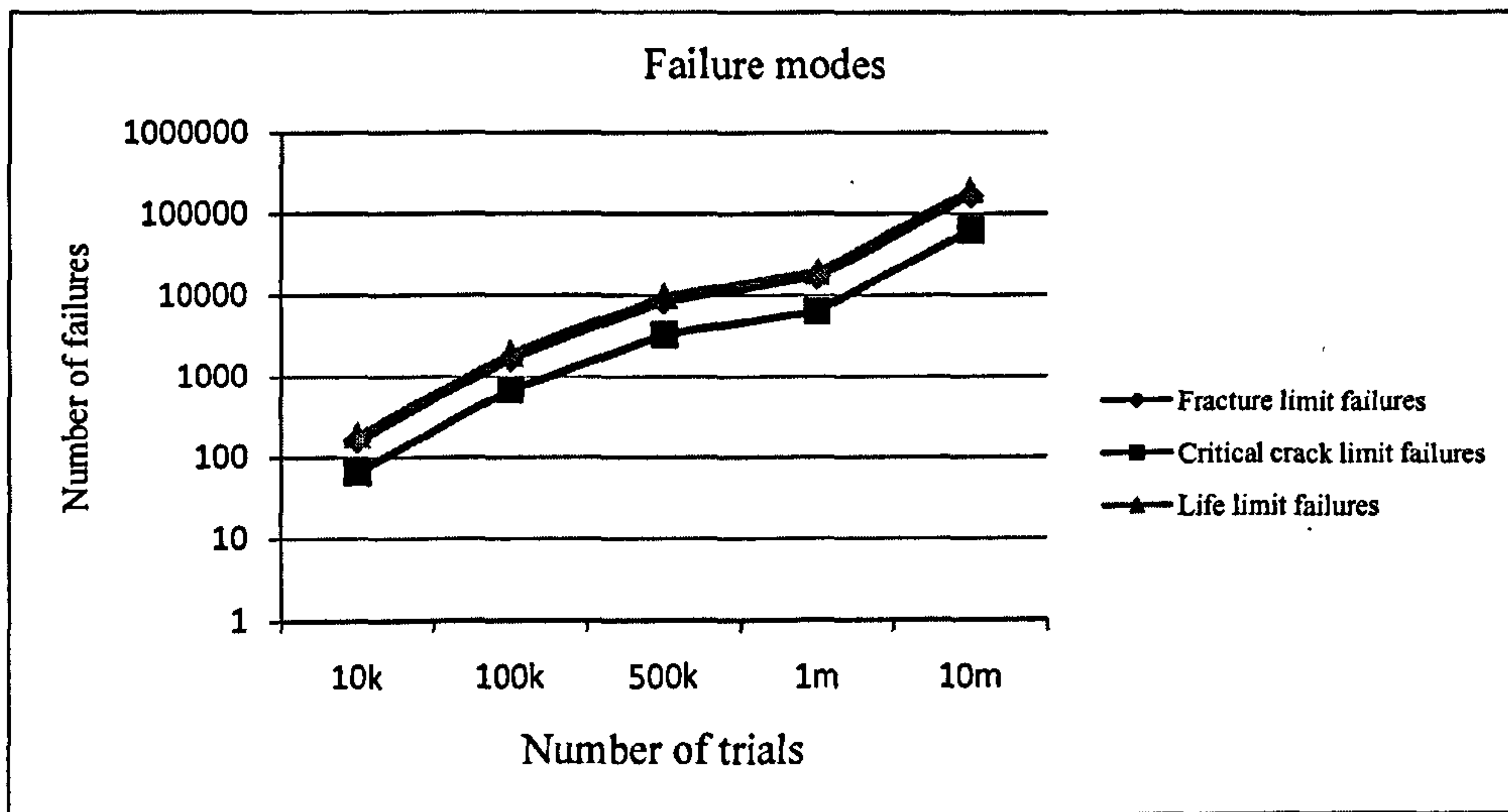


Figure (3.39) – Failure mode count comparison for different number of trials.

### 3.8.2 Sensitivity Analysis

A local sensitivity analysis (i.e. the net effect of a change in a single parameter) was carried out to partially validate the BETA-FLEXSTREM model. Key independent limit state variables were altered individually by 10% (increments and decrements where applicable). The effects on the reliability were presented in tables and graph plots.

It is expected that the changes applied to these parameters would bring about a trended change in the reliability of the structure. The graph in Figure (3.39) and Table (3.7) reveal that simulations greater than 100,000 and above generate consistent results. Therefore for the reason of efficiency for the amount of results to be generated, 100,000 simulations were deemed sufficient for the analysis.

#### 3.8.2.1 Base Model as a Sensitivity Standard

The comparative standard result to be used in this analysis is that obtained from 100,000 simulations shown in Table (3.8):

Failure Mode	Number of Failures
Limit state 1 (Stress Limit)	0
Limit State 2 (Stress intensity factor Limit)	1645
Limit State 3 (Crack Length Limit)	676
Limit state 4 ( Life limit)	1897
Total	4218
Reliability	0.95782

Table (3.8) – Base failure mode frequencies.

The values outlined in Table (3.8) serve as the zero-point (datum) for the start of the analysis. The numbers of occurrences were recorded for 100,000 simulations.

### 3.8.2.2 Fracture Toughness

The fracture toughness ( $K_{IC}$ ) – the ability of the material to resist fast fracture – has a significant bearing directly on three of the four limit states as shown in Tables (3.9) and (3.10). This in effect has a significant bearing on the reliability.

	Percentage change				
	10%	20%	30%	40%	50%
Limit State I	0	0	0	0	0
Limit State II	1941	2426	2842	3555	5629
Limit State III	693	917	1084	1700	3102
Limit State IV	1883	1975	1927	1808	1905
Total	4517	5318	5853	7063	10636
Reliability	0.95483	0.94682	0.94147	0.92937	0.89364

Table (3.9) – Effect of fracture toughness decrease on reliability.

	Percentage change				
	60%	70%	80%	90%	100%
Limit State I	0	0	0	0	0
Limit State II	8841	15338	32710	72402	100000
Limit State III	6527	12141	20403	18386	0
Limit State IV	1661	1407	716	141	0
Total	17029	28886	53829	90929	100000
Reliability	0.82971	0.71114	0.46171	0.09071	0

Table (3.10) – Effect of fracture toughness decrease on reliability.

Percentage decrease	Reliability	Percentage Change in Reliability
10	0.95483	0.31
20	0.94682	1.15
30	0.94147	1.71
40	0.92937	2.97
50	0.89364	6.70
60	0.82971	13.38
70	0.71114	25.75
80	0.46171	51.80
90	0.09071	90.53
100	0	100

Table (3.11) – Trended change in reliability (fracture toughness).

The trend in the percentage decrease outlined in Table (3.11) is plotted in Figure (3.40).

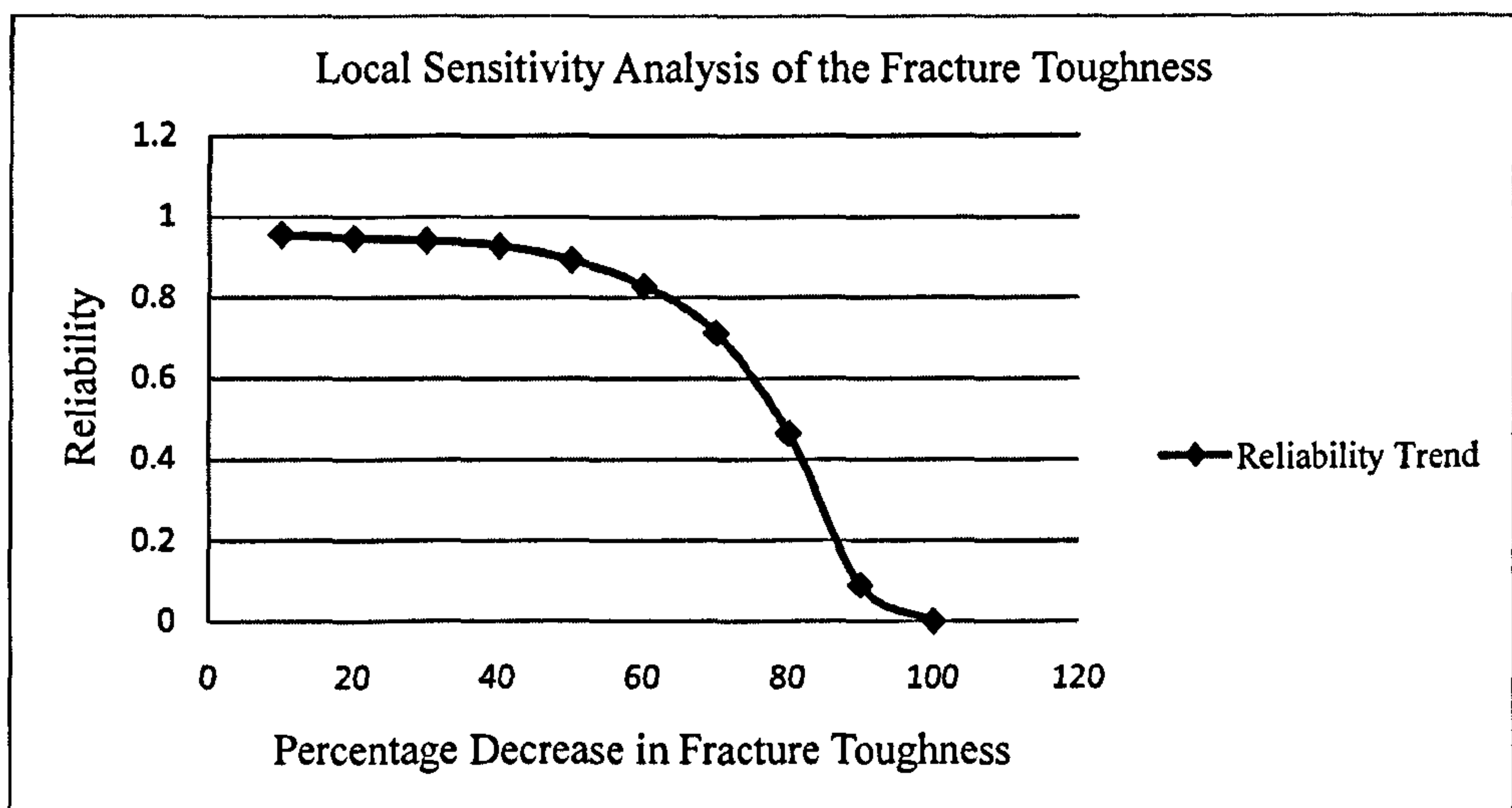


Figure (3.40) – Local sensitivity analysis of fracture toughness.

The gentle gradient is as a result of the representation in Figure (3.31). Placing this observation by the side, the decrease in the fracture toughness could be imagined as a gradual shift of the material resistance (on the right of Figure (3.31)) towards the load parameter (stress intensity factor). The initial shifts have little overlaps, hence the gentle slope. More movement (decrease in fracture toughness) towards the loads parameter results in more overlaps and thus more failures. The lognormal nature causes steeper falls in the reliability.

### 3.8.2.3 Defect (crack) Size

This is the estimated crack length on a repeatedly loaded area on a structure. From Tables (3.12) and (3.13), the effect of the changes to this parameter on three of the four limits states could be observed. The influence is very low compared to that of the fracture toughness.

	Percentage change				
	10%	20%	30%	40%	50%
Limit State I	0	0	0	0	0
Limit State II	2311	2958	3313	4194	4551
Limit State III	942	1418	1627	2088	2424
Limit State IV	2557	3286	3808	4458	4928
Total	5810	7662	8748	10740	11903
Reliability	0.9419	0.92338	0.91252	0.8926	0.88097

Table (3.12) – Effect of crack length increase on reliability.

	Percentage change				
	60%	70%	80%	90%	100%
Limit State I	0	0	0	0	0
Limit State II	5734	6363	7065	7548	8266
Limit State III	3106	3554	4153	4432	5031
Limit State IV	6032	6636	7343	7706	8154
Total	14872	16553	18561	19686	21451
Reliability	0.85128	0.83447	0.81439	0.80314	0.78549

Table (3.13) – Effect of crack length increase on reliability.

Percentage decrease	Reliability	Percentage Change in Reliability
10	0.9419	1.66
20	0.92338	3.60
30	0.91252	4.73
40	0.8926	6.81
50	0.88097	8.02
60	0.85128	11.12
70	0.83447	12.88
80	0.81439	14.97
90	0.80314	16.15
100	0.78549	17.99

Table (3.14) – Trended change in reliability (crack length).

The crack length estimation is a relative case as two similar structures could have different crack propagations (e.g. different loading scenarios and different crack lengths). As a result, where conservative values are chosen, the effects may not be as pronounced or may be overemphasized as the case may be. These values (upper and lower crack length bounds) have been increased steadily by 10%. The effect is not as great as that of the fracture toughness; however the reduction in the reliability is still significant. The percentage change in reliability in Table (3.14) follows decreasing trend though not entirely linear in Figure (3.41).

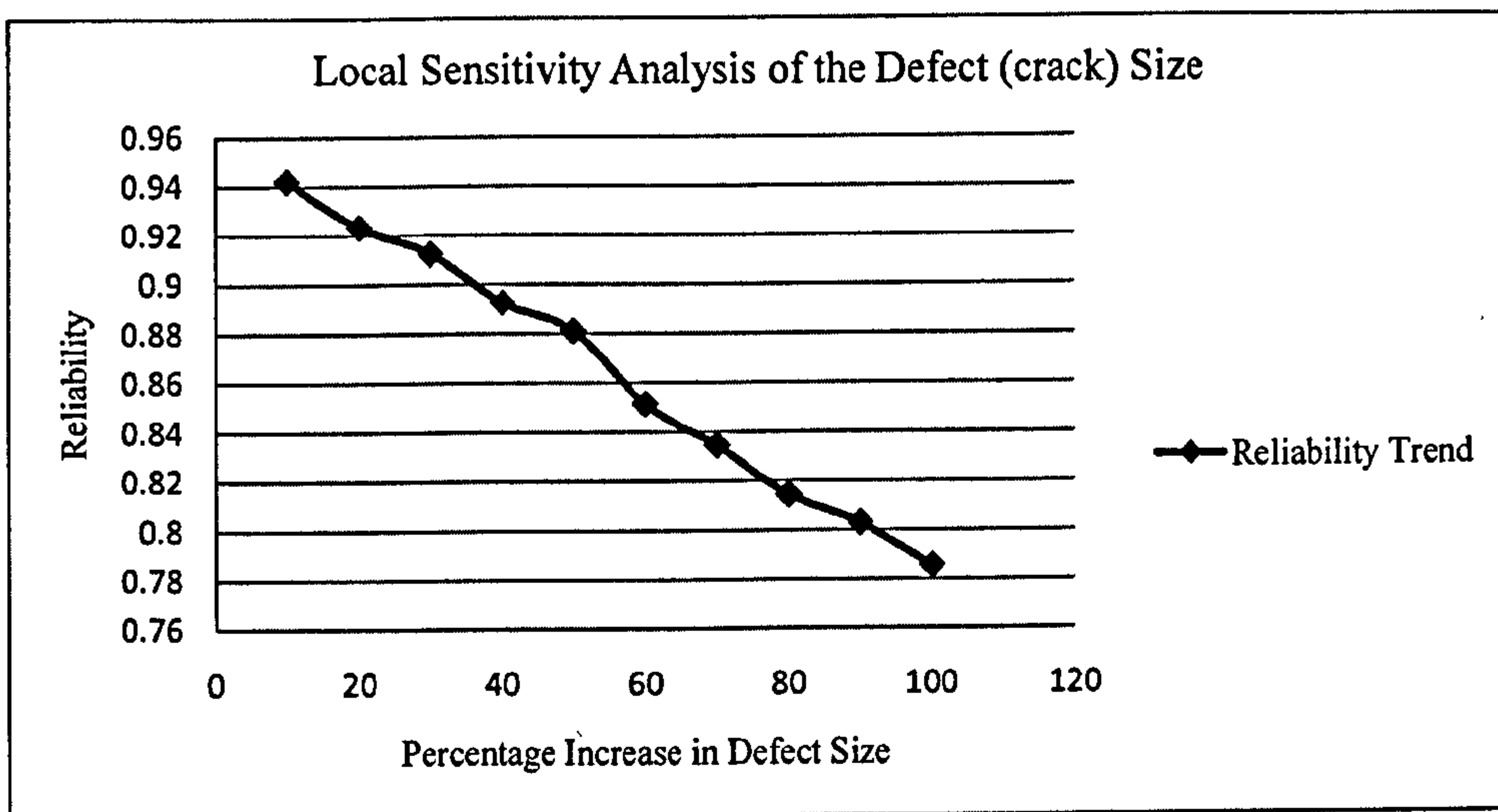


Figure (3.41) – Local sensitivity analysis of the defect (crack) size.

#### 3.8.2.4 *Planned Life*

The planned life is incorporated in the design of a structure after a consideration of several real scenarios. The amount of uncertainty present prompts the use of safety factors.

	Percentage change				
	10%	20%	30%	40%	50%
Limit State I	0	0	0	0	0
Limit State II	1781	1781	1781	1781	1781
Limit State III	662	662	662	662	662
Limit State IV	2213	2321	2424	2560	2669
Total	4656	4764	4867	5003	5112
Reliability	0.95344	0.95236	0.95133	0.94997	0.94888

Table (3.15) – Effect of planned life increase on reliability.

	Percentage change				
	60%	70%	80%	90%	100%
Limit State I	0	0	0	0	0
Limit State II	1781	1781	1781	1781	1781
Limit State III	662	662	662	662	662
Limit State IV	2702	2750	2857	2879	2947
Total	5145	5193	5300	5322	5390
Reliability	0.94855	0.94807	0.947	0.94678	0.9461

Table (3.16) – Effect of planned life increase on reliability.

From Tables (3.15) and (3.16) it can be observed that the only limit state that undergoes any significant change is limit state IV (the life limit state). This could be inferred as rational since any attempt to utilize a structure beyond its prescribed life can only increase the chances of a failure.

The data outlined in Table (3.17) shows conservative changes compared to those of the fracture toughness and crack length. The relationships could be said to be near linear as shown in Figure (3.42).

Percentage decrease	Reliability	Percentage Change in Reliability
10	0.95344	0.46
20	0.95236	0.57
30	0.95133	0.68
40	0.94997	0.82
50	0.94888	0.93
60	0.94855	0.97
70	0.94807	1.02
80	0.947	1.13
90	0.94678	1.15
100	0.9461	1.22

Table (3.17) – Trended change in reliability (planned life).

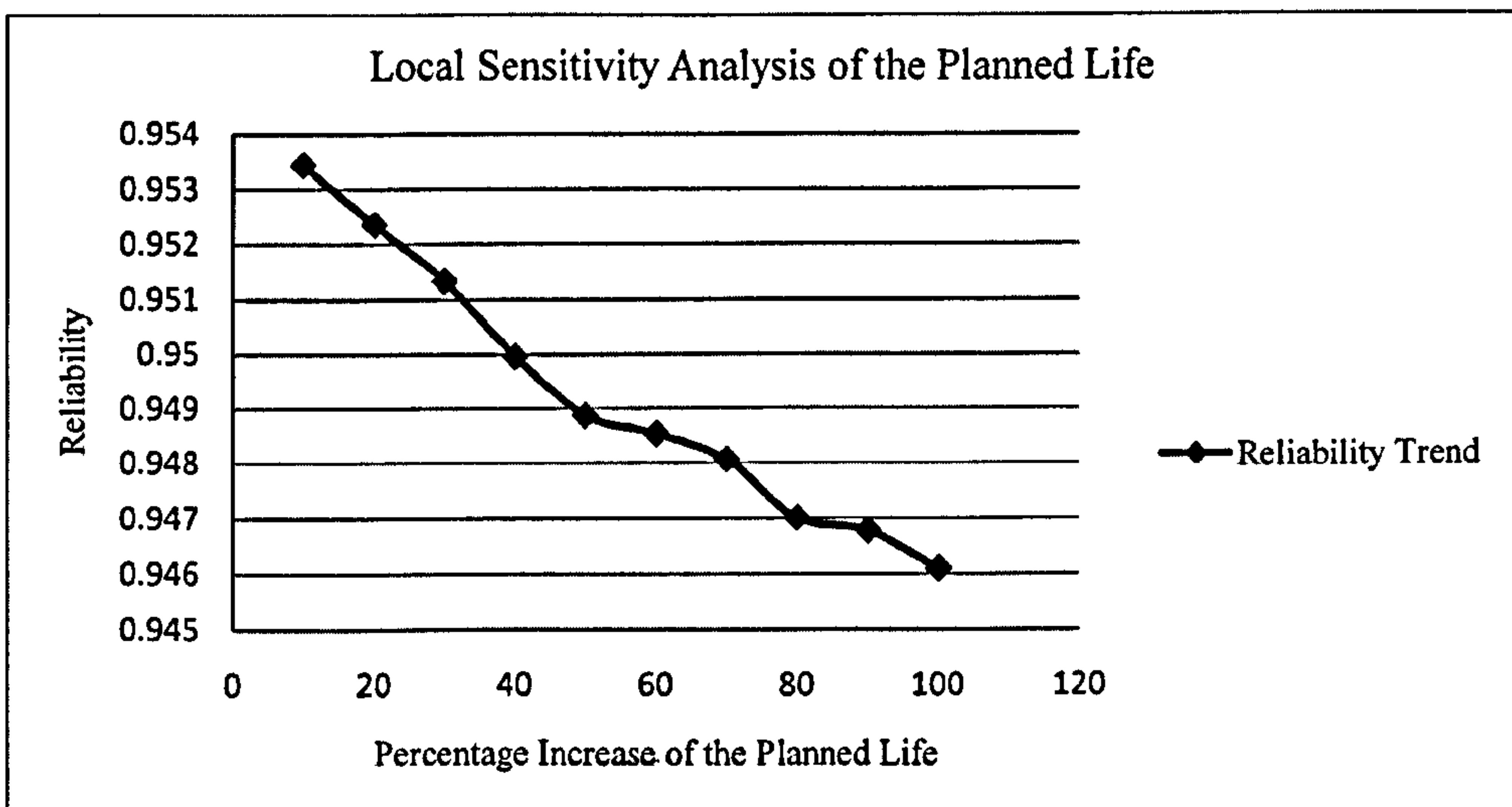


Figure (3.42) – Local sensitivity analysis of the planned life.

### 3.8.2.5 Loading

Prior to operations, working/maximum rated loads are usually designated to lifting equipment, structures, vehicles, etc. This is done to prevent mechanical failures. However the loading also has an input on the stress intensity factor, crack propagation and consequently the life of the structure.



	Percentage change				
	10%	20%	30%	40%	50%
Limit State I	0	0	0	0	0
Limit State II	1727	2027	2301	2477	2709
Limit State III	663	760	871	980	1108
Limit State IV	2072	2399	2694	2811	3244
Total	4462	5186	5866	6268	7061
Reliability	0.95538	0.94814	0.94134	0.93732	0.92939

Table (3.18) – Effect of load increase on reliability.

	Percentage change				
	60%	70%	80%	90%	100%
Limit State I	0	0	0	0	0
Limit State II	3021	2998	3118	3825	3780
Limit State III	1162	1294	1469	1730	1797
Limit State IV	3570	3675	3968	4477	4860
Total	7753	7967	8555	10032	10437
Reliability	0.92247	0.92033	0.91445	0.89968	0.89563

Table (3.19) – Effect of load increase on reliability.

Percentage decrease	Reliability	Percentage Change in Reliability
10	0.95538	0.25
20	0.94814	1.01
30	0.94134	1.72
40	0.93732	2.14
50	0.92939	2.97
60	0.92247	3.69
70	0.92033	3.91
80	0.91445	4.53
90	0.89968	6.07
100	0.89563	6.49

Table (3.20) – Trended change in reliability (loading).

From Figure (3.28) the over-design involved can be observed. This is further buttressed in Tables (3.18) and (3.19) by the zero failure in limit state I (stress limit state) at all load increment levels.

All other limit states still undergo significant changes nonetheless as a result of the relationships discussed in the model. The data from Table (3.20) is represented in Figure (3.43).

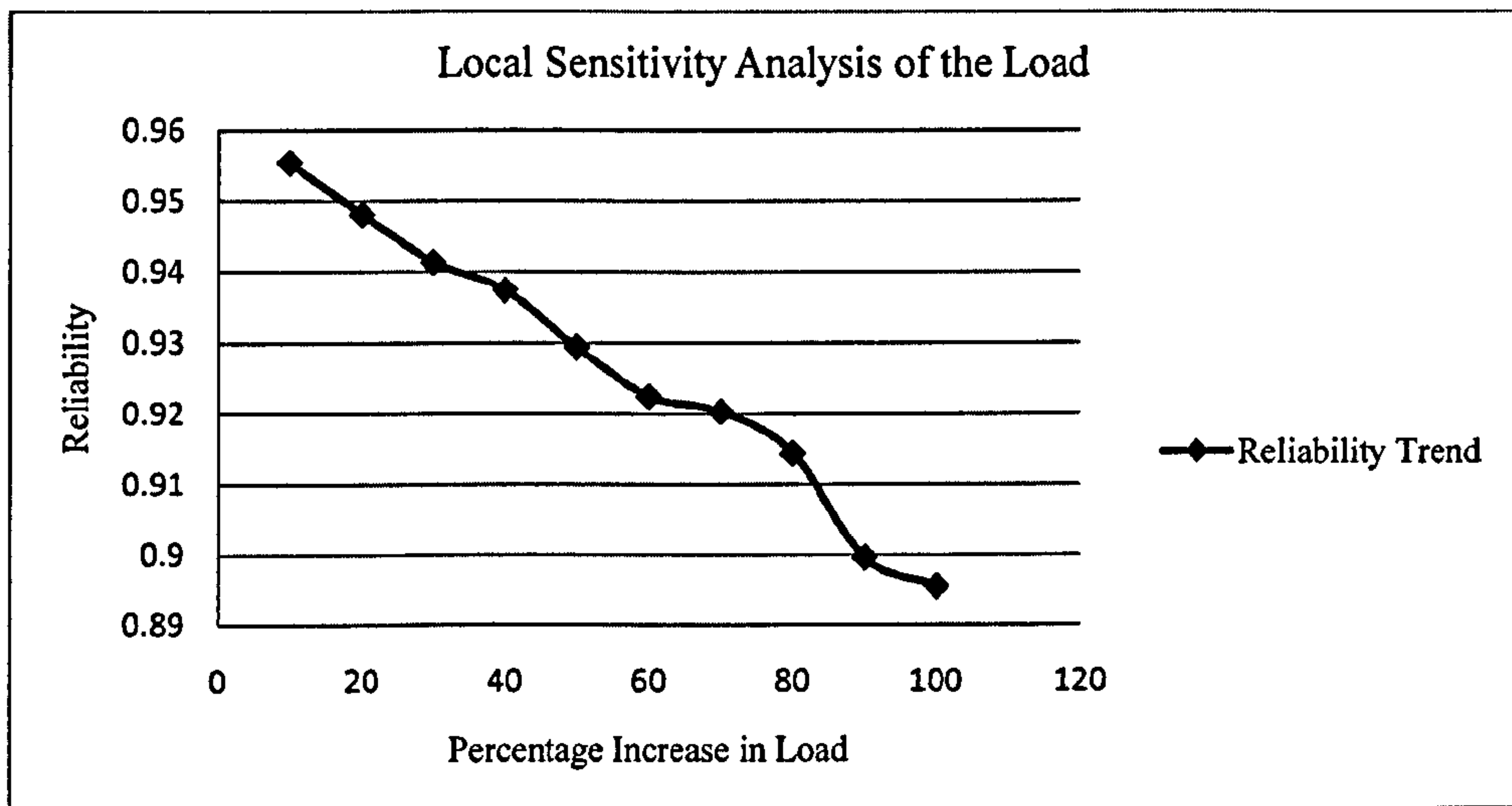


Figure (3.43) – Local sensitivity analysis of the load.

### 3.9 Conclusion

The BETA-FLEXSTREM has been developed as a method for quantifying the risk of SMSs (albeit of a specific type).

The result of the sensitivity analyses followed fairly reasonable trends. The trends suggest that better defined relationships between the system definition parameters are necessary for improvement of the algorithm.

Through the BETA-FLEXSTREM, the response of the structure, subject to inherent uncertainties, could be viewed graphically. These responses have also been subjected to limit states in order to establish the reliability of the structure. It was observed that the reliability estimations for MCS iterations/trials greater than 100,000 trials showed reasonable consistency.

The demonstration of such an algorithm is indicative of the possibilities of the MCS and limit state principles being extended to deal with more complex structures. This would lead to the development of a full version of the FLEXSTREM as would be seen in chapter 5.

## **Chapter 4:**

# **Environmental, Structural and Operational Data Requirements for Structural Analyses including Demonstrational Case Studies**

### **Summary**

*This chapter contains a discourse on system definition and case studies to be used in the subsequent chapters. The subsequent chapters draw information pertaining to the data and the given case studies for demonstration of the proposed methodologies from this chapter. The information and assumptions in this chapter are valid at all points of reference. This prevents unnecessary repetition and it enhances the organisational structure of this research.*

### **4.1 Environmental, Structural and Operational Data Requirements**

This chapter deals with the system definition step (for the most part) in the modified FSA methodology presented in chapter 1. The case studies (defined according to the system definition presented here) are also outlined. This chapter is not intended for technical discourse but for clarity purposes and to enable neat presentation without the need for bulky repetitions (especially the case studies) in the subsequent chapters.

The system definition step is highlighted in Figure (4.1). Primarily system definition in risk analysis involves some form of description of the risk scenario(s) and all the influencing factors. In the context of this research (structures), the system definition (second step of the modified FSA) involves the definition of the scenarios concerned with the identified focal area in the field of design (fatigue for this research). There are three main components necessary for the definition of the system. They include:

- Structural definition.
- Environmental definition.
- Operation definition.

This chapter only deals with these three in detail while the relationship between all three of them and the structural response is dealt with in chapter 5 – the risk quantification step. The relationship between the three main components listed above is still part of the system definition as it is also a vital description of the risk scenario. The structural response is a result of all the interactions between the main components modelled in this relationship.

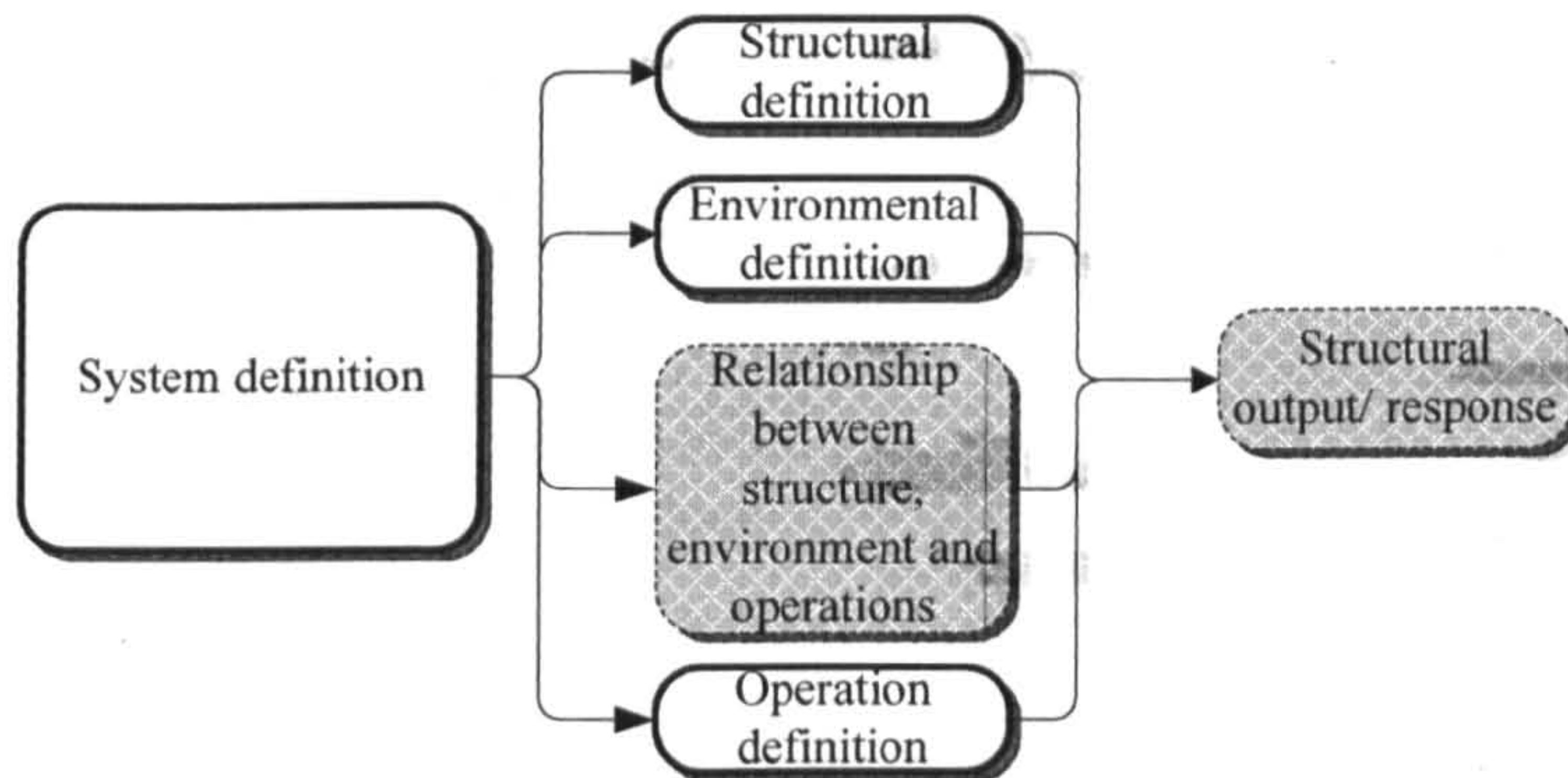


Figure (4.1) – System definition parameters highlighted.

These parameters are gathered by a part (module) of the flexible structural reliability algorithm (FLEXSTREM). There are two classes of data listed – primary and secondary data. The primary data are read directly from an input in the data gathering module. The secondary (derived) data are products of the primary data. They are listed in this chapter because they are also gathered in a data collection module before being passed on to the main algorithm(s). Table (4.1) lists the primary parameters, their symbols and units. Table (4.6) lists similar categories in addition to their derivations. Also listed are the parameters needed by both analyses types; type I – single-member structures (SMS) and type II – multi-member structures (MMS).

System definition component	Parameter name	Symbol	Unit	Type	
				I	II
Structural definition	Number of structural nodes	$N_{node}$	-	-	✓
	Number of structural elements	$N_{mem}$	-	-	✓
	Young's modulus	$E$	MPa	✓	✓
	Uniaxial yield strength	$F_y$	MPa	✓	✓
	Tensile strength	$F_{ten}$	MPa	✓	✓
	Fracture toughness	$K_{IC}$	MPam <sup>1/2</sup>	✓	✓
	Material density	$mat_d$	kg/m <sup>3</sup>	✓	✓
	Dead load	$LD_{dead}$	kg	✓	✓
	Stress intensity correction factor	$mat_\beta$	-	✓	✓
	Crack growth exponent	$mat_m$	-	✓	✓
	Crack growth rate	$mat_C$	-	✓	✓
	Initial crack length	$a_i$	m	✓	✓
	Detectable crack length	$a_d$	m	✓	✓
	Focal member of analysis	-	-	-	✓
	Focal node of analysis	-	-	-	✓
	Maximum rated load	$Max_{RL}$	kg	✓	-
	Thickness	$thk$	m	✓	-
Total length	$T_{len}$	m	✓	-	
Width*	$W_{dh}$	m	✓	-	
Operation definition	Loaded cycles/year	$N_{STL}$	-	✓	✓
	Unloaded cycles/year	$N_{STU}$	-	✓	✓
	Number of years in service	$N_{YRS}$	years	✓	✓
Environmental definition	Wind speed on structure	$w_s$	m/s	✓	✓
	Average wind force on live load	$W_{fl}$	N	✓	✓

\* not for radial members

Table (4.1) – Data required for FLEXSTREM analysis.

The parameters outlined in Tables (4.1) are sufficient for a type I (SMS) analysis (where ticked). For a type II (MMS) analysis, the following structural definition input variables for a finite element analysis (FEA) are read/initialized (in addition to those in Table (4.1)):

- structure's nodes on the x, y and z axes (3-d Cartesian coordinates) as shown in Table (4.2):

Node	Coordinates
Node index 1	[x-coordinate],[y-coordinate],[z-coordinate]
Node index 2	[x-coordinate],[y-coordinate],[z-coordinate]
etc.	etc.

Table (4.2) – Node data.

- structural member node connections horizontally placed alongside the following (illustrated in Table (4.3)):
  - a ratio of the Young’s modulus of the material of a particular member to that of the structural (principal) material (for the case of members of different materials)
  - outer diameter of the members (at this stage the FLEXSTREM covers only tubular members) (m)
  - the thickness of the cross section (for hollow/ tubular sections) (m)

Member	Node connection	Young’s Modulus ratio	Diameter	Thickness	Member group
Member index 1	[node index], [node index]	ratio	member diameter (m)	member thickness (m)	Group indicator
Member index 2	[node index], [node index]	ratio	member diameter (m)	member thickness (m)	Group indicator
etc.	etc.		etc.	etc.	etc.

Table (4.3) – Member data.

- number of zero displacement nodes (constraints)
- node(s) of zero displacement alongside direction as shown in Table (4.4):

Number of node constraints (in each direction of every node)	
Constrained node(s)	Direction
Node index 1	single coordinate (x, y or z)
Node index 2	single coordinate (x, y or z)
etc.	etc.

Table (4.4) – Constraint data.

- number of loads (live loads) on structures
- node(s) with live load(s) alongside direction(s) and a given load (MN) as shown in Table (4.5):

Number of node loadings (in each direction of every node)		
Loaded node(s)	Direction	Load value (MN)
Node index 1	single coordinate (x, y or z)	Load
Node index 2	single coordinate (x, y or z)	Load
etc.	etc.	etc.

Table (4.5) – Loading data.

#### 4.2 Secondary (Derived) Data

After the aforementioned data from section 4.1 are read, the following manipulations (Table 4.6)) take place to provide the remaining initial data for analyses:

System definition component	Parameter name	Symbol	Derivation	Unit	Type	
					I (single)	II (multi)
Operation definition	Planned life	$N_{PL}$	$N_{STL} \times N_{YRS}$	-	✓	✓
	Total life	$N_{TL}$	$(N_{STL} + N_{STU}) \times N_{YRS}$	-	✓	✓
Structural definition	Second moment of the closed section area of the beam	$I_{mont}$	$[(W_{dh} \times H_{gt})^3 / 12]^{\dagger}$	m <sup>4</sup>	✓	-
	Cross-sectional area	$C_A$	$[W_{dh} \times H_{gt}]^{\dagger}$	m <sup>2</sup>	✓	-
	Total mass	$LD_{struct}$	$C_A \times T_{len} \times mat_d$	kg	✓	-

<sup>†</sup> in the appropriate context of shape and thickness

Table (4.6) – Derived data.

#### 4.3 Data Distribution Sources

Certain distributions have been adopted for the variables in the Monte Carlo simulation. Table (4.7) presents these variables and their sources cited from literature. For the variables absent from the table, the central limit theorem is assumed (section 2.5.1.7).

Variable	Distribution	Source(s)
Wind	Gumbel	Simiu and Heckert (1996)
Stress	Gaussian	Huajian and Yongchang (1995)
Design life	lognormal	Chryssanthopoulos and Righiniotis (2006)
Defect (crack length)	exponential	Karamchandani et al (1991)
Fracture toughness	lognormal	Pillai and Prasad (1997)
Crack growth rate coefficient	lognormal	Pillai and Prasad (1997)

Table (4.7) – Data distribution and sources.



#### **4.4 Reliability Value Implication and Notation**

The figure depicting the reliability of a structure is not and should not be misconstrued for the structural integrity. The reliability is a measure, given certain parameters (limit states in this research), of the structure's performance. Limit states are benchmarks. The reliability value could be more appropriately prefixed with terms like "mechanical reliability", "fatigue reliability", etc. These show the standards by which the structure's performance was measured. No system can be completely defined; however means to ascertain its performance (and hence integrity) ought to be provided for quality and safety purposes. The absence of failure by any or a combination of benchmarks (limit states) does not mean that the integrity of a given structure is perfect. Even the benchmarks themselves are not completely defined: no benchmark is. Thus a reliability notation of 1 is misleading; it is not possible. For this reason, certain notations for scenarios depicting "reliability = 1" have been adopted in this research. For a simulation of 10000 trials which ends up with a reliability of 1, the following is denoted instead of "1":

0.9999 or

0.9<sub>4</sub>.

For 100000 trials,

0.99999 or

0.9<sub>5</sub>.

etc.

#### **4.5 Case Studies in this Research**

Two case studies are considered in this research in order to ascertain the practicability of the FLEXSTREM (and its variants). The first case study deals with the boom of an offshore crane mounted on an offshore platform. The second case study is found in numerous journals such as Kunar and Chan (1976), Sadek (1985), Coello and Christiansen (2000), Park and Sung (2002), Li and Yang (1994) to name a few. This case study has been culled from journals dealing with optimization. The results from the FLEXSTREM optimization (FLEXOPT) analysis would be compared to those from literature.

#### 4.5.1 Case Study 1: Offshore Crane Boom

An offshore crane is considered. The crane information is from a haulage company in Austria who wish to remain anonymous. The company builds several types of cranes for various operations in the maritime sector. The company's ship crane ranges are designed to handle demand on board all types of vessels including heavy lift requirements. Services to the offshore industry in the form of built-to-order lifting equipment are offered by the company. Floating cranes and bulk handlers are also available.

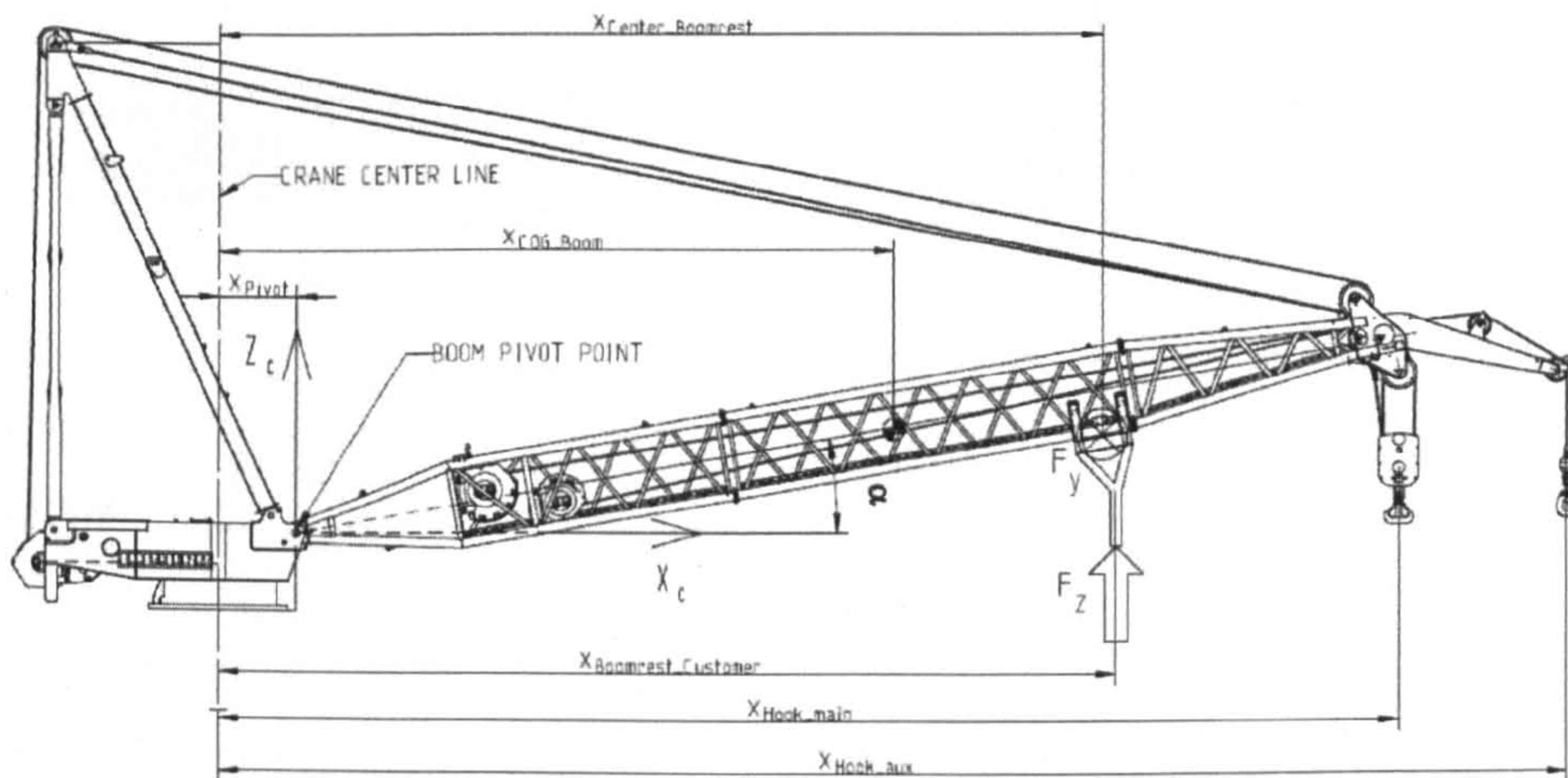


Figure (4.2) – Crane outline.

Figure (4.2) is the outline of a typical offshore crane built by the company. The crane is located on an offshore platform that operates all year round on a very busy schedule. Analysis on this crane is focused solely on the structural aspects of the boom arm (illustrated in Figure 4.3). No lifting mechanisms, machinery or auxiliary appendages were taken into consideration.

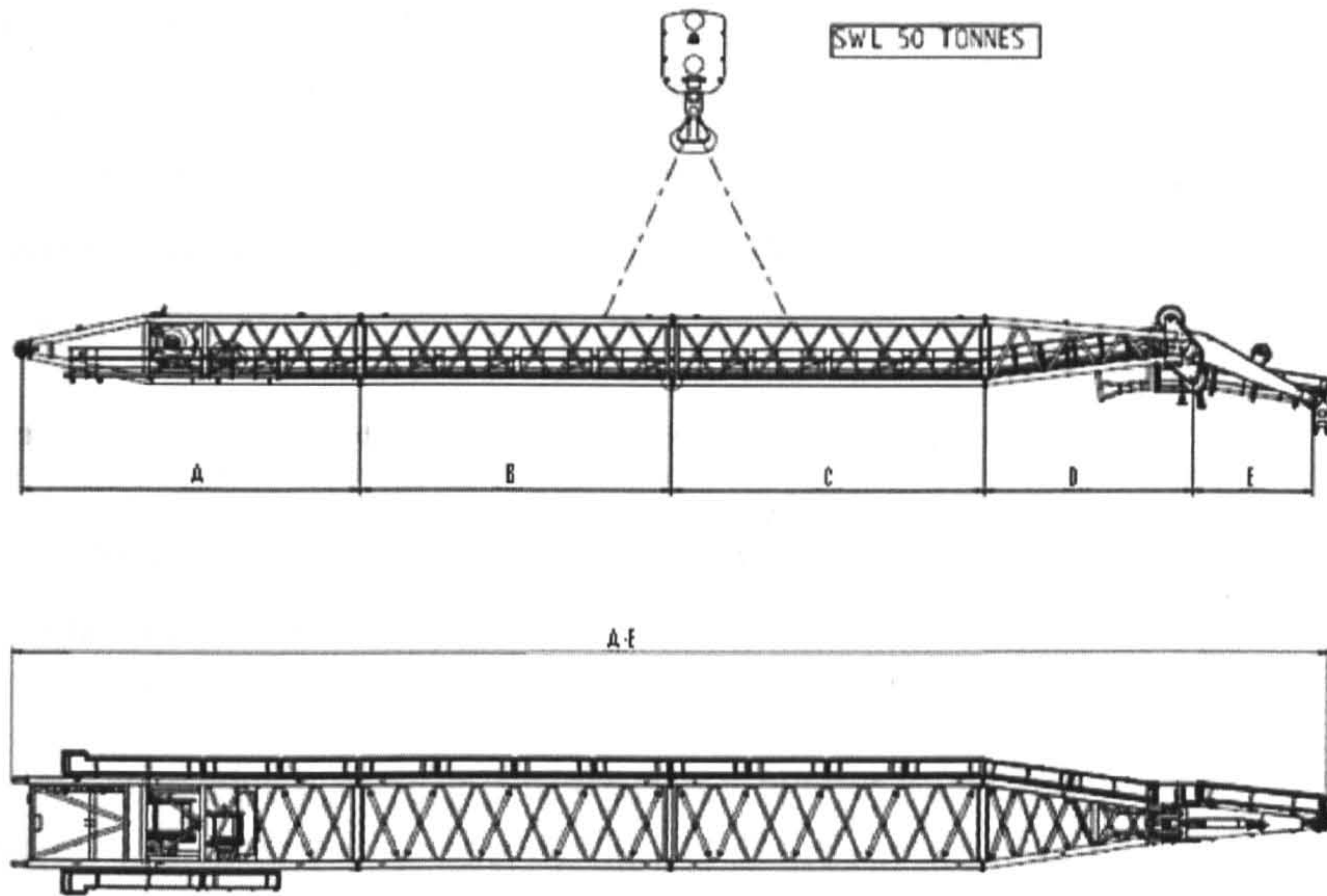


Figure (4.3) – Boom outline.

Some idealization had to be done to set up the crane boom arm up for analysis. The section E (Figure (4.3)) has been omitted.

From the idealization, the total node points (joints) on the crane boom is 121 and the total members equal 360. The maximum rated load is 50 tonnes. The hook block (dead load) is 4.6 tonnes.

The material is AISI1015 (low carbon steel). It has a density of  $7870 \text{ kg/m}^3$ . The Young's modulus of the material is 205,000 MPa. The uniaxial yield strength is 325 MPa, and the tensile strength is 385 MPa.

The design environmental wind speed average is 25 m/s. The wind force on the working load averages 3.75 kN.

The fracture toughness is  $50 \text{ MPam}^{1/2}$ . The crack growth exponent is 3 and the crack growth rate coefficient is  $4 \times 10^{-11}$ . At the nodes, the crack defect has a lower bound of 1 mm in radius and the detectable crack length is also of 1 mm radius.

The structure is 100% homogenous materially (linear behaviour). The length (x-axis) is 40 m, the height (y-axis) is 2 m and the width (z-axis) is 3 m. There are two characteristic diameters in the abstracted crane boom - the truss diameter (0.1500 m with a thickness of 0.0253 m) and the chord diameter (0.2730 m with a thickness of 0.0192 m). The overall mass of the abstracted crane boom is approximately 75000 kg.

The first two nodes (pivot) of the boom are restrained in the x and z directions only (i.e. 4 zero-displacements in total). The 121st node (load end) is the only loaded node with the load acting in the negative (downwards) y-direction.

The assumed global COV of the resistance (strength function) for all distributions is 0.06 (i.e. 6%) and 0.08 (i.e. 8%) for the demand (each stress function).

#### *Life Cycle and Loading*

The crane is located on an offshore platform that operates all year round on a very busy schedule. It is assumed that the crane is in operation for a maximum of 5 hours (~20% of the day) every day all year round. Thus for the loaded life cycle per year,  $N_{STL}$  is:

$$\begin{aligned}
 N_{STL} &= 0.2 \times \left(\frac{1 \text{ cycle}}{9 \text{ sec}}\right) \times \left(\frac{365 \text{ days}}{1 \text{ year}}\right) \times \left(\frac{24 \text{ hrs}}{1 \text{ day}}\right) \\
 &\quad \times \left(\frac{60 \text{ min}}{1 \text{ hr}}\right) \times \left(\frac{60 \text{ sec}}{1 \text{ min}}\right) \\
 &\approx 1.05 \times 10^4 \text{ cycles/yr}
 \end{aligned}
 \tag{4.1}$$

For unloaded cycles,

$$\begin{aligned}
 N_{STU} &= 0.8 \times \left(\frac{1 \text{ cycle}}{9 \text{ sec}}\right) \times \left(\frac{365 \text{ days}}{1 \text{ year}}\right) \times \left(\frac{24 \text{ hrs}}{1 \text{ day}}\right) \\
 &\quad \times \left(\frac{60 \text{ min}}{1 \text{ hr}}\right) \times \left(\frac{60 \text{ sec}}{1 \text{ min}}\right) \\
 &\approx 2.8 \times 10^6 \text{ cycles/yr}
 \end{aligned}
 \tag{4.2}$$

This crane is permitted to perform in this capacity all year round for a period of 25 years and is subjected to inspection twice a year.

It is idealized for analysis purposes and visually illustrated (using Gmsh). The tapered section of the boom where the loading takes place is much improvised; it is not

uniformly tapered on closer inspection. This would no doubt have an effect on the FEA result.

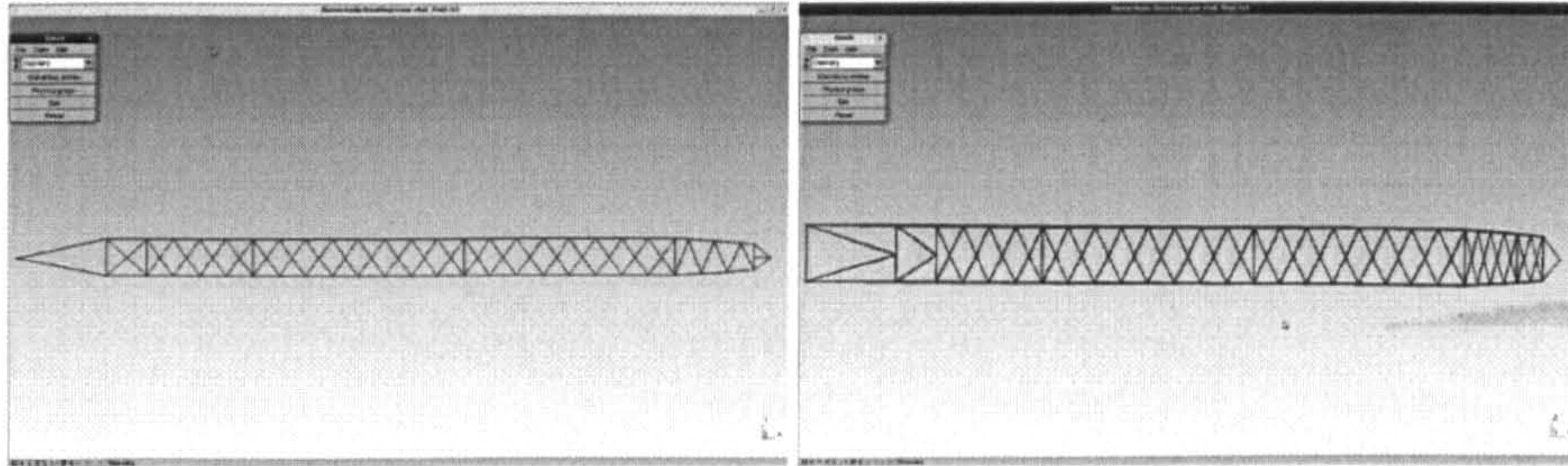


Figure (4.4) – Lateral view and top view of idealized crane boom.

Figure (4.4) shows the lateral and top view of the Gmsh construction. The lifting mechanisms (hook, auxiliary hoist, etc.) have been represented as a point end where load is exerted. Figure (4.5) shows an isometric view of the crane boom.

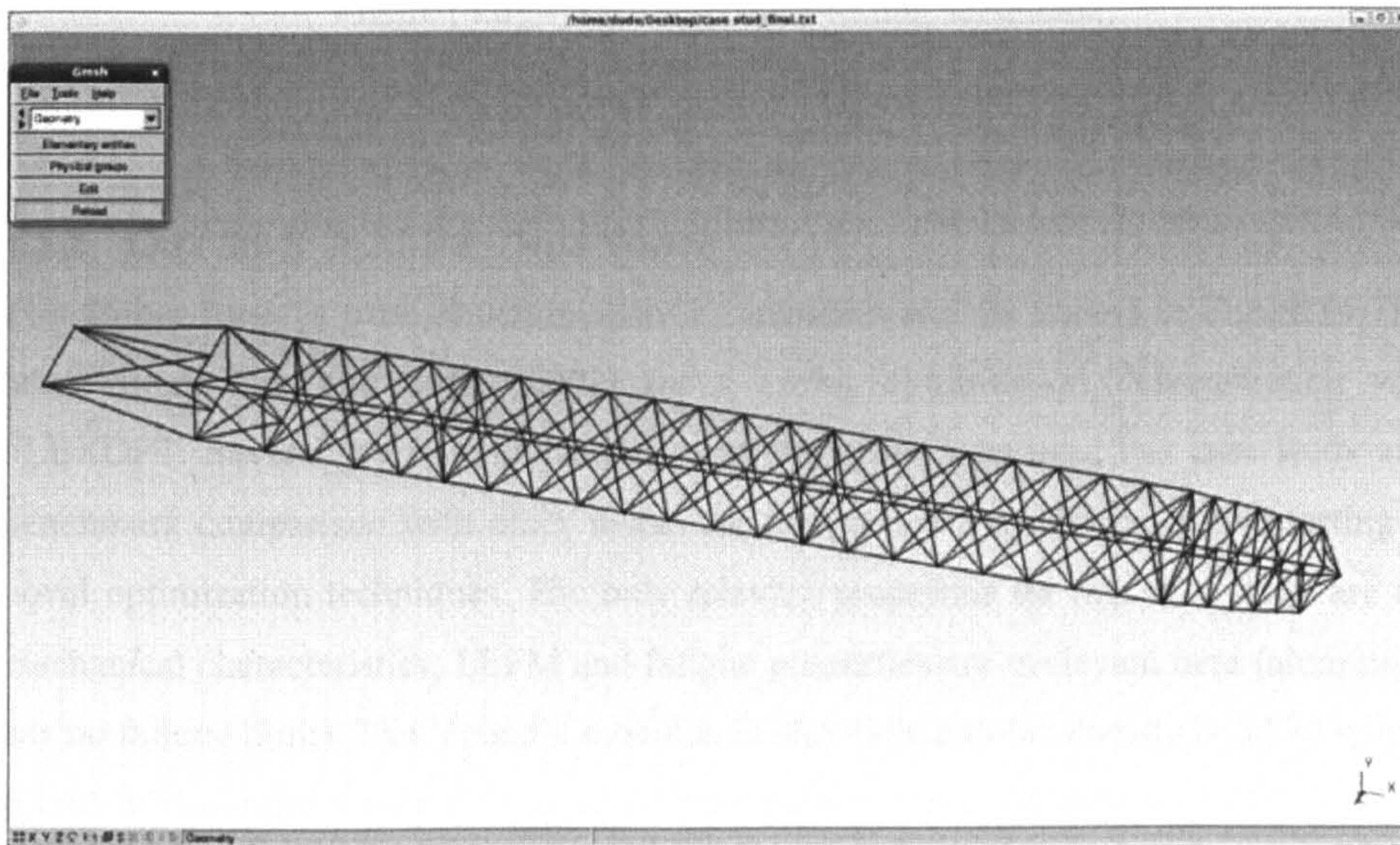


Figure (4.5) – Isometric view of the idealized crane boom.

The first two nodes (pivot) of the boom are restrained in the x and z directions only (i.e. 4 zero-displacements). The 121st node (load end) is the only loaded node with the load acting in the positive (downwards) y-direction. The constraint and loading representations are shown in Figure (4.6).

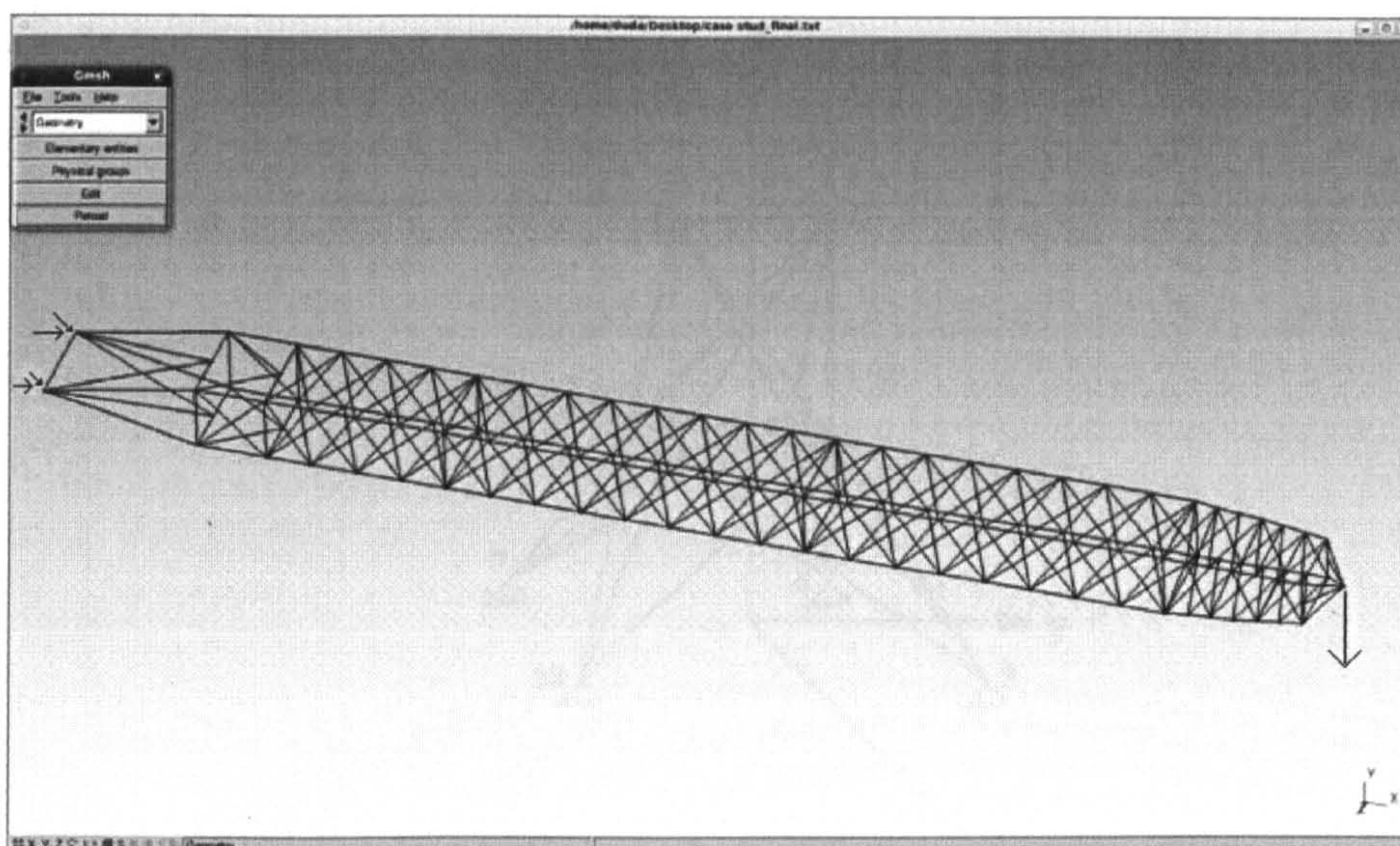


Figure (4.6) – Restraints and loading schematic.

#### 4.5.2 Case Study 2: 25-Bar Truss System

The 25-bar truss (a truss structure with 25 members and 10 nodes) in Figure (4.7) is taken from Park and Sung (2002) for a sizing optimization demonstration with FLEXOPT. Several journal publications over the years have used this case study as a benchmark comparison with other works for the purposes of efficiency and testing of novel optimization techniques. The only relevant properties for this case study are the mechanical characteristics; LEM and fatigue properties are irrelevant here (aluminium has no fatigue limit). The Young's modulus is 68.9 GPa and the density is 2,770 kg/m<sup>3</sup>. Based on these properties, it is assumed that the material is Aluminium 6061-O with a uniaxial yield strength of 55.2 MPa and uniaxial tensile strength of 124 MPa. Dummy data is put in all other data areas required in section 4.1 to avoid floating point errors during the simulation.

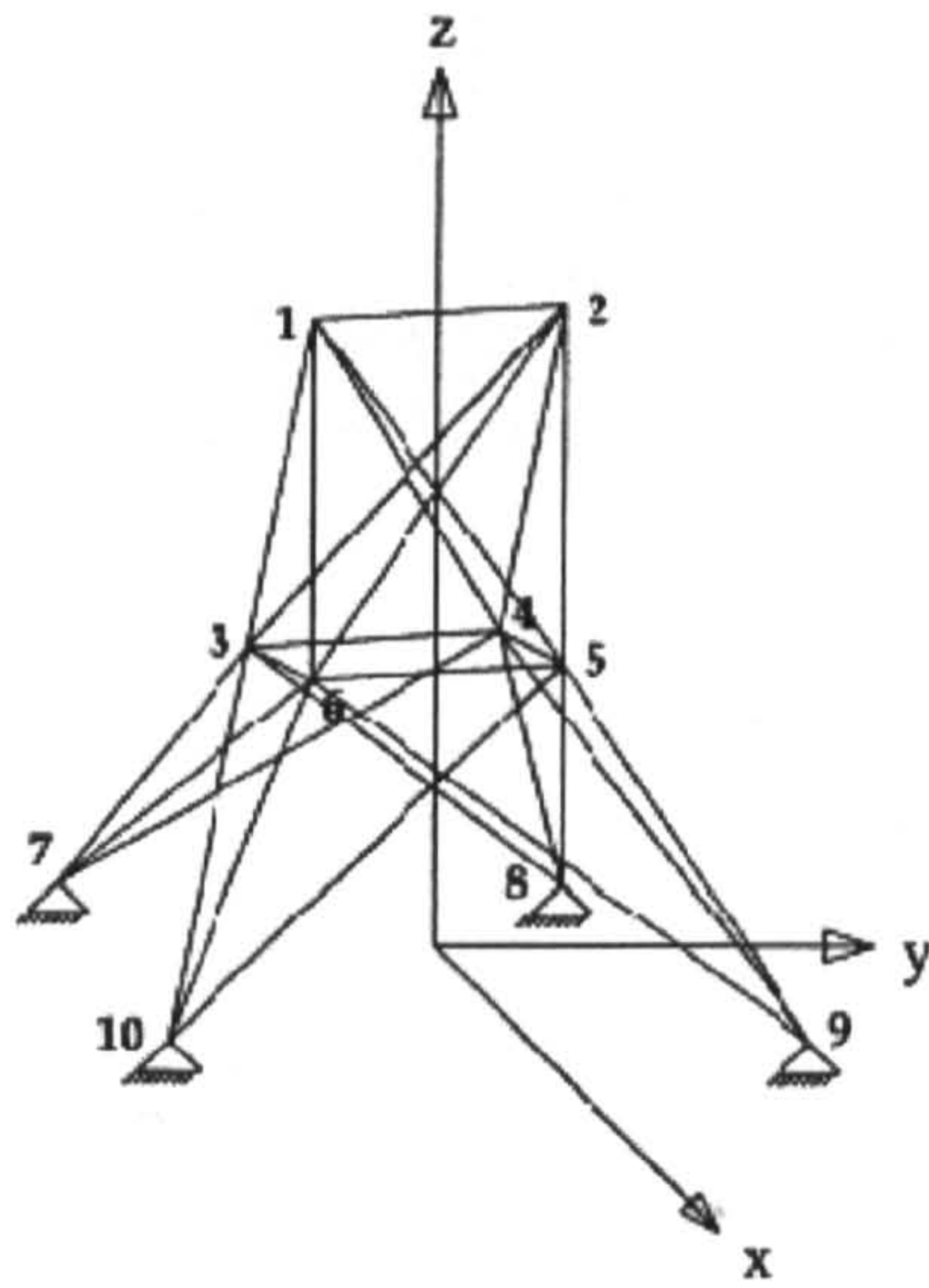


Figure (4.7) – 25-bar truss (Park and Sung (2002)).

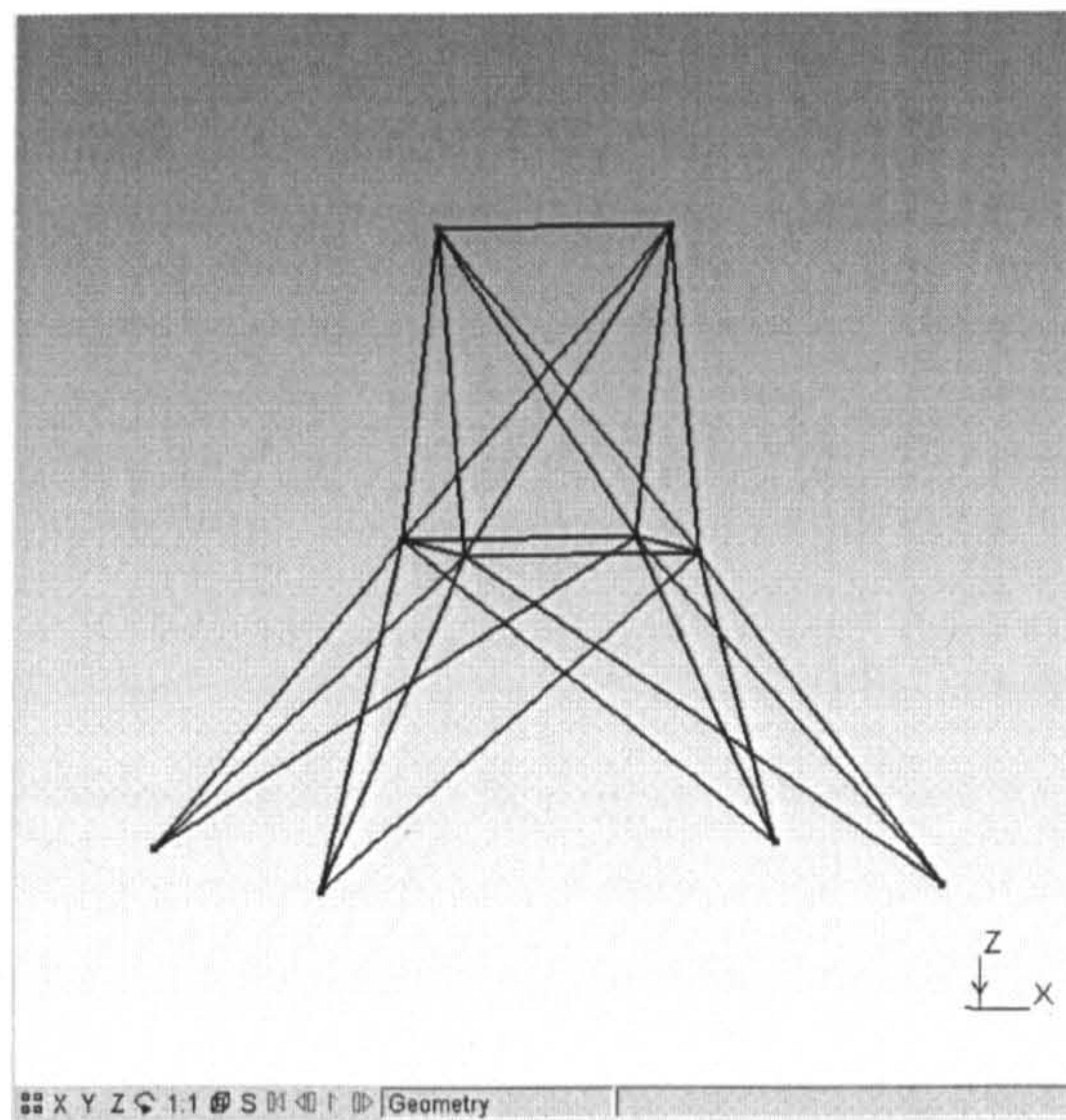


Figure (4.8) – Gmsh representation of the 25-bar truss.

Figure (4.8) shows a visual representation in Gmsh. As a starting configuration, all the member groups are assumed to have a similar configuration with 0.06 m as the diameter and 0.0015 m as the thickness.

## **Chapter 5:**

# **Flexible Structural Reliability Algorithm (FLEXSTREM): A Risk Quantification Tool for Marine/Offshore Structures**

### **Summary**

*This chapter presents a FLEXible STructural REliability algorithm (FLEXSTREM) for quantifying the risk (obtaining the reliability) of multi-member structures (MMSs). The methodology utilizes the well known finite element analysis in conjunction with the Monte Carlo simulation to carry out reliability analysis for these structures. In the model, major loading and stress scenarios are considered. A number of failure criteria (in the form of limit states) are also incorporated. A demonstration is carried out on the boom of a crane. Hereafter a partial validation by sensitivity analysis is performed.*

### **5.1 Introduction**

Structures in the offshore environment often consist of several members due to transportation, fabrication, deployment, etc. These factors share a common parameter – cost. The cost is further over-ached by safety. The safety is paramount in the transportation, fabrication and deployment of the structure. These engineering structures are designed to meet functional, economic and safety requirements (Wu and Moan (1991)).

The urgency to progress from a prescriptive design (safety factor or allowable stress design (ASD)) to a goal oriented design (reliability based) for optimum cost and integrity has been emphasized in chapter 2.

A beta version of the FLEXible STructural Reliability algorithm (BETA-FLEXSTREM) – a time-invariant technique for the quantification of risk in



marine/offshore structures was presented in chapter 3. This methodology encompassing various stress and LEFM (linear elastic fracture mechanics) models was applicable only to SMSs. The implementation via FORTRAN enabled visualisation of the structural response (stresses) as a result of the loads induced. The reliability based on the stress and LEFM models was thus determined.

Improvements to be made to the BETA-FLEXSTREM are numerous. A major development is the incorporation of the finite element analysis (FEA). It was not an exercise to reinvent the wheels for the FEA but rather, an occasion to utilize the outputs in a very efficient manner, as a means to estimate the reliability of an entire MMS while addressing each member and joint (node) individually (and not generically). In deriving this reliability, the roles of classic mechanics and linear elastic fracture mechanics (LEFM) are vital as they provide consistency to the flexibility provided by the FEA.

## 5.2 Background

Reliability in general could be determined purely on statistics (fully probabilistic) or based on modelling from first principles. Structural system failure could be modelled as a single failure event (fully probabilistic analysis) (Equation (5.1)), a union of intersections of component failure events (Equation (5.2)), or a union of component failure events (Equation (5.3)) (Wu and Moan (1991)).

$$S_{(F)} \rightarrow P_{(F)} \quad (5.1)$$

$$P_{(F)} \rightarrow (C_{(g)} \cap C_{(h)} \cap \dots C_{(l)}) \cup (C_{(j)} \cap C_{(k)} \dots \cap C_{(l)}) \cup \dots C_{(n)} \quad (5.2)$$

$$P_{(F)} \rightarrow C_{(g)} \cup C_{(h)} \cup C_{(l)} \cup C_{(j)} \dots C_{(n)} \quad (5.3)$$

where  $S_{(F)}$  is the overall structural system failure and  $P_{(F)}$  is the probability of failure (single event).  $C_{(g)}$ ,  $C_{(h)}$ ,  $C_{(l)}$ ,  $C_{(j)}$ ,  $C_{(k)}$ ,  $C_{(l)}$ , and  $C_{(n)}$  are component failure events that make up the probability of failure ( $P_{(F)}$ ).

Modelling from first principles is always subject to uncertainties. Chapter 2 deals with these uncertainties in detail. Thus incorporation of the uncertainty in the basic models (semi-probabilistic) could be said to be the other alternative to fully probabilistic models for reliability analysis. For structures, reliability based on pure statistical methods with data from sources like OREDA, WOAD, etc. is controversial as incidents

leading to structural failure are highly subjective to a vast number of variables (Shi (1991)):

- i) within the structure itself and
- ii) the operational environment as well as the interaction between the former and the latter.

Modelling from first principles involves consideration of several processes and failure modes. The shift to a reliability based design of structures requires explicit knowledge of the underlying mechano-structural processes and their interactions. Ideally, all potential failure modes must be identified and quantified in the reliability analysis of any structure, however it is sufficient to consider only dominant failure modes (Liu and Tang (2004)). The FLEXSTREM has the robust feature of incorporating as many system definition parameters (and their interactions/relationships) as possible. However no attempt is made to cover all of them in this research. Major system definition parameters and their relationships would be incorporated and applied to a real structure. The possibilities of the expansion of this methodology are vast.

### ***5.2.1 The Stochastic Finite Element Method/Analysis (SFEM/SFEA)***

The presence of non-linear effects, multiple physics, complex geometry, demanding delivery times and clamour for economic viability has propelled the use of Finite Element Analysis/Methods (FEA/FEM) to predict the behaviour and response of complex systems (Riha, D.S. et al (1999)). An outcome of the considerations of uncertainties stated so far is the development and integration of probabilistic analysis with the FEA, giving rise to the Stochastic Finite Element Analysis/Method (SFEA/SFEM). Complex structures require SFEA in order to predict structural reliability (Du et al (2005)).

The SFEA attempts to address uncertainties (Brenner and Bucher (1995)). Several SFE methods have been developed. However, only few proposed SFEM models take non-linear effects into account. Analysis of larger/complex structures remains challenging due to the amount of random variables present and numerous degrees of freedom (DOF), ranging from a few hundreds to thousands. There is need for research

addressing the challenges in the application of SFEA to structural system reliability (Liu and Tang (2004)).

### **5.2.2 SFEA Background**

This section contains excerpts from the state-of-the-art review article by Stefanou – *The stochastic finite element method: past, present and future (2009)* providing a review of past and recent developments in SFEA, pointing out possible future developments and addressing certain engineering issues to be considered in the future. An overview of efficient and accurate simulation methods of stochastic processes, Gaussian and non-Gaussian, was presented.

The most important alternative approaches to SFEA – spectral stochastic finite element method/analysis (SSFEA/SSFEM), Perturbation approach and Monte Carlo simulation (and its variants), were critically reviewed and summarized. A significant challenge is the application of SFEA to inverse and non-linear problems with stochastic data, and other scenarios where time-dependence is inherent.

Although limitations abound computationally, Monte Carlo simulation is still the only universal tool for handling these challenges. SSFEA offers a powerful alternative in certain cases with potential for improvements. The theoretical background could be more acceptable to the scientific community if more rigorous proofs of convergence properties and error estimations are provided.

Robust and efficient adaptation of developed solution techniques to parallel processing would enhance SFEA potential. Also interfacing of highly interactive SFEA software with commercial third party software (FEA) to treat large scale SFEA problems in record time would be highly beneficial.

### **5.2.3 Monte Carlo Finite Element Method**

Monte Carlo simulation (MCS) is the simplest means of handling uncertainty in SFEA. The method involves generating samples of the stochastic system matrix  $NSIM$  times

(where  $NSIM$  is the number of trials in the MCS) via a random number generator (RNG). The resulting equilibrium in Equation (4.3) is solved  $NSIM$  times to give a population data of the output vector (Stefanou (2009)).

$$X = (K_O + \Delta K)F \quad (4.3)$$

where  $X$  and  $F$  are loading and nodal displacement vectors respectively.  $K_O$  and  $\Delta K$  are the means (analytic) and fluctuating elements of the SFE matrix.

The output reliability could be thus determined on the resulting population data. The accuracy of the output depends on the size of the population data. The solution of  $NSIM$  deterministic problems requires significant computation cost particularly in cases of considerable stochastic dimensions and large scale systems (Stefanou (2009)).

Development of robust and efficient algorithms has positively impacted on the application of MCS on large-scale structures significantly. Adaptation of MCS with discretization methods involving fewer amounts of random variables could reduce computational costs (Stefanou (2009)).

Several methods of structural analysis have been proposed and developed over the years. Some of these methods in relation to the topics discussed in section 5.2 are reviewed as follows:

Riha et al (1999) interfaced NESSUS, a probabilistic analysis software, with third party FEA software (NASTRAN, ABAQUS and ANSYS) to carry out reliability analysis. The results from the presented case study revealed essential findings that are key to design and manufacturing, which would have remained unknown with conventional design (FEA) methods. Recommendations alluded to more robust interfacing of the NESSUS software with other third party FEA solvers/software, citing greater efficiency as the principal benefit.

Brenner and Bucher (1995) developed an SFE-based reliability analysis of non-linear structures incorporating randomness in the structures and the loading i.e. a combination of the SFEA and response surface method (RSM). Greater computational efficiency compared to traditional Monte Carlo methods was realized. Emphasis was made on the

more influential random variables in order to achieve this efficiency. The results obtained highlighted the strong relationship between uncertainty and probability of failure and the need for innate considerations of the former in structural modelling.

Liu and Tang (2004) presented a reliability assessment of continuum structures. The loading and structural analysis was carried via SFEA. The 'branch and bound' method was used to establish dominant failure modes. Significant computational efficiency was the hallmark achievement with a view to further development for more complex scenarios.

With the goal of achieving high accuracy while attaining considerable computational efficiency, Elhewy et al (2006) used the RSM and an artificial neural network (ANN) jointly. The structural response relationship with the random variable (input) was modelled via the ANN. Structural reliability was then determined by reliability methods. The proposed hybrid method proved to be more accurate and efficient than the conventional RSM.

Yang and Younis (2005) presented a quantification approach for system reliability taking into consideration the dependencies between components, load sharing and damage accumulation and reversal. The method is of a semi-analytic kind (semi-probabilistic); it is a blend of analytic approach - FORM and SORM at the component level and MCS at the system level. Model reduction techniques were also employed. The technique is of particular interest as it makes considerable attempts to model interaction at the component level and not just merely focusing on total system failure as a single event. Also the hybrid nature facilitated a preserve of the meticulousness of analytic methods. The level of detailed modelling of the component interaction gave greater credence to the system output, which the system reliability was part of. It was also noted that all conventional methods do not account for time factor adequately except by hardware testing.

Wong et al (2005) acknowledged that structures in reality are subjected to multiple loads rather than a single load and also, that the RSM has been used in conjunction with non-linear finite element (NLFE). An adaptive characteristic (in addition to the RSM and NLFE) was proposed and validated with MCS. This technique aimed at finding

solutions to numerical problems that arise in complex reliability scenarios. A numerical study presented was adequately addressed and the resulting reliability values were in reasonable agreement with those of the MCS.

Naess and Royset (2000) presented a procedure by which the Turkstra's rule, initially limited to linear combination of load effects and statistically independent components, could be extended to cover dependent load effect components. It was concluded that the applicability of the developed method depends on the availability of data on statistical dependence.

Floris (1998) reviewed methods of load combination modelled as Poisson processes. Demonstrations on gross loads consisting of dead loads (including floor loads) and live loads (including wind loads) were carried out in various permutations. As a result, a new practical combination rule was proposed.

### 5.3 Methodology

Having obtained a considerable level of success in carrying out a risk quantification for a relatively simpler structure, the method has been developed to cater for more complex structures (MMSs) as well as for single member structures of varying kinds. The flow of the risk quantification for structures is outlined in Figure (5.1).

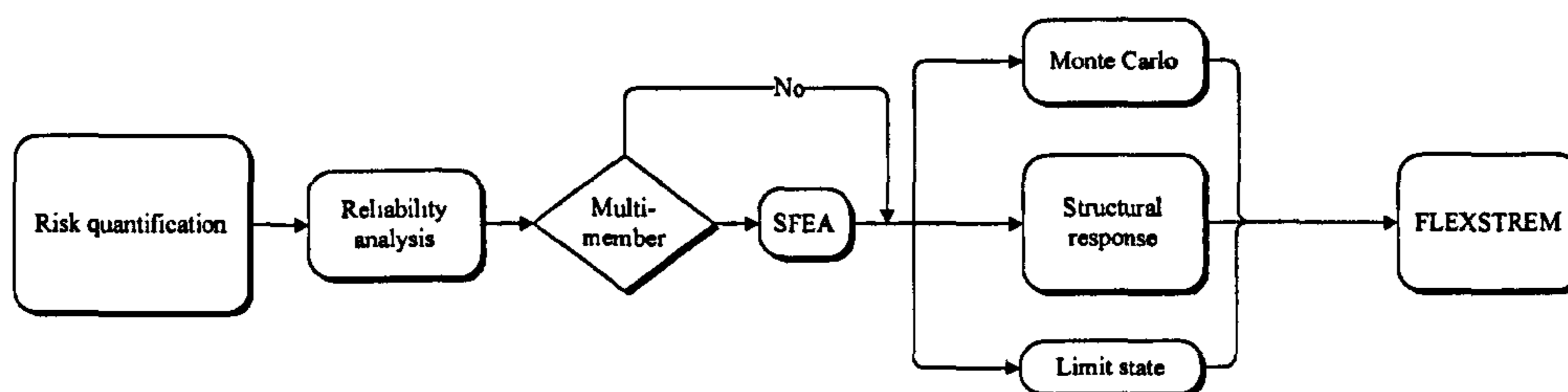


Figure (5.1) – Methodology.

The pre-existing algorithm has been further developed (in FORTRAN) to a full version capable of measuring the reliability (as a risk quantity) of more complex structures. With more complex structures more data from the system definition (chapter 4) is required when compared to the simple SMS analyzed previously. Figure (5.2) shows the structural response required for the implementation of the algorithm.

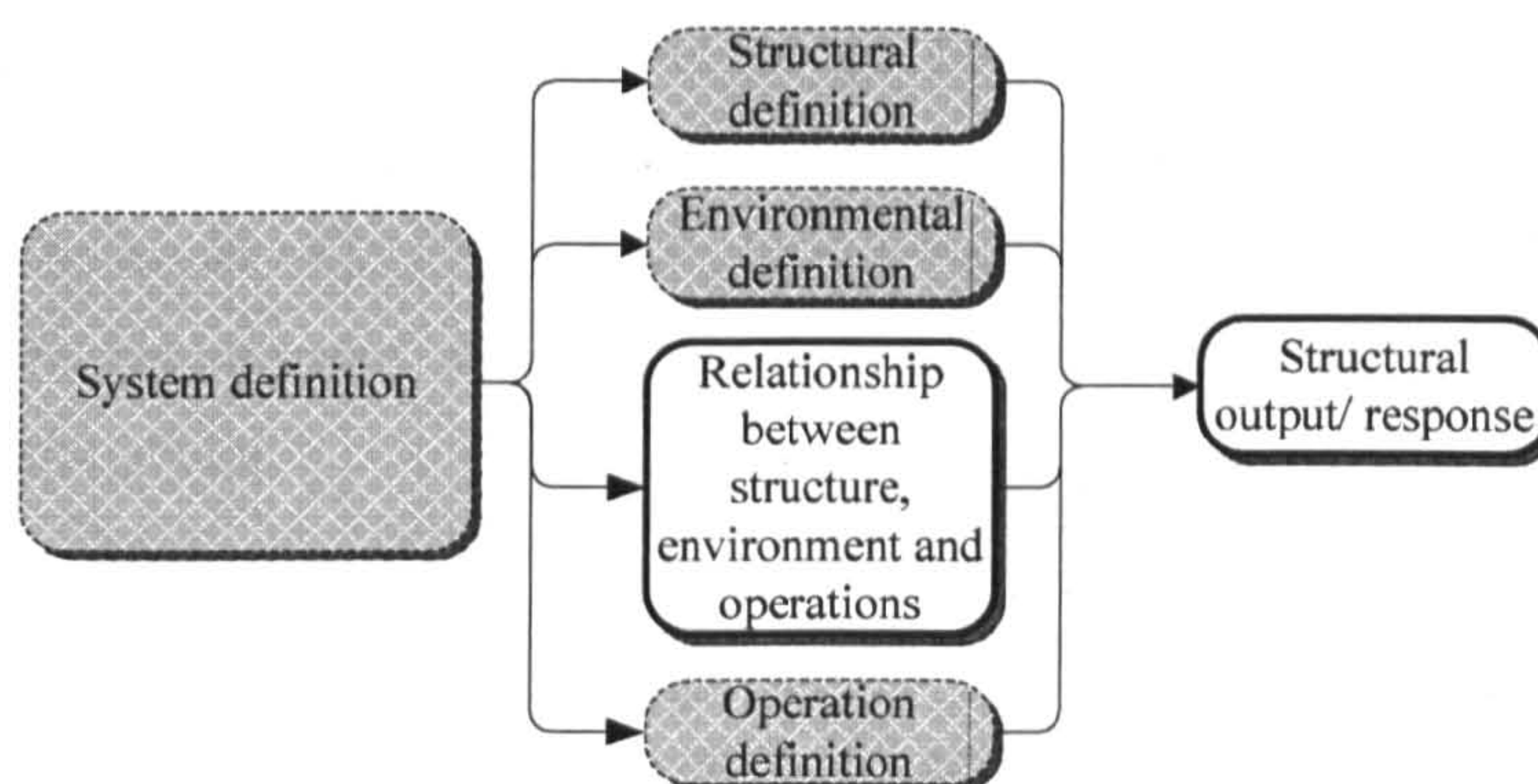


Figure (5.2) – Methodology.

The relationships between the structure, environment and the operations as well as the structural response are fully emphasized in this chapter. This method (FLEXSTREM) also forms the foundation on which subsequent methods would be developed.

#### 5.4 FLEXSTREM Overview

FLEXSTREM uses the MCS method together with specified limit states (a semi-probabilistic approach) and structural response to determine the reliability of a structure. It has been demonstrated and validated for the case of an SMS in chapter 3.

FLEXSTREM is an upgrade of the BETA-FLEXSTREM that deals with MMSs and utilizes a more robust system definition. A more pragmatic load combination has also been introduced. Furthermore, the FLEXSTREM has been developed to provide data which would be beneficial to future expansions such as sensitivity in the structural mass and dimensions.

For the purpose of dealing with MMSs, the FEA has been incorporated. The FEA module forms the backbone of FLEXSTREM. The combination of the FEA with the FLEXSTREM has facilitated a completely novel method of implementing the SFEA (without time dependency). The SFEA – a recent development, together with the classic mechanical and LFM processes (from which the limit states are derived) ensure that detailed attention is given to each structural member and joint (node) in establishing the overall reliability.

No attempt has been made to model all possible interactions between the main components of the system definition; only the major relationships ones have been modelled. The nature of FLEXSTREM allows more system definition and relationship-models to be incorporated with a few adjustments to the algorithm. The scope for improvements is wide.

There are three phases present in the FLEXSTREM: a pre-MCS processing phase (processes A and B including the immediate I/O processes), the MCS phase (C-Q), and the Post-MCS process (process R and the immediate I/O processes). A structural analysis is carried out in either of two ways in FLEXSTREM:

- Type I analysis (SMS analysis)
- Type II analysis (MMS analysis)

From the results produced by the analyses, observations could be made and between the main components of the system definition, their interactions/relationships, and ultimately, the reliability. There is a wide scope for various statistical observations and analyses of this output data.

At this stage the FLEXSTREM remains time invariant. Time dependency and variation (stochasticity) would be implemented in chapter 7.

The FLEXSTREM consists of various limit states common to unsheltered structures. The arrangement of the limit state algorithms has significant effect on the computational cost of the simulation. The labelled blocks in the FLEXSTREM algorithm in Figure (5.3) refer to the following:

- Parallelograms – I/O processes (data initializing and recording)
- Process A – Type I pre-MCS process
- Process B – Type II pre-MCS process
- Process C – MCS process
- Process D – Wind force computation
- Process E – Loading combination and determination of load increment factors
- Type I processes:
  - Process F – Bending stress analysis
  - LM I – Bending limit analysis



- Process G – Tensile stress analysis
- LM II – Tensile limit analysis
- Process H – Compressive stress analysis
- LM III – Compressive limit analysis
- Process I – Multiaxial stress analysis
- LM IV – Multiaxial limit analysis
- Process J – Crack length estimation (LEFM)
- Process K – Stress intensity factor analysis
- LM V – Fracture toughness limit analysis
- Process L – Minimum crack (required for failure) estimation
- Process M – Fracture analysis
- LM VI – Fracture limit analysis
- Process N – Life cycle assessment
- LM VII – Life limit analysis
- Type II processes:
  - Process O – Member analysis
  - LM VIII – Member limit analysis
  - Process P – Node LEFM analysis
  - LM IX – Node limit analysis
- Process Q – Reliability estimation

Processes F – N are type I procedures while processes Q and R are type II procedures. Processes F – I and O (immediate limit states included) are classical mechano-structural processes. Processes J – N and P (LM VIII included) are linear elastic fracture mechanic (LEFM) processes. LMs I to VII are fundamental limit states (type I analysis) whilst LMs VIII and IX are derived limit states consisting of LMs II and III and LMs V, VI and VII respectively (type II analysis).

There is regular syncing of data between the processes and the computer memory. This is to ensure data consistency in data transfer in the intermittent calls made by the program to the subroutines. The process of data/variable initialization and storage occurs in all processes and sub-processes. The implementation is crucial to the efficiency and accuracy of the whole algorithm. The arrangement in the FLEXSTREM

ensures that data from input files are read only once and stored in memory blocks and arrays for any other reference. This is to prevent any occurrence of I/O errors and increase the data transfer speed since access is directly to the memory and not from any external sources. Also computationally costly procedures are strategically placed to free up resources for the main procedure which is the MCS. Initialization of all limit state indicators (failure counters) is performed between processes A/B and C.

Like the previous, the current FLEXSTREM version is written in FORTRAN 95. Efficiency-enhancing features of the FORTRAN 95 have been implemented in this version. The application of this FLEXSTREM version to complex structures will be demonstrated.

The FLEXSTREM model is illustrated (Figure (5.3)).

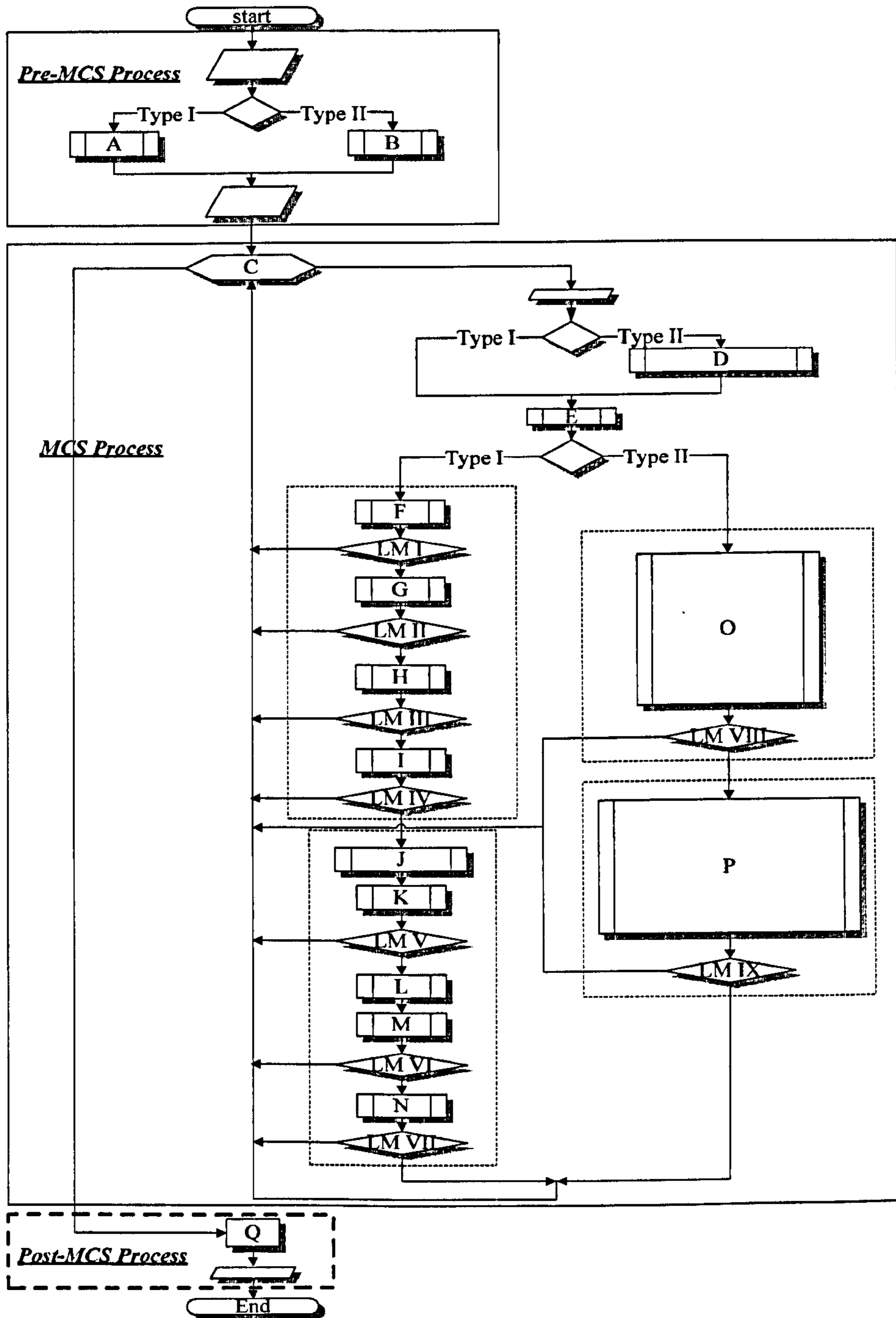


Figure (5.3) – FLEXSTREM.

### Fault Tree Representation

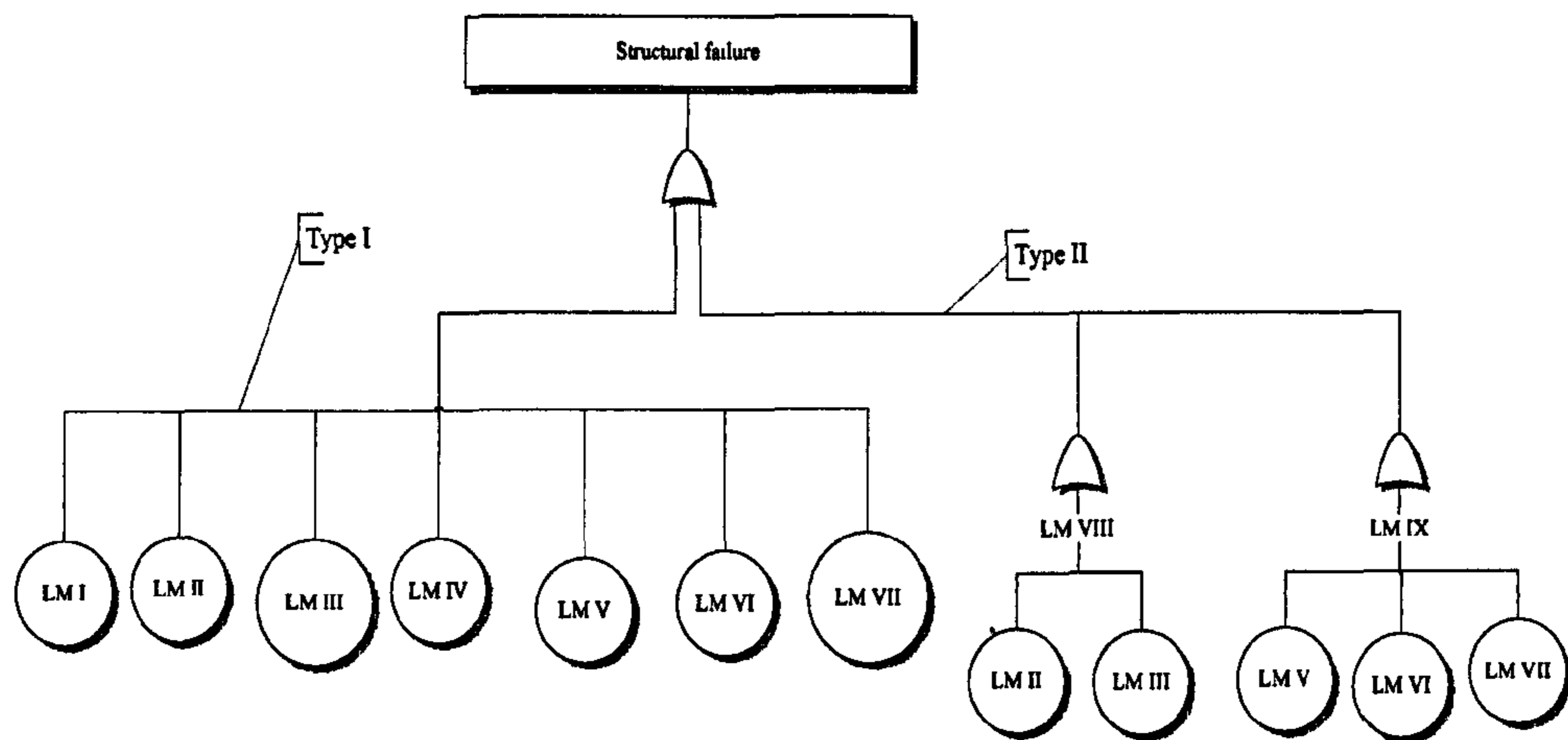


Figure (5.4) – Fault tree representation.

The underlying processes modelled in the FLEXSTREM have the fault tree representation shown in Figure (5.4). The top event (i.e. structural failure) is the probability of failure (POF) in the FLEXSTREM and is vital to structural integrity. The basic events are the limit states also on the FLEXSTREM algorithm (Figure (5.3)). From observation, statistical data on all the failure modes (basic events) are non-existent. Hands need to get 'dirty' to determine the explicit structural reliability. A partial validation where the primary variables of each of the basic events would be altered and the effects on the reliability denoted would be carried out to verify the results.

## 5.5 FLEXSTREM Preface

### 5.5.1 Coefficient of Variance (COV) and Safety Factors

The safety factor in the context of structures is intended to be some sort of compensation for the limit of structural (material) resistance to various forms of loading. It has been demonstrated in chapter 3, that this value does not truly fulfil this intention as the inherent uncertainties present could still pose significant threat to structural integrity.

The coefficient of variance (COV) is the ratio of the standard deviation to the arithmetic mean of a data set. The standard deviation could be said to be a rational measure of the

scatter present in a data set due to its variance (inherent uncertainty). This is because it has an overwhelming influence on the shape and thus ‘overlap’ of the limit state function. Components of the limit state function are subject to uncertainty, thus leading to the need for reliability analyses.

The safety factors incorporated in a structure or component could offer some insight to the expected uncertainty as a given safety factor reflects the designer’s judgement/confidence on the safe use of the structure or component (subjected to a certain loading condition). Some relationships drawn between the safety factor and the COVs of a structure’s (or component’s) definition parameters would be highly beneficial in reliability assessment.

### **5.5.2 Coefficient of Variance (COV) and Number of Random Variables**

The size of the COV becomes increasingly significant as the number of random variables in a system (i.e. system definition parameters) increases. A key source of uncertainty of any system is the impossibility to adequately model all interactions/relationships between these variables (i.e. the main components of the system definition). Also certain models are a combination of a few or more unit models. Therefore it may be convenient to infer that more variables and relationships modelled in a system (more system definition) would lead to a decrease in the level of system uncertainty. Thus, the presence of more system definition/knowledge would lead to the use of relatively lower COV(s) in the system. Figures (5.5) and (5.6) further illustrate this concept:

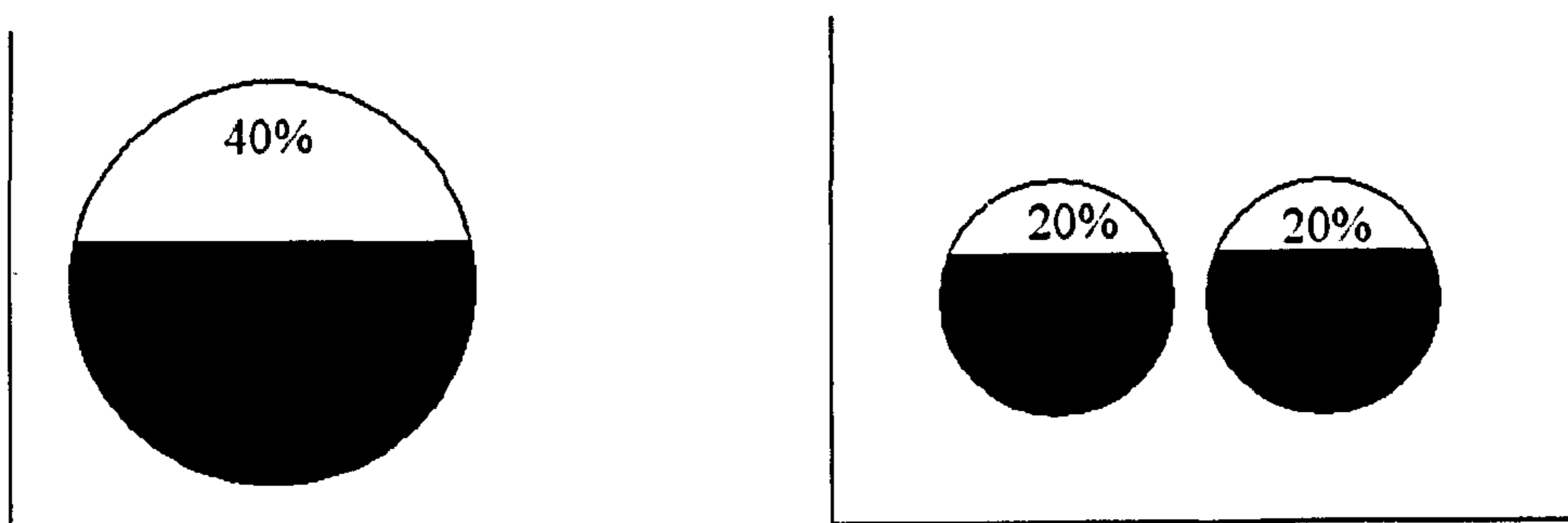


Figure (5.5) – Uncertainty at 40% and uncertainty at 20% each.

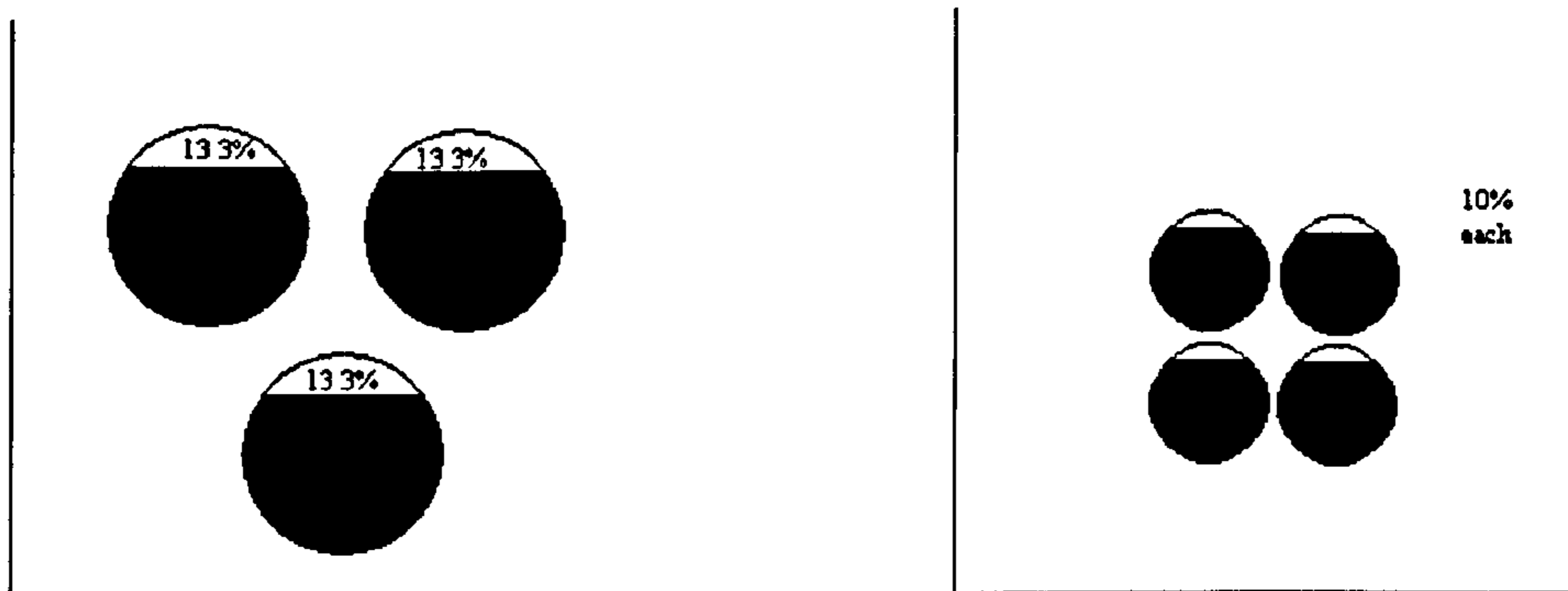


Figure (5.6) – Uncertainty at 13.3% each and uncertainty at 10% each.

The illustrations in Figures (5.5) and (5.6) assume that the child models share uncertainty equally. Figure (5.5) (left) is the parent or system model with an uncertainty (COV) of 40% (COV=0.4). The system is then further defined (broken down) to consist of two child models in Figure (5.5) (right). Further system definition gives rise to child models with less variation. As such the resulting uncertainty of each child model becomes 20%. Further system breakdown/definition to three and four child models as more system knowledge is attained (Figure (5.6)) decreases uncertainty, in this case, to 13.3% and 10%.

Non-conservative COVs at component level would result in an overall estimate far from reality and not truly representative of the system integrity. The FLEXSTREM would adopt conservative COVs as the system is considerably defined.

### 5.5.3 Coefficient of Variance (COV), Number of Simulations and Reliability

Real data from most systems exhibit different patterns of variation. These data can be modelled using the appropriate distributions. The requirements for most models are: (i) a mean and (ii) a standard deviation. The (re)generation (modelling) of a data set with the aforementioned requirements could be achieved via the MCS. The COV (the ratio of the standard deviation to the arithmetic mean) as a measure of variance and thus uncertainty of a system has a significant bearing on the number of simulations to be done in order for the generated dataset to achieve a “complete” status. A system with a small COV would require a relatively low number of simulations to achieve this “complete” status (which is translated in other scenarios as the consistency in outcomes

(reliability in this case) for infinitely increased number of simulations) compared to the number of simulations needed by a similar system with a higher COV. The following figures serve to illustrate this point:

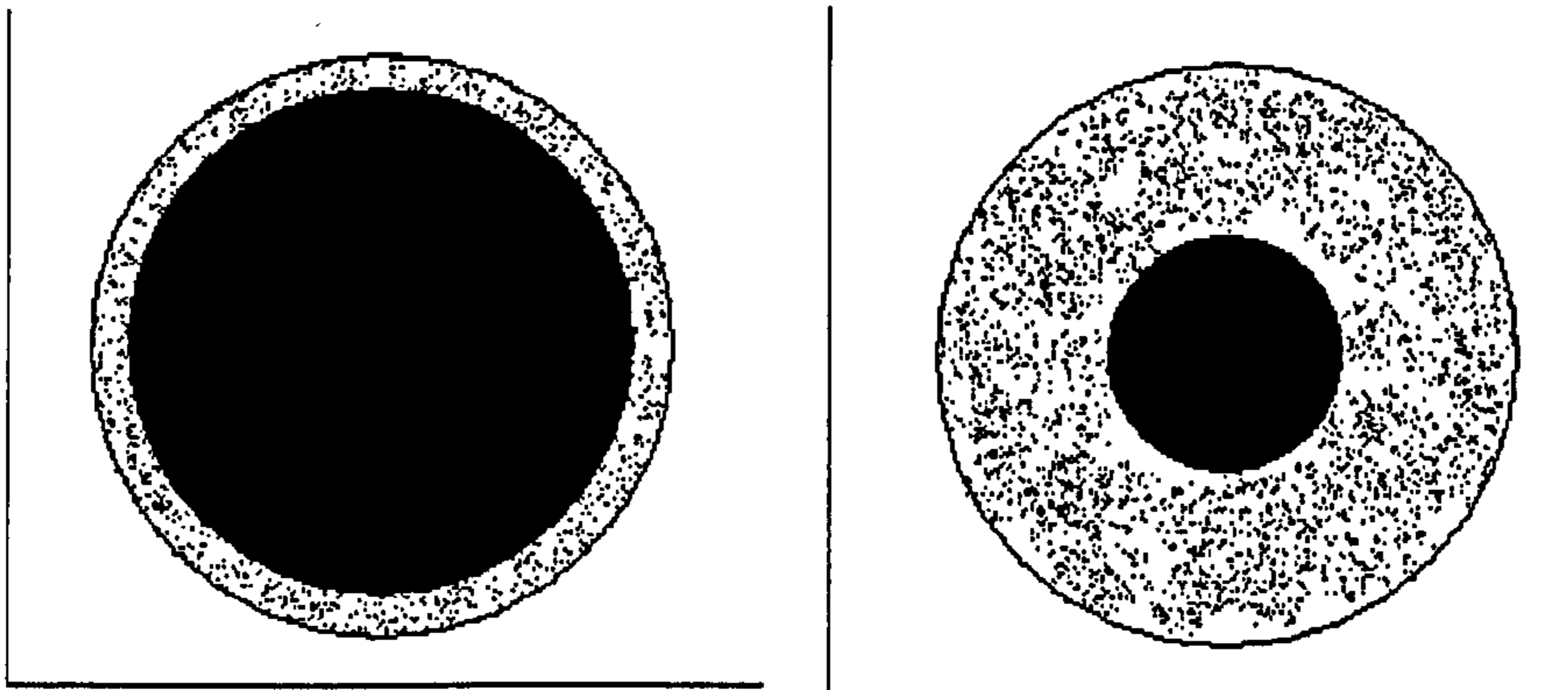


Figure (5.7) – Small COV and Large COV.

In Figure (5.7) the outer circle represents the system, the inner shaded circle represents the completely defined parameters of the system (i.e. the certainty), the area between the two circles is the system uncertainty and the dots in-between represent the simulations. From visual inference, the dots needed to “fill the void” i.e. uncertainty and form a completely shaded circle would need to be more in Figure (5.7) (right) (large COV) compared to those of Figure (5.7) (left) (small COV).

The reliability which is dependent on the COV and the number of simulations is also examined. The COV, a measure of uncertainty, has a significant relationship with the system reliability. For a given number of simulations, a higher COV would translate to more system uncertainty and thus more “unreliability” (less reliability) in the system. Conversely for the same number of simulations, a lower COV, which would also translate as less system uncertainty, would lead to a greater reliability in the system.

With smaller COVs employed in the FLEXSTREM, a relatively low number of simulations should be needed. Also, the use of small COVs should aid quick convergence of the final outcome such that a higher number of simulations would be unnecessary. The FLEXSTREM results would be extended to include comparisons

between the outcomes (reliabilities) of different numbers of simulations and COVs with respect to consistency.

#### ***5.5.4 Blind Design Concept***

The FLEXSTREM at this stage is adapted to structural frames. Common features of these frames irrespective of type and location are section properties (length, geometry, cross-sectional area, etc.) and material properties (Young's modulus, yield strength, etc.). The various modules interfaced in the FLEXSTREM conveniently deal with all these features. One of the limitations at this stage is that of section properties. Tubular sections module is the only section module present at this stage. It is desirable that in future several frame section modules would be integrated. The ultimate goal is the design and analysis of all structural frames. Shells or 'skin' modules would also be considered in the future.

#### ***5.5.5 Design Guides/Standards***

*"All models are wrong but some are useful"* - G.E.P Box

The structural design guides still rely heavily on the allowable stress design (ASD) methods. Despite the disadvantages presented hitherto, these guides are still essential to ensure concordance to an acceptable level of safety in design. Design itself requires sound engineering practice and principles regardless of the methods employed i.e. reliability based or ASD.

The models in the design guides provide the basis for limit states employed in the reliability based methods. A few of these models have been adopted for the FLEXSTREM. However, the numerical factors included in the models have been excluded in order to avoid under or over-conservativeness.

Also, some recommendations are ignored altogether as they fundamentally conflict with shared principles or are duplicates with different factors. For example the bending of a single member component and that of a whole structure may have certain factors in each



case. Thus, the governing bending formula is extracted, ignoring the factors. Analytic methods from first principle classical mechanics are also employed in setting up the limit state functions.

*Load Combinations and Wind Considerations (BS-2573-1:1983)*

There are a number of standards and guides addressing wind loading on structures. BS-2573-1:1983 was selected due to the fact that consideration was given first to individual members of the framed structure (as is the case with the crane) and ultimately to the entire structure. The following sections of the standard are considered as they totally comply with the designations for this reliability analysis.

*“Section 3 – Load and Load Combination”*

*“Clause 3.1.2.2 – for use with in-service wind states the total loading on the structure”* would be:

$$LD_{dead} + LD_{live} + H_1 + LD_{TW} \quad (5.4)$$

where,

$LD_{dead}$  – loads due to self weight

$LD_{live}$  – live loads including the hook load multiplied by an *dynamic factor*\*

$H_1$  – combined effect of the two most severe horizontal loads (not applicable)

$LD_{TW}$  – loads due to service winds acting horizontally in any direction where applicable.

\* all factors are excluded in this analysis.

*“Subsection 3.1.7 – Wind Loads”*

Before delving into this section, some background information is presented. The dynamic pressure  $P_d$ , is the property of a flowing gas or fluid expressed as:

$$P_d = \frac{1}{2} \rho v^2 \quad (5.5)$$

where  $\rho$  is the density of the fluid (air density  $\approx 1.2 \text{ kg/m}^3$ ) and  $v$  is the air velocity (m/s). This equation could be adapted for immersed structures where  $\rho$  will be water density and  $v$  will be the water velocity (current/waves).

*“Clause 3.1.7.2 – Dynamic Wind Pressure”*

$$q = 0.613 w_s^2 \quad (5.6)$$

where  $q$  is the dynamic wind pressure ( $\text{N/m}^2$ ) and  $w_s$  is the design wind speed in (m/s).

*“Clause 3.1.7.4 – Wind Load on Structure (and Members)”*

This computes the wind load for complete and part structures as well as individual members (components) of structures.

$$LD_W = \gamma C_A q C_f \quad (5.7)$$

where,

$LD_W$  – wind load (N)

$\gamma$  – factor related to design application of the calculated wind load

(\* ignored – see section 5.5.5)

$C_A$  – effective frontal area of the part under consideration

$q$  – dynamic wind pressure (clause 3.1.7.2)

$C_f$  – force coefficient in the direction of the wind for the part under consideration.

*“Clause 3.1.7.5 – Force Coefficient”*

This deals with the determination of the force coefficient  $C_f$  for each individual member of a given structure. Table 8 (see cited reference) in the document is used in conjunction with aerodynamic slenderness and section ratios to determine this coefficient.

*“Clause 3.1.7.6 – Wind Load on Sheltered Members”*

This deals with structures having multiple members that have a shielding effect on some others by virtue of their parallel position. Clause 3.1.7.4 takes care of the unsheltered (windward) areas. The wind force on the sheltered (leeward) parts is calculated from:

$$LD_{WS} = \gamma C_{SA} q C_f \varphi \quad (5.8)$$

where,

$\gamma, q, C_f$  are as defined in clause 3.1.7.4

$LD_{WS}$  – wind load on the sheltered parts (N)

$C_{SA}$  – area of the sheltered parts under consideration ( $m^2$ )

$\varphi$  – shielding factor given in Table 9 of BS-2573-1:1983 according to the solidity ratio of the front frame and the spacing ratio. The ratios are defined in Figure (3) of the BS-2573-1:1983.

The total wind force  $F_T$ , is given as:

$$LD_{TW} = LD_W + LD_{WS} \quad (5.9)$$

## **5.5.6 Algorithm Sources**

### **5.5.6.1 The Iwakuma Tetsuo FEA Code**

Central to the methodology was the development of compatible FEA code for interfacing with the FLEXSTREM code. The code written by Prof. Iwakuma Tetsuo of Tohoko University, Japan on his online repository (<http://www.civil.tohoku.ac.jp/~bear/node8.html>) for lecture purposes. The program, which was a result of years of research and publications which include Iwakuma (1990), Iura and Iwakuma (1992) and Iwakuma et al (1996), etc. to name a few, helped form the brain-box of the methodology. The code was originally written in FORTRAN 77.

The program, which was an FEA of truss structures (truss elements), was coded for 2-D structures. For this research, it was adapted to FORTRAN 95, interfaced with the original FLEXSTREM code and then modified for the analyses of 3-D structures in the FLEXSTREM. It is desired that the final version of FLEXSTREM would be made freely available with the GNU license on an online repository for use and modification by engineers and scientists.

### **5.5.6.2 Gmsh**

Gmsh is a 3D finite element grid generator with a built-in CAD engine and post-processor written in C++ by mainly Geuzaine and Remacle (2009) with contributions from a host of researchers and enthusiasts as an open source project with a special GNU license. It was used as a visualization tool for the FLEXSTREM. An interface between the Gmsh visual interface and the FLEXSTREM engine is under consideration.

## **5.6 FLEXSTREM Analysis for Structures**

### **5.6.1 Process A – Type I Pre-MCS Process**

This sets the precedent for a type I analysis (SMS). Here the external procedure A reads in the parameter values (system definition parameters) of the structural entity to be analyzed. These parameters are listed in chapter 4. From the read-in values, the derived parameters are calculated. These are then passed on to the main MCS process for analysis.

### **5.6.2 Process B – Type II Pre-MCS Process**

In this process, the initialization of the required structural parameters listed in chapter 4 is done first. Following that is the allocation of memory resources to be used in the FEA. This is done to maintain computational efficiency while reducing memory loss. The last step is the calculation of a parameter of the wind force that undergoes no further alteration (Equation (5.8)). Placing the derivation of this parameter outside the MCS process improves the efficiency of the whole algorithm. The read-in and calculated parameters are then passed on to the main MCS process for analysis.

### ***FEA Block***

As one of the most widely applied techniques in the engineering industry today, FEA needs no significant introduction. First drafted in 1941 by Hrenikoff as a solution to elasticity problems in aircraft analysis using the “frame work method”, subsequent research followed with landmarks laid by Courant (torsion – 1943) and Turner et al (stiffness matrix definition – 1956). The term “finite element” was coined by Clough in 1960. Argyris (1955 – energy theorems and matrix methods) laid the foundation for further developments of the technique. The first text on the technique (Zienkiewicz and Chung) appeared in 1967. Applications to non linear problems about that period saw the earliest text addressing the subject (Oden – 1972). With more mathematical research in the 1970’s and the advance in computer technology, FEA became readily available for use in several fields in engineering such as stress and deformation analysis of buildings, automotives, bridges, aircraft, field analysis of heat flux, fluid flow and other flow analyses.

Several literatures describing the methods are available. Ferreira (2009), Akin (2005), Mohammadi (2008), Liu and Quek (2003), Zienkiewicz and Taylor (2000) Donea and Huerta (2003), etc. are amongst a plethora of texts utilized in this research. The implementation of this process is presented in appendix B (FORTRAN code).

The nature of this research sets the scene as to what aspects of the FEA will be focused on. Several variants of the FEA application on structures exist and are employed depending on the nature of the problem and complexity of the component/structure involved. Examples of these variants include:

- truss elements
- beam elements
- frame elements

The truss element is assumed to experience forces only in the axial direction. Transverse loading and thus moment in the perpendicular directions are ignored. The beam element is assumed to experience only transverse forces. Axial forces are ignored in the analysis of beam elements. The frame element analysis is a mixture of both truss and beam element modelling conditions i.e. loading takes place in both axial and transverse directions. This analysis type is the most used in structures as it applies to real cases. The space truss (3-dimensional truss element type) is considered in this research as a successful demonstration paves way for adaptation to space frame element types.

To illustrate FEA truss analysis, the following demonstration is presented. Resources utilised in this analysis include:

- Gurley (2003) – "Direct Stiffness - Truss Application"
- Nikishkov (2004) – "Introduction to the Finite Element Method"
- Camp (2006) – "Development of Truss Elements"
- Bucciarelli (2002) – "Engineering Mechanics for Structures"

For the illustration of the theoretical processes outlined in sub-process B3, consider a typical multi-member structure – the truss. The truss structure consists of individual bar elements bounded by nodes at each end.

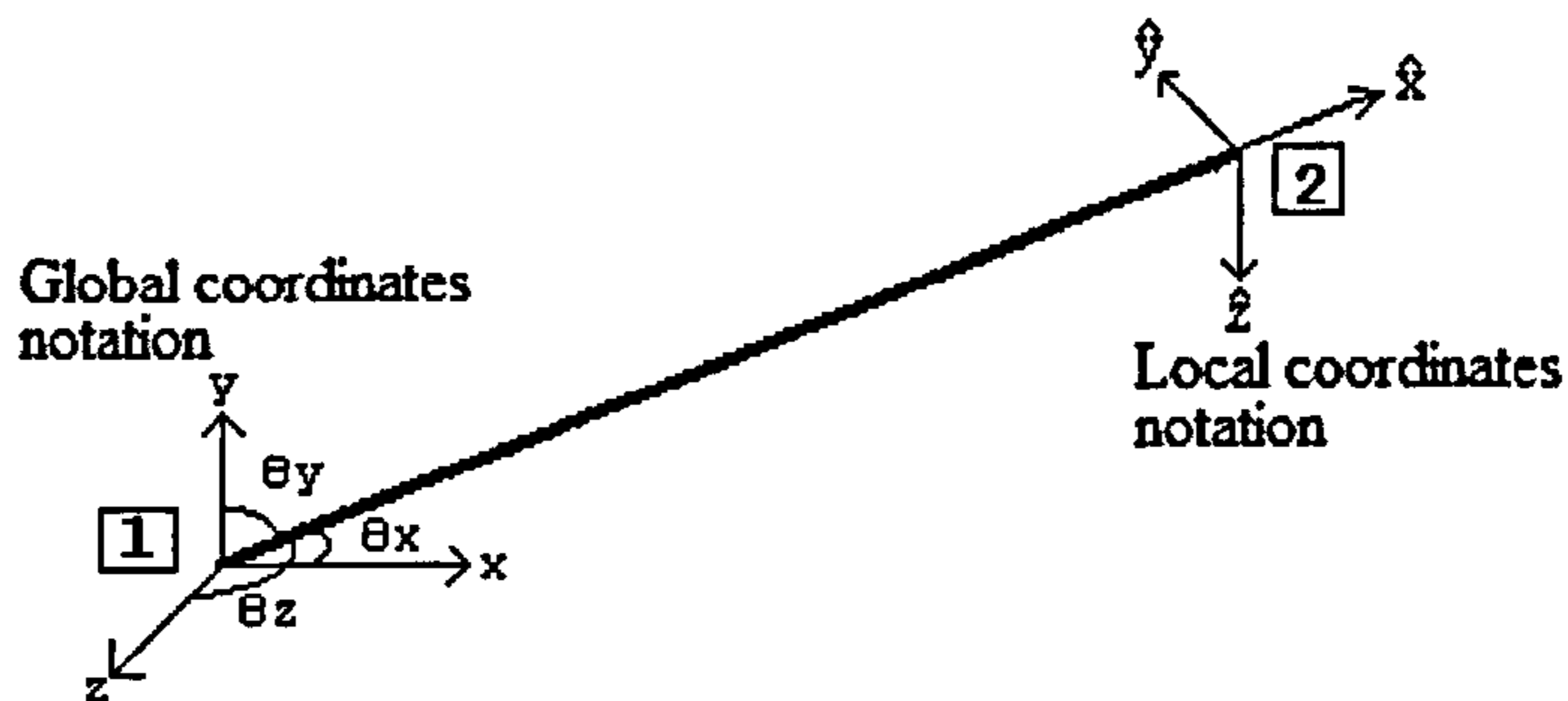


Figure (5.8) – Bar element.

At nodes 1 and 2 in Figure (5.8), are the global coordinates  $x_1, y_1, z_1$  and  $x_2, y_2, z_2$  respectively.  $x, y$  and  $z$  are the notations of the global coordinates from which the inclinations –  $\theta_x, \theta_y$  and  $\theta_z$ , are denoted.  $\hat{x}, \hat{y}$  and  $\hat{z}$  represent the local axes coordinates of the element.

A 3-dimensional vector representation is thus:

$$F = F_x i + F_y j + F_z k = \hat{F}_x \hat{i} + \hat{F}_y \hat{j} + \hat{F}_z \hat{k} \quad (5.10)$$

where  $i, j$  and  $k$  are unit vectors in the  $x, y$  and  $z$  directions (i.e. global) and  $\hat{i}, \hat{j}$  and  $\hat{k}$  are unit vectors in the  $\hat{x}, \hat{y}$  and  $\hat{z}$  directions (i.e. local). Taking dot product of Equation (5.10) with  $\hat{i}$  leads to:

$$F_x (i \cdot \hat{i}) + F_y (j \cdot \hat{i}) + F_z (k \cdot \hat{i}) = \hat{F}_x \quad (5.11)$$

where  $\hat{F}$  is a local displacement vector or global change in nodal position and  $F$  is the global displacement vector. The dot product is expanded to:

$$i \cdot \hat{i} = \frac{X_2 - X_1}{L} = C_x \quad (5.12)$$

$$j \cdot \hat{i} = \frac{Y_2 - Y_1}{L} = C_y \quad (5.13)$$

$$k \cdot \hat{i} = \frac{Z_2 - Z_1}{L} = C_z \quad (5.14)$$

where  $L$ , the bar length is given by:

$$L = \sqrt{(x_2 - x_1)^2 + (y_2 - y_1)^2 + (z_2 - z_1)^2} \quad (5.15)$$

and  $C_x = \cos \theta_x, C_y = \cos \theta_y, C_z = \cos \theta_z$

$C_x, C_y$  and  $C_z$  are projections of  $\hat{i}$  on to  $i, j$  and  $k$  respectively.

$$\hat{F}_x = C_x F_x + C_y F_y + C_z F_z \quad (5.16)$$

Transformation between local and global displacements is given as:

$$\hat{F} = TF \quad (5.17)$$

$$\begin{Bmatrix} \hat{F}_{x_1} \\ \hat{F}_{x_2} \end{Bmatrix} = \begin{bmatrix} C_x C_y C_z & 0 & 0 & 0 \\ 0 & 0 & 0 & C_x C_y C_z \end{bmatrix} \begin{Bmatrix} F_{1x} \\ F_{1y} \\ F_{1z} \\ F_{2x} \\ F_{2y} \\ F_{2z} \end{Bmatrix} \quad (5.18)$$

where  $T$ , the equilibrium matrix of projections is given as:

$$T = \begin{bmatrix} C_x C_y C_z & 0 & 0 & 0 \\ 0 & 0 & 0 & C_x C_y C_z \end{bmatrix} \quad (5.19)$$

Transformation from local to global stiffness matrix gives:

$$K = T^T \hat{k} T \quad (5.20)$$

where  $\hat{k}$  is the local stiffness matrix and  $K$ , the global stiffness matrix given as:

$$K = \begin{bmatrix} C_x & 0 \\ C_y & 0 \\ C_z & 0 \\ 0 & C_x \\ 0 & C_y \\ 0 & C_z \end{bmatrix} \frac{AE}{L} \begin{bmatrix} 1 & -1 \\ -1 & 1 \end{bmatrix} \begin{bmatrix} C_x C_y C_z & 0 & 0 & 0 \\ 0 & 0 & 0 & C_x C_y C_z \end{bmatrix} \quad (5.21)$$

where  $A$  is the cross-sectional area of the bar,  $E$  the Young's modulus and  $L$ , the bar length. Expanding the above expression gives:

$$K = \frac{AE}{L} \begin{bmatrix} C_x^2 & C_x C_y & C_x C_z & -C_x^2 & -C_x C_y & -C_x C_z \\ C_x C_y & C_y^2 & C_y C_z & -C_x C_y & -C_y^2 & -C_y C_z \\ C_x C_z & C_y C_z & C_z^2 & -C_x C_z & -C_y C_z & -C_z^2 \\ -C_x^2 & -C_x C_y & -C_x C_z & C_x^2 & C_x C_y & C_x C_z \\ -C_x C_y & -C_y^2 & -C_y C_z & C_x C_y & C_y^2 & C_y C_z \\ -C_x C_z & -C_y C_z & -C_z^2 & C_x C_z & C_y C_z & C_z^2 \end{bmatrix} \quad (5.22)$$

This can be factorized to:

$$K = \frac{AE}{L} \begin{bmatrix} \lambda & -\lambda \\ -\lambda & \lambda \end{bmatrix} \quad (5.23)$$

where  $\lambda$  is:

$$\lambda = \begin{bmatrix} C_x^2 & C_x C_y & C_x C_z \\ C_x C_y & C_y^2 & C_y C_z \\ C_x C_z & C_y C_z & C_z^2 \end{bmatrix} \quad (5.24)$$

Some of the projections are at  $0^\circ$  and some at right angles hence the presence of zeros in the matrix. The stiffness matrix  $K$  is always symmetric, positive definite and sparse:

- the symmetry enables storage of only half (diagonally) of the matrix
- the positive definite matrices contain large positive entries on the main diagonal
- the sparsity means the presence of more zeros than non-zero numbers.

The derivation of the following equations could be looked up in the recommended texts. Analysis would begin from the steps relevant to the current study.

Given,

$$T^T \hat{x} = X \quad (5.25)$$

where  $\hat{x}$  from this point on, is the individual or local member force and  $X$  is the nodal force or reaction. All other variables retain their definitions. Also,

$$\hat{k}\hat{F} = \hat{x} \quad (5.26)$$

and

$$\hat{F} = TF \quad (5.27)$$

The following is derived:

$$T^T \hat{k}\hat{F} = X \quad (5.28)$$

$$T^T \hat{k}TF = X \quad (5.29)$$

from Equation (5.20),

$$K = T^T \hat{k}T \quad (5.20)$$

thus,

$$\boxed{KF = X} \quad (5.30)$$

This is the governing FEA equation. A solution method is needed to obtain the unknown variables in matrices  $F$  and  $X$  both accurately and efficiently.

Iterative methods or direct methods are the two basic approaches that could be employed for the solution to linear system of equations. The methods are selected based on the problem size. For problems of moderate size, the direct method may be utilized. For larger problems, the iterative method becomes useful as it requires less computation time. In addition to the problem size, the matrix storage format also serves as a useful criterion for selecting the solution method.



### 5.6.2.1 Validation of the FEA-Block Output

The following example illustrated in Figure (5.9) to validate the output of the FEA-Block is culled from Camp (2006). Consider the space truss shown in Figure (5.19). The modulus of the elasticity is  $1.2 \times 10^6$  psi ( $8.27 \times 10^3$  MPa) for all elements. Node 1 is constrained from movement in the y-direction.

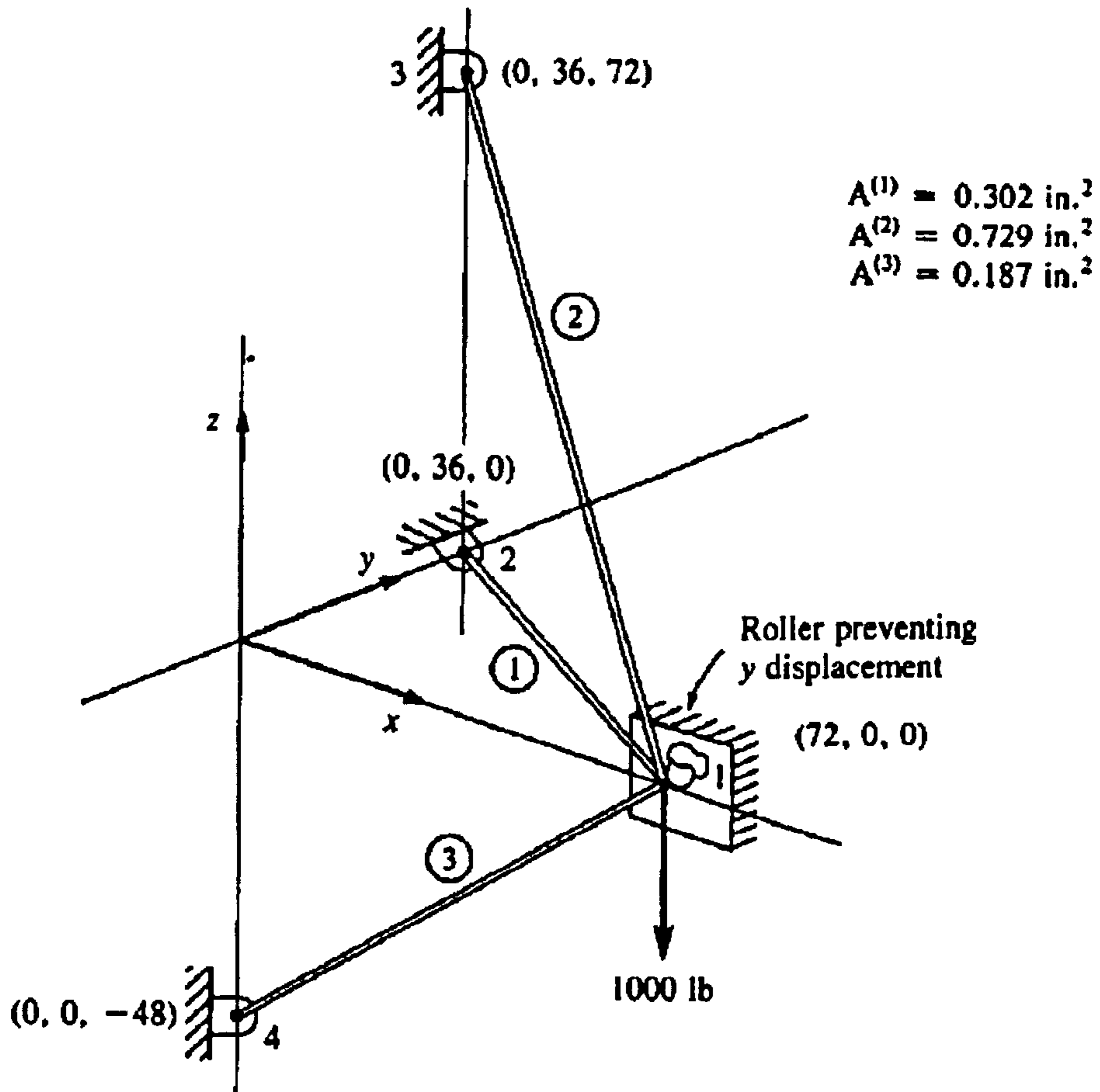


Figure (5.9) – Space truss.

Solution (Camp (2006)):

These solutions were derived from hand calculations. Given the boundary conditions:

$$d_{1y} = 0, d_{2x} = d_{2y} = d_{2z} = 0, d_{3x} = d_{3y} = d_{3z} = 0, d_{4x} = d_{4y} = d_{4z} = 0$$

where  $d$  is the displacement of a node in a particular direction (subscripts).

The solution yields the following results:

$$d_{1x} = -0.072 \text{ in } (1.829 \times 10^{-3} \text{ m}), \quad d_{1z} = -0.264 \text{ in } (6.71 \times 10^{-3} \text{ m})$$

The stress in each member/element (superscript),  $\sigma$ , is as follows:

$$\sigma^{(1)} = -955 \text{ psi } (6.584 \text{ MPa})$$

$$\sigma^{(2)} = 1423 \text{ psi } (9.811 \text{ MPa})$$

$$\sigma^{(3)} = 2843 \text{ psi } (19.6 \text{ MPa})$$

Solution (FLEXSTREM FEA block):

The space truss is represented in *Gmsh* in Figure (5.10):

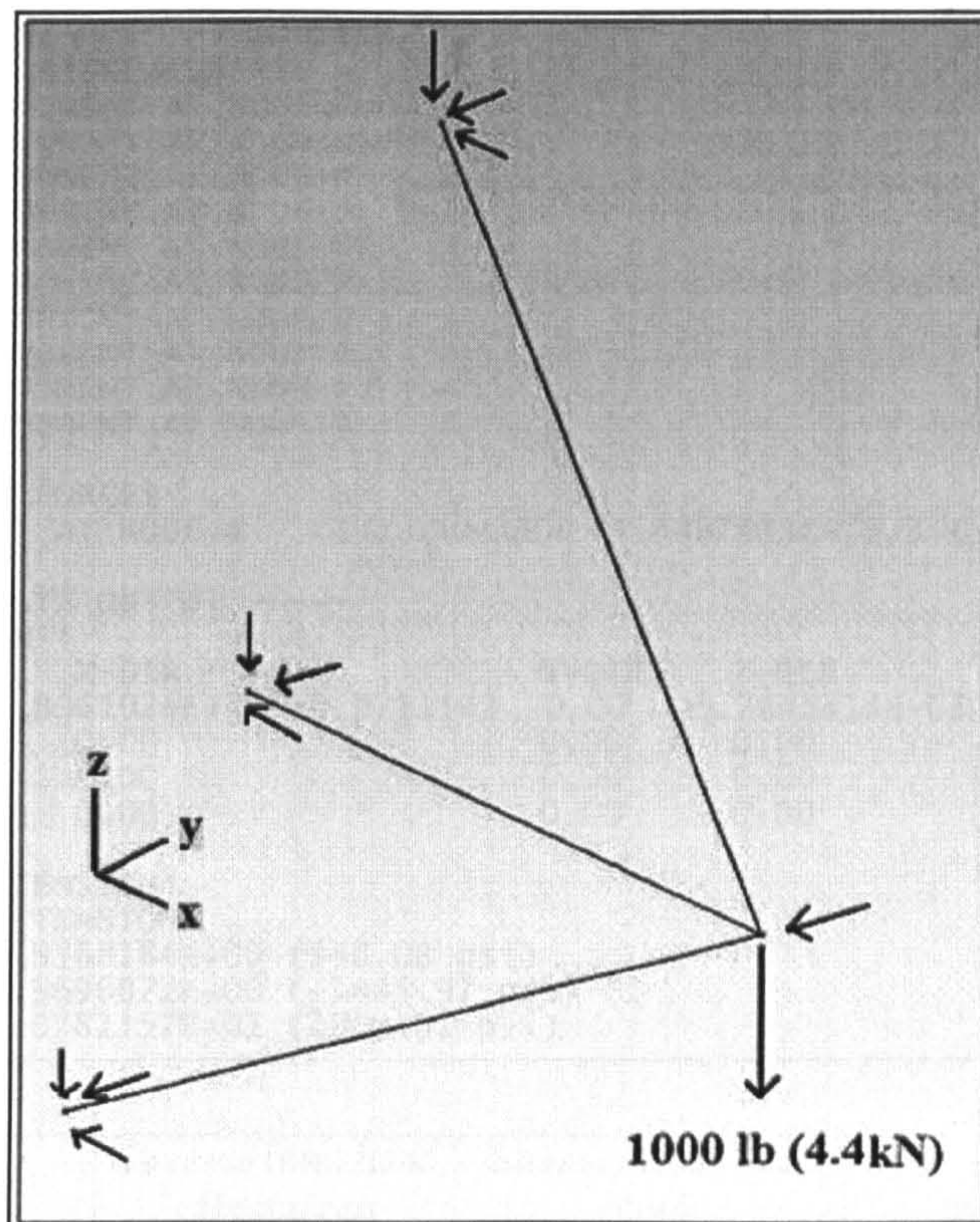


Figure (5.10) – *Gmsh* representation of the space truss.

The solution from the FLEXSTREM FEA block is presented:

```

OUTPUT
=====
FEA/3-D TRUSS ELEMENT/                               21-Oct-2010
-----
Space Truss (x-y-z) plane: Units(MN, m)
-----
# OF NODES =      4 :                               # OF ELEMENTS =      3
YOUNG-S MODULUS (E0) = 8.2737087E+03 (1.2E+6 Psi)

NODE NO.  1 :  X=  1.8288   Y=  0.00   Z=  0.00
NODE NO.  2 :  X=  0.00   Y=  9.144E-01 Z=  0.00
NODE NO.  3 :  X=  0.00   Y=  9.144E-01 Z=  1.8288
NODE NO.  4 :  X=  0.00   Y=  0.00   Z= -1.2192

ELMT NO.  1[1-2]: E/E0 =  1.00 : AREA =  1.9483800E-04 (0.302in²)
ELMT NO.  2[1-3]: E/E0 =  1.00 : AREA =  4.7032200E-04 (0.729in²)
ELMT NO.  3[1-4]: E/E0 =  1.00 : AREA =  1.2064500E-04 (0.187in²)

# OF FIXED DISPLACEMENTS =  10
  Y-COMPONENT AT NODE #  1
  X-COMPONENT AT NODE #  2
  Y-COMPONENT AT NODE #  2
  Z-COMPONENT AT NODE #  2
  X-COMPONENT AT NODE #  3
  Y-COMPONENT AT NODE #  3
  Z-COMPONENT AT NODE #  3
  X-COMPONENT AT NODE #  4
  Y-COMPONENT AT NODE #  4
  Z-COMPONENT AT NODE #  4

# OF GIVEN FORCES      =  1
Z-COMPONENT AT NODE #  1 : (VALUE= -4.4497411E-03 ) (-1000lb)

----- RESULTS OUTPUT -----
DISPLACEMENT:
  NODE      X-DIR      Y-DIR      Z-DIR
  1  -1.8061026E-03(-0.0711in)  0.00  -6.7643313E-03(-0.2663in)
  2           0.00           0.00           0.00
  3           0.00           0.00           0.00
  4           0.00           0.00           0.00

TENSION/EXTENSION:
ELEMENT      TENSION
  1  6.5368184E+00 (948.08 psi)
  2 -9.9696072E+00 (-1445.97 psi)
  3  1.9781157E+01 (2869.01 psi)
    
```

	Stresses from hand calculations	Stresses from FEA block	Percentage error
Element 1	955	948	0.73%
Element 2	1423	1445	1.55%
Element 3	2843	2869	0.91%

Table (5.1) – Percentage error in the stress results for each element by the FEA block.

From the validation analysis it can be seen that the approximations by the FEA block are in good agreement with those got from hand calculations as shown by the size of the percentage error in Table (5.1).

### 5.6.2.2 The Successive Over-Relaxation (SOR) method

An iterative approach may be applied when an  $n \times n$  matrix  $A$  is large but very sparse. The successive over relaxation (SOR) method is essentially the Gauss-Seidel method augmented by a factor called the acceleration parameter for quick convergence. In sub-process B3 the SOR method solves the unknown variables in  $F$  and  $X$  in Equation (5.31).

The stress in the members and the accompanying extension could be determined from the solution obtained from the SOR module following the equations outlined:

For stress:

$$\hat{x} = \hat{k}TF \quad (5.31)$$

$$\hat{k} = \frac{AE}{L} \begin{bmatrix} 1 & -1 \\ -1 & 1 \end{bmatrix} \quad (5.32)$$

hence the stress in a member  $\sigma$  ( $\sigma = \frac{\hat{x}}{A}$ ) is given as:

$$\sigma = \frac{E}{L} \begin{bmatrix} \gamma & -\gamma \end{bmatrix} F \quad (5.33)$$

$$\gamma = [-C_x \quad -C_y \quad -C_z] \quad (5.34)$$

The nodal stresses occur at both ends of the member. They are required for analysis on the structure nodes in later processes.

Further examination of the governing FEA Equation (5.30) is demonstrated in the following analysis:

$$\hat{x} = \hat{k}TF \quad (5.35)$$

From Equation (5.17),

$$\hat{F} = TF \quad (5.17)$$

$$\boxed{\hat{x} = \hat{k}\hat{F}} \quad (5.36)$$

The nodal reactions (forces) could be determined by a substitution of the variables derived hitherto, into the governing FEA Equation (5.30):

$$KF = X$$

Manipulation of Equation (5.36) as done by Belegundu (1984) is the most fundamental principle for efficiency of FLEXSTREM. Consider the following:

The (member) local force or reaction varies directly with the local displacement:

$$\hat{x} \propto \hat{F}$$

The constant of proportionality  $\hat{k}$ , is introduced to fully define the relationship between these two key variables, where the stiffness matrix  $\hat{k}$  depends on the following fixed parameters:

- Geometry: Element cross-sectional area  $A$  and length  $L$ .
- Material property: Element modulus of elasticity  $E$ .

$$\hat{x}^* = \hat{k}\hat{F}^* \quad (5.37)$$

this compares directly with the principal Equation (5.30):

$$\boxed{KF = X}$$

thus, an increase by a factor of  $\omega$ :

$$\hat{x} = \omega\hat{x}^* \quad (5.38)$$

would imply (substitute Equation (5.39) in (5.37)):

$$\hat{k} \cdot \hat{F} = \hat{x} = \omega \cdot \hat{x}^* \quad (5.39)$$

thus,

$$\boxed{\hat{F} = \omega \cdot \hat{F}^*} \quad (5.40)$$

while  $\hat{k}$  is left constant.

The local force  $\hat{F}$  is input as a given force (dead load). The factor  $\omega$  (which would be later known as the load/increment factor) is introduced during in MCS phase of the analysis (in process L) for limit state analyses of individual members. Without Equation (5.40) FLEXSTREM would be computationally more expensive as it would have to loop the whole FEA-block process as many time as the MCS.

#### 5.6.2.3 B4 – Reference Variable (Shielding Factor) for Wind Force Estimation

The synthesis of the shielding factor  $\varphi$ , was placed at process C outside of the main MCS loop for computational efficiency as its synthesis is independent of any random variables; it is dependent solely on fixed variables i.e. variables that would undergo no further modifications during the analysis. The implementation of the process from the tables from the referred standard (BS-2573-1:1983) is available in appendix B.

### 5.6.3 Process C – MCS Process

This is the implementation of the MCS loop as discussed in chapter 3. The distinction between an ordinary simulation, which is the emulation of the physical processes via discrete models, and the MCS, is the augmentation with a random factor. Each of the processes involved in this loop has certain distributions attributed to them. The distributions applied to the processes in this analysis include:

- Uniform distribution (applied to the external loading (live))
- Normal distribution (applied to the stress)
- Log-normal distribution (applied throughout LEFM analysis except crack growth)
- Exponential distribution (applied to crack growth)
- Gumbel (type-I extreme) distribution (applied to wind velocity)

The inverse transform method is employed for the generation of random numbers for the uniform, exponential and Gumbel distributions while the Box-Muller method is used for random number generation for the normal and lognormal distributions.

### 5.6.4 Process D – Wind Force Computation

The algorithm flow for process D is shown in Figure (5.11).

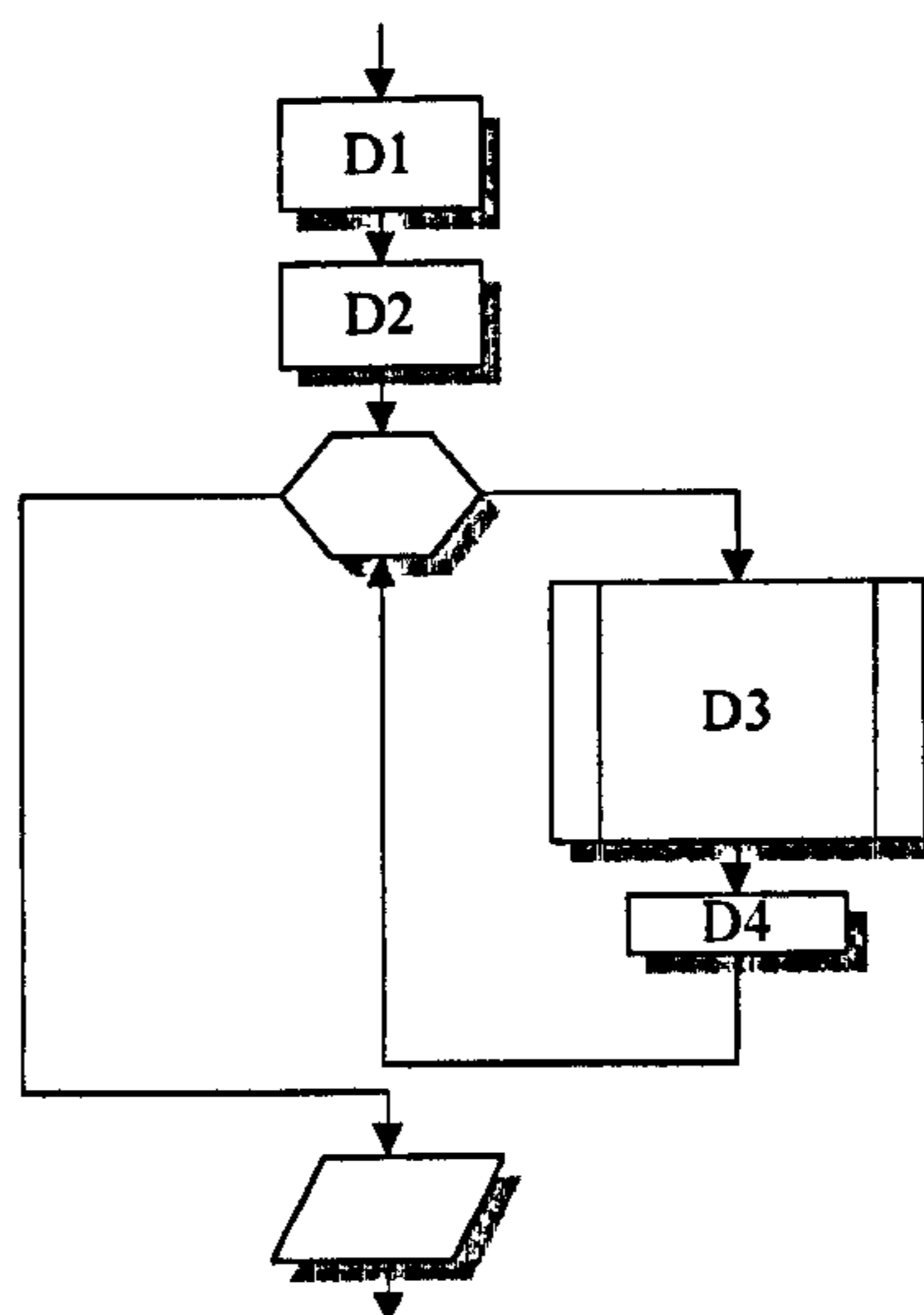


Figure (5.11) – Process F.

According to Simiu and Heckert (1996), the wind velocity in the offshore environment has a Gumbel distribution. Sub-process D1 is the transformation of the wind speed to the Gumbel distribution via a Gumbel distributed random number. This is done by the implementation in Equation (2.29).

Sub-process D2 is the derivation of the dynamic pressure of the wind using Equation (5.6). The Gumbel-transformed wind speed is used in this calculation. D3 is the computation of the wind force on windward and leeward members using Equations (5.7) and (5.8) respectively.

D4 is the culmination of the individual forces to a single total force. This force becomes the wind force acting on the whole structure as a result of the wind speed (transformed) using Equation (5.9).

#### **5.6.5 Process E – Loading Combination and Determination of Load Increment Factors**

This is another vital process utilized by FLEXSTREM. This is the FLEXSTREM normalized load combination implemented as:

$$\omega = \left[ \frac{LD_{struct} + U(LD) + LD_{TW} + X_{gb}(W_{fl}^*)}{LD_{dead}} \right] + 1 \quad (5.41)$$

where,

$\omega$  – load increment factor (dimensionless)

$LD$  – live load (N)

$LD_{struct}$  – structural weight (N)

$LD_{dead}$  – total dead load acting on the structure (N)

$LD_{TW}$  – wind force (N)

$W_{fl}$  – wind force on live load (N)

$U$  – indicates uniform distribution

$X_{gb}$  – indicates Gumbel distribution

\* optional

In this load combination culled and adapted from BS-2573-1:1983, the normalizing parameter is the total dead load used to establish the load and stress results from the FEA analysis. Where there are no explicit loads, an arbitrary value such as 1N could be assumed.

*General Form for Processes and Limit States*

The stress and strength functions which form the limit state function are set up with references mainly from Salmon and Johnson (1996) for mechanical processes unless stated otherwise. This is as a result of the recognition of the variability of strength with cross-sectional area. Adapting the analysis to suit different member configurations becomes necessary as most structures possess members with more than a unitary cross-section group.

The LFM limit state functions are set up with references from Shigley et al (2004) and derivatives of the Paris Equation (Paris et al (1961)) unless stated otherwise. From here on, processes would take the following generic structure (Figure (5.12)) unless stated otherwise:

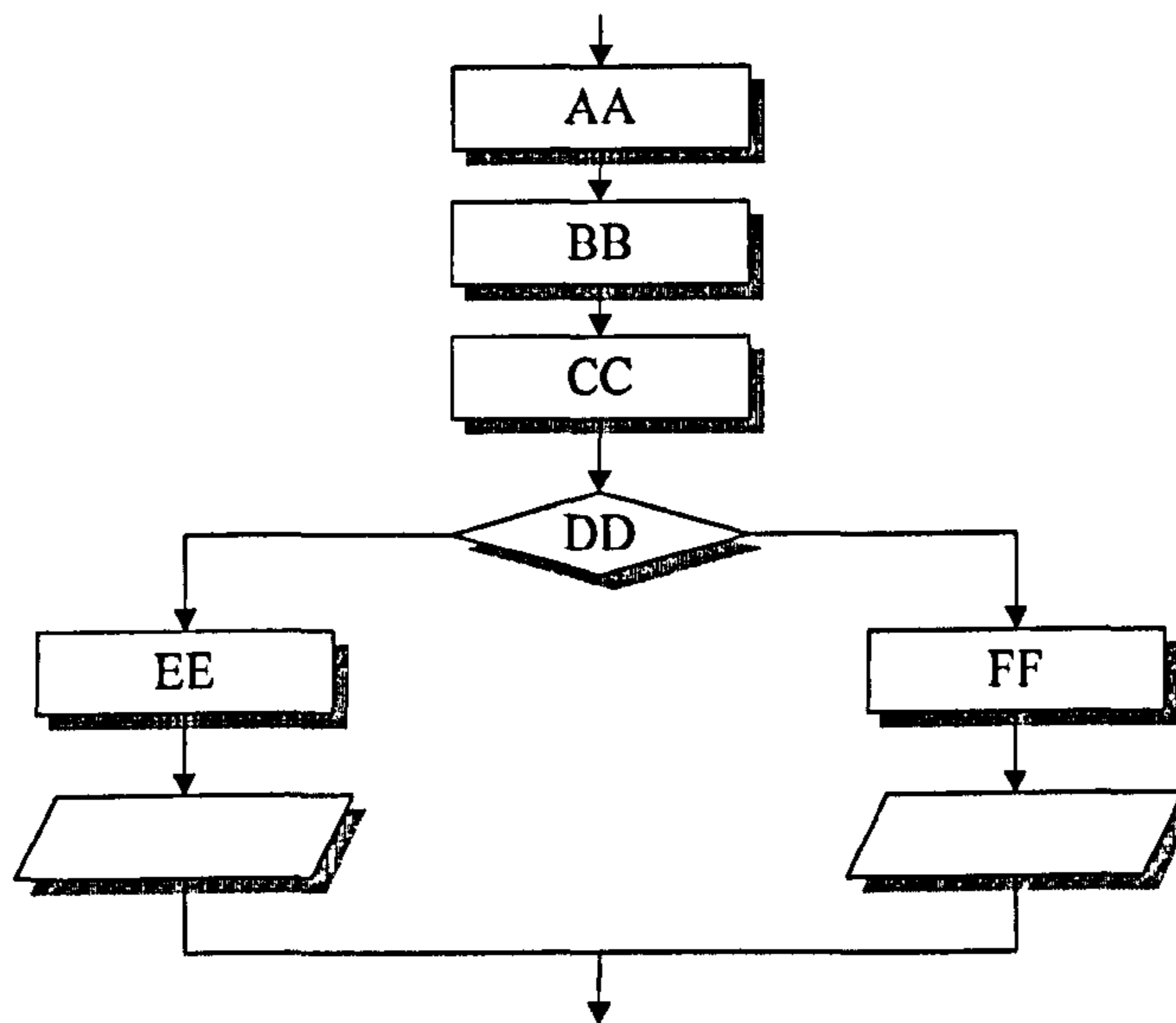


Figure (5.12) – Generic structure.



where,

AA – governing strength and stress equations

BB – transformation of the strength to the assigned strength distribution (outlined at process D)

CC – transformation of the stress to the assigned stress distribution (outlined at process D)

DD – condition:  $CC \geq BB$

EE – condition that DD = true, hence  $LMZ = true$  (i.e. failure)

FF – condition that DD = false, hence  $LMZ = false$  (i.e. survival)

LMZ – current state of the limit state function of the overarching process

Also, every limit state analysis takes the following structure unless (Figure (5.13)) otherwise stated.

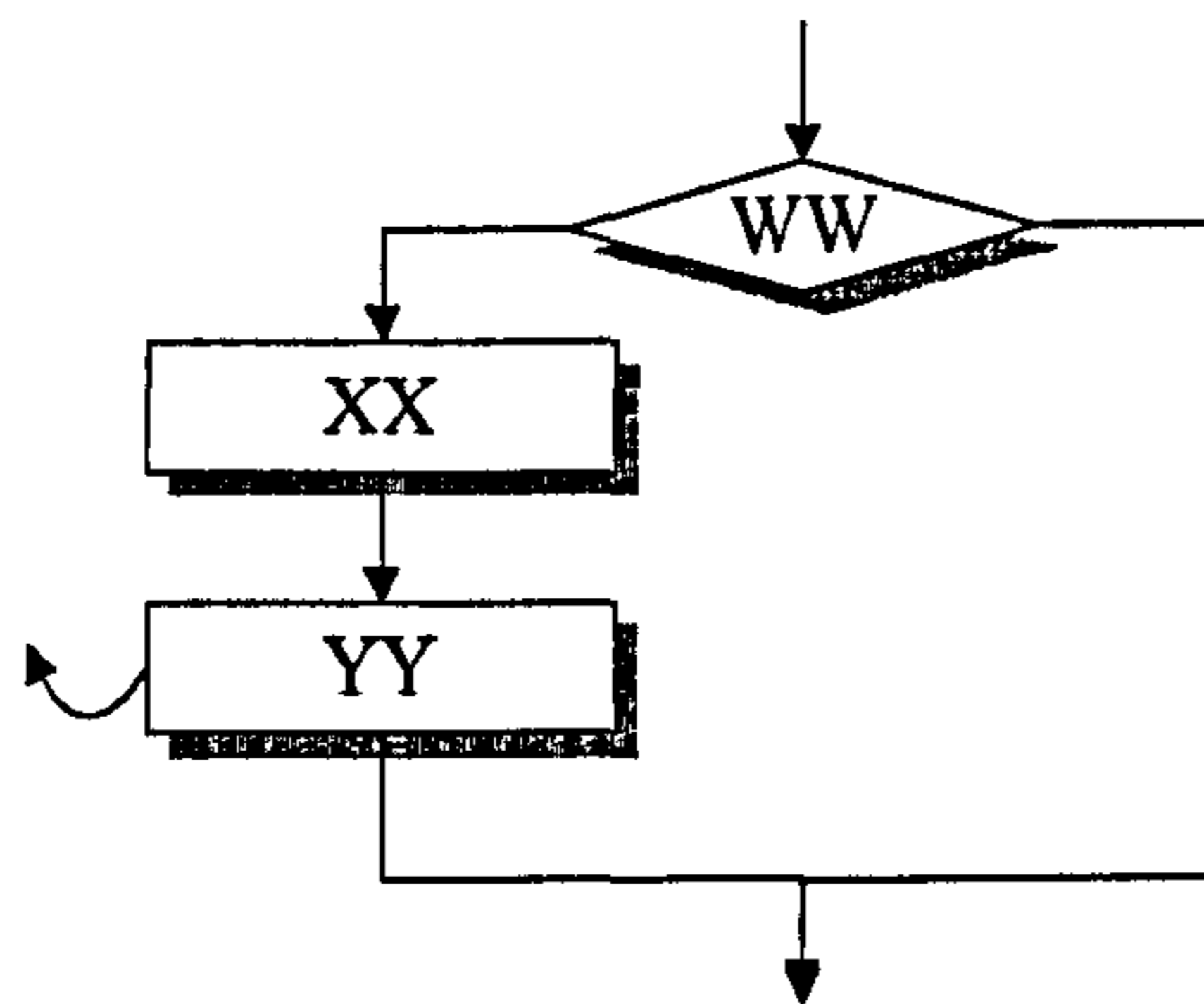


Figure (5.13) – Generic limit state.

where,

WW – condition:  $LMZ = true$

XX –  $PFC = PFC + 1$  (on the condition that  $LMZ = true$ )

YY – exit to begin MCS loop again for  $N < NSIM$

PFC – process failure counter

N – MCS simulation number

NSIM – number of MCS simulations

## 5.7 Type I (SMS Processes)

### 5.7.1 Process F – Bending Stress Analysis

The process follows the generic procedure outlined in Figure (5.12). The bending stress is given as:

$$\sigma_{bend} = \frac{M \times c}{I_{mont}} \quad (5.42)$$

where  $\sigma_{bend}$  is the bending stress (MPa),  $M$  is the moment of the section (MNm),  $I_{mont}$  is the second moment of the closed section area of the beam ( $m^4$ ) of the section and  $c$  is the centroidal distance (half the vertical cross sectional height (for uniform cross sections)) from the neutral axis (m).

The yield moment (stress) is given as:

$$y_m = \frac{I_{mont}}{c} \times F_y \quad (5.43)$$

where  $y_m$  is the yielding moment and  $F_y$  is uniaxial yield stress. The bending stress and the yielding moment are normally distributed according to Huajian and Yongchang (1995). LM I is the bending limit state analysis. It follows the generic procedure outlined in Figure (5.13).

### 5.7.2 Process G – Tensile Stress Analysis

The process follows the generic procedure outlined in Figure (5.12). The yield stress (strength function) is given as:

$$F_n = C_A F_{ten} \quad (5.44)$$

where  $F_n$  is the nominal yield stress,  $C_A$  is the cross-sectional area and  $F_{ten}$  is the uniaxial tensile strength. This becomes the strength of the section under consideration. It is against this value that the stress on the section is compared with in the limit state analysis. The tensile stress and the nominal yield stress are normally distributed. LM II is the tensile limit state analysis. It follows the generic procedure outlined in Figure (5.13).

### 5.7.3 Process H – Compressive Stress

This process also follows the pattern outlined in Figure (5.12). It also has the only strength function (mechanical) that is independent of the uniaxial yield stress of the material. The section properties and the Young's modulus are the main determinants of the survival of the said member. The compressive strength is given as:

$$P_{cr} = \frac{\pi^2 E}{(T_{len}/r)^2} C_A = F_{cr} C_A \quad (5.45)$$

$$r = \sqrt{I_{mont}/C_A} \quad (5.46)$$

where,

$P_{cr}$  – compressive strength (MPa)

$F_{cr}$  – average compressive strength (MPa)

$E$  – Young's modulus (MPa)

$C_A$  – cross-sectional area (m<sup>2</sup>)

$T_{len}$  – member length (m)

$r$  – radius of gyration (m)

$I_{mont}$  – second moment of the closed section area of the beam (m<sup>4</sup>)

The compressive strength and the axial stress are normally distributed. LM III is the compressive limit state analysis. It follows the generic procedure outlined in Figure (5.13).

### 5.7.4 Process I – Multiaxial Stress Analysis

The process follows the generic procedure in Figure (5.12). The following stress is experienced by whole structures or members subjected to a combination of the three stresses mentioned in the preceding processes. The three stresses act in only two planes however. Compression and tension stresses on one plane, while bending on a different plane. Shear stresses are not included in FLEXSTREM. The Huber-Von Mises-Hencky yield criterion (Hovgaard (1930)) is utilized and is given as:

$$\sigma_{mul} = \sqrt{(\sigma_{ten} - \sigma_{comp})^2 + \sigma_{tor}^2 - (\sigma_{tor} \times (\sigma_{ten} - \sigma_{comp}))} \quad (5.47)$$

where  $\sigma_{mul}$  is the multiaxial stress (MPa) and  $\sigma_{tor}$  is the torsion in the cross-section.

The place of  $\sigma_{tor}$  in Equation (5.48) is usually the torsion experienced by the member or structure but could be replaced by the bending stress according to Trahair and Pi (1997).

The multiaxial stress is not assigned to any distribution since its constituents are already distributed. Only the uniaxial yield stress is assigned to a distribution. LM IV is the multiaxial limit state analysis. It follows the generic procedure outlined in Figure (5.13).

### 5.7.5 Process J – Crack Length Estimation

The crack length is estimated by the following equation:

$$a_f = x_{exp} \times a_i \quad (5.48)$$

where,

$a_f$  – current length of crack (m)

$a_i$  – initial length of crack (m)

$x_{exp}$  – exponentially distributed random number

According to Karamchandani et al (1991) the crack length propagates exponentially. The cracks (and hence fatigue) in structures usually occur at the nodes especially those constrained to zero displacement in at least one direction. It is a singular step in the FLEXSTREM not following the algorithm flow set out in Figure (5.12).

### 5.7.6 Process K – Stress Intensity Factor Analysis

This estimates the stress intensity factor at a node from the LEFM fast fracture equation:

$$K_I = mat_{\beta} \sigma_{mul} \sqrt{\pi a_f} \quad (5.49)$$

where,

$K_I$  – stress intensity factor (MPa $m^{1/2}$ )

$mat_{\beta}$  – stress intensity correction factor

$\sigma_{mul}$  – multiaxial stress (MPa)

The process follows the generic procedure outlined in Figure (5.12) however the stress intensity factor itself needs no transformation (CLT). Only the fracture toughness (the strength function) needs transformation to the lognormal distribution. LM V is the

fracture toughness limit state analysis. It follows the generic procedure outlined in Figure (5.13). Here  $mat_{\beta}$ , the stress intensity correction factor is a function of certain parameters such as crack length, section width/diameter, etc, and depends on the section geometry. It could also be determined from either handbooks (based on the crack length, depth, geometry, etc.) or by use of the fractal finite element analysis (FFEA).

### 5.7.7 Process L – Minimum Crack

This is a unit step process not conforming to the pattern set out in Figure (5.12). The minimum crack length (critical crack length) required for fast fracture to occur at a discontinuity is given by:

$$a_c = \frac{1}{\pi} \left( \frac{K_{IC}}{mat_{\beta} \sigma_{mul}} \right)^2 \quad (5.50)$$

where  $a_c$  is the minimum crack and  $K_{IC}$  is the fracture toughness of the material. No transformation is necessary. The minimum crack length may also be specifically indicated as certain values or ratios.

### 5.7.8 Process M – Fracture Analysis

This process compares outputs of processes J and L (the crack length and minimum crack respectively) in a procedure similar to the operation of ‘DD’ to ‘end’ in Figure (5.12). LM VI is the fracture toughness limit state analysis. It follows the generic procedure outlined in Figure (5.13).

### 5.7.9 Process N – Life Cycle Assessment

The planned/intended/design life of the structure is the strength function while the resultant life (as a result of repeated loading) is the stress function estimated from the LEFM equation:

$$N_{OP} = \frac{1}{mat_c} \int_{a_i}^{a_f} \frac{da}{(mat_{\beta} \sigma_{mul} \times \sqrt{\pi a})^{mat_m}} \quad (5.51)$$

where,

$N_{OP}$  – resultant life of the structure (in cycles)

$mat_C$  – crack growth rate coefficient

$mat_m$  – crack growth exponent

This process follows the procedure outlined in Figure (5.12) with a key difference. The planned/intended/design life used here is the loaded life of the structure which is less than the total life. It is specified in loaded cycles. The key difference is that unlike other limit states where the stress function cannot exceed or be equal to the strength function, it is important that the resultant life (stress function) always exceeds the design life (stress function).

The transformation of  $mat_C$  to the lognormal distribution (Karamchandani (1991)) is done at process AA in Figure (5.12). The resultant life  $N_{OP}$  is not transformed (CLT). The planned/intended/design life is lognormally distributed (Chryssanthopoulos and Righiniotis (2006)). LM VII is the life limit state analysis. It follows the generic procedure outlined in Figure (5.13).

## 5.8 Type II (Multi-Member Processes)

### 5.8.1 Process O – Member Analyses

The flow of the procedure is outlined as follows (Figure (5.14)):

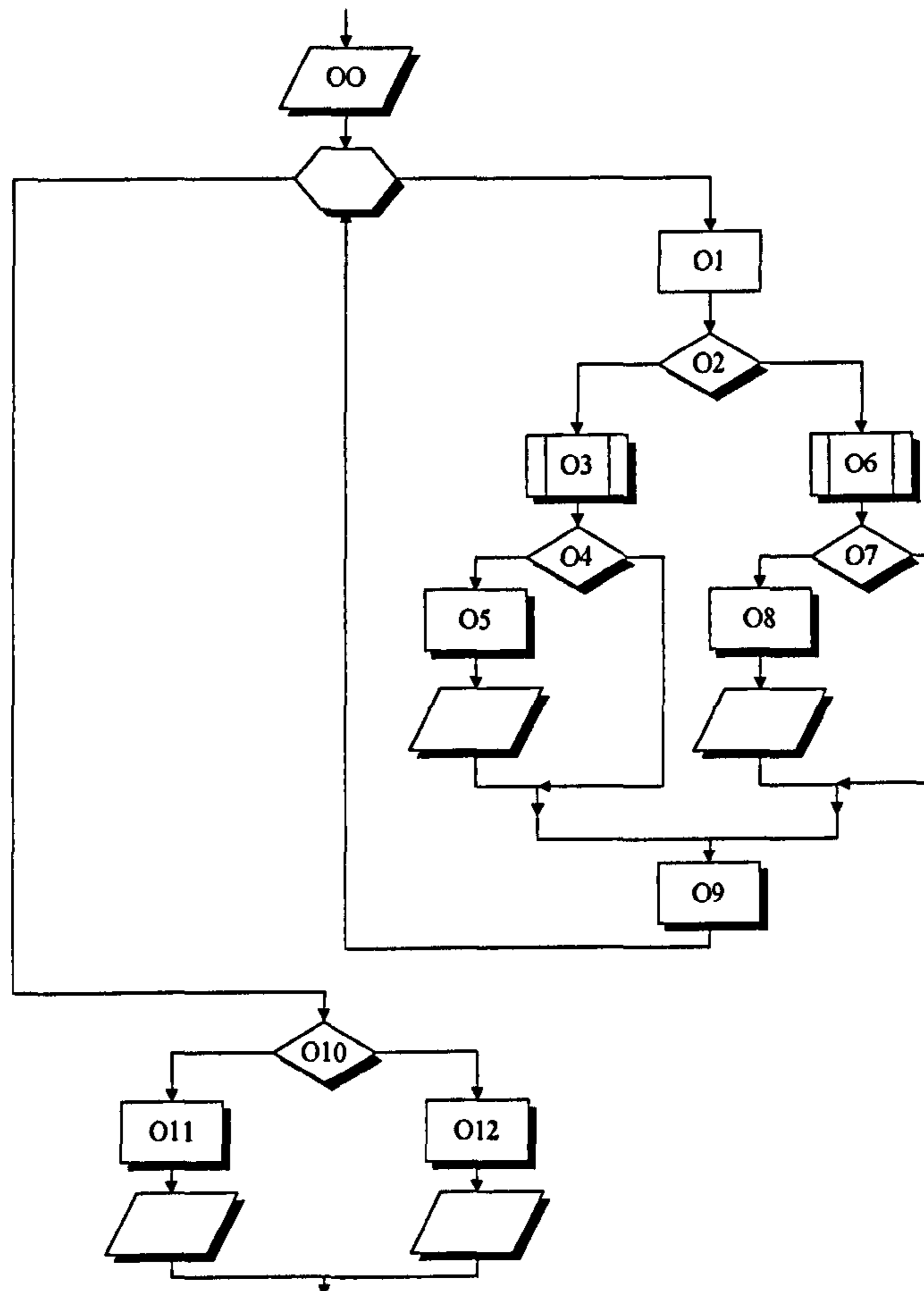


Figure (5.14) – Member analysis.

The procedure takes advantage of the FLEXSTREM governing Equation (5.40). At I/O process OO, the system (structural) definition including all members and their respective configurations are initialized. Also, the output structural response (stresses experienced by individual members as a result of the dead load(s)) is output from process B. Furthermore, the load (as a result of the increment factor) exerted on the structure is output from process E. This load (different/changes at each MCS iteration) leads to a new structural response which is reflected in the stress present in each of the

structure members. For a given member, the new stress it experiences is equivalent to the product of the load/increment factor  $\omega$ , and the datum (pre-existing) response (which is constant (from process B, stored in memory)), as a result of a dead load. In this way, considerable time and resources are saved compared to a situation where the whole FEA (sub-process B3) is repeated (looped) continually. The attention to individual structural members is illustrated in Figure (5.15).

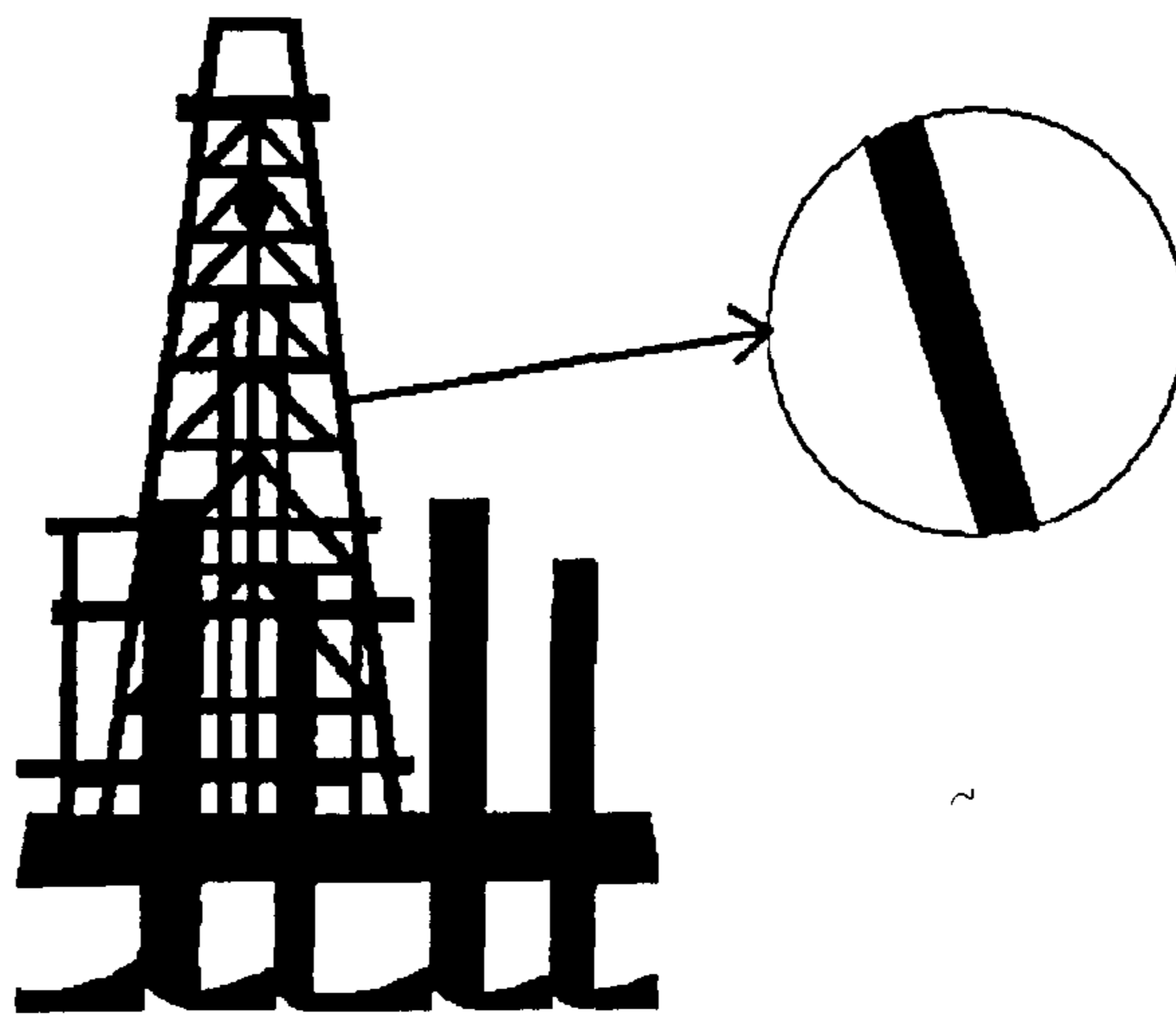


Figure (5.15) – Member analysis illustration.

At O1, the following takes place:

$$\sigma_{mem} = \omega \cdot \sigma_{mem} \quad (5.52)$$

The stress  $\sigma_{mem}$ , when positive indicates a member under tension and when negative indicates a member under compression. O2 serves to ascertain this stress status.

O3 follows if the stress (from O2) is positive (i.e. tensile). O3 is similar to process I:

$$F_{n(mem)} = C_{A(mem)} F_{ten(mem)} \quad (5.53)$$

A sub-limit analysis in O3 reveals failure or survival of the member under tension. The survival report is then passed to O4. On failure O5 is initialized. O5 is a tensile failure counter.

O6 follows if the stress (from O2) is negative. As a compression analysis, process similarities are exact as in process J:



$$P_{cr(mem)} = \frac{\pi^2 E}{(T_{len(mem)}/r_{(mem)})^2} C_A = F_{cr(mem)} C_{A(mem)} \quad (5.54)$$

$$r_{(mem)} = \sqrt{I_{mont(mem)}/C_{A(mem)}} \quad (5.55)$$

A sub-limit analysis in O6 reveals failure or survival of the member under tension. The survival report is then passed to O7. On failure O8 is initialized. O8 is a compressive failure counter.

O9 totals any failure occurrences in O5 and O8. O10, O11 and O12 are akin to DD, EE and FF in Figure (5.12) respectively. Here, data recording is done only for the particular member selected for analysis. All member responses are not recorded at once. For analyses covering beam or frame elements, a bending analysis would be included and would also embody a multiaxial stress analysis. LM VIII is the member limit state analysis. It follows the generic procedure outlined in Figure (5.13).

### 5.8.2 Process P – Node (Joint) LEFM Analyses

The flow of the procedure is outlined as follows (Figure (5.16)):

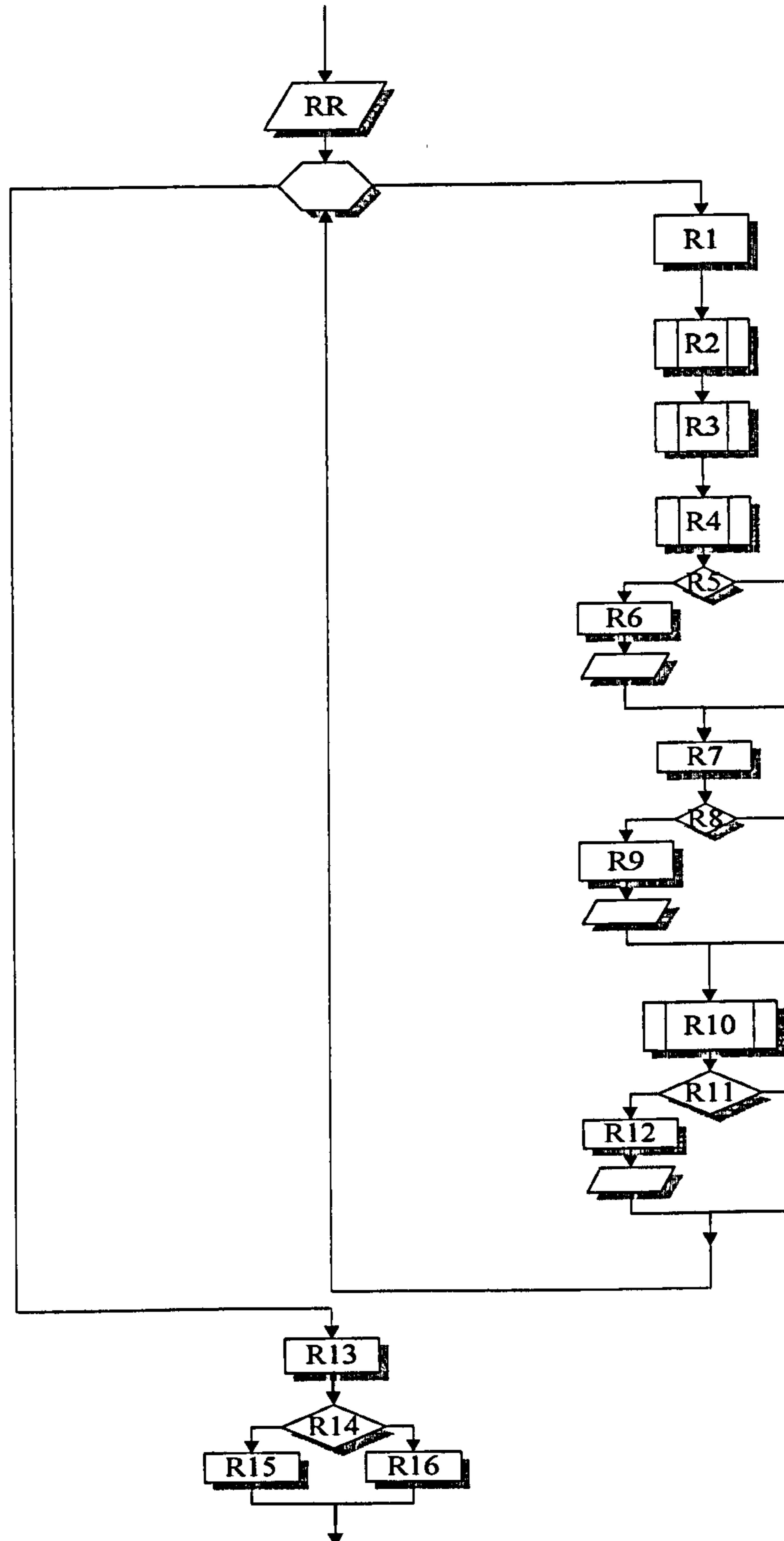


Figure (5.16) – Joint (node) analyses.

This is another configuration specific analysis. Mechanical (axial stress related) failures usually occur on the members. However the most dominant niche of failure on multi-member structures is at the joints (nodes) of the structure (Bucciarelli (2002)). The nodes are thus analyzed using the LEFM approach as the cracks and fatigue failure mechanisms are in operation here.

At RR, the system (structural) definition parameters including all nodes and their respective configurations are initialized. The displacements in all three coordinates at each node are also initialized. The FLEXSTREM governing equation is applied in this procedure. It should be noted that the initialized displacements are a result of a given force – the dead load(s) (MN). The load increment factor  $\omega$  (by which new displacements (part of the structural response) would be derived) is also initialized. The attention to individual structural nodes (joints) is illustrated in Figure (5.17).

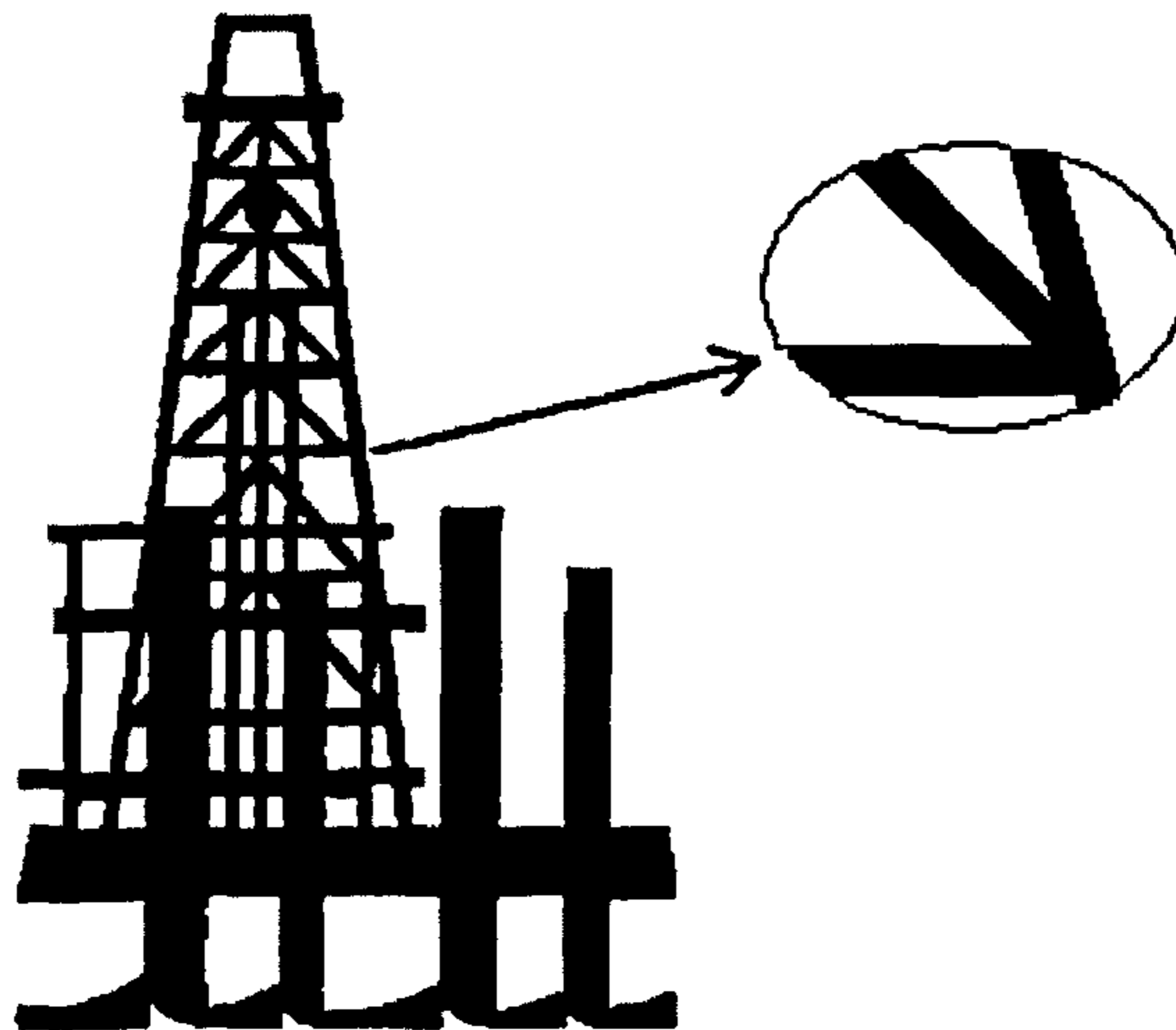


Figure (5.17) – Node analyses illustration.

At R1, the nodal stress derived from the FEA solution process is multiplied by the load/increment factor:

$$\sigma_{mul(nd)} = \omega \times \sigma_{str(nd)} \quad (5.56)$$

where,

$\sigma_{mul(nd)}$  – factored stress at node in (MPa)

$\sigma_{str(nd)}$  – nodal stress from FEA block (MPa)

It is then transformed to the Gaussian (normal) distribution and sent to the external procedure R3 (similar to process J) which returns the estimated crack length propagated at each node:

$$a_{f(nd)} = X_{exp}(a_{i(nd)}) \quad (5.57)$$

R4 is an external procedure (similar to process M). The hitherto derived nodal multiaxial stress and nodal crack length are input alongside  $mat_{\beta}$  to obtain the nodal stress intensity factor  $K_{I(nd)}$  via Equation (5.59):

$$K_{I(nd)} = mat_{\beta} \sigma_{mul(nd)} \sqrt{\pi a_{f(nd)}} \quad (5.58)$$

$$mat_{\beta} = F\left(\frac{r_i}{r_o}, \frac{a_f}{thk}\right) \quad (5.59)$$

The outputs: the fracture toughness (transformed lognormally) and the stress intensity factor are compared within this external procedure. The outcome (a logical value depicting failure or survival) is fed back through a logic variable. This logic variable is input at R5. On failure, the value (at which failure occurred) and the event are recorded at R6 for each node.

#### *Stress Intensity Correction Factor for Tubular Multi-Member Structures*

The stress intensity correction factor  $mat_{\beta}$ , is a function of the crack length, depth, width, thickness, angle of propagation and geometry of component (joint) (Etube et al (1999)). This value is very shape dependent. In the fatigue analyses of structures, very many assumptions are made (e.g. flat surface, symmetry etc) in the determination of this value. It is indeed difficult to establish a general relationship between these parameters mentioned hitherto, as the designated empirical solutions available throughout literature are often very specimen (and geometry) specific. The specific nature of the empirical formulations inhibits application to a wide range of structures as this research attempts to do. A probabilistic approach is also hampered by the lack of an assigned distribution in literatures. Various literatures have dealt mainly with the stress intensity correction factor of a single component of given type obtained empirically. Those that focused on complex structures mostly referred to handbooks or the use of the fractal FEA (FFEA) to obtain this value. Generally, approximated stress intensity correction factors are used to determine the stress intensity factor and hence the life of the structure.

EXCLUDED  
UNDER  
INSTRUCTION  
FROM  
UNIVERSITY

The crack propagation very much depends on the loading on the structure (Etube et al (1999)). Very little attention is given to the effect of variable amplitude loading. The “rainflow counting method” introduced by Matsuishi and Endo (1968) is a prominent method of reducing the variable amplitudes of loading into simple loadings and reversals. “Most of the existing models [stress intensity correction factor formulations] do not allow for interaction effects to be accounted for. Those that attempt to model interaction effects are based on a cycle by cycle analysis with emphasis on single overloads or underloads. This often makes their use on engineering structures impractical”. This research considers a wide range of structures consisting of K-connections, T-connections, Y-connections, etc. and their adjacent permutations. There are also multiple thicknesses at the structure joint.

For an accurate model of these types of structures, a flexible method of obtaining the stress intensity correction factors such as the FFEA would be highly recommended. In the absence of this a limitation is thus imposed on the FLEXSTREM proposed in this research. As only tubular members are dealt with presently, the stress intensity correction factor formulation for an external circumferential crack in a thick walled cylinder from Tada et al (2000) is proposed. Also, appropriate  $mat_{\beta}$  values or functions that suit the geometrical specification of other cross-sections could be introduced. The randomness already present in the overall model should suffice for any short falls from the values obtained from the proposed model.

Figure (5.18) – External circumferential crack in a thick walled cylinder (Tada et al (2000)).

where  $p$  in Figure (5.18) is the stress in the cylinder,  $a$  is the crack length,  $t$  is the thickness and  $r_i$  and  $r_o$  are the inner and outer radii of the cylinder respectively.

The value of  $mat_\beta$  is determined from the graph depicted in Figure (5.19). To do this, two primary parameters are initially required:

- the ratio of the crack length  $a$  to the thickness  $t$ ;
- the ratio of the inner diameter  $r_i$  to the outer diameter  $r_o$ .

Methods: Integral Transform - Integral Equations ( $a/t \leq 0.6$ ), Interpolation ( $a/t > 0.6$ )  
Accuracy: Solid curves ( $0.1 \leq r_i/r_o \leq 0.9; a/t \leq 0.6$ ) are based on values with better than 1% accuracy;  
2% for  $a/t > 0.6$ .  
References: Erdogan 1982; Tada 1985

Figure (5.19) – Plot of the function in Equation (5.61) (Tada (2000)).

Placing these parameters into the graph in Figure (5.19) gives of a value,  $val$  (read off the y-axis). This value is an outcome of the function expressed in Equation (5.60):

$$\frac{\sqrt{1 - \frac{a}{t}}}{1 + \frac{r_o}{r_i}} mat_{\beta} = val \quad (5.60)$$

To determine the value of the stress intensity correction factor,  $mat_{\beta}$ , Equation (5.61) is utilized:

$$mat_{\beta} = \frac{val}{\frac{\sqrt{1 - \frac{a}{t}}}{1 + \frac{r_o}{r_i}}} \quad (5.61)$$

The model is limited to tubular sections where the ratio of the crack length to the wall thickness does not exceed 0.8.



*Validation of the Stress Intensity Correction Factor*

The values of  $val$  generated from the FLEXSTREM in Tables (5.2) and (5.3) are to be compared with those seen on the graph shown in Figure (5.19). The  $val$  and  $mat_{\beta}$  values have been determined for  $r/r_o$  ratios ranging from 0.01-1.0. Linear interpolations have been utilized where necessary.

$r/r_o$ Range	$Val$	Crack length ( $a$ )	$r/r_o$	thickness( $t$ )	$a/t$	$mat_{\beta}$
0-0.1	0.0100	0.001	0.0100	0.99000	0.00101	1.0105
	0.0125	0.002	0.0125	0.98745	0.00203	1.0136
	0.0453	0.003	0.0453	0.95475	0.00314	1.0469
	0.0767	0.004	0.0767	0.92331	0.00433	1.0790
	0.1050	0.005	0.1063	0.89369	0.00559	1.0963
0.1-0.2	0.1000	0.001	0.1000	0.90000	0.00111	1.1006
	0.1020	0.002	0.1025	0.89745	0.00223	1.0983
	0.1282	0.003	0.1353	0.86475	0.00347	1.0779
	0.1534	0.004	0.1667	0.83331	0.00480	1.0759
	0.1770	0.005	0.1963	0.80369	0.00622	1.0823
0.2-0.3	0.1800	0.001	0.2000	0.80000	0.00125	1.0807
	0.1822	0.002	0.2025	0.79745	0.00251	1.0829
	0.2100	0.003	0.2353	0.76475	0.00392	1.1046
	0.2367	0.004	0.2667	0.73331	0.00545	1.1273
	0.2619	0.005	0.2963	0.70369	0.00711	1.1497
0.3-0.4	0.2650	0.001	0.3000	0.70000	0.00143	1.1492
	0.2665	0.002	0.3025	0.69745	0.00287	1.1491
	0.2862	0.003	0.3353	0.66475	0.00451	1.1423
	0.3050	0.004	0.3667	0.63331	0.00632	1.1404
	0.3228	0.005	0.3963	0.60369	0.00828	1.1420
0.4-0.5	0.3250	0.001	0.4000	0.60000	0.00167	1.1384
	0.3263	0.002	0.4025	0.59745	0.00335	1.1387
	0.3426	0.003	0.4353	0.56475	0.00531	1.1328
	0.3583	0.004	0.4667	0.53331	0.00750	1.1304
	0.3732	0.005	0.4963	0.50369	0.00993	1.1306

Table (5.2) – Validation of the stress intensity correction factor for  $r/r_o$  ratio: 0.0 – 0.5.

$r/r_o$ Range	$Val$	Crack length ( $a$ )	$r/r_o$	thickness( $t$ )	$a/t$	$mat_{\beta}$
0.5-0.6	0.3750	0.001	0.5000	0.50000	0.00200	1.1261
	0.3765	0.002	0.5025	0.49745	0.00402	1.1280
	0.3962	0.003	0.5353	0.46475	0.00646	1.1400
	0.4150	0.004	0.5667	0.43331	0.00923	1.1527
	0.4328	0.005	0.5963	0.40369	0.01239	1.1658
0.6-0.7	0.4350	0.001	0.6000	0.40000	0.00250	1.1615
	0.4356	0.002	0.6025	0.39745	0.00503	1.1616
	0.4438	0.003	0.6353	0.36475	0.00822	1.1472
	0.4517	0.004	0.6667	0.33331	0.01200	1.1360
	0.4591	0.005	0.6963	0.30369	0.01646	1.1277
0.7-0.8	0.4600	0.001	0.7000	0.30000	0.00333	1.1190
	0.4610	0.002	0.7025	0.29745	0.00672	1.1210
	0.4741	0.003	0.7353	0.26475	0.01133	1.1253
	0.4867	0.004	0.7667	0.23331	0.01714	1.1312
	0.4985	0.005	0.7963	0.20369	0.02455	1.1386
0.8-0.9	0.5000	0.001	0.8000	0.20000	0.00500	1.1278
	0.5009	0.002	0.8025	0.19745	0.01013	1.1308
	0.5123	0.003	0.8353	0.16475	0.01821	1.1361
	0.5233	0.004	0.8667	0.13331	0.03001	1.1445
	0.5337	0.005	0.8963	0.10369	0.04822	1.1574
0.9-1.0	1	0.001	0.9000	0.10000	0.01000	2.1217
	1	0.002	0.9025	0.09745	0.02052	2.1299
	1	0.003	0.9353	0.06475	0.04633	2.1189
	1	0.004	0.9667	0.03331	0.12009	2.1688

Table (5.3) – Validation of the stress intensity correction factor for  $r/r_o$  ratio: 0.6 – 1.0.

From Tables (5.2) and (5.3), it could be seen that the  $val$  values obtained from the FLEXSTREM module are in good agreement with those from the graph in Figure (5.19).

R7 (similar to process N) determines the minimum crack length that would cause failure at each node from Equation (5.62):

$$a_{c(nd)} = \frac{1}{\pi} \left( \frac{K_{IC(nd)}}{mat_{\beta} \sigma_{mul(nd)}} \right)^2 \quad (5.62)$$

R8 compares this length with the estimated crack length from R3. On failure the event and failure values are recorded at R9 for each node.

R10 is an external procedure similar to process P requiring the same variables in the current context. The structural planned/intended/design life (loading phase) is compared with the resultant life (as a result of repeated loading) of each node.

$$N_{OP(nd)} = \frac{1}{mat_c} \int_{a_l(nd)}^{a_f(nd)} \frac{da_{(nd)}}{(mat_{\beta} \sigma_{mul(nd)} \times \sqrt{\pi a_{(nd)}})^{mat_m}} \quad (5.63)$$

The logical output denoting failure or survival is input in R11. On failure, R12 records the event and failure value at a node and the algorithm proceeds to analyze the next node.

R13 assesses the occurrence of any failure event from R6, R9 and R12. A survival is recorded at R16 and a failure at R15. LM IX is the node LEM limit analysis. It follows the generic procedure outlined in Figure (5.13).

### 5.8.3 Process S – Reliability Estimation

This is the only post-MCS process besides data culmination. It estimates the overall reliability R, of the structure derived from the computation:

$$POF = \frac{\sum PFC}{NSIM} \quad (5.64)$$

thus,

$$R = 1 - POF \quad (5.65)$$

A case study is presented for demonstration and partial validation of FLEXSTREM.

### 5.9 Results/Discussion

An analysis (type II) is carried out on the crane boom arm shown in chapter 4. The analysis is purely from a structural perspective and takes no significant consideration of the crane in its entirety. The sample results and graphs showing the distribution (strength and resistance) of each component of the process limit states are presented in appendix A.2. The graphs produced are a result of the relationships/interactions between the components of the system definition in the MCS process chain. The following (Table (5.4)) is a summary of the entire FLEXSTREM process.

Analysis type	Type II (multi-member structure)
No of simulations	10000
Primary failure mode(s)	Nodal failure (1379)
Secondary failure mode(s)	Life limit violation (1379)
POF	0.1379
Reliability	0.8621

Table (5.4) – FLEXSTREM result for crane boom.

The failures in the analysis came from only 2 nodes (welded joints): nodes 118 and 120. Node 118 had a total of 226 failures ( $\approx 16\%$ ) while node 120 had a total of 1153 failures ( $\approx 84\%$ ). This is as a result of the high amount of stress in the surrounding locale on the structure. These are the highest points of stress anywhere on the structure. In this analysis there are strong relationships between the various process-models compared to the BETA-FLEXSTREM. These are highlighted using a sensitivity analysis. Tables (5.5) and (5.6) show a sample of the FLEXSTREM results from 15 trials. The “F” in the limit states column represents the logical connotation of “false” which signifies no violation of the referred limit state. The last 3 columns in Table (5.5) show the mechanical analysis results (this section is applicable to the members only). Any member could be specified in the data file. Table (5.6) shows the LEFM analysis results (this section is only applicable to the nodes). Any particular node could be specified in the data file. Member 75 and node 120 are picked for analysis.

**FLEXSTREM ANALYSIS FOR MULTI-MEMBER STRUCTURES/COMPONENTS. FOCAL JOINT: 120; FOCAL MEMBER: 75**

Simulation No	Wind Speed (m/s)	Wind Force (MN)	Load Factor	Member Strength (MPa)	Stress in Member (MPa)	Member Limit Failure?
1	19.62	0.011	18.007	7.28E+01	6.88E-03	F
2	25.92	0.017	20.53	7.58E+01	8.60E-03	F
3	27.93	0.019	27.798	7.10E+01	8.78E-03	F
4	25.99	0.017	22.398	7.62E+01	9.36E-03	F
5	25.76	0.017	20.476	7.89E+01	7.11E-03	F
6	31.24	0.024	20.008	8.59E+01	6.77E-03	F
7	25.95	0.017	22.343	7.05E+01	8.68E-03	F
8	28.12	0.02	24.614	7.94E+01	9.34E-03	F
9	27.05	0.018	19.755	7.47E+01	7.62E-03	F
10	28.75	0.021	20.741	7.93E+01	8.29E-03	F
11	26.06	0.017	25.214	6.81E+01	9.41E-03	F
12	23.98	0.014	23.292	7.50E+01	9.02E-03	F
13	23.02	0.013	24.666	7.91E+01	1.03E-02	F
14	24.76	0.015	18.61	8.25E+01	6.91E-03	F
15	29.47	0.022	25.938	7.35E+01	8.94E-03	F

Table (5.5) – Sample result table from FLEXSTREM. (a)

Simulation No	Nodal Multiaxial Stress (MPa)	Nodal Stress Intensity Factor (MPa√m)	Fracture Toughness (MPa√m)	Fracture Limit Failure?	Existing Crack Length (m)	Critical Crack length (m)	Crack Limit Failure?	Planned Life (Cycles)	Resultant Life (cycles)	Life Limit Failure?
1	5.09E+01	2.33E+00	4.84E+01	F	5.11E-04	2.20E-01	F	2.59E+05	1.34E+06	F
2	5.56E+01	3.59E+00	4.49E+01	F	9.96E-04	1.56E-01	F	2.36E+05	1.02E+06	F
3	8.21E+01	8.17E+00	4.58E+01	F	2.25E-03	7.04E-02	F	2.64E+05	2.92E+05	F
4	6.99E+01	6.60E+00	5.55E+01	F	2.04E-03	1.45E-01	F	2.59E+05	4.73E+05	F
5	6.32E+01	3.01E+00	4.67E+01	F	5.53E-04	1.33E-01	F	2.78E+05	6.41E+05	F
6	4.72E+01	1.79E+00	4.43E+01	F	3.54E-04	2.17E-01	F	2.62E+05	1.89E+06	F
7	5.98E+01	3.19E+00	4.27E+01	F	6.88E-04	1.23E-01	F	2.66E+05	8.12E+05	F
8	6.07E+01	1.54E+00	5.20E+01	F	1.59E-04	1.82E-01	F	2.51E+05	8.31E+05	F
9	6.53E+01	5.11E+00	5.13E+01	F	1.44E-03	1.45E-01	F	2.28E+05	6.09E+05	F
10	6.66E+01	2.20E+00	5.02E+01	F	2.69E-04	1.40E-01	F	2.66E+05	6.13E+05	F
11	7.94E+01	5.41E+00	4.59E+01	F	1.11E-03	7.97E-02	F	2.57E+05	3.11E+05	F
12	7.79E+01	6.73E+00	5.17E+01	F	1.73E-03	1.02E-01	F	2.73E+05	3.43E+05	F
13	8.42E+01	9.54E+00	5.14E+01	F	2.84E-03	8.23E-02	F	2.79E+05	2.55E+05	T
14	5.40E+01	4.53E+00	5.55E+01	F	1.64E-03	2.45E-01	F	2.55E+05	1.06E+06	F
15	6.61E+01	1.42E+00	5.24E+01	F	1.14E-04	1.55E-01	F	2.63E+05	5.94E+05	F

Table (5.6) – Sample result table from FLEXSTREM. (b)

Several data and data analyses could be derived from the FLEXSTREM results. Tables (5.5) and (5.6) are samples of these data analyses. Other representations are available in appendix A.4. The wind speed data in Table (5.5) is plotted in Figure (5.20). The Gumbel distribution was assigned to this variable, thus leading to the observed pattern.

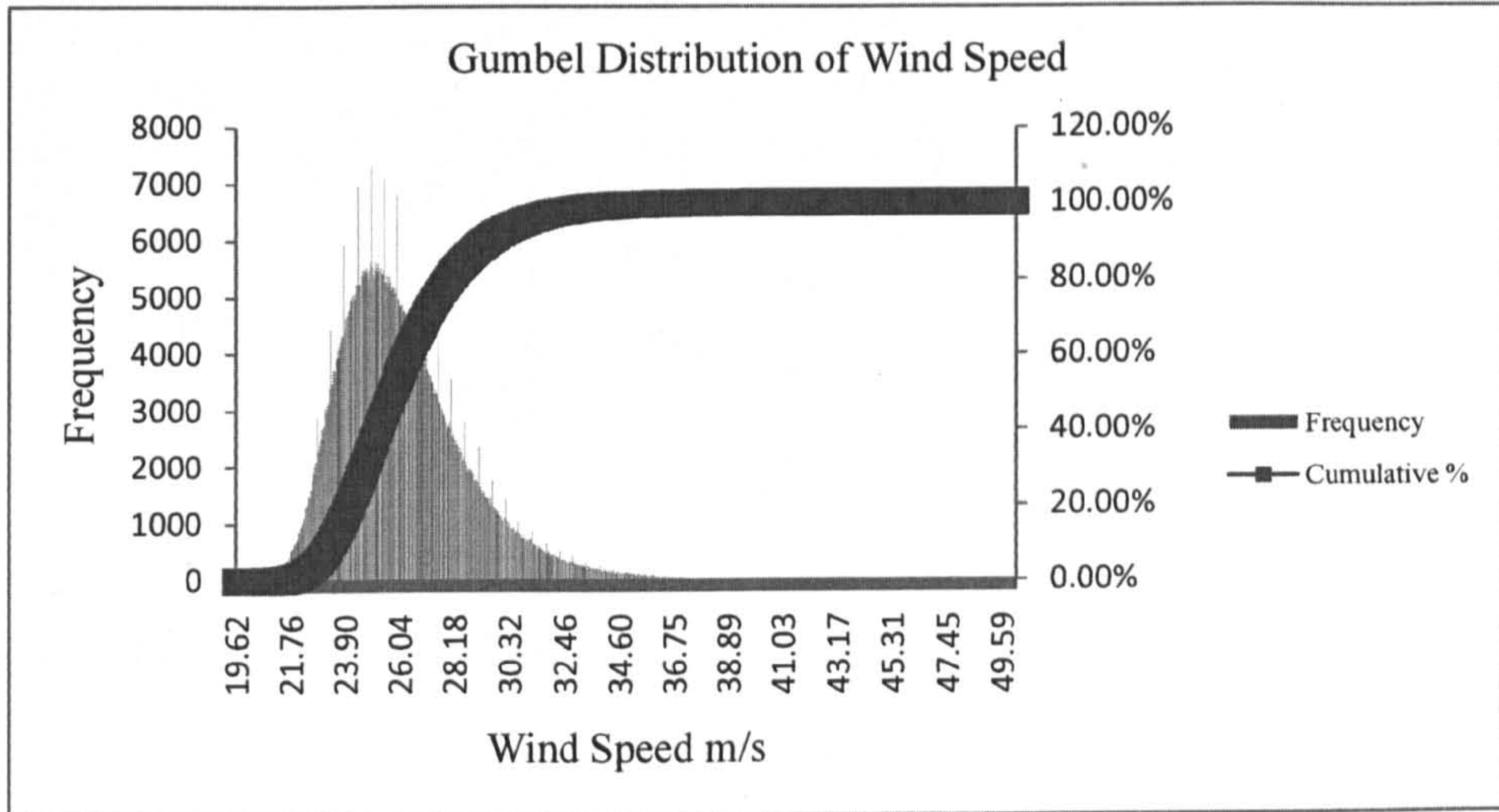


Figure (5.20) – Gumbel distribution of wind speed.

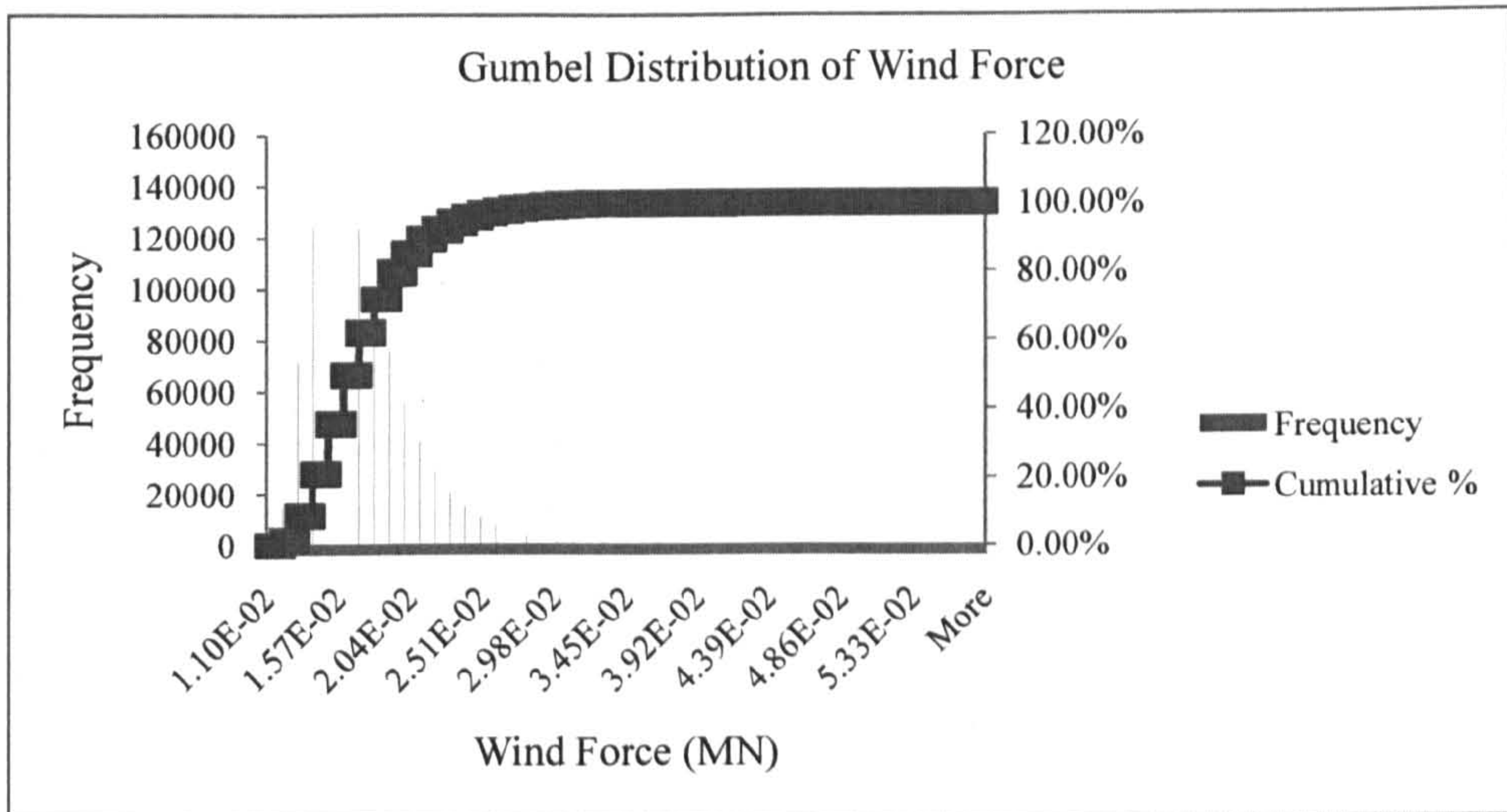


Figure (5.21) – Gumbel distribution of wind force.

Section 5.5.5 showed the source of the derivation of the wind force. The nearly-discrete nature of the graph in Figure (5.21) shows the high level of rigidity (highly

deterministic nature) in the adopted model. Incorporation of a more flexible model such as computational fluid dynamics (CFD) should greatly reduce this effect.

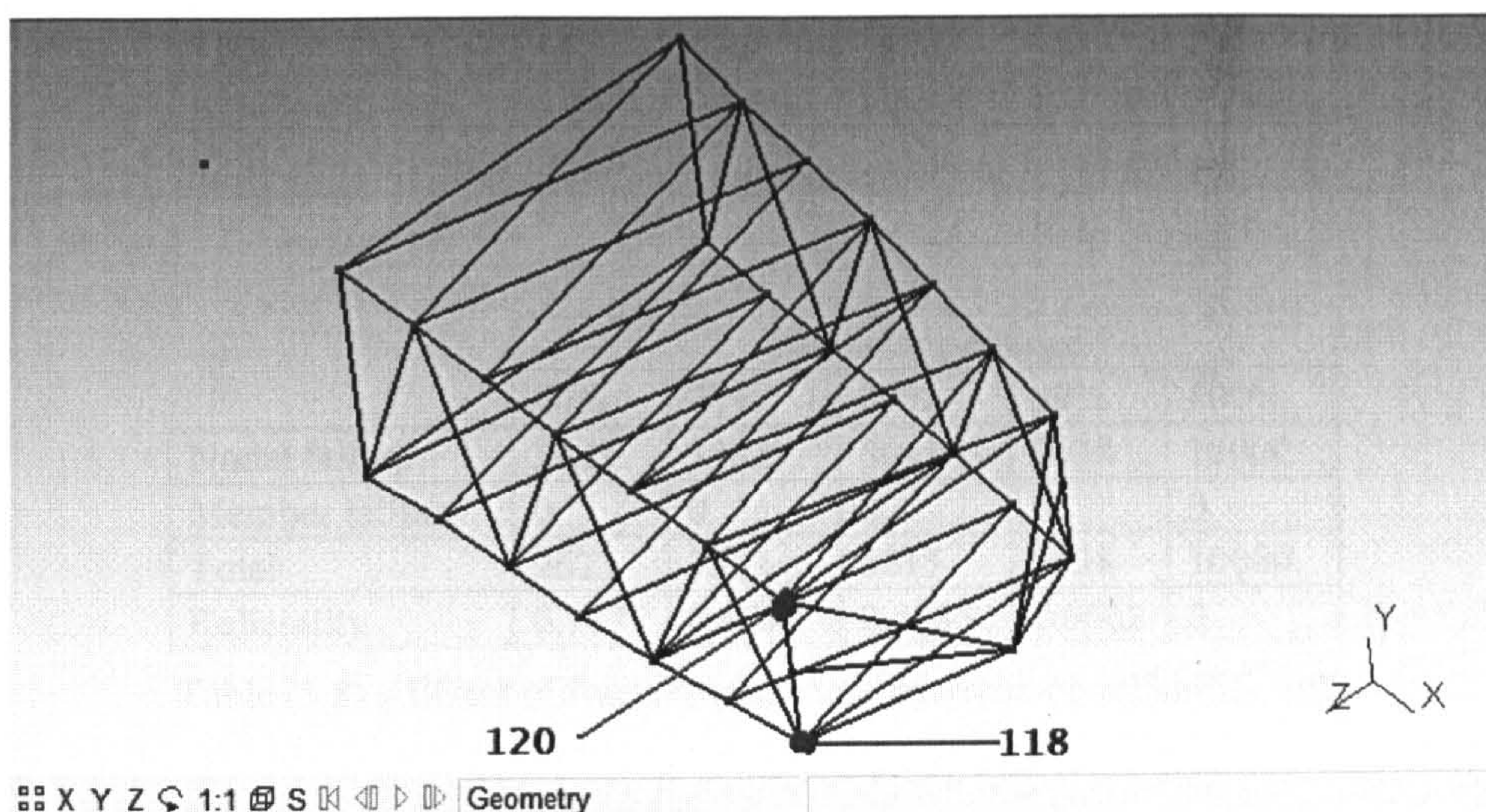


Figure (5.22) – Highly stressed points on crane boom.

Figure (5.22) shows the highly stressed points on the structure: nodes 118 and 120. The non-uniformity of the tapering towards the loaded node (Figure (4.6)) can be observed here. Also the proximity of these highly stressed nodes to the loaded node can be observed as well.

### 5.9.1 Sensitivity Analysis

A sensitivity analysis is carried out for partial validation of the FLEXSTREM. Key independent limit state variables were altered individually by 10%. The effects on the reliability were presented in tables and graph plots. It is expected that the changes applied to these parameters would bring about trended changes in the reliability of the structure.

#### 5.9.1.1 Fracture Toughness

The fracture toughness ( $K_{IC}$ ) – the ability of the material to resist fast fracture – has a significant bearing on the nodal failure as shown in Tables (5.7) and (5.8). This in effect has a significant bearing on the reliability.



	Percentage change				
	10%	20%	30%	40%	50%
Nodal failure	1450	1568	1694	1884	2152
Member failure	0	0	0	0	0
Total	1450	1568	1694	1884	2152
Reliability	0.855	0.8432	0.8306	0.8116	0.7848

Table (5.7) – Effect of fracture toughness decrease on reliability. (a)

	Percentage change				
	60%	70%	80%	90%	100%
Nodal failure	2623	3382	5015	9338	10000
Member failure	0	0	0	0	0
Total	2623	3382	5015	9338	10000
Reliability	0.7377	0.6618	0.4985	0.0662	0

Table (5.8) – Effect of fracture toughness decrease on reliability. (b)

Percentage decrease	Reliability	Percentage change in Reliability
10	0.855	0.82
20	0.8432	2.19
30	0.8306	3.65
40	0.8116	5.86
50	0.7848	8.97
60	0.7377	14.43
70	0.6618	23.23
80	0.4985	42.18
90	6.62E-02	92.32
100	0	100

Table (5.9) – Trended change in reliability (fracture toughness).

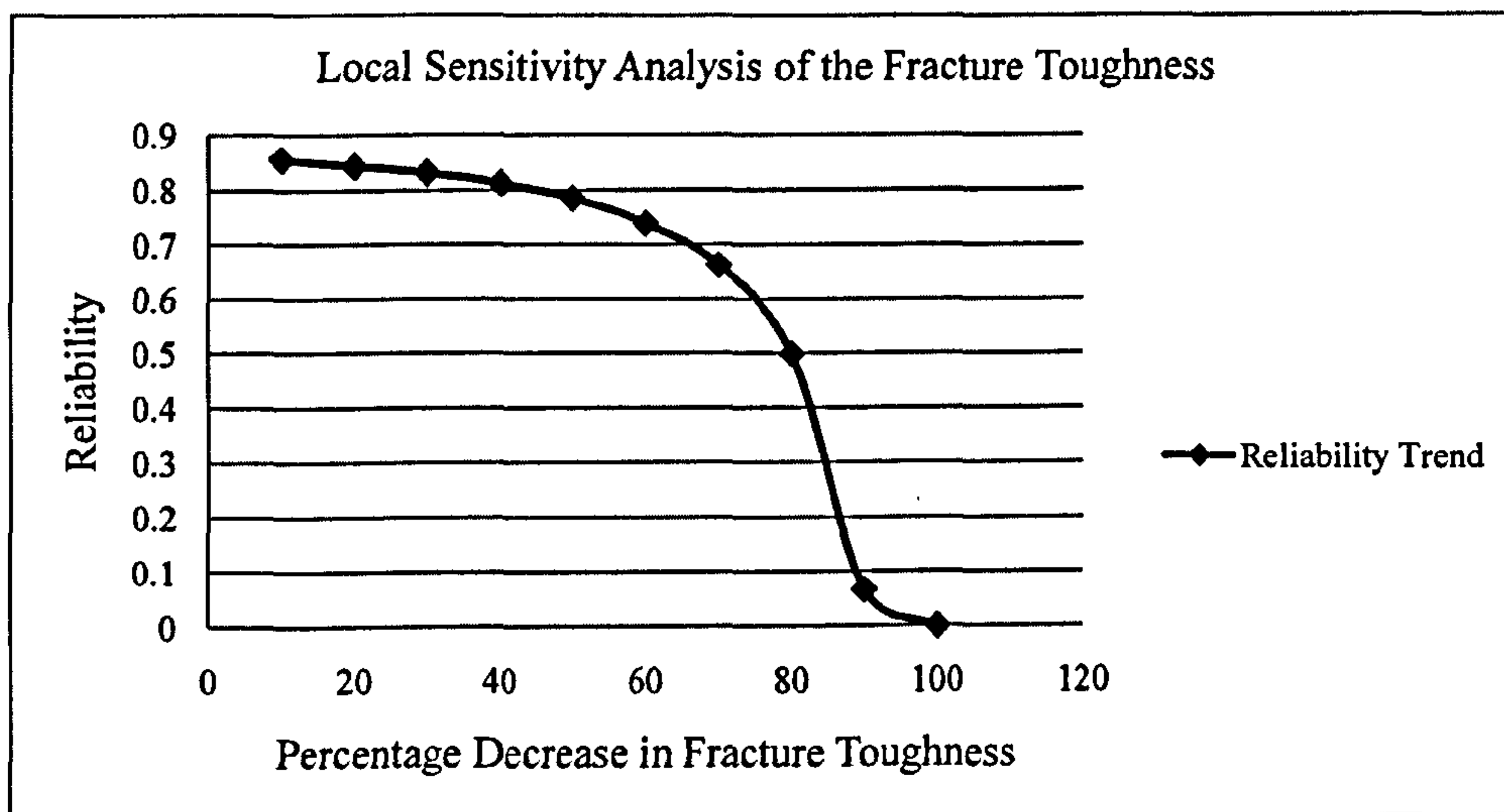


Figure (5.23) – Local sensitivity analysis of the fracture toughness.

The trended change in reliability recorded in Table (5.9) is plotted in Figure (5.23). A gentle slope (or rate of change) is observed from a 10% decrease through till about 80%. From the 90% decrease, the reliability becomes very low as the material essentially loses its ability to resist fast fracture. Without this ability (fracture toughness), the reliability logically is zero at a 100% decrease.

5.9.1.2 Defect Size (Crack Length)

This is the estimated crack length on a repeatedly loaded area on a structure. From Tables (5.10) and (5.11), the effect of the changes to this parameter on nodal failure could be observed. The influence is low compared to that of the fracture toughness.

	Percentage change				
	10%	20%	30%	40%	50%
Nodal failure	1744	2116	2511	2885	3220
Member failure	0	0	0	0	0
Total	1744	2116	2511	2885	3220
Reliability	0.8256	0.7884	0.7489	0.7115	0.678

Table (5.10) – Effect of crack length increase on reliability. (a)

	Percentage change				
	60%	70%	80%	90%	100%
Nodal failure	3545	3841	4138	4375	4636
Member failure	0	0	0	0	0
Total	3545	3841	4138	4375	4636
Reliability	0.6455	0.6159	0.5862	0.5625	0.5364

Table (5.11) – Effect of crack length increase on reliability. (b)

Percentage increase	Reliability	Percentage change in Reliability
10	0.8256	4.23
20	0.7884	8.55
30	0.7489	13.13
40	0.7115	17.47
50	0.678	21.35
60	0.6455	25.12
70	0.6159	28.56
80	0.5862	32.00
90	0.5625	34.75
100	0.5364	37.78

Table (5.12) – Trended change in reliability (crack length).

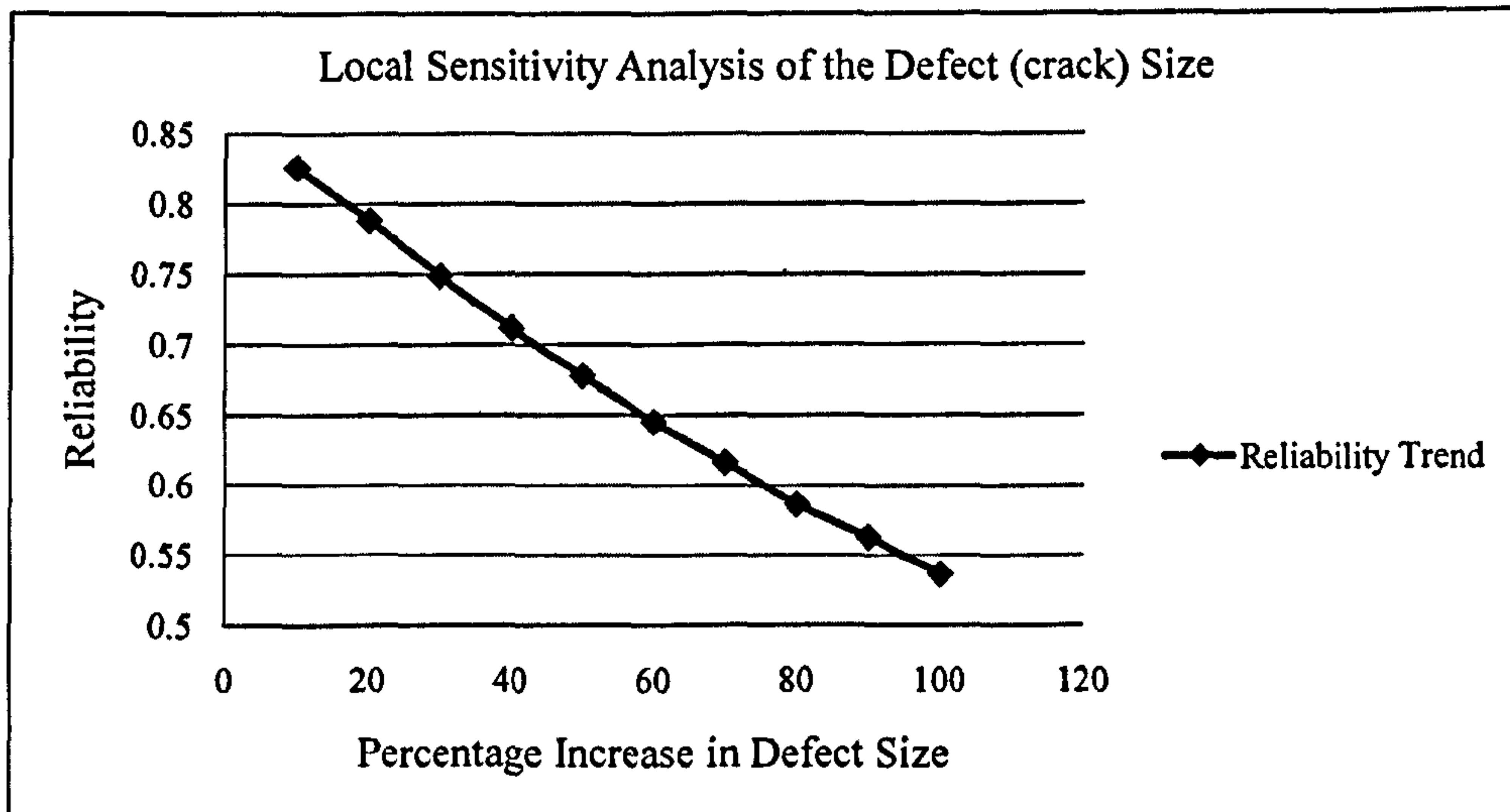


Figure (5.24) – Local sensitivity analysis of the defect (crack) size.

The trended reliability change in Table (5.12) is plotted in Figure (5.24). The rate of change of the reliability with respect to the decrease is largely linear.

### 5.9.1.3 *Planned/Design Life*

The changes in nodal failure due to increments to the design life of the structure are observed in Tables (5.13) and (5.14). These changes could be compared to a scenario where the utility of the structure was extended beyond its stipulated life time.

	Percentage change				
	10%	20%	30%	40%	50%
Nodal failure	1966	2543	3148	3662	4186
Member failure	0	0	0	0	0
Total	1966	2543	3148	3662	4186
Reliability	0.8034	0.7457	0.6852	0.6338	0.5814

Table (5.13) – Effect of planned life increase on reliability. (a)

	Percentage change				
	60%	70%	80%	90%	100%
Nodal failure	4630	5026	5428	5812	6134
Member failure	0	0	0	0	0
Total	4630	5026	5428	5812	6134
Reliability	0.537	0.4974	0.4572	0.4188	0.3866

Table (5.14) – Effect of planned life increase on reliability. (b)

Percentage decrease	Reliability	Percentage change in Reliability
10	0.8034	6.81
20	0.7457	13.50
30	0.6852	20.52
40	0.6338	26.48
50	0.5814	32.56
60	0.537	37.71
70	0.4974	42.30
80	0.4572	46.97
90	0.4188	51.42
100	0.3866	55.16

Table (5.15) – Trended change in reliability (planned life).

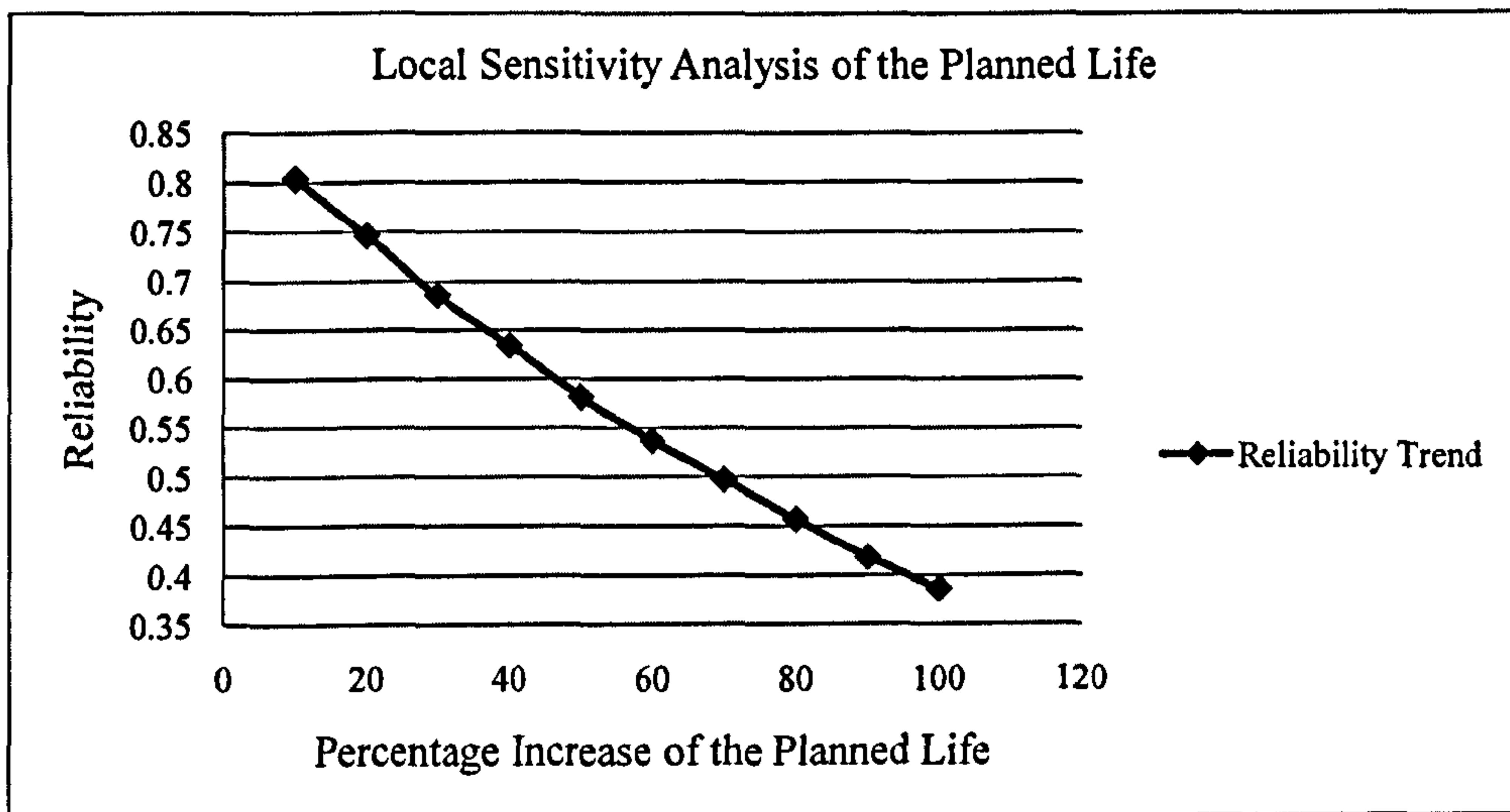


Figure (5.25) – Local sensitivity analysis of the planned life.

The changes to the reliability in Table (5.15) are plotted in Figure (5.25). The rate of change of the reliability with respect to the increase in planned life is also largely linear in this scenario.

#### 5.9.1.4 Load Factor

In this scenario, the maximum limit of the loading on the structure (all load combinations) is increased steadily. The effects on the structural reliability are outlined in Tables (5.16) and (5.17).

	Percentage change				
	10%	20%	30%	40%	50%
Nodal failure	1980	2559	3100	3625	4081
Member failure	0	0	0	0	0
Total	1980	2559	3100	3625	4081
Reliability	0.802	0.7441	0.69	0.6375	0.5919

Table (5.16) – Effect of load factor increase on reliability. (a)

	Percentage change				
	60%	70%	80%	90%	100%
Nodal failure	4445	4768	5050	5322	5545
Member failure	0	0	0	0	0
Total	4445	4768	5050	5322	5545
Reliability	0.5555	0.5232	0.495	0.4678	0.4455

Table (5.17) – Effect of load factor increase on reliability. (b)

Percentage increase	Reliability	Percentage change in Reliability
10	0.802	6.97
20	0.7441	13.69
30	0.69	19.96
40	0.6375	26.05
50	0.5919	31.34
60	0.5555	35.56
70	0.5232	39.31
80	0.495	42.58
90	0.4678	45.74
100	0.4455	48.32

Table (5.18) – Trended change in reliability (load factor).

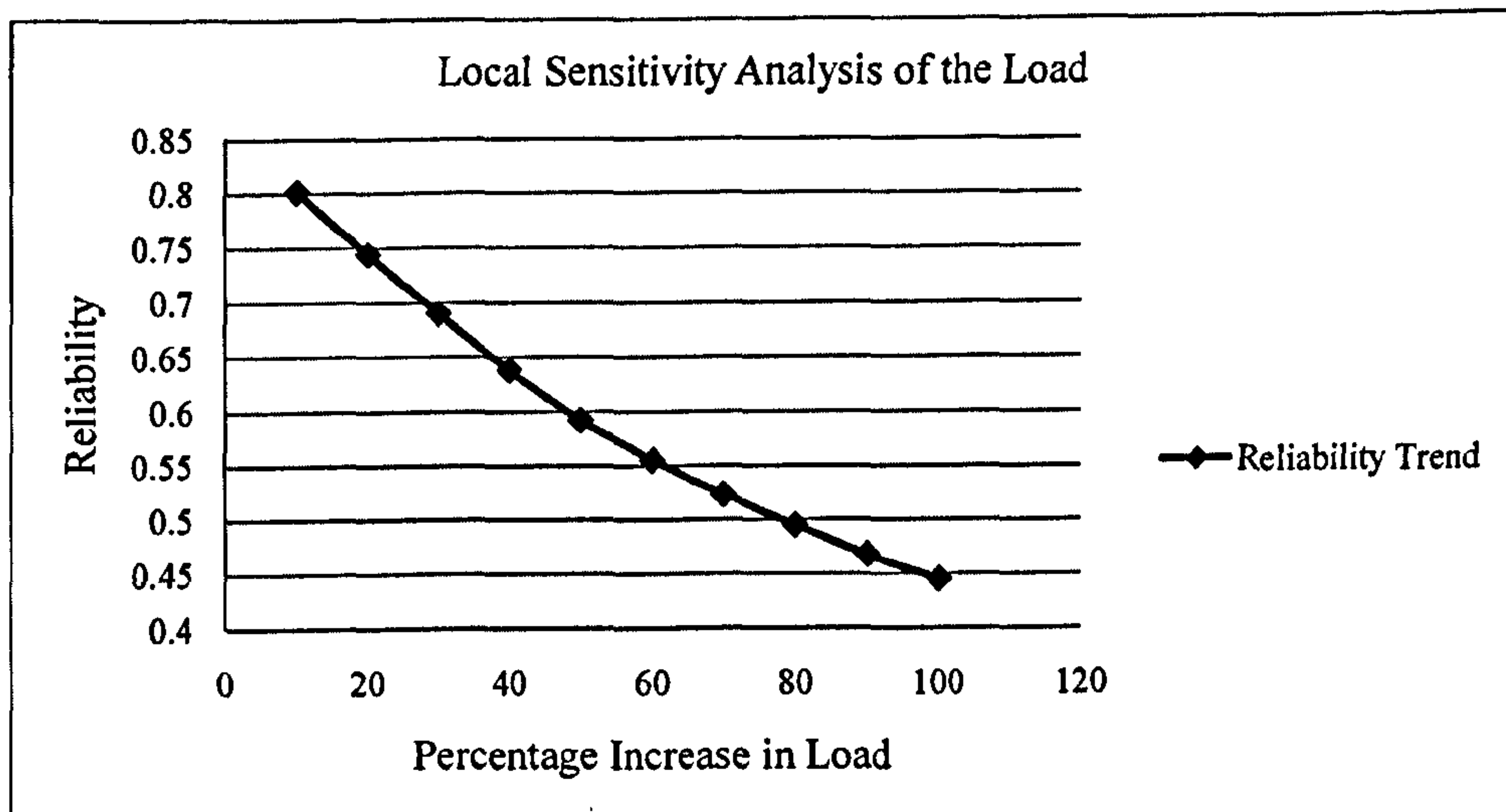


Figure (5.26) – Local sensitivity analysis of the load.

The changes in reliability outlined in Table (5.18) are plotted in Figure (5.26). Once again a reasonably linear relationship is found to exist between the rate of change of the reliability and the load factor increase.

### **5.9.2 The COV-Number of Simulations-Reliability Relationship**

Another analysis that could be carried out from the FLEXSTREM results is the COV analysis from the preambles stated in section 5.5. Table (5.19) and the graphs in Figures (5.27) and (5.28) are samples of what this analysis entails. Subsequent tables and graphs comparing outcomes of other permutations in the increase and decrease of both the strength/resistance component COV(R) and the stress/demand COV(D), and the number of simulations are presented in appendix A.3. As stated earlier, the COV (of the system definition parameters), could be said to be a measure of the uncertainty in a system. From the analysis, it could be inferred that a link exists between the reliability and the COV (both of resistance and demand components) and number of simulations. To establish more understanding the word uncertainty and COV are used interchangeably in this research. The reliability is a variable dependent on the number of simulations and the COV, which are independent variables. The COV consists of a COV(R) (strength/resistance) component and a COV(D) (stress/demand) component. There are 3 main parameters to be analysed: the COV, the reliability and the number of simulations. Thus in this analysis, there are a number of observations to be made:

- Changes in the reliability value as a result of reduction or increment of the COV (or a COV component (COV(R) or COV(D))).
- Consistency of the reliability value as the number of simulations increases (for a fixed COV).
- How the consistency of the reliability value is affected by changes in the COV as the number of simulations increases.

Case 1:

Reliability values obtained at different numbers of simulations while keeping COV(R) constant and increasing COV(D).

Coefficient of Variation status			Reliability per no of simulations				Average
COV(D)	% change in COV(D)	COV(R)	1K	10K	100K	1M	
0.08	0	0.06	0.87	0.8621	0.86107	0.861762	0.863733
0.12	50	0.06	0.822	0.8107	0.81077	0.812726	0.814049
0.16	100	0.06	0.766	0.7638	0.76173	0.763818	0.763837
0.2	150	0.06	0.72	0.718	0.71611	0.717759	0.71796725
0.24	200	0.06	0.68	0.6756	0.67321	0.675391	0.67605025
0.28	250	0.06	0.633	0.6345	0.6345	0.637735	0.63493375
0.32	300	0.06	0.605	0.5995	0.60656	0.605239	0.60407475
0.36	350	0.06	0.566	0.5715	0.5772	0.576537	0.57280925
0.4	400	0.06	0.541	0.5477	0.5514	0.552559	0.54816475

Table (5.19) – Keeping COV(R) constant and increasing COV (D) at different numbers of simulations.

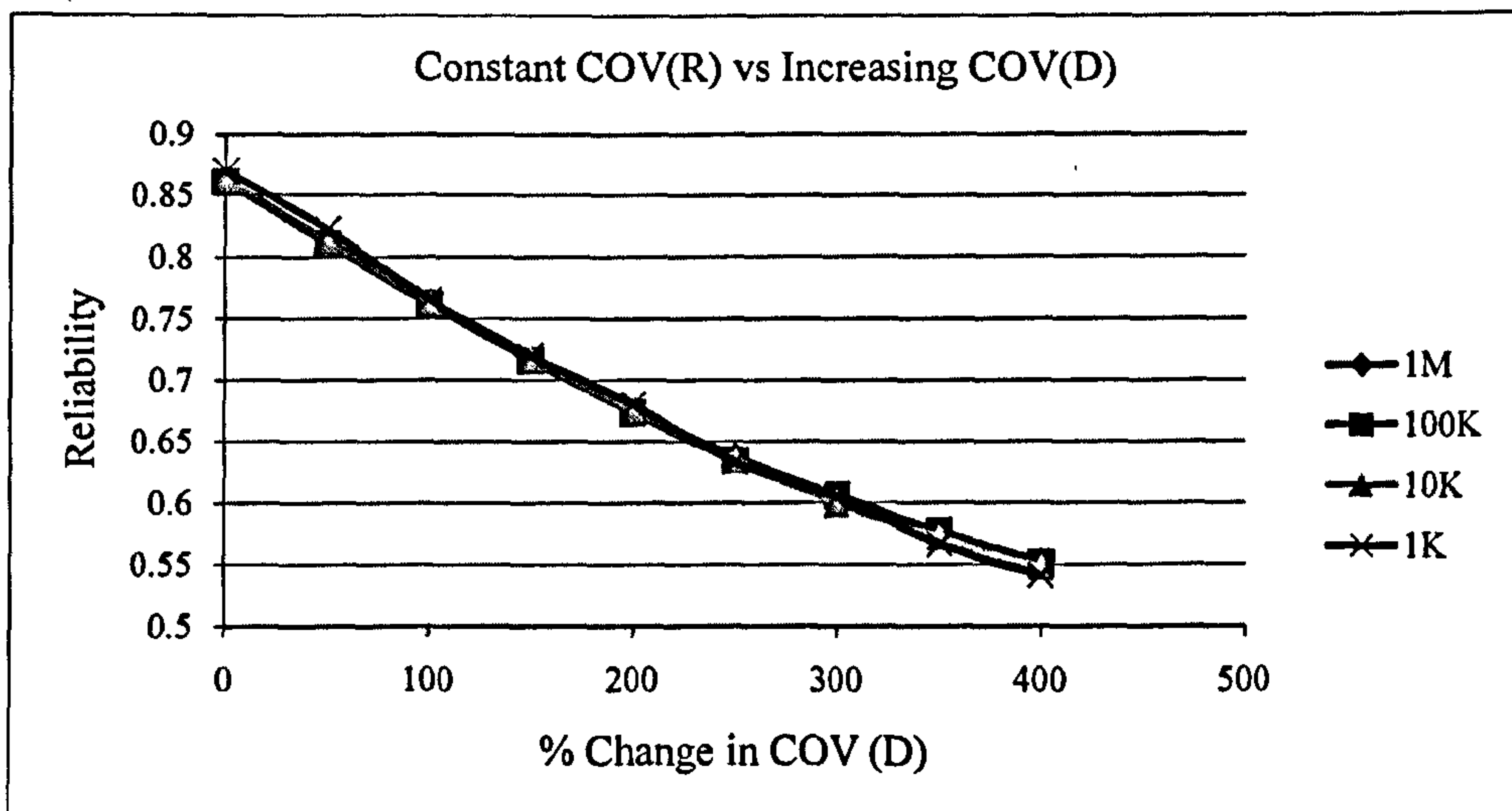


Figure (5.27) – Constant COV(R) vs. increasing COV(D).



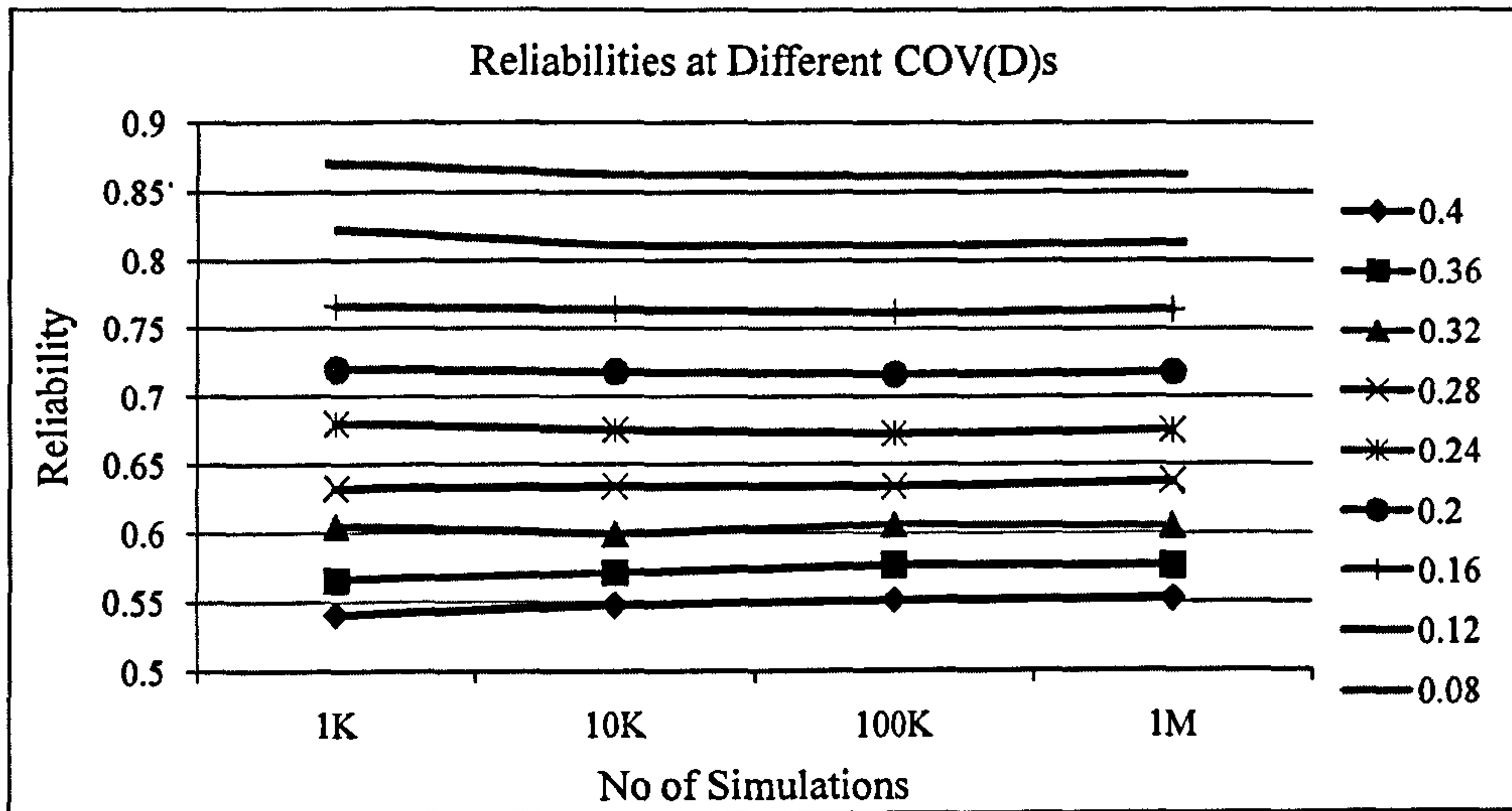


Figure (5.28) – Reliability at different COV(D)s.

The COV (R) component of the COV has a very marginal contribution to the reliability outcome (due to the low value chosen) for this particular case study. It would have to be increased significantly in order for it to have a considerable impact on the reliability. Future work would ensure that the required increments are made. Thus, the COV(D) is the de facto representation of the COV in this section as its contribution to the reliability is the most significant.

From the analysis of all the results (including those in appendix A.3), the following axioms apply:

1. Increase in the COV (uncertainty in a system) would bring about a reduction in the reliability of the system. Conversely, as the COV of a system decreases the reliability increases.
2. As the COV increases, the reliability value for a specified number of simulations (say 1000) is less accurate (or has more round-off errors) when compared to the reliability value of a higher number of simulations (say 10000). This is true for the reliability values of subsequently higher number of simulations (100000, 1000000, etc.). The round-off errors or inaccuracies get worse as the COV increases.

3. As the COV decreases, the reliability value for a specified number of simulations (say 1000) is more accurate (or has less round-off errors) when compared to the reliability value of a higher number of simulations (say 10000). This is true for the reliability values of subsequently higher number of simulations (100000, 1000000, etc.). The round-off errors or accuracies improve as the COV decreases.
4. As system COV increases, a higher number of simulations are required to have less of these round-off errors. This is seen with the case of the reliability values obtained for 1000 simulations compared to the reliability values obtained for subsequently higher number of simulations.

Finally, it could be observed that 10k represented a balanced trade off simulation number in terms of efficiency and accuracy.

### **5.10 Conclusion**

The FLEXSTREM has been successfully developed to handle more complicated scenarios. The patterns of the output graphs in the sensitivity analysis suggest better defined relationships between components of the system (structural) definition compared to those of the BETA-FLEXSTREM. As a result, FLEXSTREM could be better relied for the quantification of the risks associated with fatigue for a wide range of structure types. The SFEA method has allowed for the thorough and efficient risk quantification of structures. In addition to the statistical graphical output, the FLEXSTREM has also been developed to analyse the COV (uncertainty) associated with the system (structural) definition parameters.

The model presented forms a solid framework on which other mechanical, structural, mathematical and programming techniques could be built on. This framework is in itself subject to vast expansion and improvement in current models. Several models especially those within the FEA field like CFD and LEFM fields like corrosion could be integrated in the future. More section properties and configurations as well as an upgrade to the frame-element type in the FEA module could also be undertaken. The

model in its current state, built on practicability grounds, is applicable within limits to real cases.

Recently developed methods have provided flexibility; classical methods have provided consistency.

“If in doubt (uncertain), increase the COV (measure of uncertainty)”.

## **Chapter 6:**

# **FLEXSTREM Optimization (FLEXOPT): A FLEXSTREM Based Structural Optimization Tool for Risk Control using Cost-Safety Criteria**

### **Summary**

*This chapter presents a tool for providing possible solutions that improve the reliability of the structure as a means of mitigating risks associated with fatigue failure. In this chapter, an adaptation of the pre-existing validated FLEXible STuctural REliability algorithm (FLEXSTREM) for optimization purposes – FLEXOPT is presented. The mass as a function of cost is utilized alongside reliability to present better structural configurations for a given structure. The optimization technique is a novel procedure. The case of a crane boom is presented for optimization. Also the well known 25-bar truss case is optimized and compared alongside other optimization results from literatures obtained by different techniques. This serves as a comparative benchmarking for the FLEXOPT model.*

### **6.1 Introduction**

According to Dean and Marks (1965), optimization methods are used in the determination of 'best' or optimal decision policies where parameter values are unknown. Throughout the history of modern engineering, decision making to aid selection(s) of these 'best' parameters like weight, dimensions, shape, etc. are numerous. There is generally no concrete or 'more correct' way to achieve the intended goal. The 'search' for the best (optimal) parameter(s) (solution(s)) could be broadly classified under constrained and unconstrained types.

Some methods of optimization include:

- Newton method
- gradient search
- conjugate gradient method
- linear and non-linear programming
- quadratic programming
- Lagrangian methods
- 

Most optimization techniques are iterative in nature. The invention of the electronic computers has greatly impacted on the development and application of the various methods particularly in the areas of structural design, aerospace, mechanical and nuclear engineering.

## **6.2 Background**

Broadly speaking, structural engineering may be considered as “the rational establishment of a structural design that is the best of all possible designs within a prescribed objective and given a set of geometrical and/or structural limitation” (Lam et al (2000)).

Structural optimization may be split into two groups: the first group consisting of optimization concepts useful for obtaining good insight into optimization of a given structure and the second being the mathematical principles required to obtain the explicit optimal design of the structure (i.e. the means to obtain elements in the first group) (Lam et al (2000)).

The first group is further subdivided into 3 main areas (Lam et al (2000)):

- sizing optimization
- shape optimization
- topology optimization

The second group could be spread broadly under 3 areas (Lam et al (2000)) :

- optimality criteria methods

- mathematical methods
- heuristic methods (genetic algorithms (GA), evolutionary method and biological growth technique)

### ***6.2.1 Sizing Optimization***

Here the topology and shape of the structure is held constant while the key parameters (usually the cross-section and thickness) are varied towards optimal values. Sizing optimization could also be an outcome of topology and shape optimization (Lam et al (2000)).

### ***6.2.2 Shape Optimization***

Here the topology is held constant while the shape is varied. Node position and finite mesh adjustment (variation) are the methods applied by various techniques in this area (Lam et al (2000)).

### ***6.2.3 Topology Optimization***

Here everything (shape, topology and sizing) becomes variable (Lam et al (2000)). A design boundary is usually imposed and may have some degree of flexibility. This optimization type is more cumbersome to solve as design variables and constraints become too numerous. Practically the topology and shape of most structures are determined before optimization techniques are applied; this makes sizing optimization the most important. Its relative simplicity also becomes a huge advantage.

In this chapter a FLEXSTREM based optimization technique (FLEXOPT) is presented. FLEXOPT utilizes the sizing optimization (cross-sectional area and thickness) against specified targets – high reliability and optimal cost (material savings).

Khot et al, (1973) developed an efficient optimization method based on the finite element analysis (FEA). The method utilized strain energy distribution and numerical search for minimization of the structural weight of structures made up of composite

materials whilst being subjected to multiple loads. The method demonstrated on an airplane wing yielded satisfactory results in weight minimization and optimal stiffness.

Rao (1980) introduced uncertainty (variance) while attempting to find the minimal cost design for structures. Two cases were considered: a deterministic case (no uncertainties (variance)) and a probabilistic case. This approach was applied to the design of a cable stayed box girder. The major finding was the effect of the uncertainty on the optimum design of the girder. Expansion of the methodology to cover other areas was also deemed possible.

Svanberg's (1981) work aimed at minimizing the weight of a 3 dimensional truss structure in the presence of displacements, stress and buckling as a result of multiple loads. This method focused on the geometry but not the topology of the said structure. The method was demonstrated on a 3-bar structure and a 39-bar structure. The results showed a considerable saving in material (hence costs) with further scope for applications to a wider range of structures.

Xu (1989) presented a two-phase method optimization based on the well known fuzzy set theory. At phase one, the fuzzy solution is obtained by means of the Level Cuts method. At phase two, the crisp solution is obtained from the fuzzy solution by the bound search method. This technique was applied to a 3-bar truss and a corrugated bulkhead. The outcomes recorded considerable savings in material. The results were accorded greater credence due to the realistic fuzzy modelling of structural constraints.

Reliability based structural analysis program RBSA and its optimization counterpart RBSA-OPT were one of the early software tools aimed at interactively carrying out reliability based optimization. Nakib and Frangopol (1990) conducted an optimization procedure on a 13-bar bridge truss with the help of these software tools. The software achieved a material savings of 50% whilst undergoing further development.

Xie and Steven (1993) presented a very unique technique for determining the optimum (or near optimum) topology of a structure using an evolutionary approach. Having FEA as a foundation, the technique metamorphoses to an optimal shape by deleting areas

below a specified stress ratio (with respect to the maximum structural stress). Demonstration on several structures was carried out with interesting outcomes. Possible refinements and more research on this method would yield appealing solutions.

Hajela and Lee (1995) like the previous presented a technique for optimal structural topology using genetic algorithms (GA). The method is an adaptation of the ground structure topology optimization technique implemented in a two phase search (based on GA). The method proved useful for obtaining a very good idea of how the optimal structural topology ought to be. This greatly reduces the workload for a more precise algorithm whose role is to obtain local optimum cross-sections and configurations.

Gil and Andreu (2001) presented a method to address optimal shape and optimal cross-section configuration simultaneously. The method combines full stress design optimization with the conjugate gradient optimization. The combination was intended to mitigate the complexities of the result due to combination of variables (nodes, cross-sections, etc.) of different orders of magnitude. Demonstrations were carried out on early 20<sup>th</sup> century bridges. The objectives were met as the results produced were concise, intuitive and stable.

Park and Sung (2002) developed an algorithm based on the simulated annealing (SA) method for optimization under several constraints. The need to fully utilize the capabilities of a cluster of computers (PC's) led to the development of two phases of the algorithm: simulated quenching (SQ) and SA. The results from the demonstrations on a 21-story regular steel braced frame and an irregular counterpart recorded significant computational efficiency and yielded more stable convergence histories.

### **6.3 Methodology**

The next step in the modified FSA is the risk control option/cost benefit analyses. This basically refers to methods by which risk is mitigated while considering cost. The method presented in this chapter is the one of two methods which may be used to achieve this aim.



Optimization, as hitherto elaborated upon, attempts to proffer solutions which are constantly reviewed and then ranked/selected for the given design problem. The method is developed with two main optimization criteria – a safety quantity (i.e. reliability) and a cost quantity (i.e. structural mass). These quantities are already existent as outputs from the FLEXSTEM, thus an optimization module is incorporated. The resultant algorithm is a FLEXSTEM based optimization procedure – FLEXOPT. This is illustrated in Figure (6.1):

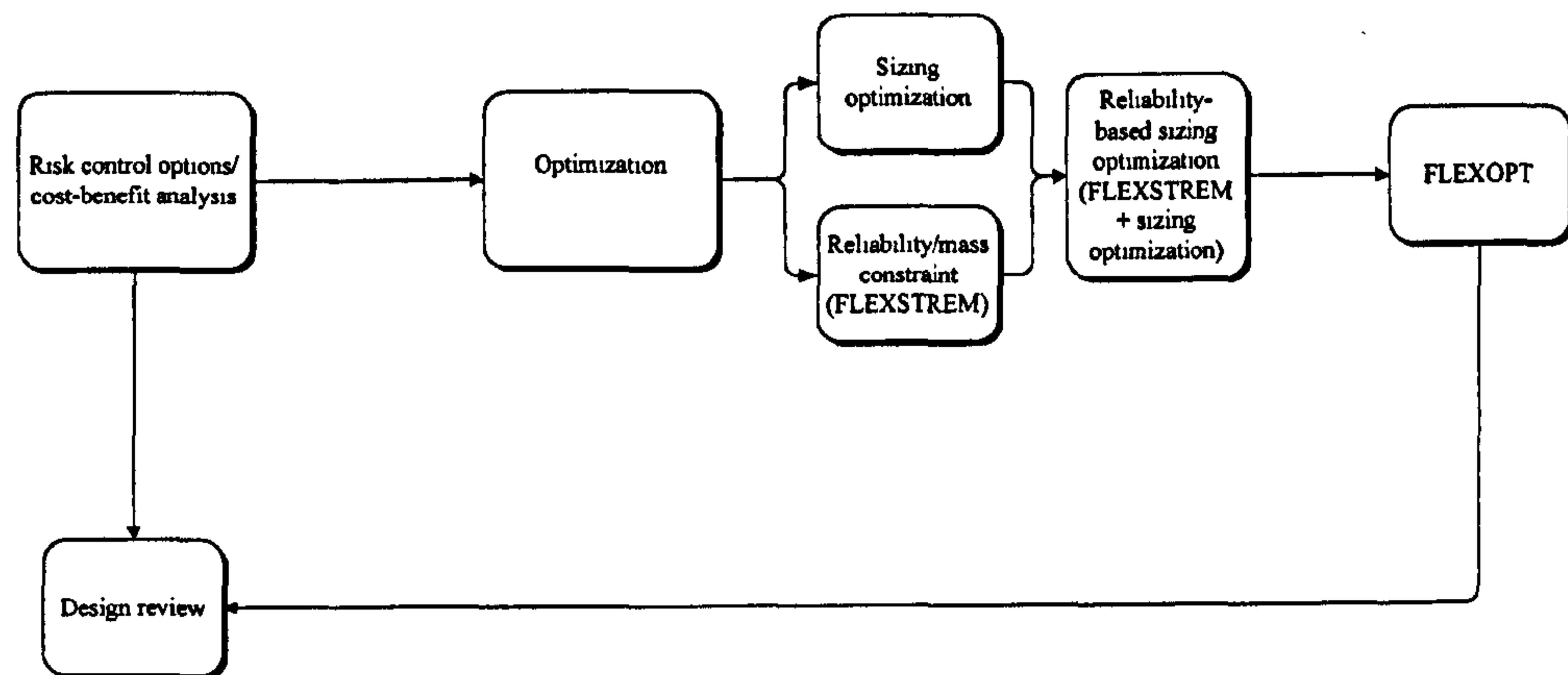


Figure (6.1) – FLEXOPT algorithm.

The optimization module essentially generates new structural configurations (diameter and thicknesses) and passes them to FLEXSTEM (within FLEXOPT), which then evaluates them. The reliability and mass values returned by FLEXSTEM are then compared to the target reliability and mass input in FLEXOPT. If they meet all the criteria, they are recorded in the “best result” category. If the configuration(s) fail(s) to meet the criteria, the result is ignored and the next configurations are then analysed. A separate sensitivity analysis for FLEXOPT is not necessary as the FLEXSTEM algorithm has already been subjected to one previously.

The type of optimization employed is the sizing optimization. The algorithm attempts to determine the best dimension that the member(s) could assume for optimal cost and reliability. The algorithm is also implemented in FORTRAN.

## **6.4 FLEXOPT Overview**

FLEXOPT is based on the validated FLEXSTREM algorithm. The FLEXSTREM forms the main engine of the FLEXOPT algorithm and is only slightly modified.

With the cost and safety as the primary foci (goals), FLEXOPT manipulates certain physical variables – the size variables (thicknesses and diameters), affecting these foci (goals) and in turn selects the best results based on the constraint margins placed on the goals and the selected optimization level. The size variables are selected because they could be quite easily manipulated physically and are not abstract e.g. it is easier to manipulate structural dimension (in design phase) than to alter global wind velocity.

The underlying model – FLEXSTREM on which FLEXOPT is built is of utmost significance as more realistic evolutions of the algorithm (FLEXSTREM) would yield more realistic optimal results. The FLEXSTREM, for now, is time invariant and its finite element analysis (FEA) engine is based on the truss element type. Future improvements to the FLEXSTREM, which could include the implementation of time variance (stochasticity) and modification of the FEA engine to frame element type, would significantly impact on the optimal solution(s) from FLEXOPT. In the absence of such improvements (and thus more system definition), the level of uncertainty in the system (the coefficient of variance (COV) size) in the FLEXSTREM could be increased as a compensation. This is a strong advantage of probabilistic modelling.

A FLEXOPT analysis can be carried out in the following ways:

- Type I analysis – level 1 convergence
- Type II analysis – level 1 convergence
- Type I analysis – level 2 convergence
- Type II analysis – level 2 convergence

Level 1 convergence is based on reliability only regardless of mass while level 2 convergence is based on both reliability and structural mass. Level 1 convergence is too “loose” to be modelled and may be replaced by a manual/visual selection criterion from recorded results. Results are recorded twice: firstly, for all outcomes and secondly for the best outcome(s).

The darkened shapes with “dashed” borders in Figure (6.2) are pre-existing FLEXSTREM processes while the “continuous” line bordered shapes are the new or modified algorithms introduced in FLEXOPT. The processes involved in the FLEXOPT are:

- Level convergence specification
- Specification of the number of combinations to perform
- Specification of the upper and lower boundaries of optimization percentage
- Designation of the target reliability and tolerance
- Generation and shuffling of the optimization coefficient arrays
- FLEXOPT loop
- FLEXSTREM FEA block modification
- Convergence conditions
- Result sorting operations

#### **6.4.1 Level Convergence Criteria**

The level-convergence concept classifies structural design according to these two selection criteria (costs incurred and consequences of failure). A two-tier classification for the design optimization of a structure could take the form shown in Table (6.1).

Level	Cost	Consequence
Level 1	LI	HI
Level 2	HI	HI

Table (6.1) – Levels of design.

Key

LI	Little or no importance
HI	High importance

Some engineering applications would require less attention to cost and focus more on safety. These would fall into the level 1 category. An example of such an application is the front lights of a vehicle. Though it is inexpensive, its absence or malfunction poses a significant level of risk.

Also some other engineering applications require considerable attention to both cost and safety. These would fall into the level 2. An example of such an application is a typical building structure.

### 6.5 FLEXOPT Structural Analysis

Figure (6.2) (below) shows the algorithm flow for FLEXOPT.

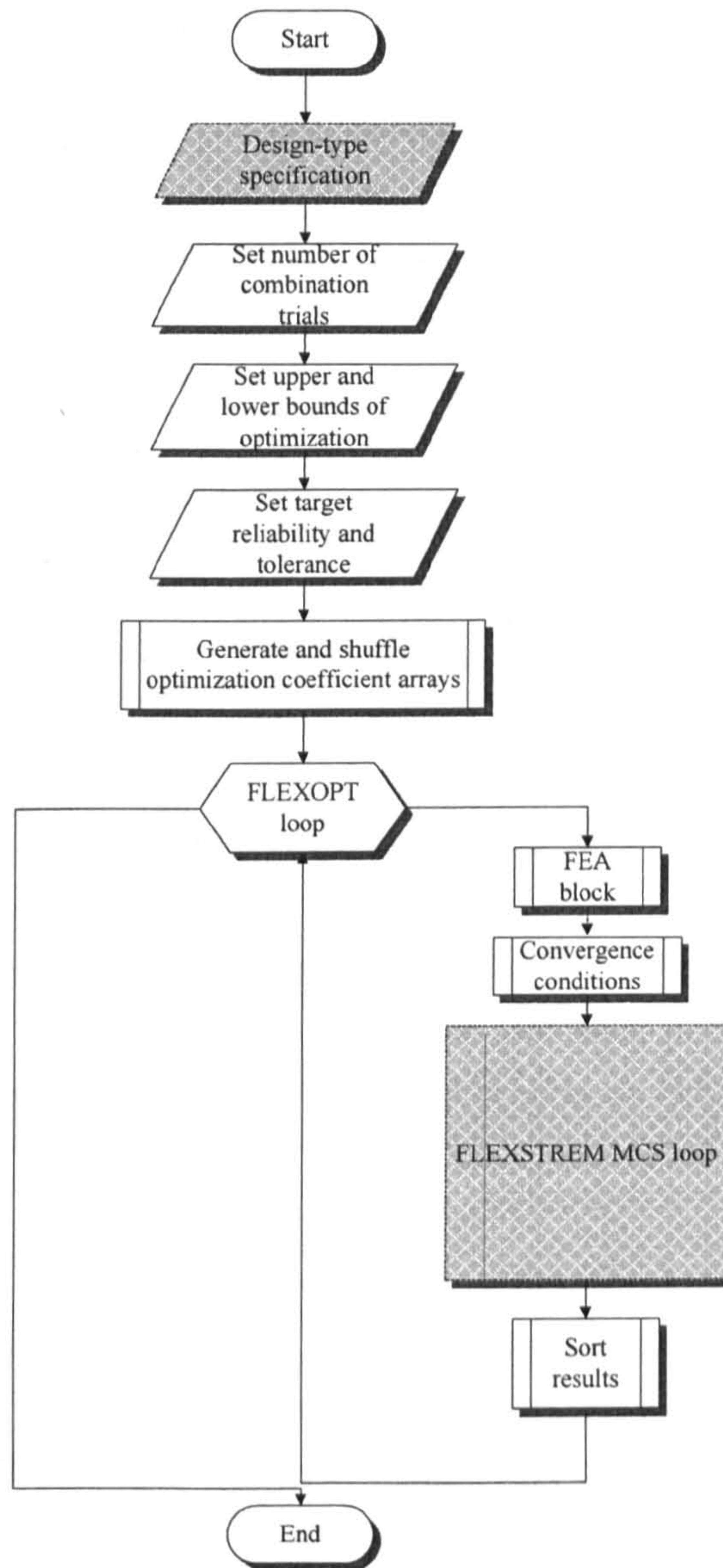


Figure (6.2) – FLEXOPT algorithm.

### 6.5.1 Level Convergence Specification

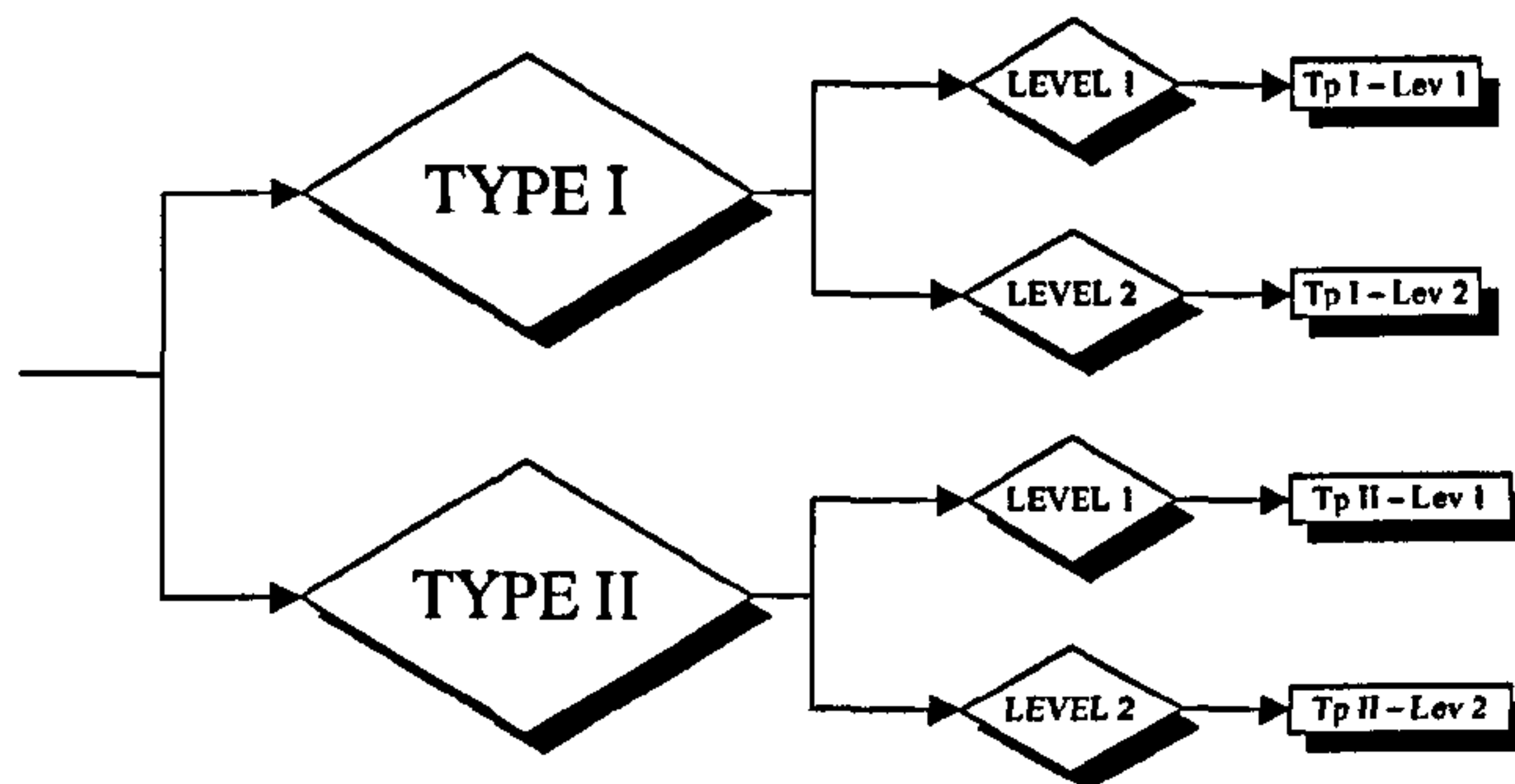


Figure (6.3) – Level convergence specification.

This is a data entry process. The data entered specifies the convergence parameters of the entire FLEXOPT procedure. From the flow in Figure (6.3), analysis is possible in four ways:

- Type I analysis – level 1 convergence
- Type II analysis – level 1 convergence
- Type I analysis – level 2 convergence
- Type II analysis – level 2 convergence

The type analysis is selected first before the level convergence criterion.

### 6.5.2 Specification of the Number of Combinations to Perform

This is another data entry process. The data entered here specifies *NCOM* – the amount of optimization iterations to be performed by FLEXOPT. It is also the size of the coefficient vectors (1-D arrays) to be generated for each of the shape variables (thicknesses and diameters). The number entered must be an even integer for reasons specified in section 6.5.5.1.

### 6.5.3 Specification of the Upper and Lower Boundaries of Optimization Percentage

This is a data entry process. The data entered here determines the highest and the lowest values of the coefficient vectors. These values are percentages; they determine the percentage by which a variable is increased or decreased. The lower bound value of the coefficient vectors must be greater than zero to avoid floating point errors. The choice

of these values is based on a “feel” of where the best results of the FLEXOPT procedure lie. If there is no idea of where these values (best results) are, a lower bound value greater than 0% and less than 1% (e.g. 0.1%) and an upper bound value of 100% are recommended for an initial trial. Knowledge gained from the initial results should enable better calibrations of these boundaries in subsequent analyses. A relatively narrow distance (search region) between both boundaries could be beneficial for computation time (quick convergence) and for target parameters (goals) that are sensitive to minute changes.

Figures (6.4) and (6.5) show the “search” region (between  $\psi_{min}$  – the lower bound value and  $\psi_{max}$  – the upper bound value) in which FLEXOPT operates to obtain the best result. The size of the search region has an impact on the computation time for convergence. The convergence time for an optimization procedure based on boundaries stated in Figure (6.4) (i.e. 75% - 100% and its mirror in the negative number line) should be less than the convergence time for the same optimization procedure based on the boundaries stated in Figure (6.5) (i.e. 0.1% - 100% and its mirror in the negative number line).

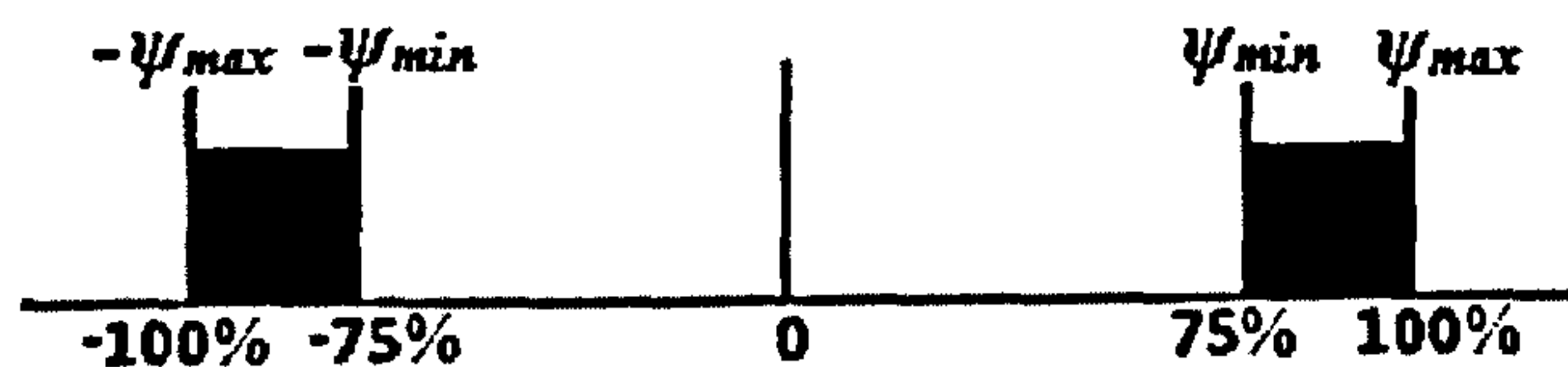


Figure (6.4) – Narrow search distance between optimization percentage boundaries.

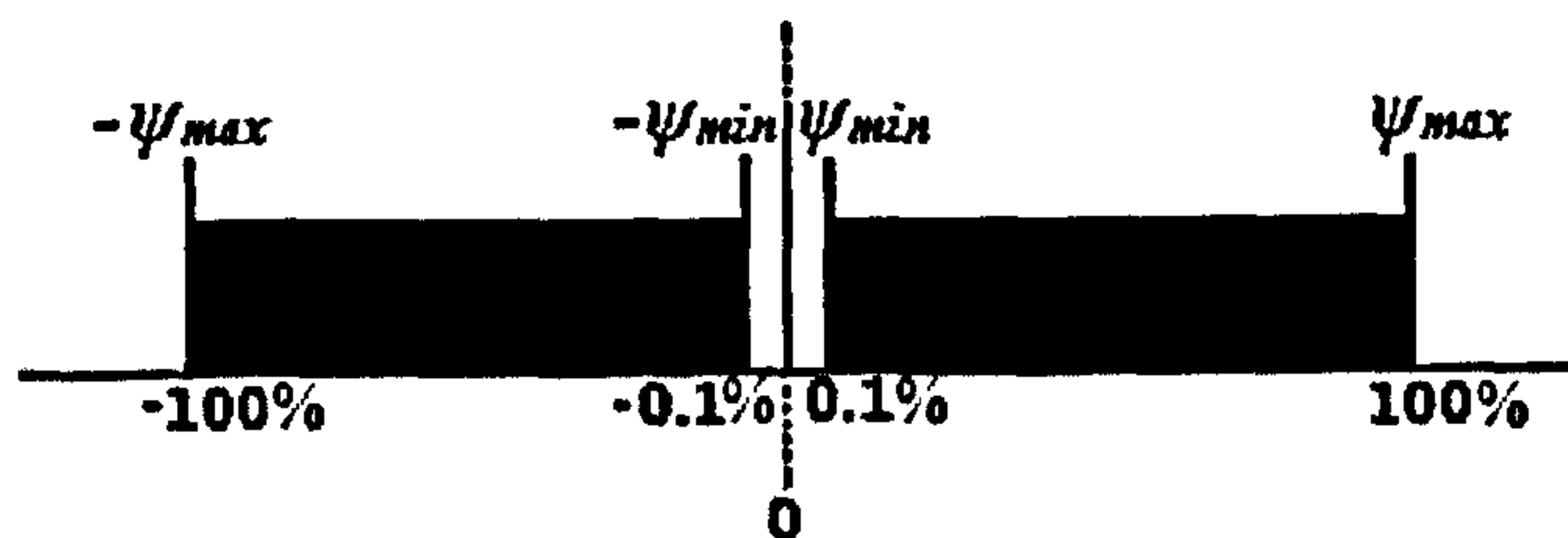


Figure (6.5) – Wide search distance between optimization percentage boundaries.

Although the maximum coefficient vector value,  $\psi_{max}$  is depicted as 100% in Figures (6.4) and (6.5),  $\psi_{max}$  could be specified at a much higher value. However, changes of this kind are limited to only the positive coefficients ( $+\psi_i$ ) as the negative coefficients

( $+\psi_i$ ) are pegged at -100% and no lower. This is explained via Equations (6.10) and (6.11) in section 6.5.7.

#### **6.5.4 Designation of the Target Reliability and Tolerance**

This is a data entry process. The selection of the highest structural reliability is the part of the principal aims of FLEXOPT. This is reflected in its presence in both of the outlined convergence criteria – level 1 and level 2. From chapter 5, the reliability,  $R$  in FLEXSTREM is defined as:

$$R = 1 - POF$$

where the probability of failure ( $POF$ ) is given as:

$$POF = \frac{\sum PFC}{NSIM}$$

where PFC is the process failure counter – a culmination instances at which the modelled limit states were violated and  $NSIM$  is the number of MCS trials in the FLEXSTREM MCS loop. Thus the uppermost reliability value ( $R_{max}$ ) closest to 1 (as reliability is never 1) which could be entered (designated) as the target reliability to be specified for a given FLEXOPT analysis dependent on a given number of MCS iterations,  $NSIM$ , is given as:

$$R_{max} = 1 - 10^{-Q} \quad (6.1)$$

$$Q = \log_{10} NSIM \quad (6.2)$$

Following this is the data entry of a tolerance value. The tolerance value is entered as a percentage. This value dictates how close a value can be to the target reliability in order to be considered in the “best results” category and by doing so aids in the convergence of the optimization process. This enables the FLEXOPT to access a given range or reliability values for different configurations to compare (alongside weight) and thus choose optimal solutions (based on the level selected). A relatively low tolerance would enable selection of reliability values closer to the target reliability values. A relatively large tolerance is less “strict” on the best reliability values selected.

### 6.5.5 Generation and Shuffling of the Optimization Coefficient Arrays

This process utilizes  $NCOM$  (section 6.4.2) and the values of the upper and lower boundaries of the optimization coefficient value (percentage) (section 6.4.3). It is predominantly in 3 phases as shown in Figure (6.6).

#### 6.5.5.1 A1 – Generation of the Positive Optimization Coefficients

Firstly, the  $NCOM$  value must be a positive even number because the first half of the optimization coefficients of a given size variable (in the analysis) is to the right of zero on the number line (positive) while the other half is to the left (negative).

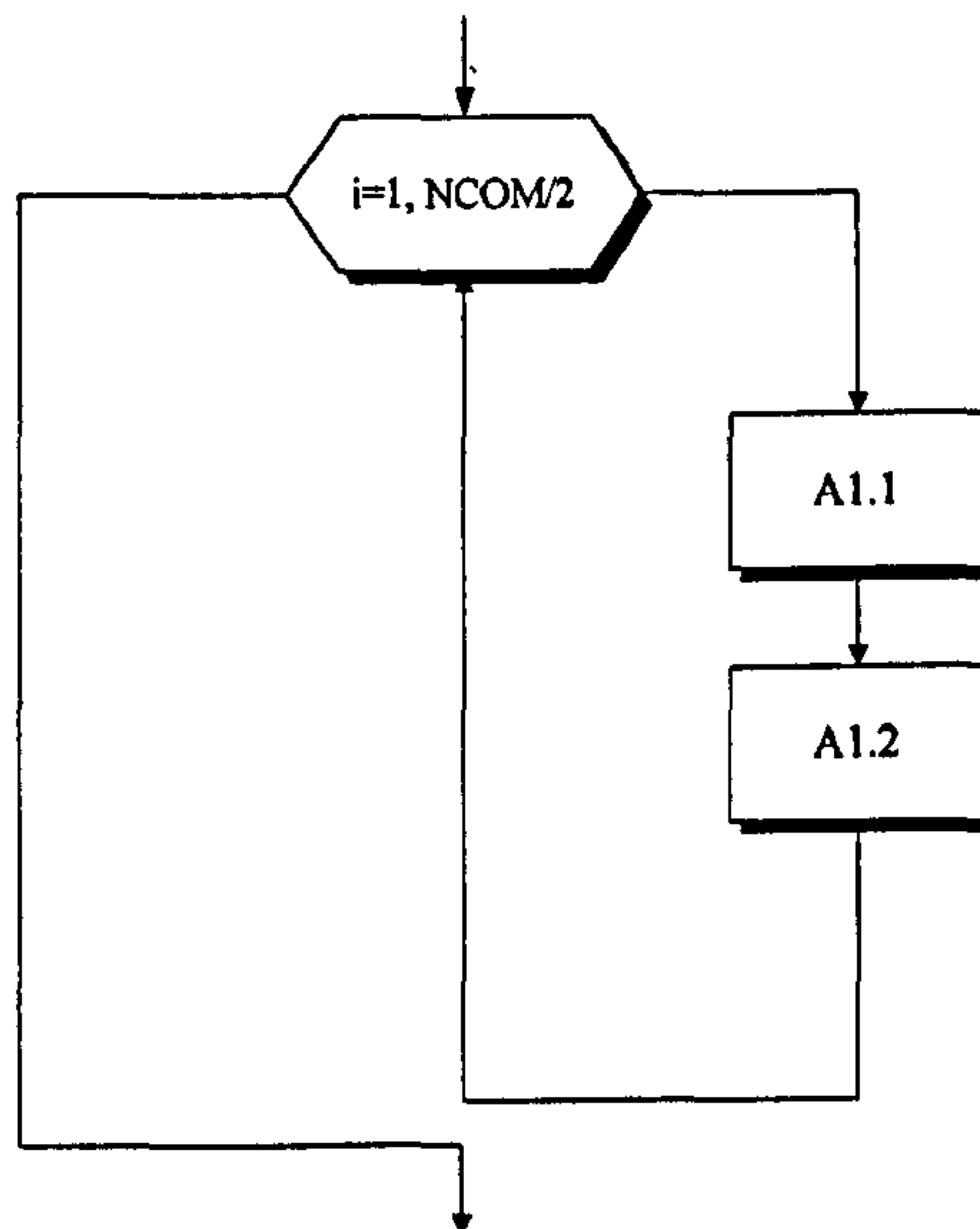


Figure (6.6) – Generation of positive optimization coefficients.

From Figure (6.7), at A1.1 random values are sampled from a uniform distribution. At A1.2 the uniform random numbers are utilized to form coefficients using the following equation:

$$\psi_i = RN_i \times (\psi_{max} - \psi_{min}) + \psi_{min} \quad (6.3)$$

where,

$RN$  is a uniform random number

$\psi$  is the coefficient array of a variable to be optimized

$i$  is the counting index of the first half of the optimization coefficients of the size variable (i.e. the index is between 1 and  $NCOM/2$ ).



6.5.5.2 A2 – Generation of Negative Optimization Coefficients

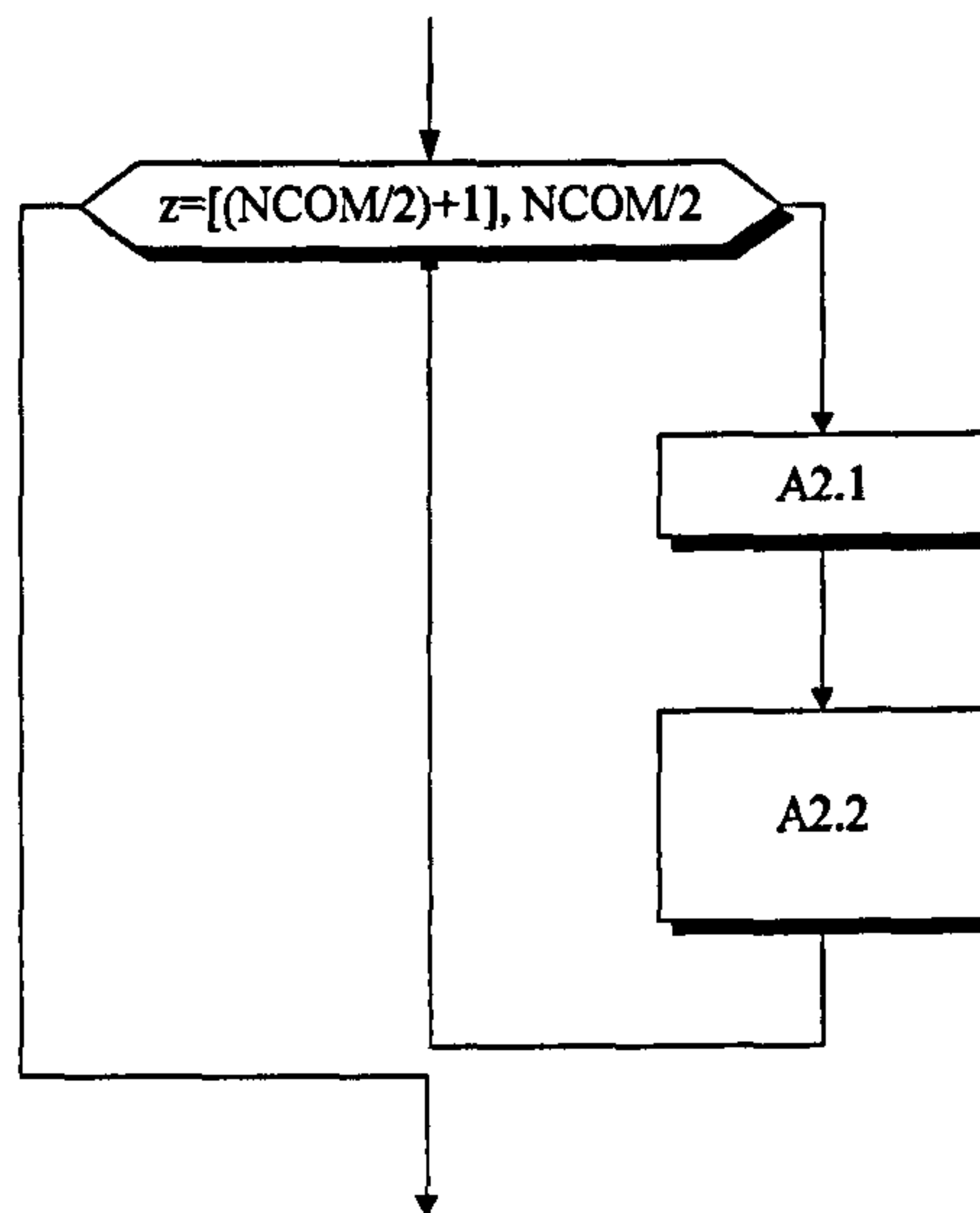


Figure (6.7) – Generation of negative optimization coefficients.

The flow of A2 is presented in Figure (6.7). A2.1 computes a step increase (i.e. 1) from the starting point of the second half of the optimization coefficients of a variable using the following equation:

$$z = \frac{NCOM}{2} + 1 \quad (6.4)$$

where,  $z$  is the counting index of the second half of the optimization coefficients of the size variable (i.e. the index is between  $NCOM/2+1$  and  $NCOM$ ).

At A2.2, a reversal of the sign of each coefficient in the first half of  $NCOM$  from positive to negative takes place:

$$\psi_z = -\psi_l \quad (6.5)$$

At this point the coefficient array of two size variables  $a$  and  $b$  would look like this (Figure (6.8)):

$$\begin{array}{ll}
 \Psi_{(1)a} & \Psi_{(1)b} \\
 \Psi_{(2)a} & \Psi_{(2)b} \\
 \Psi_{(3)a} & \Psi_{(3)b} \\
 \Psi_{(4)a} & \Psi_{(4)b} \\
 \Psi_{(5)a} & \Psi_{(5)b} \\
 -\Psi_{(6)a} & -\Psi_{(6)b} \\
 -\Psi_{(7)a} & -\Psi_{(7)b} \\
 -\Psi_{(8)a} & -\Psi_{(8)b} \\
 -\Psi_{(9)a} & -\Psi_{(9)b} \\
 -\Psi_{(10)a} & -\Psi_{(10)b}
 \end{array}$$

Figure (6.8) – Initial coefficients array (before shuffling).

For optimization procedures involving a single variable, such an array could suffice. However the presence of more than one variable implies that interaction of these coefficients in this state would only bring about biased outcome as the variables would be either exclusively positive or exclusively negative. For example, a relationship between two size variables  $a$  and  $b$  is an additive operation; the following occurs:

$$\psi_g a + \psi_g b = \Delta\chi \quad (6.6)$$

$$\psi_h a + \psi_h b = \nabla\chi \quad (6.7)$$

where,

$g$  is any value between 6 and 10 in Figure (6.8)

$h$  is any value between 1 and 5 in Figure (6.8)

$\chi$  is the outcome of the additive operation between size variables  $a$  and  $b$

$\Delta$  indicates an increase

$\nabla$  indicates a decrease

This problem leads to A3.

### 6.5.5.3 A3 – Shuffling of Optimization Coefficient Arrays

A3 is a modern implementation of the Fischer-Yates shuffler (Fischer and Yates (1938)) intended for use on computers – on which the first implementation was introduced by Durstenfeld (1964) and popularized by Knuth (1969). The algorithm essentially

redistributes all coefficient values of an array in a non-biased manner and without duplicates.

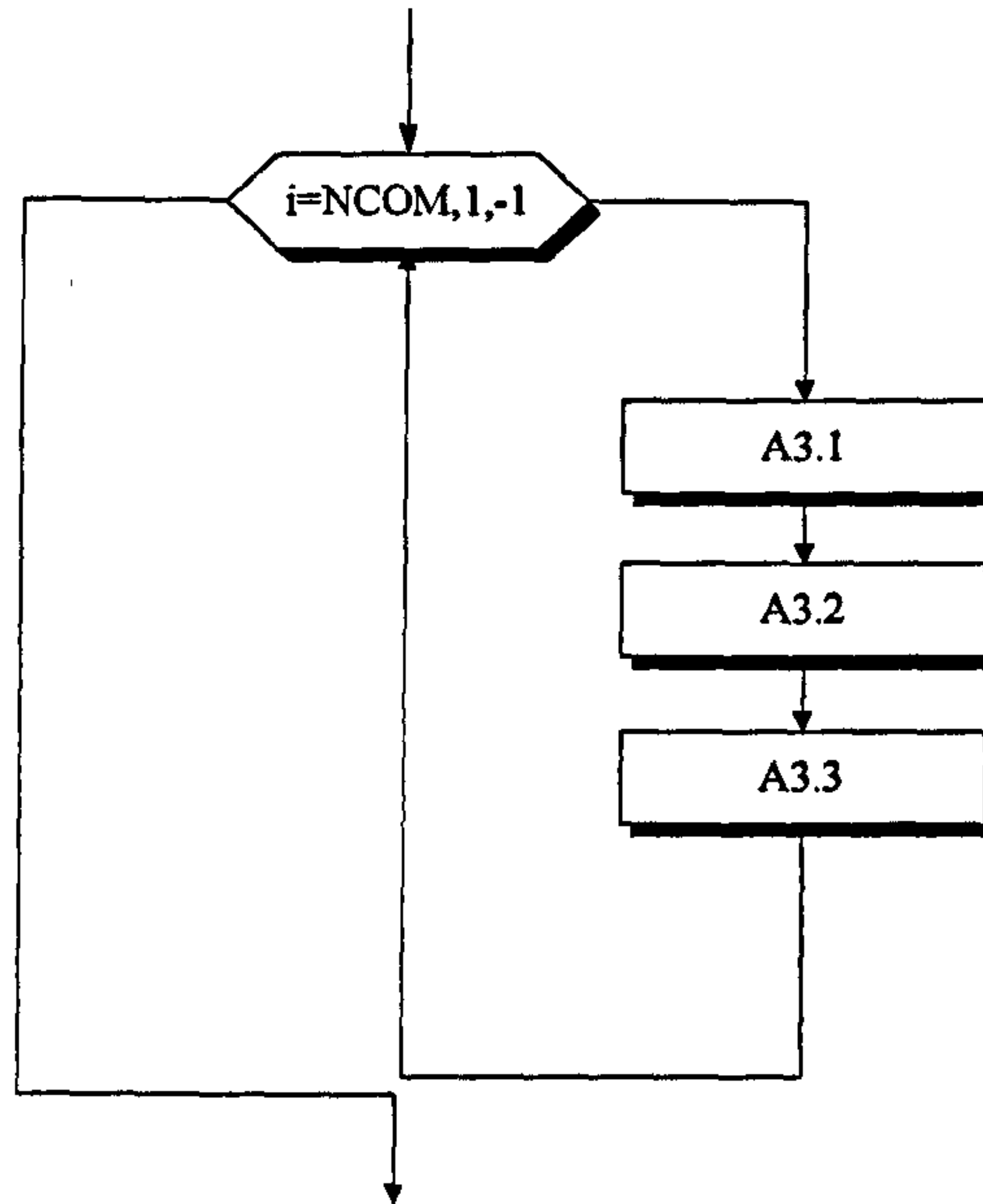


Figure (6.9) – Shuffling of optimization coefficient arrays.

The loop in Figure (6.9) is a regressing loop, regressing from the largest value of  $NCOM$  to 1 i.e. the first value of the loop is  $NCOM$  and it decreases by 1 until its value is 1.

At A3.1 a random number from a uniform distribution is selected. At A3.2 a random array index  $p$ , of a size variable (having a unique optimization coefficient index from the optimization coefficient vector) is generated from the gradually diminishing value of  $NCOM$  following Equation(6.8):

$$p = RN(NCOM) \quad (6.8)$$

A3.3 assigns the coefficient value at index  $i$  to that of the non-biased random index  $p$  using:

$$\psi_p = \psi_i \quad (6.9)$$

The resulting arrangement of the coefficients of variables  $a$  and  $b$  is now random (Figure (6.10)):

$$\begin{array}{r}
 \psi_{(3)a} \quad -\psi_{(8)b} \\
 -\psi_{(8)a} \quad \psi_{(4)b} \\
 \psi_{(1)a} \quad -\psi_{(10)b} \\
 -\psi_{(6)a} \quad -\psi_{(7)b} \\
 -\psi_{(10)a} \quad \psi_{(1)b} \\
 \psi_{(4)a} \quad \psi_{(5)b} \\
 -\psi_{(9)a} \quad \psi_{(2)b} \\
 \psi_{(2)a} \quad -\psi_{(6)b} \\
 -\psi_{(7)a} \quad \psi_{(3)b} \\
 \psi_{(5)a} \quad -\psi_{(9)b}
 \end{array}$$

Figure (6.10) – Shuffled coefficients.

The first coefficients of the size variable are set to zero to signify the initial status of the optimization procedure.

#### **6.5.6 FLEXOPT Loop**

This is the start of the iterative optimization procedure. The specified *NCOM* is the number of iterations to be carried out.

#### **6.5.7 FLEXSTREM FEA Block Modification**

As stated earlier, there are two criteria by which the best results/optimal solutions may be selected in FLEXOPT – the safety (reliability) and the cost (structural mass). The reliability obtained from FLEXSTREM is dependent on the limit states modelled as demonstrated in chapter 5. Most of these limit states are predominantly dependent on the material properties. The material properties are a set of attributes peculiar to a given material. At design stage, a selected material property (from the set of properties of the said material) cannot be changed independently. Rather, a new material with the desired property (within a set of acceptable properties) is selected. Thus the material properties could be said to be un-modifiable. For example, for an application Z, the following material properties are required (Table (6.2)):

Material property	Minimum requirement for application Z
Tensile strength	79 MPa
Yield strength	150 MPa
Fracture toughness	49 MPa ( $\sqrt{m}$ )

Table (6.2) – Minimum material requirement for application Z.

For the application Z, a material X has been suggested. Material X has the following properties (Table (6.3)):

Material property	Minimum requirement for application Z	Material X properties
Tensile strength	79 MPa	80 MPa
Yield strength	150 MPa	160 MPa
Fracture toughness	49 MPa ( $\sqrt{m}$ )	45 MPa ( $\sqrt{m}$ )

Table (6.3) – Material property X against minimum requirements for application Z.

From Table (6.3), it could be seen that material X falls short in the fracture toughness requirement. A solution to this would involve a new material selection as the fracture toughness property of material X cannot be altered independently. A new material Y is proposed for the application (Table (6.4)):

Material property	Minimum requirement for application Z	Material Y properties
Tensile strength	79 MPa	83 MPa
Yield strength	150 MPa	155 MPa
Fracture toughness	49 MPa ( $\sqrt{m}$ )	55 MPa ( $\sqrt{m}$ )

Table (6.4) – Material property Y against minimum requirements for application Z.

Material Y, from Table (6.4) meets the minimum requirement for application Z. This example illustrates the un-modifiable nature of material property (within the scope of this research).

The material property is un-modifiable, however the structural configuration (and hence weight) could be altered. The structural weight depends on the volume (made up of individual member volumes for multi member structures) and the material density. The material density cannot be altered independently as it is a material property. However, the thickness and the outer diameter are the only parameters that could be altered. Also, the nodes of the structure are fixed (in sizing optimization); changes in the lengths of individual members would alter the position of the nodes and effectively the structure

shape, hence no manipulations could be made to it. Thus, the volume, which depends on the length, outer diameter and thickness (for tubular sections) could be altered.

Structures predominantly consist of groups of members having similar geometry properties for ease of fabrication, cost, analyses, etc. among other reasons. The required data procedure in chapter 4 section 4.1, Table (4.3) enables the indication of member groups. These member groups could be indicated by the simple addition of a character to aid recognition by the FLEXOPT program. An illustration of the grouping is presented in Table (6.5) (rightmost column):

Node 1	Node 2	Diameter (m)	Thickness (m)	Member Group
3	4	0.030	0.008	C
3	5	0.015	0.005	T
4	5	0.030	0.008	C

Table (6.5) – Structural group identification.

As stated earlier, a group has two size variables of interest – thickness and outer diameter. These size variables are each assigned a coefficient vector. For two member groups, four coefficient vectors (1-D arrays) would be needed, for three member groups, six coefficient vectors, etc.

The coefficient vectors are fed into the FEA block to modify the default values of each of the two size variables (thickness and diameter) for the different member groups at each step of *NCOM* iterations. The modification to variables *a* and *b* would take the form:

$$a = a + \left( \frac{\psi_i}{100} \times a \right) \quad (6.10)$$

$$b = b + \left( \frac{\psi_i}{100} \times b \right) \quad (6.11)$$

where,

*a* and *b* are the thickness and outer diameter of a group.

This modification affects several variables shown in section 5.6.2 of chapter 5. From the Equations (6.9) and (6.10) it could be observed that while coefficients ( $\psi_i$ ) greater than 100% would maintain values of *a* and *b* greater than zero, coefficients ( $\psi_i$ ) equal to or less than -100% would reduce *a* and *b* to values less than zero.

### 6.5.8 Convergence Conditions

The convergence conditions are based on the convergence specification at the start of the analysis (section 6.5.1). Level 1 convergence is based on only the reliability while the structural mass is ignored. The Level 1 algorithm flow is shown in Figure (6.11):

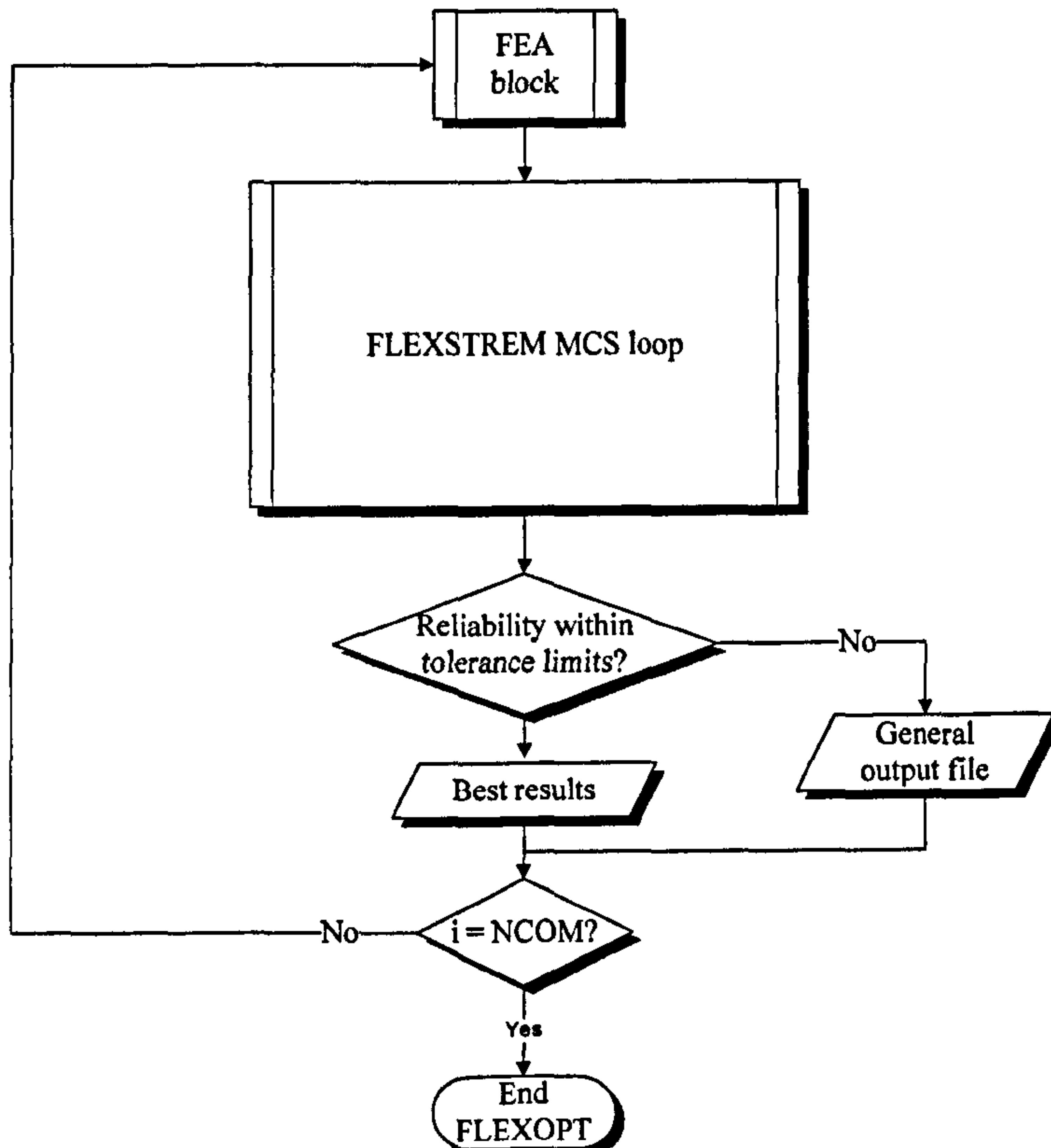


Figure (6.11) – Level 1 convergence flow.

The Level 2 convergence is based on both reliability and mass. This speeds up the computation as higher structural masses are ignored regardless of their reliability values. The flow of the Level 2 convergence is shown in Figure (6.12).

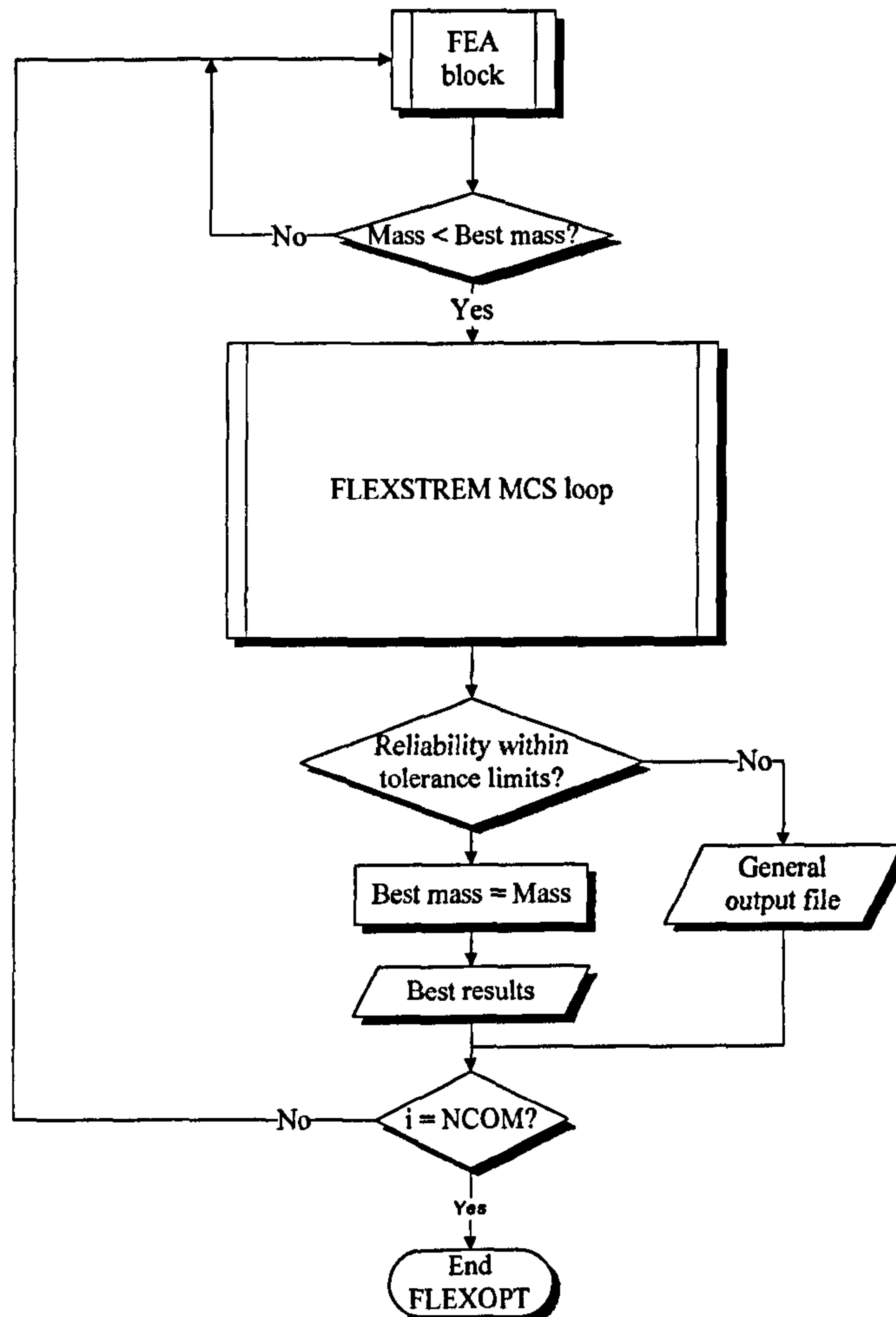


Figure (6.12) – Level 2 convergence flow.

### 6.5.9 Result Sorting Operations

Generally a lot of iterations would be expected. The outcome of each FLEXOPT analysis is recorded in a general output file. The results that meet the specified convergence condition are sent to a different output file for design review. This ensures that the best results are not lost in the general output file. This process is also illustrated in Figures (6.11) and (6.12).



## 6.6 Result/Discussion

### 6.6.1 Optimization of Crane Boom

The abstracted crane boom arm configuration shown in chapter 4 (section 4.5.1) is presented for a size optimization. The crane boom is made up of two member groups; thus, 4 coefficient vectors are needed as each variable (diameter or thickness) in the set of size variables (diameter and thickness) for each member group (A and B (Table (6.6)) is optimized independently. A maximum optimization reliability goal of 0.9999 with a reliability tolerance of 0.1% is set. The maximum coefficient vector value is 125% and the minimum is 0.1%. The total number of iterations for this analysis (also the size of the coefficient vector) is 2500. The result is outlined in Tables (6.6):

#### Level 2 optimization for 2500 combinations within the limits of 125.000% and 0.100% with a target reliability of 0.9999:

Iteration number	Member failure count	Nodal failure count	Reliability	POF	Structural mass (kg)	Percentage change in structural group configurations (optimal size variable coefficients)			
						Group A percentage change in thickness	Group A percentage change in diameter	Group B percentage change in thickness	Group B percentage change in diameter
1	0	1379	0.8621	0.1379	75447.0	0	0	0	0

Table (6.6) – FLEXOPT optimization result. (a)

Based on a two member-group configuration, no mass lower than the original with reliability within the set tolerance was found.

### 6.6.2 Optimization and Comparison of the 25-bar Truss Tower

A comparative verification of the FLEXOPT is presented for the 25-bar truss tower shown in chapter 4. The aim is to compare the results from FLEXOPT with those of other methods for benchmarking and efficiency purposes. The 25-bar truss tower is made up of 8 member-groups. Thus, 16 coefficient vectors for each size variable are required. The result is shown in Tables (6.7 – 6.9):

**Level 2 optimization for 100000 combinations within the limits of 100.000% and 0.100% with a target reliability of 0.9999:**

Iteration number	Member failure count	Nodal failure count	Reliability	POF	Structural mass (kg)
1	0	0	0.9999	0	493.4
32	0	0	0.9999	0	454.9
101	9	0	0.9991	0.0009	268.3
144	0	0	0.9999	0	251.5
163	0	0	0.9999	0	202.3
1374	0	0	0.9999	0	184.7
2668	0	0	0.9999	0	184.2
4777	0	0	0.9999	0	151.8
8927	0	0	0.9999	0	142.7
25696	0	0	0.9999	0	88.8

Table (6.7) – FLEXOPT 25-bar truss optimization result. (a)

Iteration number	Percentage change in structural group configurations (optimal size variable coefficients)							
	Group A percentage change in thickness	Group A percentage change in diameter	Group B percentage change in thickness	Group B percentage change in diameter	Group C percentage change in thickness	Group C percentage change in diameter	Group D percentage change in thickness	Group D percentage change in diameter
1	0	0	0	0	0	0	0	0
32	-2.65	-46.97	84.32	75.25	-0.44	8.69	76.18	64.72
101	-69.38	90.9	-64.9	-20.81	-36.99	12.45	12.22	-46.9
144	-1.84	49.06	-26.74	4.06	-63.9	37.53	-93.62	-20.21
163	0.25	40.39	-81.23	4.54	54.14	-6.99	-70.51	26.51
1374	8.1	-69.41	-87.22	27.52	-48.05	-23.03	-88.99	-58.72
2668	-48.95	65.69	-91.78	94.78	-5.73	-19.73	16.06	-42.03
4777	-34.98	-44.91	-61.16	69.45	-58.34	8.47	93.1	-42.36
8927	-58.26	15.05	-60.51	-39.94	-30.98	-29.18	-65.18	27.4
25696	-69.34	6.42	-69.62	-22.86	-72.96	-1.09	-77.38	-39.09

Table (6.8) – FLEXOPT 25-bar truss optimization result. (b)

Iteration number	Percentage change in structural group configurations (optimal size variable coefficients)							
	Group E percentage change in thickness	Group E percentage change in diameter	Group F percentage change in thickness	Group F percentage change in diameter	Group G percentage change in thickness	Group G percentage change in diameter	Group H percentage change in thickness	Group H percentage change in diameter
1	0	0	0	0	0	0	0	0
32	-95.82	56.5	-82.42	35.78	-98.93	-17.44	-78.97	51.58
101	-8.42	19.99	-3.97	-48.48	-23.55	13.83	-83.29	-66.93
144	-57.84	3.08	-70.58	-5.41	-82.17	92.15	35.85	-45.05
163	-85.1	-15.5	-13.62	-21.34	-99.29	14.97	-93.39	13.98
1374	-34.68	51.7	-68.72	84.89	-65.44	-71.56	-76.05	-7.29
2668	76.3	-15	-81.5	-28.82	-86.86	27.7	-42.61	-23.68
4777	-99.39	-94.01	-94.68	35.53	92.34	-48.57	25.7	-50.69
8927	-93.39	-73.08	-88.25	30.97	9.06	-52.58	-2.31	-58.3
25696	-27.49	-75.69	-73.93	-70.36	-94.02	50.26	60.61	-51.33

Table (6.9) – FLEXOPT 25-bar truss optimization result. (c)

With the given number of iterations and optimization boundaries, the lowest mass within the confines of the specified reliability tolerance was found to be 88.8 kg. There is approximately a difference of 405 kg (in material and hence cost) when compared to the initial structural mass of 493.4 kg.

From a selection of literatures, the following sizing optimization results have been obtained:

Author	Weight (kg)
NDM <sup>(1)</sup>	246.73
Li and Wood <sup>(3)</sup>	243.43
Shih and Lee <sup>(2)</sup>	96.58
Li and Yang <sup>(4)</sup>	84.1
<b>This research</b>	<b>88.8</b>

Table (6.10) – Optimization comparison for 25-bar truss.

where,

- 1- Park and Sung (2002).
- 2- Shih and Lee (2006).
- 3- Li and Wood (2009).
- 4- Li and Yang (1994).

The dimensions of the optimization results in Table (6.10) are also available in the cited literature. It should be noted that the FLEXOPT optimization of the 25-bar truss was carried out without any factor or ratios as the general presentation of the 25-bar truss from several literatures contained little or no restrictions.

### 6.6.3 Recommendation for a New Crane Boom Configuration

From chapter 5 it could be observed that the root causes of the failure are located within the highly stressed tapered region shown in Figure (5.22). Thus this region is designated a different member group so as to enable optimization to be favourable enough to its demands (high stress) without subjection to the “best” dimensions for the other member groups. This is a step towards reducing uncertainty as inferred in section 5.5.3. The number of member groups is increased to 3. The third member group (tapered region – Figure (5.22)) is assigned an initial diameter of 0.3 m with a thickness of 0.013 m. The analysis is presented in Table (6.11):

#### Level 2 optimization for 2500 combinations within the limits of 125.000% and 0.100% with a target reliability of 0.9999

Iteration number	Member failure count	Nodal failure count	Reliability	POF	Structural mass (kg)	Percentage change in structural group configurations (optimal size variable coefficients)						
						Group A percentage change in thickness	Group A percentage change in diameter	Group B percentage change in thickness	Group B percentage change in diameter	Group C percentage change in thickness	Group C percentage change in diameter	Group C percentage change in diameter
11	0	0	0.9999	0	70178	3.28	-26.94	-8.27	-72.09	36.35	117.97	
25	0	1	0.9999	0.0001	64841.2	70.34	-34.56	58.98	-37.68	-30.99	68.28	
109	0	0	0.9999	0	45678.5	113.53	-58.8	-5.7	-22.1	52.42	21.19	
713	0	0	0.9999	0	42992.2	46.76	-54.71	-24.74	-32.46	27.65	5.83	
815	0	0	0.9999	0	36913.6	-29.23	-64.86	121.05	-63.07	-30	87.22	
1973	0	0	0.9999	0	21469.2	27.57	-65.48	44.77	-81.94	57.48	-41.37	

Table (6.11) – FLEXOPT optimization for new crane section configuration.

From the results, the improvements to the reliability and weight values could be noted. Three configurations are to be noted in this analysis:

- (1) Configuration 1 – original configuration (the original configuration of the crane boom members: mass = 75447 kg, reliability = 0.8621).
- (2) Configuration 2 – robust configuration (the most robust (most weight) of the optimization solutions from Table (6.14): mass = 70178 kg, reliability = 0.9999).
- (3) Configuration 3 – optimal configuration (the best (lowest weight and high reliability) from the optimization solutions in Table (6.14): mass = 21469.2 kg, reliability = 0.9999).

These configurations would be subject to a different type of analysis in chapter 7.

## **6.7 Conclusion**

A method aimed at presenting solutions that improve structural reliability while considering cost has been developed. Flexibility in the form of options to either focus on safety (reliability) alone or on safety and cost (mass) simultaneously has been achieved in this chapter.

A benchmarking analysis on the 25-bar truss showed the optimization levels that could be achieved using the FLEXOPT method. The importance of FLEXSTREM as the foundational method for the risk quantification was also shown. The solutions proffered were tested by the validated FLEXSTREM. Improvements to the underlying FLEXSTREM model would lead to improvements in the optimal solutions generated from FLEXOPT which could bring about optimal utilization of resources and a good level of safety in the design/modification of structures.

In the crane case study, optimization of the crane boom consisting initially of 2 member groups did not offer any significant improvements both cost-wise (structural mass) and safety-wise (reliability). The introduction of a third grouping to cover the highly stressed region (and thus fashion solutions solely suited to the region) brought about considerable savings in cost and an improved reliability level.

## **Chapter 7:**

# **Stochastic FLEXSTREM (STOFLEX): A Stochastic Implementation of FLEXSTREM for Risk Control in Structural Maintenance and Repair Scheduling**

### **Summary**

*In this chapter, another risk control option/cost benefit analysis is presented. A stochastic adaptation of the FLEXible SStructural RELiability algorithm (FLEXSTREM) - STOFLEX to predict crack propagation within a structure given a stochastic loading scenario is developed. It also assesses the performance of structures subject to various loads and thus aids in the scheduling of inspection and maintenance activities that would preserve the integrity of the structure. For existing structures such analysis would also give insight on life extension. The method is demonstrated on a crane boom arm for three separate configurations.*

### **7.1 Introduction**

Fatigue is one of the failure modes experienced by structures under cyclic loadings (Aghakouchak and Steiner (2001)). Fatigue has for a very long time posed serious considerations in the design of various structures (Yao et al (1986)). These structures cut across several engineering fields. Mechanical engineering examples include turbines, propeller shafts, pressure vessels, pipings, etc. Aeronautic engineering examples include aircraft structures, jet engines, etc. Civil engineering examples include offshore structures, nuclear power-plants, highway and railway bridges, etc.

STOFLEX – an adaptation of the FLEXSTREM is presented in this chapter. Modelled strongly on the basis of probability and statistics, the adaptation fulfils the criteria



needed for a phenomenon highly subjected to uncertainty such as fatigue. The method is modelled to simulate crack growth simultaneously in all joints (nodes) of a structure. Any one joint could be monitored in an analysis. This implies that the performance of a structure subject to a certain pattern of inspection could be monitored. Thus better inspection and maintenance intervals could be scheduled. Also, recommendations could be made for structures that are at the end of their prescribed lives such that more years could be safely and economically added.

## **7.2 Background**

Many public infrastructures are ageing and consequently attention has been directed to existing structures for evaluation and reassessment (Aghakouchak and Steiner (2001)). These structures often need in-service inspections for repair and maintenance to avoid sudden failure from fatigue (Meng et al (2007)).

The most common type of offshore structure is the steel jacket platform (Baker and Descamps (1999), Aghakouchak and Steiner (2001)). These structures were intended to be in service for about 25-30 years (Baker and Descamps (1999)).

Fatigue failure has been one of the most dominant failure modes in tubular connections of offshore structures especially in harsh environments such as the North Sea (Aghakouchak and Steiner (2001)). Some of these structures like deep water structures have very little redundancy with very severe consequences of fatigue failures compared to steel jacket platforms in shallow waters (Skjong and Torhaug (1991)). Tubular members of offshore structures are the most prone to fatigue failures for reasons of connection geometries, welds at joints and cyclic loading (especially by forces in the immediate environment) (Aghakouchak and Steiner (2001)).

Despite the solid establishment of fracture mechanics and numerous standards available, the fatigue phenomenon is not completely understood (Yao et al (1986)); much uncertainty abounds still in both process and variable values (Aghakouchak and Steiner (2001)), thus making the damage analysis of structural systems a challenging task (Yao et al (1986)). As a result it is deemed necessary to carry out laboratory experiments to

determine the property of new materials, geometries, loading and environmental conditions.

Still, there exists a considerably large scatter in laboratory tests even for identical specimens. It thus becomes desirable to incorporate statistical methods to somewhat represent this scatter (Yao et al (1986), Aghakouchak and Steiner (2001), Wu et al (2004)). However cases of insufficient data in new structural configurations and large/costly structures (most civil engineering structures) impede the implementation of the statistical methods (Yao et al (1986)). The incorporation of variability as a property in the analysis and design of these components is of great importance due to the uncertainty present in both material fatigue strength (resistance) and structural loading (stress).

Fatigue reliability, in terms of crack growth, has been developed and adopted by the offshore industry since the 1980s and early 1990s (Righiniotis (2004)). Fatigue limit states govern the dimension in several parts of an offshore structure in many cases (Skjong and Torhaug (1991)). For cases where fatigue becomes the determining factor of several aspects of the structure, e.g. inspection, dimensions and operations, etc., it is imperative that the fatigue information maintains high accuracy.

Fatigue failure probability is defined as the probability of an initial crack length reaching or exceeding the critical crack length in a given period of time (Meng et al (2007)). Fatigue reliability analysis carried out should be based on (Skjong and Torhaug (1991)):

- Physical and mechanical models of the environment
- Loading
- Response analysis
- Fatigue strength
- Damage accumulation

A reflection of the uncertainty (randomness) in all phases of this analysis should be done by describing all parameters as random variables with their various characteristics (Skjong and Torhaug (1991)). The probabilistic model must also contain uncertainty

models to explicitly account for the limitations of physical and mechanical modes due to lack of knowledge and model abstraction. The derived computed reliabilities are measures of confidence in the structural reliability. The reliability is not a structural property due to the presence of epistemic uncertainties (which reduce with the availability of more data). The availability of these data (reduction of uncertainty) reflects in the computed reliability. Also, the computed reliabilities cannot be interpreted as expected failure frequencies. They are rather used as yardsticks for comparing structural reliabilities of different possible structural configurations.

Welding induces some defects which initialize cracks on a micro-scale (Lukic and Cremona (2001)). Cracks are often localized at the weld where they could propagate under loading and ultimately lead to joint failure. From field observations and laboratory tests it has been observed that (Aghakouchak and Steiner (2001)):

- A fatigue crack initiates from the weld toe hotspot connection (tubular) and gradually propagates around the intersection and through the wall thickness.
- A fatigue crack usually occurs at the joints of members of large diameters.
- On through-thickness penetration of the crack, a reduction in joint stiffness is observed. This is considered as the end of the fatigue life of the joint.

The conditions governing this crack growth include (Lukic and Cremona (2001)):

- Structural geometry
- Initiation site
- Loading
- Material characteristics.

All the conditions are random, thus the analysis is better treated probabilistically (Lukic and Cremona (2001)). The two methods used in modelling components subject to fatigue are the S-N method and the linear elastic fracture mechanics (LEFM) method (Aghakouchak and Steiner (2001)).

Several authors have proposed various inspection strategies based on two different phases of fatigue failure (Meng et al (2007)):

- Crack initiation

- Crack propagation.

The strategies are mainly based on the Paris-Erdogan model with the crack initiation phase neglected. This view makes the model suited to welded joints (Meng et al (2007)).

Structural safety depends not only on initial structural design and high fabrication standards but also on appropriate amount of in-service inspection and when necessary, repair (Baker and Descamps (1999)). The main objective of inspection planning is to protect lives, minimize damage, reduce lifetime cost and minimize downtime. The inspection of steel structures is aimed at the early detection of fatigue, corrosion and other types of damage. The stakes in the inspection of offshore structures is higher than that of onshore structure for the following reasons (Baker and Descamps (1999)):

- Submerged parts cannot easily be seen.
- Sudden failure could lead to release of hydrocarbons and thus large scale pollution.
- More variables (environmental) compared to onshore structures.

The advances in drilling technology have meant that more reserves could be tapped by using devices on the existing offshore platforms (Baker and Descamps (1999)). This has led to the prolongation of the lives of the structures. As a result, inspections have become a high priority and more cost sensitive due to the effectiveness and frequency.

Traditional safety and inspection qualitatively combine criteria such as fatigue lives, member criticality, stress levels, past inspection data, previous experience and cost consideration to produce an inspection plan (Onofriou (1999)). For deep water structures, repair and maintenance intervals could be very challenging (Skjong and Torhaug (1991)) as the monitoring of the integrity and performance of offshore structures by underwater inspection comes at a significant cost to the operators (Onofriou (1999)).

The most common offshore structure, the jacket offshore structure possesses welded joints ranging from hundreds to thousands (Baker and Descamps (1999)). The inspection of such structures using divers (humans) is very costly. This makes the cost management of high priority.

Structural maintenance constitutes a complementary and necessary approach in design in order to reduce risk of failure (Lukic and Cremona (2001)). Design fatigue-lives (with augmented safety factors usually calculated from a design code) are often used to determine inspection intervals in spite of the well established fact that there is little correspondence (weak relationship/link) between design life and resultant life of the structure (Skjong and Torhaug (1991)). Inspection intervals have to be strategically chosen such that risk of failure (fatigue) is controlled (Lukic and Cremona (2001)).

Fatigue or crack may occur earlier than expected due to larger (than projected) residual stresses and stress concentration factors (SCFs), undetected initial defects in highly stressed parts of a weld, higher stress ranges due to a larger structural response for particular sea states, undetected initial defects in highly stressed parts of a weld, or also as a result of undetected gross defects such as misalignments of the joint, or poor welding conditions (Baker and Descamps (1999)).

Fatigue safety factors (deterministic) are usually large enough to ensure that even in adverse conditions, fatigue failure occurrence throughout the design life of the structure is minimal (Baker and Descamps (1999)). Increasing the safety factor such that inspection becomes irrelevant is extremely uneconomic. It is more economic to ensure that occurrence of fatigue during service life is minimal and to plan optimal inspection intervals that arrest crack growth.

Inspection exercises are cost dependent and thus must rely on a healthy compromise between cost and safety (Lukic and Cremona (2001)) as too many (frequent) inspections cause prolonged downtime and increased cost (Meng et al (2007)), whilst too few inspections increase risk of failure in terms of loss of lives and property. An optimal inspection plan maintains a suitable balance between cost (inspection, maintenance and repair) and safety.

### **7.3 Methodology**

As stated in the previous chapter, the risk control option/cost benefit analysis step in the modified FSA is aimed at mitigating risk while considering the cost involved. The

methodology presented in this chapter is the second of two methods which attempts to achieve this aim. In this chapter, a method which attempts to provide best optimal inspection intervals in which maintenance and repair activities could be carried out is introduced. In order to achieve this, the method has to be, in addition to the attributes of the pre-existing FLEXSTREM:

- A time dependent (stochastic) analysis
- Capable of predicting fatigue failure

This is further illustrated in Figure (7.1):

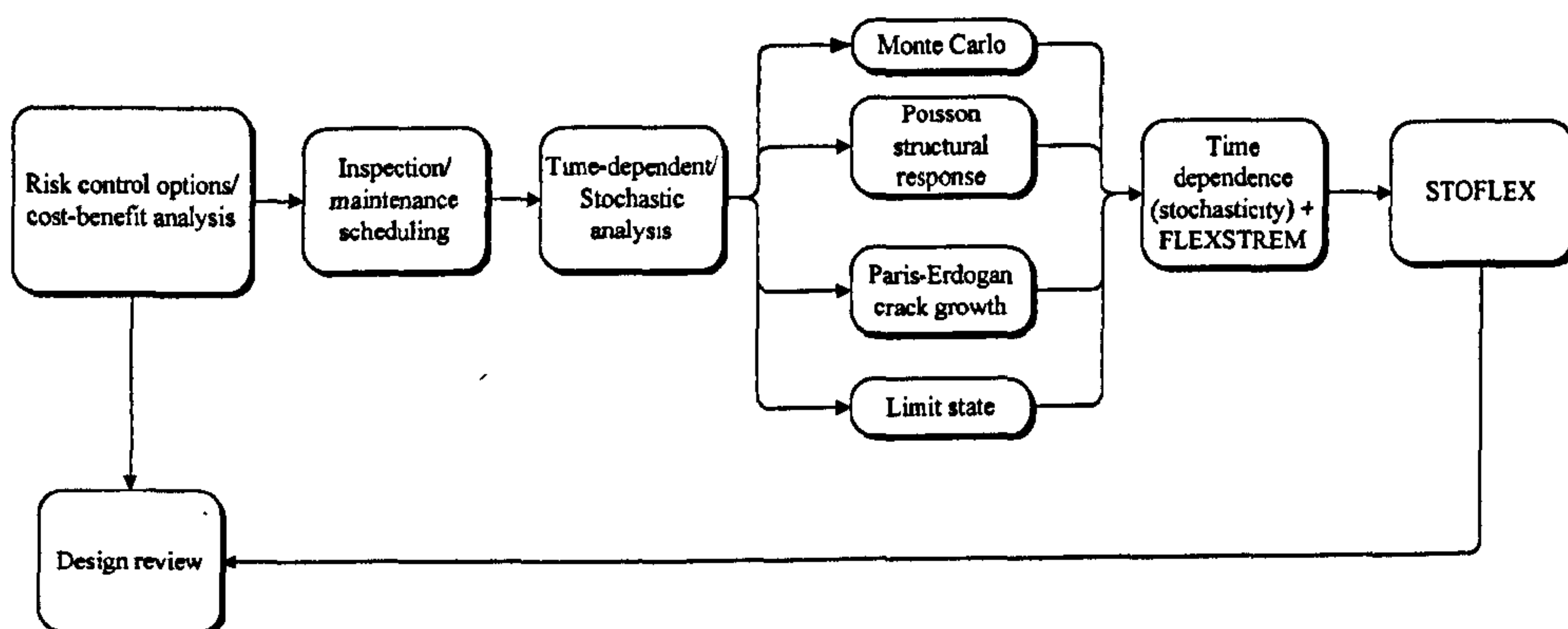


Figure (7.1) – Methodology.

The challenge is to incorporate these new attributes outlined above into the pre-existing FLEXSTREM. This would involve creation of new modules that model time dependent relationships between the structural, environmental and operation components which would produce a Poisson structural response. This Poisson structural response is then fed into a fatigue prediction model – the Paris-Erdogan crack growth model. The Paris-Erdogan crack growth model replaces the LEFM crack length estimation models already present in the FLEXSTREM. The final algorithm is essentially a time dependent (stochastic) version of FLEXSTREM, shortened to STOFLEX. The STOFLEX algorithm is also implemented in FORTRAN.

The new modules have only the following differences from the original FLEXSTREM:

- Replacement of  $NSIM$  (the total number of Monte Carlo simulations (MCS)) with  $N_{TL}$  (the total life of the structure).
- Introduction of an “unloaded” state during specific iteration intervals.

- Replacement of the existing crack/defect length estimation model with a crack/defect growth (Paris-Erdogan model).

The FLEXSTREM still retains every other mechanism, even more than the FLEXSTREM optimization (FLEXOPT). Again the partial validation of the foundational method, FLEXSTREM is sufficient for STOFLEX. Also the Paris-Erdogan model is widely accepted and has been in use since 1963.

#### 7.4 STOFLEX Overview

STOFLEX is the implementation of stochasticity (i.e. time dependency) in the loading for the existing FLEXSTREM framework. To the FLEXSTREM, there is the introduction of a stochastic initialization process S-S (between the Pre-MCS and MCS processes), the introduction of a loading and inspection interval process (S-R) at the start of the MCS process and the substitution of the LEFM crack length estimation process (in both analysis types (J and R3)) with an LEFM crack growth process (S-J and S-R3 respectively). The MCS variable  $NSIM$  is also replaced with  $N_{TL}$ , the total life of the structure (i.e. loaded + unloaded cycles). These are the only tweaks that FLEXSTREM needs for adaptation to STOFLEX. The whole of STOFLEX is based on the widely acknowledged (validated) Paris-Erdogan model. STOFLEX feeds this model with stochastic loads modelled in real time.

As with FLEXSTREM, an analysis could be either of type I or type II. A very salient point is STOFLEX's capability to cater for both new and existing structures. As most of the processes have already been introduced hitherto, only the following additions which are responsible for the adaptation from FLEXSTREM to STOFLEX would be examined in this chapter:

- Process S-S – Stochastic initialization
- Process S-R – Loading and inspection interval
- Process S-J – LEFM crack growth process (type I)
- Process S-R3 – LEFM crack growth process (type II)
- Perfect and imperfect repair
- STOFLEX for existing structures

The processes are outlined in Figure (7.2). The dash-lined capsules are the modules needed to adapt FLEXSTREM to STOFLEX. The method would be demonstrated on the crane boom case study in 3 configurations provided in chapter 6 (FLEXOPT). The configurations are:

- (1) Configuration 1 – original configuration (the original configuration of the crane boom members: mass = 75447 kg, reliability = 0.8621).
- (2) Configuration 2 – robust configuration (the most robust (most weight) of the optimization solutions from Table (6.14): mass = 70178 kg, reliability = 0.9999).
- (3) Configuration 3 – optimal configuration (the best (lowest weight and high reliability) from the optimization solutions in Table (6.14): mass = 21469.2 kg, reliability = 0.9999).



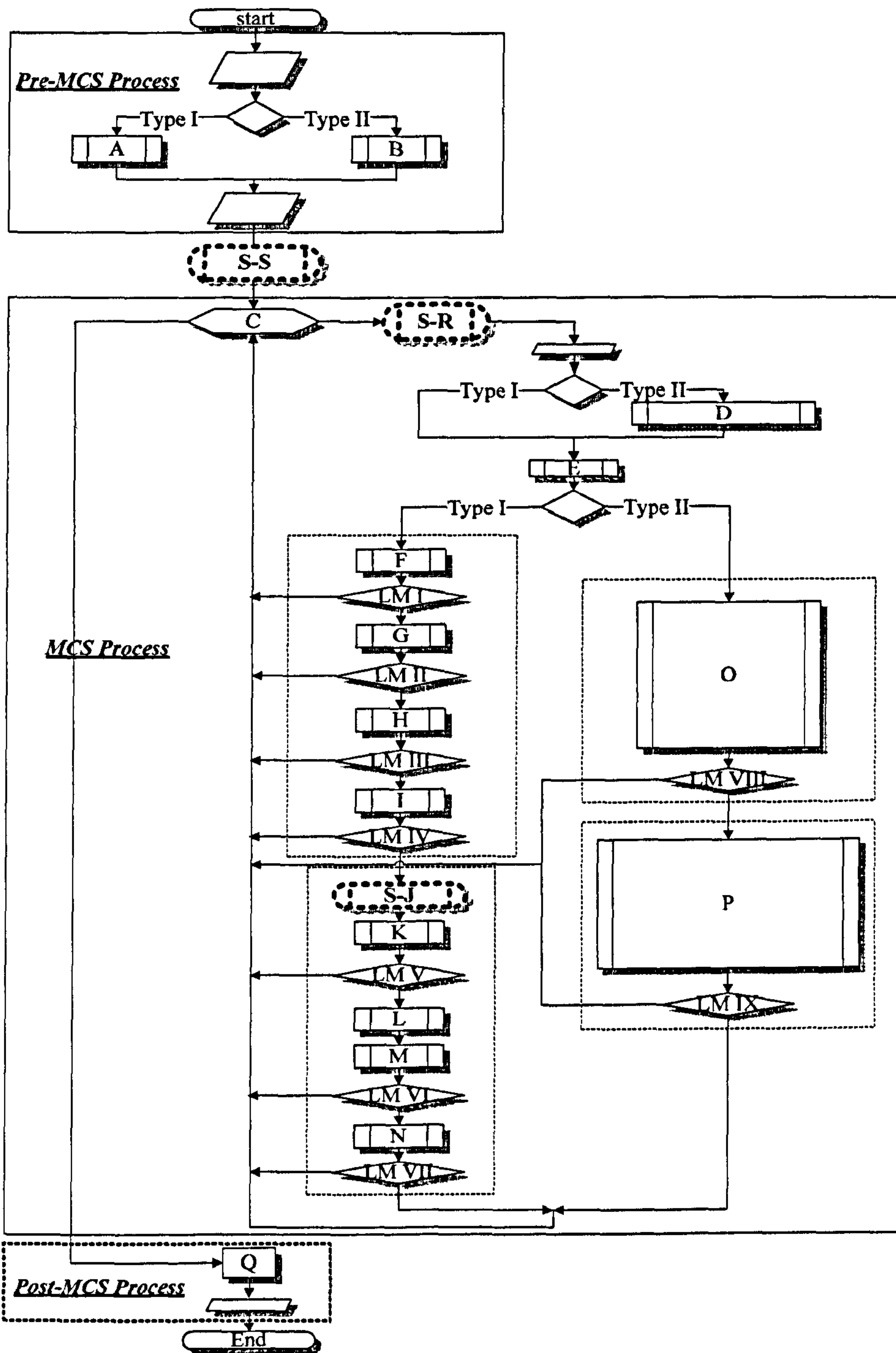


Figure (7.2) – FLEXSTREM adaptation to STOFLEX.

#### 7.4.1 Process S-S: Stochastic Initialization

There are five variables to be initialized from this process. The MCS process count,  $NSIM$  is replaced with the total life of the structure,  $N_{TL}$ . The calculation in chapter 4 shows the loading percentage per day. Therefore from the loaded and unloaded cycles which are given in cycles per year, the daily cycles need to be determined.

$$U_{cy} = N_{STU}/365 \quad (7.1)$$

$$L_{cy} = N_{STL}/365 \quad (7.2)$$

where,

$U_{cy}$  – structure's daily unloaded cycles

$L_{cy}$  – structure's daily loaded cycles

$N_{STU}$  – structure's yearly unloaded life cycles

$N_{STL}$  – structure's yearly loaded life cycles

Also the total life of the structure is obtained from the following equation:

$$N_{TL} = (N_{STU} + N_{STL}) \times N_{YRS} \quad (7.3)$$

where,

$N_{YRS}$  – number of years left/to be in service

The non-linear load pattern derived from Equations (7.1) and (7.2) is illustrated in Figure (7.3).

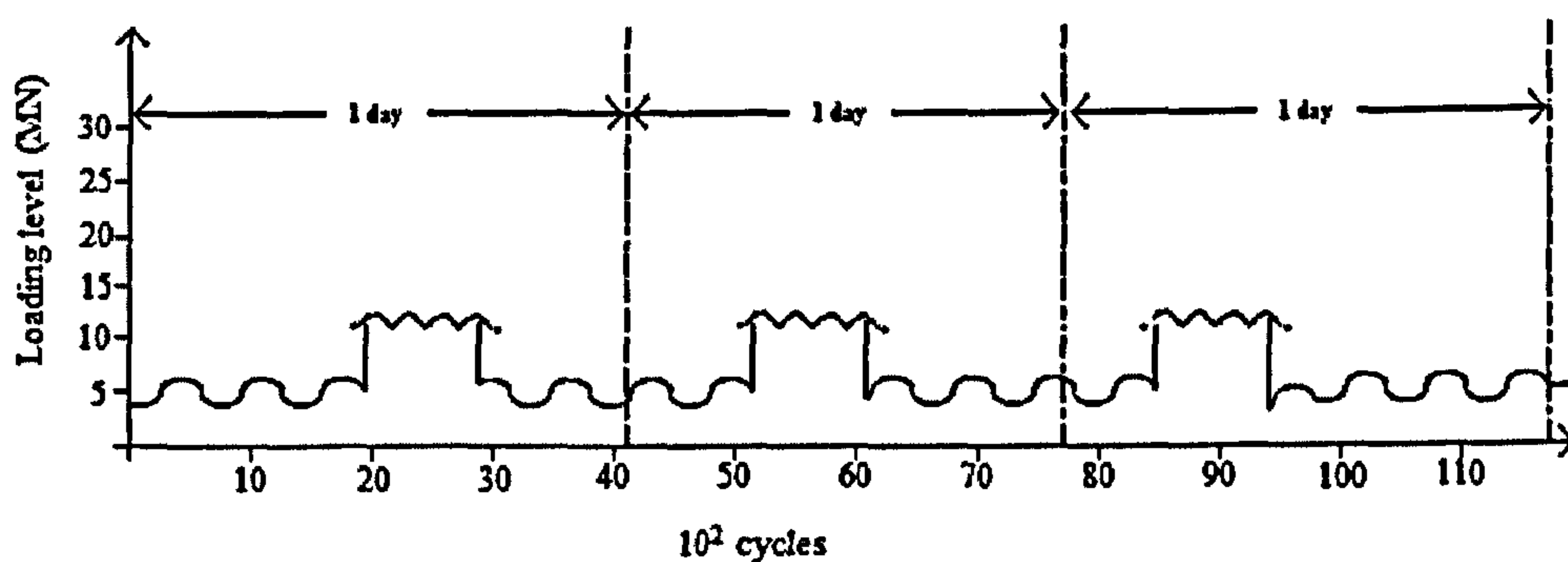


Figure (7.3) – STOFLEX daily loading pattern.

Figure (7.3) (not drawn to scale) depicts the levels of loading experienced every day as a Poisson loading process. The regular sinusoids represent the environmental and dead loads inherent whilst the heightened sinusoids represent the live loading on the structure.

This is a common loading pattern for several structures. The pattern could be altered for special cases where the norm becomes the exception.

Finally, a generic inspection period of twice per annum is chosen for the model. The inspections are at equally spaced intervals  $INS_1$  and  $INS_2$  by the following equations:

$$INS_1 = (N_{STU} + N_{STL})/2 \quad (7.4)$$

$$INS_2 = (N_{STU} + N_{STL}) \quad (7.5)$$

where,

$INS_1$  – first inspection period (cycles)

$INS_2$  – second inspection period (cycles)

These are the parameters required for the stochastic analysis. Process S-R checks the MCS count (cycle by cycle). Depending on the cycle, loading on the structure occurs. Repair and maintenance also depends on this MCS count value.

#### 7.4.2 Process S-J and SR3: LEFM Crack Growth Process

On the first run of STOFLEX, data is entered indicating whether the scenario is that of a perfect repair (PR) or not. This happens only at the start of the STOFLEX. Next, the algorithm determines whether there is an inspection/repair to be made. For an inspection cycle, the inspection counter records a value indicating that an inspection interval has occurred including its numeric order. The algorithm then holds the Boolean value of the inspection status.

Next, the algorithm carries out the following for all joints (nodes) in a type II (MMS) analysis (by looping), or for a single joint under a type I (SMS) analysis (no looping). The use of the dotted line on the loop initiator in Figure (7.4) illustrates this option.

- For the first run of the STOFLEX, the algorithm initializes the critical crack length value from the system definition parameters supplied (chapter 4).
- For subsequent runs, the crack is grown via the Paris-Erdogan crack growth model (Equations (7.6-7.8)).
- Next, if there are repairs to be carried out during an inspection interval, the repair module is run (perfectly or imperfectly depending on the scenario) (see section (7.4.3)).

- The results from these processes are then recorded.

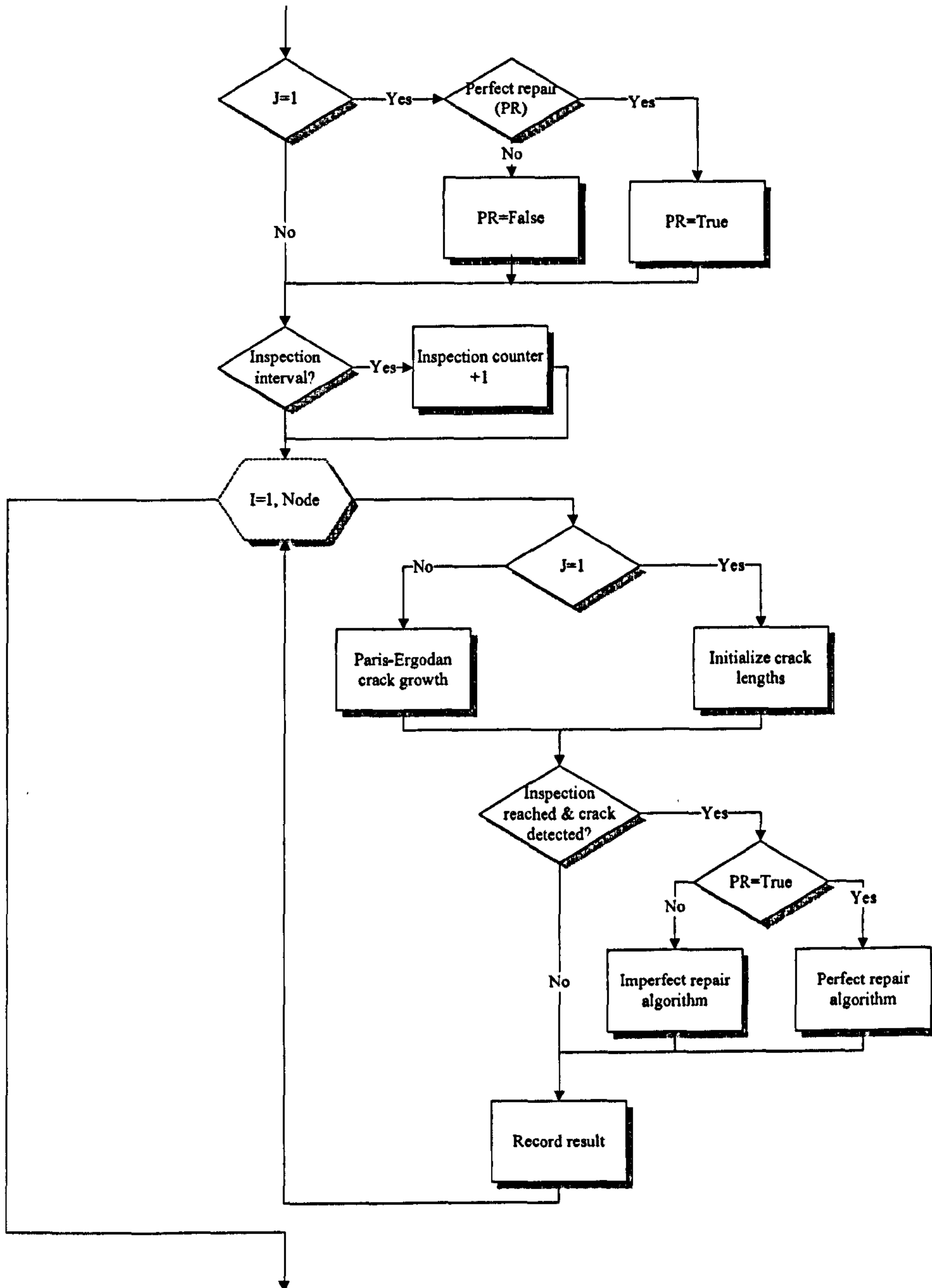


Figure (7.4) – Crack growth/propagation algorithm.

A vital module of the STOFLEX analysis is the crack propagation algorithm. The algorithm is shown in Figure (7.4). The crack propagation is modelled from the well known Paris-Erdogan relationship given as (Paris and Erdogan (1963)):

$$\frac{da}{dN_{TL}} = mat_c (\Delta K_I)^{mat_m} \quad (7.6)$$

$$da = dN_{TL} \times [mat_c (\Delta K_I)^{mat_m}] \quad (7.7)$$

$$a_f = a_{(f-1)} + da \quad (7.8)$$

where,

$da$  – instantaneous crack growth (m)

$dN_{TL}$  – instantaneous life cycle

$a_f$  – (instantaneous) crack length (m)

$a_{(f-1)}$  – previous crack length (m)

Processes S-J and S-R3 are similar; the only difference being that S-R3 is node/joint specific.

### 7.4.3 Perfect and Imperfect Repair

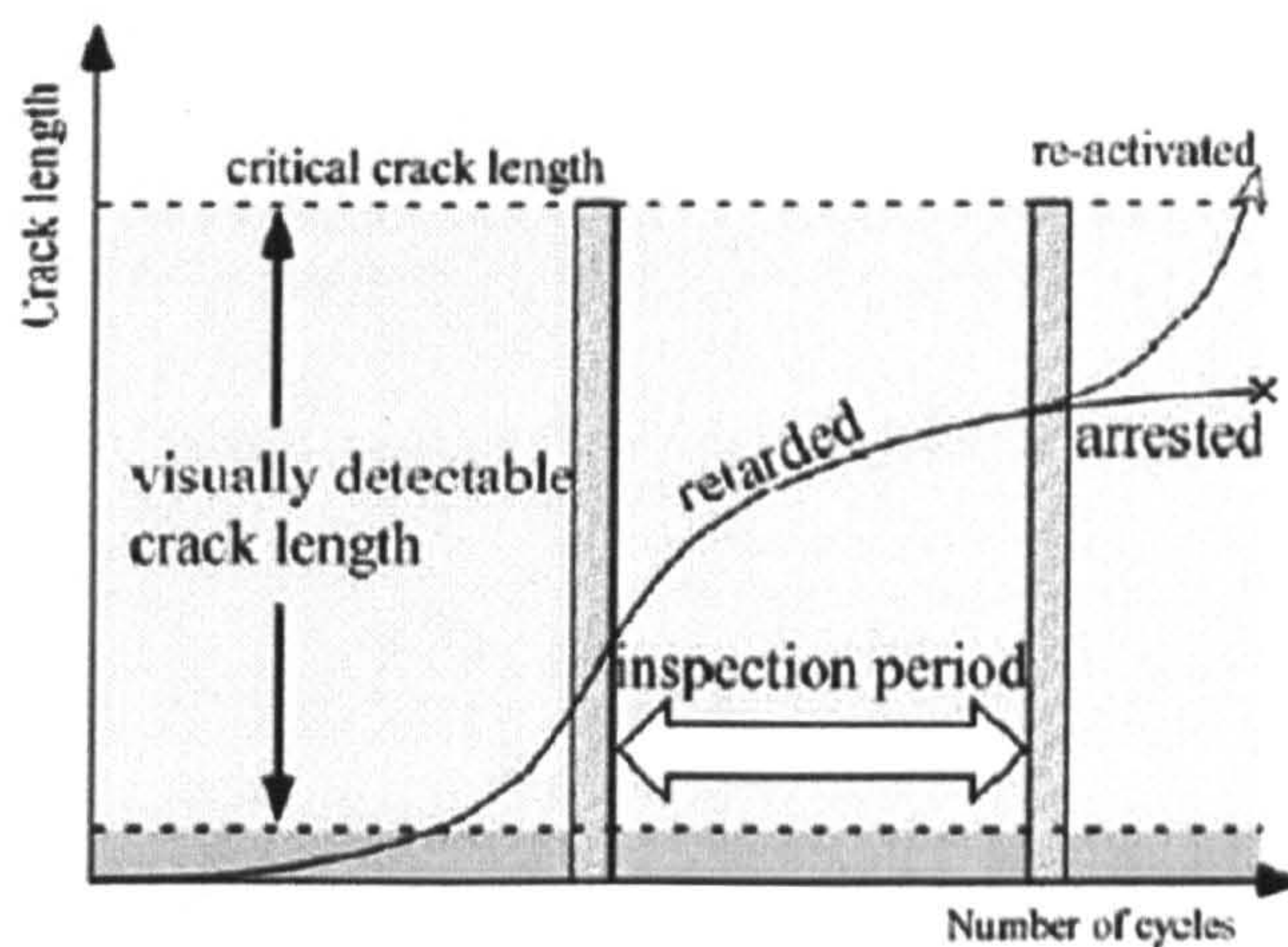


Figure (7.5) – Proposed concept of fatigue crack management in a welded structure (Okawa and Sumi (2008)).

The repair criterion used in the STOFLEX is based on a detectable defect length during the inspection interval. Figure (7.5) is a concept of the effects of repair operations on

crack propagation. The repair is implemented during the maintenance (inspection) intervals. In the case of perfect repair, the propagated crack length at a joint is completely repaired (i.e. the joint reverted to its original status (100%)) while for the case of imperfect repair the crack length is only repaired to a certain degree but not completely (i.e. the joint is worse off compared to its original status (< 100%)). Notwithstanding, deterioration effects still take place at all the structure's nodes and is specified as a percentage (0-100%) within STOFLEX.

#### ***7.4.4 STOFLEX for existing structures***

New structures could be analysed as well as existing structures. The only data required for analysis of existing structures is the remaining number of years in use in place of the total (which is specified for new structures) outlined in chapter 4. With this, the loaded and unloaded life cycles and loading and inspections intervals could be determined. These are then input as required in processes S-S, S-R and S-J (S-R3).

## 7.5 Results/Discussion

The STOFLEX would be demonstrated on the crane boom case study in 3 configurations provided in chapter 6 for fatigue, inspection and maintenance purposes in a perfect repair scenario. The configurations are:

- (1) Configuration 1 – original configuration (the original configuration of the crane boom members: mass = 75447 kg, reliability = 0.8621).
- (2) Configuration 2 – robust configuration (the most robust (most weight) of the optimization solutions from Table (6.14): mass = 64799 kg, reliability = 0.09999).
- (3) Configuration 3 – optimal configuration (the best (lowest weight and high reliability) from the optimization solutions in Table (6.14): mass = 14317.7 kg, reliability = 0.09999).

The most loaded node (node 120) is selected for analyses in all 3 cases. For these 3 cases, 3 types of analyses are carried out; they are:

- Crack propagation analysis
- Stress intensity factor analysis
- Inspection and maintenance scheduling.

### 7.5.1 Crack Propagation

The crack propagation analysis is a test to determine the durability of a joint/node in a given structure. The analysis entails recording the increase in crack/defect in a joint under Poisson loading. The test is run to failure. To do this, the inspection/repair module is disabled in the STOFLEX.

The crack propagation analysis is carried out for the three configurations. The node focused on in the analysis (as mentioned earlier) is node 120. This node is the comparative basis for all three crane configurations.

Based on the crack growth rate, three phases have been selected. The phases were selected based on significant changes in the rate of crack propagation. For the crack growth analyses for each configuration, a graph showing all phases is presented

(Figures (7.6-7.8)). For these graphs, the length of each phase and the corresponding crack length are importantly noted. Finally the cycle range at which failure occurs is noted. Table (7.1) shows these values:

	Configuration 1	Configuration 2	Configuration 3
Phase I	0 – 360000 cycles	0 – $11.09 \times 10^6$ cycles	0 – $5.86 \times 10^6$ cycles
Crack length (m)	0.0005 – 0.001	0.0005 – 0.001	0.0005 – 0.001
Phase II	$360000 - 1.02 \times 10^6$ cycles	$11.09 \times 10^6 - 31.1 \times 10^6$ cycles	$5.86 \times 10^6 - 16.73 \times 10^6$ cycles
Crack length (m)	0.001 – 0.01	0.001 – 0.01	0.001 – 0.01
Phase III	$1.02 \times 10^6 - 1.05 \times 10^6$ cycles	$31.1 \times 10^6 - 32.15 \times 10^6$ cycles	$16.73 \times 10^6 - 17.53 \times 10^6$ cycles
Crack length (m)	0.01 – 0.014	0.01 – 0.02	0.01 – 0.025
Failure cycle	$1.05 \times 10^6$ cycles	$32.15 \times 10^6$ cycles	$17.53 \times 10^6$ cycles

Table (7.1) – Crack propagation data for the 3 crane configurations.

For the individual phase plots (see appendix A.4), the slope (rate of change of crack propagation) in addition to the phase length and crack length, is noted. It should be noted that the first stage of crack propagation which is the crack opening/initiation phase has been ignored in this (and subsequent) analyses according to (Meng et al (2000)). Also, the cracks in the analyses may grow past certain lengths at which the node/joint would definitely have failed; however the point is to show the critical crack lengths at which fast fracture would occur.

### 7.5.1.1 Crane Configuration 1

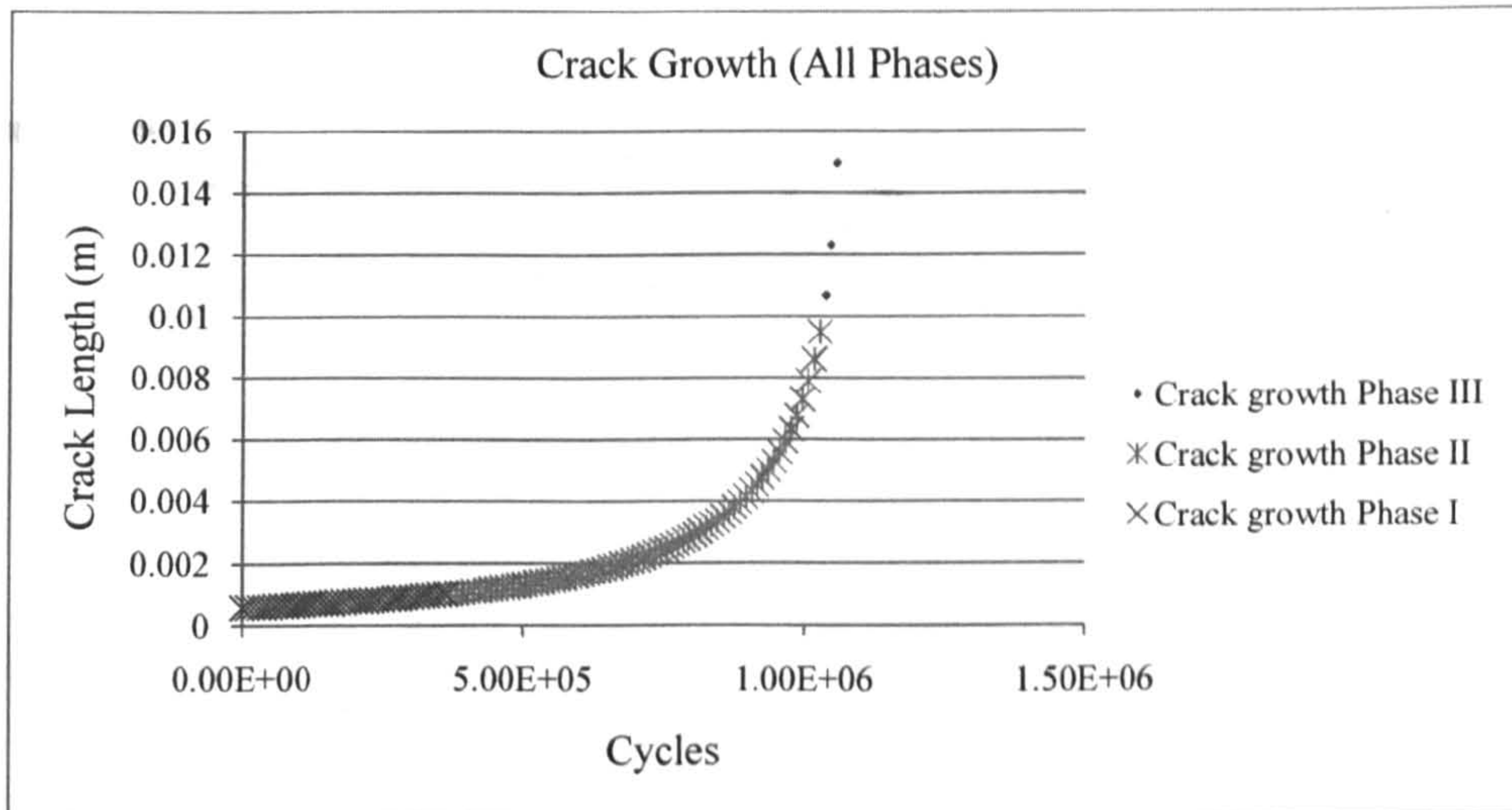


Figure (7.6) – Crack propagation (all phases).



For crane configuration 1 crack growth (propagation) (Figure (7.6)), the life of the joint/node before the fast fracture (failure) is estimated at about 1.05 million cycles. As mentioned earlier, the phases are demarcated based on the significant changes in rate of crack propagation. From about 0 – 360000 cycles, the lowest rate of crack propagation can be observed. In this phase, a crack length of 0.5 mm grows to 1 mm.

The next phase covers about 650000 cycles, ranging from approximately 360000 – 1.02 million cycles. This is the longest phase for this configuration. The crack grows from 1 mm to 10 mm.

Phase III, the failure phase, earmarks the beginning of the failure of the joint/node. It ranges from about 1.02 million cycles to 1.05 million cycles. Within this relatively short period, the crack grows from about 10 mm to 14 mm. The rate of crack propagation is at its highest here. The graphs of the individual phases are presented in appendix A.6.

#### 7.5.1.2 Crane Configuration 2

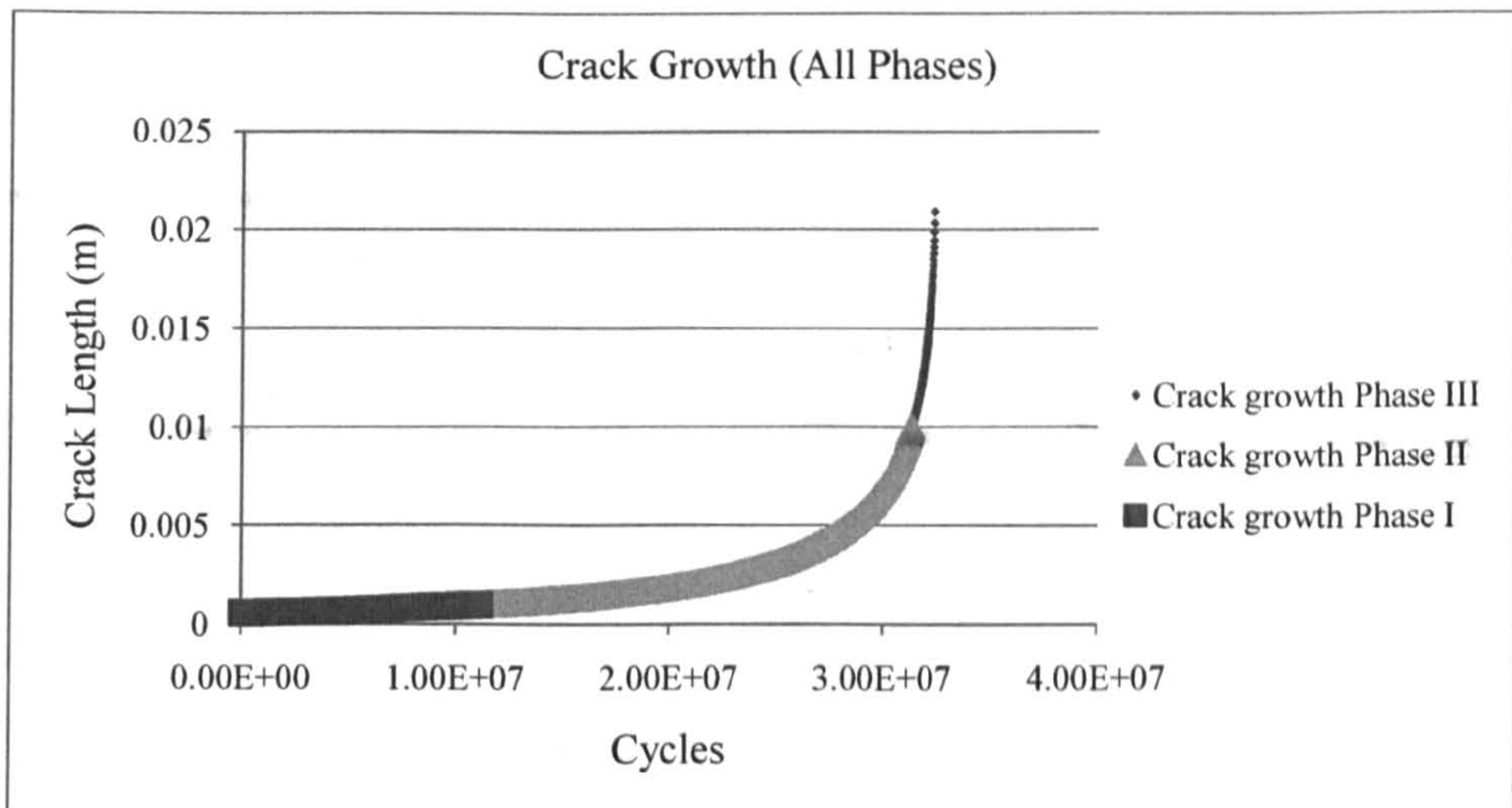


Figure (7.7) – Crack propagation (all phases)

For crane configuration 2 (Figure (7.7)), the life of the joint before fast fracture is estimated to be about 32.5 million cycles (roughly 30 times that of configuration 1). Phase I of the crack propagation for this configuration ranges from about 0 – 11 million cycles. In this phase, a node defect/crack of 0.5 mm grows to 1 mm.

The next phase ranges from about 11 million cycles – 31 million cycles. This is the longest phase in the crack propagation analysis. Here the crack grows from about 1 mm to 10 mm.

Phase III, the final phase, ranges from about 31 million cycles to 32.5 million cycles. This is the shortest phase for this configuration. Within these final cycles, the crack length grows from 10 mm to about 20 mm. The graphs of the individual phases are presented in appendix A.6.

### 7.5.1.3 Crane Configuration 3 (Optimal Configuration)

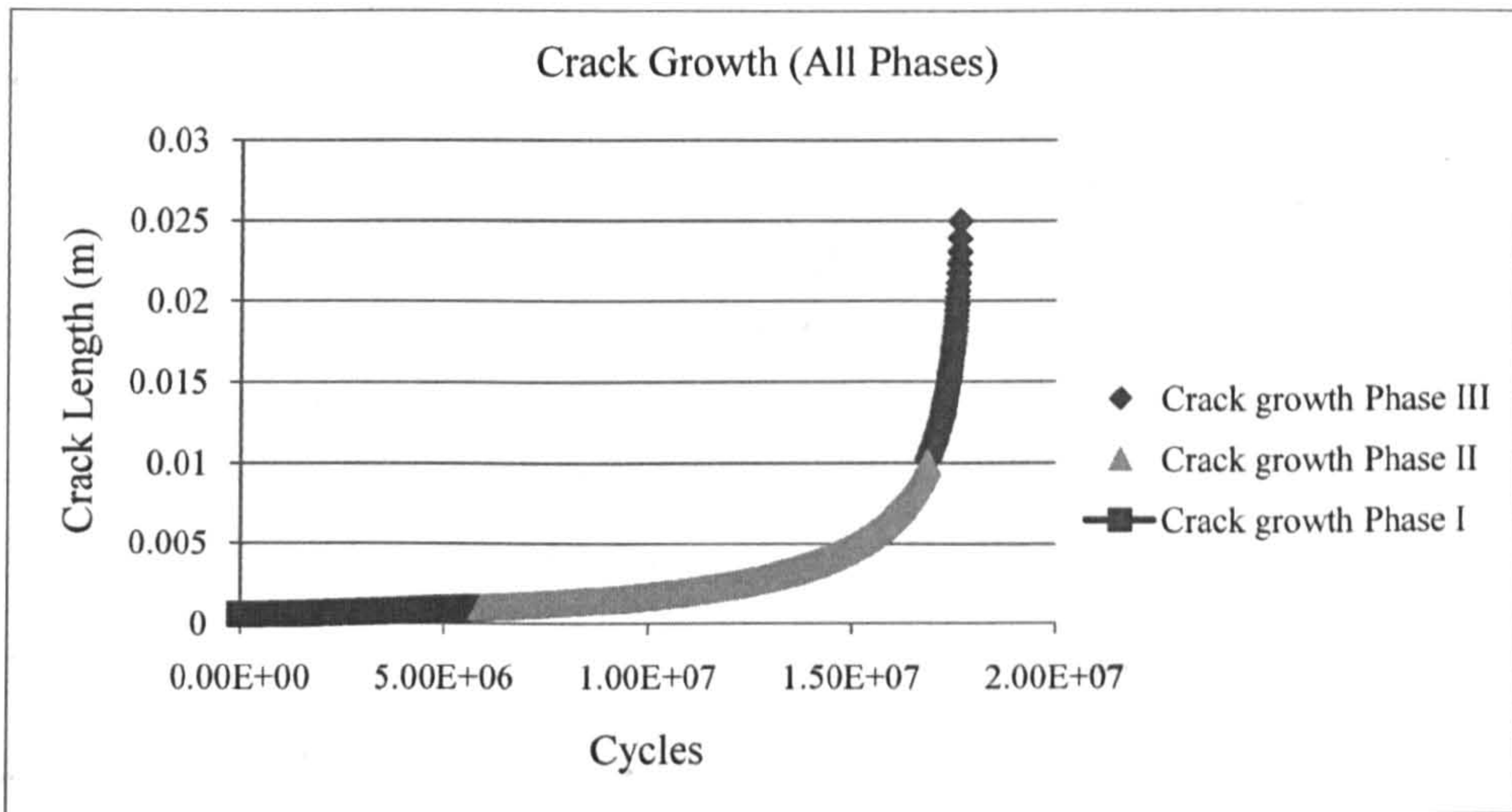


Figure (7.8) – Crack propagation (all phases).

For crane configuration 3 (Figure (7.8)), the estimated life before fast fracture (fatigue failure) is about 17.5 million cycles (about 17 times that of configuration 1). Phase 1 occurs at about 0 – 6 million cycles. In this phase a node defect/crack grows from about 0.5 mm to about 1 mm. The rate of crack growth is at its lowest in this phase.

Phase II ranges from approximately 6 million cycles – 17 million cycles. This is the longest phase for this configuration. In this phase the crack length grows a further 9 mm to approximately 10 mm.

The next (the final phase) ranges from about 17 million cycles to about 17.5 million cycles. Here, the crack grows from about 10 mm to approximately 100 mm. The graphs of the individual phases are also presented in appendix A.6.

### 7.5.2 Stress Intensity Factor Analysis

A fatigue crack propagation rate ( $da/dN$ ) vs. the stress-intensity factor ( $\Delta K_I$ ) graph is plotted. It is important to note the range of the stress intensity factor and the crack growth rate. The linear region (region II) of the generic  $da/dN$ -  $\Delta K_I$  curve (Figure (2.2)) has been modelled in the STOFLEX (Equation (7.6)) and is thus represented in the plotted graphs (Figures (7.9 – 7.11)).

For configuration 1 (Figure (7.9)), the crack propagates fastest. From the data plot, it could be seen (by the relatively few marks) joint records comparatively very little activity in its operational life. The endurance of the joint becomes minimal as it quickly approaches the higher  $\Delta K_I$  regions (which are indicative of the higher crack propagation rates). On reaching higher values of the stress intensity factor, a “fizzling out” of the data point starts to occur as the material experiences fast fracture.

In crane configuration 2 (Figure (7.10)), the crack propagation is minimal. Here the most parts of the stress intensity factor amplitudes on the joint/node are well spread in the tolerable regions of  $\Delta K_I$ . This is indicative of the low crack propagation rate which enables the joint to be in operation for comparatively longer periods without reaching the critical stress intensity factor range.

In crane configuration 3 (Figure (7.11)), most of the stress intensity factor amplitudes also occur in the tolerable  $\Delta K_I$  region where the crack propagation is relatively low. The rate of this propagation begins to increase as a result of the increase in the stress intensity factor. The joint in this configuration could also be said to have good fatigue resistance during its operational life.

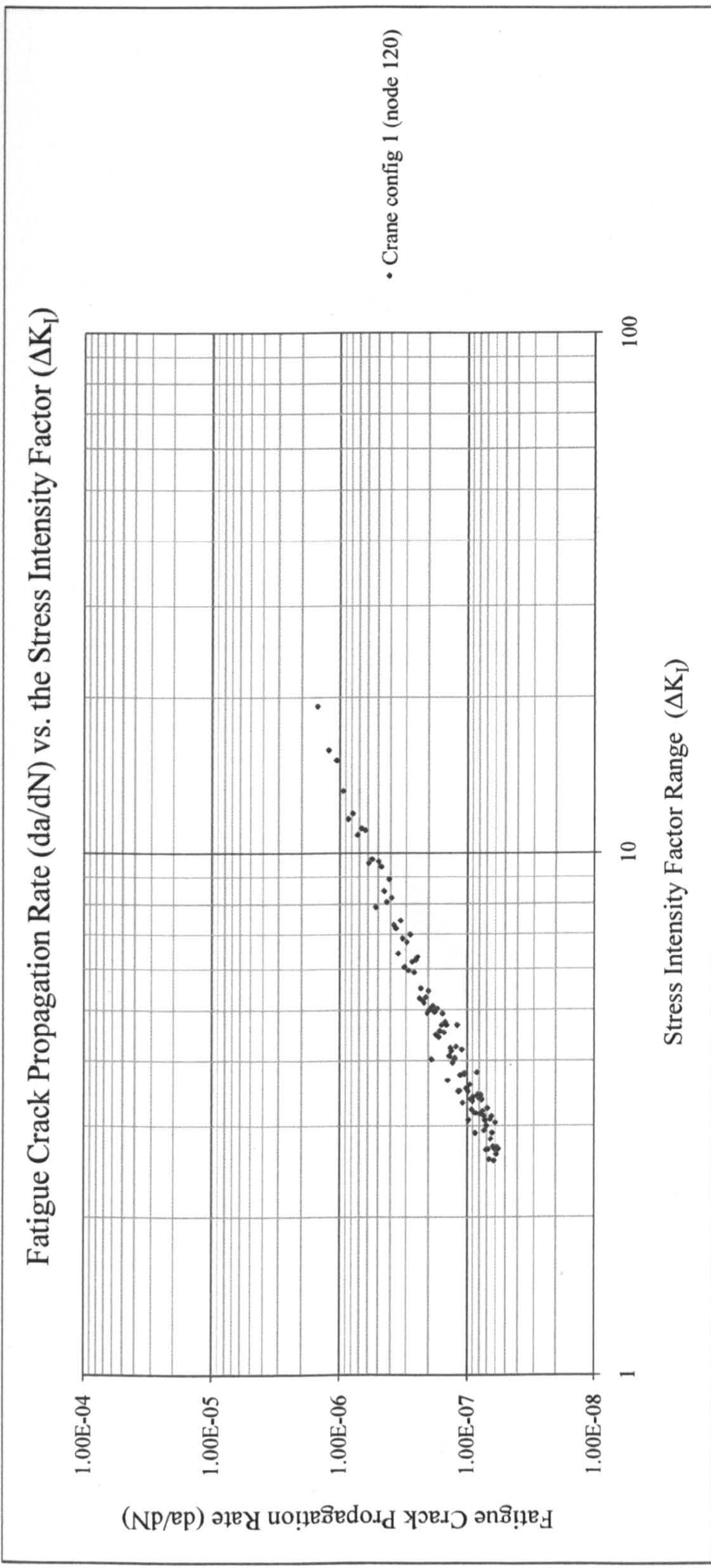


Figure (7.9) – Fatigue crack propagation rate (da/dN) vs. the stress intensity factor (ΔK<sub>I</sub>) (crane configuration 1).

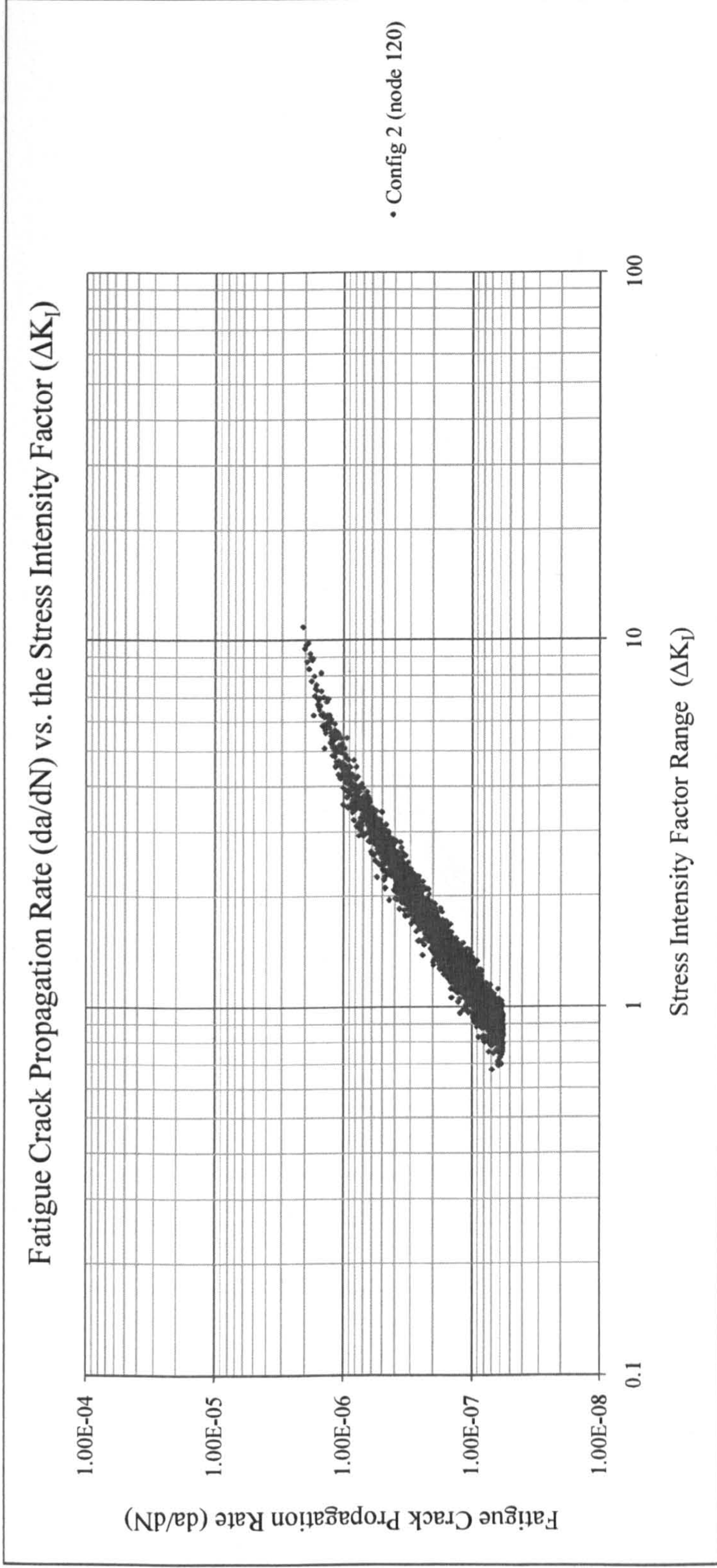


Figure (7.10) – Fatigue crack propagation rate (da/dN) vs. the stress intensity factor ( $\Delta K_I$ ) (crane configuration 2).

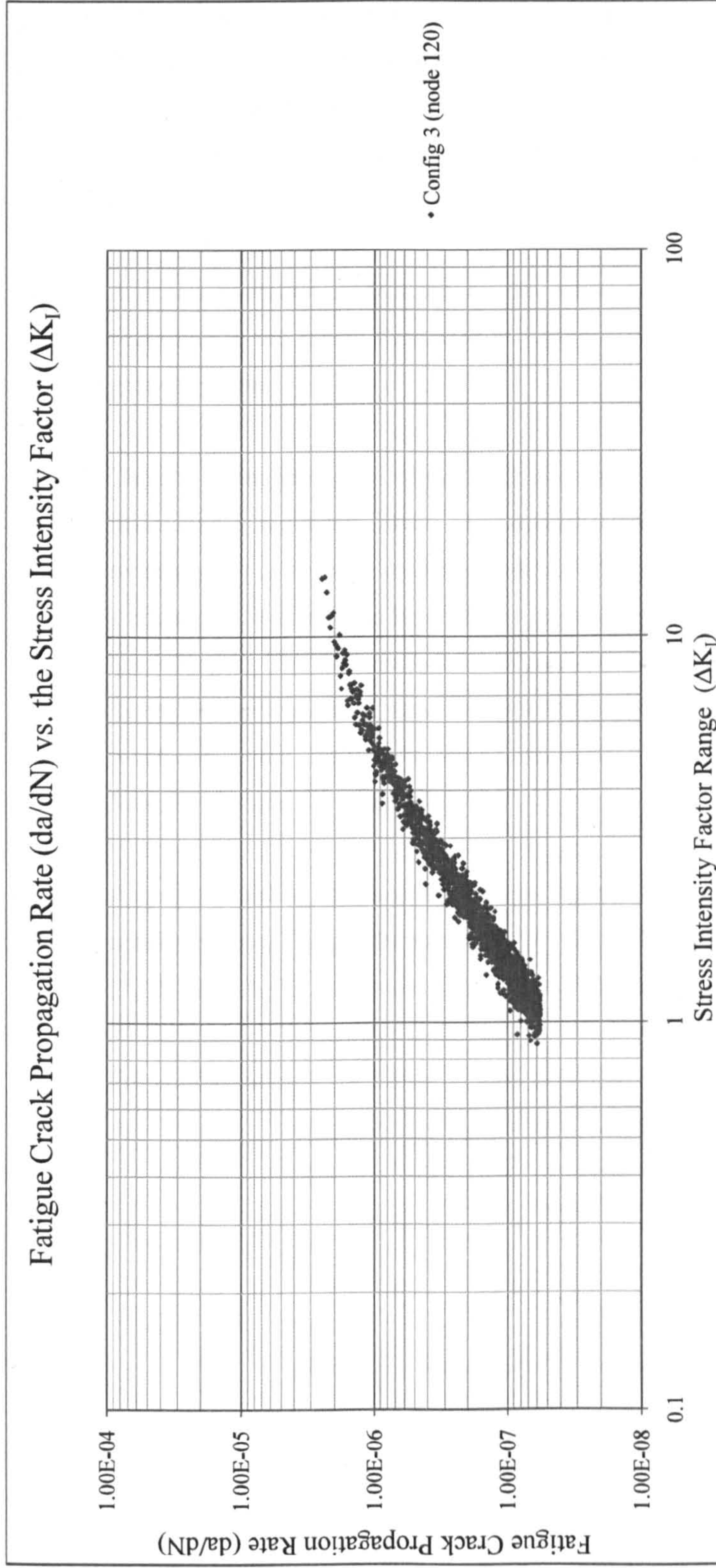


Figure (7.11) – Fatigue crack propagation rate (da/dN) vs. the stress intensity factor ( $\Delta K_I$ ) (crane configuration 3 (optimal configuration)).

### 7.5.3 Inspection and Maintenance Scheduling

Inspection takes place in the structure when the cycles (totalling  $N_{TL}$ ) reach the inspection intervals ( $INS1$  or  $INS2$ ) in process S-S. On reaching the inspection intervals, repairs are carried out if the existing crack has grown up to or beyond the detectable crack length.

A repair operation is depicted by the retardation of the crack growth in the graph according to the model illustrated in Figure (7.5). After the repair operation the crack growth resumes.

The aim of the prediction of the crack growth is to aid the scheduling of inspection and maintenance regimes. These maintenance regimes could be set prescriptively (e.g. twice a year) or by some criterion such as the ratio of a predicted crack length present in a node/joint. It could also be set based on the length of an existing crack (e.g. detectable crack length). The maintenance is critical to the cost and the safety of the structure and therefore any scheduling must be done with respect to the cost and safety. Following a twice-per-annum inspection regime and detectable crack length repair criteria the following graphs are presented.

A graph depicting maintenance scheduling and monitoring is plotted for the 3 crane configurations. The graphs are similar to the crack propagation analysis graphs (Figures (7.12 – 7.14)). For this analysis, the inspection module on STOFLEX is re-enabled.

For configuration 1, the following occurred (Table (7.2)):

Node/Joint	No of repairs
120	50
118	30
109	8
115	1
116	1
	Total 90

Table (7.2) – Repair operations for crane configuration 1.

This information is plotted in Figure (7.12) (for repairs on node 120 only). There was a lot of downtime following the complete failure of some nodes/joints before the inspection intervals.

For configuration 2, the following occurred (Table (7.3)):

Node/Joint	No of repairs
120	6
91	9
92	1
118	1
	Total 17

Table (7.3) – Repair operations for crane configuration 2.

No downtime occurred for this crane configuration. The data is plotted (for repairs on node 120 only) in Figure (7.13).

For configuration 3, the following occurred (Table (7.4)):

Node/Joint	No of repairs
120	13
91	4
118	1
	Total 18

Table (7.4) – Repair operations for crane configuration 3.

No downtime occurred for this configuration. The data is plotted (for repairs on node 120 only) in Figure (7.14).



Crane Configuration 1 (Perfect Repair Scenario)

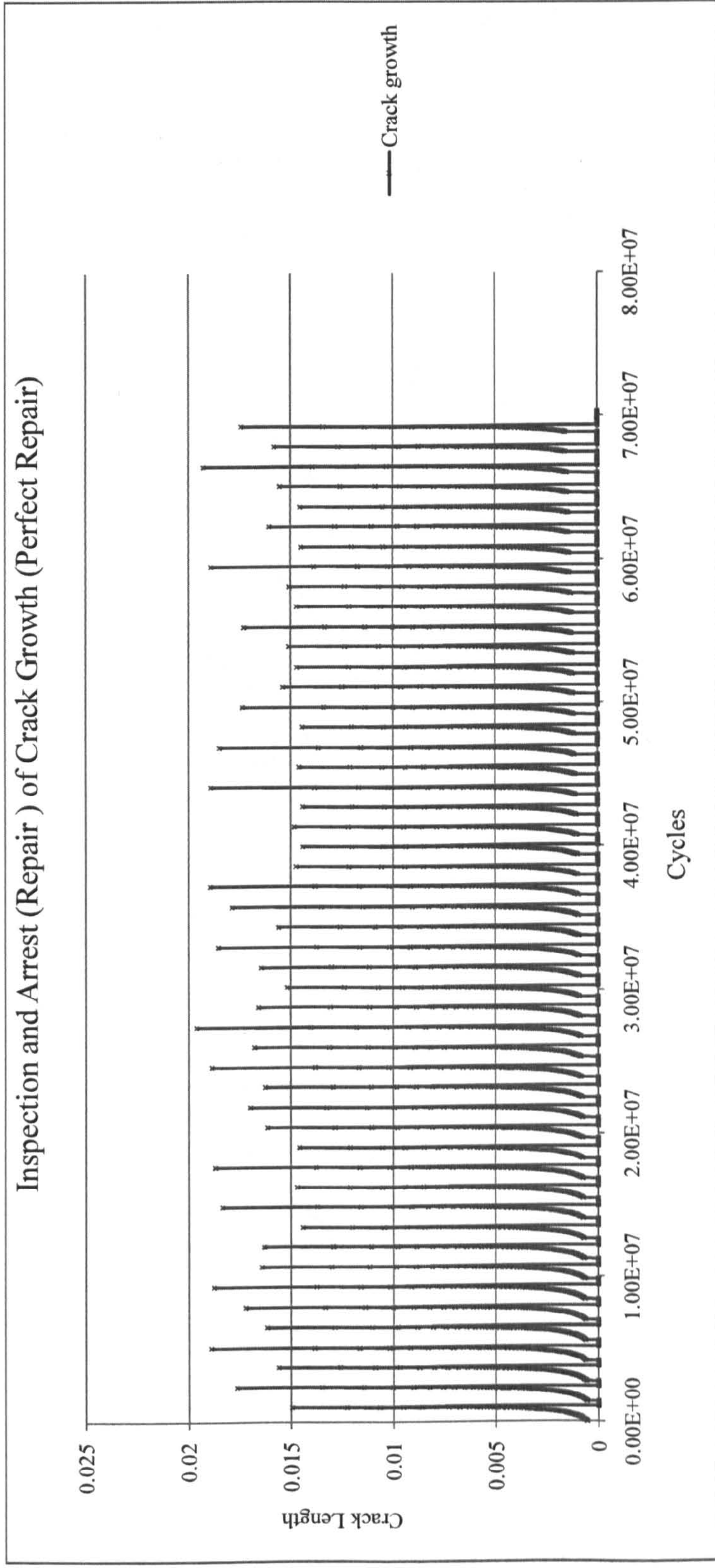


Figure (7.12) – Inspection and perfect repair scenario.

Crane Configuration 2 (Perfect Repair Scenario) (No Failure)

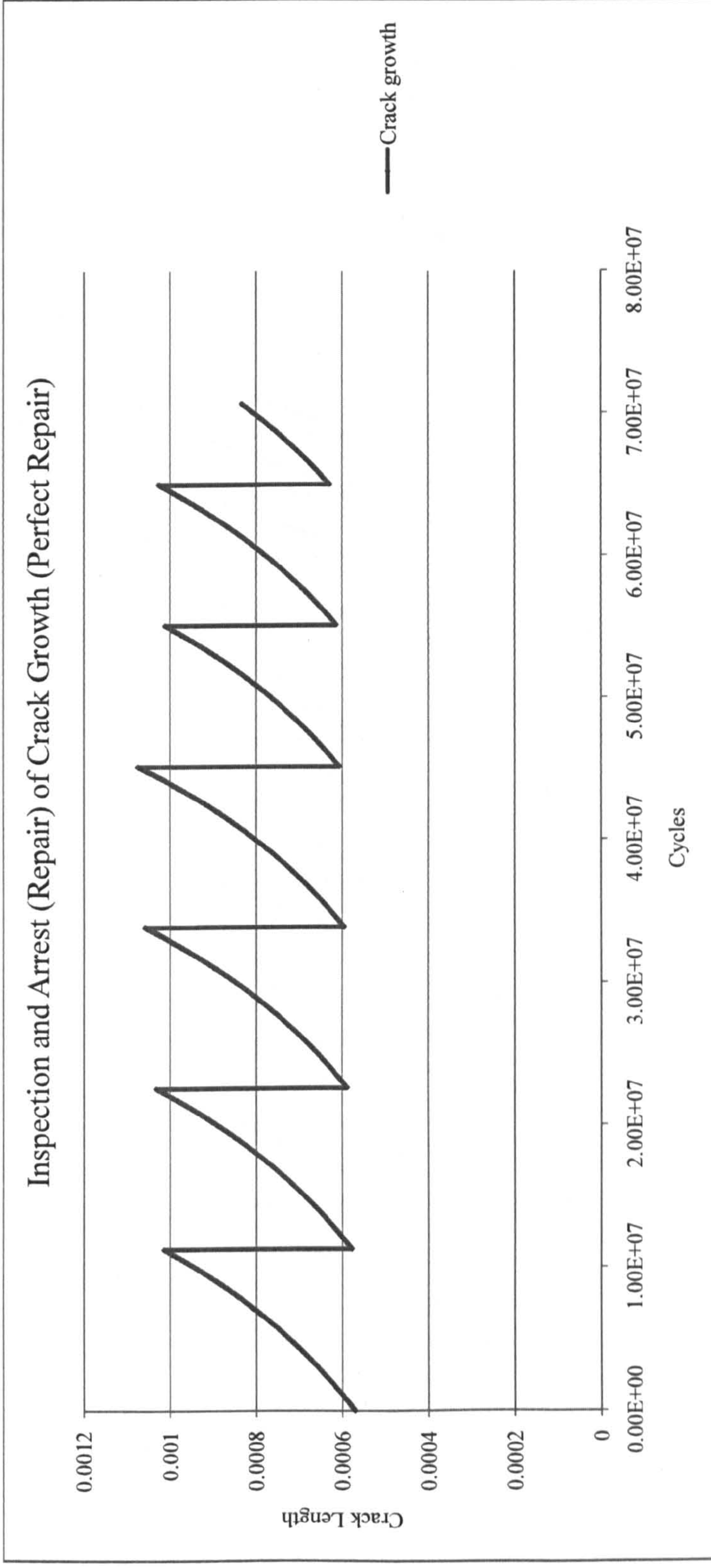


Figure (7.13) – Inspection and perfect repair scenario.

Crane Configuration 3 (Optimal Configuration) (No Failure)

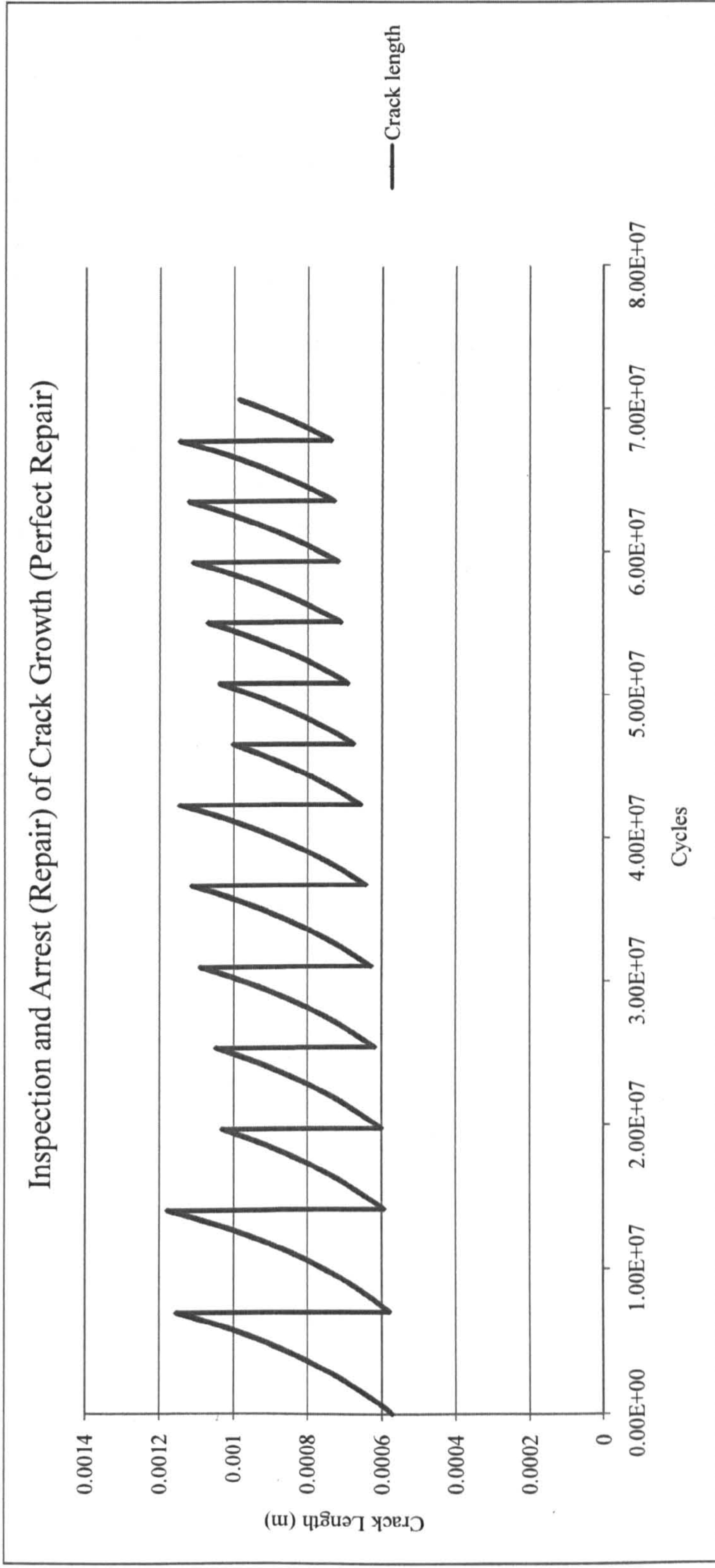


Figure (7.14) – Inspection and repair (none) scenario.

## **7.6 Conclusion**

A method to aid in the scheduling of maintenance and repair activities (thereby maintaining structural integrity and reducing risk while making optimal use of resources) was developed. New modules were developed and integrated into the validated FLEXSTREM to produce the STOFLEX.

The STOFLEX produced results which were broken down for further analyses. The case of the abstracted offshore crane boom was presented for analyses. 3 separate analyses were performed for 3 configurations of the crane boom.

The first analysis was the crack propagation analysis. In this analysis, the structure was loaded until it failed (without repair operations). It was found that the configuration 1 was the least durable while the configuration 2 was the most durable. Configuration 3 was also significantly durable.

The second analysis was a damage tolerance test. In this analysis, it was found that the most damage tolerant configuration was configuration 2 while the least damage tolerant was configuration 1. Crane configuration 3 had a high level of damage tolerance.

In the last analysis (the inspection and maintenance scheduling), it was found that configuration 1, as expected (from previous analysis), had the worst structural performance with several repairs, failures and a lot of downtime while configuration 2 had the best performance with the least repairs, no failures and zero downtime. Configuration 3 had a very good performance with no downtime, little repairs and no failures.

Overall, with respect to cost and safety, crane configuration 3 would be recommended as the best design as it possesses a high level of safety, while costing relatively less in design and operations.

## Chapter 8: Discussion and Conclusion

### Summary

*A summary of the research is presented. The contributions of the research to the risk-based design of structures are also stated. Finally, the limitations and the scope for further research are presented.*

### 8.1 Introduction

A review of the contributions to research aimed at reducing the overall risks posed to structure within the marine/offshore environments has been presented. From the literature review chapter, the need to provide an overarching framework that includes specialist solution to design and maintenance in a “root-to-fruit” fashion was identified. This research was carried out with the aim of providing a platform for such a solution.

### 8.2 Findings

During the course of this research, a number of achievements with regards to the main aim were recorded. These are as follows:

- A formal safety assessment (FSA) framework for the design maintenance and inspection for marine and offshore structures was sufficiently developed. This framework is outlined in chapter 1 (Figure (1.1)). Within this framework, three novel specialist techniques were proposed.
- The first of these techniques was the quantification of the risk associated with marine/offshore structures. Following the description of the offshore scenario (system definition) via models, present uncertainties (randomness) were taken in to consideration using the Monte Carlo simulation. The structure was then

subjected to survival tests by the use of limit state modelling. This quantification method was first tested for the case of a single member structure (SMS) (chapter 3) and was later developed and adapted for use on a multi-member structure (MMS) (chapter 5).

- The second of the specialized techniques is the optimization method (as a risk control option (RCO)/cost benefit analyses (CBA)) presented in chapter 6. The method offered a means to obtain better structural configurations that provide a good level of structural integrity while maintaining an optimal cost value.
- The final method introduced was aimed at providing a guideline for the inspection and maintenance activities to be carried out on marine/offshore structures (also as an RCO/CBA). Using time dependent loading and the Paris crack growth model, the life of a structure subjected to a given number of inspections were simulated. The results obtained from such an analysis ought to provide a means for scheduling the inspection and maintenance of a marine/offshore structure so as to maintain its integrity while carrying out cost effective maintenance practices.

### **8.3 Research Contribution**

An overarching framework (modified FSA) for the design of offshore structures in the proposed manner has been developed. Having identified fatigue as a major hazard of structural events and having defined considerably the system parameters involved with fatigue, this research has utilized specialist knowledge in implementing the steps outlined by the framework. The risk quantification/reliability estimation of structures has been demonstrated. The optimization of structural configurations (as a risk reduction/cost benefit measure) has also been demonstrated. Such optimization could also be extended to include cost-wise adaptation to existing structures. Finally the stochastic (time dependency) implementation has provided a framework by which the lives of existing structures could be extended (also as a risk reduction/ cost benefit measure) as well as maintenance and inspection scheduled in a manner that ensures that the structure's integrity is not compromised.

#### **8.4 Limitations and Future Work**

The foundational method could be improved with the incorporation of other processes such as corrosion (due to salinity), microbial growth (subsea structures), wave loading, etc. The wind model utilized could be replaced by recently developed methods such as computational fluid dynamics (CFD). Updating the model to accommodate other loading scenarios could also be achieved by using “frame-element” types as opposed to the truss type used. Gmsh currently serves as a loosely bound visual interface. Future considerations could involve using proper visual interfaces that would make users appreciate more of the behind-the-scenes operations. For optimization, shape and topology optimization techniques could be introduced to proffer more efficient solutions to structural design and adaptation. Currently the stress intensity correction factor (and thus the fatigue model) is limited to structures having 0.8 as the ratio of the crack length to tube thickness. The scope of the model could be further advanced with the use of the fractal finite element analysis (FFEA). More flexible inspection intervals could be incorporated to determine optimal inspection periods. Also more repair criterion, such as the crack length to critical crack length ratio, could be incorporated to provide possible cost effect maintenance solutions.

## References

Aghakouchak, A. A. and Stiemer, S. F. (2001). Fatigue Reliability Assessment of Tubular Joints of Existing Offshore Structures. *Canadian Journal of Civil Engineering*. Vol. 28, pp. 691–698.

Akin, J. E. (2005). *Finite Element Analysis with Error Estimators*. Great Britain: Elsevier Butterworth-Heinemann. ISBN: 0750667222.

Amadio, C. Moschino, D. and Fragiaco, M. (2006). *Probabilistic Analysis of a PR Steel-Concrete Composite Frame*. London: Taylor & Francis Group, ISBN 0-415-40824-5

American Bureau of Shipping (1991). *Guide for Certification of Cranes*. U.S.A: ABS.

Au, S. K., Wang, Z. H. and Lo, S. M. (2007). Compartment Fire Risk Analysis by Advanced Monte Carlo Simulation. *Engineering Structures*. Vol. 29, pp. 2381–2390.

Avena, T., Vinnem, J. E. and Wiencke, H. S. (2007). A Decision Framework for Risk Management, with Application to the Offshore Oil and Gas Industry. *Reliability Engineering and System Safety*. Vol. 92, pp. 433–448.

Ayyub, B. M. and McCuen, R. H. (2003) *Probability, Statistics and Reliability for Engineers and Scientists*. 2nd Edition, Chapman & Hall/CRC Press LLC, ISBN 1 58488 286 7.

Baker, M. J. and Descamps, B. (1999). Reliability-Based Methods in the Inspection Planning of Fixed Offshore Steel Structures. *Journal of Constructional Steel Research*. Vol. 52, pp. 117–131.

Balasubramanian, V. and Guha, B. (1999). Effect of Weld Size on Fatigue Crack Growth Behaviour of Cruciform Joints by Strain Energy Density Factor Approach. *Theoretical and Applied Fracture Mechanics*. Vol. 31, pp. 141-148.



Beck, A. T. and Melchers, R. E. (2004). On the Ensemble Crossing Rate Approach to Time Variant Reliability Analysis of Uncertain Structures. *Probabilistic Engineering Mechanics*. Vol. 19, pp. 9-19.

Belegundu, A. D. (1984). Design-Independent Calculation in FEM-Based Optimization Programs. *Computers and Structures*. Vol. 19 (4), pp. 631-633.

Boresi, A. P., Schmidt, J. A., Sidebottom, O. M. (1993). *Advanced Mechanics of Materials*. Canada: John Wiley & Sons Inc., ISBN 0-471-55157-0.

Box, G. E. P. and Muller, M. E. (1958). A Note on the Generation of Random Normal Deviates. *The Annals of Mathematical Statistics*. Vol. 29 (2), pp. 610-611.

Brandsæter, A. (2002). Risk Assessment in the Offshore Industry. *Safety Science*. Vol. 40, pp. 231-269.

Brenner, C. E. and Bucher, C. (1995). A Contribution to the SFE-Based Reliability Assessment of Nonlinear Structures under Dynamic Loading. *Probabilistic Engineering Mechanics*. Vol. 10, pp. 265-273.

British Standard (1983) BS-2573-1:1983. Rules for the Design of Cranes. Great Britain: BSI 10-1999.

Bucciarelli, L. (2002). "Engineering Mechanics for Structures", Lecture Notes Distributed in the Topic Engineering Mechanics for Structures. Massachusetts Institute of Technology, Department of Civil and Environmental Engineering.

Camp, C. (2006). "Development of Truss Elements", Lecture Notes Distributed in the Topic Civil 7117 - Finite Element Methods in Structural Mechanics. University of Memphis, Department of Civil Engineering on 2/6/2006.

Carassale, L. and Solari, G. (2006). Monte Carlo Simulation of Wind Velocity Fields on Complex Structures. *Journal of Wind Engineering and Industrial Aerodynamics*. Vol. 94, pp. 323–339.

Cheng, J., Xiao, R. C., Xiang, H. F. and Jiang, J. J. (2003). NASAB: A Finite Element Software for the Nonlinear Aerostatic Stability Analysis of Cable-Supported Bridges. *Advances in Engineering Software*. Vol. 34, pp. 287–296.

Ching, J. and Hsu, W. C. (2008). Transforming Reliability Limit-State Constraints Into Deterministic Limit-State Constraints. *Structural Safety*. Vol. 30, pp. 11-33.

Chryssanthopoulos, M. K. and Righiniotis, T. D. (2006). Fatigue Reliability of Welded Steel Structures. *Journal of Constructional Steel Research*. Vol. 62, pp. 1199–1209.

Coello, C. A. and Christiansen, A. D. (2000). Multiobjective Optimization of Trusses Using Genetic Algorithms. *Computers and Structures*. Vol. 75, pp. 647-660.

Dean, B. V. and Marks, E. S. (1965). Optimal Design of Optimization Experiments. *Operations Research*. Vol. 13 (4), pp. 647-673.

Det Norske Veritas (2004). DNV-OS-C101. Design of Offshore Steel Structures, General (LRFD Method). Norway: DNV.

Donea, J. and Huerta, A. (2003). Finite Element Methods for Flow Problems. Great Britain: John Wiley & Sons, Ltd. ISBN: 0471496669.

Du, S., Ellingwood, B. R. and Cox, J. V. (2005). Solution Methods and Initialization Techniques in SFE Analysis of Structural Stability. *Probabilistic Engineering Mechanics*. Vol. 20, pp. 179–187.

Durstenfeld, R. (1964). Algorithm 235: Random Permutation. *Communications of the ACM*. Vol. 7 (7), pp. 420.

Elhewy, A. H., Mesbahi, E. and Pu, Y. (2006). Reliability Analysis of Structures Using Neural Network Method. *Probabilistic Engineering Mechanics*. Vol. 21, pp. 44-53.

Etube, L. S., Brennan, F. P. and Dover, W. D. (1999). Review of Empirical and Semi-Empirical Y Factor Solutions for Cracked Welded Tubular Joints. *Marine Structures*. 12, pp. 565-582.

Faber, M. H. (2000). Reliability Based Assessment of Existing Structures. *Prog. Struct. Engng Mater*. Vol. 2, pp. 247-253.

Falck, A., Skramstad, E. and Berg, M. (2000). Use of QRA for Decision Support in the Design of an Offshore Oil Production Installation. *Journal of Hazardous Materials*. Vol. 71, pp. 179–192.

Ferreira, A. J. M. (2008). *Matlab Codes for Finite Element Analysis*. New York: Springer-Verlag New York Inc. ISBN: 1402091990.

Fisher, R. A. and Yates, F. (1938). *Statistical Tables for Biological, Agricultural and Medical Research* (3rd ed.). London: Oliver & Boyd. pp. 26–27.

Floris, C. (1998). Stochastic Analysis of Load Combination. *Journal of Engineering Mechanics*. Vol. 124 (9), pp. 929-938.

Geuzaine, C. and Remacle, J. F. (2009). Gmsh: A Three-Dimensional Finite Element Mesh Generator With Built-in Pre- and Post-Processing Facilities [Online]. [Accessed 29-03-2010]. Available From: <<http://www.geuz.org/gmsh/>>.

Gil, L. and Andreu, A. (2001). Shape and Cross-Section Optimisation of a Truss Structure. *Computers and Structures*. Vol. 79, pp. 681-689.

Gray, A. W. and Melchers, R. E. (2006). Load Combination Analysis by 'Directional Simulation in the Load Space'. *Probabilistic Engineering Mechanics*. Vol. 21, pp. 159-170.

Gray, A. W. and Melchers, R. E. (2006). Modifications to the 'Directional Simulation in the Load Space' Approach to Structural Reliability Analysis. *Probabilistic Engineering Mechanics*. Vol. 21, pp. 148–158.

Grime, A. J. and Langley, R. S. (2008). Lifetime Reliability Based Design of an Offshore Vessel Mooring. *Applied Ocean Research*. Vol. 30, pp. 221-234.

Grooteman, F. (2008). A Stochastic Approach to Determine Lifetimes and Inspection Schemes for Aircraft Components. *International Journal of Fatigue*. Vol. 30, pp.138-149.

Gumbel, E. J. (1947). The Distribution of the Range. *The Annals of Mathematical Statistics*. Vol. 18 (3), pp. 384-412.

Guoliang, J., Lin, C. and Jiamei, D. (1993). Monte Carlo Finite Element Method of Structure Reliability Analysis. *Reliability Engineering and System Safety*. Vol. 40, pp. 77-83.

Gurley, K. R. (2003). "Direct Stiffness - Truss Application", Lecture Notes Distributed in the Topic Ces 4141 - Stress Analysis. University of Florida, Department of Civil and Coastal Engineering.

Hajela, P. and Lee, E. (1995). Genetic Algorithms in Truss Topological Optimization. *Solids Structures*. Vol. 32 (22), pp. 3341-3357.

Hanna, S. Y. and Karsan, D. I. (1991). Fatigue Data for Reliability-Based Offshore Platform Inspection and Repair. *Journal of Structural Engineering*. Vol. 117 (10), pp. 3168-3185.

Hill, R. (1948). A Theory of the Yielding and Plastic Flow of Anisotropic Metals. *Proceedings of the Royal Society of London. Series A, Mathematical and Physical Sciences*. Vol. 193 (1033), pp. 281-297.

Hu, S., Fang, Q., Xia, H. and Xi, Y. (2007). Formal Safety Assessment Based on Relative Risks Model in Ship Navigation. *Reliability Engineering and System Safety*. Vol. 92, pp. 369–377.

Huajian, C. and Yongchang, S. (1995). A Practical Reliability Analysis Method for Engineers. *Reliability Engineering and System Safety*. Vol. 47, pp. 93-95.

International Energy Agency (IEA), 2003. *World Energy Investment Outlook: 2003 Insights*. OECD/IEA, Paris.

Iura, M. and Iwakuma, T. (1992). Dynamic Analysis of the Planar Timoshenko Beam with Finite Displacement. *Computers and Structures*. Vol. 45 (1), pp. 173-179.

Iwakuma, T. (1990). Timoshenko Beam Theory with Extension Effect and its Stiffness Equation for Finite Rotation. *Computers and Structures*. Vol. 34 (2), pp. 239-250.

Iwakuma, T., Ikeda, K. and Nishino, F. (1996). Consistency of Straight-Beam Approximation of a Thin-Walled Circular Beam. *Computers and Structures*. Vol. 60 (1), pp. 87-93.

Iwakuma, T. (2010). Lecture Note for Structural Mechanics and Fem Programs [Online]. [Accessed 29-03-2010]. Available From: <<http://www.civil.tohoku.ac.jp/~bear/node8.html>>.

Jovanovic, A. (2003). Risk-Based Inspection and Maintenance in Power and Process Plants in Europe. *Nuclear Engineering and Design*. Vol. 226, pp. 165–182.

Kaiser, M. J. (2007). World Offshore Energy Loss Statistics. *Energy Policy*. Vol. 35 (6), 3496–3525.

Karamchandani, A., Dalane, J. I. and Bjerager, P. (1991). Systems Reliability of Offshore. Structures Including Fatigue and Extreme Wave Loading. *Marine Structures*. Vol. 4, pp. 353-379.

Kececioglu, D. (2003). *Robust Engineering Design by Reliability with Emphasis on Mechanical Components and Structural Reliability*. Pennsylvania, U.S.A: DEStech Publications, ISBN 1-932078-07-X.

Khan, F. I. and Haddara, M. (2004). A New Approach for Process Plant Inspection and Maintenance. *Process Safety Progress*. Vol. 23 (4), pp. 252-265.

Khot, N. S., Venkayya, V. B., Johnson, C. D. and Tischler, V. A. (1973). Optimization Of Fiber Reinforced Composite Structures. *Solids Structures*. Vol. 9, pp. 1225-1236.

Knuth, D. E. (1969). *The Art of Computer Programming volume 2: Seminumerical algorithms*. Reading, MA: Addison–Wesley. pp. 124–125.

Kreiner, J. H. and Putcha, C. S. (1994). A Computer Aided Technique for Shaft Design through Monte Carlo Simulation. *Computers and Structures*. Vol. 52 (2), pp. 367-371.

Kunar, R. R. and Chan, A. S. L. (1976). A Method for the Configurational Optimisation of Structures. *Computer Methods in Applied Mechanics and Engineering*. Vol. 7, pp. 331-350.

Lam, Y.C., Manickarajah, D. and Bertolini, A. (2000). Performance Characteristics of Resizing Algorithms for Thickness Optimization of Plate Structures. *Finite Elements in Analysis and Design*. Vol. 34, pp. 159-174.

Li, J. P. and Wood, A. S. (2009). An Adaptive Species Conservation Genetic Algorithm for Multimodal Optimization. *International Journal for Numerical Methods in Engineering*. Vol. 79, pp. 1633–1661.

Li, W. and Yang, L. (1994). An Effective Optimization Procedure Based on Structural Reliability. *Computers and Structures*. Vol. 52 (5), pp. 1061-1067.

Liu, N. and Tang, W. H. (2004). System Reliability Evaluation of Nonlinear Continuum Structures – A Probabilistic Fem Approach. *Finite Elements in Analysis and Design*. Vol. 40, pp. 595–610.

Lukic, M. and Cremona, C. (2001). Probabilistic Optimization of Welded Joints Maintenance vs. Fatigue and Fracture. *Reliability Engineering and System Safety*. Vol. 72, pp. 253-264.

Matsuishi, M. and Endo, T. (1968). Fatigue of Metals Subjected to Varying Stress. In: *Proceedings of the Kyushu Branch of Japan Society of Mechanical Engineering, Fukuoka, Japan (in Japanese) 1968*, pp. 37–40.

Manners, W. (1989). A First-Order Reliability Method for Certain System and Load Combination Calculations. *Structural Safety*. Vol. 6, pp.39-51.

Mao, H. and Mahadevan, S. (2000). Reliability Analysis of Creep–Fatigue Failure. *International Journal of Fatigue*. Vol. 22, pp.789-797.

Melchers, R. E. and Ahammed, M. (2004). A Fast Approximate Method for Parameter Sensitivity Estimation in Monte Carlo Structural Reliability. *Computers and Structures*. Vol. 82, pp. 55–61.

Meng, G., Li, F., Sha, L. and Zhou, Z. (2007). Prediction of Optimal Inspection Time for Structural Fatigue Life. *International Journal of Fatigue*. Vol. 29, pp. 1516–1522.

Moan, T. (2005). Reliability-Based Management of Inspection, Maintenance and Repair of Offshore Structures. *Structure and Infrastructure Engineering*. Vol. 1 (1), pp. 33 - 62.

Moan, T. and Jiao, G. (1992). Reliability-Based Fatigue and Fracture Design Criteria for Welded Offshore Structures. *Engineering Fracture Mechanics*. Vol. 41 (2), pp.271-282.

Mohammadi, S. (2008). *Extended Finite Element Method: for Fracture Analysis of Structures*. Great Britain: Blackwell Publishing Ltd. ISBN: 9781405170604.

Mori, Y. Kato, T. and Murai, K. (2003). Probabilistic Models of Combinations of Stochastic Loads for Limit State Design. *Structural Safety*. Vol. 25, pp.69-97.

Naess, A. and Royset, J. (2000). Extensions of Turkstra's Rule and their Application to Combination of Dependent Load Effects. *Structural Safety*. Vol. 22, pp. 129-143.

Naess, A., Gaidai, O. and Haver, S. (2007). Efficient Estimation of Extreme Response of Drag-Dominated Offshore Structures by Monte Carlo Simulation. *Ocean Engineering*. Vol. 34, pp. 2188–2197.

Nakib, R. and Frangopol, D. M. (1990). RBSA and RBSA-OPT: Two Computer Programs for Structural System Reliability Analysis and Optimization. *Computers and Structures*. Vol. 36 (1), pp. 13-27.

Neal, R. M. (2001). *Bayesian Mixture Modelling by Monte Carlo Simulation*. University of Toronto: Canada.

Nikishkov, G. P. (2004). "Introduction to the Finite Element Method", Lecture Notes Distributed in the Topic General Lecture. University of Aizu, Department of Computer Software.

Okawa, T. and Sumi, Y. (2008). A Computational Approach for Fatigue Crack Propagation in Ship Structures under Random Sequence of Clustered Loading. *Journal of Marine Science and Technology*. Vol. 13 (4), pp. 416-427.

Onofriou, T. (1999). *Reliability Based Inspection Planning of Offshore Structures*. *Marine Structures*. Vol. 12, pp. 521-539.

Paris, P. C., Gomez, M. P. and Anderson, P. E. (1961). A Rational Analytic Theory of Fatigue. *The Trend in Engineering*. Vol. 13, pp. 9-14.



Paris, P. and Erdogan, F. (1963). A Critical Analysis of Crack Propagation Laws. *Journal of Basic Engineering*. Vol. 85 (4), pp. 528-534.

Park, H. S. and Sung, C. W. (2002). Optimization of Steel Structures using Distributed Simulated Annealing Algorithm on a Cluster of Personal Computers. *Computers and Structures*. Vol. 80, pp. 1305–1316.

Pate-Cornell, M. E. (1994). Quantitative Safety Goals for Risk Management of Industrial Facilities. *Structural Safety*. Vol. 13, pp. 145-157.

Pillai, T. M. M. and Prasad, A. M. (2000). Fatigue Reliability Analysis in Time Domain for Inspection Strategy of Fixed Offshore Structures. *Ocean Engineering*. Vol. 27, pp. 167–186.

Quek, S. S. and Liu, G. R. (2003). *Finite Element Method: A Practical Course*. Great Britain: Butterworth-Heinemann. ISBN: 0750658665.

Rahman, S. and Wei, D. (2006). A Univariate Approximation at Most Probable Point for Higher-Order Reliability Analysis. *International Journal of Solids and Structures*. Vol. 43, pp. 2820–2839.

Rao, S. S. (1980). *Structural Optimization by Chance Constrained Programming Techniques*. *Computers and Structures*. Vol. 12, pp. 777-781.

Rashedi, R. and Moses, F. (1986). Application of Linear Programming to Structural System Reliability. *Computers and Structures*. Vol. 24 (3), pp. 375-384.

Riha, D. S., Thacker, B. H., Hall, D. A., Auel, T. R. and Pritchard, S. D (1999). Capabilities and Applications of Probabilistic Methods in Finite Element Analysis. in: *Fifth ISSAT International Conference On Reliability and Quality in Design*, August 11-13, Las Vegas, Nevada, U.S.A.

- Rubinstein, R. Y. (1981). *Simulation and the Monte Carlo Method*. 1 ed. U.S.A: John Wiley & Sons, Inc, ISBN 0-471-08917-6.
- Ruud, S. and Mikkelsen, A. (2008). Risk-based Rules for Crane Safety Systems. *Reliability Engineering and System Safety*. Vol. 93, pp. 1369–1376.
- Sadek, E. A. (1985). Dynamic Optimization of Framed Structures. *Computers and Structures*. Vol. 21 (6), pp. 1313-1323.
- Salmon, C. G., and Johnson, J. E. (1996). *Steel Structures: Design and Behaviour*. 4th ed. New York: Harpercollins College Publishers.
- Schoefs, F. (2008). Sensitivity Approach for Modelling the Environmental Loading of Marine Structures through a Matrix Response Surface. *Reliability Engineering and System Safety*. Vol. 93, pp. 1004–1017.
- Sharp, J. V., Billingham, J. and Robinson, M. J. (2001). The Risk Management of High-Strength Steels in Jack-Ups in Seawater. *Marine Structures*. Vol. 14, pp. 537-551.
- Shaw, S. J. (1992). Use of Risk Assessment as an Offshore Design Tool. *Journal of Loss Prevention in the Process Industries*. Vol. 5 (1), pp. 10-17.
- Shi, W. B. (1991). Stochastic Load Combinations with Particular Reference to Marine Structures. *Marine Structures*. Vol. 4, pp. 435-453.
- Shih, C. J. and Lee, H. W. (2006). Modified Double-Cuts Approach in 25-Bar and 72-Bar Fuzzy Truss Optimization. *Computers and Structures*. Vol. 84, pp. 2100-2104.
- Shigley, J. E., Mischke, C. R. and Budynas, R. G. (2004). *Mechanical Engineering Design*. 7th ed. Berkshire, U.K: McGraw Hill Education, ISBN 13-9780072520378.
- Shiraki, W. (1993). Probabilistic Load Combinations for Steel Piers at Ultimate Limit States. *Structural Safety*. Vol. 13, pp. 67-81.

Shooman, M. L. (1990). Probabilistic Reliability: An Engineering Approach. 2 ed. New York: McGraw-Hill Book Co.

Siddiqui, N. A. and Ahmad, S. (2001). Fatigue and Fracture Reliability of TLP Tethers under Random Loading. Marine Structures. Vol. 14, pp. 331-352.

Simiu, E. and Heckert, N. A. (1996). Extreme Wind Distribution Tails: A "Peaks over Threshold" Approach. Journal of Structural Engineering. Vol. 122 (5), pp. 539-547.

Skjong, R. and Torhaug, R. (1991). Rational Methods for Fatigue Design and Inspection Planning of Offshore Structures. Marine Structures. Vol. 4, pp.381-406.

Smith, E. J. (1995). Risk Management in the North Sea Offshore Industry: History, Status and Challenges. Acta Astronautica. Vol. 37, pp. 513-523.

Stefanou, G. (2009). The Stochastic Finite Element Method: Past, Present and Future. Computer Methods in Applied Mechanics and Engineering. Vol. 198, pp. 1031–1051.

Svanberg, K. (1981). Optimization of Geometry in Truss Design. Computer Methods in Applied Mechanics and Engineering. Vol. 28, pp. 63-80.

Tada, H., Paris, P. C. and Irwin, G. R. (2000). The Stress Analysis of Cracks Handbook. 3rd ed. New York: Wiley-Blackwell, ISBN 0791801535.

Trahair, N. S. and Pi, Y. L. (1997). Torsion, Bending and Buckling of Steel Beams. Engineering Structure. Vol. 19 (5), pp. 372-377.

Tveit, O. J. (1994). Safety Issues on Offshore Process Installations - An overview. Journal of Loss Prevention in the Process Industries. Vol. 7 (4), pp. 267-272.

van de Lindt, J. W. and Goh, G. (2004). Effect of Earthquake Duration on Structural Reliability. Engineering Structures. Vol. 26, pp. 1585–1597.

- Vinnem, J. E. (1998). Evaluation of Methodology for QRA in Offshore Operations. *Reliability Engineering and System Safety*. Vol. 61, pp. 39-52.
- Wang, J. (2000). A Subjective Modelling Tool Applied to Formal Ship Safety Assessment. *Ocean Engineering*. Vol. 27, pp. 1019–1035.
- Willis. (2004). Willis Energy Loss Database. Available: [www.willis.com](http://www.willis.com). Last accessed 10 April 2009.
- Wong, S. M., Hobbs, R. E. and Onof, C. (2005). An Adaptive Response Surface Method for Reliability Analysis of Structures with Multiple Loading Sequences. *Structural Safety*. Vol. 27, pp. 287-308.
- Wu, Y. F, and Lewins, J. D. (1992). Monte Carlo Studies of Engineering System Reliability. *Annals of Nuclear Energy*. Vol. 19 (10-12), pp. 825-859.
- Wu, W. F., and Ni, C. C. (2004). Probabilistic Models of Fatigue Crack Propagation and their Experimental Verification. *Probabilistic Engineering Mechanics*. Vol. 19, pp. 247–257.
- Wu, Y. L. and Moan, T. (1991). An Incremental Load Formulation for Limit States in the Reliability Analysis of Nonlinear Systems. *Structural Safety*. Vol. 10, pp. 307-325.
- Xie, Y. M. and Steven, G. P. (1993). A Simple Evolutionary Procedure for Structural Optimization. *Computers and Structures*. Vol. 49 (5), pp. 885-896.
- Xu, C. (1989). Fuzzy Optimization of Structures by the Two-Phase Method. *Computers and Structures*. Vol. 31 (4), pp. 575-580.
- Yang, G. (2002). A Monte Carlo Method of Integration. IB Diploma Programme Thesis, Nørre Gymnasium, Denmark.

Yang, K. and Younis, H. (2005). A Semi-Analytical Monte Carlo Simulation Method for System's Reliability with Load Sharing and Damage Accumulation. *Reliability Engineering and System Safety*. Vol. 87, pp. 191-200.

Yao, J. T. P., Kozin, F., Wen, Y. -K., Yang, J. -N., Schueller, G. I. and Ditlevsen, O. (1986). Stochastic Fatigue, Fracture and Damage Analysis. *Structural Safety*. Vol. 3, pp. 231-267.

Zhu, W. Q., Lin Y. K. and Lei, Y. (1992). On Fatigue Crack Growth under Random Loading. *Engineering Fracture Mechanics*. Vol. 43 (1), pp.1-12.

Zienkiewicz, O. C. and Taylor, R. L. (2000). *The Finite Element Method for Fluid Dynamics*, Vol. 3. Great Britain: Butterworth-Heinemann. ISBN: 0750650508.

Zou, M., Yu, B., Feng, Y. and Xu, P. (2007). A Monte Carlo Method for Simulating Fractal Surfaces. *Physica A*. Vol. 386, pp. 176–186.

## Appendices

### Appendix A

#### Appendix A.1

```

|*****
| PROGRAM: BETA-FLEXSTREM
| PROGRAMMER: Echezona C. Chukwuka
|*****
PROGRAM BETA-FLEXSTREM
USE IFPORT
IMPLICIT NONE
REAL::A_C
REAL::N_EFF          !Cycles to failure
REAL::N_STL_TRANS
REAL::Y_STR_TRANS
REAL::STR_TRANS
REAL::K
REAL::K_STL_TRANS   !Fracture toughness
REAL::A             !Crack length
REAL::STR           !Stress (from loading)
REAL::L             !Load
REAL::C_MAT
REAL::POF
REAL::BETA
REAL::RELIABILITY
REAL::V_RELIABILITY
REAL::NRN           !NORMAL RANDOM NUMBER
REAL::ERN           !EXPONENTIAL RANDOM NUMBER
INTEGER::N1=100000 !No of simulations
INTEGER::I          !Loop index
INTEGER::COUNTER1,COUNTER2,&
                COUNTER3,COUNTER4 !Failure counters
INTEGER::IERROR,UNIT !Format parameters

COUNTER1=0
COUNTER2=0
COUNTER3=0
COUNTER4=0

DO I=1,N1
  CALL GAUSSIAN_RANDOM_NUMBER(NRN)
  CALL EXPO_RANDOM_NUMBER(ERN)
  CALL LOAD(L)
  CALL NOMINAL_STRESS(STR)
  CALL STRESS_TRANSFORMATION(STR_TRANS,Y_STR_TRANS)
  IF (STR_TRANS .GE. Y_STR_TRANS) THEN
    COUNTER1=COUNTER1+1
    GOTO 143
  ELSE !(NO FAIL)
  END IF
  CALL STRESS_FRACTURE(K,K_STL_TRANS,BETA)
  IF (K .GE. K_STL_TRANS) THEN
    COUNTER2=COUNTER2+1
    GOTO 147
  ELSE !(NO FAIL)
  END IF
  CALL MINIMUM_CRACK(A_C)
  CALL CRACK_LENGTH(A)
  IF (A .GE. A_C) THEN
    COUNTER3=COUNTER3+1
    GOTO 162
  ELSE !(NO FAIL)
  END IF
  CALL LIFE_CYCLE(N_EFF,N_STL_TRANS,C_MAT)
  IF (N_EFF .LE. N_STL_TRANS) THEN
    COUNTER4=COUNTER4+1
    GOTO 151
  ELSE !(NO FAIL)
  END IF
151 OPEN(20,FILE='N_STL_TRANS-VALUE.TXT',STATUS='REPLACE',ACTION='WRITE',IOSTAT=IERROR)
  WRITE(20,240)N_STL_TRANS
  240 FORMAT (' ',F20.10)
  OPEN(25,FILE='N_EFF-VALUE.TXT',STATUS='REPLACE',ACTION='WRITE',IOSTAT=IERROR)
  WRITE(25,250) N_EFF
  250 FORMAT (' ',F20.4)
162 OPEN(32,FILE='A-VALUE.TXT',STATUS='REPLACE',ACTION='WRITE',IOSTAT=IERROR)
  WRITE(32,260) A

```

```

260 FORMAT (' ',F6.4)
OPEN(58,FILE='A_C-VALUE.TXT',STATUS='REPLACE',ACTION='WRITE',IOSTAT=IERROR)
WRITE(58,450) A_C
450 FORMAT (' ',F12.6)
147 OPEN(21,FILE='K-VALUE.TXT',STATUS='REPLACE',ACTION='WRITE',IOSTAT=IERROR)
WRITE(21,220) K
220 FORMAT (' ',F14.10)
OPEN(22,FILE='K_STL_TRANS-
VALUE.TXT',STATUS='REPLACE',ACTION='WRITE',IOSTAT=IERROR)
WRITE(22,230) K_STL_TRANS
230 FORMAT (' ',F14.10)
143 OPEN(23,FILE='STR_TRANS-VALUE.TXT',STATUS='REPLACE',ACTION='WRITE',IOSTAT=IERROR)
WRITE(23,200) STR_TRANS
200 FORMAT (' ',F13.3)
OPEN(28,FILE='Y_STR_TRANS-
VALUE.TXT',STATUS='REPLACE',ACTION='WRITE',IOSTAT=IERROR)
WRITE(28,280) Y_STR_TRANS
280 FORMAT (' ',F10.4)
OPEN(38,FILE='C_MAT_TRANS-
VALUE.TXT',STATUS='REPLACE',ACTION='WRITE',IOSTAT=IERROR)
WRITE(38,270) C_MAT
270 FORMAT (' ',F14.13)
IF (N_EFF .LE. N_STL_TRANS.OR.A .GE. A_C.OR.K .GE. K_STL_TRANS.OR.STR_TRANS .GE.
Y_STR_TRANS) THEN
OPEN(44,FILE='COUNTERS.TXT',STATUS='REPLACE',ACTION='WRITE',IOSTAT=IERROR)
WRITE(44,290) COUNTER1,COUNTER2,COUNTER3,COUNTER4
290 FORMAT (' ',COUNTER1 = ',I4,/, &
1X,COUNTER2 = ',I4,/, &
1X,COUNTER3 = ',I4,/, &
1X,COUNTER4 = ',I4,/)
ELSE
END IF
END DO

POF=(REAL(COUNTER1+COUNTER2+COUNTER3+COUNTER4)/N1)
RELIABILITY=(1-POF)
V_RELIABILITY=COUNTER4-(COUNTER1+COUNTER2+COUNTER3)

PRINT*,'POF',POF
PRINT*,'RELIABILITY',RELIABILITY
PRINT*,'V_RELIABILITY',V_RELIABILITY
OPEN(89,FILE='RESULT.TXT',STATUS='REPLACE',ACTION='WRITE',IOSTAT=IERROR)
WRITE(89,590) POF,RELIABILITY,V_RELIABILITY
590 FORMAT (' ',PROBABILITY OF FAILURE = ',E13.6,/, &
1X,RELIABILITY = ',F12.10,/, &
1X,VIRTUAL RELIABILITY = ',F8.4)

STOP
END PROGRAM CHAP_1_OPT
!-----
SUBROUTINE GAUSSIAN_RANDOM_NUMBER(NORMRND)
USE IFPORT
IMPLICIT NONE

REAL,INTENT(OUT)::NORMRND
REAL::RL,Y1,Y2
REAL,SAVE ::Z
LOGICAL,SAVE ::NORM=.FALSE.

IF (NORM) THEN
NORMRND=Z
NORM=.FALSE.
ELSE
DO
CALL SEED(1975)
CALL RANDOM_NUMBER(Y1)
CALL SEED(1865)
CALL RANDOM_NUMBER(Y2)
Y1=(2.0*Y1)-1.0
Y2=(2.0*Y2)-1.0
RL=(Y1*Y1)+(Y2*Y2)
IF (RL > 0.0 .AND. RL < 1.0) EXIT
END DO

RL=SQRT(-2.0*LOG(RL)/RL)
NORMRND=Y1*RL
Z=Y2*RL
NORM=.TRUE.
END IF

END SUBROUTINE GAUSSIAN_RANDOM_NUMBER
!-----
SUBROUTINE EXPO_RANDOM_NUMBER(EXPRND)

USE IFPORT
IMPLICIT NONE

```

```

REAL,INTENT(OUT)::EXPRND
REAL::R

CALL SEED(1294)
CALL RANDOM_NUMBER(R)
EXPRND=-LOG(R)

END SUBROUTINE EXPO_RANDOM_NUMBER
!=====
SUBROUTINE LOAD(LD)

IMPLICIT NONE

REAL,INTENT(OUT)::LD ! Load in kn
REAL::RAND
INTEGER::Q,I4,N4=1
INTEGER::I
INTEGER*4 TIMEARRAY(3)

CALL ITIME(TIMEARRAY)

I = RAND( TIMEARRAY(1)+TIMEARRAY(3) )

DO I = 1, 1
END DO

DO I4=1,N4
  Q=INT(RAND(0)*1000)
  SELECT CASE (Q)
  CASE (1:100)
    LD=5.
  CASE (101:200)
    LD=10.
  CASE (201:300)
    LD=15.
  CASE (301:400)
    LD=20.
  CASE (401:500)
    LD=25.
  CASE (501:600)
    LD=30.
  CASE (601:700)
    LD=35.
  CASE (701:800)
    LD=40.
  CASE (801:900)
    LD=45.
  CASE (901:1000)
    LD=50.
  IF (Q .LT. 1) EXIT
  END SELECT
END DO

END SUBROUTINE LOAD
!=====
SUBROUTINE NOMINAL_STRESS(STRESS)

IMPLICIT NONE

REAL,INTENT(OUT)::STRESS
REAL,PARAMETER::ALF=0.000015 !Coefficient of expansion of steel
REAL,PARAMETER::T1=293. !Average temperature (design temperature) 20*C
REAL,PARAMETER::O_L=5. !Full length of jib m
REAL,PARAMETER::DIST=4.7 !Perpendicular distance (for moment calculation)m
REAL,PARAMETER::W=34. !weight of jib boom in kn
REAL,PARAMETER::FH=0.04 !Flange height
REAL,PARAMETER::FW=0.3 !flange width in metres
REAL,PARAMETER::WW=0.03 !web width
REAL,PARAMETER::WH=0.5 !web height
REAL::T2,MONT,I_MONT,A,RAND,CH,CD
REAL::DIST_1,FW_1,WH_1 !New dimensions after expansion
REAL::LD !Load parameter nomenclature
INTEGER::I
INTEGER*4 TIMEARRAY(3)

CALL ITIME(TIMEARRAY)
I = RAND( TIMEARRAY(1)+TIMEARRAY(2)+TIMEARRAY(3) )

DO I = 1, 1
END DO

CALL LOAD(LD)
T2=RAND(0)*(303.-273.)+273.
CH=ALF*(T2-T1)
DIST_1=(O_L*CH)+DIST
FW_1=(FW*CH)+FW

```



```

WH_1=(WH*CH)+WH
A=FW_1*FH
MONT=(LD*DIST_1)+(DIST_1*0.5*W)
I_MONT=2*A*((WH_1*0.5)+(FH*0.5))*((WH_1*0.5)+(FH*0.5)) +(WW*(WH_1*WH_1*WH_1)/12)
CD=FH+(WH_1*0.5)
STRESS=MONT*CD/I_MONT

END SUBROUTINE NOMINAL_STRESS
!-----
SUBROUTINE STRESS_TRANSFORMATION(STS,YRANS)

IMPLICIT NONE

REAL,INTENT(OUT)::STS !TRANSFORMED STRESS
REAL,INTENT(OUT)::YRANS !TRANSFORMED STRESS
REAL,PARAMETER::Y_STR=351.571 !YIELD STRESS MATERIAL PROPERTY IN kN/m^2
REAL::S_Y_STR,S_STR,STR_1,GRNJ
CALL NOMINAL_STRESS(STR_1)

CALL GAUSSIAN_RANDOM_NUMBER(GRNJ)
S_STR=0.158*STR_1*0.001
STS=(STR_1*0.001)+(GRNJ*S_STR)
S_Y_STR=0.1*Y_STR
YRANS=Y_STR+(GRNJ*S_Y_STR)

END SUBROUTINE STRESS_TRANSFORMATION
!-----
SUBROUTINE CRACK_LENGTH(A_LEN)

IMPLICIT NONE

REAL,INTENT(OUT)::A_LEN
REAL,PARAMETER::AI=0.00175 !Initial crack length m
REAL,PARAMETER::AF=0.107002 !0.010056 !Final crack length m
REAL::A_EFF,AF_TRANS,AI_TRANS,I_A,EXRN,R1
INTEGER::I,N_2=100000

CALL EXPO_RANDOM_NUMBER(EXRN)
AF_TRANS=EXRN*AF
AI_TRANS=EXRN*AI
A_EFF=0

DO I=1,N_2
  CALL RANDOM_NUMBER(R1)
  I_A=R1*(AF_TRANS-AI_TRANS)+AI_TRANS
  A_EFF=(A_EFF+I_A)
END DO

A_LEN=(REAL(A_EFF)/N_2)

END SUBROUTINE CRACK_LENGTH
!-----
SUBROUTINE STRESS_FRACTURE(K_0,KRANS,BETA)

IMPLICIT NONE

REAL,INTENT(OUT)::K_0
REAL,INTENT(OUT)::KRANS,BETA
REAL,PARAMETER::K_STL=70. !Design fracture Toughness (steel) kNm^0.5
REAL,PARAMETER::PI=3.14159265 !The value of Pi
REAL::S_K_STL,LEN_1,STS_2,YRANS_2,K_COV,CONV,S_K_STL_LOG,K_STL_LOG,LN_K,GRNI

CALL GAUSSIAN_RANDOM_NUMBER(GRNI)
CALL STRESS_TRANSFORMATION(STS_2,YRANS_2)
CALL CRACK_LENGTH(LEN_1)
CALL EDGE_CRACK_PURE_BEND_SPEC (PI,LEN_1,W,BETA)

K_0=BETA*STS_2*(SQRT(PI*LEN_1))
S_K_STL=0.1*K_STL
K_COV=S_K_STL/K_STL
CONV=LOG(1+(K_COV*K_COV))
S_K_STL_LOG=SQRT(CONV)
K_STL_LOG=LOG(K_STL)-(0.5*CONV)
LN_K=K_STL_LOG+(GRNI*S_K_STL_LOG)
KRANS=EXP(LN_K)
END SUBROUTINE STRESS_FRACTURE
!-----
SUBROUTINE EDGE_CRACK_PURE_BEND_SPEC (PI,A,W,F)
IMPLICIT NONE

REAL, INTENT(IN)::A,W,PI
REAL, INTENT(OUT)::F
REAL::X

X = (PI*A)/(2*W)
F = SQRT((1./X)*TAN(X))*((0.923+0.199*(1-SIN(X))**4)/COS(X))

```

```

END SUBROUTINE EDGE_CRACK_PURE_BEND_SPEC
|=====
SUBROUTINE MINIMUM_CRACK(A_C)

IMPLICIT NONE

REAL,INTENT(OUT)::A_C
DOUBLE PRECISION::PI=3.14159265      !The value of Pi
REAL,PARAMETER::BETA=1.12           !Beta(material Property)
REAL::SIM,STS_1,YRANS_1,K_1,KRANS_1

CALL STRESS_TRANSFORMATION(STS_1,YRANS_1)
CALL STRESS_FRACTURE(K_1,KRANS_1)
SIM=KRANS_1/(BETA*STS_1)
A_C=1/PI*(SIM*SIM)

END SUBROUTINE MINIMUM_CRACK
|=====
SUBROUTINE LIFE_CYCLE(N_EFF,N_STL_TRANS,C_MAT_TRANS)

IMPLICIT NONE

REAL,INTENT(OUT)::N_EFF
REAL,INTENT(OUT)::N_STL_TRANS
REAL,INTENT(OUT)::C_MAT_TRANS
DOUBLE PRECISION::C_MAT=0.0000000004 !c (material property)
REAL,PARAMETER::N_STL=108000.        !Life (design) cycle of steel
INTEGER,PARAMETER::M_PWR=3
REAL::S_N_STL,GRNK,K_3,KRANS_3,N_COV,CONVN,S_N_STL_LOG,N_STL_LOG,LN_N
REAL::S_C_MAT,C_COV,CONVC,S_C_MAT_LOG,C_MAT_LOG,LN_C

CALL GAUSSIAN_RANDOM_NUMBER(GRNK)
CALL STRESS_FRACTURE(K_3,KRANS_3)
S_C_MAT=0.1*C_MAT
C_COV=S_C_MAT/C_MAT
CONVC=LOG(1+(C_COV*C_COV))
S_C_MAT_LOG=SQRT(CONVC)
C_MAT_LOG=LOG(C_MAT)-(0.5*CONVC)
LN_C=C_MAT_LOG+(GRNK*S_C_MAT_LOG)
C_MAT_TRANS=EXP(LN_C)
N_EFF=(1/C_MAT_TRANS)*(1/K_3)*(1/K_3)*(1/K_3)
S_N_STL=0.1*N_STL
N_COV=S_N_STL/N_STL
CONVN=LOG(1+(N_COV*N_COV))
S_N_STL_LOG=SQRT(CONVN)
N_STL_LOG=LOG(N_STL)-(0.5*CONVN)
LN_N=N_STL_LOG+(GRNK*S_N_STL_LOG)
N_STL_TRANS=EXP(LN_N)

END SUBROUTINE LIFE_CYCLE

```

Appendix A.2

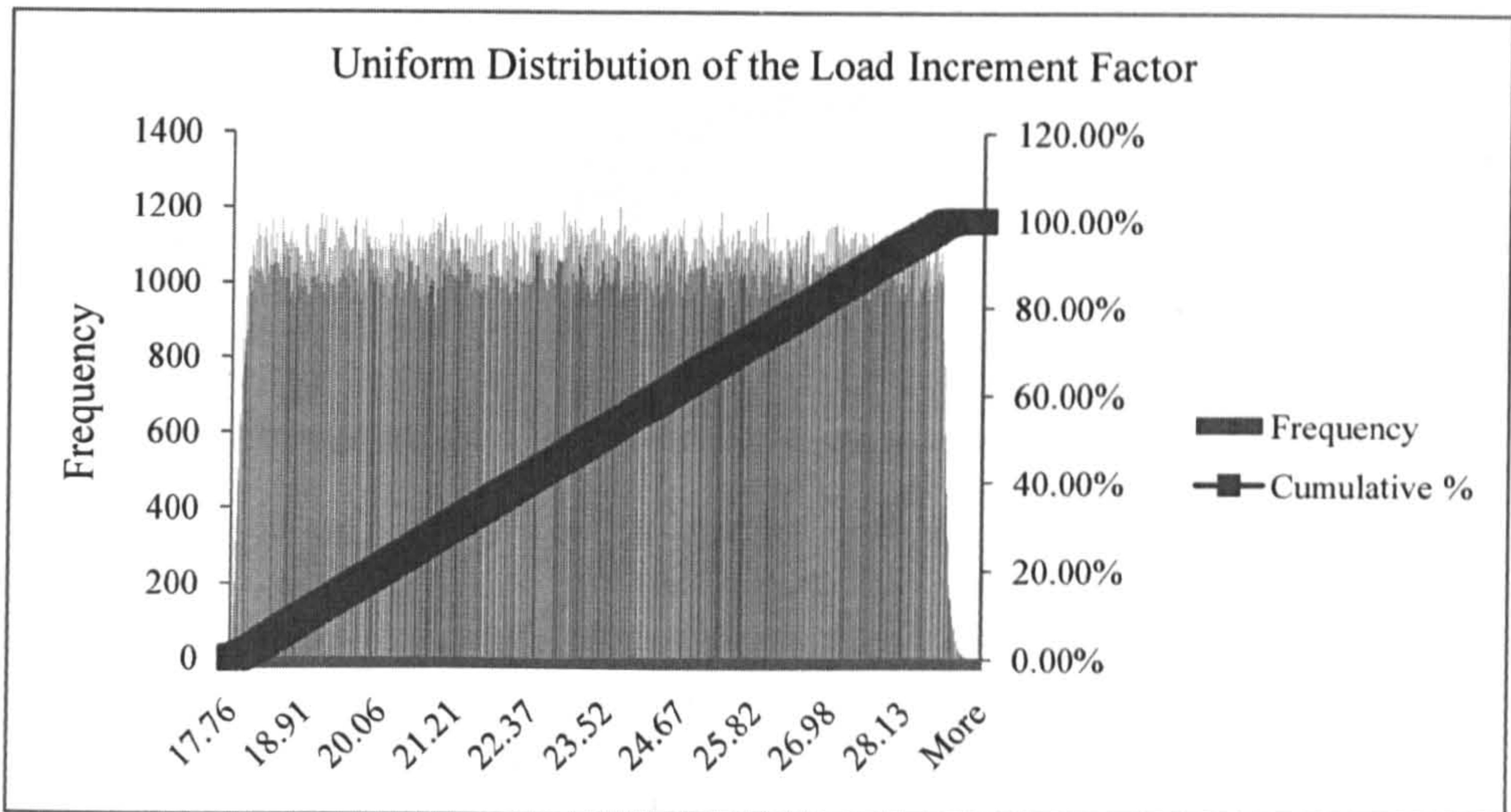


Figure (A.1) – Uniform distribution of the load increment factor.

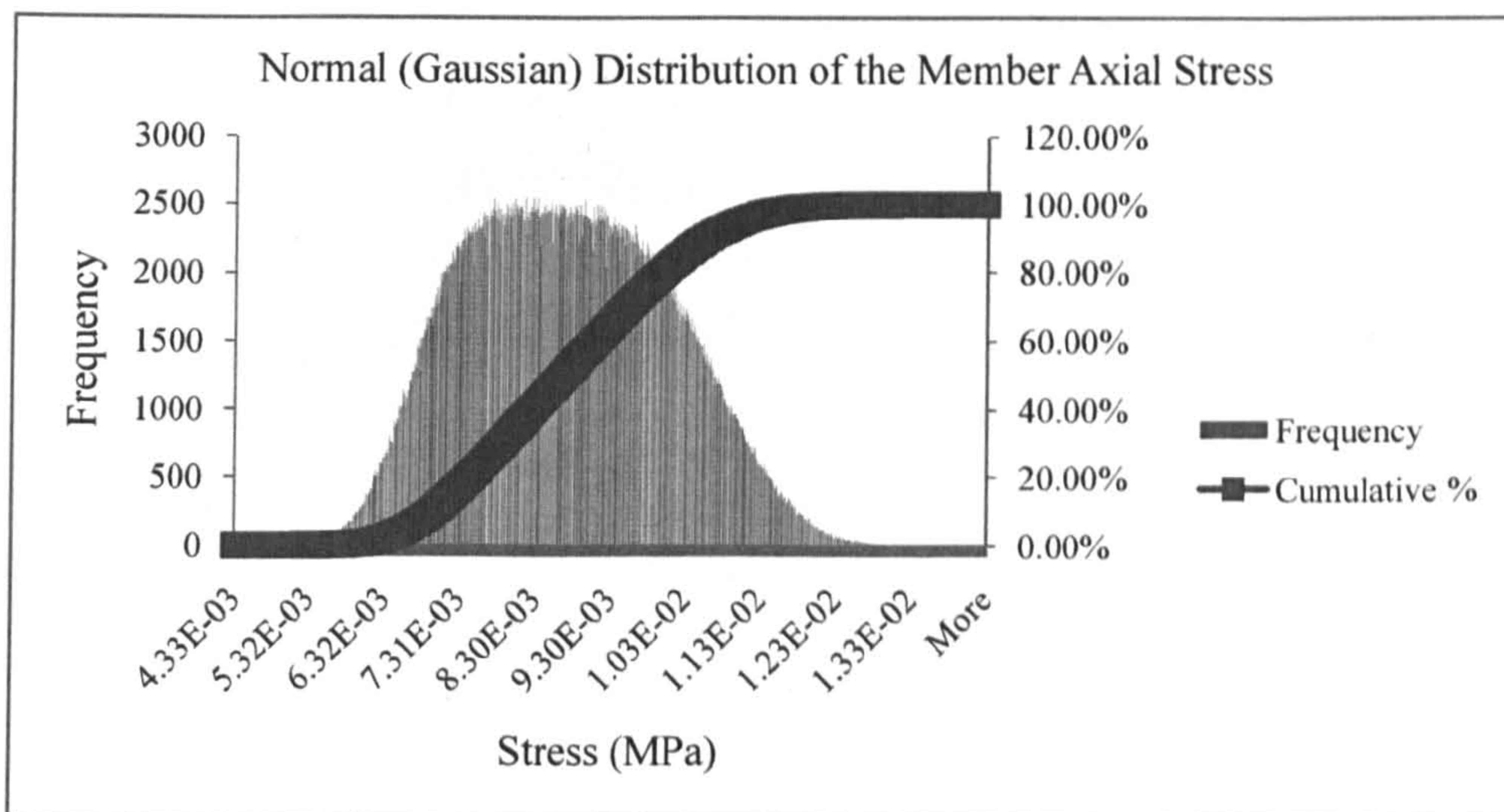


Figure (A.2) – Normal distribution of the axial stress in structural member.

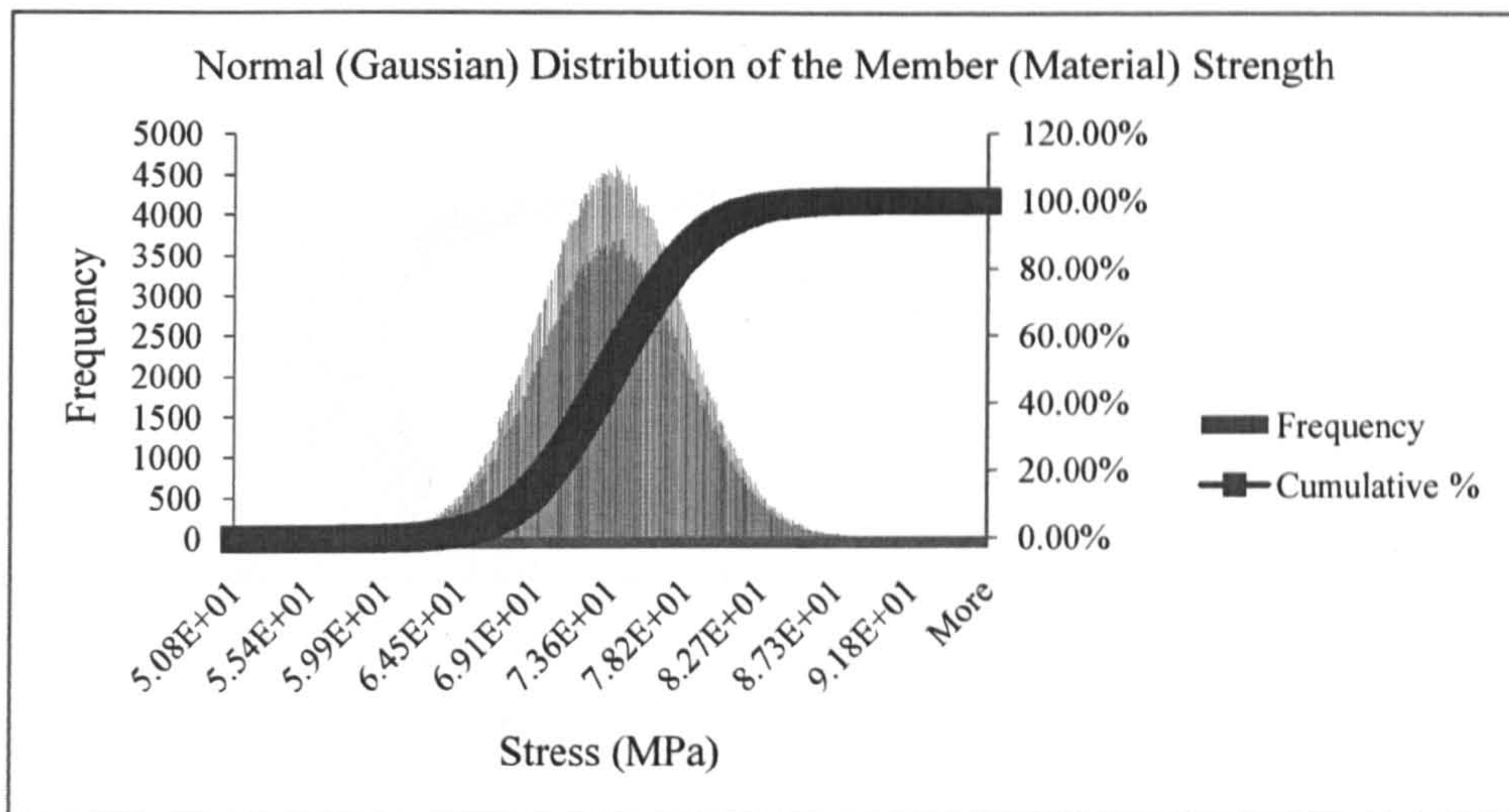


Figure (A.3) – Normal distribution of the member (material) strength.

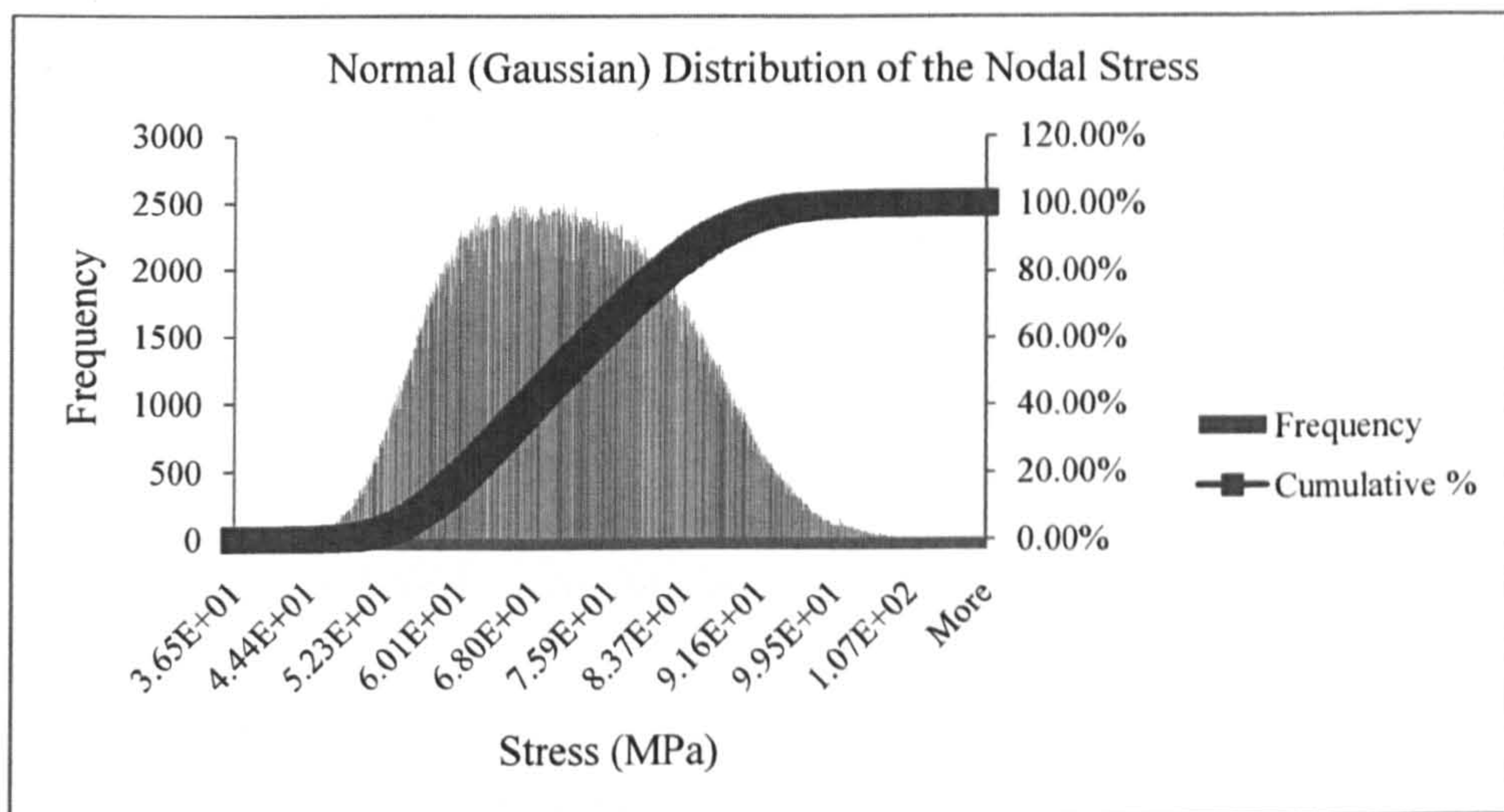


Figure (A.4) – Normal distribution of the nodal stress.

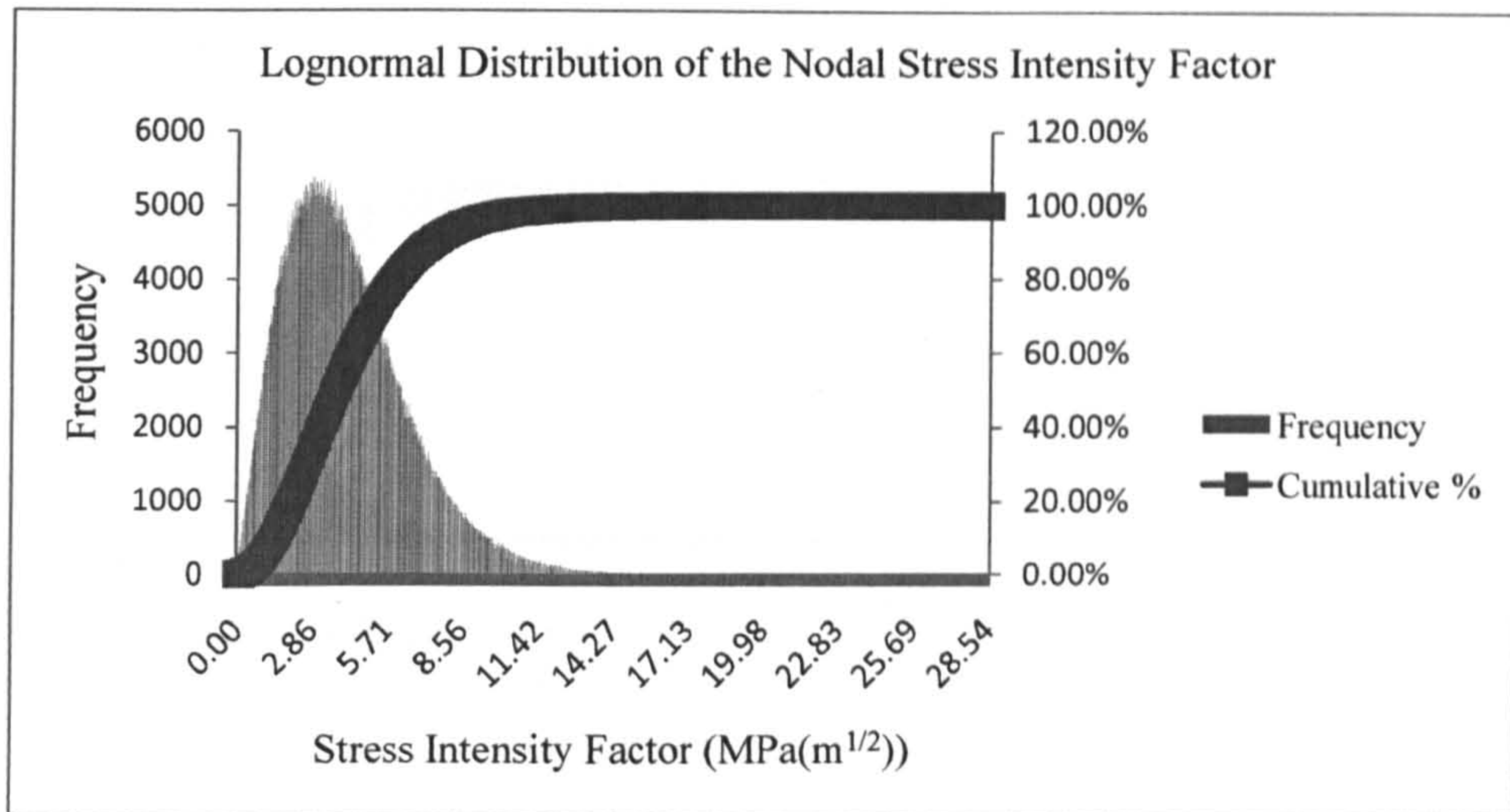


Figure (A.5) – Lognormal distribution of the nodal stress intensity factor.

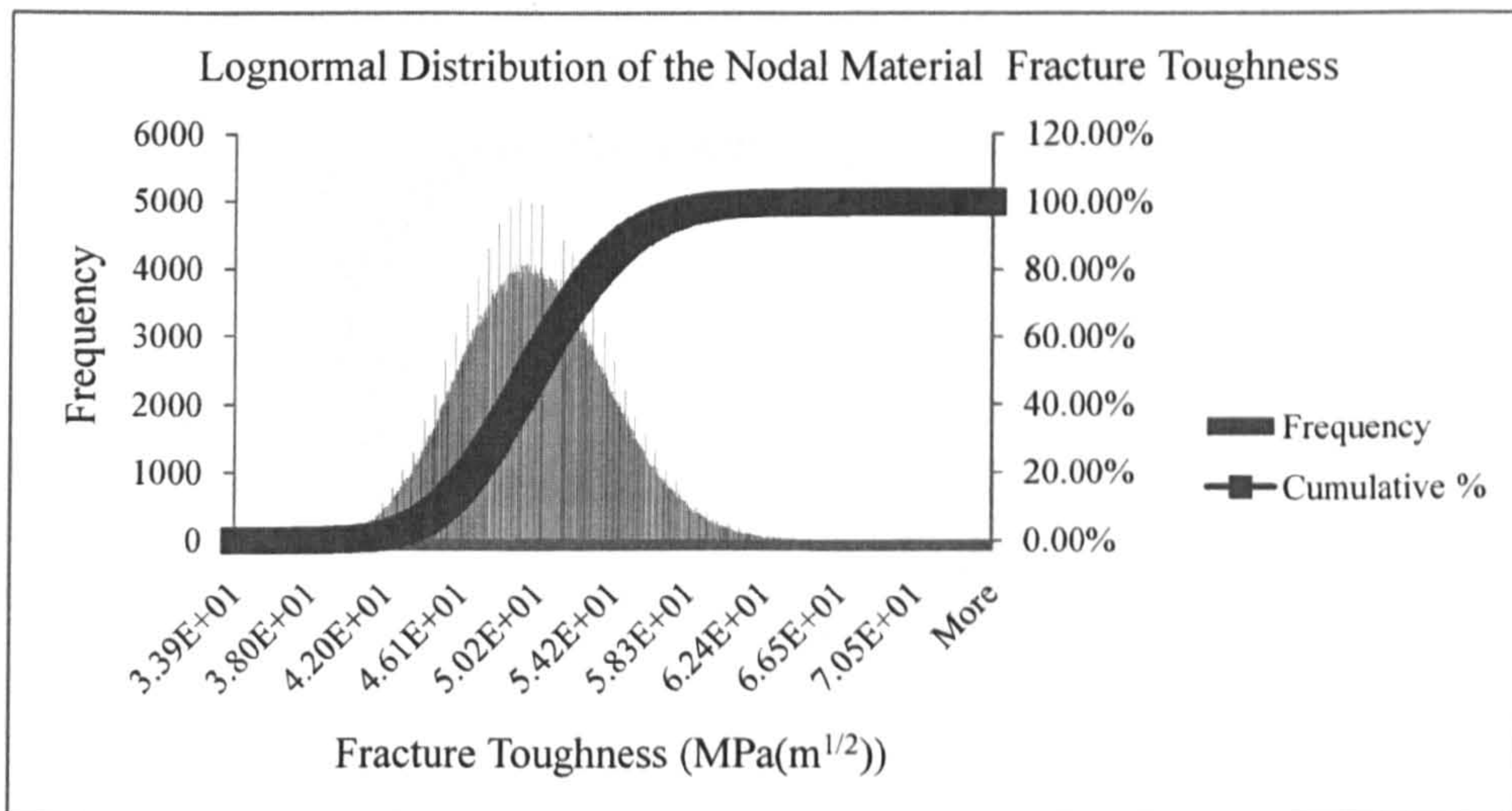


Figure (A.6) – Lognormal distribution of the nodal material fracture toughness.

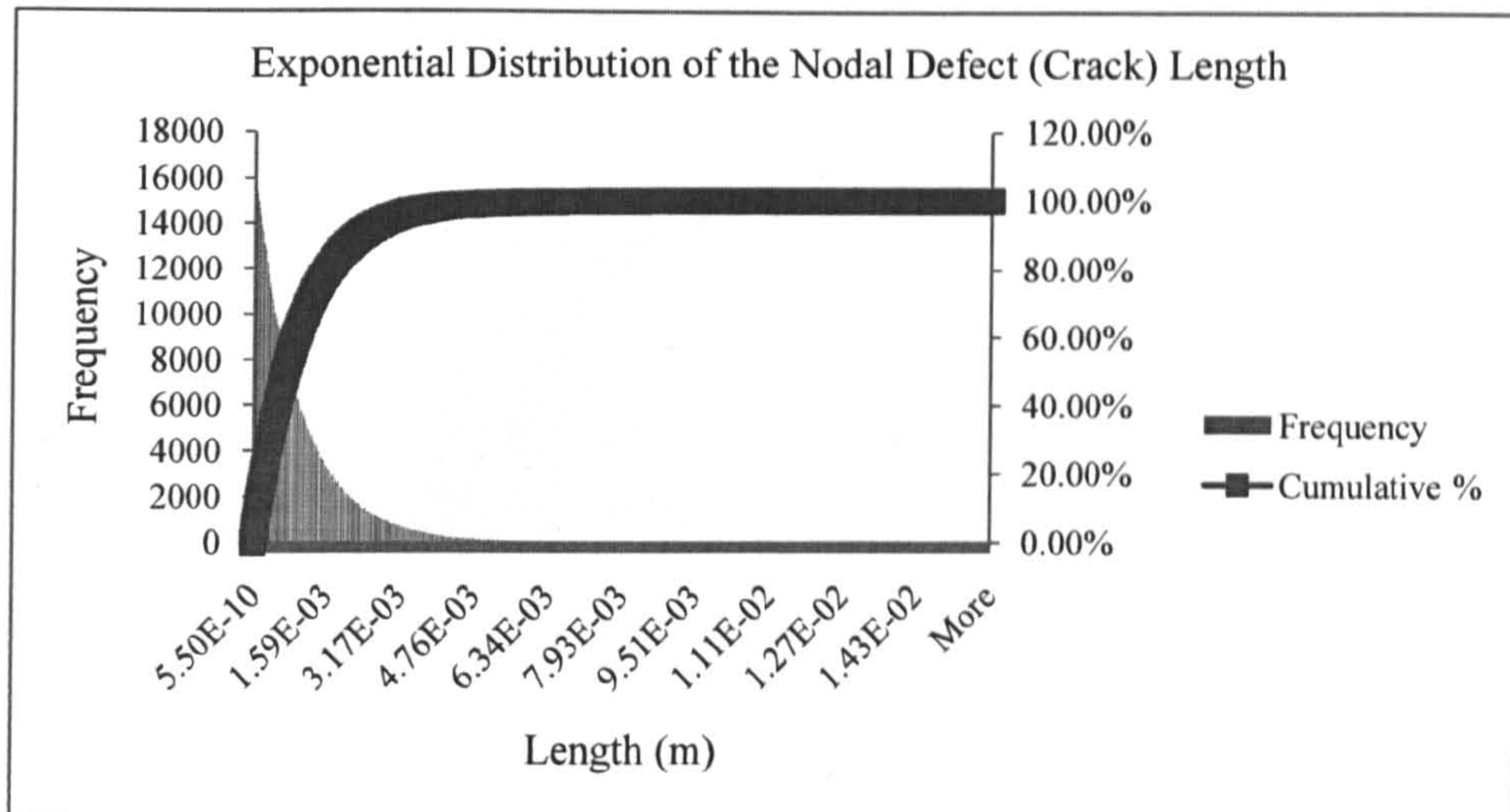


Figure (A.7) – Exponential distribution of the nodal defect.

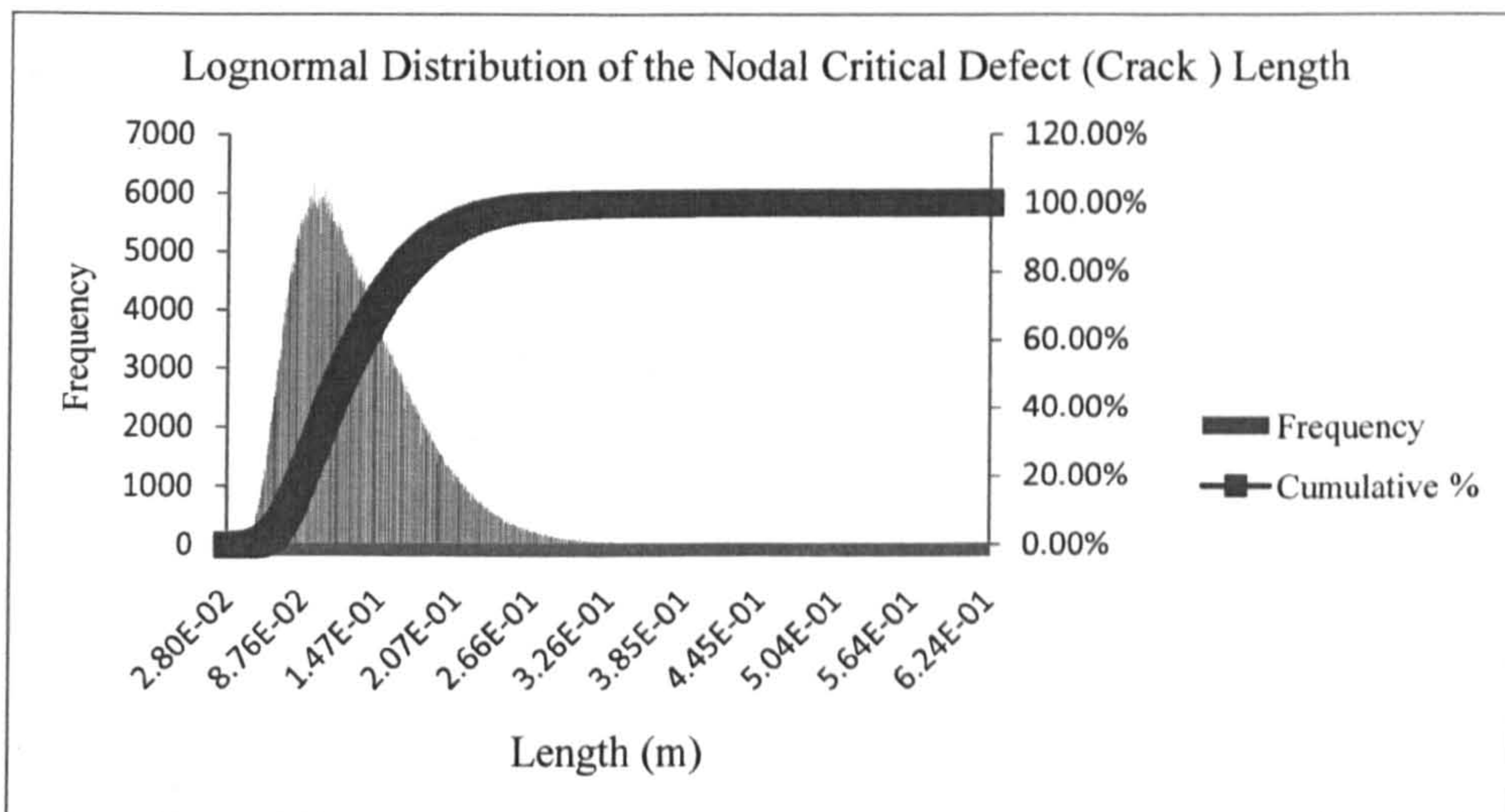


Figure (A.8) – Lognormal distribution of the nodal critical crack length.

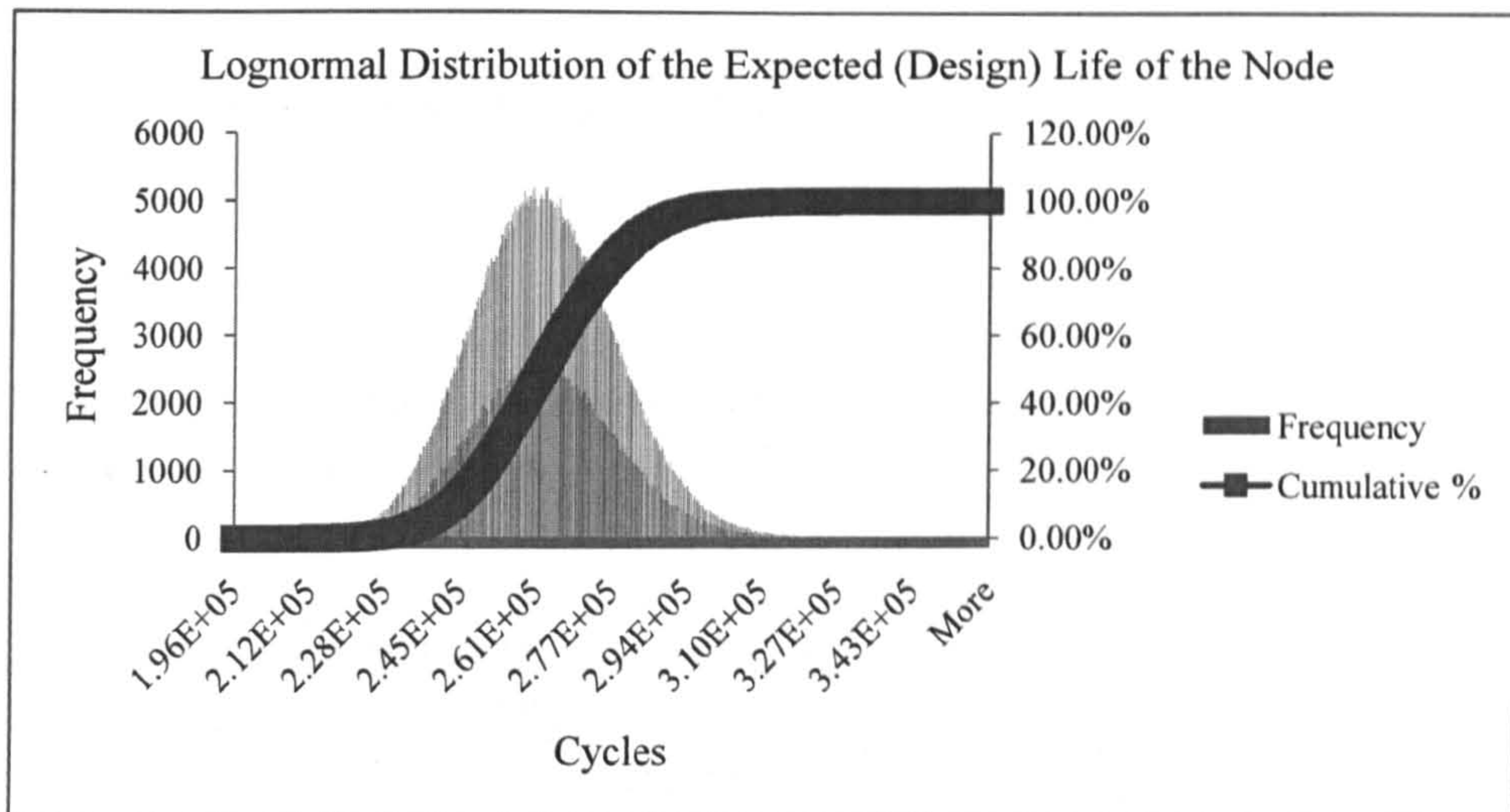


Figure (A.9) – Lognormal distribution of the expected life of the node.

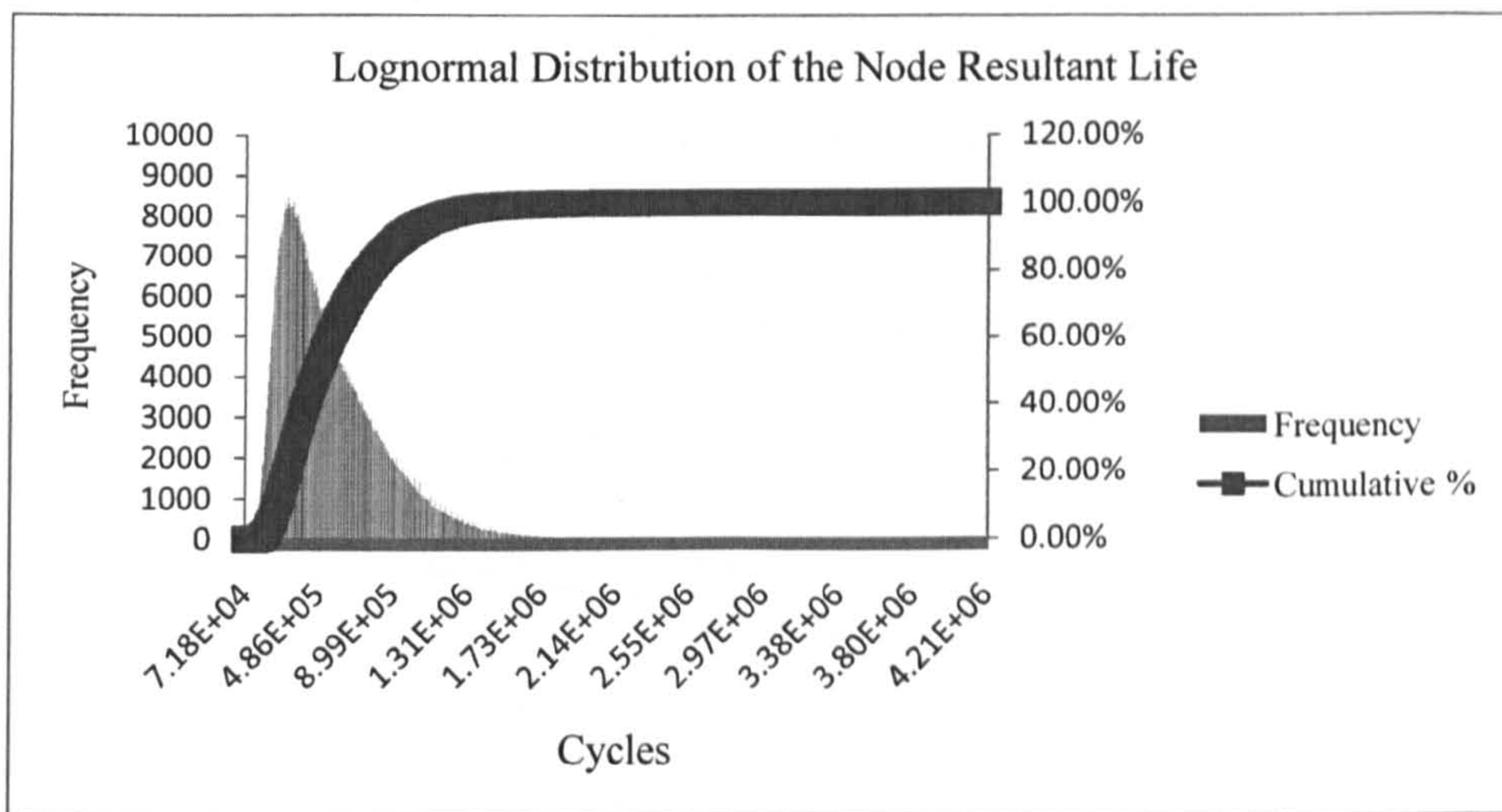


Figure (A.10) – Lognormal distribution of the node resultant life.

Appendix A.3

Changes in the reliability values due to changes in the COV components – COV(D) and COV(R).

Case 2:

Reliability values obtained at different numbers of simulations while keeping COV(D) constant and increasing COV(R).

Coefficient of Variation status			Reliability per no of simulations				Average
COV(D)	COV(R)	% change in COV(R)	1K	10K	100K	1M	
0.08	0.06	0	0.87	0.8621	0.86107	0.861762	0.863733
0.08	0.09	50	0.866	0.8611	0.85945	0.85967	0.861555
0.08	0.12	100	0.86	0.8552	0.85585	0.856705	0.85693875
0.08	0.15	150	0.859	0.851	0.85267	0.852975	0.85391125
0.08	0.18	200	0.861	0.847	0.84891	0.849074	0.851496
0.08	0.21	250	0.856	0.839	0.844	0.844248	0.845812
0.08	0.24	300	0.827	0.837	0.83301	0.834681	0.83292275
0.08	0.27	350	0.799	0.8004	0.79946	0.800555	0.79985375
0.08	0.3	400	0.689	0.6999	0.70289	0.704357	0.69903675

Table (A.1) – COV(D) constant; increasing COV(R).

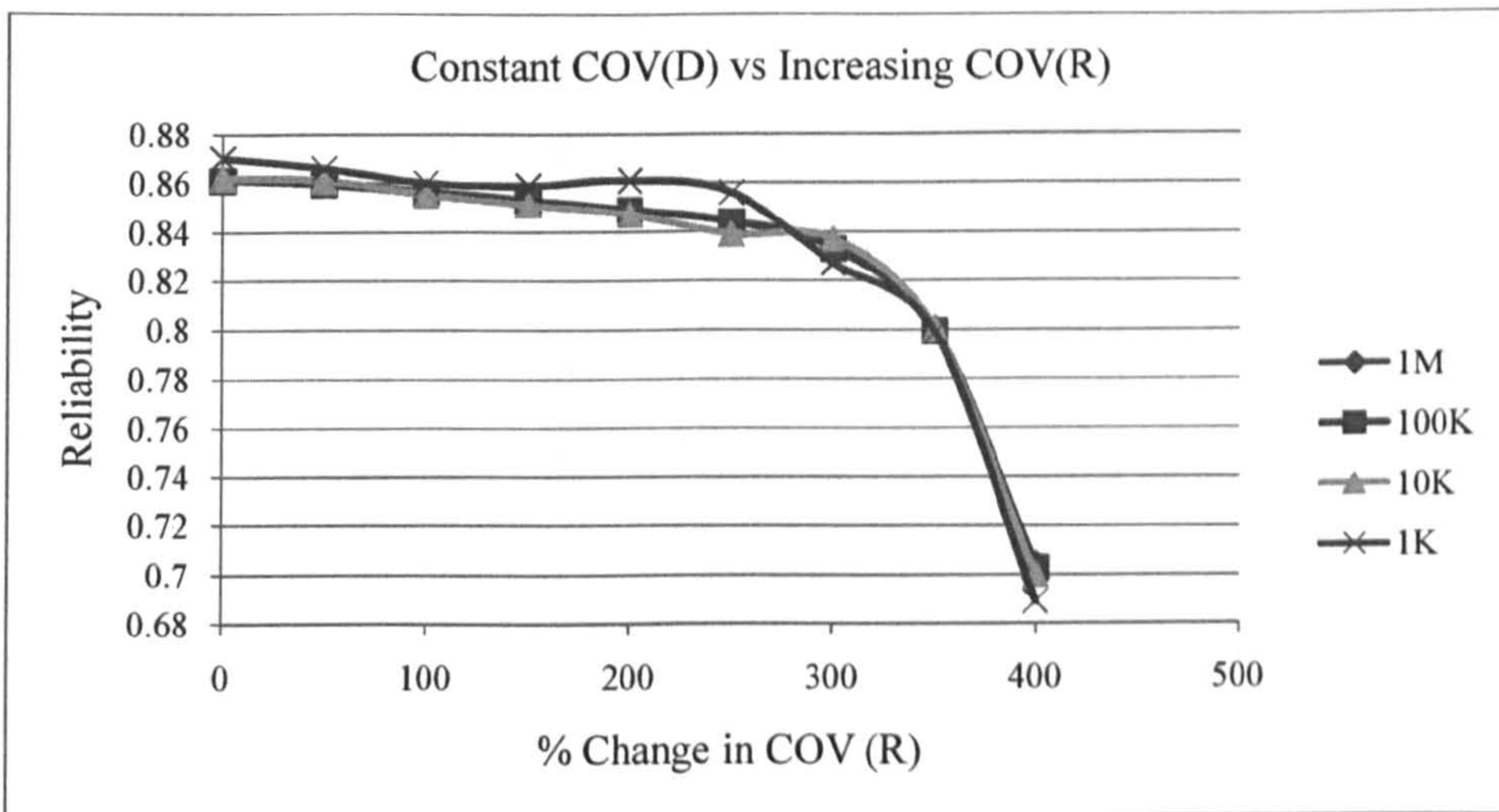


Figure (A.11) – Constant COV(D) vs. Increasing COV(R)



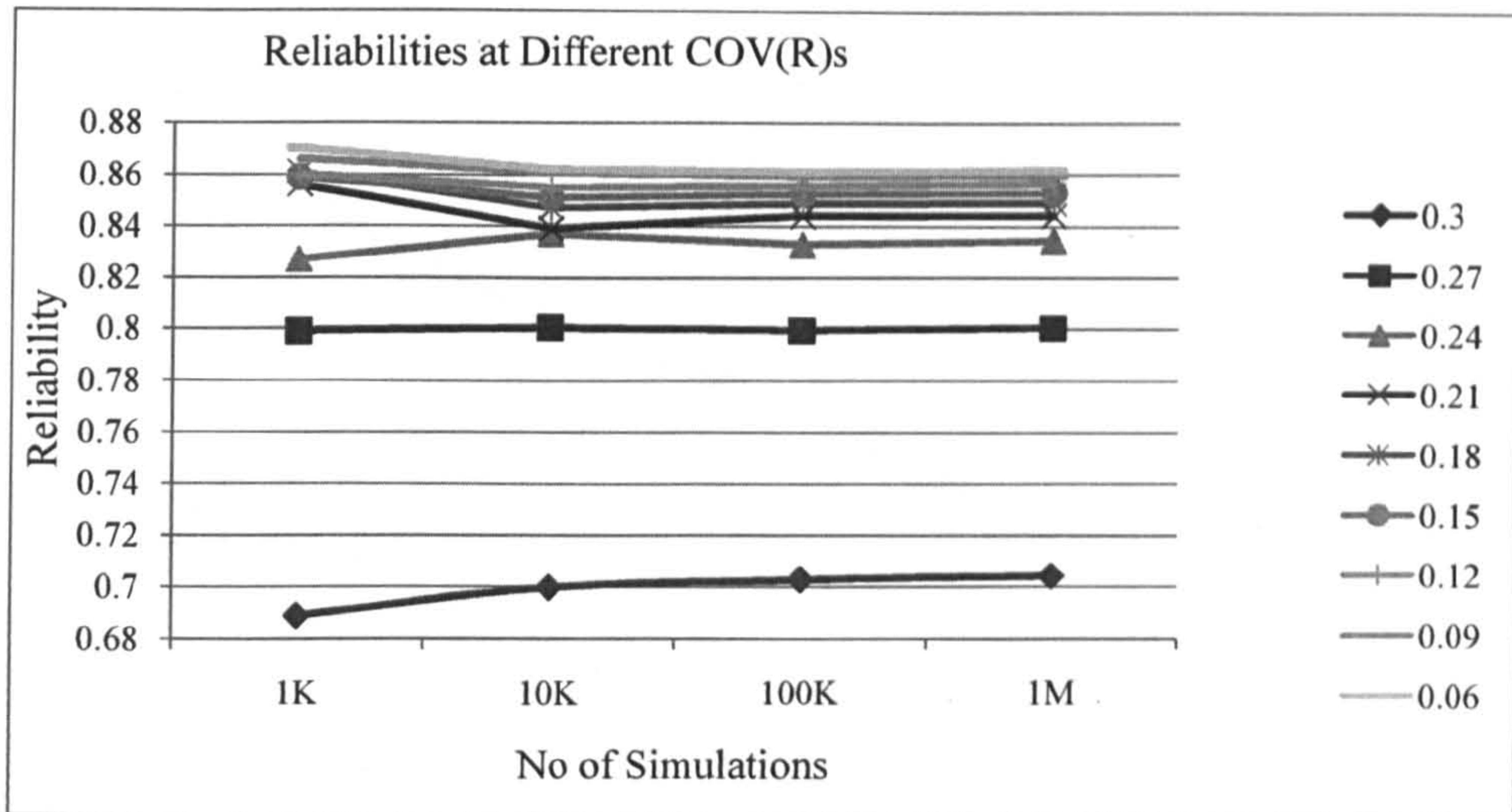


Figure (A.12) – Reliabilities at different COVs.

Case 3:

Reliability values obtained at different numbers of simulations while simultaneously increasing COV (D) and COV (R).

Coefficient of Variation status				Reliability per no of simulations				Average
COV (D)	% change in COV(D)	COV (R)	% change in COV(R)	1K	10K	100K	1M	
0.08	0	0.06	0	0.87	0.8621	0.86107	0.861762	0.863733
0.12	50	0.09	50	0.821	0.8111	0.81004	0.811356	0.813374
0.16	100	0.12	100	0.766	0.7613	0.76056	0.762208	0.762517
0.2	150	0.15	150	0.715	0.714	0.71473	0.716396	0.7150315
0.24	200	0.18	200	0.677	0.6744	0.67208	0.675435	0.67472875
0.28	250	0.21	250	0.632	0.6369	0.64009	0.639438	0.637107
0.32	300	0.24	300	0.598	0.6096	0.60478	0.605522	0.6044755
0.36	350	0.27	350	0.524	0.5504	0.55676	0.559453	0.54765325
0.4	400	0.3	400	0.457	0.4784	0.47451	0.476633	0.47163575

Table (A.2) – COV(D) and COV(R) simultaneously increased.

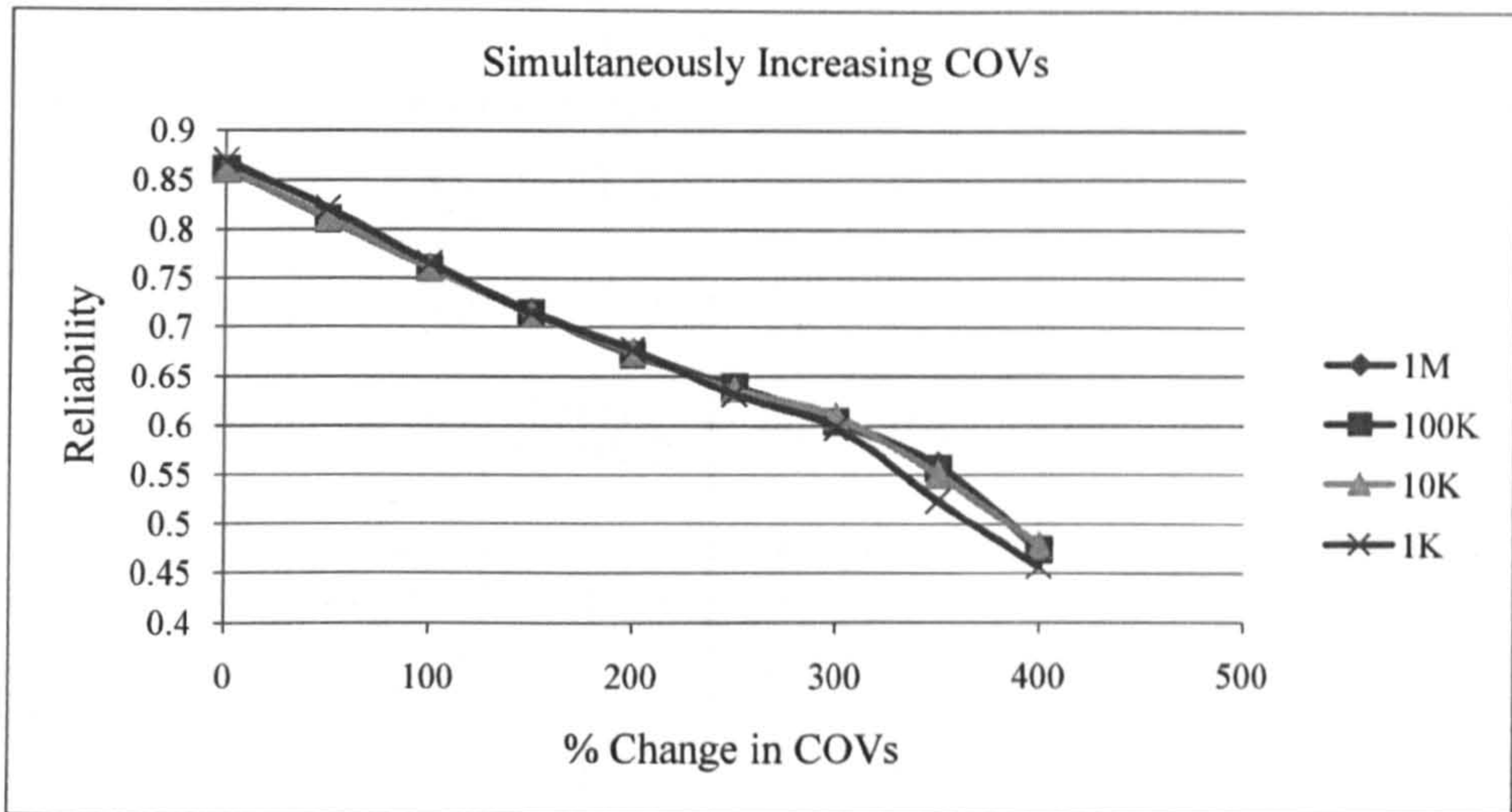


Figure (A.13) – Simultaneously increasing COVs.

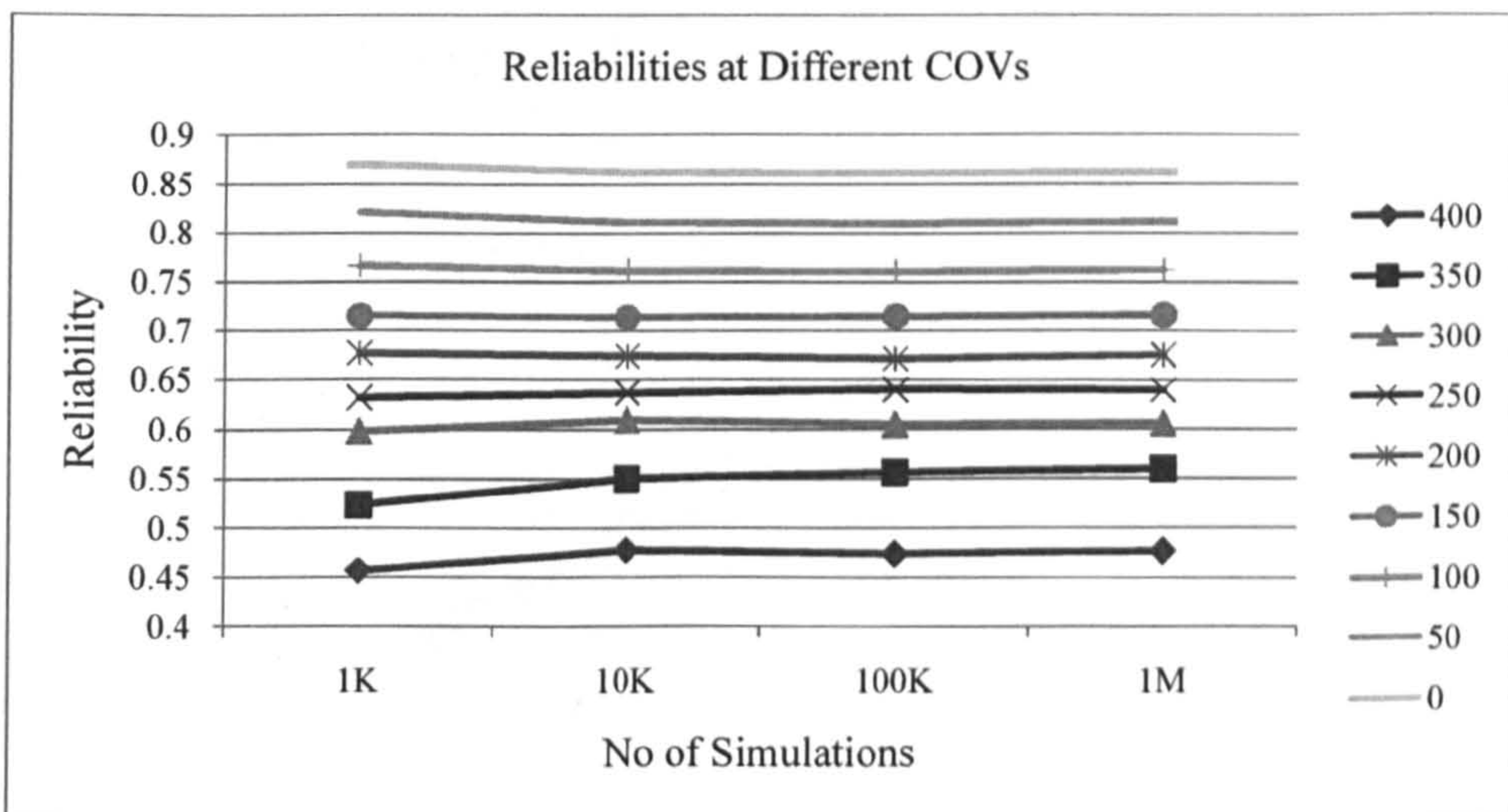


Figure (A.14) – Reliabilities at different COVs.

Case 4:

Reliability values obtained at different numbers of simulations while simultaneously decreasing COV (D) and COV (R).

Coefficient of Variation status				Reliability per no of simulations				Average
COV (D)	% change in COV(D)	COV (R)	% change in COV(R)	1K	10K	100K	1M	
0.08	0	0.06	0	0.87	0.8621	0.86107	0.861762	0.863733
0.07	-12.5	0.0525	-12.5	0.88	0.8731	0.87288	0.874006	0.8749965
0.06	-25	0.045	-25	0.889	0.8836	0.88493	0.885818	0.885837
0.05	-37.5	0.0375	-37.5	0.9	0.8949	0.8958	0.896948	0.896912
0.04	-50	0.03	-50	0.913	0.9045	0.90613	0.907178	0.907702
0.03	-62.5	0.0225	-62.5	0.925	0.9161	0.91551	0.916224	0.9182085
0.02	-75	0.015	-75	0.933	0.924	0.92273	0.923326	0.925764
0.01	-87.5	0.0075	-87.5	0.939	0.9285	0.92823	0.928334	0.931016
0	-100	0	-100	0.94	0.9309	0.93029	0.929768	0.9327395

Table (A.3) – COV(D) decreasing; COV(R) decreasing.

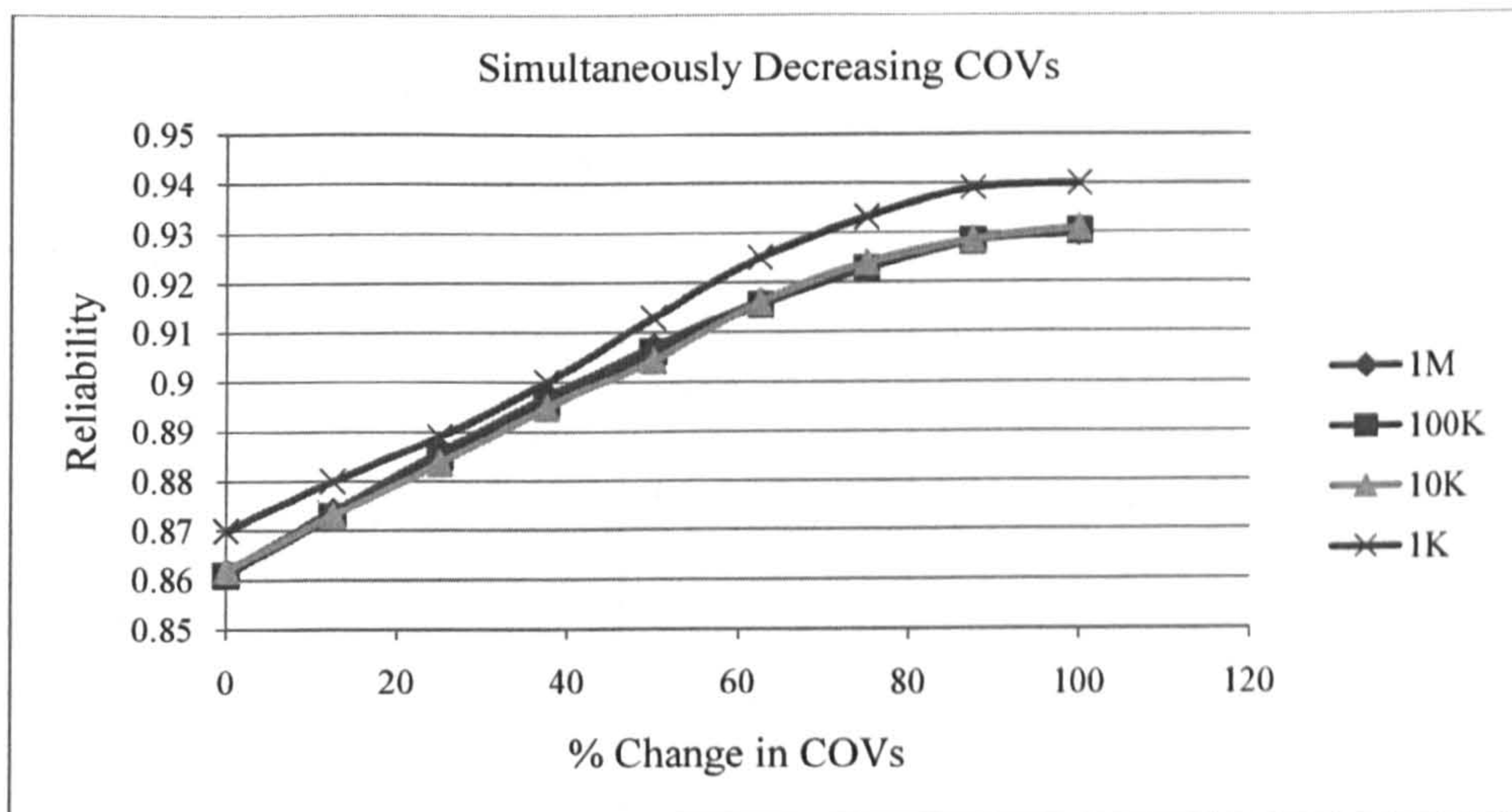


Figure (A.15) – Simultaneously decreasing COVs.

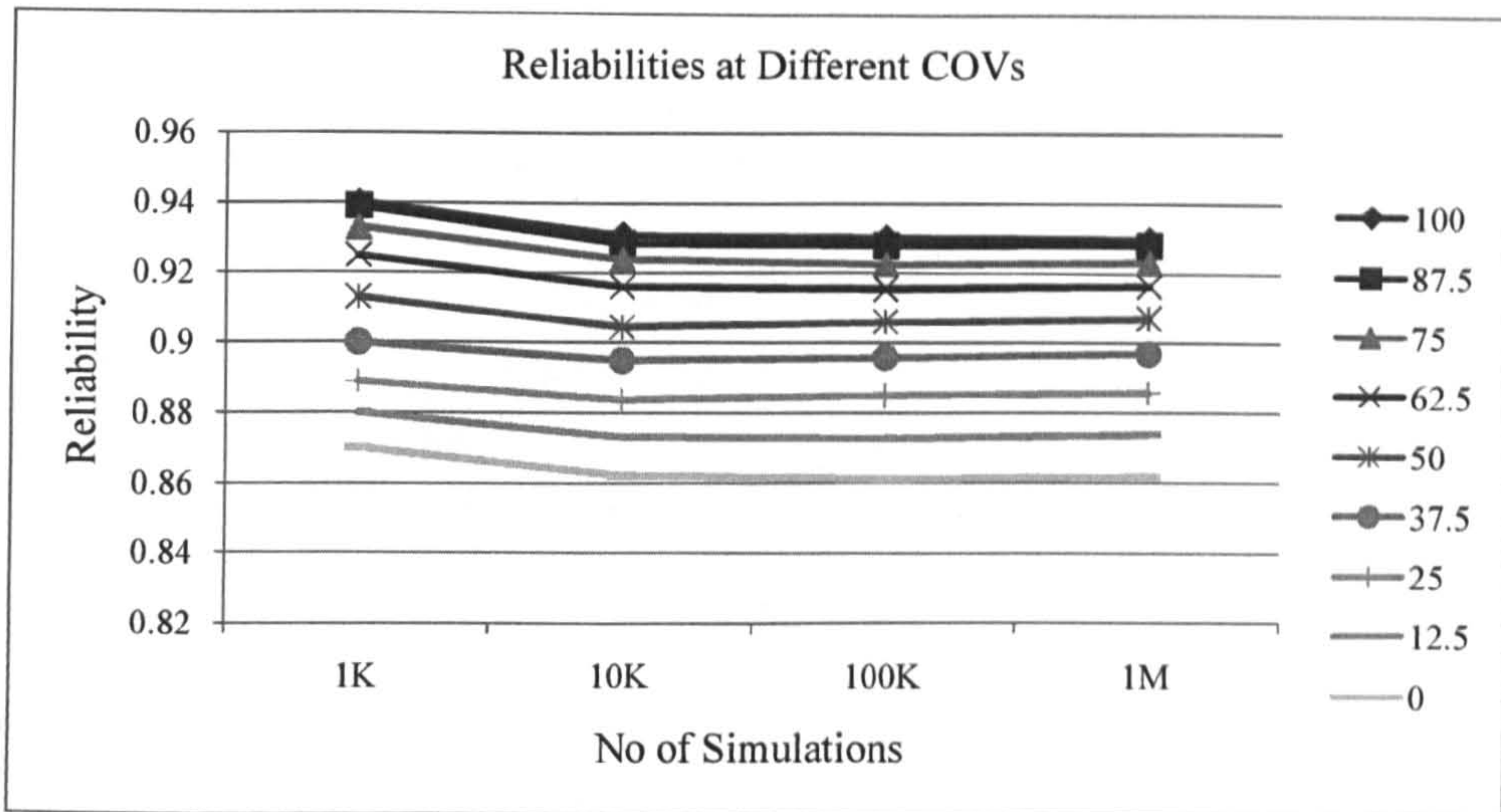


Figure (A.16) – Reliabilities at different COVs.

Case 5:

Reliability values obtained at different numbers of simulations while keeping COV (R) constant and decreasing COV (D).

Coefficient of Variation status			Reliability per no of simulations				Average
COV (D)	% change in COV(D)	COV (R)	1K	10K	100K	1M	
0.08	0	0.06	0.87	0.8621	0.86107	0.861762	0.863733
0.07	-12.5	0.06	0.877	0.8716	0.8728	0.873529	0.87373225
0.06	-25	0.06	0.889	0.8833	0.8842	0.884945	0.88536125
0.05	-37.5	0.06	0.9	0.8934	0.89488	0.895566	0.8959615
0.04	-50	0.06	0.912	0.9028	0.90473	0.905025	0.90613875
0.03	-62.5	0.06	0.919	0.9107	0.9129	0.913249	0.91396225
0.02	-75	0.06	0.923	0.9192	0.91965	0.919876	0.9204315
0.01	-87.5	0.06	0.93	0.9242	0.925	0.924426	0.9259065
0	-100	0.06	0.934	0.9267	0.92727	0.92641	0.928595

Table (A.4) – COV(R) constant; COV(D) decreased.

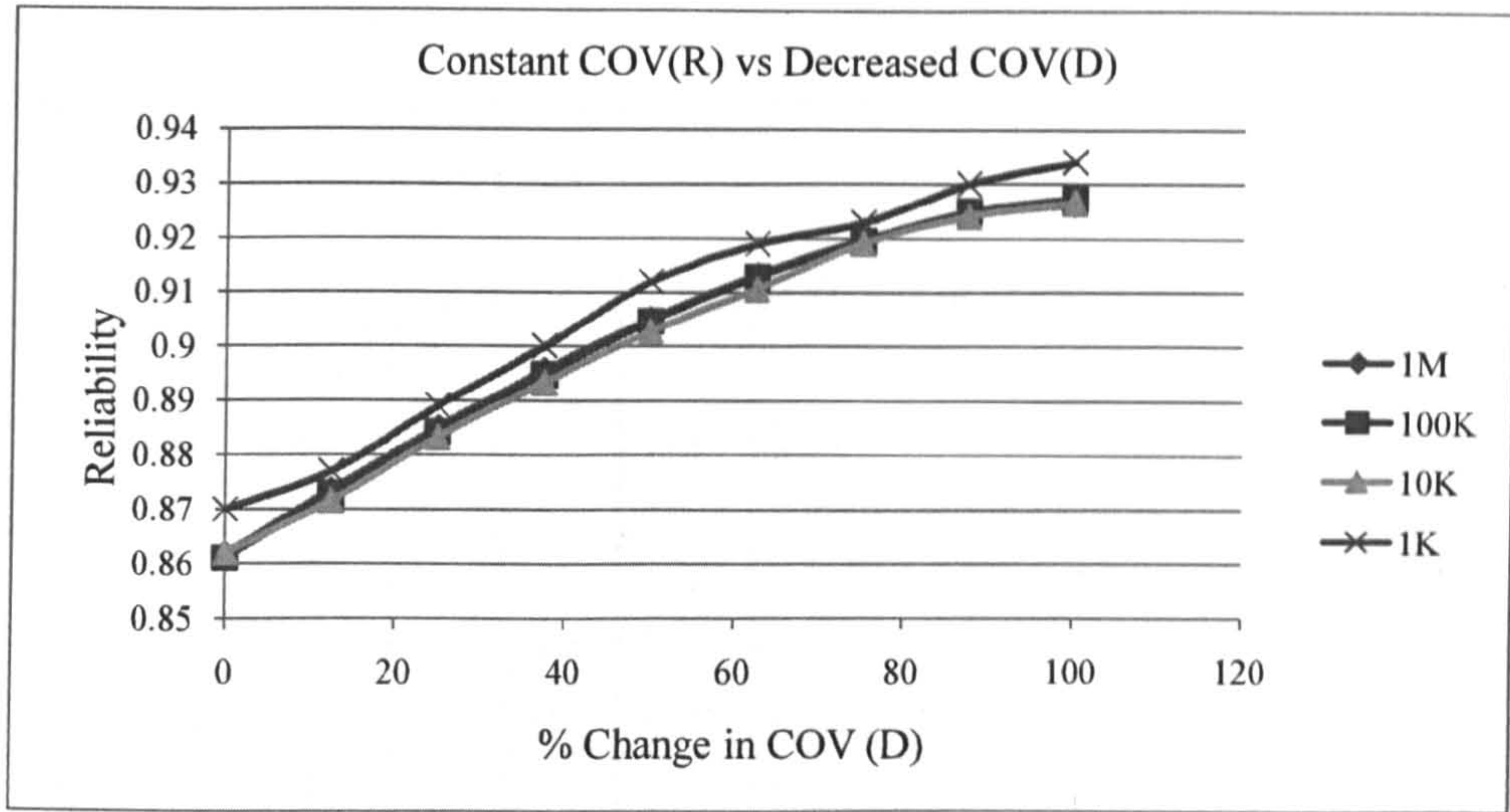


Figure (A.17) – Constant COV(R) vs. decreased COV(D).

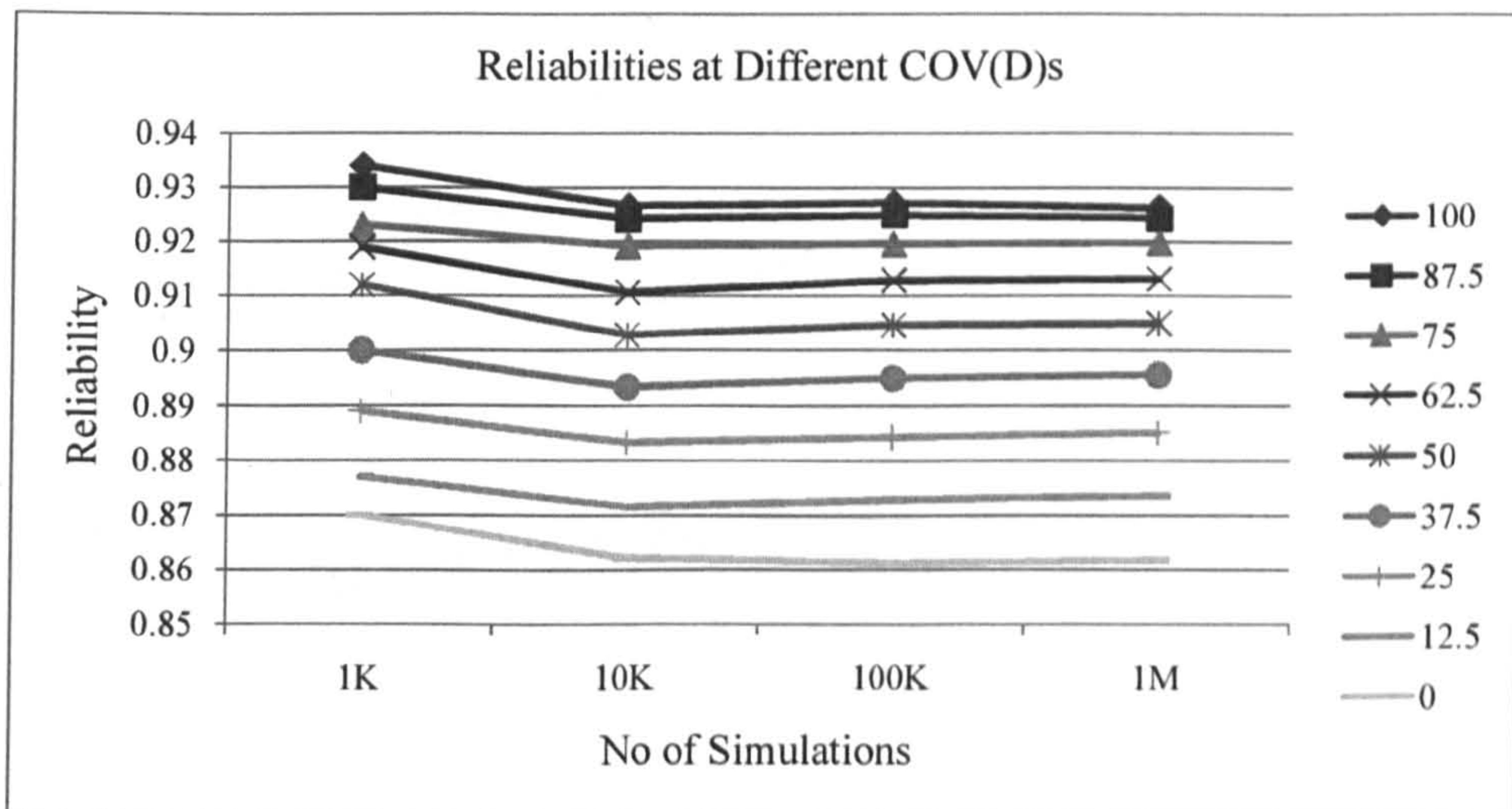


Figure (A.18) – Reliabilities at different COV(D)s.

Case 6:

Reliability values obtained at different numbers of simulations while keeping COV (D) constant and decreasing COV (R).

Coefficient of Variation status			Reliability per no of simulations				Average
COV (D)	COV (R)	% change in COV(R)	1K	10K	100K	1M	
0.08	0.06	0	0.87	0.8621	0.86107	0.861762	0.863733
0.08	0.0525	-12.5	0.872	0.8624	0.86136	0.862181	0.86448525
0.08	0.045	-25	0.874	0.8629	0.8617	0.862545	0.86528625
0.08	0.0375	-37.5	0.871	0.8631	0.86204	0.862959	0.86477475
0.08	0.03	-50	0.871	0.8634	0.86263	0.863237	0.86506675
0.08	0.0225	-62.5	0.872	0.8642	0.86298	0.863412	0.865648
0.08	0.015	-75	0.873	0.8633	0.86307	0.863621	0.86574775
0.08	0.0075	-87.5	0.871	0.8632	0.86324	0.86369	0.8652825
0.08	0	-100	0.868	0.8631	0.8631	0.863728	0.864482

Table (A.5) – COV(D) constant; COV(R) decreased.

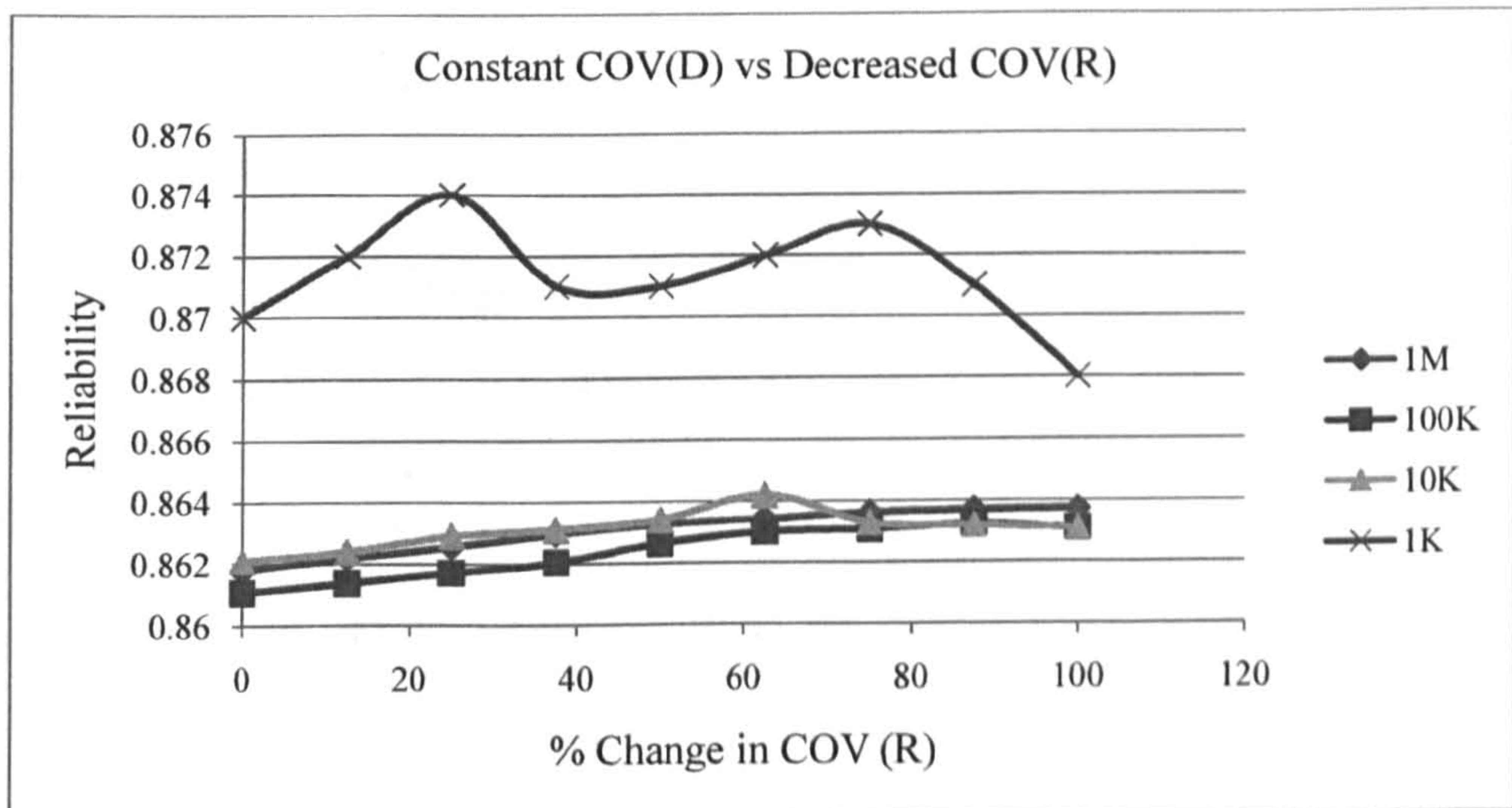


Figure (A.19) – Constant COV(D) vs. decreased COV(R).

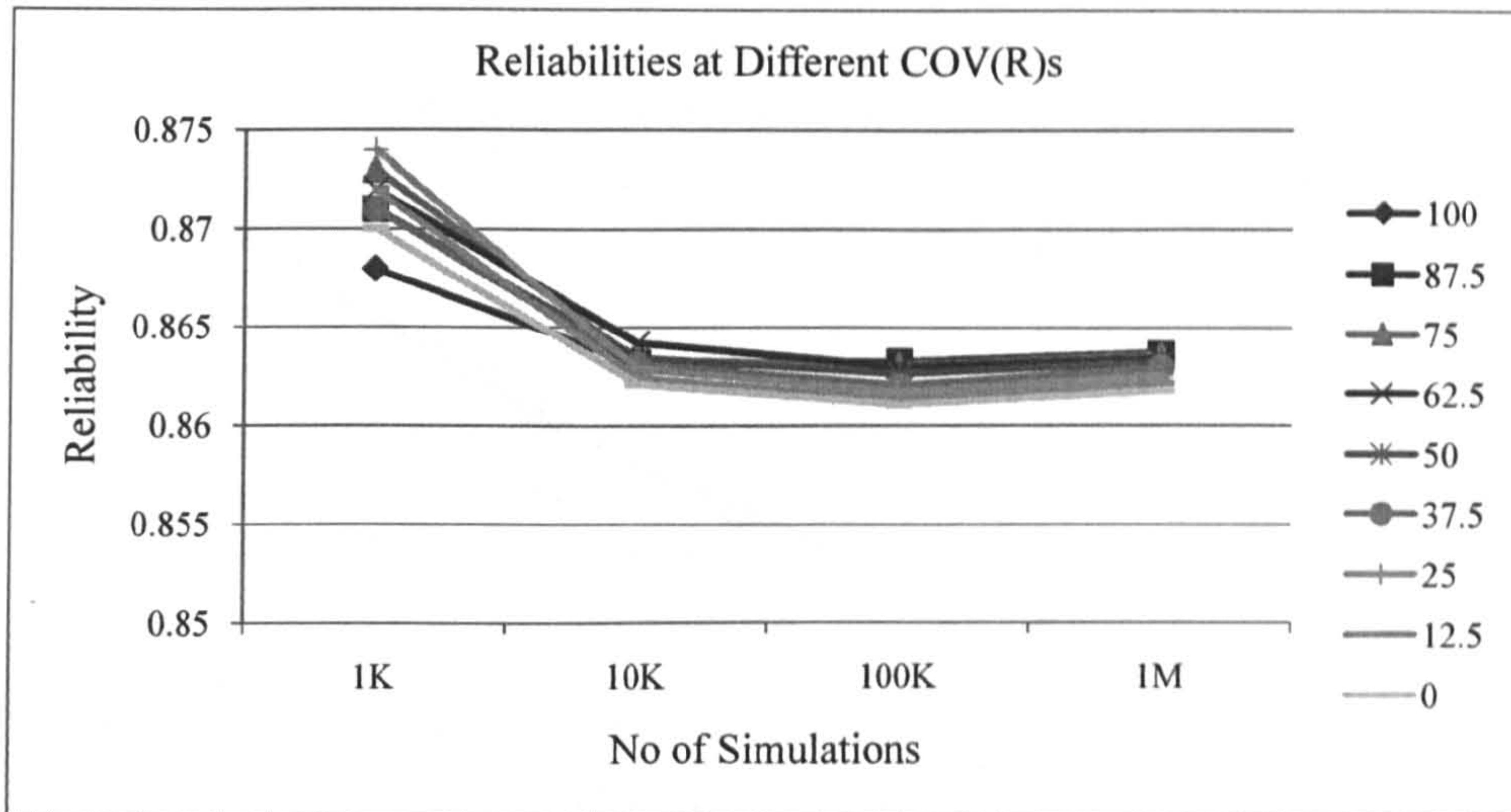


Figure (A.20) – Reliabilities at different COVs.

Case 7:

Reliability values obtained at different numbers of simulations while decreasing COV (R) and increasing COV (D).

Coefficient of Variation status				Reliability per no of simulations				Average
COV (D)	% change in COV(D)	COV (R)	% change in COV(R)	1K	10K	100K	1M	
0.08	0	0.06	0	0.87	0.8621	0.86107	0.861762	0.863733
0.12	50	0.0525	-12.5	0.82	0.8111	0.81116	0.812972	0.813808
0.16	100	0.045	-25	0.768	0.7648	0.76211	0.764119	0.76475725
0.2	150	0.0375	-37.5	0.722	0.7166	0.71603	0.718065	0.71817375
0.24	200	0.03	-50	0.677	0.6723	0.6728	0.675463	0.67439075
0.28	250	0.0225	-62.5	0.635	0.6337	0.63438	0.637597	0.63516925
0.32	300	0.015	-75	0.604	0.599	0.60639	0.605108	0.6036245
0.36	350	0.0075	-87.5	0.568	0.5702	0.57685	0.576243	0.57282325
0.4	400	0	-100	0.546	0.5444	0.55109	0.552002	0.548373

Table (A.6) – COV(D) increased; COV(R) decreased.

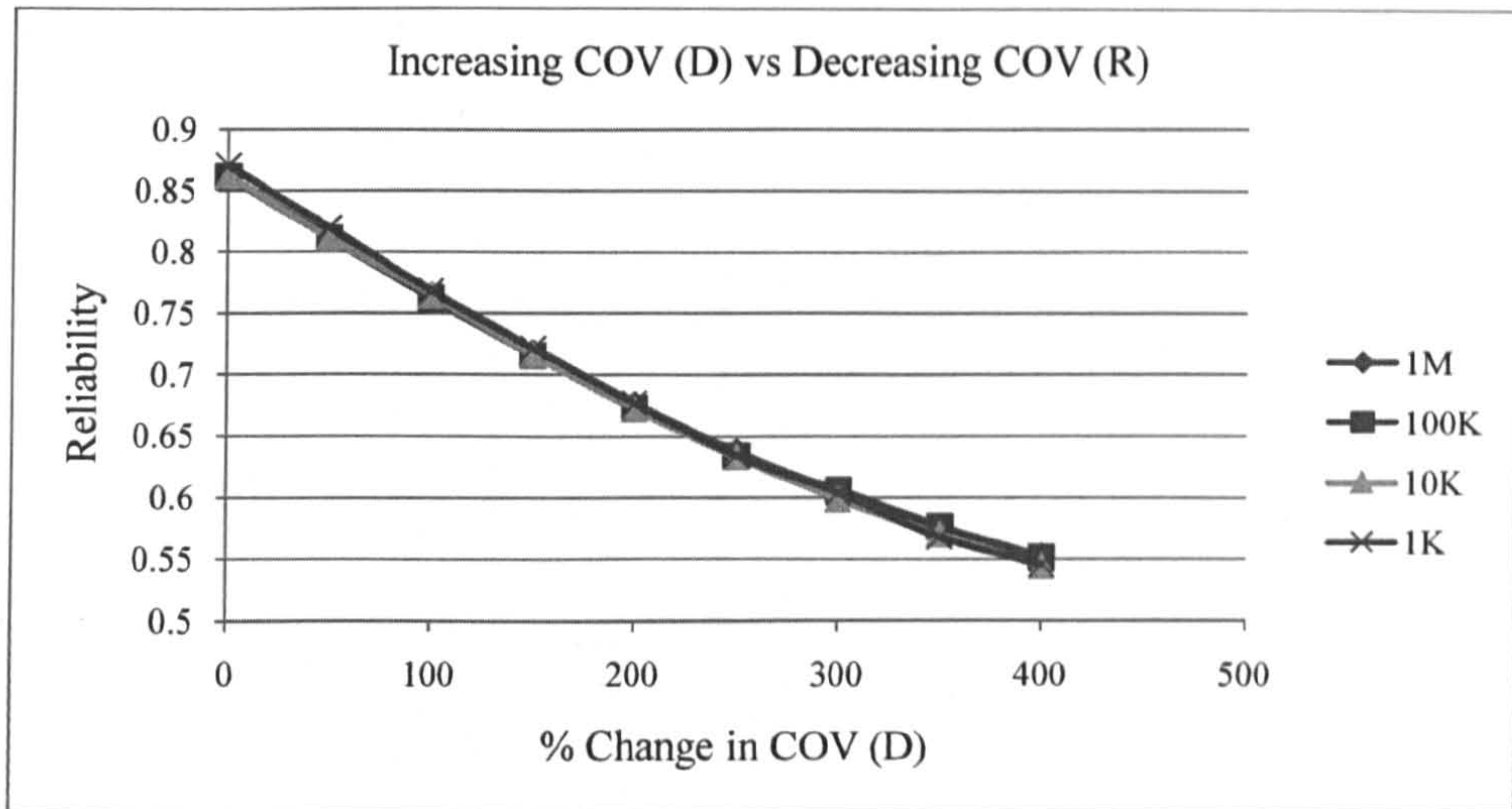


Figure (A.21) – Increasing COV(D) vs. decreasing COV(R).

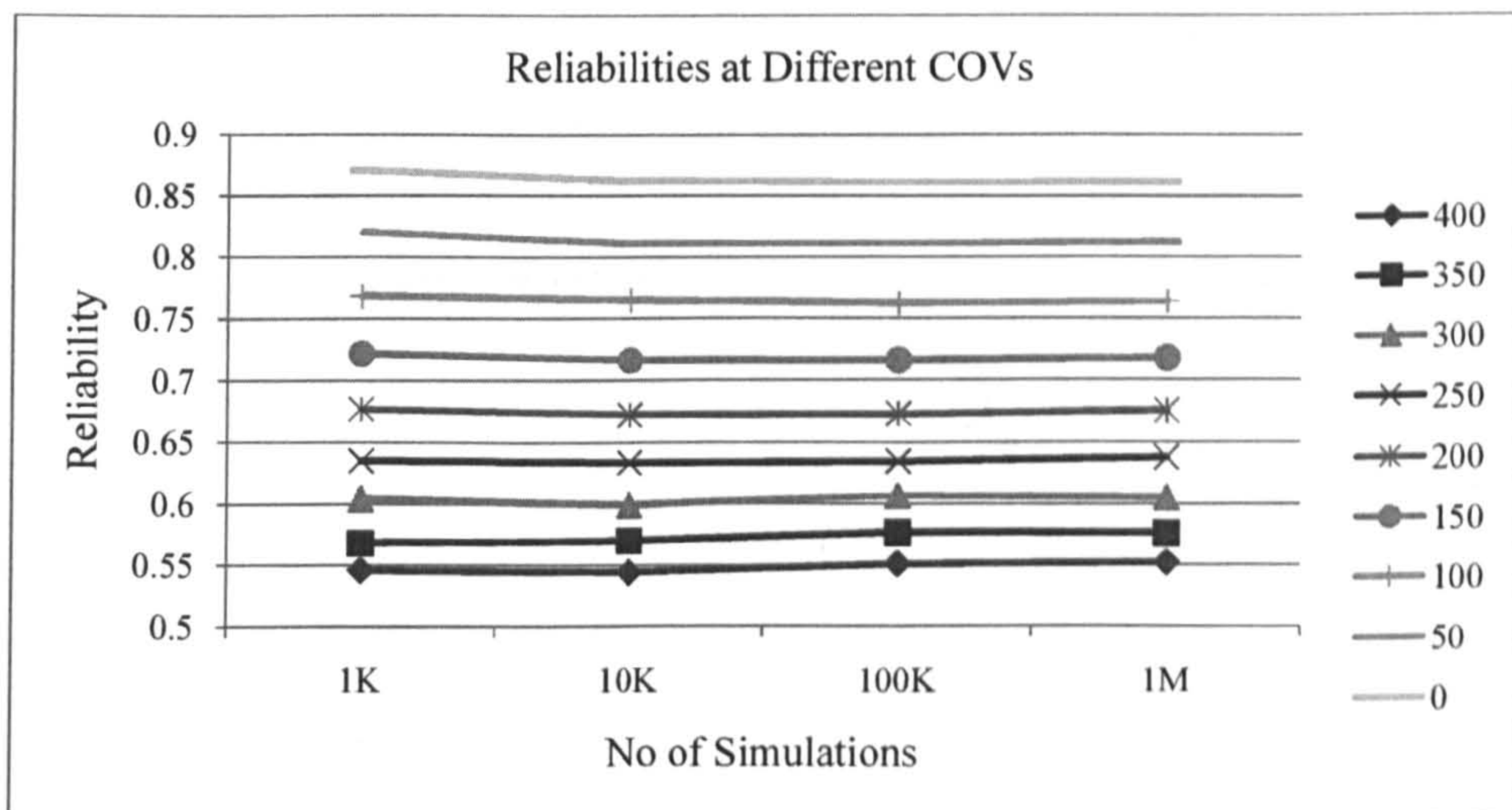


Figure (A.22) – Reliabilities at different COVs.



Case 8:

Reliability values obtained at different numbers of simulations while decreasing COV (D) and increasing COV (R).

Coefficient of Variation status				Reliability per no of simulations				Average
COV (D)	% change in COV(D)	COV (R)	% change in COV(R)	1K	10K	100K	1M	
0.08	0	0.06	0	0.87	0.8621	0.86107	0.861762	0.863733
0.07	-12.5	0.09	50	0.877	0.8703	0.87083	0.871175	0.87232625
0.06	-25	0.12	100	0.885	0.8765	0.87828	0.878331	0.87952775
0.05	-37.5	0.15	150	0.888	0.8811	0.88338	0.883016	0.883874
0.04	-50	0.18	200	0.887	0.8841	0.88636	0.885428	0.885722
0.03	-62.5	0.21	250	0.883	0.8794	0.88413	0.884319	0.88271225
0.02	-75	0.24	300	0.861	0.8747	0.8754	0.875859	0.87173975
0.01	-87.5	0.27	350	0.828	0.8349	0.83941	0.839983	0.83557325
0	-100	0.3	400	0.717	0.7325	0.73667	0.738105	0.73106875

Table (A.7) – COV(D) decreased; COV(R) increased.

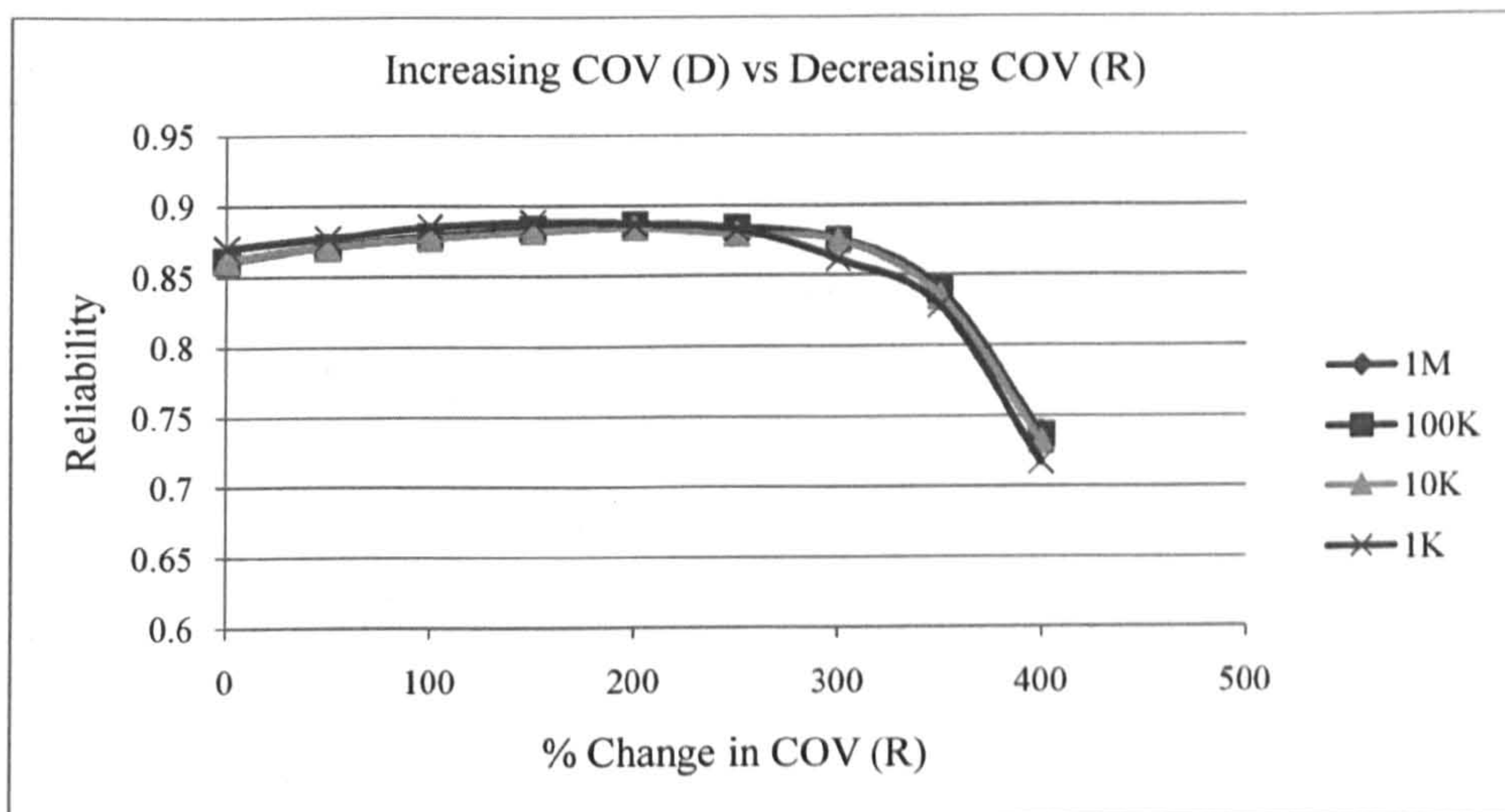


Figure (A.23) – Increasing COV(D) vs. decreasing COV(R).

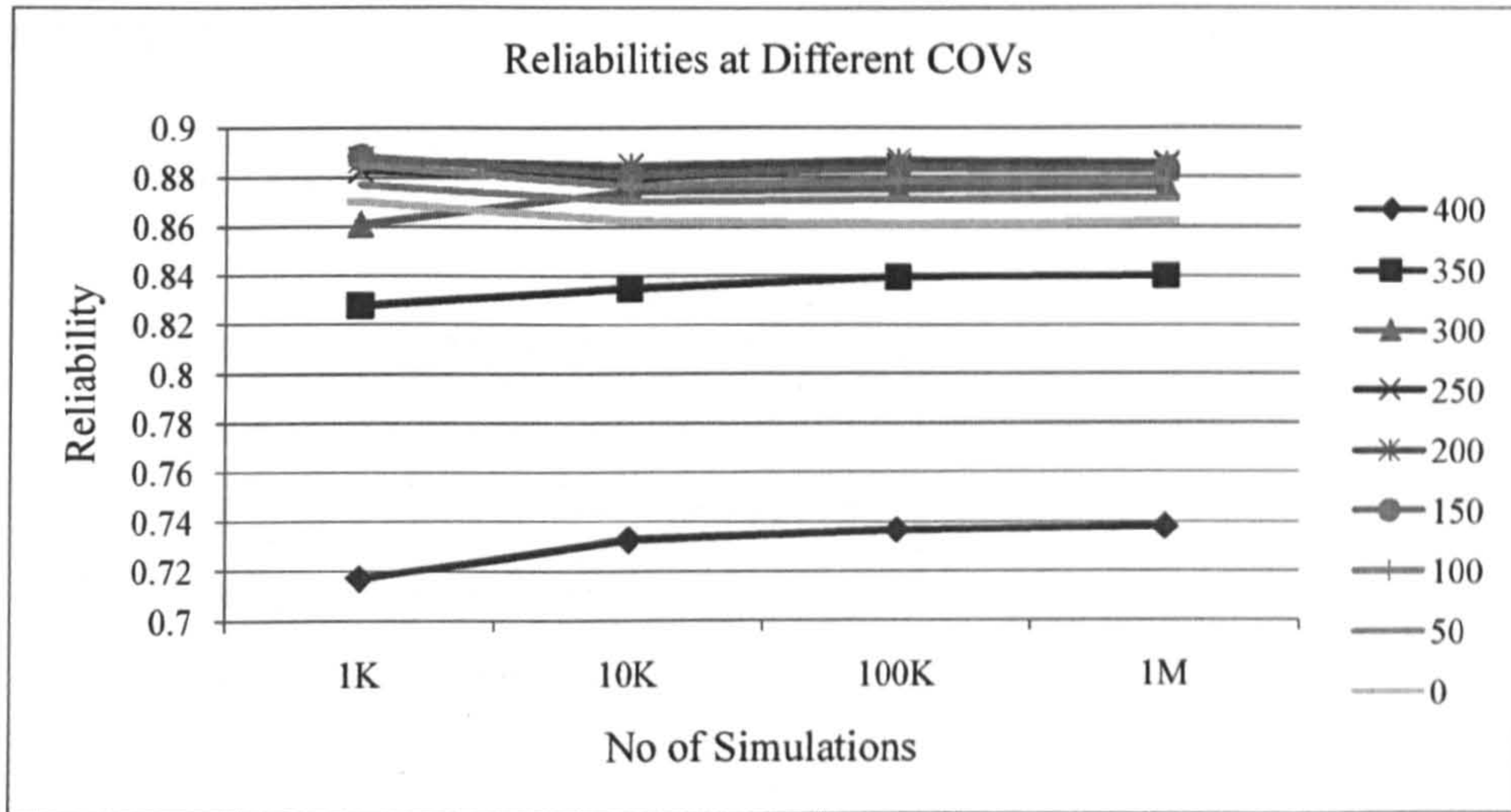


Figure (A.24) – Reliabilities at different COVs.

Appendix A.4

Crane Configuration 1:

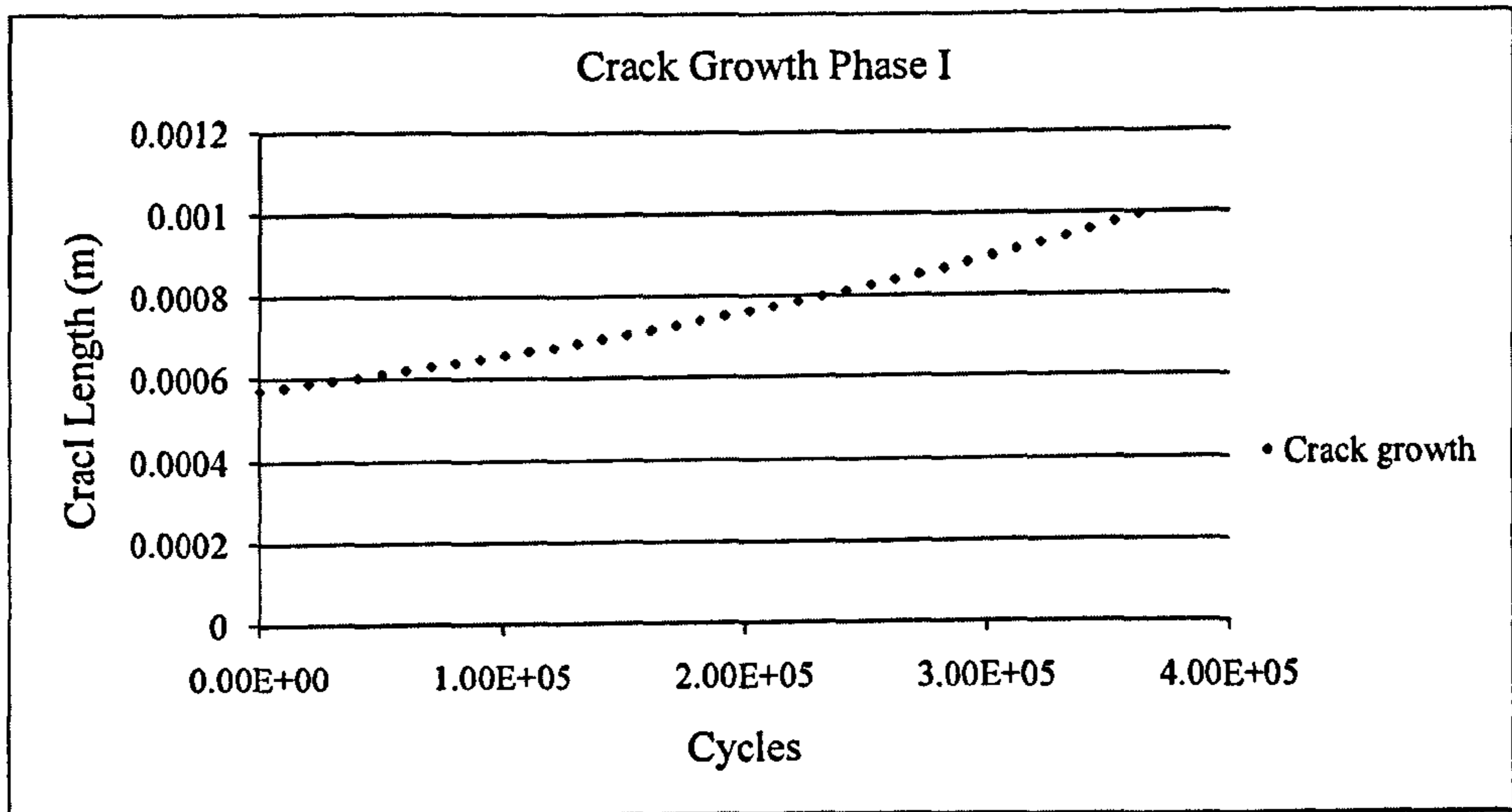


Figure (A.25) – Crack propagation phase 1.

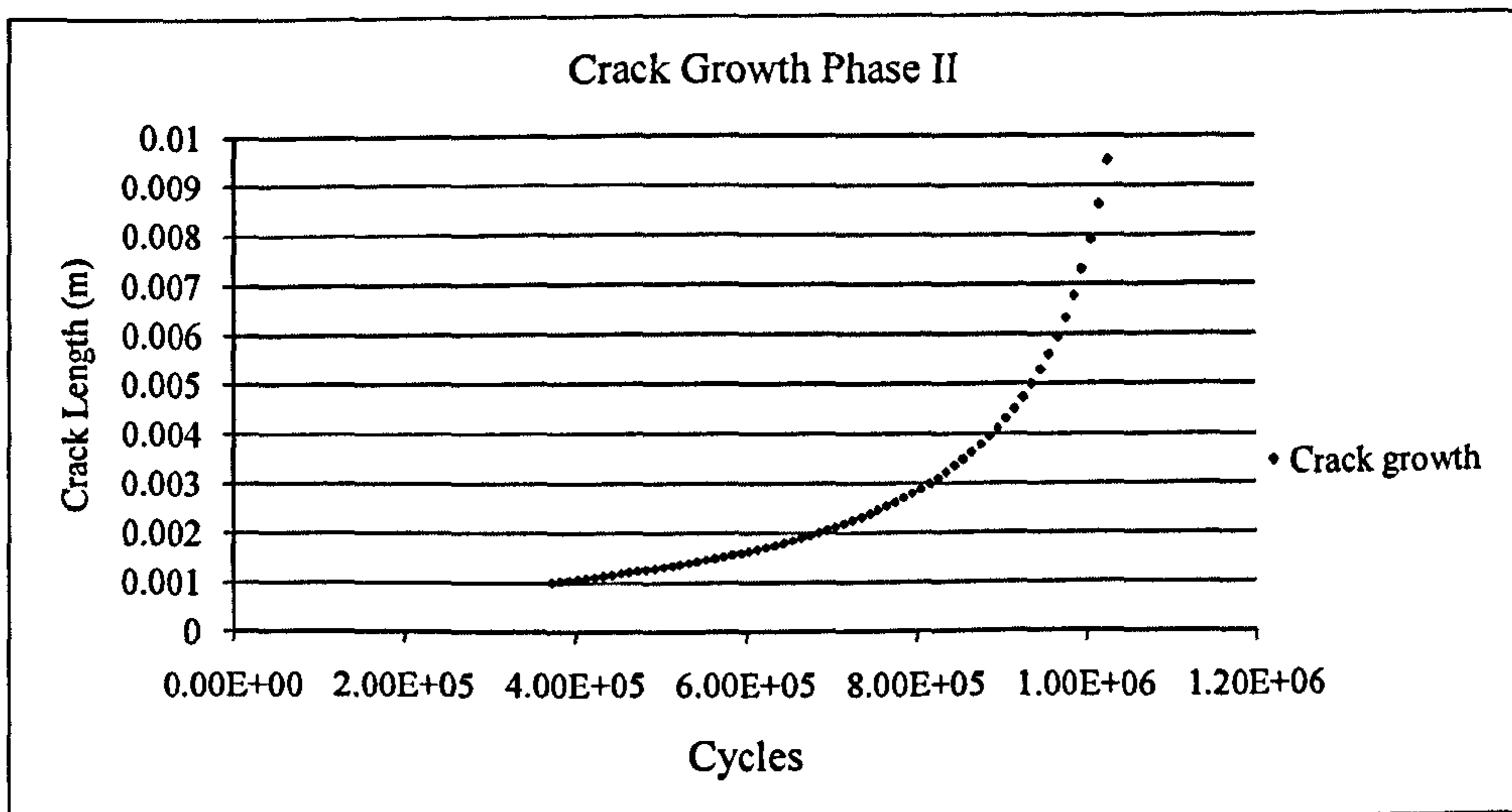


Figure (A.26) – Crack propagation phase 2.

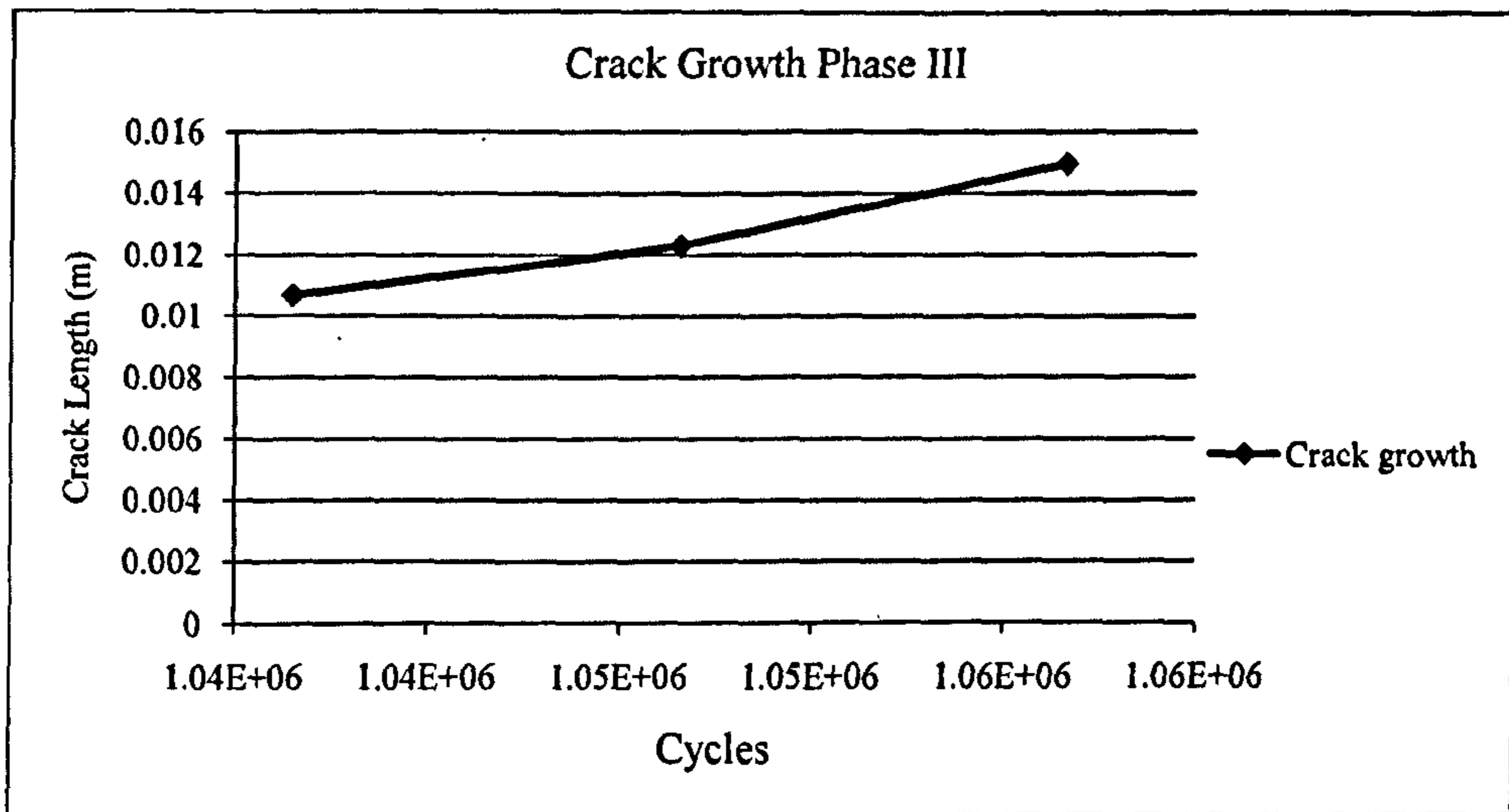


Figure (A.27) – Crack propagation phase 3.

Crane Configuration 2:

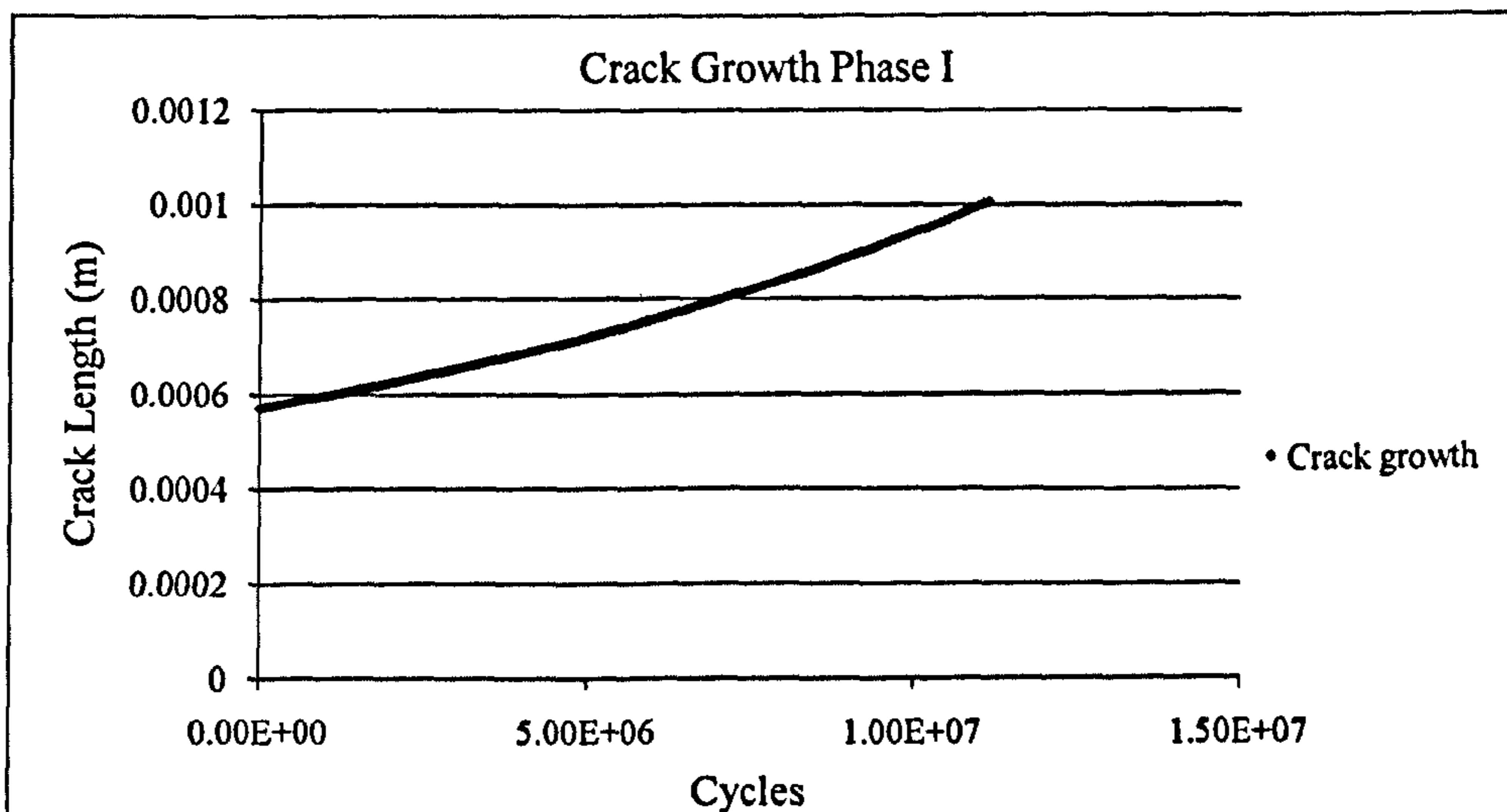


Figure (A.28) – Crack propagation phase 1.

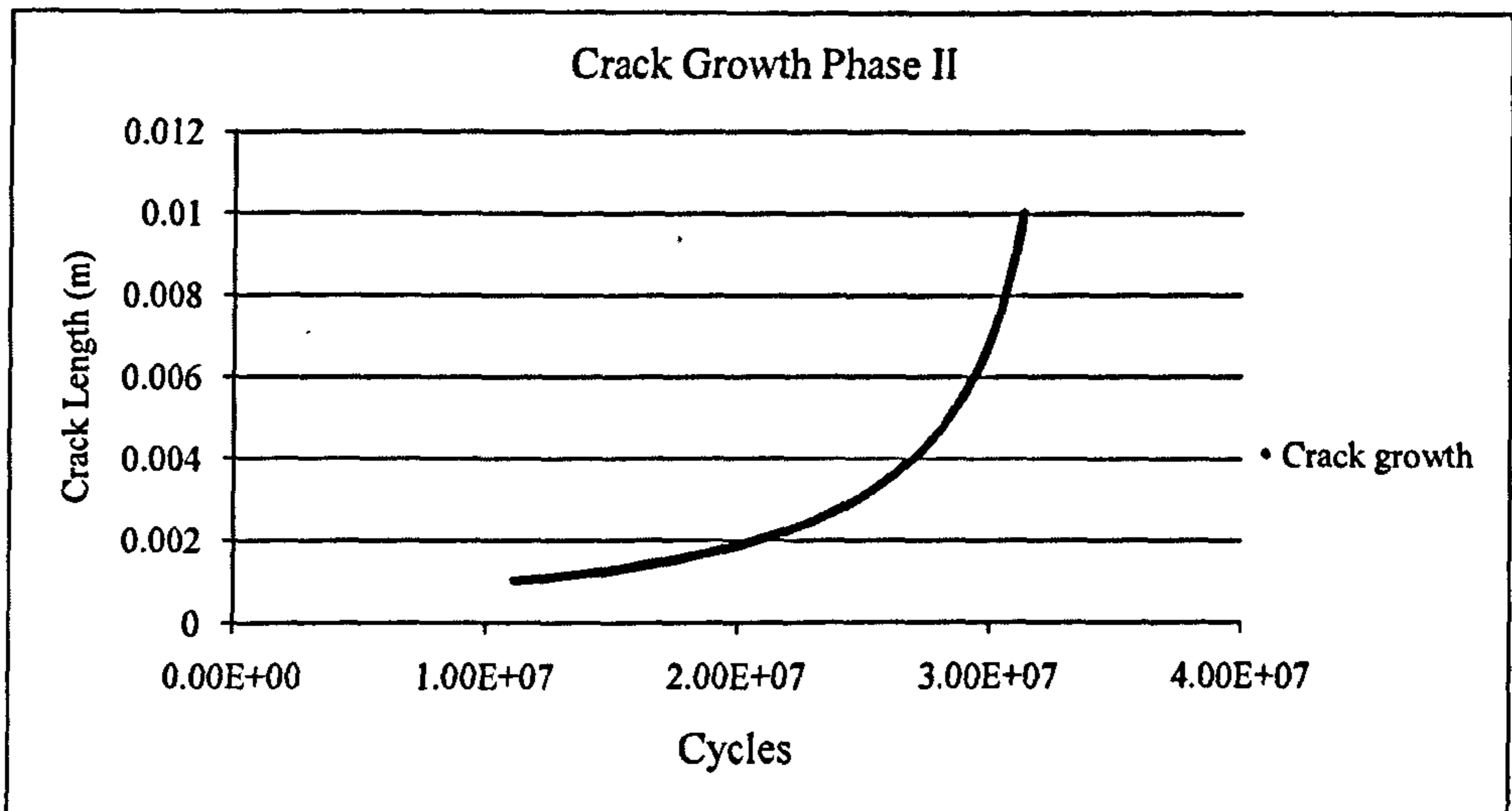


Figure (A.29) – Crack propagation phase 2.

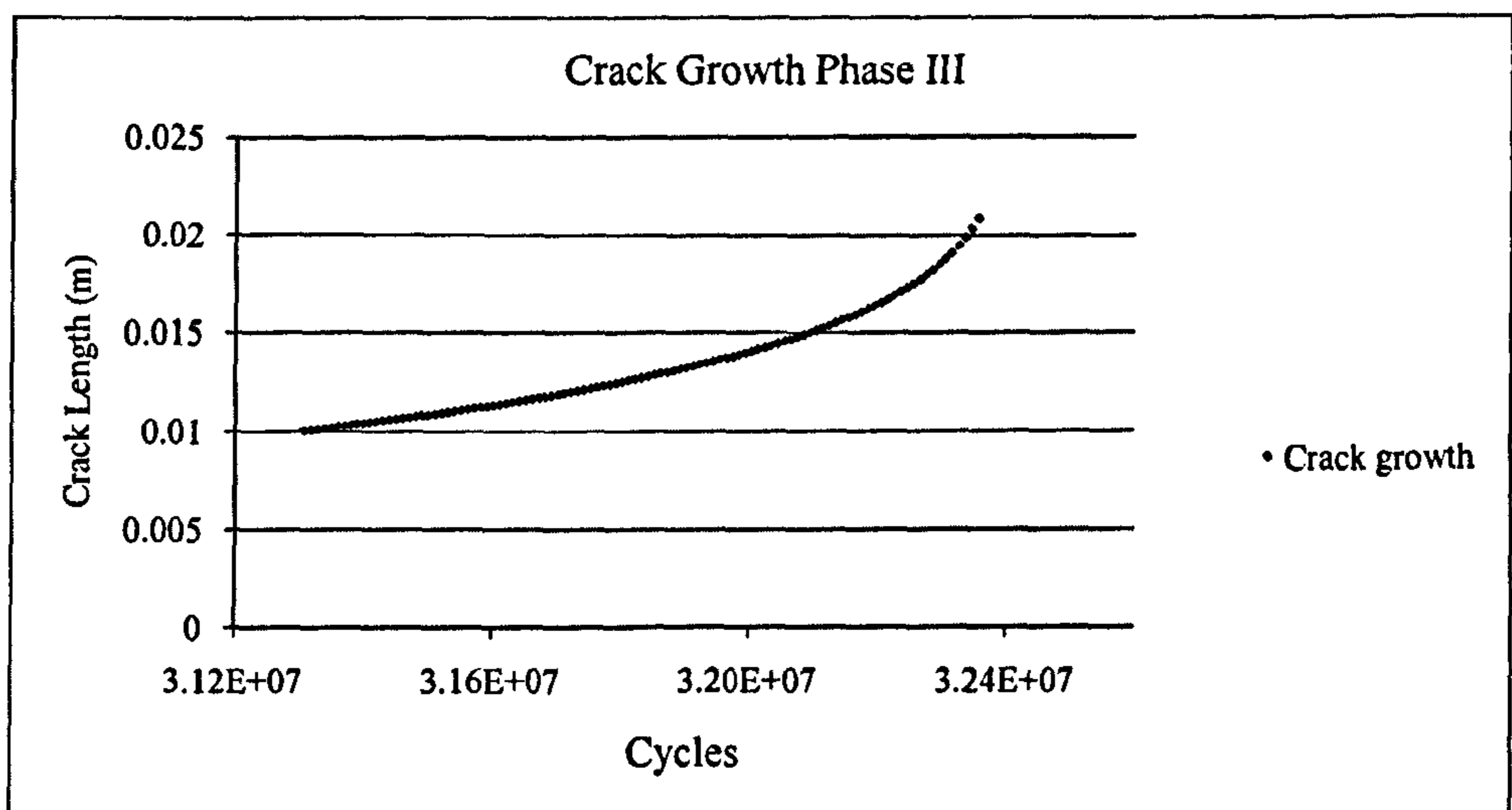


Figure (A.30) – Crack propagation phase 3.

Crane Configuration 3:

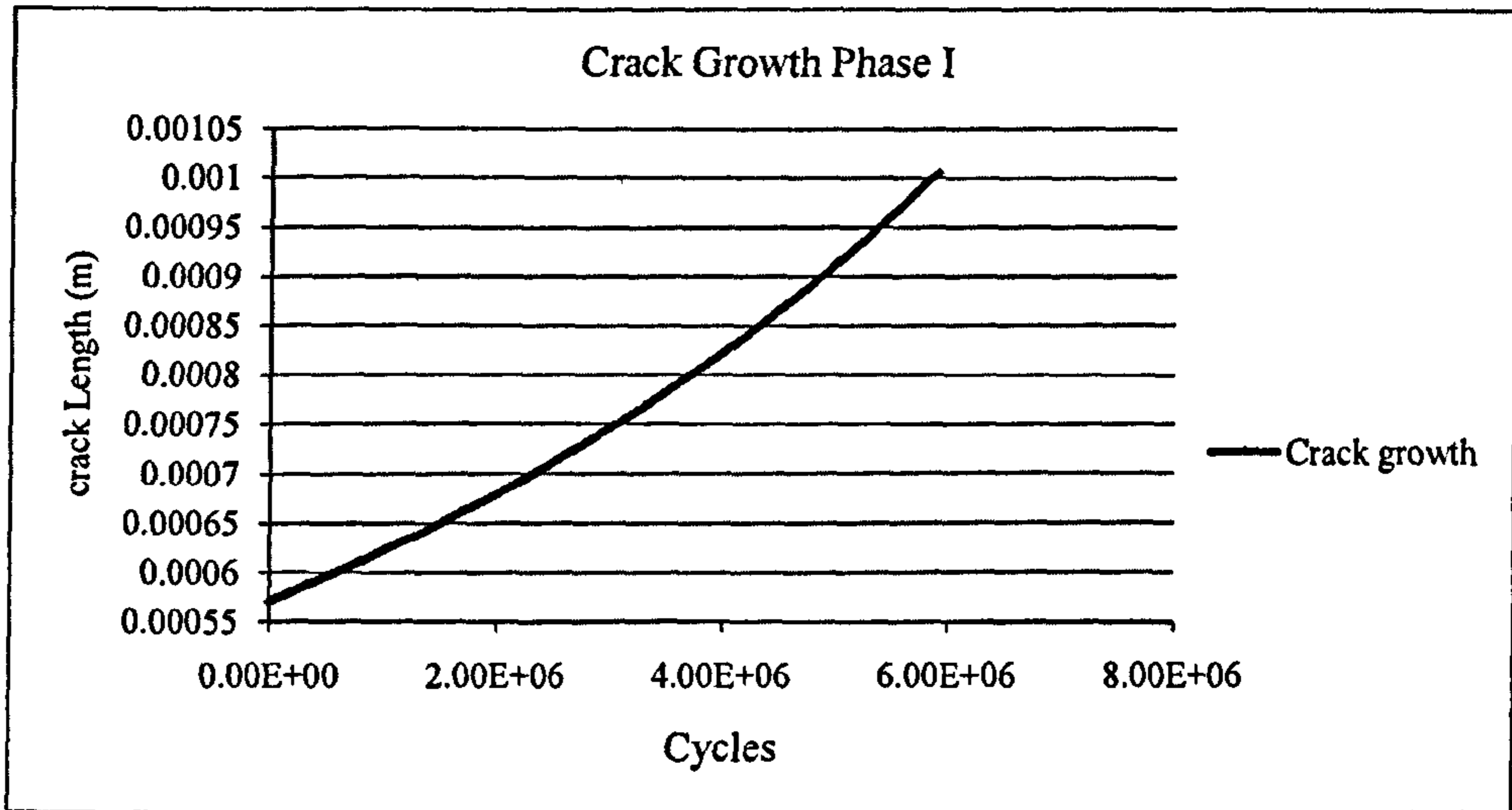


Figure (A.32) – Crack propagation phase 1.

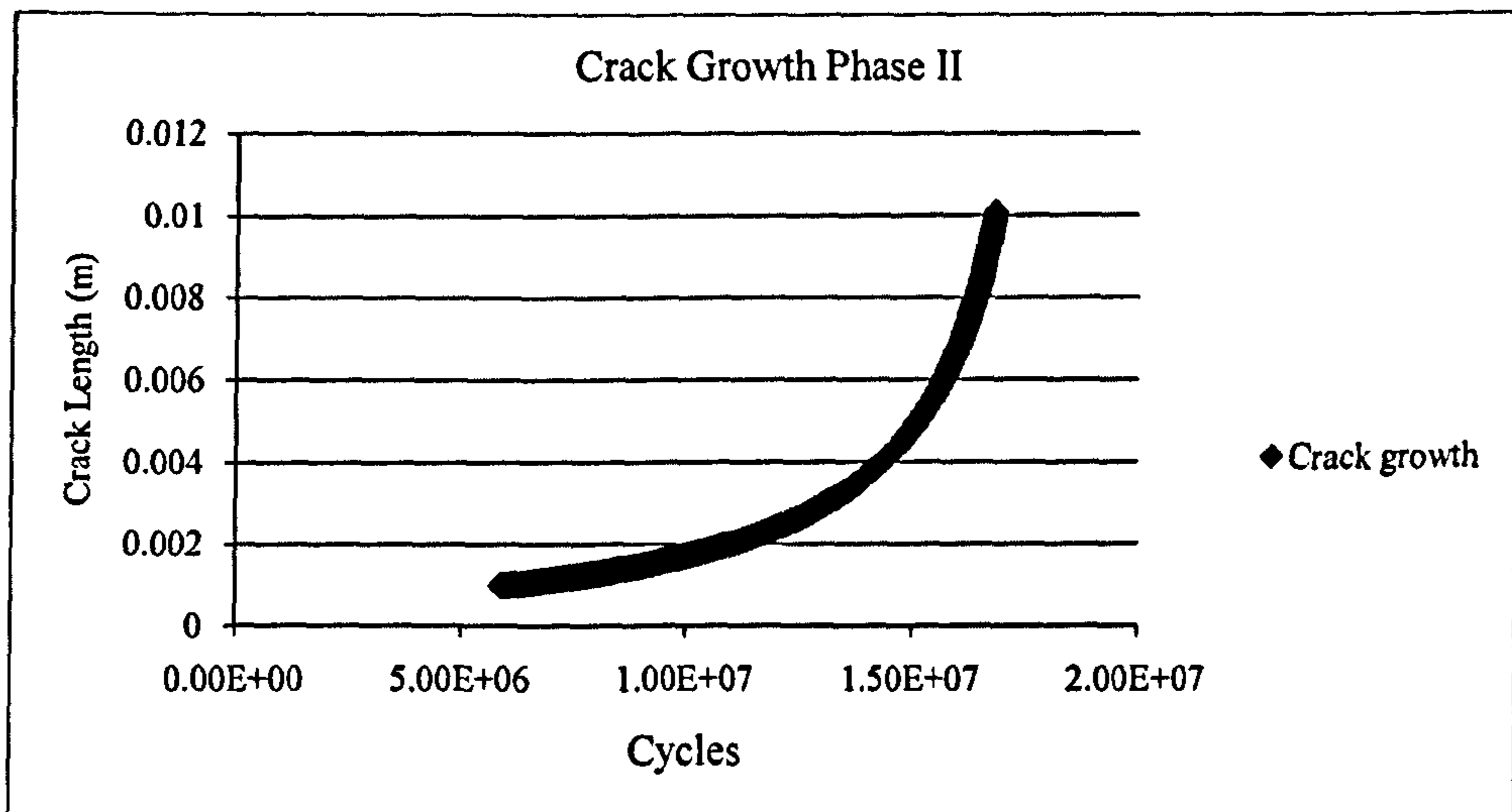


Figure (A.33) – Crack propagation phase 2.

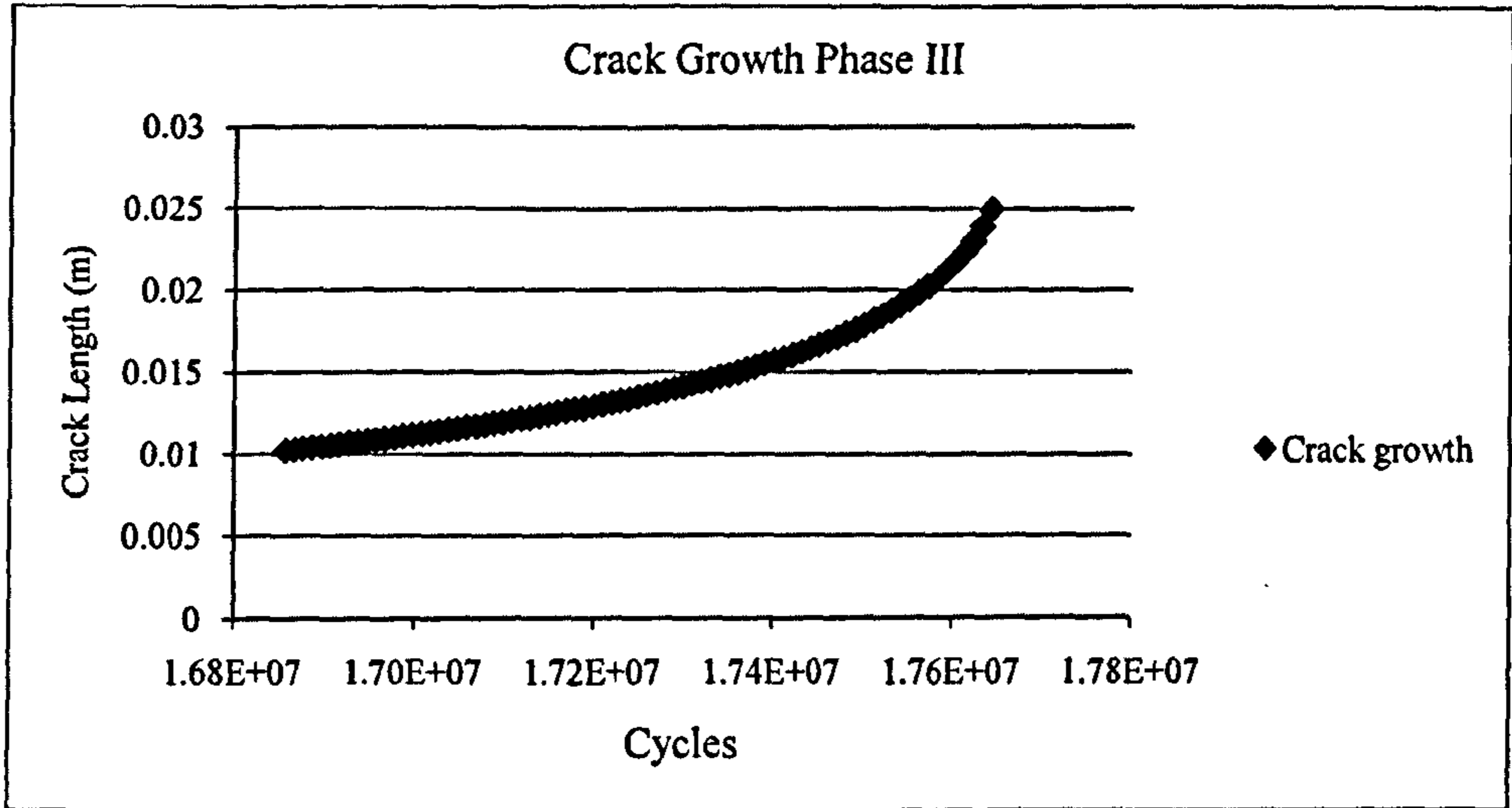


Figure (A.34) – Crack propagation phase 3.

## Appendix B

### Appendix B.1

```

C:\Users\dude\Documents\Visual Studio 2008\Projects\FLEXSTREM_V2(FINAL)\FLEXSTREM_V2(FINA...
Enter analysis type: SINGLE MEMBERED STRUCTURE or MULTI-MEMBERED STRUCTURE
1
2
The system is NOT diagonally dominant
STRUCTURAL MASS = 41643.0706062317
END OF FEA BLOCK SUBROUTINE
    
```

```

!*****
! PROGRAM: FLEXSTREM
! PURPOSE: TO CARRY OUT A DETAILED RELIABILITY ANALYSIS OF A STRUCTURE.
! DATE PROGRAMMER DESCRIPTION OF CHANGE
! =====
! 22-10-2010 ECHEZONA CHUKWUKA FINAL VERSION
!*****
PROGRAM FLEXSTREM
IMPLICIT NONE
!=====STRUCTURAL PARAMETERS=====
REAL(8)::FY, FT, K, WS, EE, MAX_RL, BETA, D_LOAD, AI, M_PWR,&
C_MAT, WF_LD, DECT_CRACK, DENS
INTEGER:: NODE, NEL, N_PL, NN, MEMBER, JOINT
!=====FEA VARIABLES=====
REAL(8):: MEM_LEN, H, W, D_G, I_MNT, C_A, TM
REAL(8),ALLOCATABLE, DIMENSION(:):: DIA, AREA, THK
REAL(8),ALLOCATABLE, DIMENSION(:):: TLEN, TEN, SLEN
REAL(8),ALLOCATABLE, DIMENSION(:)::ND_STR,N_THK,N_DIA
!=====MECH ANALYSES VARIABLES=====
REAL(8)::SF, W_FORCE, OMEGA, D_BEND, D_COMPRESS, D_TENSILE,&
MUL_STR
!=====FRAC ANALYSES VARIABLES=====
REAL(8)::AF, KRANS, A_CR, K_LOAD
!=====GEN & SIM VARS=====
INTEGER(8), PARAMETER::N1 = 10000
REAL(8)::POF, REL
CHARACTER::TITLE
INTEGER::J
INTEGER::Z, FLEX_TYPE
INTEGER::BEND_COUNTER, TENS_COUNTER, COMP_COUNTER,&
MULSTR_COUNTER, MEM_COUNTER, FRAC_COUNTER, FRACT_COUNTER,&
LIFE_COUNTER, ND_LEFM_COUNTER
LOGICAL::LGC_1, LGC_2, LGC_3, LGC_4, LGC_5, LGC_6, LGC_7,&
LGC_8, LGC_9
!=====
DO
WRITE(*,*)'ENTER ANALYSIS TYPE: SINGLE MEMBERED STRUCTURE OR&
MULTI-MEMBERED STRUCTURE '
WRITE(*,*)' 1 &
2 ,
READ(*,*)Z
IF(Z == 1)THEN
FLEX_TYPE = 1
EXIT
ELSE IF(Z == 2)THEN
FLEX_TYPE = 2
EXIT
ELSE
END IF
    
```



```

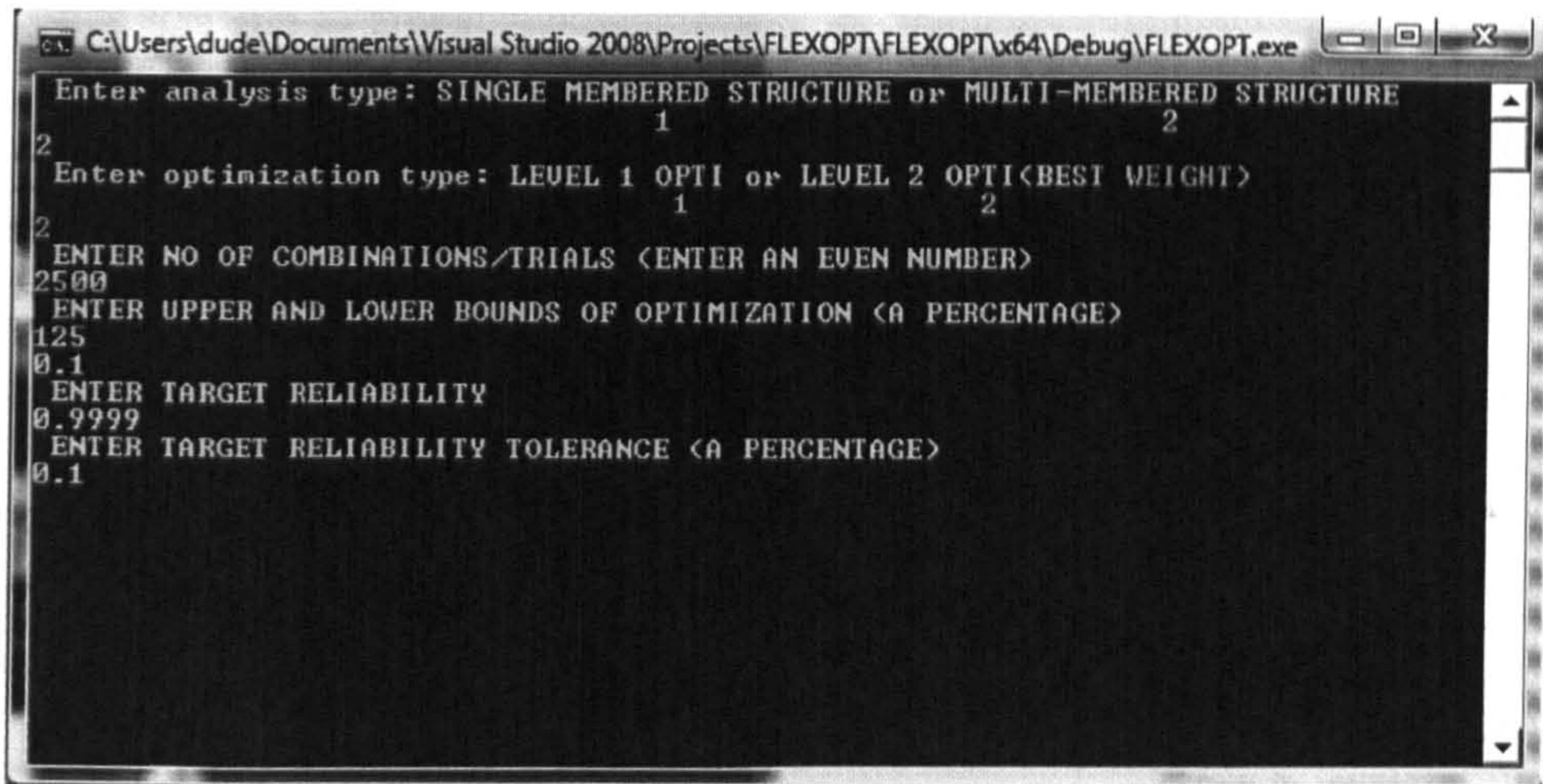
END DO
IF(FLEX_TYPE == 1)THEN
  W_FORCE = 0.
  WF_LD = 0.
  CALL SINGLE_MEM(M_PWR, FY, FT, K, EE, MAX_RL, BETA, D_LOAD,&
    AI, DECT_CRACK, N_PL, C_MAT, MEM_LEN, H,&
    I_MNT, C_A, TM)
ELSE IF(FLEX_TYPE == 2)THEN
  CALL STR_PAR(NODE, NEL, NN, M_PWR, FY, FT, K, WS, EE, WF_LD,&
    BETA, MAX_RL, AI, DECT_CRACK, N_PL, C_MAT, DENS,&
    MEMBER, JOINT)
  ALLOCATE(TLEN(NEL), TEN(NEL), SLEN(NEL), DIA(NEL), AREA(NEL),&
    THK(NEL), ND_STR(NODE), N_THK(NODE), N_DIA(NODE))
  CALL FEA_BLOCK(NODE, NEL, NN, EE, DENS, MEM_LEN, H, W, D_G,&
    TM, D_LOAD, TLEN, TEN, SLEN, DIA, AREA,&
    THK, ND_STR, N_THK, N_DIA)
  CALL TABLES_SF(MEM_LEN, H, W, D_G, SLEN, DIA, NEL, SF)
END IF
BEND_COUNTER = 0
TENS_COUNTER = 0
COMP_COUNTER = 0
MULSTR_COUNTER = 0
MEM_COUNTER = 0
FRAC_COUNTER = 0
FRACT_COUNTER = 0
LIFE_COUNTER = 0
ND_LEFM_COUNTER = 0
OPEN(20, FILE='FLEXSTREM_RESULTS.FLX')
IF(FLEX_TYPE == 1)THEN
  CALL DATREC_1
ELSE
  CALL DATREC_2(JOINT, MEMBER)
END IF
!*****START SIMULATION*****
DO J = 1, N1
!*****MECHANICAL ANALYSES*****
  WRITE(20, 230, ADVANCE='NO')J
  IF(FLEX_TYPE == 2)THEN
    CALL WIND_FORCE(WS, SF, SLEN, DIA, NEL, W_FORCE)
  ELSE
    END IF
  CALL LOAD_COMBINATION(D_LOAD, TM, OMEGA, W_FORCE, WF_LD,&
    MAX_RL)
  IF(FLEX_TYPE == 1)THEN
    CALL BENDING_STRESS(OMEGA, MEM_LEN, I_MNT, H, FY, D_BEND,&
      LGC_1)
    IF(LGC_1 == .TRUE.)THEN
      BEND_COUNTER = BEND_COUNTER + 1
      CYCLE
    ELSE
      END IF
    CALL TENSILE_STRESS(OMEGA, FT, C_A, D_TENSILE, LGC_2)
    IF(LGC_2 == .TRUE.)THEN
      TENS_COUNTER = TENS_COUNTER + 1
      CYCLE
    ELSE
      END IF
    CALL COMPRESSIVE_STRESS(OMEGA, MEM_LEN, I_MNT, C_A, EE, &
      D_COMPRESS, LGC_3)
    IF(LGC_3 == .TRUE.)THEN
      COMP_COUNTER = COMP_COUNTER + 1
      CYCLE
    ELSE
      END IF
    CALL MULTIAXIAL_STRESS(D_TENSILE, D_COMPRESS, D_BEND, FY, &
      MUL_STR, LGC_4)
    IF(LGC_4 == .TRUE.)THEN
      MULSTR_COUNTER = MULSTR_COUNTER + 1
      CYCLE
    ELSE
      END IF
    !***** FRACTURE ANALYSES*****
    CALL CRACK_LENGTH(AI, AF)
    CALL FRACT_TOUGH(MUL_STR, AF, K, BETA, K_LOAD, KRANS, &
      LGC_6)
    IF(LGC_6 == .TRUE.)THEN
      FRACT_COUNTER = FRACT_COUNTER + 1
      CYCLE
    ELSE
      END IF
    CALL MINIMUM_CRACK(MUL_STR, KRANS, BETA, A_CR)
    CALL FRAC_ANALYSIS(AF, A_CR, LGC_7)
    IF(LGC_7 == .TRUE.)THEN
      FRAC_COUNTER = FRAC_COUNTER + 1
      CYCLE
    ELSE

```

```

        END IF
        CALL LIFE_CYCLE(N_PL, C_MAT, M_PWR, BETA, MUL_STR, AI, &
                      A_CR, LGC_8)
        IF(LGC_8 == .TRUE.)THEN
            LIFE_COUNTER = LIFE_COUNTER + 1
            CYCLE
        ELSE
            END IF
            !*****MEMBER ANALYSIS(LEVEL 3)*****
        ELSE !IF(FLEX_TYPE==2)THEN
            CALL MEM_ANALYSIS(MEMBER, OMEGA, FT, EE, TLEN, AREA, DIA, &
                             THK, TEN, NEL, LGC_5)
            IF(LGC_5 == .TRUE.)THEN
                MEM_COUNTER = MEM_COUNTER + 1
                CYCLE
            ELSE
                END IF
            CALL ND_LEFM_ANALYSIS(JOINT, NODE, ND_STR, N_THK, N_DIA, EE, K, &
                                 C_MAT, M_PWR, N_PL, OMEGA, AI,
LGC_9)
            IF(LGC_9 == .TRUE.)THEN
                _COUNTER = ND_LEFM_COUNTER + 1
            ELSE
                END IF
            END IF
        END DO
        !*****END OF SIMULATION*****
        !-----DISPLAY RELIABILITY-----
        POF = (DBLE(BEND_COUNTER+TENS_COUNTER+COMP_COUNTER+MULSTR_COUNTER+&
                  MEM_COUNTER+FRACT_COUNTER+FRAC_COUNTER+LIFE_COUNTER+&
                  ND_LEFM_COUNTER)/N1)
        REL = DBLE(1.-POF)
        WRITE(20, 240)BEND_COUNTER, TENS_COUNTER, COMP_COUNTER, &
                    MULSTR_COUNTER, MEM_COUNTER, FRACT_COUNTER, FRAC_COUNTER, &
                    LIFE_COUNTER, ND_LEFM_COUNTER, REL, POF

        WRITE(*,*)REL
        STOP 'END OF ANALYSIS'
        CLOSE(20)
        230  FORMAT(1 X, I8)
        240  FORMAT(/, /, ' ', 'BEND_COUNTER = ', I4, /, 1 X, 'TENS_COUNTER =&
        ', I4, /, 1 X, 'COMP_COUNTER = ', I4, /, 1 X, 'MULSTR_COUNTER = &
        ', I4, /, 1 X, 'MEM_COUNTER = ', I4, /, 1 X, 'FRACT_COUNTER = ', &
        I4, /, 1 X, 'FRAC_COUNTER = ', I4, /, 1 X, 'LIFE_COUNTER = ', &
        I4, /, 1 X, 'ND_LEFM_COUNTER = ', I4, /, 1 X, 'RELIABILITY = ', &
        F10.5, /, 1 X, 'POF(1-REL)= ', F10.7)
        END
    
```



```

!*****
! PROGRAM: FLEXOPT
! PURPOSE: TO CARRY OUT A DETAILED FLEXSTREM V2 BASED OPTIMIZATION A STRUCTURE.
! DATE          PROGRAMMER          DESCRIPTION OF CHANGE
! =====
! 10-06-2010    ECHEZONA CHUKWUKA    FINAL VERSION.
!*****
PROGRAM FLEXOPT
IMPLICIT NONE
!=====STRUCTURAL PARAMETERS=====
REAL(8)::FY, FT, K, WS, EE, MAX_RL, BETA, D_LOAD, AI, M_PWR,&
          C_MAT, WF_LD, DECT_CRACK, DENS
INTEGER::NODE, NEL, N_PL, NN, MEMBER, JOINT
!=====FEA VARIABLES=====
REAL(8)::MEM_LEN, H, W, D_G, I_MNT, C_A, TM
REAL(8),ALLOCATABLE,DIMENSION(:)::DIA, AREA, THK
REAL(8),ALLOCATABLE,DIMENSION(:)::TLEN, TEN, SLEN
REAL(8),ALLOCATABLE,DIMENSION(:)::ND_STR,N_THK,N_DIA
!=====MECH ANALYSES VARIABLES=====
REAL(8)::SF, W_FORCE, OMEGA, D_BEND, D_COMPRESS, D_TENSILE,&
          MUL_STR
!=====FRAC ANALYSES VARIABLES=====
REAL(8)::AF, KRANS, A_CR, K_LOAD
!=====FLEXOPT VARIABLES=====
INTEGER::N_COM, ERR, OPT_LEV, K1, F, ALL_OK
REAL(8)::PERCENT, PERCENT_MIN, TAR_REL, TAR_REL_TOL,&
          REAL_TOL_MIN, REAL_TOL_MAX, BEST_TM, HUGEY, BIG, R_LIM
REAL(8),ALLOCATABLE::T_DIA(:), T_THK(:), C_DIA(:), C_THK(:),&
          T_25(:, :), T25(:)
REAL(8), ALLOCATABLE::MOD_DIA(:), MOD_THK(:)
CHARACTER, ALLOCATABLE::B_CHR(:)
LOGICAL::NEG
!=====GEN & SIM VARS=====
INTEGER(8), PARAMETER::N1 = 10000
REAL(8)::POF, REL
CHARACTER::TITLE
INTEGER::J, I, J1
INTEGER::Z, FLEX_TYPE
INTEGER::BEND_COUNTER, TENS_COUNTER, COMP_COUNTER,&
          MULSTR_COUNTER, MEM_COUNTER, FRAC_COUNTER, FRACT_COUNTER,&
          LIFE_COUNTER, ND_LEFM_COUNTER
LOGICAL::LGC_1, LGC_2, LGC_3, LGC_4, LGC_5, LGC_6, LGC_7,&
          LGC_8, LGC_9
!=====
ALL_OK = 0
HUGEY = HUGE(BIG)
DO
  WRITE(*,*)'ENTER ANALYSIS TYPE: SINGLE MEMBERED STRUCTURE OR&
  MULTI-MEMBERED STRUCTURE '
  WRITE(*,*)'                1                &
                2                '
  READ(*,*)Z
  IF(Z == 1)THEN
    FLEX_TYPE = 1
  EXIT

```

```

        ELSE IF(Z == 2)THEN
            FLEX_TYPE = 2
            EXIT
        ELSE
            END IF
    END DO
DO
    WRITE(*,*)'ENTER OPTIMIZATION TYPE: LEVEL 1 OPTI OR LEVEL 2 &
                OPTI(BEST WEIGHT)'
    WRITE(*,*)'                2                1                &
    READ(*,*)Z
    IF(Z == 1)THEN
        OPT_LEV = 1
        EXIT
    ELSE IF(Z == 2)THEN
        OPT_LEV = 2
        EXIT
    ELSE
        END IF
    END DO
! START FLEXOPT LOOP HERE=====
DO
    WRITE(*,*)'ENTER NO OF COMBINATIONS/TRIALS(ENTER AN EVEN&
                NUMBER)'
    READ(*,*)N_COM
    CALL EVEN_NUMBER_CHECKER(N_COM, ERR)
    IF(ERR == 1)THEN
        CYCLE
    ELSE
        EXIT
    END IF
    END DO
DO
    WRITE(*,*)'ENTER UPPER AND LOWER BOUNDS OF OPTIMIZATION(A&
                PERCENTAGE)'
    READ(*,*)PERCENT, PERCENT_MIN
    IF(PERCENT == 0. .OR. PERCENT_MIN == 0.)THEN
        CYCLE
    ELSE IF(PERCENT_MIN .GE. PERCENT)THEN
        WRITE(*,*)'UPPER BOUND MUST BE GREATER THAN LOWER BOUND'
        CYCLE
    ELSE
        EXIT
    END IF
    END DO
DO
    WRITE(*,*)'ENTER TARGET RELIABILITY'
    READ(*,*)TAR_REL
    R_LIM = 1. -(1./(10**(LOG10(DBLE(N1)))))
    IF(TAR_REL .GT. R_LIM .OR. TAR_REL .LE. 0.)THEN
        WRITE(*,*)'MUST BE LESS THAN ', R_LIM, ' AND GREATER THAN&
                ZERO'
        CYCLE
    ELSE
        END IF
    WRITE(*,*)'ENTER TARGET RELIABILITY TOLERANCE(A PERCENTAGE)'
    READ(*,*)TAR_REL_TOL
    IF((TAR_REL_TOL/100.).GE. 1.)THEN
        WRITE(*,*)'MUST BE LESS THAN 100%'
        CYCLE
    ELSE
        REAL_TOL_MIN = TAR_REL -(TAR_REL*(TAR_REL_TOL/100.))
        REAL_TOL_MAX = TAR_REL +(TAR_REL*(TAR_REL_TOL/100.))
        EXIT
    END IF
    END DO
K1 = 6 !STRUCTURAL GROUPS * 2 {WHERE 2=DIAMETER & THICKNESS GROUPS}
ALLOCATE(T_25(N_COM, K1), T25(K1))
CALL OPT_VAR_ARR_T25(T_25, K1, N_COM, PERCENT, PERCENT_MIN)
OPEN(20, FILE='BEST_FLEXOPT_RESULTS.FLX')
OPEN(22, FILE='FLEXOPT_RESULTS.FLX')
IF(FLEX_TYPE == 1)THEN
    WRITE(20, 320)N_COM, PERCENT, PERCENT_MIN, TAR_REL
ELSE IF(FLEX_TYPE == 2)THEN
    WRITE(20, 350)N_COM, PERCENT, PERCENT_MIN, TAR_REL
ELSE
    END IF
BEST_TM = HUGEY
DO I = 1, N_COM
    REL = 0.
    IF(I == 1)THEN
        DO J1 = 1, K1
            T_25(I, J1) = 0.
        END DO
    ELSE

```

```

END IF
DO F = 1, K1
  IF ((T_25(I,F).LT.0.).AND.(T_25(I,F).GE.100.))THEN
    T25(F)=ABS(T_25(I,F))
  ELSE
    T25(F)=T_25(I,F)
  END IF
END DO
IF(FLEX_TYPE == 1)THEN
  CALL SINGLE_MEM(T25, K1, M_PWR, FY, FT, K, EE, MAX_RL,&
    BETA, D_LOAD, AI, DECT_CRACK, N_PL,&
    C_MAT, MEM_LEN, H, I_MNT, C_A, TM)

  W_FORCE = 0.
  WF_LD = 0.
ELSE IF(FLEX_TYPE == 2)THEN
  CALL STR_PAR(NODE, NEL, NN, M_PWR, FY, FT, K, WS, EE,&
    WF_LD, BETA, MAX_RL, AI, DECT_CRACK,&
    N_PL, C_MAT, DENS, MEMBER, JOINT)
  ALLOCATE(TLEN(NEL), TEN(NEL), SLEN(NEL), DIA(NEL),&
    AREA(NEL), THK(NEL), ND_STR(NODE), N_THK(NODE), N_DIA(NODE))
  IF(I == 1)THEN
    ALLOCATE(B_CHR(NEL), MOD_THK(NEL), MOD_DIA(NEL))
    B_CHR = '!'
    MOD_DIA = 0.
    MOD_THK = 0.
  ELSE
    END IF
  CALL FEA_BLOCK(T25, K1, NODE, NEL, NN, EE, DENS, MEM_LEN,&
    H, W, D_G, TM, D_LOAD, TLEN, TEN, SLEN, DIA,&
    AREA, THK, ND_STR, N_THK, N_DIA, ALL_OK, FT,
MOD_DIA,&
    MOD_THK, B_CHR)
  CALL TABLES_SF(MEM_LEN, H, W, D_G, SLEN, DIA, NEL, SF)
ELSE
  END IF
IF(FLEX_TYPE == 2)THEN
  DO J1 = 1, NEL
    IF((AREA(J1).LT. 0.).OR.(ALL_OK .EQ. 1))THEN
      NEG = .TRUE.
      DEALLOCATE(TLEN, TEN, SLEN, DIA, AREA, THK, ND_STR, N_THK, N_DIA)
      EXIT
    ELSE
      NEG = .FALSE.
    END IF
  END DO
ELSE !FLEXTYPE =1
  IF(TM .LT. 0.)THEN
    NEG = .TRUE.
  ELSE
    END IF
END IF
IF(NEG == .TRUE.)THEN !IF THERE ARE NEGATIVE DIMENSIONS
  CYCLE
ELSE
  END IF
IF(OPT_LEV == 1)THEN
  BEST_TM = HUGEY
ELSE
  END IF
IF(TM .GT. BEST_TM)THEN
  IF(FLEX_TYPE == 2)THEN
    DEALLOCATE(TLEN, TEN, SLEN, DIA, AREA, THK, ND_STR, N_THK, N_DIA)
  ELSE
    END IF
  CYCLE
ELSE
  END IF
BEND_COUNTER = 0
TENS_COUNTER = 0
COMP_COUNTER = 0
MULSTR_COUNTER = 0
MEM_COUNTER = 0
FRAC_COUNTER = 0
FRACT_COUNTER = 0
LIFE_COUNTER = 0
ND_LEFM_COUNTER = 0
!*****START SIMULATION*****
DO J = 1, N1
!*****MECHANICAL ANALYSES*****
  IF(FLEX_TYPE == 2)THEN
    CALL WIND_FORCE(WS, SF, SLEN, DIA, NEL, W_FORCE)
  ELSE
    END IF
  CALL LOAD_COMBINATION(D_LOAD, TM, OMEGA, W_FORCE, WF_LD,&
    MAX_RL)
  IF(FLEX_TYPE == 1)THEN

```

```

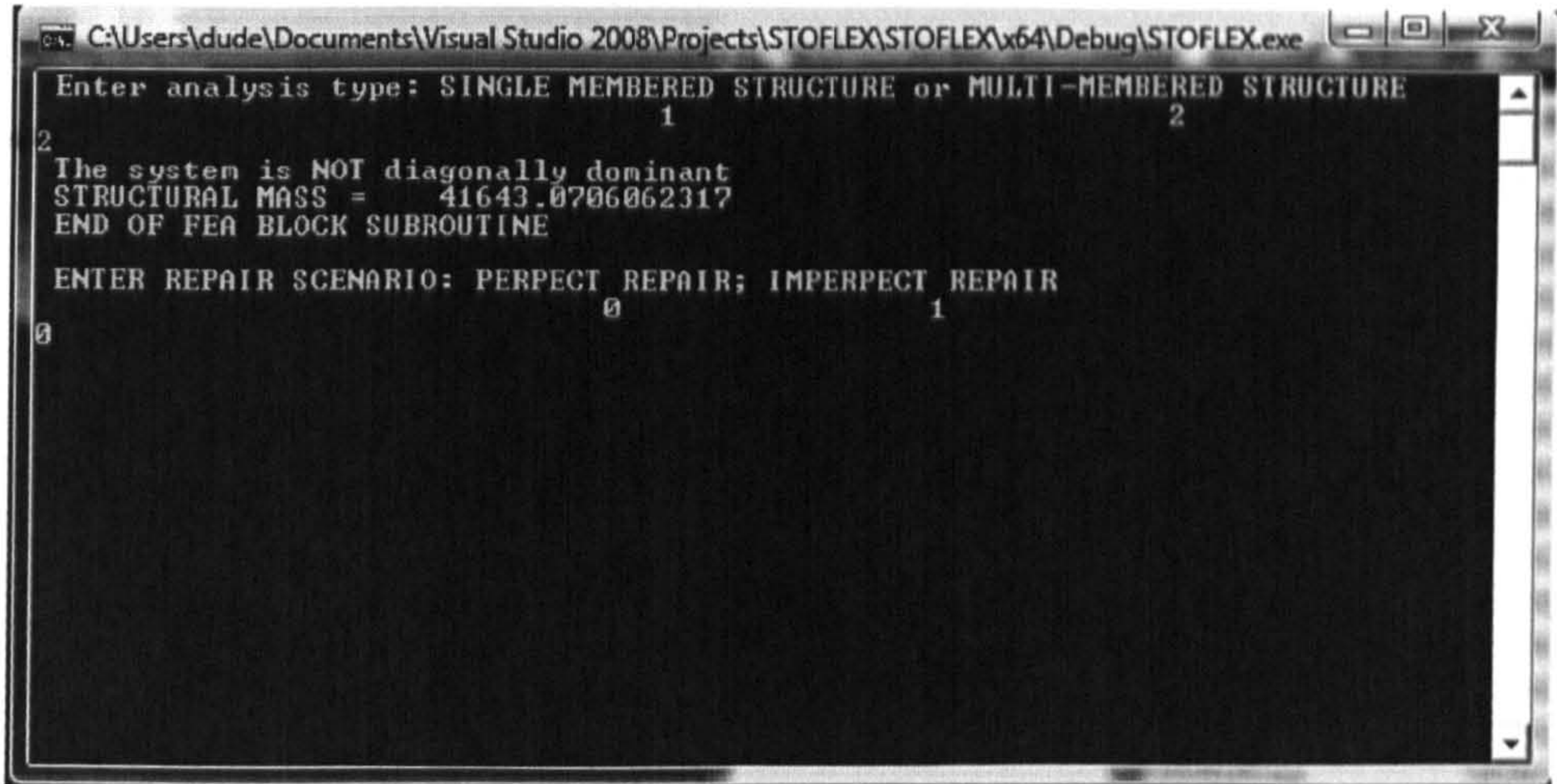
CALL BENDING_STRESS(OMEGA, MEM_LEN, I_MNT, H, FY,&
                   D_BEND, LGC_1)
IF(LGC_1 == .TRUE.)THEN
    BEND_COUNTER = BEND_COUNTER + 1
    CYCLE
ELSE
    END IF
CALL TENSILE_STRESS(OMEGA, FT, C_A, D_TENSILE, LGC_2)
IF(LGC_2 == .TRUE.)THEN
    TENS_COUNTER = TENS_COUNTER + 1
    CYCLE
ELSE
    END IF
CALL COMPRESSIVE_STRESS(OMEGA, MEM_LEN, I_MNT, C_A, EE,&
                       D_COMPRESS, LGC_3)
IF(LGC_3 == .TRUE.)THEN
    COMP_COUNTER = COMP_COUNTER + 1
    CYCLE
ELSE
    END IF
CALL MULTIAXIAL_STRESS(D_TENSILE, D_COMPRESS, D_BEND, &
                      FY, MUL_STR, LGC_4)
IF(LGC_4 == .TRUE.)THEN
    MULSTR_COUNTER = MULSTR_COUNTER + 1
    CYCLE
ELSE
    END IF
!***** FRACTURE ANALYSES*****
CALL CRACK_LENGTH(AI, AF)
CALL FRACT_TOUGH(MUL_STR, AF, K, BETA, K_LOAD, KRANS, &
                LGC_6)
IF(LGC_6 == .TRUE.)THEN
    FRACT_COUNTER = FRACT_COUNTER + 1
    CYCLE
ELSE
    END IF
CALL MINIMUM_CRACK(MUL_STR, KRANS, BETA, A_CR)
CALL FRAC_ANALYSIS(AF, A_CR, LGC_7)
IF(LGC_7 == .TRUE.)THEN
    FRAC_COUNTER = FRAC_COUNTER + 1
    CYCLE
ELSE
    END IF
CALL LIFE_CYCLE(N_PL, C_MAT, M_PWR, BETA, MUL_STR, AI, &
               A_CR, LGC_8)
IF(LGC_8 == .TRUE.)THEN
    LIFE_COUNTER = LIFE_COUNTER + 1
    CYCLE
ELSE
    END IF
!*****MEMBER ANALYSIS(LEVEL 3)*****
ELSE !IF(FLEX_TYPE==2)THEN
    CALL MEM_ANALYSIS(OMEGA, FT, EE, TLEN, AREA, DIA, THK, &
                    TEN, NEL, LGC_5)
    IF(LGC_5 == .TRUE.)THEN
        MEM_COUNTER = MEM_COUNTER + 1
        CYCLE
    ELSE
        END IF
    CALL ND_LEFM_ANALYSIS(NODE, ND_STR, N_THK, N_DIA, EE, K, C_MAT, &
                        M_PWR, N_PL, OMEGA, AI, LGC_9)
    IF(LGC_9 == .TRUE.)THEN
        ND_LEFM_COUNTER = ND_LEFM_COUNTER + 1
    ELSE
        END IF
    END IF
END DO
!*****END OF SIMULATION*****
!-----DISPLAY RELIABILITY-----
POF = (DBLE(BEND_COUNTER+TENS_COUNTER+COMP_COUNTER+&
           MULSTR_COUNTER+MEM_COUNTER+FRACT_COUNTER+FRAC_COUNTER+&
           LIFE_COUNTER+ND_LEFM_COUNTER)/N1)
REL = DBLE(1.-POF)
IF((TM .LT. BEST_TM).AND.(REL .GE. REAL_TOL_MIN .AND. REL &
 .LE. REAL_TOL_MAX))THEN
    BEST_TM = TM
    WRITE(20, 240, ADVANCE='NO')I, BEND_COUNTER, &
                                TENS_COUNTER, COMP_COUNTER, MULSTR_COUNTER,&
                                MEM_COUNTER, FRACT_COUNTER, FRAC_COUNTER,&
                                LIFE_COUNTER, ND_LEFM_COUNTER, REL, POF, TM
DO F = 1, K1 - 1
    WRITE(20, '(2X,F7.2)', ADVANCE='NO')T25(F)
END DO
WRITE(20, '(2X,F7.2,"|")')T25(K1)
ELSE
    WRITE(22,240,ADVANCE='NO')I,BEND_COUNTER,TENS_COUNTER, COMP_COUNTER,&

```

```

MULSTR_COUNTER, MEM_COUNTER, FRACT_COUNTER,&
FRAC_COUNTER, LIFE_COUNTER, ND_LEFM_COUNTER,&
REL, POF, TM
DO F = 1, K1 - 1
  WRITE(22, '(2X,F7.2)', ADVANCE='NO')T25(F)
END DO
WRITE(22, '(2X,F7.2,"|")')T25(K1)
END IF
WRITE(*,*)'REL=', REL
IF(FLEX_TYPE == 2)DEALLOCATE(TLEN, TEN, SLEN, DIA, AREA, &
THK, ND_STR,N_THK,N_DIA)
END DO
STOP 'END OF ANALYSIS'
CLOSE(20)
320 FORMAT('LEVEL 1 OPTIMIZATION FOR ', I8, 1 X, 'COMBINATIONS&
WITHIN THE LIMITS OF ', F7.3, '% AND ', F7.3, '% ',&
'WITH TARGET REL=', F7.6, '/')
350 FORMAT('LEVEL 2 OPTIMIZATION FOR ', I8, 1 X, 'COMBINATIONS&
WITHIN THE LIMITS OF ', F7.3, '% AND ', F7.3, '% ',&
'WITH TARGET REL=',F7.6, '/')
240 FORMAT(I8, 2 X, '|', 'BEND_COUNTER=', I4, 1 X, '|',&
'TENS_COUNTER=', I4, 1 X, '|', 'COMP_COUNTER=',&
I4, 1 X, '|', 'MULSTR_COUNTER=', I4, 1 X, '|',&
'MEM_COUNTER=', I4, 1 X, '|', 'FRACT_COUNTER=',&
I4, 1 X, '|', 'FRAC_COUNTER=', I4, 1 X, '|', 'LIFE_COUNTER=',&
I4, 1 X, '|', 'ND_LEFM_COUNTER=', I4, 1 X, '|', 'RELIABILITY=',&
F10.8, 1 X, '|', 'POF=', F10.7, 1 X, '|', F10.1, 1 X, '|')
END

```



```

!*****
! PROGRAM: STOFLEX
! PURPOSE: TO CARRY OUT A STOCHASTIC AND REPAIR ANALYSIS OF A STRUCTURE.
! DATE PROGRAMMER DESCRIPTION OF CHANGE
! =====
! 27-05-2010 ECHEZONA CHUKWUKA
!*****
PROGRAM STOFLEX
IMPLICIT NONE
!=====STRUCTRAL PARAMETERS=====
REAL (8) :: FY, FT, K, WS, EE, MAX_RL, BETA, D_LOAD, AI, M_PWR, &
           C_MAT, WF_LD, DECT_CRACK, DENS
INTEGER :: NODE, NEL, N_PL, NN, MEMBER, JOINT
!=====FEA VARIABLES=====
REAL (8) :: MEM_LEN, H, W, D_G, I_MNT, C_A, TM
REAL (8), ALLOCATABLE, DIMENSION (:), :: DIA, AREA, THK
REAL (8), ALLOCATABLE, DIMENSION (:), :: TLEN, TEN, SLEN
REAL (8), ALLOCATABLE, DIMENSION (:), :: ND_STR, N_THK, N_DIA
!=====MECH ANALYSES VARIABLES=====
REAL (8) :: SF, W_FORCE, OMEGA, D_BEND, D_COMPRESS, D_TENSILE, &
           MUL_STR
!=====FRAC ANALYSES VARIABLES=====
REAL (8) :: AF, KRANS, A_CR, K_LOAD
REAL (8), ALLOCATABLE :: A_F (:), N_EFF (:), RP_PERF (:)
!=====STOFLEX VARS=====
INTEGER(8) :: N1, NT, U_CY, L_CY, N_STU, N_YRS, N_STL, L_T, U_T,
INTEGER :: LOAD_STAT, INSPEC, INSPEC_1, INSPEC_2, INS_1, INS_2
!=====GEN & SIM VARS=====
REAL (8) :: POF, REL
CHARACTER :: TITLE
INTEGER :: J
INTEGER :: Z, FLEX_TYPE
INTEGER :: BEND_COUNTER, TENS_COUNTER, COMP_COUNTER, &
           MULSTR_COUNTER, MEM_COUNTER, FRAC_COUNTER, FRACT_COUNTER, &
           LIFE_COUNTER, ND_LEFM_COUNTER
LOGICAL :: LGC_1, LGC_2, LGC_3, LGC_4, LGC_5, LGC_6, LGC_7, &
           LGC_8, LGC_9
!=====
DO
  WRITE (*,*) 'ENTER ANALYSIS TYPE: SINGLE MEMBERED STRUCTURE OR&
  MULTI-MEMBERED STRUCTURE '
  WRITE (*,*) ' 1
  2
  READ (*,*) Z
  IF (Z == 1) THEN
    FLEX_TYPE = 1
    EXIT
  ELSE IF (Z == 2) THEN
    FLEX_TYPE = 2
    EXIT
  ELSE
    END IF
END DO
IF (FLEX_TYPE == 1) THEN
  W_FORCE = 0.

```



```

WF_LD = 0.
CALL SINGLE_MEM (M_PWR, FY, FT, K, EE, MAX_RL, BETA, D_LOAD, &
  AI, DECT_CRACK, N_STL, N_STU, N_YRS, C_MAT, MEM_LEN, H, &
  I_MNT, C_A, TM)
ELSE IF (FLEX_TYPE == 2) THEN
  CALL STR_PAR (NODE, NEL, NN, M_PWR, FY, FT, K, WS, EE, WF_LD, &
    BETA, MAX_RL, AI, DECT_CRACK, N_STL, N_STU, N_YRS, C_MAT, &
    DENS, MEMBER, JOINT)
  ALLOCATE (TLEN(NEL), TEN(NEL), SLEN(NEL), DIA(NEL), AREA(NEL), &
    THK(NEL), ND_STR(NODE), A_F(NODE), N_EFF(NODE), &
    RP_PERF(NODE), N_THK(NODE), N_DIA(NODE))
  CALL FEA_BLOCK (NODE, NEL, NN, EE, DENS, MEM_LEN, H, W, D_G, &
    TM, D_LOAD, TLEN, TEN, SLEN, DIA, AREA, THK, ND_STR, N_THK, N_DIA)
  !
  CALL TABLES_SF (MEM_LEN, H, W, D_G, SLEN, DIA, NEL, SF)
ELSE
  END IF
BEND_COUNTER = 0
TENS_COUNTER = 0
COMP_COUNTER = 0
MULSTR_COUNTER = 0
MEM_COUNTER = 0
FRAC_COUNTER = 0
FRACT_COUNTER = 0
LIFE_COUNTER = 0
ND_LEFM_COUNTER = 0
OPEN (20, FILE='STOFLEX_RESULTS.FLX')
OPEN (15, FILE='STOFLEX_GROWTH_RESULTS.FLX')
OPEN (8, FILE='INSPECTION_INTERVALS.FLX')
IF (FLEX_TYPE == 1) THEN
  CALL DATREC_1
ELSE
  CALL DATREC_2 (JOINT, MEMBER)
END IF
CALL STOFLEX_VAR (N_STL, N_STU, N_YRS, N_PL, U_CY, L_CY, &
  INSPEC_1, INSPEC_2)
NT = 0
L_T = L_CY + U_CY
U_T = U_CY
INS_1 = INSPEC_1
INS_2 = INSPEC_2
!*****START SIMULATION*****
DO J = 1, N_PL
  !-----LOADING INTERVAL-----
  LOAD_STAT = 0
  IF ((NT >= (U_T+1)) .AND. (NT <= L_T)) THEN
    LOAD_STAT = 1
    ELSE IF (NT == (L_T+1)) THEN
      NT = 0
      U_T = (U_CY+L_CY) + U_T
      L_T = U_T + L_CY
    ELSE
      END IF
    NT = NT + 1
  !-----INSPECTION CONDITIONS-----
  INSPEC = 0
  IF (J == INS_1) THEN
    INS_1 = INS_1 + INSPEC_1
    INSPEC = 1
  ELSE IF (J == INSPEC_2) THEN
    INS_2 = INS_2 + INSPEC_2
    INSPEC = 1
  ELSE
    END IF
  !*****MECHANICAL ANALYSES*****
  IF (FLEX_TYPE == 2) THEN
    CALL WIND_FORCE (WS, SF, SLEN, DIA, NEL, W_FORCE)
  ELSE
    END IF
  CALL S_LOAD_COMBINATION (LOAD_STAT, D_LOAD, TM, OMEGA, W_FORCE, WF_LD, MAX_RL)
  IF (FLEX_TYPE == 1) THEN
    CALL BENDING_STRESS (OMEGA, MEM_LEN, I_MNT, H, FY, D_BEND, &
      LGC_1)
    IF (LGC_1 == .TRUE.) THEN
      BEND_COUNTER = BEND_COUNTER + 1
      CYCLE
    ELSE
      END IF
    CALL TENSILE_STRESS (OMEGA, FT, C_A, D_TENSILE, LGC_2)
    IF (LGC_2 == .TRUE.) THEN
      TENS_COUNTER = TENS_COUNTER + 1
      CYCLE
    ELSE
      END IF
    CALL COMPRESSIVE_STRESS (OMEGA, MEM_LEN, I_MNT, C_A, EE, &
      D_COMPRESS, LGC_3)

```

```

IF (LGC_3 == .TRUE.) THEN
  COMP_COUNTER = COMP_COUNTER + 1
  CYCLE
ELSE
  END IF
CALL MULTIAXIAL_STRESS (D_TENSILE, D_COMPRESS, D_BEND, FY, &
MUL_STR, LGC_4)
IF (LGC_4 == .TRUE.) THEN
  MULSTR_COUNTER = MULSTR_COUNTER + 1
  CYCLE
ELSE
  END IF
!***** FRACTURE ANALYSES*****
CALL CRACK_GROWTH (AI, AF, DECT_CRACK, BETA, C_MAT, M_PWR, &
MUL_STR, J, INSPEC)
CALL FRACT_TOUGH (MUL_STR, AF, K, BETA, K_LOAD, KRANS, &
LGC_6)
IF (LGC_6 == .TRUE.) THEN
  FRACT_COUNTER = FRACT_COUNTER + 1
  CYCLE
ELSE
  END IF
CALL MINIMUM_CRACK (MUL_STR, KRANS, BETA, A_CR)
CALL FRAC_ANALYSIS (AF, A_CR, LGC_7)
IF (LGC_7 == .TRUE.) THEN
  FRAC_COUNTER = FRAC_COUNTER + 1
  CYCLE
ELSE
  END IF
CALL LIFE_CYCLE (N_PL, C_MAT, M_PWR, BETA, MUL_STR, AI, &
A_CR, LGC_8)
IF (LGC_8 == .TRUE.) THEN
  LIFE_COUNTER = LIFE_COUNTER + 1
  CYCLE
ELSE
  END IF
!*****MEMBER ANALYSIS (LEVEL 3)*****>>>
ELSE !IF (FLEX_TYPE==2) THEN
  CALL MEM_ANALYSIS (MEMBER, OMEGA, FT, EE, TLEN, AREA, DIA, &
THK, TEN, NEL, LGC_5)
IF (LGC_5 == .TRUE.) THEN
  MEM_COUNTER = MEM_COUNTER + 1
  CYCLE
ELSE
  END IF
CALL ND_LEFM_ANALYSIS (JOINT, NODE, ND_STR, N_THK, N_DIA, EE, K, &
C_MAT, M_PWR, N_PL, OMEGA, AI, A_F, N_EFF, RP_PERF, &
DECT_CRACK, J, INSPEC, LGC_9)
IF (LGC_9 == .TRUE.) THEN
  ND_LEFM_COUNTER = ND_LEFM_COUNTER + 1
ELSE
  END IF
END IF
END DO
!*****END OF SIMULATION*****
!-----DISPLAY RELIABILITY-----
POF = (DBLE(BEND_COUNTER+TENS_COUNTER+COMP_COUNTER+MULSTR_COUNTER+&
MEM_COUNTER+FRACT_COUNTER+FRAC_COUNTER+LIFE_COUNTER+&
ND_LEFM_COUNTER)/N1)
REL = DBLE (1.-POF)
WRITE (20, 240) BEND_COUNTER, TENS_COUNTER, COMP_COUNTER, &
MULSTR_COUNTER, MEM_COUNTER, FRACT_COUNTER, FRAC_COUNTER, &
LIFE_COUNTER, ND_LEFM_COUNTER, REL, POF
WRITE (*,*) REL
STOP 'END OF ANALYSIS'
CLOSE (20)
CLOSE (15)
CLOSE (8)
230 FORMAT (1 X, I8)
240 FORMAT (/, /, ' ', 'BEND_COUNTER = ', I4, /, 1 X, 'TENS_COUNTER =&
', I4, /, 1 X, 'COMP_COUNTER = ', I4, /, 1 X, 'MULSTR_COUNTER = &
', I4, /, 1 X, 'MEM_COUNTER = ', I4, /, 1 X, 'FRACT_COUNTER = ', &
I4, /, 1 X, 'FRAC_COUNTER = ', I4, /, 1 X, 'LIFE_COUNTER = ', &
I4, /, 1 X, 'ND_LEFM_COUNTER = ', I4, /, 1 X, 'RELIABILITY = ', &
F10.5, /, 1 X, 'POF(1-REL) = ', F10.7)
END
=====
REAL FUNCTION S_FORCE_CO(M,N,Q,CO,SFO)
IMPLICIT NONE
REAL(8),INTENT(IN)::M !Length
REAL(8),INTENT(IN)::N !Diameter
REAL(8),INTENT(IN)::Q !Dymanic pressure
REAL(8),INTENT(IN)::CO !Force coefficient
REAL(8),INTENT(IN)::SFO !shielding factor
REAL(8),PARAMETER::PI=4.D0*ATAN(1.D0)
REAL(8),PARAMETER::Y=1.

```

```

REAL(8)::U
U=PI*0.5
S_FORCE_CO=(Y*U*M*N*Q*CO*SFO)
END FUNCTION S_FORCE_CO

```

```

REAL FUNCTION MASS(LE,AR,DEN)
IMPLICIT NONE
REAL(8),INTENT(IN)::LE !Length m
REAL(8),INTENT(IN)::AR !AREA (thickness already considered)
REAL(8),INTENT(IN)::DEN!Density kg/m^3
REAL(8),PARAMETER::PI=4.D0*ATAN(1.D0)
REAL(8)::R1
REAL(8)::R2
REAL(8)::V
V=LE*AR
MASS=V*DEN
END FUNCTION MASS

```

```

REAL FUNCTION LOGN_TRANS(X,Y)
IMPLICIT NONE
REAL(8),INTENT(IN)::X !Variable
REAL(8),INTENT(IN)::Y !Coefficient of variance of variable
REAL(8)::S_X,GRN,Z,T,LN_X,MN
CALL GAUSSIAN_RANDOM_NUMBER(GRN)
S_X=Y*X
Z=LOG(X)-(0.5*LOG(1.+(S_X*S_X)/(X*X)))
T=LOG(1.+(S_X*S_X)/(X*X))
LN_X=Z+(GRN*SQRT(T))
LOGN_TRANS=EXP(LN_X)
END FUNCTION LOGN_TRANS

```

```

REAL FUNCTION LINEAR_INTER(X,Y,X1,Y1,SL_R)
IMPLICIT NONE
REAL(8),INTENT(IN)::X
REAL(8),INTENT(IN)::Y
REAL(8),INTENT(IN)::X1
REAL(8),INTENT(IN)::Y1
REAL(8),INTENT(IN)::SL_R
LINEAR_INTER=((Y1-Y)*(SL_R-X)/(X1-X))+Y
END FUNCTION LINEAR_INTER

```

```

REAL FUNCTION GUMBEL_TRANS(X,Y)
IMPLICIT NONE
REAL(8),INTENT(IN)::X !Variable
REAL(8),INTENT(IN)::Y !Coefficient of variance of variable
REAL(8)::S_X!Standard deviation of X
REAL(8)::GMRND
CALL GUMBEL_MAX_RANDOM_NUMBER(GMRND)
S_X=Y*X
GUMBEL_TRANS=X+(S_X*(GMRND))
END FUNCTION GUMBEL_TRANS

```

```

REAL FUNCTION GAUSS_TRANS(X,Y)
IMPLICIT NONE
REAL(8),INTENT(IN)::X
REAL(8),INTENT(IN)::Y
REAL(8)::S_X
REAL(8)::GRNJ
CALL GAUSSIAN_RANDOM_NUMBER(GRNJ)
S_X=Y*X
GAUSS_TRANS=X+(GRNJ*S_X)
END FUNCTION GAUSS_TRANS

```

```

REAL FUNCTION FORCE_CO(M,N,Q,CO)
IMPLICIT NONE
REAL(8),INTENT(IN)::M
REAL(8),INTENT(IN)::N
REAL(8),INTENT(IN)::Q
REAL(8),INTENT(IN)::CO
REAL(8),PARAMETER::PI=4.D0*ATAN(1.D0)
REAL(8),PARAMETER::Y=1.
REAL(8)::U
U=PI*0.5
FORCE_CO=(Y*U*M*N*Q*CO)
END FUNCTION FORCE_CO

```

```

REAL FUNCTION AREA(P,B)
IMPLICIT NONE
REAL(8),INTENT(IN)::P !length
REAL(8),INTENT(IN)::B !diameter
REAL(8),PARAMETER::PI=4.D0*ATAN(1.D0)
REAL(8)::U
!AREA=PI*0.5*D_T*H ! surface area of half cylinder
!body (excluding both ends)

U=PI*0.5
AREA=(U*P*B)
END FUNCTION AREA

```

```

MODULE DIMENSIONS
IMPLICIT NONE
SAVE
REAL(8),PARAMETER::PI=4.D0*ATAN(1.D0) !value of PI
REAL(8),PARAMETER::G=9.81 !Acceleration due to gravity m/s^2
REAL(8),PARAMETER::DTR=real(PI/180.) !conversion factor of degrees to
!radians
REAL(8),PARAMETER::MEGA=1.0E-6 !conversion factor to Mega (i.e.
!divide by a million)
REAL(8),PARAMETER::COV_R=0.06 !Coefficient of Variance resistance parameter
REAL(8),PARAMETER::COV_D=0.08 !Coefficient of Variance for demand parameter
END MODULE DIMENSIONS

```

```

SUBROUTINE SINGLE_MEM (M_PWR, FY, FT, K, EE, MAX_RL, BETA, D_LOAD, AI, &
& DECT_CRACK, N_PL, C_MAT, MEM_LEN, H, I_MNT, C_A, TM)
IMPLICIT NONE
REAL (8), INTENT (OUT):: EE !YOUNG'S MODULUES MPA
REAL (8), INTENT (OUT):: C_MAT, BETA !C (MATERIAL CONSTANT) (MPA^-4)(M^-1),BETA
(MATERIAL CONSTANT)
REAL (8), INTENT (OUT):: K !FRACTURE TOUGHNESS MPAM^1/2
REAL (8), INTENT (OUT):: AI !INITIAL CRACK LENGTH BOUNDS M
REAL (8), INTENT (OUT):: FY, FT !UNIAXIAL YIELD STRESS MPA AND TENSILE STRENGTH MPA
INTEGER, INTENT (OUT):: N_PL !PLANNED/INTENDED/DESIGN LIFE CYCLE OF STRUCTURE
REAL (8), INTENT (OUT):: MAX_RL, D_LOAD !MAXIMUM RATED LOAD (LIVE LOAD) KG, DEAD LOAD KG
REAL (8), INTENT (OUT) :: M_PWR !M (MATERIAL CONSTANT)
REAL (8), INTENT (OUT) :: DECT_CRACK !DETECTABLE CRACK LENGTH M
REAL (8), INTENT (OUT) :: I_MNT, C_A
REAL (8), INTENT (OUT) :: H
REAL (8), INTENT (OUT) :: TM
REAL (8), INTENT (OUT) :: MEM_LEN
REAL (8) :: DENS, W, THK
INTEGER :: N_STL, N_STU, N_YRS
CHARACTER (15) :: DATE
CHARACTER (70) :: TITLE
OPEN (25, FILE='SINGLE STRUCTURE PARAMETERS.DAT')
OPEN (16, FILE='RESULT_SING.DAT')
CALL DATE4 (DATE)
WRITE (16, 200) DATE
DO
  READ (25, 500) TITLE
  WRITE (16, 600) TITLE
  IF (TITLE == 'END') EXIT
  READ (25,*) M_PWR, FY, FT, K, DENS, N_STL, N_STU, N_YRS, &
  MAX_RL
  READ (25,*) BETA, D_LOAD, AI, DECT_CRACK, C_MAT, EE, W, H, THK
  READ (25,*) MEM_LEN
  N_PL = N_YRS * N_STL
  !=====I->THE SECOND MOMENT OF THE CLOSED SECTION AREA OF THE BEAM=====
  I_MNT = ((W*H*H*H)-((W-THK)*(H-THK)*(H-THK)*(H-THK))) / 12.
  !((W*H^3)-(W*THK^3))/12
  !=====C_A->THE X-SECTIONAL AREA OF THE BOX SECTION(FROM FRONT VIEW)=====
  C_A = (H*W) - ((H-THK)*(W-THK))
  TM = C_A * MEM_LEN * DENS
  WRITE (16, 150) FY, FT, K, DENS, N_STL, N_STU, N_YRS, MAX_RL, &
  D_LOAD, BETA, M_PWR, C_MAT, AI, DECT_CRACK, EE, MEM_LEN, W, &
  H, THK
END DO
150 FORMAT (' ', 'UNIAXIAL YIELD STRENGTH =', PD11.3, ' MPA' /, ' ',
'TENSILE STRENGTH =', PD11.3, ' MPA', /, ' ', 'FRACTURE TOUGHNESS &
=', PD11.3, ' MPA(M^0.5)' /, ' ',
'MATERIAL DENSITY =', PD11.3, ' KG/(M^3)', /, ' ', 'LOADED CYCLES/YR&
=', I8 /, ' ', 'UNLOADED CYCLES/YR =',
I8, /, ' ', 'NO OF YRS IN SERVICE =', I5 /, ' ', 'MAXIMUM RATED LOA&
D (LIVE) =', PD11.3, ' KG' /, ' ',
'DEAD LOAD =', PD11.3, ' KG' /, ' ', 'LEFM BETA =', PD10.3, ' ', ' ', &
'LEFM M =', PD10.3, ' ', ' ',

```

```
'LEFM C =', PD11.3, / ' ', 'INITIAL CRACK LENGTH =', PD10.3, ' M' &
/, ' ', 'DETECTABLE CRACK LENGTH =', PD10.3,
'M', / ' ', 'YOUNG-S MODULUS =', D10.3, ' MPA' /, ' ', 'STRUCTUR&
E/COMPONENT LENGTH =', D10.3, ' M', / ' ',
'STRUCTURE/COMPONENT CROSS-SECTIONAL WIDTH =', D10.3, ' M', / ' ',&
'STRUCTURE/COMPONENT CROSS-SECTIONAL HEIGHT =',
D10.3, ' M', / ' ', 'STRUCTURE/COMPONENT CROSS-SECTIONAL THICKNES&
S =', D10.3, ' M', /)
200 FORMAT (' ', 'FEA/3-D TRUSS ELEMENT/', 52 X, A15 /)
500 FORMAT (A70)
600 FORMAT (/ ' ', 70 ('-') / ' ', A70 / ' ', 70 ('-'))
CLOSE (25)
CLOSE (16)
RETURN
END SUBROUTINE SINGLE_MEM
```

```
-----
SUBROUTINE STR_PAR (NODE, NEL, NN, M_PWR, FY, FT, K, WS, EE, WF_LD, &
& BETA, MAX_RL, AI, DECT_CRACK, N_PL, C_MAT, DENS, MEMBER, JOINT)
IMPLICIT NONE
REAL (8), INTENT (OUT) :: EE !YOUNG'S MODULUES MPA
REAL (8), INTENT (OUT) :: C_MAT, BETA !C (MATERIAL CONSTANT) (MPAA-4)(MA-1), BETA
(MATERIAL CONSTANT)
REAL (8), INTENT (OUT) :: K, WS !FRACTURE TOUGHNESS MPAMA1/2, WIND SPEED IN STRUTURE'S
ENVIRONMENT
REAL (8), INTENT (OUT) :: AI !INITIAL CRACK LENGTH BOUNDS M
REAL (8), INTENT (OUT) :: FY, FT !UNIAXIAL YIELD STRESS MPA AND TENSILE STRENGTH MPA
INTEGER, INTENT (OUT) :: N_PL !PLANNED/INTENDED/DESIGN LIFE CYCLE OF STRUCTURE
REAL (8), INTENT (OUT) :: MAX_RL !MAXIMUM RATED LOAD (LIVE LOAD) KG
INTEGER, INTENT (OUT) :: NEL, NODE !TOTAL NUMBER OF MEMBERS, TOTAL NUMBER OF NODES
INTEGER, INTENT (OUT) :: NN !STIFFNESS MATRIX DIMENSION
INTEGER, INTENT (OUT) :: MEMBER !FOCAL MEMBER OF ANALYSIS
INTEGER, INTENT (OUT) :: JOINT !FOCAL JOINT OF ANALYSIS
REAL (8), INTENT (OUT) :: M_PWR !M (MATERIAL CONSTANT)
REAL (8), INTENT (OUT) :: DENS !MATERIAL DENSITY KG/MA3
REAL (8), INTENT (OUT) :: WF_LD !WIND FORCE ON DEAD LOAD N
REAL (8), INTENT (OUT) :: DECT_CRACK !DETECTABLE CRACK LENGTH M
INTEGER :: N_STL, N_STU, N_YRS
REAL (8) :: D_LOAD !DEAD LOAD KG
CHARACTER (15) :: DATE
CHARACTER (70) :: TITLE
OPEN (25, FILE='STRUCTURE PARAMETERS.DAT')
OPEN (6, FILE='RESULT.DAT')
CALL DATE4 (DATE)
WRITE (6, 200) DATE
DO
  READ (25, 500) TITLE
  IF (TITLE == 'END') EXIT
  WRITE (6, 600) TITLE
  READ (25,*) NODE, NEL, M_PWR
  READ (25,*) FY, FT, K, DENS, WS, N_STL, N_STU, N_YRS, MAX_RL
  READ (25,*) WF_LD, BETA, D_LOAD, AI, DECT_CRACK, C_MAT, EE
  READ (25,*) MEMBER, JOINT
  NN = 3 * NODE
  N_PL = N_YRS * N_STL
  WRITE (6, 100) NODE, NEL, EE
  WRITE (6, 150) FY, FT, K, DENS, WS, N_STL, N_STU, N_YRS, &
  MAX_RL, D_LOAD, WF_LD, BETA, M_PWR, C_MAT, AI, DECT_CRACK, &
  MEMBER, JOINT
END DO
100 FORMAT (' ', '# OF NODES =', I5, ' :', 16 X, '# OF ELEMENTS =', &
I5/' ', 'YOUNG-S MODULUS (E0) =', PD15.7 /)
150 FORMAT (' ', 'UNIAXIAL YIELD STRENGTH =', PD11.3, ' MPA' /, ' ',
'TENSILE STRENGTH =', PD11.3, ' MPA' /, ' ', 'FRACTURE TOUGHNESS &
=', PD11.3, ' MPA(MA0.5)' /, ' ', 'MATERIAL DENSITY =', PD11.3,
' KG/(MA3)' /, ' ', 'WIND SPEED ON STRUCTURE =', PD10.3, ' M/S' &
/, ' ', 'LOADED CYCLES/YR =', I8 / ' ', 'UNLOADED CYCLES/YR =',
I8, / ' ', 'NO OF YRS IN SERVICE =', I5 / ' ', 'MAXIMUM RATED LOA&
D (LIVE) =', PD11.3, ' KG' /, ' ', 'LIVE LOAD =', PD11.3, ' KG', / &
' AVERAGE WIND FORCE ON LIVE LOAD =', PD11.3, ' N', / ' ', 'LEFM B&
ETA =', PD10.3, ' ', 'LEFM M =', PD10.3, ' ', 'LEFM C =',
PD11.3, / ' ', 'INITIAL CRACK LENGTH =', PD10.3, ' M' /, ' ', 'DE&
TECTABLE CRACK LENGTH =', PD10.3, ' M', / ' ', 'FOCAL MEMBE
OF ANALYSIS =', I5, / ' ', 'FOCAL NODE OF ANALYSIS =', I5, /
200 FORMAT (' ', 'FEA/3-D TRUSS ELEMENT/', 52 X, A15 /)
500 FORMAT (A70)
600 FORMAT (/ ' ', 70 ('-') / ' ', A70 / ' ', 70 ('-'))
CLOSE (25)
RETURN
END SUBROUTINE STR_PAR
```

```
-----
SUBROUTINE GUMBEL_MAX_RANDOM_NUMBER(GUMBRND)
```

```

IMPLICIT NONE
REAL(8),INTENT(OUT)::GUMBRND
REAL(8)::R
CALL SEED(1294)
CALL RANDOM_NUMBER(R)
GUMBRND=-LOG(-LOG(R))
!The expected value is expressed here
!http://www.resacorp.com/gumbel\_expectedvalue.htm
!where alpha and beta, the shape and scale parameters
!respectively are the mean and standard deviation (also respectively).
RETURN
END SUBROUTINE GUMBEL_MAX_RANDOM_NUMBER

```

```

-----
SUBROUTINE EXPO_RANDOM_NUMBER(EXPRND)
IMPLICIT NONE
REAL(8),INTENT(OUT)::EXPRND
REAL(8)::R
CALL SEED(1294)
CALL RANDOM_NUMBER(R)
EXPRND=-LOG(R)
RETURN
END SUBROUTINE EXPO_RANDOM_NUMBER

```

```

-----
SUBROUTINE GAUSSIAN_RANDOM_NUMBER(NORMRND)
IMPLICIT NONE
REAL(8),INTENT(OUT)::NORMRND
REAL(8)::RL,Y1,Y2
REAL(8),SAVE ::Z
LOGICAL,SAVE ::NORM=.FALSE.
IF (NORM) THEN
  NORMRND=Z
  NORM=.FALSE.
ELSE
  DO
    CALL SEED(1975)
    CALL RANDOM_NUMBER(Y1)
    CALL SEED(1865)
    CALL RANDOM_NUMBER(Y2)
    Y1=(2.0*Y1)-1.0
    Y2=(2.0*Y2)-1.0
    RL=(Y1*Y1)+(Y2*Y2)
    IF (RL > 0.0 .AND. RL < 1.0) EXIT
  END DO
  RL=SQRT(-2.0*LOG(RL)/RL)
  NORMRND=Y1*RL
  Z=Y2*RL
  NORM=.TRUE.
END IF
RETURN
END SUBROUTINE GAUSSIAN_RANDOM_NUMBER

```

```

=====
SUBROUTINE TABLES_SF (MEM_LEN, H, W, D_G, SLEN, DIA, NEL, SF)
USE DIMENSIONS
IMPLICIT NONE
!TABLE TO BE USED DETERMINATION OF SHIELDING FACTOR SF (APPLICABLE TO WHOLE
!STRUCTURE, I.E. NO NEED FOR INPUTTING DIFFERENT CHARACTERISTIC DIMENSIONS
!AMONG THE DUMMY ARGUMENTS)
REAL :: LINEAR_INTER !FUNCTION USED FOR LINEAR INTERPOLATION (TO DETERMINE THE SHIELDING
FACTOR)
REAL :: AREA
INTEGER, INTENT (IN) :: NEL !NUMBER OF MEMBERS
REAL (8), DIMENSION (NEL), INTENT (IN) :: SLEN !LENGTHS OF INDIVIDUAL WINDWARD(& ALSO
LEEWARD) MEMBERS M
REAL (8), DIMENSION (NEL), INTENT (IN) :: DIA !DIAMETERS OF MEMBERS M
REAL (8), INTENT (IN) :: MEM_LEN, H, W, D_G !LENGTH, HEIGHT, WIDTH AND THICKNESS(D_G) OF
MAIN STRUCTURE M
REAL (8), INTENT (OUT) :: SF !SHIELDING FACTOR
REAL (8) :: X, Y, X1, Y1 !INTERPOLATION ARGUMENTS
REAL (8) :: A, TA !AREA OF SOLID PARTS M^2
REAL (8) :: S_L_R !SOLIDITY RATIO
REAL (8) :: AE !ENCLOSED AREA M^2
REAL (8) :: S_R !SPACING RATIO
INTEGER :: J
INTEGER, SAVE :: N
TA = 0.
DO J = 1, NEL
  A = AREA (SLEN(J), DIA(J))
  TA = TA + A
END DO
AE = MEM_LEN * (H+(2.*D_G))
S_R = W / H

```

```

SL_R = TA / AE
IF ((S_R > 0.) .AND. (S_R <= 0.5)) THEN
  IF ((SL_R > 0.) .AND. (SL_R <= 0.1)) THEN
    X = 0
    Y = 0
    X1 = 0.1
    Y1 = 0.75
    SF = LINEAR_INTER (X, Y, X1, Y1, SL_R)
    ELSE IF ((SL_R > 0.1) .AND. (SL_R <= 0.2)) THEN
    X = 0.1
    Y = 0.75
    X1 = 0.2
    Y1 = 0.40
    SF = LINEAR_INTER (X, Y, X1, Y1, SL_R)
    ELSE IF ((SL_R > 0.2) .AND. (SL_R <= 0.3)) THEN
    X = 0.2
    Y = 0.40
    X1 = 0.3
    Y1 = 0.32
    SF = LINEAR_INTER (X, Y, X1, Y1, SL_R)
    ELSE IF ((SL_R > 0.3) .AND. (SL_R <= 0.4)) THEN
    X = 0.3
    Y = 0.32
    X1 = 0.4
    Y1 = 0.21
    SF = LINEAR_INTER (X, Y, X1, Y1, SL_R)
    ELSE IF ((SL_R > 0.4) .AND. (SL_R <= 0.5)) THEN
    X = 0.4
    Y = 0.21
    X1 = 0.5
    Y1 = 0.15
    SF = LINEAR_INTER (X, Y, X1, Y1, SL_R)
    ELSE IF ((SL_R > 0.5) .AND. SL_R >= 0.6) THEN
    SF = 0.1
    ELSE
    END IF
  ELSE
  END IF
  IF ((S_R > 0.5) .AND. (S_R <= 1.)) THEN
    IF ((SL_R > 0.) .AND. (SL_R <= 0.1)) THEN
    X = 0
    Y = 0
    X1 = 0.1
    Y1 = 0.92
    SF = LINEAR_INTER (X, Y, X1, Y1, SL_R)
    ELSE IF ((SL_R > 0.1) .AND. (SL_R <= 0.2)) THEN
    X = 0.1
    Y = 0.92
    X1 = 0.2
    Y1 = 0.75
    SF = LINEAR_INTER (X, Y, X1, Y1, SL_R)
    ELSE IF ((SL_R > 0.2) .AND. (SL_R <= 0.3)) THEN
    X = 0.2
    Y = 0.75
    X1 = 0.3
    Y1 = 0.59
    SF = LINEAR_INTER (X, Y, X1, Y1, SL_R)
    ELSE IF ((SL_R > 0.3) .AND. (SL_R <= 0.4)) THEN
    X = 0.3
    Y = 0.59
    X1 = 0.4
    Y1 = 0.43
    SF = LINEAR_INTER (X, Y, X1, Y1, SL_R)
    ELSE IF ((SL_R > 0.4) .AND. (SL_R <= 0.5)) THEN
    X = 0.4
    Y = 0.43
    X1 = 0.5
    Y1 = 0.25
    SF = LINEAR_INTER (X, Y, X1, Y1, SL_R)
    ELSE IF ((SL_R > 0.5) .AND. SL_R >= 0.6) THEN
    SF = 0.1
    ELSE
    END IF
  ELSE
  END IF
  IF ((S_R > 1.) .AND. (S_R <= 2.)) THEN
    IF ((SL_R > 0.) .AND. (SL_R <= 0.1)) THEN
    X = 0
    Y = 0
    X1 = 0.1
    Y1 = 0.95
    SF = LINEAR_INTER (X, Y, X1, Y1, SL_R)
    ELSE IF ((SL_R > 0.1) .AND. (SL_R <= 0.2)) THEN
    X = 0.1
    Y = 0.95
    X1 = 0.2

```

```

Y1 = 0.80
SF = LINEAR_INTER (X, Y, X1, Y1, SL_R)
  ELSE IF ((SL_R > 0.2) .AND. (SL_R <= 0.3)) THEN
X = 0.2
Y = 0.80
X1 = 0.3
Y1 = 0.63
SF = LINEAR_INTER (X, Y, X1, Y1, SL_R)
  ELSE IF ((SL_R > 0.3) .AND. (SL_R <= 0.4)) THEN
X = 0.3
Y = 0.63
X1 = 0.4
Y1 = 0.5
SF = LINEAR_INTER (X, Y, X1, Y1, SL_R)
  ELSE IF ((SL_R > 0.4) .AND. (SL_R <= 0.5)) THEN
X = 0.4
Y = 0.5
X1 = 0.5
Y1 = 0.33
SF = LINEAR_INTER (X, Y, X1, Y1, SL_R)
  ELSE IF ((SL_R > 0.5) .AND. SL_R >= 0.6) THEN
SF = 0.2
  ELSE
  END IF
ELSE
END IF
IF ((S_R > 2.) .AND. (S_R <= 4.)) THEN
  IF ((SL_R > 0.) .AND. (SL_R <= 0.1)) THEN
X = 0
Y = 0
X1 = 0.1
Y1 = 1.
SF = LINEAR_INTER (X, Y, X1, Y1, SL_R)
  ELSE IF ((SL_R > 0.1) .AND. (SL_R <= 0.2)) THEN
X = 0.1
Y = 1.
X1 = 0.2
Y1 = 0.88
SF = LINEAR_INTER (X, Y, X1, Y1, SL_R)
  ELSE IF ((SL_R > 0.2) .AND. (SL_R <= 0.3)) THEN
X = 0.2
Y = 0.88
X1 = 0.3
Y1 = 0.76
SF = LINEAR_INTER (X, Y, X1, Y1, SL_R)
  ELSE IF ((SL_R > 0.3) .AND. (SL_R <= 0.4)) THEN
X = 0.3
Y = 0.76
X1 = 0.4
Y1 = 0.66
SF = LINEAR_INTER (X, Y, X1, Y1, SL_R)
  ELSE IF ((SL_R > 0.4) .AND. (SL_R <= 0.5)) THEN
X = 0.4
Y = 0.66
X1 = 0.5
Y1 = 0.55
SF = LINEAR_INTER (X, Y, X1, Y1, SL_R)
  ELSE IF ((SL_R > 0.5) .AND. SL_R >= 0.6) THEN
SF = 0.45
  ELSE
  END IF
ELSE
END IF
IF ((S_R > 4.) .AND. (S_R <= 5.)) THEN
  IF ((SL_R > 0.) .AND. (SL_R <= 0.1)) THEN
X = 0
Y = 0
X1 = 0.1
Y1 = 1.
SF = LINEAR_INTER (X, Y, X1, Y1, SL_R)
  ELSE IF ((SL_R > 0.1) .AND. (SL_R <= 0.2)) THEN
X = 0.1
Y = 1.
X1 = 0.2
Y1 = 0.95
SF = LINEAR_INTER (X, Y, X1, Y1, SL_R)
  ELSE IF ((SL_R > 0.2) .AND. (SL_R <= 0.3)) THEN
X = 0.2
Y = 0.95
X1 = 0.3
Y1 = 0.88
SF = LINEAR_INTER (X, Y, X1, Y1, SL_R)
  ELSE IF ((SL_R > 0.3) .AND. (SL_R <= 0.4)) THEN
X = 0.3
Y = 0.88
X1 = 0.4

```



```

Y1 = 0.81
SF = LINEAR_INTER (X, Y, X1, Y1, SL_R)
  ELSE IF ((SL_R > 0.4) .AND. (SL_R <= 0.5)) THEN
X = 0.4
Y = 0.81
X1 = 0.5
Y1 = 0.75
SF = LINEAR_INTER (X, Y, X1, Y1, SL_R)
  ELSE IF ((SL_R > 0.5) .AND. SL_R >= 0.6) THEN
SF = 0.68
  ELSE
  END IF
ELSE
END IF
IF (S_R > 5.0) THEN
  SF = 1.
ELSE
END IF
RETURN
END SUBROUTINE TABLES_SF

```

```

-----
SUBROUTINE TABLES_CF(L,D,VS,CF)
USE DIMENSIONS
IMPLICIT NONE
!Table to be used in determination of Force coefficient CF (applicable
!to individual members i.e. different characteristic dimensions are entered
!amongst the dummy arguments)
REAL::LINEAR_INTER      !Function used for linear interpolation
                        !(to determine the force coefficient)
REAL(8),INTENT(OUT)::CF  !Force coefficient
REAL(8),INTENT(IN)::L    !Characteristic length m
REAL(8),INTENT(IN)::D    !Characteristic diameter m
REAL(8),INTENT(IN)::VS   !Gumbel distributed wind speed m/s
REAL(8)::X,Y,X1,Y1      !Interpolation arguments
REAL(8)::A_S            !Aerodynamic slenderness (dimless)
REAL(8)::C              !Coefficient for circular sections (dimless)
A_S=L/D
C=D*VS
IF (C < 6.) THEN
  IF ((A_S>0.) .AND. (A_S<= 5.)) THEN
    X=0 ; Y=0
    X1=5 ; Y1=0.75
    CF=LINEAR_INTER(X,Y,X1,Y1,A_S)
  ELSE IF ((A_S>5.) .AND. (A_S<= 10.))THEN
    X=5 ; Y=0.75
    X1=10 ; Y1=0.80
    CF=LINEAR_INTER(X,Y,X1,Y1,A_S)

  ELSE IF ((A_S>10.) .AND. (A_S<= 20.)) THEN
    X=10 ; Y=0.80
    X1=20 ; Y1=0.90
    CF=LINEAR_INTER(X,Y,X1,Y1,A_S)
  ELSE IF ((A_S>20.) .AND. (A_S<=30.)) THEN
    X=20 ; Y=0.90
    X1=30 ; Y1=0.95
    CF=LINEAR_INTER(X,Y,X1,Y1,A_S)
  ELSE IF ((A_S>30.) .AND. (A_S<= 40.)) THEN
    X=30 ; Y=0.95
    X1=40 ; Y1=1.0
    CF=LINEAR_INTER(X,Y,X1,Y1,A_S)
  ELSE IF ((A_S>40.) .AND. (A_S<= 50.)) THEN
    X=40 ; Y=1.0
    X1=50 ; Y1=1.1
    CF=LINEAR_INTER(X,Y,X1,Y1,A_S)
  ELSE
  END IF
ELSE
CF=1.2
END IF
IF (C >= 6.) THEN
  IF ((A_S>0.) .AND. (A_S<= 5.)) THEN
    X=0 ; Y=0
    X1=5 ; Y1=0.60
    CF=LINEAR_INTER(X,Y,X1,Y1,A_S)
  ELSE IF ((A_S>5.) .AND. (A_S<= 10.))THEN
    X=5 ; Y=0.60
    X1=10 ; Y1=0.65
    CF=LINEAR_INTER(X,Y,X1,Y1,A_S)
  ELSE IF ((A_S>10.) .AND. (A_S<= 20.)) THEN
    X=10 ; Y=0.65
    X1=20 ; Y1=0.70
    CF=LINEAR_INTER(X,Y,X1,Y1,A_S)
  ELSE IF ((A_S>20.) .AND. (A_S<=30.)) THEN
    X=20 ; Y=0.70

```

```

        X1=30 ; Y1=0.70
        CF=LINEAR_INTER(X,Y,X1,Y1,A_S)
    ELSE IF ((A_S>30.) .AND. (A_S<= 40.)) THEN
        X=30 ; Y=0.70
        X1=40 ; Y1=0.75
        CF=LINEAR_INTER(X,Y,X1,Y1,A_S)
    ELSE IF ((A_S>40.) .AND. (A_S<= 50.)) THEN
        X=40 ; Y=0.75
        X1=50 ; Y1=0.80
        CF=LINEAR_INTER(X,Y,X1,Y1,A_S)
    ELSE
    END IF
ELSE
CF=0.8
END IF
RETURN
END SUBROUTINE TABLES_CF

```

```

-----
SUBROUTINE WIND_FORCE(WS,SF,SLEN,DIA,NEL,W_FORCE)
USE DIMENSIONS
IMPLICIT NONE
REAL::FORCE_CO          !Function to determine force coefficient
REAL::S_FORCE_CO        !Function to determine shielding factor
REAL::GUMBEL_TRANS      !Function to transform variable to Gumbel distribution
INTEGER,INTENT(IN)::NEL !number of members to be analyzed
REAL(8),DIMENSION(NEL),INTENT(IN)::SLEN !Lengths of individual windward
                                         !(& also leeward) members m
REAL(8),DIMENSION(NEL),INTENT(IN)::DIA !Diameters of members m
REAL(8),INTENT(IN)::WS,SF !WIND SPEED (m/s) & Shielding factor
REAL(8),INTENT(OUT)::W_FORCE !Total wind force on main structure N
REAL(8)::Q                !Dynamic wind pressure KPa
REAL(8)::VS               !wind velocity m/s
REAL(8)::F_WIND,TF_WIND   !wind load on windward parts N
REAL(8)::F_SHEL,TF_SHEL  !wind load on sheltered parts N
REAL(8)::CF               !Force coefficient
INTEGER::I
VS=GUMBEL_TRANS(WS,COV_D)
Q=0.613*(VS*VS)
TF_WIND=0.
TF_SHEL=0.
DO I=1,NEL
    IF (SLEN(I) .NE. 0.)THEN
        CALL TABLES_CF(SLEN(I),DIA(I),VS,CF)
        F_WIND=FORCE_CO(SLEN(I),DIA(I),Q,CF)
        F_SHEL=S_FORCE_CO(SLEN(I),DIA(I),Q,CF,SF)
    ELSE
        F_WIND=0.
        F_SHEL=0.
    END IF
    TF_WIND=TF_WIND+F_WIND
    TF_SHEL=TF_SHEL+F_SHEL
    W_FORCE=TF_WIND+TF_SHEL
END DO
WRITE (20,130,ADVANCE="NO")VS,W_FORCE*MEGA !commented in STOFLEX & FLEOPT
130 FORMAT (10X,F5.2,7X,F10.3)
RETURN
END SUBROUTINE WIND_FORCE

```

```

=====
SUBROUTINE FEA_BLOCK(NODE,NEL,NN,EE,DENS,MEM_LEN,H,W,D_G,TM,D_LOAD ,TLEN,&
                    TEN,SLEN,DIA,AREA,THK,ND_STR,N_THK,N_DIA)
USE DIMENSIONS
USE IFPORT
IMPLICIT NONE
REAL::MASS              !Function to determine mass of individual members
!INTEGER,INTENT(IN)::DOF !DEGREE OF FREEDOM = 3 (3-D)
INTEGER,INTENT(IN)::NN !Total degrees of freedom (DOF * node)
INTEGER,INTENT(IN)::NODE !Total number of nodes
INTEGER,INTENT(IN)::NEL !Total number of members
REAL(8),INTENT(IN)::EE,DENS !Young's modulus MPa
REAL(8),INTENT(OUT)::MEM_LEN !length of member (boom arm) m
REAL(8),INTENT(OUT)::H,W !Height m, width m
REAL(8),INTENT(OUT)::D_G !Chord diameter (Shell thickness) m
REAL(8),INTENT(OUT)::TM,D_LOAD !Total mass of structure,total dead load on
structure
REAL(8),DIMENSION(NODE),INTENT(OUT)::ND_STR,N_THK,N_DIA !Nodal stress MPa,
Thicknesses & diameters (m)
REAL(8),DIMENSION(NEL),INTENT(OUT)::TLEN !Lengths of individual members m
REAL(8),DIMENSION(NEL),INTENT(OUT)::TEN !Individual member stresses (as a result
lof
unit force) MPa
REAL(8),DIMENSION(NEL),INTENT(OUT)::SLEN !Lengths of individual windward(& also
leeward) members m

```

```

REAL(8),DIMENSION(NEL),INTENT(OUT)::DIA      !Diameters of members m
REAL(8),DIMENSION(NEL),INTENT(OUT)::AREA,THK !Area m^2 and thickness m of individual
members
CHARACTER(1),DIMENSION(3)::DIR=('/X','Y','Z'/)
INTEGER,ALLOCATABLE::IND(:),EFT(:)        !Solution vector for LU decomposition and
!global

matrix builder
INTEGER,ALLOCATABLE::NBAR(:,:)            !Member vertices (2 sets of coordinates
describing                                !their
start and end positions)
REAL(8),ALLOCATABLE::SL(:,:),RE(:)       !Local stiffness matrix and Young's modulus
ratio

(for the case of diff materials)
REAL(8),ALLOCATABLE,DIMENSION(:,:)::SR,S  !Global stiffness matrix (real and dummy
matrix)
REAL(8),ALLOCATABLE,DIMENSION(:,:)::X,Y,Z !Node coordinates (Cartesian)
REAL(8),ALLOCATABLE::FR(:),F(:),DIS(:),N_AREA(:) !Force vector matrix (real and dummy
vectors)
REAL(8)::FF                                !Unit load on structure MN
INTEGER::NDIS,NFORC                         !No of nodes having zero displacements and
!no of loads (force) acting
on structure
REAL(8)::MSS,D_T,Z_MAX,N_STR
INTEGER::I,II,J,J0,JJ,K,L,M,NJ,NI,I1,I2
CHARACTER(70)::TITLE
INTEGER::DOF,GMSH
DOF=3
ALLOCATE(IND(NN),EFT(6),NBAR(2,NEL),SR(NN,NN),S(NN,NN),SL(6,6),&
RE(NEL),X(1,NODE),Y(1,NODE),Z(1,NODE),FR(NN),F(NN),&
DIS(NN),N_AREA(NODE))
OPEN(5,FILE='STRUCTURE.DAT')
OPEN(9,FILE='GMSH_INPUT.DAT')
! node data/ element data *****
DO I=1,NODE
CALL NEW_COORD(X(1,I),Y(1,I),Z(1,I),I)
END DO
WRITE(6,100)
DO I=1,NEL
CALL NEW_NODE(NBAR(:,I),RE(I),AREA(I),DIA(I),THK(I),I)
END DO
SR=0.
S=0.
! local and global stiffness matrices *****
DO I=1,NEL
NI = NBAR(1,I)
NJ = NBAR(2,I)
DO II=1,1
JJ=1
CALL NEW_LOCALS(X(JJ,NI),X(JJ,NJ),Y(JJ,NI),Y(JJ,NJ),Z(JJ,NI),&
Z(JJ,NJ),RE(I),AREA(I),SL)
END DO
EFT(1) = DOF*(NI-1)+1      !SAME AS M=(J*DOF)-DOF+K .. SEE BELOW
EFT(2) = EFT(1)+1
EFT(3) = EFT(2)+1
EFT(4) = DOF*(NJ-1)+1
EFT(5) = EFT(4)+1
EFT(6) = EFT(5)+1
DO J=1,6
J0=EFT(J)
DO K=1,6
JJ=EFT(K)
S(J0,JJ)=S(J0,JJ)+SL(J,K)
END DO
END DO
END DO
!-----write properly formatted stiffness matrix to file-----
!OPEN(15,FILE='MATR.DAT')
!DO I = 1,NN
!WRITE (15,3123) (SR(I,J), J=1,NN)
!3123 FORMAT (364(1X,F15.8))
!END DO
! fixed displacement boundary conditions *****
READ(5,*) NDIS
WRITE(6,200) NDIS
DO I=1,NDIS
READ(5,*) J,K
WRITE(6,300) DIR(K),J
M=(J*DOF)-DOF+K
DO L=1,NN
S(M,L)=0.D0
S(L,M)=0.D0
END DO
S(M,M)=1.D0
END DO

```

```

F=0.
! force boundary conditions *****
D_LOAD=0.
READ(5,*) NFORC
WRITE(6,400) NFORC
DO I=1,NFORC
  READ(5,*) J,K,FF
  WRITE(6,600) DIR(K),J,FF
  M=(J*DOF)-DOF+K
  F(M)=FF
  D_LOAD=D_LOAD+ABS(FF)
END DO
! solve it !! *****
S=S*EE
DIS=0.
CALL GS_SOR(S,F,DIS,NN,I)
! displacement output *****
WRITE(6,700)
DO I=1,NODE
  J=DOF*I-2 !CHANGED FROM 2 TO DOF & FROM 1 TO 2
  WRITE(6,800) I,DIS(J),DIS(J+1),DIS(J+2) !displacement in each axis
                                         ! (I.E
Y=J+1...etc)
END DO
! tension/extension output
WRITE(6,900)
ND_STR=0.
N_AREA=0.
DO I=1,NEL
  NI = NBAR(1,I)
  NJ = NBAR(2,I)
  I1=(DOF*NI)-2 !CHANGED FROM 2 TO DOF & FROM 1 TO 2
  I2=(DOF*NJ)-2 !CHANGED FROM 2 TO DOF & FROM 1 TO 2
  DO II=1,1
    JJ=1
    CALL NEW_TENDON (X(JJ,NI),X(JJ,NJ),Y(JJ,NI),Y(JJ,NJ),Z(JJ,NI),&
                     Z(JJ,NJ),RE(I),AREA(I),DIS(I1),DIS(I2),EE,TLEN(I),TEN(I),N_STR,I)
  END DO
  ND_STR(NI)=ND_STR(NI)+N_STR
  ND_STR(NJ)=ND_STR(NJ)+(-N_STR)
  N_AREA(NI)=N_AREA(NI)+AREA(I)
  N_AREA(NJ)=N_AREA(NJ)+AREA(I)
!*****PRINCIPAL THICKNESS*****
!***** (LEAST THICK SECTION) FOR NODE LEFM ANALYSIS*****
  N_THK(NI)=MIN(THK(NI),THK(NJ))
  IF (THK(NI)<=THK(NJ))THEN
    N_DIA(NI)=DIA(NI)
  ELSE
    N_DIA(NI)=DIA(NJ)
  END IF
  N_THK(NJ)=MIN(N_THK(NI),THK(NJ))
  IF (N_THK(NI)<=THK(NJ))THEN
    N_DIA(NJ)=DIA(NI)
  ELSE
    N_DIA(NJ)=DIA(NJ)
  END IF
!*****
END DO
! reaction forces
WRITE(6,950)
DO I=1,NN
  FR(I)=0.D0
  DO J=1,NN
    FR(I)=FR(I)+S(I,J)*DIS(J)
  END DO
END DO
DO I=1,NODE
  J=DOF*I-2 !CHANGED FROM 2 TO DOF & FROM 1 TO 2
  WRITE(6,800) I,FR(J),FR(J+1),FR(J+2)
END DO
WRITE(6,1050)
DO I=1,NODE
  WRITE(6,809) I,ND_STR(I)
END DO
!===== DERIVED DATA =====
H=MAXVAL(Y)-MINVAL(Y)
W=MAXVAL(Z)-MINVAL(Z)
D_T=MINVAL(DIA)
D_G=MAXVAL(DIA)
MEM_LEN=MAXVAL(X)
!=====TM-> total mass of the whole structure=====
TM=0.
DO I=1,NEL
  MSS=MASS(TLEN(I),AREA(I),DENS)
  TM=TM+MSS
END DO

```

```

WRITE(*,*)'STRUCTURAL MASS = ',TM,'kg'
!=====SLEN-> Lengths of individual windward(& also leeward) truss
members=====
Z_MAX=MAXVAL(Z)
DO I=1,NEL
  NI = NBAR(1,I)
  NJ = NBAR(2,I)
  CALL WIND_MEM(X(1,NI),X(1,NJ),Y(1,NI),Y(1,NJ),Z(1,NI),Z(1,NJ),Z_MAX,SLEN(I))
END DO
!+++++E.N.D+++++
READ(5,500) TITLE
WRITE(6,610) TITLE
! end main routine *****
CLOSE (5)
CLOSE (6)
CLOSE (9)
DEALLOCATE(IND,EFT,NBAR,SR,S,SL,RE,X,Y,Z,FR,F,DIS,N_AREA)
TYPE *,'END OF FEA BLOCK SUBROUTINE'
!GMSH=RUNQQ('gmsH','GMSH_INPUT.DAT')
RETURN
500 FORMAT(A70)
610 FORMAT(/' ',70('-'))/' ',A70/' ',70('-'))
100 FORMAT()
200 FORMAT(/' ', '# OF FIXED DISPLACEMENTS =',I5)
300 FORMAT(' ',5X,A1,'-COMPONENT AT NODE #',I5)
400 FORMAT(/' ', '# OF GIVEN FORCES =',I5)
600 FORMAT(' ',5X,A1,'-COMPONENT AT NODE #',I5,' ; (VALUE=',1PD15.7,' )')
700 FORMAT(/' ', '----- RESULTS OUTPUT -----'/' ', 'DISPLACEMENT:'/' ', '&
  NODE',7X,'X-DIR',10X,'Y-DIR',10X,'Z-DIR')
800 FORMAT(' ',I5,3X,1PD15.7)
809 FORMAT(' ',I5,3X,1PD15.7)
900 FORMAT(/' ', 'TENSION/EXTENSION:'/' ', 'ELEMENT' 4X, 'TENSION',8X, 'EXTENSION')
950 FORMAT(/' ', 'REACTION (OR APPLIED) FORCES:'/' ', ' NODE',7X,'X-DIR',10X,&
  'Y-DIR',10X,'Z-DIR')
1050 FORMAT(/' ', 'NODAL STRESSES:'/' ', ' NODE',7X,'STRESS')
354 FORMAT(F6.4)
364 FORMAT(F6.4)
374 FORMAT(F6.4)
END SUBROUTINE FEA_BLOCK

```

```

-----
SUBROUTINE OPT_FEA_BLOCK(T25,K1,NODE,NEL,NN,EE,DENS,MEM_LEN,H,W,D_G,TM,&
  D_LOAD,TLEN,TEN,SLEN,DIA,AREA,THK,ND_STR,N_THK,N_DIA,ALL_OK,&
  FT,MOD_DIA,MOD_THK,B_CHR)
USE DIMENSIONS
IMPLICIT NONE
REAL::MASS !Function to determine mass of individual members
!INTEGER,INTENT(IN)::DOF !DEGREE OF FREEDOM = 3 (3-D)
!-----
INTEGER,INTENT(IN)::K1
REAL(8),INTENT(INOUT)::T25(K1)
REAL(8),INTENT(INOUT)::MOD_DIA(NEL),MOD_THK(NEL)
CHARACTER,INTENT(INOUT)::B_CHR(NEL)
!-----
INTEGER,INTENT(IN)::NN !Total degrees of freedom (dof x node)
INTEGER,INTENT(IN)::NODE !Total number of nodes
INTEGER,INTENT(IN)::NEL !Total number of members
INTEGER,INTENT(INOUT)::ALL_OK !0=NO FAULT; 1= FAULT
REAL(8),INTENT(IN)::EE,DENS,FT !Young's modulus MPa
REAL(8),INTENT(OUT)::MEM_LEN !length of member (boom arm) m
REAL(8),INTENT(OUT)::H,W !Height m, width m
REAL(8),INTENT(OUT)::D_G !chord diameter (Shell thickness) m
REAL(8),INTENT(OUT)::TM,D_LOAD !Total mass of structure kg, total dead loads on
structure kg
REAL(8),DIMENSION(NODE),INTENT(OUT)::ND_STR,N_THK,N_DIA !Nodal stress MPa
Thicknesses & diameters m
REAL(8),DIMENSION(NEL),INTENT(OUT)::TLEN !Lengths of individual members m
REAL(8),DIMENSION(NEL),INTENT(OUT)::TEN !Individual member stresses
!-----
a result of unit force) MPa
REAL(8),DIMENSION(NEL),INTENT(OUT)::SLEN !Lengths of individual windward(& also
leeward) members m
REAL(8),DIMENSION(NEL),INTENT(OUT)::DIA !Diameters of members m
REAL(8),DIMENSION(NEL),INTENT(OUT)::AREA,THK !Area m^2 and thickness m of individual
members
CHARACTER(1),DIMENSION(3)::DIR=('/X','Y','Z'/)
INTEGER,ALLOCATABLE::IND(:),EFT(:) !solution vector for LU decomposition and
! global
matrix builder
INTEGER,ALLOCATABLE::NBAR(:,:) !Member vertices (2 sets of coordinates
!describing
their start and end positions)
REAL(8),ALLOCATABLE::SL(:,:),RE(:) !Local stiffness matrix and Young's
!modulus
ratio (for the case of diff materials)

```

```

REAL(8),ALLOCATABLE,DIMENSION(:,:)::SR,S      !Global stiffness matrix (real and dummy
matrix)
REAL(8),ALLOCATABLE,DIMENSION(:,:)::X,Y,Z    !Node coordinates (cartesian)
REAL(8),ALLOCATABLE::FR(:),F(:),DIS(:),N_AREA(:) !Force vector matrix (real and
dummy vectors)
REAL(8)::FF                                  !Unit load on structure MN
INTEGER::NDIS,NFORC                          !No of nodes having zero displacements and
                                              !no of loads (force) acting
on structure
REAL(8)::MSS,D_T,Z_MAX,N_STR
INTEGER::I,II,J,J0,JJ,K,L,M,NJ,NI,I1,I2
CHARACTER(70)::TITLE
INTEGER::STATUS(NEL),STATUS_2(NEL),MECH_CHECK,DIM_CHECK
CHARACTER::CHR(NEL)
INTEGER::DOF
LOGICAL::LGC,LGC_1
REAL(8)::CF,RN,LL,UL
STATUS_2=0
DIM_CHECK=0
MOD_DIA=0.
MOD_THK=0.
DO
  MECH_CHECK=0
  STATUS=0
  DOF=3
  ALLOCATE(IND(NN),EFT(6),NBAR(2,NEL),SR(NN,NN),S(NN,NN),&
           SL(6,6),RE(NEL),X(1,NODE),Y(1,NODE),Z(1,NODE),FR(NN),F(NN),&
           DIS(NN),N_AREA(NODE))
  OPEN(5,FILE='STRUCTURE.DAT')
! node data/ element data *****
  DO I=1,NODE
    CALL NEW_COORD(X(1,I),Y(1,I),Z(1,I),I)
  END DO
  WRITE(6,100)
  DO I=1,NEL
    CALL
NEW_NODE(T25,K1,NBAR(:,I),RE(I),AREA(I),DIA(I),THK(I),MOD_DIA(I),MOD_THK(I),ALL_OK,&
        DIM_CHECK,MECH_CHECK,B_CHR,CHR(I),I,NEL)
  END DO
  S=0.
  SR=0.
! local and global stiffness matrices *****
  DO I=1,NEL
    NI = NBAR(1,I)
    NJ = NBAR(2,I)
    DO II=1,1
      JJ=1
      CALL
NEW_LOCALS(X(JJ,NI),X(JJ,NJ),Y(JJ,NI),Y(JJ,NJ),Z(JJ,NI),Z(JJ,NJ),RE(I),AREA(I),SL)
    END DO
    EFT(1) = DOF*(NI-1)+1      !SAME AS M=(J*DOF)-DOF+K .. SEE BELOW
    EFT(2) = EFT(1)+1
    EFT(3) = EFT(2)+1
    EFT(4) = DOF*(NJ-1)+1
    EFT(5) = EFT(4)+1
    EFT(6) = EFT(5)+1
    DO J=1,6
      J0=EFT(J)
      DO K=1,6
        JJ=EFT(K)
        S(J0,JJ)=S(J0,JJ)+SL(J,K)
      END DO
    END DO
  END DO
!-----write properly formatted stiffness matrix to file-----
!OPEN(15,FILE='MATR.DAT')
!DO I = 1,NN
!WRITE (15,3123) (SR(I,J), J=1,NN)
!3123 FORMAT (364(1X,F15.8))
!END DO
! fixed displacement boundary conditions *****
  READ(5,*) NDIS
  WRITE(6,200) NDIS
  DO I=1,NDIS
    READ(5,*) J,K
    WRITE(6,300) DIR(K),J
    M=(J*DOF)-DOF+K
    DO L=1,NN
      S(M,L)=0.D0
      S(L,M)=0.D0
    END DO
    S(M,M)=1.D0
  END DO
  F=0.
! force boundary conditions *****
  D_LOAD=0.

```

```

READ(5,*) NFORC
WRITE(6,400) NFORC
DO I=1,NFORC
  READ(5,*) J,K,FF
  WRITE(6,600) DIR(K),J,FF
  M=(J*DOF)-DOF+K
  F(M)=FF
  D_LOAD=D_LOAD+ABS(FF)
END DO
! solve it !! *****
S=S*EE
DIS=0.
CALL GS_SOR(S,F,DIS,NN,I)
! displacement output *****
WRITE(6,700)
DO I=1,NODE
  J=DOF*I-2 !CHANGED FROM 2 TO DOF & FROM 1 TO 2
  WRITE(6,800) I,DIS(J),DIS(J+1),DIS(J+2) !displacement in each axis (I.E
Y=J+1...etc)
END DO
! tension/extension output
WRITE(6,900)
ND_STR=0.
N_AREA=0.
DO I=1,NEL
  NI = NBAR(1,I)
  NJ = NBAR(2,I)
  I1=(DOF*NI)-2 !CHANGED FROM 2 TO DOF & FROM 1 TO 2
  I2=(DOF*NJ)-2 !CHANGED FROM 2 TO DOF & FROM 1 TO 2
  DO II=1,1
  JJ=1
    CALL NEW_TENDON (X(JJ,NI),X(JJ,NJ),Y(JJ,NI),Y(JJ,NJ),Z(JJ,NI),&
Z(JJ,NJ),RE(I),AREA(I),DIS(I1),DIS(I2),EE,TLEN(I),TEN(I),N_STR,I)
  END DO
  ND_STR(NI)=ND_STR(NI)+N_STR
  ND_STR(NJ)=ND_STR(NJ)+(-N_STR)
  N_AREA(NI)=N_AREA(NI)+AREA(I)
  N_AREA(NJ)=N_AREA(NJ)+AREA(I)
!*****PRINCIPAL THICKNESS*****
!*****LEAST THICK SECTION) FOR NODE LEFM ANALYSIS*****
  N_THK(NI)=MIN(THK(NI),THK(NJ))
  IF (THK(NI)<=THK(NJ)) THEN
    N_DIA(NI)=DIA(NI)
  ELSE
    N_DIA(NI)=DIA(NJ)
  END IF
  N_THK(NJ)=MIN(N_THK(NI),THK(NJ))
  IF (N_THK(NI)<=THK(NJ)) THEN
    N_DIA(NJ)=DIA(NI)
  ELSE
    N_DIA(NJ)=DIA(NJ)
  END IF
!*****
END DO
!-----Check dimensions-----
B_CHR='!'
STATUS_2=0
DO I=1, NEL
  IF ((DIA(I).LE.0.).OR.(THK(I).LE.0.)) THEN
    B_CHR(I)=CHR(I)
    STATUS(I)=1
  ELSE
    MOD_DIA(I)=DIA(I)
    MOD_THK(I)=THK(I)
    STATUS(I)=0
  END IF
  IF (MAXVAL(STATUS)==1) CYCLE
  IF ((MAXVAL(STATUS)==1).AND.(I==NEL)) EXIT
  IF (TEN(I)<0.) THEN !Compression
    CALL MEM_COMP(AREA(I),DIA(I),THK(I),TLEN(I),TEN(I),EE,LGC)
    IF (LGC==.TRUE.) THEN
      STATUS_2(I)=1
      B_CHR(I)=CHR(I)
    ELSE
      MOD_DIA(I)=DIA(I)
      MOD_THK(I)=THK(I)
      STATUS_2(I)=0
    END IF
  ELSE !Tension
    CALL MEM_TENS(AREA(I),TEN(I),FT,LGC_1)
    IF (LGC_1==.TRUE.) THEN
      STATUS_2(I)=1
      B_CHR(I)=CHR(I)
    ELSE
      MOD_DIA(I)=DIA(I)

```

```

                MOD_THK(I)=THK(I)
                STATUS_2(I)=0
            END IF
        END IF
    END DO
    DIM_CHECK=0
    IF (MAXVAL(STATUS)==1)DIM_CHECK=1
    IF (MAXVAL(STATUS_2)==1)MECH_CHECK=1
! -----reaction forces-----
    WRITE(6,950)
    DO I=1,NN
        FR(I)=0.D0
        DO J=1,NN
            FR(I)=FR(I)+S(I,J)*DIS(J)
        END DO
    END DO
    DO I=1,NODE
        J=DOF*I-2 !CHANGED FROM 2 TO DOF & FROM 1 TO 2
        WRITE(6,800) I,FR(J),FR(J+1),FR(J+2)
    END DO
    WRITE(6,1050)
    DO I=1,NODE
        WRITE(6,809) I,ND_STR(I)
    END DO
! ----- DERIVED DATA -----
    H=MAXVAL(Y)-MINVAL(Y)
    W=MAXVAL(Z)-MINVAL(Z)
    D_T=MINVAL(DIA)
    D_G=MAXVAL(DIA)
    MEM_LEN=MAXVAL(X)
! -----TM-> total mass of the whole structure-----
    TM=0.
    DO I=1,NEL
        MSS=MASS(TLEN(I),AREA(I),DENS)
        TM=TM+MSS
    END DO
    WRITE(*,*)'STRUCTURAL MASS = ',TM,'kg'
! -----SLEN-> Lengths of individual windward(& also leeward) truss
members-----
    Z_MAX=MAXVAL(Z)
    DO I=1,NEL
        NI = NBAR(1,I)
        NJ = NBAR(2,I)
        CALL WIND_MEM(X(1,NI),X(1,NJ),Y(1,NI),Y(1,NJ),Z(1,NI),Z(1,NJ),Z_MAX,SLEN(I))
    END DO
!+++++E.N.D+++++
    READ(5,500) TITLE
    WRITE(6,610) TITLE
! end main routine *****
    CLOSE (5)
    CLOSE (6)
    CLOSE (9)
    DEALLOCATE(IND,EFT,NBAR,SR,S,SL,RE,X,Y,Z,FR,F,DIS,N_AREA)
    TYPE *, 'END OF FEA BLOCK SUBROUTINE'
    !GMSH=RUNQQ('gmsb','GMSH_INPUT.DAT')
    IF ((MECH_CHECK==0).AND.(DIM_CHECK==0)) THEN
        ALL_OK=0
    ELSE
        ALL_OK=1
    END IF
    IF (ALL_OK==0) THEN
        B_CHR='!'
        EXIT
    ELSE
        END IF
    END DO
    RETURN
500 FORMAT(A70)
610 FORMAT('/' ,70('-')/' ',A70/' ',70('-'))
100 FORMAT()
200 FORMAT('/' , '# OF FIXED DISPLACEMENTS =',I5)
300 FORMAT(' ',5X,A1,'-COMPONENT AT NODE #',I5)
400 FORMAT('/' , '# OF GIVEN FORCES =',I5)
600 FORMAT(' ',5X,A1,'-COMPONENT AT NODE #',I5,' : (VALUE=',1PD15.7,' )')
700 FORMAT('/' , '----- RESULTS OUTPUT -----/' , 'DISPLACEMENT:'/' ', 'NODE',7X,'X-
DIR',10X,'Y-DIR',10X,'Z-DIR')
800 FORMAT(' ',I5,3X,1P3D15.7)
809 FORMAT(' ',I5,3X,1PD15.7)
900 FORMAT('/' , 'TENSION/EXTENSION:'/' ', 'ELEMENT',4X,'TENSION',8X,'EXTENSION')
950 FORMAT('/' , 'REACTION (OR APPLIED) FORCES:'/' ', 'NODE',7X,'X-DIR',10X,'Y-
DIR',10X,'Z-DIR')
1050 FORMAT('/' , 'NODAL STRESSES:'/' ', 'NODE',7X,'STRESS')
354 FORMAT(F6.4)
364 FORMAT(F6.4)
374 FORMAT(F6.4)
END SUBROUTINE FEA_BLOCK

```



```

-----
! INPUT NODE NO. OF ONE ELEMENT *****
SUBROUTINE NEW_NODE(NBAR,RE,AREA,DIA,THK,I)
USE DIMENSIONS
IMPLICIT NONE
INTEGER,INTENT(IN)::I
INTEGER,INTENT(OUT)::NBAR(2)
REAL(8),INTENT(OUT)::RE
REAL(8),INTENT(OUT)::AREA
REAL(8),INTENT(OUT)::DIA
REAL(8),INTENT(OUT)::THK
CHARACTER::CHR
READ(5,*) NBAR(1),NBAR(2),RE,DIA,THK,CHR
AREA=PI*THK*(DIA-THK)
WRITE(6,200) I,NBAR(1),NBAR(2),RE,AREA
WRITE(9,950) I,NBAR(1),NBAR(2)
RETURN
200 FORMAT(' ', 'ELMT NO.', I5, ' [', I5, ' -', I5, ' ] : E/E0 =', 1PD15.7, &
' : AREA =', D15.7)
950 FORMAT('Line(', I3, ') = {', I3, ', ', I3, ' } ;')
END
-----

```

```

-----
! INPUT NODE NO. OF ONE ELEMENT *****
SUBROUTINE OPT_NEW_NODE(T25,K1,NBAR,RE,AREA,DIA,THK,MOD_DIA,MOD_THK,&
ALL_OK,DIM_CHECK,MECH_CHECK,B_CHR,CHR,I,NEL)
USE DIMENSIONS
IMPLICIT NONE
!-----
INTEGER,INTENT(IN)::K1,NEL
REAL(8),INTENT(INOUT)::T25(K1)
!-----
INTEGER,INTENT(IN)::I
INTEGER,INTENT(OUT)::NBAR(2)
REAL(8),INTENT(OUT)::RE
REAL(8),INTENT(OUT)::AREA
REAL(8),INTENT(OUT)::THK,DIA
REAL(8),INTENT(OUT)::MOD_THK,MOD_DIA
CHARACTER,INTENT(IN)::B_CHR(NEL)
INTEGER,INTENT(IN)::DIM_CHECK,MECH_CHECK,ALL_OK
INTEGER::J
CHARACTER::CHR,FLT
READ(5,*) NBAR(1),NBAR(2),RE,DIA,THK,CHR
IF ((DIM_CHECK==1).OR.(MECH_CHECK==1)) THEN la group dimension was faulty
DO J=1,NEL
IF (CHR==B_CHR(J)) THEN
FLT=B_CHR(J)
ELSE
END IF
END DO
IF (CHR=='A') THEN
IF ('A'==FLT) THEN
T25(1)=ABS(T25(1)) ; T25(2)=ABS(T25(2))
THK=THK+((T25(1)/100.)*THK)
DIA=DIA+((T25(2)/100.)*DIA)
ELSE
THK=MOD_THK; DIA=MOD_DIA
END IF
ELSE IF (CHR=='B') THEN
IF ('B'==FLT) THEN
T25(3)=ABS(T25(3)) ; T25(4)=ABS(T25(4))
THK=THK+((T25(3)/100.)*THK)
DIA=DIA+((T25(4)/100.)*DIA)
ELSE
THK=MOD_THK; DIA=MOD_DIA
END IF
ELSE IF (CHR=='C') THEN
IF ('C'==FLT) THEN
T25(5)=ABS(T25(5)) ; T25(6)=ABS(T25(6))
THK=THK+((T25(5)/100.)*THK)
DIA=DIA+((T25(6)/100.)*DIA)
ELSE
THK=MOD_THK; DIA=MOD_DIA
END IF
ELSE IF (CHR=='D') THEN
IF ('D'==FLT) THEN
T25(7)=ABS(T25(7)) ; T25(8)=ABS(T25(8))
THK=THK+((T25(7)/100.)*THK)
DIA=DIA+((T25(8)/100.)*DIA)
ELSE
THK=MOD_THK; DIA=MOD_DIA
END IF
ELSE IF (CHR=='E') THEN

```

```

IF ('E'==FLT) THEN
  T25(9)=ABS(T25(9)) ; T25(10)=ABS(T25(10))
  THK=THK+((T25(9)/100.)*THK)
  DIA=DIA+((T25(10)/100.)*DIA)
ELSE
  THK=MOD_THK; DIA=MOD_DIA
END IF
ELSE IF (CHR=='F') THEN
  IF ('F'==FLT) THEN
    T25(11)=ABS(T25(11)) ; T25(12)=ABS(T25(12))
    THK=THK+((T25(11)/100.)*THK)
    DIA=DIA+((T25(12)/100.)*DIA)
  ELSE
    THK=MOD_THK; DIA=MOD_DIA
  END IF
ELSE IF (CHR=='G') THEN
  IF ('G'==FLT) THEN
    T25(13)=ABS(T25(13)) ; T25(14)=ABS(T25(14))
    THK=THK+((T25(13)/100.)*THK)
    DIA=DIA+((T25(14)/100.)*DIA)
  ELSE
    THK=MOD_THK; DIA=MOD_DIA
  END IF
ELSE IF (CHR=='H') THEN
  IF ('H'==FLT) THEN
    T25(15)=ABS(T25(15)) ; T25(16)=ABS(T25(16))
    THK=THK+((T25(15)/100.)*THK)
    DIA=DIA+((T25(16)/100.)*DIA)
  ELSE
    THK=MOD_THK; DIA=MOD_DIA
  END IF
ELSE
  THK=MOD_THK; DIA=MOD_DIA
END IF
AREA=PI*THK*(DIA-THK)
WRITE(6,200) I,NBAR(1),NBAR(2),RE,AREA
RETURN
END IF
IF (ALL_OK==0) THEN !No fault in group dimensions
  IF (CHR=='A') THEN
    THK=THK+((T25(1)/100.)*THK)
    DIA=DIA+((T25(2)/100.)*DIA)
  ELSE IF (CHR=='B') THEN
    THK=THK+((T25(3)/100.)*THK)
    DIA=DIA+((T25(4)/100.)*DIA)
  ELSE IF (CHR=='C') THEN
    THK=THK+((T25(5)/100.)*THK)
    DIA=DIA+((T25(6)/100.)*DIA)
  ELSE IF (CHR=='D') THEN
    THK=THK+((T25(7)/100.)*THK)
    DIA=DIA+((T25(8)/100.)*DIA)
  ELSE IF (CHR=='E') THEN
    THK=THK+((T25(9)/100.)*THK)
    DIA=DIA+((T25(10)/100.)*DIA)
  ELSE IF (CHR=='F') THEN
    THK=THK+((T25(11)/100.)*THK)
    DIA=DIA+((T25(12)/100.)*DIA)
  ELSE IF (CHR=='G') THEN
    THK=THK+((T25(13)/100.)*THK)
    DIA=DIA+((T25(14)/100.)*DIA)
  ELSE IF (CHR=='H') THEN
    THK=THK+((T25(15)/100.)*THK)
    DIA=DIA+((T25(16)/100.)*DIA)
  ELSE
    THK=THK ; DIA=DIA
  END IF
  AREA=PI*THK*(DIA-THK)
  WRITE(6,200) I,NBAR(1),NBAR(2),RE,AREA
  RETURN
END IF
AREA=PI*THK*(DIA-THK)
WRITE(6,200) I,NBAR(1),NBAR(2),RE,AREA
RETURN
)100 FORMAT(2I5,3F10.0)
200 FORMAT(' ', 'ELMT NO.', I5, ' [' , I5, ' -', I5, ' ] : E/E0 =', 1PD15.7, ' : AREA =', D15.7)
END

```

```

! input node no. and its coordinates *****
SUBROUTINE NEW_COORD(X,Y,Z,I)
IMPLICIT NONE
INTEGER, INTENT(IN)::I
REAL(8), INTENT(OUT)::X,Y,Z
READ(5,*) X,Y,Z
WRITE(6,200) I,X,Y,Z

```

```

WRITE(9,750) I,X,Y,Z
RETURN
200 FORMAT(' ', 'NODE NO.', I5, ' : X=', 1PD15.7, ' Y=', D15.7, ' Z=', D15.7)
750 FORMAT('Point(', I3, ') = {', F5.2, ', ', F5.2, ', ', F5.2, ', 0.01} ;')
END

```

```

-----
! FORM LOCAL STIFFNESS MATRIX *****
SUBROUTINE NEW_LOCALS ( X1,X2,Y1,Y2,Z1,Z2,RE,AREA,SL )
USE DIMENSIONS
IMPLICIT NONE
REAL(8), INTENT(IN):: X1,X2,Y1,Y2,Z1,Z2,AREA
REAL(8), INTENT(IN):: RE
REAL(8), INTENT(OUT):: SL(6,6)
REAL(8):: CTZ,CTY,CTX,THY,THX,THZ,TLEN
INTEGER:: I,J
THX=X2-X1           !X-DISTANCE BTW 2 POINTS ON X-PLANE
THY=Y2-Y1           !Y-DISTANCE BTW 2 POINTS ON Y-PLANE
THZ=Z2-Z1           !Z-DISTANCE BTW 2 POINTS ON Z-PLANE
TLEN=SQRT(THX*THX+THY*THY+THZ*THZ) !LENGTH BTW THE 2 POINTS (CARTESIAN COORD.)
CTX=THX/TLEN
CTY=THY/TLEN
CTZ=THZ/TLEN
SL(1,1:3)=(/(CTX*CTX),(CTX*CTY),(CTX*CTZ)/)
SL(2,1:3)=(/(CTX*CTY),(CTY*CTY),(CTY*CTZ)/)
SL(3,1:3)=(/(CTX*CTZ),(CTY*CTZ),(CTZ*CTZ)/)
SL(4:6,4:6)=SL(1:3,1:3)
SL(1:3,4:6)=-SL(1:3,1:3)
SL(4:6,1:3)=SL(1:3,4:6)
SL=SL*RE*AREA/TLEN
RETURN
END

```

```

-----
SUBROUTINE GS_SOR(A,B,X,N,ITER)
! =====
! SOLUTIONS TO A SYSTEM OF LINEAR EQUATIONS A*X=B
! METHOD: THE SUCCESSIVE-OVER-RELAXATION (SOR)
! ALEX G. (NOVEMBER 2009)
! =====
! INPUT ...
! A(N,N) - ARRAY OF COEFFICIENTS FOR MATRIX A
! B(N)   - ARRAY OF THE RIGHT HAND COEFFICIENTS B
! X(N)   - SOLUTIONS (INITIAL GUESS)
! N      - NUMBER OF EQUATIONS (SIZE OF MATRIX A)
! OMEGA  - THE OVER-RALAXATION FACTOR
! EPS    - CONVERGENCE TOLERANCE
! OUTPUT ...
! X(N)   - SOLUTIONS
! ITER   - NUMBER OF ITERATIONS TO ACHIEVE THE TOLERANCE
! COMMENTS ...
! KMAX   - MAX NUMBER OF ALLOWED ITERATIONS
! =====
IMPLICIT NONE
INTEGER, PARAMETER::KMAX=100
INTEGER N
DOUBLE PRECISION A(N,N), B(N), X(N)
DOUBLE PRECISION C, OMEGA, EPS, DELTA, CONV, SUM
INTEGER I, J, K, ITER, FLAG
EPS=0.00001
OMEGA=1.0
! CHECK IF THE SYSTEM IS DIAGONALLY DOMINANT
FLAG = 0
DO I=1,N
  SUM = 0.0
  DO J=1,N
    IF(I == J) CYCLE
    SUM = SUM+ABS(A(I,J))
  END DO
  IF(ABS(A(I,I)) < SUM) FLAG = FLAG+1
END DO
IF(FLAG > 0) WRITE(*,*) 'THE SYSTEM IS NOT DIAGONALLY DOMINANT'
DO K=1,KMAX
  CONV = 0.0
  DO I=1,N
    DELTA = B(I)
    DO J=1,N
      DELTA = DELTA - A(I,J)*X(J)
    END DO
    X(I) = X(I)+OMEGA*DELTA/A(I,I)
    IF(ABS(DELTA) > CONV) CONV=ABS(DELTA)
  END DO
  IF(CONV < EPS) EXIT
END DO

```

```

ITER = K
IF(K == KMAX) WRITE (*,*) 'THE SYSTEM FAILED TO CONVERGE'
END SUBROUTINE GS_SOR

```

```

-----
! TENSION/EXTENSION CALCULATION *****
SUBROUTINE NEW_TENDON ( X1,X2,Y1,Y2,Z1,Z2,RE,AREA,D1,D2,EE,TLEN,TEN,N_STR,IEL )
USE DIMENSIONS
IMPLICIT NONE
REAL(8),INTENT(IN)::X1,X2,Y1,Y2,Z1,Z2,AREA
REAL(8),INTENT(IN)::D1(3),D2(3)
REAL(8),INTENT(IN)::RE,EE
REAL(8),INTENT(OUT)::TLEN,TEN,N_STR
INTEGER,INTENT(IN)::IEL
REAL(8)::CTX,CTY,CTZ,THY,THX,THZ,EXT
THX=X2-X1      !X-DISTANCE BTW 2 POINTS ON X-PLANE
THY=Y2-Y1      !Y-DISTANCE BTW 2 POINTS ON Y-PLANE
THZ=Z2-Z1      !Z-DISTANCE BTW 2 POINTS ON Z-PLANE
TLEN=SQRT(THX*THX+THY*THY+THZ*THZ)
CTX=THX/TLEN ; CTY=THY/TLEN ; CTZ=THZ/TLEN
TEN=((CTX*D1(1))+(CTY*D1(2))+(CTZ*D1(3))-(CTX*D2(1))-(CTY*D2(2))-(CTZ*D2(3)))*RE*EE/TLEN
N_STR=TEN
EXT=TEN/(EE*RE)
WRITE(6,100) IEL,TEN,EXT
RETURN
100 FORMAT(' ',I5,2X,1P2D15.7)
200 FORMAT(F15.10)
END

```

```

-----
SUBROUTINE WIND_MEM( X1,X2,Y1,Y2,Z1,Z2,Z_MAX,SLEN )
IMPLICIT NONE
REAL(8),INTENT(IN):: X1,X2,Y1,Y2,Z1,Z2
REAL(8),INTENT(IN)::Z_MAX
REAL(8),INTENT(OUT)::SLEN !Lengths of individual windward(& also leeward) truss members
m
REAL(8)::THY,THX,THZ
IF ((Z1==Z_MAX) .AND. (Z2==Z_MAX)) THEN
  THX=X2-X1      !X-DISTANCE BTW 2 POINTS ON X-PLANE
  THY=Y2-Y1      !Y-DISTANCE BTW 2 POINTS ON Y-PLANE
  THZ=Z2-Z1      !Z-DISTANCE BTW 2 POINTS ON Z-PLANE
  SLEN=SQRT(THX*THX+THY*THY+THZ*THZ)      !LENGTH BTW THE 2 POINTS (CARTESIAN COORD.)
ELSE
  SLEN=0.
END IF
RETURN
END

```

```

=====
SUBROUTINE LOAD_COMBINATION(D_LOAD,TM,OMEGA,W_FORCE,WF_LD,MAX_RL)
USE DIMENSIONS
IMPLICIT NONE
SAVE
REAL::GUMBEL_TRANS      !Function to transform variable to Gumbel (maximum)
distribution
REAL(8),INTENT(IN)::WF_LD      !wind force on acting on load in N
REAL(8),INTENT(IN)::W_FORCE      !wind force N
REAL(8),INTENT(IN)::MAX_RL      !Load N,
REAL(8),INTENT(IN)::TM          !total mass of structure kg
REAL(8),INTENT(IN)::D_LOAD      !weight of dead load (hook block) kg
REAL(8),INTENT(OUT)::OMEGA      !multiplier (total load on analyzed member)
REAL(8)::T_LOAD              !Total load MN
REAL(8)::RN
CALL RANDOM_NUMBER(RN)
IF (MAX_RL .GT. 0.) THEN
  IF ((W_FORCE .GT. 0.) .AND. (WF_LD .GT. 0.)) THEN
    T_LOAD=(((G*MAX_RL*RN)+(TM*G)+W_FORCE+(GUMBEL_TRANS(WF_LD,COV_D)))&
    *MEGA /D_LOAD)+1.      !Converted to MN to keep uniformity
  ELSE
    T_LOAD=(((G*MAX_RL*RN)+(TM*G))*MEGA/D_LOAD)+1.
  END IF
ELSE
  IF ((W_FORCE .GT. 0.) .AND. (WF_LD .GT. 0.)) THEN
    T_LOAD=(((TM*G)+W_FORCE+(GUMBEL_TRANS(WF_LD,COV_D)))*MEGA/D_LOAD)+1.      !Co
    nverted to MN to keep uniformity
  ELSE
    T_LOAD=(((TM*G))*MEGA/D_LOAD)+1.
  END IF
END IF
OMEGA=T_LOAD
WRITE (20,130,ADVANCE="NO")OMEGA !commented out in FLEXOPT
130 FORMAT (8X,F10.3)
RETURN
END SUBROUTINE LOAD_COMBINATION

```

```

SUBROUTINE S_LOAD_COMBINATION(LOAD_STAT,D_LOAD,TM,OMEGA,W_FORCE,WF_LD,MAX_RL)
USE DIMENSIONS
IMPLICIT NONE
SAVE
REAL::GUMBEL_TRANS      !Function to transform variable to Gumbel (maximum)
distribution
REAL(8),INTENT(IN)::WF_LD  !wind force on acting on load in N
REAL(8),INTENT(IN)::W_FORCE !wind force N
REAL(8),INTENT(IN)::MAX_RL  !Load N,
REAL(8),INTENT(IN)::TM      !total mass of structure kg
REAL(8),INTENT(IN)::D_LOAD  !weight of dead load (hook block) kg
REAL(8),INTENT(OUT)::OMEGA  !Multiplier (total load on analyzed member)
INTEGER,INTENT(IN)::LOAD_STAT !Loading status 0=false, 1=true
REAL(8)::T_LOAD           !Total load MN
REAL(8)::RN
CALL RANDOM_NUMBER(RN)
IF (LOAD_STAT==0)THEN
  IF ((W_FORCE .GT. 0.).AND.(WF_LD .GT. 0.))THEN
    T_LOAD=(((TM*G)+W_FORCE+(GUMBEL_TRANS(WF_LD,COV_D))))&
    *MEGA/D_LOAD)+1. !Converted to MN to keep uniformity
  ELSE
    T_LOAD=(((TM*G))*MEGA/D_LOAD)+1.
  END IF
  OMEGA=T_LOAD
ELSE !LOAD_STAT=1
  IF (MAX_RL .GT. 0.)THEN
    IF ((W_FORCE .GT. 0.).AND.(WF_LD .GT. 0.))THEN
      T_LOAD=(((G*MAX_RL*RN)+(TM*G)+W_FORCE+(GUMBEL_TRANS(WF_LD,COV_D))))&
      *MEGA/D_LOAD)+1. !Converted to MN to keep uniformity
    ELSE
      T_LOAD=(((G*MAX_RL*RN)+(TM*G))*MEGA/D_LOAD)+1.
    END IF
  ELSE
    IF ((W_FORCE .GT. 0.).AND.(WF_LD .GT. 0.))THEN
      T_LOAD=(((TM*G)+W_FORCE+(GUMBEL_TRANS(WF_LD,COV_D))))&
      *MEGA/D_LOAD)+1. !Converted to MN to keep uniformity
    ELSE
      T_LOAD=(((TM*G))*MEGA/D_LOAD)+1.
    END IF
  END IF
  OMEGA=T_LOAD
END IF
RETURN
END SUBROUTINE LOAD_COMBINATION

```

```

SUBROUTINE TENSILE_STRESS(OMEGA,FT,C_A,D_TENSILE,LGC_2)
USE DIMENSIONS
IMPLICIT NONE
REAL::GAUSS_TRANS      !Function to transform variable to a normal(Gaussian)
distribution.
REAL(8),INTENT(IN)::OMEGA
REAL(8),INTENT(IN)::FT      !Tensile strength MPa
REAL(8),INTENT(IN)::C_A     !Cross sectional area m^2
REAL(8),INTENT(OUT)::D_TENSILE !Tensile demand (exerted by loads) MPa
LOGICAL,INTENT(OUT)::LGC_2  !TRUE==FAILED, FALSE==SURVIVED
REAL(8)::AXIAL_STR        !Axial stress MPa
REAL(8)::NF_T             !Nominal tensile strength MPa
REAL(8)::R_TENSILE        !Tensile strength (Gaussian distributed) MPa
AXIAL_STR=OMEGA/C_A
NF_T=C_A*FT
R_TENSILE=GAUSS_TRANS(NF_T,COV_R)
D_TENSILE=GAUSS_TRANS(AXIAL_STR,COV_D)
IF (D_TENSILE >= R_TENSILE) THEN
  LGC_2=.TRUE.
  WRITE (20,130)R_TENSILE,D_TENSILE,LGC_2
ELSE
  LGC_2=.FALSE.
  WRITE (20,130,ADVANCE="NO")R_TENSILE,D_TENSILE,LGC_2
END IF
130 FORMAT (T5,2(5X,F10.3),L10) !commented in FLEXOPT and STOFLEX
RETURN
END SUBROUTINE TENSILE_STRESS

```

```

SUBROUTINE COMPRESSIVE_STRESS(OMEGA,MEM_LEN,I_MNT,C_A,EE,D_COMPRESS,LGC_3)
USE DIMENSIONS
IMPLICIT NONE
REAL::GAUSS_TRANS      !Function to transform variable to a normal(Gaussian)
distribution.
REAL(8),INTENT(IN)::OMEGA
REAL(8),INTENT(IN)::MEM_LEN !Member (LV1) length m

```

```

REAL(8),INTENT(IN)::I_MNT,C_A,EE      !second moment of the closed section area of the
beam m^4,
                                !cross-sectional area m^2, Young's Modulus MPa
REAL(8),INTENT(OUT)::D_COMPRESS      !Compressive demand (Gaussian distributed) (exerted
by loads) MPa
LOGICAL,INTENT(OUT)::LGC_3           !TRUE==FAILED, FALSE==SURVIVED
REAL(8)::AXIAL_STR                   !Axial stress MPa
REAL(8)::PCR                          !Basic compressive strength MPa
REAL(8)::R_COMPRESS                  !Compressive strength (Gaussian distributed) MPa
REAL(8)::R                            !Radius of gyration m
REAL(8)::A                            !Cross-sectional area in compression m^2
AXIAL_STR=OMEGA/C_A
R=SQRT(I_MNT/C_A)
PCR=C_A*(PI*PI*EE/(MEM_LEN/R)**2)
R_COMPRESS=GAUSS_TRANS(PCR,COV_R)
D_COMPRESS=GAUSS_TRANS(AXIAL_STR,COV_D)
IF (D_COMPRESS >= R_COMPRESS) THEN
    LGC_3=.TRUE.
    WRITE (20,130)R_COMPRESS,D_COMPRESS,LGC_3
    ELSE
    LGC_3=.FALSE.
    WRITE (20,130,ADVANCE="NO")R_COMPRESS,D_COMPRESS,LGC_3
END IF
130 FORMAT (T5,2(5X,F10.3),L10) !commented in FLEXOPT and STOFLEX
RETURN
END SUBROUTINE COMPRESSIVE_STRESS

```

```

-----
SUBROUTINE BENDING_STRESS(OMEGA,MEM_LEN,I,H,FY,D_BEND,LGC_1)
USE DIMENSIONS
IMPLICIT NONE
REAL::GAUSS_TRANS !Function to transform variable to a normal(Gaussian) distribution.
REAL(8),INTENT(IN)::FY !Axial stress MPa, Yield stress MPa
REAL(8),INTENT(IN)::MEM_LEN,H !Member length m, member height m
REAL(8),INTENT(IN)::OMEGA,I !multiplier, second moment of the closed section area of
the beam m^4
REAL(8),INTENT(OUT)::D_BEND !Bending demand (exerted by loads)(Gaussian transformed)
MPa
LOGICAL,INTENT(OUT)::LGC_1 !TRUE==FAILED, FALSE==SURVIVED
REAL(8)::C !H*0.5 Distance to neutral axis m
REAL(8)::B_STR !Basic bending stress MPa
REAL(8)::M_FORCE !Moment of force MNm
REAL(8)::Y_M !Yield moment MPam^3
REAL(8)::R_BEND !Bending strength (Gaussian distributed) MPa
REAL(8)::S
C=H*0.5
S=I/C
M_FORCE=OMEGA*MEM_LEN*0.5 !*0.5 assumes all loads in boom are conc. at the centre
B_STR=M_FORCE/S
Y_M=S*FY
R_BEND=GAUSS_TRANS(Y_M,COV_R)
D_BEND=GAUSS_TRANS(B_STR,COV_D)
IF (D_BEND >= R_BEND) THEN
    LGC_1=.TRUE.
    WRITE (20,130)R_BEND,D_BEND,LGC_1
    ELSE
    LGC_1=.FALSE.
    WRITE (20,130,ADVANCE="NO")R_BEND,D_BEND,LGC_1
END IF
130 FORMAT (T5,2(5X,F10.3),L15) !commented in FLEXOPT and STOFLEX
RETURN
END SUBROUTINE BENDING_STRESS

```

```

-----
SUBROUTINE MULTIAXIAL_STRESS(D_TENSILE,D_COMPRESS,D_BEND,FY,MUL_STR,LGC_4)
USE DIMENSIONS
IMPLICIT NONE
REAL::GAUSS_TRANS !Function to transform variable to a normal(Gaussian) distribution.
REAL(8),INTENT(IN)::D_TENSILE,D_COMPRESS ! Tensile stress MPa, Compressive stress MPa
REAL(8),INTENT(IN)::D_BEND,FY !Bending stress MPa, Yield stress MPa
REAL(8),INTENT(OUT)::MUL_STR !Multiaxial stress (yield criterion) MPa
LOGICAL,INTENT(OUT)::LGC_4 !TRUE==FAILED, FALSE==SURVIVED
REAL(8)::T !Tensile stress MPa
REAL(8)::C !Compressive stress MPa
REAL(8)::B !Bending stress MPa
REAL(8)::Y_STR !Multiaxial yield strength (Gaussian distributed) MPa
T=D_TENSILE
C=D_COMPRESS
B=D_BEND
MUL_STR=SQRT(((T-C)**2)+(B**2)-(B*(T-C)))
Y_STR=GAUSS_TRANS(FY,COV_R)
IF (MUL_STR >= Y_STR) THEN
    LGC_4=.TRUE.
    WRITE (20,130)MUL_STR,Y_STR,LGC_4

```

```

      ELSE
      LGC_4=.FALSE.
      WRITE (20,130,ADVANCE="NO")Y_STR,MUL_STR,LGC_4
    END IF
130 FORMAT (T5,2(5X,F10.3),L15) !commented in FLEXOPT and STOFLEX
    RETURN
  END SUBROUTINE MULTIAXIAL_STRESS

```

```

=====
SUBROUTINE MEM_ANALYSIS(MEMBER,OMEGA,FT,EE,TLEN,AREA,DIA,THK,TEN,NEL,LGC_5)
  IMPLICIT NONE
  INTEGER,INTENT(IN)::MEMBER !Focal member of analysis
  INTEGER,INTENT(IN)::NEL !Number of members in structure
  REAL(8),DIMENSION(NEL),INTENT(IN)::DIA !Individual diameters m
  REAL(8),DIMENSION(NEL),INTENT(IN)::THK !Individual thicknesses m
  REAL(8),DIMENSION(NEL),INTENT(IN)::TLEN !Individual lengths m
  REAL(8),DIMENSION(NEL),INTENT(IN)::AREA !Individual areas m^2
  REAL(8),DIMENSION(NEL),INTENT(IN)::TEN !Individual member stresses (as a result of
  unit force) MPa
  REAL(8),INTENT(IN)::OMEGA,FT,EE !multiplier, Tensile strength MPa, Young's modulus
  MPa
  LOGICAL,INTENT(OUT)::LGC_5 !TRUE==FAILED, FALSE==SURVIVED
  INTEGER::I,COUNT,COMP_COUNT,TEN_COUNT !Failure counters
  REAL(8)::MEM_TESN(NEL) !Member stresses augmented by multiplier
  LOGICAL,DIMENSION(NEL)::LGC_1,LGC_2 !TRUE==FAILED, FALSE==SURVIVED
  REAL(8),DIMENSION(NEL)::R_COMPRESS,D_COMPRESS,R_TENSILE,D_TENSILE
  LGC_5=.FALSE.
  COUNT=0 ; COMP_COUNT=0 ; TEN_COUNT=0
  DO I=1, NEL
    MEM_TESN(I)=TEN(I)*OMEGA
    IF (MEM_TESN(I)<0.) THEN
      CALL MEM_COMP(AREA(I),DIA(I),THK(I),TLEN(I),MEM_TESN(I),EE,&
        D_COMPRESS(I),R_COMPRESS(I),LGC_1(I))
      IF (LGC_1(I)==.TRUE.) THEN
        COMP_COUNT=COMP_COUNT+1
        WRITE(14,78) I,MEM_TESN(I)
        IF (I>=MEMBER) EXIT
      ELSE
      END IF
    ELSE
      CALL MEM_TENS(AREA(I),MEM_TESN(I),FT,D_TENSILE(I),R_TENSILE(I),&
        LGC_2(I))
      IF (LGC_2(I)==.TRUE.) THEN
        TEN_COUNT=TEN_COUNT+1
        WRITE(14,88) I,MEM_TESN(I)
        IF (I>=MEMBER) EXIT
      ELSE
      END IF
    END IF
  END DO
  COUNT=COMP_COUNT+TEN_COUNT
  IF (COUNT >0) THEN
    LGC_5=.TRUE.
  ELSE
    LGC_5=.FALSE.
  END IF
  !-----This section is commented out in FLEXOPT and STOFLEX-----
  IF ((MEM_TESN(MEMBER)>0.) .AND. (LGC_5.EQV. .TRUE.)) THEN
    WRITE (20,100)R_TENSILE(MEMBER),D_TENSILE(MEMBER),LGC_2(MEMBER)
    ELSE IF ((MEM_TESN(MEMBER)>0.) .AND. (LGC_5.EQV. .FALSE.)) THEN
      WRITE
      (20,100,ADVANCE="NO")R_TENSILE(MEMBER),D_TENSILE(MEMBER),LGC_2(MEMBER)
    ELSE
  END IF
  IF ((MEM_TESN(MEMBER)<0.) .AND. (LGC_5.EQV. .TRUE.)) THEN
    WRITE (20,100)R_COMPRESS(MEMBER),D_COMPRESS(MEMBER),LGC_1(MEMBER)
    ELSE IF ((MEM_TESN(MEMBER)<0.) .AND. (LGC_5.EQV. .FALSE.)) THEN
      WRITE
      (20,100,ADVANCE="NO")R_COMPRESS(MEMBER),D_COMPRESS(MEMBER),LGC_1(MEMBER)
    ELSE
  END IF
100 FORMAT(2(10X,ES10.3),L10)
78 FORMAT ('COMP FAIL=',I5,5X,F10.3)
88 FORMAT ('TEN FAIL=',I5,5X,F10.3)
  !-----
  RETURN
END SUBROUTINE MEM_ANALYSIS

```

```

=====
SUBROUTINE MEM_TENS(AR,TENSN,FT,D_TENSILE,R_TENSILE,LGC)
  USE DIMENSIONS
  IMPLICIT NONE
  REAL::GAUSS_TRANS !Function to transform variable to a normal(Gaussian)
  distribution.

```

```

REAL(8),INTENT(IN)::FT      !Tensile strength MPa
REAL(8),INTENT(IN)::AR      !Area m^2
REAL(8),INTENT(IN)::TENSN   !Tensile demand (exerted by loads) MPa
LOGICAL,INTENT(OUT)::LGC    !TRUE==FAILED, FALSE==SURVIVED
REAL(8)::NT_S               !Nominal tensile strength MPa
REAL(8)::D_TENSILE,R_TENSILE
NT_S=AR*FT
R_TENSILE=GAUSS_TRANS(NT_S,COV_R)
D_TENSILE=GAUSS_TRANS(TENSN,COV_D)
IF (D_TENSILE .GE. R_TENSILE) THEN
    LGC=.TRUE.
    ELSE
    LGC=.FALSE.
END IF
RETURN
END SUBROUTINE

```

```

SUBROUTINE MEM_COMP(AR,DIA,THK,LENG,TENSN,EE,D_COMPRESS,R_COMPRESS,LGC)
USE DIMENSIONS
IMPLICIT NONE
REAL::GAUSS_TRANS          !Function to transform variable to a normal(Gaussian)
distribution.
REAL(8),INTENT(IN)::EE      !YOUNG'S MODULUS
REAL(8),INTENT(IN)::AR      !AREA m^2
REAL(8),INTENT(IN)::DIA     !
REAL(8),INTENT(IN)::THK     !
REAL(8),INTENT(IN)::LENG    !LENGTH OF MEMBER
REAL(8),INTENT(IN)::TENSN   !Tensile demand (exerted by loads) MPa
LOGICAL,INTENT(OUT)::LGC    !TRUE==FAILED, FALSE==SURVIVED
REAL(8),INTENT(OUT)::D_COMPRESS,R_COMPRESS !Compressive strength MPa, Compressive
demand (exerted by loads) MPa (both Gaussian distributed)
REAL(8)::PCR                !Basic compressive strength MPa
REAL(8)::R                  !radius of gyration m
REAL(8)::A                  !Cross-sectional area in compression m^2
REAL(8)::I,RD               !second moment of the closed section area of the beam m^4, radius m
REAL(8)::TENSN_D
RD=(DIA)/2.                 !RADIUS (net)
I=AR*RD*RD*.25              !second moment of the closed section area of the beam OF HOLLOW
CYLINDER
R=SQRT(I/AR)
PCR=AR*(PI*PI*EE/(LENG/R)**2)
R_COMPRESS=GAUSS_TRANS(PCR,COV_R)
TENSN_D=ABS(TENSN)
D_COMPRESS=GAUSS_TRANS(TENSN_D,COV_D)
IF (D_COMPRESS .GE. R_COMPRESS) THEN
    LGC=.TRUE.
    ELSE
    LGC=.FALSE.
END IF
RETURN
END SUBROUTINE

```

```

SUBROUTINE MINIMUM_CRACK(MUL_STR,KRANS,BETA,A_CR)
USE DIMENSIONS
IMPLICIT NONE
REAL(8),INTENT(IN)::MUL_STR,BETA !Multiaxial stress MPa, Beta (material constant
REAL(8),INTENT(IN)::KRANS !Lognormally distributed value of the fracture toughness
(K)MPam^0.5
REAL(8),INTENT(OUT)::A_CR !Minimum crack length required to cause fracture m
REAL(8)::SIM
SIM=KRANS/(BETA*MUL_STR)
A_CR=1./PI*(SIM*SIM)
RETURN
END SUBROUTINE MINIMUM_CRACK

```

```

SUBROUTINE CRACK_LENGTH(AI,AF)
IMPLICIT NONE
REAL(8),INTENT(IN)::AI          !Lower bound of crack length m
REAL(8),INTENT(OUT)::AF         !Upper bound of crack length m
REAL(8)::EXRN
CALL EXPO_RANDOM_NUMBER(EXRN)
AF=EXRN*AI
RETURN
END SUBROUTINE CRACK_LENGTH

```

```

SUBROUTINE CRACK_GROWTH(AI,AF,DECT_CRACK,BETA,C_MAT,M_PWR,MUL_STR,J,INSPEC)
USE DIMENSIONS
IMPLICIT NONE
SAVE

```



```

REAL::LOGN_TRANS
REAL(8),INTENT(IN)::AI          !Lower bound of crack length m
REAL(8),INTENT(OUT)::AF         !Upper bound of crack length m
REAL(8),INTENT(IN)::MUL_STR
REAL(8),INTENT(IN)::M_PWR
REAL(8),INTENT(IN)::BETA
REAL(8),INTENT(IN)::C_MAT
INTEGER,INTENT(IN)::J
INTEGER,INTENT(IN)::INSPEC      !Inspection status (0==FALSE, 1==TRUE)
REAL(8),INTENT(IN)::DECT_CRACK !1mm
REAL(8)::X,A,C_MAT_TRANS_N,C_MAT_TRANS_A,EXRN
REAL(8)::RP_PERF              !initial state of joint
REAL(8)::D_A,D_N,N_EFF
INTEGER::COUNT_REC
IF ((INSPEC==1) .AND. (AF>=DECT_CRACK)) THEN
    A=RP_PERF                  !i.e. perfect repair
    WRITE(8,*)INSPEC,A
ELSE
END IF
C_MAT_TRANS_A=LOGN_TRANS(C_MAT,COV_D)
C_MAT_TRANS_N=LOGN_TRANS(C_MAT,COV_D)
IF (J==1) THEN
    D_N=0.
    COUNT_REC=J+9999
    WRITE (15,130)J,N_EFF,AF
    DO
        CALL EXPO_RANDOM_NUMBER(EXRN)
        A=AI*EXRN
        CALL EXPO_RANDOM_NUMBER(EXRN)
        AF=AI*EXRN
        RP_PERF=AF
        IF ((A>AI).AND.(AF>AI)) EXIT
    END DO
ELSE
    X=DBLE(BETA*MUL_STR*DSQRT(PI*AF))
    D_A=DBLE(C_MAT_TRANS_A*DEXP(M_PWR*DLOG(X)))
    D_N=D_A/(C_MAT_TRANS_N*DEXP(M_PWR*DLOG(X)))
END IF
CALL EXPO_RANDOM_NUMBER(EXRN)
A=A+(D_A*EXRN)
AF=A
N_EFF=N_EFF+D_N
IF (J==COUNT_REC)THEN
    COUNT_REC=COUNT_REC+10000
    WRITE (15,130)J,N_EFF,AF
ELSE
END IF
130 FORMAT (I8,5X,F10.0,6X,F14.8)
RETURN
END SUBROUTINE CRACK_GROWTH

```

```

SUBROUTINE FRAC_ANALYSIS(AF,A_CR,LGC_7)
IMPLICIT NONE
REAL(8),INTENT(IN)::AF          !Estimated crack length m
REAL(8),INTENT(IN)::A_CR        !Minimum crack length required for failure m
LOGICAL,INTENT(OUT)::LGC_7      !TRUE==FAILED, FALSE==SURVIVED
IF (AF >= A_CR) THEN
    LGC_7=.TRUE.
    WRITE (20,130)AF,A_CR,LGC_7
ELSE
    LGC_7=.FALSE.
    WRITE (20,130,ADVANCE="NO")AF,A_CR,LGC_7
END IF
130 FORMAT (2(10X,F8.4),L12)
RETURN
END SUBROUTINE FRAC_ANALYSIS

```

```

SUBROUTINE FRACT_TOUGH(MUL_STR,AF,K,BETA,K_LOAD,KRANS,LGC_6)
USE DIMENSIONS
IMPLICIT NONE
REAL::LOGN_TRANS                !Function transforming input variables to a lognormal
distribution
REAL(8),INTENT(IN)::MUL_STR,AF  !multiaxial stress MPa, estimated crack length m
REAL(8),INTENT(IN)::K,BETA      !Fracture toughness MPam0.5, Beta (material constant)
REAL(8),INTENT(OUT)::K_LOAD     !Stress intensity factor induced by multiaxial stress
MPam0.5
REAL(8),INTENT(OUT)::KRANS      !Lognormally distributed value of the fracture
toughness (K)MPam0.5
LOGICAL,INTENT(OUT)::LGC_6      !TRUE==FAILED, FALSE==SURVIVED
K_LOAD=BETA*MUL_STR*(SQRT(PI*AF))
KRANS=LOGN_TRANS(K,COV_D)
IF (K_LOAD .GE. KRANS) THEN

```

```

LGC_6=.TRUE.
WRITE (20,130)K_LOAD,KRANS,LGC_6
ELSE
LGC_6=.FALSE.
WRITE (20,130,ADVANCE="NO")K_LOAD,KRANS,LGC_6
END IF
130 FORMAT (14X,F6.3,17X,F6.3,L15)
RETURN
END SUBROUTINE FRACT_TOUGH

```

```

-----
SUBROUTINE LIFE_CYCLE(N_PL,C_MAT,M_PWR,BETA,MUL_STR,AI,A_CR,LGC_8)
!
USE DIMENSIONS
IMPLICIT NONE
REAL::LOGN_TRANS      !Function transforming input variables to a lognormal
distribution
!
INTEGER,INTENT(IN)::N_PL      !Planned/intended/design Life cycle of structure in use
REAL(8),INTENT(IN)::C_MAT      !c (material constant) (MPa^-4)(m^-1)
REAL(8),INTENT(IN)::AI        !Initial crack length m
REAL(8),INTENT(IN)::A_CR      !final crack length(critical crack length to cause
brittle fracture) m
REAL(8),INTENT(IN)::MUL_STR    !stress in material MPa
REAL(8),INTENT(IN)::BETA      !Beta material property (constant)
REAL(8),INTENT(IN)::M_PWR     !m (material constant)
LOGICAL,INTENT(OUT)::LGC_8    !TRUE==FAILED, FALSE==SURVIVED
REAL(8)::R_N_PL
REAL(8)::N_EFF                !Resultant life of the structure
REAL(8)::A_INTEG              !Integration result
REAL(8)::N_PL_TRANS           !Life (design) cycle of structure in use (lognormally
transformed)
REAL(8)::C_MAT_TRANS           !c (material constant) (MPa^-4)(m^-1) (lognormally
transformed)
C_MAT_TRANS=LOGN_TRANS(C_MAT,COV_D)
R_N_PL=DBLE(N_PL)
N_PL_TRANS=LOGN_TRANS(R_N_PL,COV_R)
CALL CRACK_INTEG(M_PWR,AI,A_CR,A_INTEG)
N_EFF=A_INTEG*1/(C_MAT_TRANS*EXP(M_PWR*LOG(BETA*MUL_STR*SQRT(PI))))
IF (N_PL_TRANS >= N_EFF) THEN
LGC_8=.TRUE.
ELSE
LGC_8=.FALSE.
END IF
WRITE (20,130)N_PL_TRANS,N_EFF,LGC_8 !commented in FLEXOPT and STOFLEX
130 FORMAT (2(8X,ES10.3),L15)
RETURN
END SUBROUTINE LIFE_CYCLE

```

```

-----
SUBROUTINE CRACK_INTEG(M_PWR,AI,A_CR,A_INTEG)
IMPLICIT NONE
REAL::LOGN_TRANS      !Function transforming input variables to a lognormal
distribution
REAL(8),INTENT(IN)::AI        !Initial crack length m
REAL(8),INTENT(IN)::A_CR      !final crack length(critical crack length to cause
brittle fracture) m
REAL(8),INTENT(IN)::M_PWR     !m (material constant)
REAL(8),INTENT(OUT)::A_INTEG  !Integration result
REAL(8)::X,R_AI,R_ACR
X=(M_PWR/2.)-1.
R_AI=1./(X*DEXP(X*DLOG(AI)))
R_ACR=-1./(X*DEXP(X*DLOG(A_CR)))
A_INTEG=R_AI+R_ACR
RETURN
END SUBROUTINE CRACK_INTEG

```

```

=====
SUBROUTINE ND_LEFM_ANALYSIS(JOINT,NODE,ND_STR,N_THK,N_DIA,E,K,C_MAT,M_PWR,&
N_PL,OMEGA,AI,LGC_9)
USE DIMENSIONS
IMPLICIT NONE
INTEGER,INTENT(IN)::JOINT      !Focal joint of analysis
INTEGER,INTENT(IN)::NODE       !Total no of joints(nodes) in structure
REAL(8),INTENT(IN)::M_PWR     ! m (material constant)
REAL(8),INTENT(IN)::ND_STR(NODE) !Nodal stresses MPa
REAL(8),INTENT(IN)::OMEGA     !The nodal multiplier
REAL(8),INTENT(IN)::E,K       !Young's modulus MPa, fracture toughness MPam^1/2
REAL(8),INTENT(IN)::C_MAT     !c (material constant)
INTEGER,INTENT(IN)::N_PL      !Planned/intended/design Life cycle of structure
REAL(8),INTENT(IN)::AI        !Initial crack length bounds m
LOGICAL,INTENT(OUT)::LGC_9    !TRUE==FAILED, FALSE==SURVIVED
INTEGER::COUNT,STR_INT_COUNT,CRLN_COUNT,ND_LIFE_COUNT !Failure counters
INTEGER::I,J

```

```

REAL(8)::AREA           !Node area m^2
REAL(8)::EXPRND         !Exponential random number
REAL(8),DIMENSION(NODE)::BETA      ! Stress intensity correction factor
REAL(8),DIMENSION(NODE)::AF,A_I    !Crack length m
REAL(8),DIMENSION(NODE)::ND_MULSTR,KRANS,K_LOAD !Nodal multiaxial
                                           !stress MPa,nodal stress intensity factor
MPam^1/2
REAL(8)::A_CR(NODE)     !Minimum crack length required to cause fracture at node m
LOGICAL::LGC,LGC_1,LGC_2 !TRUE==FAILED, FALSE==SURVIVED
REAL(8)::GG
LGC_9=.FALSE.; BETA=0.; AF=0.; A_I=0.; ND_MULSTR=0.; KRANS=0.; K_LOAD=0.; A_CR=0.
COUNT=0 ; STR_INT_COUNT=0 ; CRLEN_COUNT=0 ; ND_LIFE_COUNT=0
DO I=1, NODE
  CALL MULSTR(JOINT,I,OMEGA,ND_STR(I),ND_MULSTR(I))
  A_I(I)=AI
  CALL ND_CRACK_LEN(A_I(I),AF(I))
  CALL ND_FT_SI(JOINT,I,ND_MULSTR(I),AF(I),K,BETA(I),K_LOAD(I),KRANS(I),LGC)
  IF (LGC==.TRUE.) THEN
    STR_INT_COUNT=STR_INT_COUNT+1
    WRITE(19,68) I,K_LOAD(I) !commented out in FLEXOPT
    IF(I>=JOINT) EXIT
  ELSE
    END IF
  GG=KRANS(I)/(BETA(I)*ND_MULSTR(I))
  A_CR(I)=(GG*GG)*1./PI !DETERMINE MINIMUM CRACK
  IF (AF(I)>= A_CR(I)) THEN
    CRLEN_COUNT=STR_INT_COUNT+1
    WRITE(19,78) I,AF(I),A_CR(I)
    IF (I==JOINT) WRITE (20,140)AF(I),A_CR(I) !commented out in FLEXOPT
    IF(I>=JOINT) EXIT !commented out in FLEXOPT
  ELSE
    IF (I==JOINT) WRITE (20,150,ADVANCE="NO")AF(I),A_CR(I)
  END IF
  CALL ND_LIFE(JOINT,I,N_PL,C_MAT,M_PWR,BETA(I),ND_MULSTR(I),A_I(I),A_CR(I),LGC_1)
  IF (LGC_1==.TRUE.) THEN
    ND_LIFE_COUNT=STR_INT_COUNT+1
    WRITE(19,88) I !commented out in FLEXOPT
  ELSE
    END IF
END DO
COUNT=STR_INT_COUNT+CRLEN_COUNT+ND_LIFE_COUNT
IF (COUNT >0) THEN
  LGC_9=.TRUE.
ELSE
  LGC_9=.FALSE.
END IF
68 FORMAT ('STRESS INS=',I5,5X,F15.3)
78 FORMAT ('CRK LENS=',I5,5X,2F10.3)
88 FORMAT ('LIFE FAIL=',I5,5X)

140 FORMAT(2(8X,ES10.3),8X,'T')
150 FORMAT(2(8X,ES10.3),8X,'F')
RETURN
END SUBROUTINE ND_LEFM_ANALYSIS

```

```

-----
SUBROUTINE ND_CRACK_LEN(AI,AF)
IMPLICIT NONE
REAL(8),INTENT(IN)::AI           !Lower bound of crack length m
REAL(8),INTENT(OUT)::AF          !Upper bound of crack length mREAL(8)::EXRN
CALL EXPO_RANDOM_NUMBER(EXRN)
AF=EXRN*AI
RETURN
END SUBROUTINE ND_CRACK_LEN

```

```

-----
SUBROUTINE MULSTR(JOINT,I,OMEGA,ND_STR,ND_MULSTR)
USE DIMENSIONS
IMPLICIT NONE
REAL::GAUSS_TRANS !Function to transform variable to a normal(Gaussian) distribution.
INTEGER,INTENT(IN)::JOINT,I
REAL(8),INTENT(IN)::OMEGA
REAL(8),INTENT(IN)::ND_STR !Nodal stress MPa
REAL(8),INTENT(OUT)::ND_MULSTR !stress (Transformed) MPa
REAL(8)::STR
STR=OMEGA*ABS(ND_STR)
ND_MULSTR=GAUSS_TRANS(STR,COV_D)
IF (I==JOINT) WRITE (20,100,ADVANCE="NO")ND_MULSTR !commented in FLEXOPT and STOFLEX
100 FORMAT(10X,ES10.3)
RETURN
END SUBROUTINE MULSTR

```

```

-----
SUBROUTINE ND_FT_SI(JOINT,I,MUL_STR,AF,K,THK,DIA,BETA,K_LOAD,KRANS,LGC)

```

```

USE DIMENSIONS
IMPLICIT NONE
REAL::LOGN_TRANS      !Function transforming input variables to a lognormal
distribution
INTEGER,INTENT(IN)::JOINT,I
REAL(8),INTENT(IN)::MUL_STR,AF !multiaxial stress MPa, estimated crack length m
REAL(8),INTENT(IN)::K,THK,DIA !Fracture toughness MPam0.5, thickness & diameter
REAL(8),INTENT(OUT)::BETA
REAL(8),INTENT(OUT)::K_LOAD !stress intensity factor induced by multiaxial stress
kNm0.5
REAL(8),INTENT(OUT)::KRANS !Lognormally distributed value of the fracture toughness
(K)kNm0.5
LOGICAL,INTENT(OUT)::LGC !TRUE==FAILED, FALSE==SURVIVED
CALL EXTERNAL_CRACK_TUBE (AF,THK,DIA,BETA)
K_LOAD=BETA*MUL_STR*(SQRT(PI*AF))
KRANS=LOGN_TRANS(K,COV_D)
IF (K_LOAD .GE. KRANS) THEN
  LGC=.TRUE.
  IF (I==JOINT) WRITE (20,130)K_LOAD,KRANS,LGC !commented out in FLEXOPT & STOFLEX
  ELSE
  LGC=.FALSE.
  IF (I==JOINT) WRITE (20,130,ADVANCE="NO")K_LOAD,KRANS,LGC !commented out in
FLEXOPT & STOFLEX
END IF
130 FORMAT (2(10X,ES10.3),L15)
RETURN
END SUBROUTINE ND_FT_SI

```

```

SUBROUTINE ND_LIFE(JOINT,I,N_PL,C_MAT,M_PWR,BETA,MUL_STR,AI,A_CR,LGC_8)
USE DIMENSIONS
IMPLICIT NONE
REAL::LOGN_TRANS      !Function transforming input variables to a lognormal
distribution
INTEGER,INTENT(IN)::JOINT,I
INTEGER,INTENT(IN)::N_PL !Planned/intended/design Life cycle of structure in use
REAL(8),INTENT(IN)::C_MAT !c (material constant) (MPa-4)(m-1)
REAL(8),INTENT(IN)::AI !Initial crack length m
REAL(8),INTENT(IN)::A_CR !final crack length(critical) crack length to cause
brittle fracture) m
REAL(8),INTENT(IN)::MUL_STR !stress in material MPa
REAL(8),INTENT(IN)::BETA !Beta material property (constant)
REAL(8),INTENT(IN)::M_PWR !m (material constant)
LOGICAL,INTENT(OUT)::LGC_8 !TRUE==FAILED, FALSE==SURVIVED
REAL(8)::R_N_PL
REAL(8)::N_EFF !Resultant life of the structure
REAL(8)::A_INTEG !Integration result
REAL(8)::N_PL_TRANS !Life (design) cycle of structure in use (lognormally
transformed)
REAL(8)::C_MAT_TRANS !c (material constant) (MPa-4)(m-1) (lognormally
transformed)
C_MAT_TRANS=LOGN_TRANS(C_MAT,COV_D)
R_N_PL=DBLE(N_PL)
N_PL_TRANS=LOGN_TRANS(R_N_PL,COV_R)
CALL CRACK_INTEG(M_PWR,AI,A_CR,A_INTEG)
N_EFF=A_INTEG*1/(C_MAT_TRANS*EXP(REAL(M_PWR)*LOG(BETA*MUL_STR*SQRT(PI))))
IF (N_PL_TRANS >= N_EFF) THEN
  LGC_8=.TRUE.
  ELSE
  LGC_8=.FALSE.
END IF
IF (I==JOINT) WRITE (20,130)N_PL_TRANS,N_EFF,LGC_8 ! commented in FLEXOPT and STOFLEX
130 FORMAT (2(8X,ES10.3),L10)RETURN
END SUBROUTINE ND_LIFE

```

```

SUBROUTINE ND_CRACK_GROWTH(NODE,OMEGA,AF,AI,DECT_CRACK,N_EFF,RP_PERF,N_THK,N_DIA, &
C_MAT,M_PWR,ND_STR,ND_MULSTR,J,INSPEC,JOINT)
USE DIMENSIONS
IMPLICIT NONE
SAVE
REAL::GAUSS_TRANS
REAL::LOGN_TRANS
INTEGER,INTENT(IN)::NODE
INTEGER,INTENT(IN)::JOINT !Focal joint of analysis
REAL(8),INTENT(IN)::AI !Lower bound of crack length m
REAL(8),INTENT(INOUT)::AF(NODE) !Upper bound of crack length m
REAL(8),INTENT(INOUT)::N_EFF(NODE)
REAL(8),INTENT(INOUT)::RP_PERF(NODE)
REAL(8),INTENT(OUT)::ND_MULSTR(NODE)
REAL(8),INTENT(IN)::OMEGA
REAL(8),INTENT(IN)::ND_STR(NODE),N_THK(NODE),N_DIA(NODE) !Nodal stress MPa ,Thk & Dia m
REAL(8),INTENT(IN)::M_PWR
REAL(8),INTENT(IN)::C_MAT

```

```

INTEGER, INTENT(IN)::J, INSPEC
REAL(8), INTENT(IN)::DECT_CRACK
REAL, PARAMETER::IMP_U=96.1, IMP_L=93.3      !Upper and lower bound of imperfection
coefficent
REAL, PARAMETER::DEP_U=99.2, DEP_L=97.1      !Upper and lower bound of depreciation
coefficent
REAL(8)::A, C_MAT_TRANS_N(NODE), C_MAT_TRANS_A(NODE), EXRN_1, EXRN, RN
REAL(8)::X(NODE), D_A(NODE), D_N(NODE), STR(NODE), DEP, IMP, BETA
INTEGER::INSP_COUNT, COUNT_REC, I
LOGICAL::PERF_REP
IF (J==1) THEN
  DO
    WRITE(*,*)'
    WRITE(*,*)'ENTER REPAIR SCENARIO: PERFECT REPAIR; IMPERPECT REPAIR'
    WRITE(*,*)'
    READ(*,*)I
    IF ((I /= 0).AND.(I /= 1))THEN
      WRITE(*,*)'ENTER 0 OR 1'
      CYCLE
    ELSE
      EXIT
    END IF
  END DO
  IF (I==0) THEN
    PERF_REP=.TRUE.
  ELSE
    PERF_REP=.FALSE.
  END IF
ELSE
  END IF
IF (INSPEC==1) INSP_COUNT=INSP_COUNT+1
DO I=1, NODE
  ND_MULSTR(I)=0.
  STR(I)=OMEGA*ABS(ND_STR(I))
  ND_MULSTR(I)=GAUSS_TRANS(STR(I), COV_D)
  IF (J==1) THEN
    DO
      CALL EXPO_RANDOM_NUMBER(EXRN)
      AF(I)=AI*EXRN
      IF (AF(I)<AI)EXIT
    END DO
    RP_PERF(I)=AF(I)
    D_N(I)=0.
    N_EFF(I)=0.
    INSP_COUNT=0
    COUNT_REC=J+9999
  ELSE
    C_MAT_TRANS_A(I)=LOGN_TRANS(C_MAT, COV_D)
    C_MAT_TRANS_N(I)=LOGN_TRANS(C_MAT, COV_D)
    CALL EXTERNAL_CRACK_TUBE (AF(I), N_THK(I), N_DIA(I), BETA)
    X(I)=ND_MULSTR(I)*BETA*SQRT(PI*AF(I))
    D_A(I)=C_MAT_TRANS_A(I)*EXP(M_PWR*LOG(X(I)))
    D_N(I)=D_A(I)/(C_MAT_TRANS_N(I)*EXP(M_PWR*LOG(X(I))))
    CALL EXPO_RANDOM_NUMBER(EXRN)
    AF(I)=AF(I)+(D_A(I)*EXRN)
    N_EFF(I)=N_EFF(I)+D_N(I)
  END IF
  IF ((INSPEC==1) .AND. (AF(I)>=DECT_CRACK)) THEN
    CALL RANDOM_NUMBER(RN)
    IF (PERF_REP .EQ. .TRUE.)THEN
      !-----perfect repair-----
      DEP=(RN*(DEP_U-DEP_L))+DEP_L
      AF(I)=RP_PERF(I)*(100./DEP)
      RP_PERF(I)=AF(I)
      WRITE(8, 35)I, INSP_COUNT, AF(I), DEP
    ELSE
      !-----imperfect repair-----
      IMP=(RN*(IMP_U-IMP_L))+IMP_L
      AF(I)=(RP_PERF(I)*(100./DEP))*(100./IMP)
      RP_PERF(I)=AF(I)
      WRITE(8, 55)I, INSP_COUNT, AF(I), IMP, DEP
    !-----
  END IF
  ELSE
  END IF
  IF ((J==1).AND.(I==JOINT))WRITE (15, 130)J, I, N_EFF(I), AF(I), X(I)
  IF ((J==COUNT_REC).AND.(I==JOINT))THEN !1 FOR RESULTS ON ONLY 1ST NODE
    COUNT_REC=COUNT_REC+10000
    WRITE (15, 130)J, I, N_EFF(I), AF(I), X(I)
  ELSE
  END IF
END DO
130 FORMAT (I8, 5X, I4, 5X, F10.0, 2X, F18.12, 2X, F10.3)
35 FORMAT ("PERF", 2X, I3, 2X, I2, 2X, F8.7, 2X, F6.3)
55 FORMAT ("IMPERF", 2X, I3, 2X, I2, 2X, F8.7, 2X, F6.3, 2X, F6.3)
RETURN

```

END SUBROUTINE ND\_CRACK\_GROWTH

```

=====
SUBROUTINE ND_LEFM_ANALYSIS(JOINT,NODE,ND_STR,N_THK,N_DIA,EE,K ,C_MAT,M_PWR,&
      N_PL,OMEGA,AI,AF,N_EFF,RP_PERF,DECT_CRACK,J,INSPEC,LGC_9)
USE DIMENSIONS
IMPLICIT NONE
SAVE
INTEGER,INTENT(IN)::JOINT   !Focal joint of analysis
INTEGER,INTENT(IN)::NODE   !Total no of joints(nodes) in structure
REAL(8),INTENT(IN)::M_PWR  ! m (material constant)
REAL(8),INTENT(IN)::ND_STR(NODE),N_THK(NODE),N_DIA(NODE) !Nodal stresses at nodes MPa
REAL(8),INTENT(IN)::OMEGA  !The nodal multiplier
REAL(8),INTENT(IN)::EE,K   !Young's modules MPa, fracture toughness MPam1/2,
REAL(8),INTENT(IN)::C_MAT  !c (material constant)
INTEGER,INTENT(IN)::N_PL,J  !Planned/intended/design Life cycle of structure
INTEGER,INTENT(IN)::INSPEC  !Inspection status (1==TRUE, 0==FALSE)
REAL(8),INTENT(IN)::AI     !Initial crack length bounds m
REAL(8),INTENT(IN)::DECT_CRACK
REAL(8),INTENT(INOUT)::AF(NODE)
REAL(8),INTENT(INOUT)::N_EFF(NODE) !Resultant life of node
REAL(8),INTENT(INOUT)::RP_PERF(NODE)
LOGICAL,INTENT(OUT)::LGC_9 !TRUE==FAILED, FALSE==SURVIVED
INTEGER::I,COUNT,STR_INT_COUNT,CRLEN_COUNT,ND_LIFE_COUNT !Failure counters
REAL(8),DIMENSION(NODE)::BETA !stress intensity correction factor
REAL(8),DIMENSION(NODE)::ND_MULSTR,KRANS,K_LOAD !Nodal multiaxial stress MPa,
!nodal stress intensity factor
MPam1/2
REAL(8)::A_CR(NODE) !Minimum crack length required to cause fracture at node m
LOGICAL::LGC,LGC_1,LGC_2 !TRUE==FAILED, FALSE==SURVIVED
REAL(8)::GG,EXRN

LGC_9=.FALSE.; BETA=0.; ND_MULSTR=0.; KRANS=0.; A_CR=0. ; K_LOAD=0.
COUNT=0 ; STR_INT_COUNT=0 ; CRLEN_COUNT=0 ; ND_LIFE_COUNT=0
ND_MULSTR=0. ; K_LOAD=0.
CALL ND_CRACK_GROWTH(NODE,OMEGA,AF,AI,DECT_CRACK,N_EFF,RP_PERF,N_THK,N_DIA,
      C_MAT,M_PWR,ND_STR,ND_MULSTR,J,INSPEC,JOINT)
DO I=1, NODE
  CALL ND_FT_SI(JOINT,I,ND_MULSTR(I),AF(I),K,BETA(I),K_LOAD(I),KRANS(I),LGC)
  IF (LGC==.TRUE.) THEN
    STR_INT_COUNT=STR_INT_COUNT+1
    WRITE(20,68) J,I,K_LOAD(I)
    IF(I>=JOINT) EXIT
  ELSE
    END IF
    GG=KRANS(I)/(BETA(I)*ND_MULSTR(I))
    A_CR(I)=(GG*GG)*1./PI !DETERMINE MINIMUM CRACK
    IF (AF(I)>= A_CR(I)) THEN
      CRLEN_COUNT=STR_INT_COUNT+1
      WRITE(20,78) J,I,AF(I),A_CR(I)
      IF(I>=JOINT) EXIT
    ELSE
      END IF
      CALL
ND_LIFE(JOINT,I,N_PL,C_MAT,M_PWR,BETA(I),ND_MULSTR(I),RP_PERF(I),A_CR(I),LGC_1)
  IF (LGC_1==.TRUE.) THEN
    ELSE
  END IF
END DO
COUNT=STR_INT_COUNT+CRLEN_COUNT+ND_LIFE_COUNT
IF (COUNT >0) THEN
  LGC_9=.TRUE.
  ELSE
  LGC_9=.FALSE.
  END IF
68  FORMAT (I10,11X,'STRESS INS',11X,'@ NODE',I5,6X,F15.3)
78  FORMAT (I10,11X,'CRK LENGTH',11X,'@ NODE',I5,6X,2F10.3)
88  FORMAT (I10,11X,'LIFE CYCLE',11X,'@ NODE',I5)
RETURN
END SUBROUTINE ND_LEFM_ANALYSIS
=====

```

```

SUBROUTINE EXTERNAL_CRACK_TUBE (A,T,EXT_DIA,F)
IMPLICIT NONE

```

```

REAL(8), INTENT(IN)::A,T,EXT_DIA
REAL(8), INTENT(OUT)::F
REAL(8)::X,Y,G,RI,RO

```

```

RO=EXT_DIA/2.
RI=RO-T
X = A/T; Y = RI/RO
CALL G_VAL(X,Y,G)
F = G/(SQRT(1-(X))/(1+(1/Y)))

```

```
RETURN
END SUBROUTINE EXTERNAL_CRACK_TUBE
```

```
=====
SUBROUTINE G_VAL(X,Y,G)
IMPLICIT NONE
```

```
REAL :: LINEAR_INTER
```

```
REAL(8), INTENT(IN):: X,Y
REAL(8), INTENT(OUT):: G
REAL(8)::G1,G2,Y1,Y2
```

```
IF ((X>0.) .AND. (X<= 0.8)) THEN
!
!   IF ((Y>0.) .AND. (Y<= 0.1)) THEN
!       G1=0. ; Y1=0.
!       G2=0.1 ; Y2=0.1
!       G=LINEAR_INTER(Y1,G1,Y2,G2,Y)
!
!   ELSE IF ((Y>0.1) .AND. (Y<= 0.2))THEN
!       G1=0.1 ; Y1=0.1
!       G2=0.18 ; Y2=0.2
!       G=LINEAR_INTER(Y1,G1,Y2,G2,Y)
!
!   ELSE IF ((Y>0.2) .AND. (Y<= 0.3)) THEN
!       G1=0.18 ; Y1=0.2
!       G2=0.265 ; Y2=0.3
!       G=LINEAR_INTER(Y1,G1,Y2,G2,Y)
!
!   ELSE IF ((Y>0.3) .AND. (Y<=0.4)) THEN
!       G1=0.265 ; Y1=0.3
!       G2=0.325 ; Y2=0.4
!       G=LINEAR_INTER(Y1,G1,Y2,G2,Y)
!
!   ELSE IF ((Y>0.4) .AND. (Y<= 0.5)) THEN
!       G1=0.325 ; Y1=0.4
!       G2=0.375 ; Y2=0.5
!       G=LINEAR_INTER(Y1,G1,Y2,G2,Y)
!
!   ELSE IF ((Y>0.5) .AND. Y<=0.6) THEN
!       G1=0.375 ; Y1=0.5
!       G2=0.435 ; Y2=0.6
!       G=LINEAR_INTER(Y1,G1,Y2,G2,Y)
!
!   ELSE IF ((Y>0.6) .AND. Y<=0.7) THEN
!       G1=0.435 ; Y1=0.6
!       G2=0.46 ; Y2=0.7
!       G=LINEAR_INTER(Y1,G1,Y2,G2,Y)
!
!   ELSE IF ((Y>0.7) .AND. Y<=0.8) THEN
!       G1=0.46 ; Y1=0.7
!       G2=0.5 ; Y2=0.8
!       G=LINEAR_INTER(Y1,G1,Y2,G2,Y)
!
!   ELSE IF ((Y>0.8) .AND. Y<=0.9) THEN
!       G1=0.5 ; Y1=0.8
!       G2=0.535 ; Y2=0.9
!       G=LINEAR_INTER(Y1,G1,Y2,G2,Y)
!
!   ELSE IF (Y>0.9) THEN
!       G = 1.
!   ELSE
!   END IF
```

```
ELSE IF (X>.8) THEN
    G = 1.
ELSE
```

```
END IF
```

```
END SUBROUTINE G_VAL
```

```
=====
SUBROUTINE OPT_VAR_ARR_T25(T_25,L,K,PERCENT,MIN)
IMPLICIT NONE
INTEGER,INTENT(IN)::L,K !L=DIVISIONS/TRIALS
REAL(8),INTENT(IN)::PERCENT
REAL(8),INTENT(IN)::MIN
REAL(8),INTENT(INOUT)::T_25(L,K)
REAL(8)::P,Q,R,S
INTEGER::I,J,M
DO I=1,L/2
```

```

      DO M=1,K
        CALL RANDOM_NUMBER(P)
        T_25(I,M)=P*(PERCENT-MIN)+MIN
      END DO
    END DO
  DO I=1,L/2
    J=(L/2)+I
    DO M=1,K
      T_25(J,M)=-T_25(I,M)
    END DO
  END DO
  !===== SHUFFLE THE ARRAYS =====
  CALL KNUTH_SHUFFLER_T25 (T_25,L,K)
  !=====
  RETURN
END SUBROUTINE OPT_VAR_ARR_T25

```

```

-----
SUBROUTINE KNUTH_SHUFFLER_T25 (T_25,L,K)
!THE SUBROUTINE SHUFFLES ARRAYS IN A NON-BIASED MANNER
!PUBLISHED BY DONALD E. KNUTH IN VOLUME 2 OF HIS BOOK
!THE ART OF COMPUTER PROGRAMMING AS "ALGORITHM P"
!IT IS ESSENTIALLY THE DURSTENFIELD IMPLEMENTATION OF
!THE FISCHER-YATES SHUFFLER
IMPLICIT NONE
REAL(8),INTENT(INOUT)::T_25(L,K)
INTEGER,INTENT(IN)::L,K
REAL::B,A
INTEGER::I,J,M
DO I=L,1,-1
  DO M=1,K
    CALL RANDOM_NUMBER(A)
    J=INT(A*(L)+1)
    B=T_25(J,M)
    T_25(J,M)=T_25(I,M)
    T_25(I,M)=B
  END DO
END DO
RETURN
END SUBROUTINE KNUTH_SHUFFLER_T25

```

```

-----
SUBROUTINE EVEN_NUMBER_CHECKER(NUM,ERR)
!THIS SUBROUTINE CHECKS IF THE NUMBER ENTERED IS EVEN
IMPLICIT NONE
INTEGER,INTENT(IN)::NUM
INTEGER,INTENT(OUT)::ERR !ZERO=SUCCESS, 1=FAILURE;RETRY
INTEGER::Y
REAL::X,Z
IF (NUM==0)THEN
  ERR=1
  RETURN
ELSE
END IF
X=REAL(NUM/2.)
Y=INT(NUM/2)
Z=REAL(X-Y)
IF (Z==0.)THEN
  ERR=0
  RETURN
ELSE
  ERR=1
END IF
RETURN
END SUBROUTINE EVEN_NUMBER_CHECKER

```

```

=====
SUBROUTINE STOFLEX_VAR(N_STL,N_STU,N_YRS,N_PL,U_CY,L_CY,INSPEC_1,INSPEC_2)
USE DIMENSIONS
IMPLICIT NONE
INTEGER,INTENT(IN)::N_STL !Loaded structural cycle
INTEGER,INTENT(IN)::N_STU !Unloaded structural cycle
INTEGER,INTENT(IN)::N_YRS
INTEGER,INTENT(OUT)::N_PL !Total life cycle
INTEGER,INTENT(OUT)::U_CY !Unloaded cycles per day
INTEGER,INTENT(OUT)::L_CY !Loaded cycles per day
INTEGER,INTENT(OUT)::INSPEC_1 !First annual inspection
INTEGER,INTENT(OUT)::INSPEC_2 !Second annual inspection
INTEGER,PARAMETER::DAY=365
U_CY=N_STU/DAY
L_CY=N_STL/DAY
N_PL=(N_STL+N_STU)*N_YRS
INSPEC_1=(N_STL+N_STU)/2
INSPEC_2=N_STL+N_STU

```



```
RETURN
END SUBROUTINE STOFLEX_VAR
```

```
=====
SUBROUTINE STO_DATREC_2(JOINT, MEMBER)
IMPLICIT NONE
INTEGER, INTENT(IN) :: JOINT, MEMBER
WRITE(20, 210) JOINT, MEMBER
WRITE(20, 220)
WRITE(15, 230)
WRITE(15, 240)
210 FORMAT ('STOFLEX ANALYSIS FOR MULTI-MEMBERED STRUCTURES/COMPONENTS.', ' FOCAL
JOINT:', I5, &
           ', FOCAL MEMBER:', I5 //, &
           3X, 'CYCLE', 8X, 'BASIC FAILURE EVENT', 5X, 'FAILURE
LOCATION', 3X, 'VALUE')
220 FORMAT (2X, '-----', 6X, '-----', 5X, '-----', 3X, '-----')
230 FORMAT (1X, 'CYCLE', 7X, 'JOINT', 7X, 'N + DN', 11X, 'A + DA', 13X, 'K')
240 FORMAT ('-----', 4X, '-----', 2X, '-----', 5X, '-----', 7X, '-----')
RETURN
END SUBROUTINE STO_DATREC_2
=====
```

```
SUBROUTINE DATREC_1
IMPLICIT NONE
WRITE(20, 210)
WRITE(20, 220)
210 FORMAT ('FLEXSTREM ANALYSIS FOR SINGLE MEMBERED STRUCTURES/COMPONENTS.' //, &
           3X, 'SIM NO', 8X, 'LOAD(MN)', &
           7X, 'INCRMNT FACTR', 2X, 'BEND STRGTH(MPA)', 1X, 'BENDING STR(MPA)', &
           3X, 'BEND LIM ST', 2X, 'TENS STRGTH(MPA)', 2X, 'TENS STR(MPA)', 2X, 'TENS LIM
ST', 1X, &
           'COMP STRGTH(MPA)', 1X, 'COMP STR(MPA)', 1X, 'COMP LIM ST', 2X, 'YLD
STRGTH(MPA)', 2X, &
           'MULTIAXIAL(MPA)', 3X, 'STRGTH LIM ST', 1X, 'FRACT LOAD(MPAMA0.5)', &
           1X, 'FRACT TGHNS(MPAMA0.5)', 1X, 'FRACT LIM ST', 3X, 'CRACK LGTH(M)', 4X, 'MIN
CRACK(M)', 2X, &
           'CRACK LIM ST', 2X, 'PLANNED LIFE(CY)', 1X, 'RESULTANT LIFE(CY)', 2X, 'LIFE LIM
ST')
220 FORMAT ('-----', 8X, '-----', &
           7X, '-----', 2X, '-----', 1X, '-----', &
           3X, '-----', 2X, '-----', 2X, '-----', 2X, '-----'
           ', 1X, &
           '-----', 1X, '-----', 1X, '-----', 2X, '-----'
           -, 2X, &
           '-----', 3X, '-----', 1X, '-----', &
           1X, '-----', 1X, '-----', 3X, '-----', 4X, '-----'
           -----', 2X, &
           '-----', 2X, '-----', 1X, '-----', 2X, '-----'
           ---')
RETURN
END SUBROUTINE DATREC_1
=====
```

```
SUBROUTINE DATREC_2(JOINT, MEMBER)
IMPLICIT NONE
INTEGER, INTENT(IN) :: JOINT, MEMBER
WRITE(20, 210) JOINT, MEMBER
WRITE(20, 220)
OPEN(14, FILE='FAILED_MEMBERS.FLX')
OPEN(19, FILE='FAILED_NODES.FLX')
210 FORMAT ('FLEXSTREM ANALYSIS FOR MULTI-MEMBERED STRUCTURES/COMPONENTS.', &
           ' FOCAL JOINT:', I5, ' FOCAL MEMBER:', I5 //, &
           3X, 'SIM NO', 4X, 'WIND SPD(M/S)', 5X, 'WIND FORCE(MN)', &
           3X, 'INCRMNT FACTR', 3X, 'MEM STRGTH(MPA)', 4X, 'MEM STRESS(MPA)', 4X, &
           'MEM LIM ST', 1X, 'NODAL MUL AXLSTR(MPA)', 2X, 'STR
INSTY(MPAMA0.5)', 1X, &
           'FRACT TGH(MPAMA0.5)', 2X, 'FRCT LIM ST', 2X, 'EXSTNG CRCK(M)', 4X, &
           'CRIT CRCK(M)', 2X, 'CRCK LIM ST', 2X, 'PLANNED LIFE(CY)', 1X, &
           'RESULTANT LIFE(CY)', 1X, 'LIFE LIM ST')
220 FORMAT ('-----', 8X, '-----', 4X, '-----', 5X, '-----', &
           3X, '-----', 3X, '-----', 4X, '-----', 4X, &
           '-----', 1X, '-----', 2X, '-----'
           ', 1X, &
           '-----', 2X, '-----', 2X, '-----', 4X, &
           '-----', 2X, '-----', 2X, '-----', &
           1X, '-----', 1X, '-----')
RETURN
END SUBROUTINE DATREC_2
=====
```

Appendix B.2

(Sub-) Programs	Function(s)	Author (Programmer)	Process	Type 1	Type 2	FLEXSTREM	FLEXOPT	STOFLEX
flexstrem	to carry out a comprehensive structural reliability	E.C.C	FLEXSTREM	X	X	X	X	X
flexopt	to carry out structural size optimization based on FLEXSTREM	E.C.C	FLEXOPT	X	X		X	
stoflex	stochastic FLEXSTREM for inspection and maintenance scheduling	E.C.C	STOFLEX	X	X			X
area	to get the surface area of a member (component)	E.C.C	N/A	X	X	X	X	X
mass	to get the mass of a member (component)	E.C.C	N/A	X	X	X	X	X
force_co	to calculate the force coefficient on a member	E.C.C	D3.	X	X	X	X	X
s_force_co	to calculate the force coefficient on a shielded member	E.C.C	D3.	X	X	X	X	X
gumbel_trans	to transform a variable to the Gumbel (maximum) distribution	E.C.C	N/A	X	X	X	X	X
linear_inter	for linear interpolation	E.C.C	N/A	X	X	X	X	X

logn_trans	to transform a variable to the lognormal distribution	E.C.C	N/A	X	X	X	X	X	X
gauss_trans	to transform a variable to the normal (Gaussian) distribution	E.C.C	N/A	X	X	X	X	X	X
dimensions	contains useful constants	E.C.C	N/A	X	X	X	X	X	X
str_par	reads data for multimember structures	E.C.C	B	X		X		X	
single_mem	reads data for single member structures	E.C.C	A		X			X	
expo_random_number	generates an exponential random number	E.C.C	N/A	X		X		X	
gauss_random_number	generates a normal (Gaussian) random number	Numerical recipes	N/A	X		X		X	
gumbel_max_random_number	generates a Gumbel (maximum) random number	E.C.C	N/A	X		X		X	
table_cf	reference table for force coefficients	E.C.C	D3		X			X	
table_sf	reference table for force coefficients for shielded members	E.C.C	B4		X			X	

wind_force		E.C.C	D			X	X	X	X	X
load_combination	calculates the total wind force on the structure	E.C.C	E	X	X	X	X	X	X	X
sto_load_combination	combines all loading on the structure to produce the loading/increment factor	E.C.C	E	X	X	X	X	X	X	X
tensile_stress	stochastic load combination (	E.C.C	G	X	X	X	X	X	X	X
bending_stress	tensile stress calculation	E.C.C	F	X	X	X	X	X	X	X
compressive_stress	bending stress calculation	E.C.C	H	X	X	X	X	X	X	X
multiaxial_stress	compressive stress calculation	E.C.C	I	X	X	X	X	X	X	X
mem_analysis	multiaxial stress calculation	E.C.C	O	X	X	X	X	X	X	X
mem_tens	member analysis (failure of survival)	E.C.C	03	X	X	X	X	X	X	X
mem_comp	member tension	E.C.C	06	X	X	X	X	X	X	X
minimum_crack	member compression	E.C.C	L/R7	X	X	X	X	X	X	X
	calculates minimum crack length that would lead to fast fracture	E.C.C								

crack_length	calculates current crack length in structure	E.C.C	J	X		X	X	X	
crack_growth	paris-erdogan crack growth model	E.C.C	S-J	X				X	
external_crack_tube	evaluates the stress intensity correction factor of an external crack in a thick tube	E.C.C	N/A		X	X	X		X
frac_analysis	failure or survival analysis for fracture	E.C.C	M	X		X	X	X	
fract_tough	transforms fracture toughness to given distribution	E.C.C	K	X		X	X	X	
g_val	helps in determining the stress intensity correction factor	E.C.C	N/A		X	X	X	X	
life_cycle	LEFM estimation of the remaining life of the structure	E.C.C	N	X		X	X	X	
crack_integ	integration in lefm life cycle formulae	E.C.C	N./R10.	X		X	X	X	
nd_lefm_analysis	failure or survival lefm analysis for structure nodes	E.C.C	P		X	X	X	X	
sto_nd_lefm_analysis	stochastic adaptation of FLEXSTREM nd_lefm_analysis	E.C.C	N/A		X				X

nd_crack_len	calculates current crack length in structure	E.C.C	R3				X	X	X	
nd_crack_growth	paris-erdogan crack growth model for multi joints (nodes)	E.C.C	S-R3				X			X
nd_ft_si	fracture toughness-stress intensity factor analysis	E.C.C	R4				X	X	X	
mulstr	transforms nodal stress to given distribution	E.C.C	R1				X	X	X	
nd_life	LEFM estimation of the remaining life of the node	E.C.C	R10				X	X	X	
fea_block	FEA analysis	E.C.C	B3				X	X	X	
opt_fea_block	optimization implementation for FEA analysis	E.C.C	B3				X	X	X	
new_node	reads in section properties for main FEA analysis	E.C.C	B3.				X	X	X	
opt_new_node	reads in section properties (based on groups) for main FEA analysis	E.C.C	B3.				X	X	X	
new_coord	reads in structure node coordinates	E.C.C	B3.				X	X	X	
new_locals	builds local stiffness matrix	E.C.C	B3.				X	X	X	
gs_sor	solution for unknown in the FEA equation (KF=X)	ALEXANDER L. GURDINOV	B3.				X	X	X	
new_tendon	calculates the stress in each member	E.C.C	B3.				X	X	X	

wind_mem	Determines the sheltered members from the set of all structure members	E.C.C	B3.		X	X	X	X
even_number_checker	checks if entered number is even	E.C.C	N/A	X	X	X		
opt_var_arr_t25	generation of optimization coefficients	E.C.C	FLEXOPT-A1/A2	X	X	X		
knuth_shuffle_t25	shuffles optimization coefficients	E.C.C	FLEXOPT-A3	X	X	X		
stoflex_var	initializes stochastic data for stoflex	E.C.C	N/A	X	X			X
sto_datrec2	data recording for stoflex	E.C.C	N/A		X			X
datrec_1	data recording for flexstream (level 1)	E.C.C	N/A	X			X	
datrec_2	data recording for flexstream (level 2)	E.C.C	N/A		X		X	

### Appendix C

#### The GNU General Public License

The programs by E. C. C (Thesis Author) are free software: you can redistribute it and/or modify it under the terms of the GNU General Public License as published by the Free Software Foundation, either version 3 of the License, or (at your option) any later version.

This program is distributed in the hope that it will be useful, but **WITHOUT ANY WARRANTY**; without even the implied warranty of **MERCHANTABILITY or FITNESS FOR A PARTICULAR PURPOSE**. See the GNU General Public License for more details.

You should have received a copy of the GNU General Public License along with this program. If not, see <http://www.gnu.org/licenses/>.